Design, Synthesis and Characterisation of Tool Compounds to Define the Roles of Serine Racemase and Dual-specificity Tyrosine Phosphorylation-regulated Kinase 1A in Diseases of the Central Nervous System

Scott Henry Henderson

Submitted for the degree of Doctor of Philosophy

University of Sussex

June 2019

Declaration

I hereby declare that this thesis has not been and will not be, submitted in whole or in part to another University for the award of any other degree.

The contributions of other persons that have produced results that are exhibited in this thesis are outlined below:

Dr. Chloe Koulouris (University of Sussex) carried out all protein production and purification, biological assays and crystallography in support of the Serine Racemase project.

In relation to the DYRK1A project, Dr. Fiona Sorrell (SGC, University of Oxford) carried out protein-ligand crystallography; Mr. James Bennett (TDI, University of Oxford) conducted the ligand-binding displacement assay; Dr. Paulo Godoi (SGC, UNICAMP) carried out the thermal shift kinase selectivity assay; Dr. Roberta Ruela de Sousa (SGC, UNICAMP) carried out the NanoBRET cellular activity assay. A number of assays and analytical results were carried out by commercial vendors. %ee determination was conducted by Reach Separations Ltd. Biological activity and selectivity of DYRK1A inhibitors were determined at ProQinase GmbH and DiscoveRx Corporation. Cyprotex Ltd. conducted MDCK-MDR1 permeability assay. The synthesis and characterisation of compounds **287**, **288**, **289**, **290**, **277** and **299** was carried out by Mr. Malacky Coleman Balaam as part of his MChem award at the University of Sussex. Small molecule x-ray crystallography was carried out by Dr. Mark Roe (University of Sussex). Mr. Marcus Hanley (University of Sussex) and Mr. Thomas Keating (University of Sussex) conducted metabolic stability and thermodynamic solubility assays.

Interpretation and subsequent decision making based on the data generated by those listed above is wholly my own.

Signed……

S. H. Henderson

Acknowledgements

I would like to thank my supervisors, Professor Simon Ward and Professor John Atack for their guidance, faith and expertise. Your supervision has enabled me to develop into an independent researcher. I would also like to acknowledge the BBSRC, Evotec UK Ltd and the University of Sussex for providing funding and support during this research project.

I would like to thank the members of the Structural Genomics Consortium (SGC) who I have had the pleasure of collaborating with during the DYRK1A project. Dr. Jonathan Elkins, Dr. Fiona Sorrell, Mr. James Bennett, Dr. Paulo Godoi and Dr. Roberta Ruela de Sousa, thank you for your invaluable insights, advice and contributions that has resulted in this work. I would like to thank my industrial supervisor Dr. Daryl Walter for his input, advice and enthusiasm. I would like to acknowledge Evotec for hosting me at their research labs in Abingdon, Oxfordshire, and all of the scientists at Evotec who made the experience both valuable and enjoyable.

I am grateful to past and present members of the Sussex Drug Discovery Centre – special thanks to Chloe Koulouris for her collaboration on the Serine Racemase project. Ryan West and Mark Honey, it was great to bounce ideas and chat chemistry. Irina Chuckowree, Tristan Reuillon and Ben Wahab thank you for your support, expertise and approachability during the early stages of my PhD. Thank you to Malacky Coleman Balaam, the MChem student that I had the opportunity to supervise. To all of those at the SDDC that I have failed to mention by name but whom I have had the pleasure of working alongside for the past four years, thank you. I would also like to acknowledge the shared facility managers at the University of Sussex, Dr. Mark Roe, Dr. Alaa Abdul-Sada and Dr. Iain Day, for their support and guidance in regards to x-ray crystallography, mass spectrometry and NMR spectroscopy. I would like to thank Dr. Robert Mart (University of Cardiff) for the use of the polarimeter.

Finally, I would like to thank my family, who I can never truly thank enough for their support; my parents Beverly and Michael Henderson, my brother Phil and sister Sarah. I'd especially like to thank my wife Gemma for your love, support and for always being there for me. "You're beautiful because for you, politeness is instinctive, not a marketing campaign".

This thesis is dedicated to those born with Trisomy 21 and to those who develop Alzheimer's disease later in life. I sincerely hope that in some way this research contributes to providing you with answers and improving your prospects. So it goes.

Abstract

The inherent challenges associated with delivering novel treatments for diseases of the central nervous system (CNS) have resulted in significant reductions in research capacity within the global biopharma industry, despite the growing societal burden of CNS diseases within ageing populations. This thesis describes the design and synthesis of small molecule inhibitors of two enzymes implicated in diseases of the CNS, Serine racemase (SR) and Dual-specificity tyrosine phosphorylation-regulated kinase 1A (DYRK1A).

SR is an enzyme responsible for the production of the *N*-methyl-*D*-aspartate receptor (NMDA-R) co-agonist *D*-serine. Hyperactivation and hypoactivation of the NMDA-Rs is implicated in numerous diseases of the CNS. Inhibition of SR has the potential to attenuate the activity of the NMDA-Rs without the side effects associated with conventional NMDA-R antagonists. A multifaceted approach is taken to identify a hit series on which to develop a molecular probe for SR; a molecule (A) derived from a historical fragment-screening campaign carried out by Evotec is investigated as a chemotype to deliver a SR tool compound. Published peptidomimetics (B) that represent one of the most potent classes of SR inhibitors are further modified with the aim of increasing inhibitory potency. Preliminary SR inhibition data in our assay format suggests that neither of these two chemotypes inhibit SR.

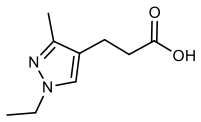

A

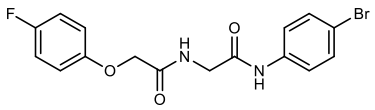

B

DYRK1A is a protein kinase that plays an essential role in the regulation of cellular processes involved in maintaining normal brain development and function. Overexpression of DYRK1A is believed to be responsible for the intellectual impairment, early onset Alzheimer's disease and characteristic phenotype exhibited by patients with Down's syndrome.

Three distinct series of inhibitors that were identified from publically available kinase profiling data were investigated in parallel for their potential to furnish a selective and drug-like chemical probe of DYRK1A. A program of chemical optimisation, heavily influenced by predictive *in silico* design strategies, was prosecuted around each of these scaffolds with the aims of improving DYRK1A binding affinity and selectivity. In addition the physicochemical properties of each series was refined in order to produce a kinase inhibitor capable of permeating the CNS. Structure-activity relationships established during the course of this project, specifically during investigation of the pyrazolo[1,5-*b*]pyridazine series, identified key regions of DYRK1A that if

targeted appropriately afforded kinome-wide selectivity and unprecedented levels of isoform selectivity. A unique collection of Type I DYRK1A inhibitors that are potent, selective and have the potential to be developed as *in vivo* tools are reported in this thesis.

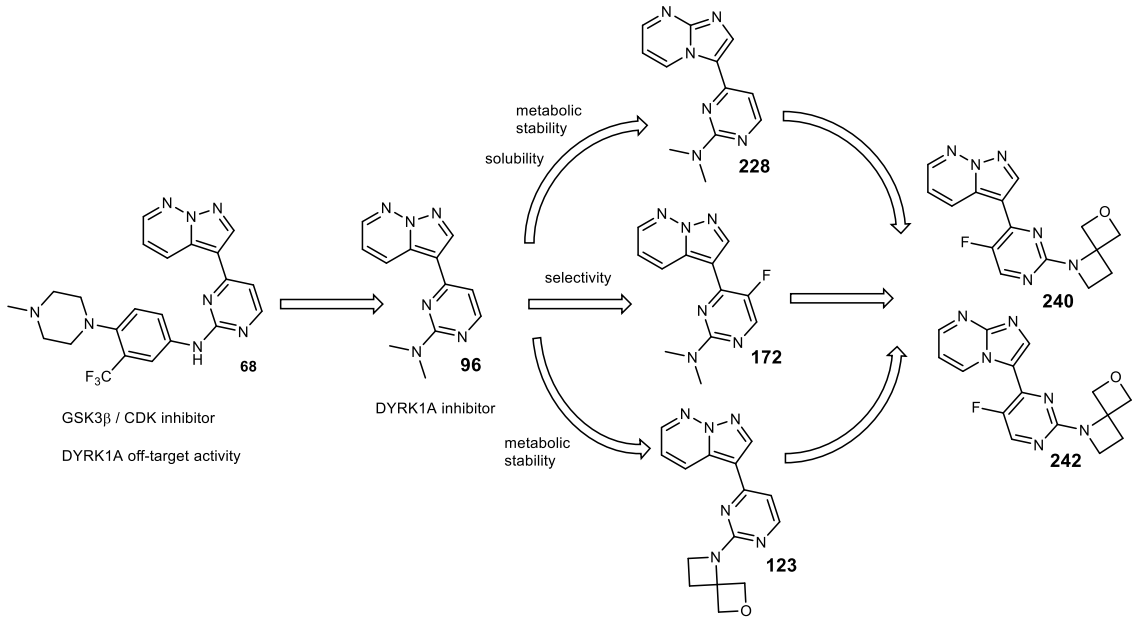

Table of Contents

Abbreviations

3D-RISM	3 Dimensional Reference Interaction Site Model
-ve	Negative
+ve	Positive
°C	Degree Celcius
δ	Chemical shift
µ	Micro
µwave	Microwave irradiation
Å	Angstrom
Aβ	Beta-Amyloid peptide
Ac	Acetyl
AD	Alzheimer's disease
ADME(T)	Absorption, distribution, metabolism, excretion, (toxicology)
ALS	Amyloid lateral scerlosis
APP	Amyloid precursor protein
ASF	Alternative splicing factor
AMKL	Acute megakaryoblastic leukaemia
ASD	Autism spectrum disorder
ATP	Adenosine triphosphate
BBB	Blood brain barrier
Boc	*Tert*-Butyloxycarbonyl
Bt	Benzotriazole
CCG	Chemical Computing Group
CDI	1'-Carbonyldiimidazole
CDKs	Cyclin dependent kinases
ChEMBLdb	ChEMBL database
CKs	Casein kinases
CLKs	CDC-like kinases
CMGC	Including cyclin-dependent kinases (CDKs), mitogen-activated protein kinases (MAP kinases), glycogen synthase kinases (GSK) and CDK-like kinases

CNS	Central nervous system
CNS MPO	Central nervous system multi-parameter optimisation
CREB	cAMP response element binding
CSD	Cambridge Structural Database
CYP	Cytochrome P450 oxidase
Da	Dalton
DAO	*D*-amino acid oxidase
DBU	1,8-Diazabicyclo[5.4.0]undec-7-ene
DIPEA	*N*,*N*-diisopropylethylamine
DMF	*N*,*N*-dimethylformamide
DMF-DMA	*N*,*N*-dimethylformamide dimethyl acetal
DMSO	Dimethylsufoxide
DNA	Deoxyribonucleic acid
dppf	1,1'-Ferrocenediyl-bis(diphenylphosphine)
DSCR	Down's syndrome critical region
DSF	Differential Scanning Fluorimetry
DYRKs	Dual-specificity tyrosine phosphorylation-regulated kinases
EDC	1-Ethyl-3-(3-dimethylaminopropyl)carbodiimide
EGCG	Epigallocatechin gallate
EGFR	Epidermal growth factor receptor
eIF2B	Elongation factor 1-beta
EtOAc	Ethyl acetate
EtOH	Ethanol
F	Phenylalanine
FDA	Food and drug administration
FGFR	Fibroblast growth factor receptor
Gli1	Glioma-associated oncogene
Glu	Glutamic acid
Gly	Glycine
GSKs	Glycogen synthase kinases
H2L	Hit to lead

h	Hour (s)
HBA	Hydrogen bond acceptor
HBD	Hydrogen bond donor
HD	Huntington's disease
hERG	Human ether-a-go-go-related gene
Hip-1	Huntingtin interacting protein 1
HLM	Human liver microsomes
HRMS	High-resolution mass spectrometry
HTS	High-throughput screening
Hz	Hertz
IC_{50}	Concentration for inhibition of 50% of the maximal response
IR	Infrared
kDa	Kilodalton
KNIME®	Konstanz Information Miner
LC-MS	Liquid chromatography-mass spectrometry
LE	Ligand efficiency
LEHA	L-*erythro*-3-hydroxyaspartate
Leu	Leucine
LLE	Lipophilic ligand efficiency
LipE	Lipophilic ligand efficiency
LO	Lead optimisation
LRMS	Low-resolution mass spectrometry
LTP	Long-term potentiation
Lys	Lysine
M	Molar (moles per Litre)
MAO-A	Monoamine oxidase A
MAPKs	Mitogen-activated protein kinases
m-CPBA	3-Chloroperbenzoic acid
MDCK-MDR1	Madin-Darby canine kidney cells transfected with the human MDR1 gene
Me	Methyl

Met	Methionine
MeOH	Methanol
mg	Milligram
min	Minute (s)
m.p.	Melting point
MOE	Molecular Operating Environment
mol	Mole
mRNA	Messenger ribonucleic acid
Mwt	Molecular weight
m/z	Mass-to-charge ratio
NFATs	Nuclear factor of activated T-cells
NFTs	Neurofibrillary tangles
NLS	Nuclear localisation signal
nm	Nanometre
NMDA-R	*N*-methyl-*D*-aspartate receptor
NMR	Nuclear magnetic resonance
OPLS3	Optimised potentials for liquid simulations
PAINS	Pan-assay interference compounds
P_{app}	Apparent permeability rate in MDCK-MDR1 assay
PD	Parkinson's disease
PDB	Protein databank
P-gp	P-glycoprotein
PK	Pharmacokinetic
PKIS	Published Kinase Inhibitor Set
PLP	Pyridoxal-5'-phosphate
PNS	Peripheral nervous system
ppm	Part(s) per million
QC	Quality control
QSAR	Quantitative structure-activity relationship
R	Unspecified functional group
R&D	Research and Development

R*f*	Retention factor
RLM	Rat liver microsomes
RMSD	Root-mean-square deviation
RNF	Ring-finger protein
rt	Room temperature
S	Serine
SAR	Structure-activity relationship
sat.	Saturated
SBDD	Structure-based drug design
SDDC	Sussex Drug Discovery Centre
SDH	Serine dehydratase
Ser	Serine
SF	Splicing factor
SFI	Solubility forecast index
SGC	Structural Genomics Consortium
*si*RNA	small interfering ribonucleic acid
SR	Serine racemase
STAT	Signal transducer and activator of transcription protein
T	Threonine
T3P	Propanephosphonic acid anhydride
TEA	Triethylamine
THF	Tetrahydrofuran
TMS	Trimethylsilyl
TPSA	Topological polar surface area
UV	Ultraviolet
vs	Versus
v/v	Volume for volume
Wnt	Wingless/int protein
XED	EXtended Electron Distributions
Y	Tyrosine

CHAPTER 1. The Need for High Quality Chemical Probes in Drug Discovery

Chapter 1 serves as an introduction to the drug discovery process and highlights the need for quality molecular probes to be used during the early-stages of research undertaken on novel drug targets. The metrics and design strategies employed to identify high quality probes are described below. A brief introduction to an emerging field in synthetic organic radical chemistry, namely photoredox catalysis, which has been used in this thesis for late-stage functionalization of probe compounds, is provided at the end of the chapter.

1.1. Drug Discovery

The identification of a biological target that has been implicated in the progression of a disease is the traditional starting point of a drug discovery program. The target is validated through specifically designed target- and disease-related screening protocols. Compounds that display activity against the target ("hit" compounds) are found by screening chemical libraries of synthetic molecules and natural products against the target. Structure-activity relationships (SAR) are established through close analogue synthesis of hits, most often with the aim of improving potency against the primary target. Analogues with improved affinity and well-balanced molecular properties are termed "lead" compounds. The leads are progressed through preliminary *in vitro* and *in vivo* studies to give an early indication of the toxicology and pharmacokinetic (PK) properties of the molecules. A labour intensive period of further analogue synthesis is carried out until a compound with optimal properties is nominated as a clinical candidate - a molecule which is entered into clinical trials subject to passing a series of studies imposed by regulatory authorities. In the majority of cases the initial clinical candidate is withdrawn from the process or fails due to efficacy, toxicity and poor pharmacokinetics.[1] An overview of the drug discovery process is shown in Figure 1.

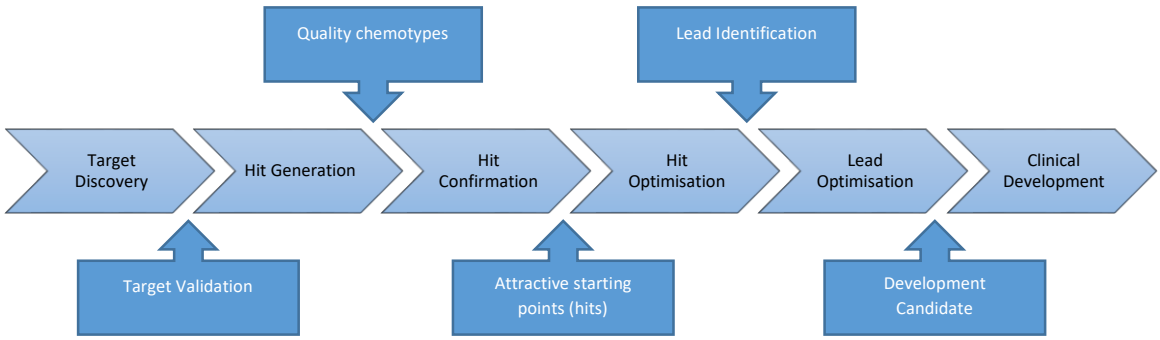

Figure 1. Overview of the Drug Discovery Process.

1.1.1. Target Discovery and Hypothesis Generation

The majority of drug discovery programs begin with the identification of a biological target implicated in the cause or progression of a disease. Confidence in the target is provided when the cell biology, clinical biomarkers and human genetic evidence all connect the target to the disease. Various techniques such as 'omic' technologies, bioinformatics, genetic associations, reverse genetics and *in vivo* studies can all be used to identify a potential target.[2,3]

1.1.2. Target Validation

A 'druggability' assessment of the target is undertaken once the evidence is strong enough to link the target to the disease. Often druggability assessments are carried out with small molecule probes that attenuate the activity of the target and are used to demonstrate the role of the target in cellular and animal models of the disease state. Structural data and bioinformatics data can be studied to determine whether there are known ligand binding sites on the target that may be drugged.

Alternative strategies include the use of antisense technology to target mRNA; small interfering RNA (*si*RNA) prevents gene expression, halting the production of the target of interest.[4] Comparing the phenotypic response of an active molecular probe with the effects of antisense technologies can be an effective method of identifying targets. Other than small molecules, peptides[5] and antibodies[6] that display high specificity for the target have also been effective in the modulation and validation of targets.

In vivo models, such as transgenic or knockout animal models, can represent a more complex disease paradigm and provide an opportunity to observe the effect of gene manipulation expressed in the phenotype of the animal model. The quality of the molecular probe being employed in the animal model heavily impacts the results and interpretation of experiments. Low quality molecular probes that lack selectivity and exhibit poor *in vivo* pharmacokinetics may not give an accurate portrayal of target attenuation and overall role in disease. This is especially true when the results of the animal studies are extrapolated to man.[7]

1.1.3. Hit Generation and Identification[8]

A hit is a compound with confirmed activity against a drug target. Once a target has been validated, hit identification is initiated using a target based approach or a phenotypic approach. High-throughput screening (HTS) against the target using company compound collections (> 10 k compounds) or focused libraries of compounds remains the primary tool for hit generation. DNA-encoded libraries (DEL) can also be screened as a method of finding hits. The oligonucleotide sequence appended to a compound allows rapid identification of the small molecule hit, resolving a major obstacle of conventional combinatorial chemistry. Molecular 'Fragments' (Mwt < 250 Da) can be screened against soluble targets and 3D structural information of the target can be generated with a technique such as x-ray crystallography. Structure-aided drug design can then be employed to improve affinity and selectivity for the target during the hit-to-lead (H2L) phase. If the 3D structure of the target is known or active ligands are known, an *in silico* approach can be taken to identify hits. Virtual screening and Target-based *De Novo* Design are two approaches that can be taken if the 3D target structure is known. Scaffold hopping and searches based on a pharmacophore model derived from ligand data (QSAR data) can also be used to generate hit matter.

During phenotypic screens compounds are screened against the cell, tissue or organism. Hits can then be identified as the molecules that are inducing an observable disease-modifying effect. The identity of the target can then be elucidated.

Hit I.D. and selection affects all later stages of the drug discovery process, consequently much thought should be given to the selection of a hit molecule for H2L optimisation. The hit needs to balance suitable potency against the target with well-balanced physicochemical properties, synthetic feasibility, toxicophores, metabolic stability and selectivity.

1.1.4. Hit Optimisation (H2L) or Lead Identification

A lead compound has palpable scope after further optimisation to deliver a preclinical candidate to test a clinical hypothesis. After a hit or more likely, multiple hit series are identified, a period

of analogue synthesis is undertaken with the purpose of establishing SAR and determining whether a series warrants further investment and resource required for Lead Optimisation (LO).

Multifactorial optimisation of potency, selectivity, physicochemical properties, absorption, distribution, metabolism, excretion and toxicology (ADMET) are undertaken in iterative design cycles that focus on identifying SAR and weaknesses within the series. Screening cascades are in place that often involve the use of orthogonal assays, selectivity assessments (related receptors and off-targets, hERG and CYP inhibition), metabolic stability (*in vitro* and *in vivo*), in addition to cross-species assays. During the H2L phase the lead profile is identified as well as the objectives for LO defined.

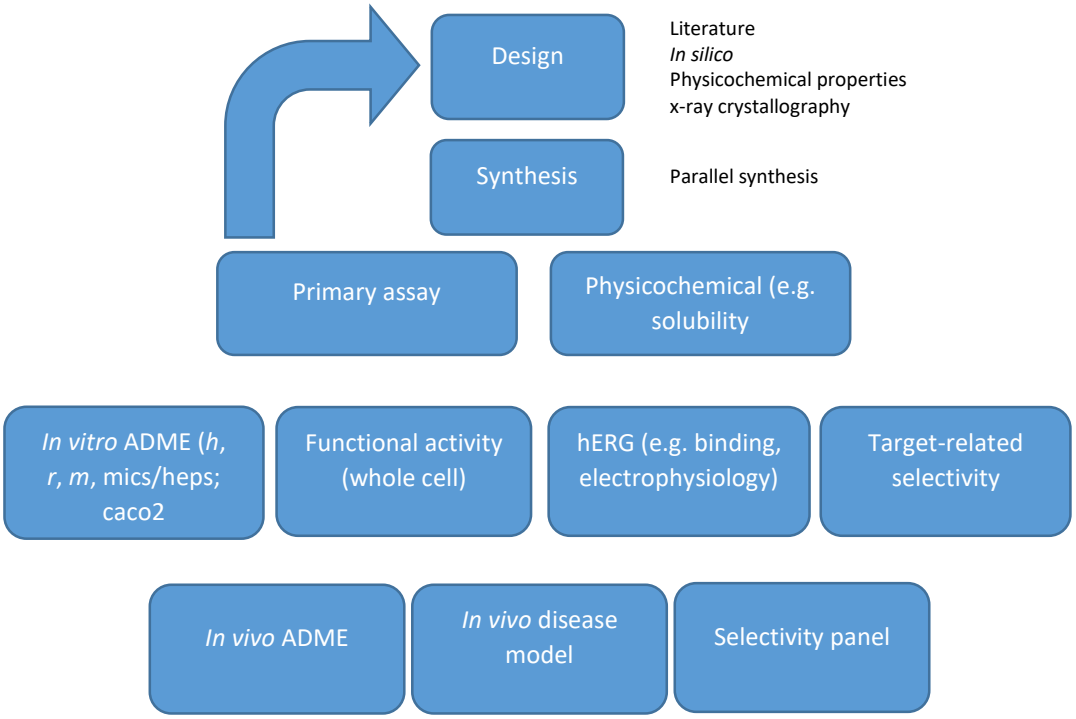

Figure 2. Typical Hit Optimisation cascade leading to Lead Identification. hERG = human ether-a-go-go-related gene; *h* = human; *r* = rat, *m* = murine; mics = microsomes; heps = hepatocytes; caco2 = human epithelial colorectal adenocarcinoma cells.

1.1.5. Lead Optimisation (LO)

As a more focussed and resource intensive extension of H2L, during LO further improvements are sought in *in vitro* and *in vivo* potency, selectivity (versus closely related targets, hERG, phospholipidosis), *in vitro* and *in vivo* pharmacokinetics (metabolic stability in line with desired dosing regimen and intended use) to deliver a preclinical candidate. Consideration is given to

whether the lead is soluble and whether a particular formulation will be required. Small scale *in vivo* toxicology and safety pharmacology studies are undertaken before the lead becomes a candidate. The candidate is then subjected to any studies outlined by regulatory authorities before clinical testing.

1.1.6. Compound Attrition

In spite of technological improvements, greater expenditure on R&D and in theory a wider selection of potential targets unearthed after the human genome was elucidated, the number of medicines reaching the market is in decline with high levels of compound attrition during drug development.[9] Safety concerns and a lack of efficacy are the major factors that have contributed to compound attrition over the past 20 years.[9] The use of high quality molecular probes during the fundamental stages of drug discovery programs may contribute to lowering the high attrition rate.[9]

1.2. The Importance of Choosing the Right Starting Point

1.2.1. Definition of a Chemical Probe

Arrowsmith *et al*. define a chemical probe as *" …a selective small-molecule modulator of a protein's function that allows the user to ask mechanistic and phenotypic questions about its molecular target in biochemical, cell-based or animal studies"*.[10]

Chemical probes should (i) permit the interrogation of a therapeutic hypothesis, (ii) probe on-target safety and facilitate the assessment of mechanistic toxicity and (iii) give confidence that the target is tractable for the following drug discovery program.[10, 11] As a result high quality chemical probes allow an earlier analysis of the target and ultimately enable a 'Go/No-Go' decision to be made at an earlier and less expensive stage of the drug discovery process.[11]

1.2.2. High-Quality Probes = Meaningful Biological Data

Selecting a high quality chemical probe with a desirable balance of properties is important. Choosing a promiscuous probe will result in promiscuous pharmacology, which will confuse the interpretation of data and may result in incorrect decisions being taken around the druggability of a target and the tractability of a chemical series.[10,11] A number of publications have recommended guidelines or 'rules of thumb' for probe selection, these were summarised and further developed by Workman and Collins to produce "fitness factors".[12]

Fitness factors are classified into four main categories: (1) **chemical properties** (structure, stability, solubility and permeability of the chemical probe); (2) **biological potency** (biochemical

and cellular activity, the existence of analogues of the probe with similar activity, and *in vivo* pharmacokinetics to achieve exposure at the target); (3) **biological selectivity** (knowledge of chemotype specific off-targets, the existence of an analogue with no primary target activity, the existence of probes from a different chemical class that exert a similar effect and an awareness of other activities associated with the chemical class); (4) **context of use** (knowledge of whether the probe has been fully characterised and is available for use without restriction, whether complementary experiments are possible such as RNAi and/or mutants of the target availability, ultimately the probe must test specific biological hypotheses).[12]

In spite of numerous publications that advocate the use of high quality probes during the early stages of the drug discovery process, much fundamental biological research that draws mechanistic conclusions is based on unsuitable chemical probes.[13] A classic example is the natural product, Epigallocatechin-3-gallate (EGCG), which is known to be a promiscuous pan-assay interference compound (PAINS),[10,14] yet this has not prevented its use in *in vivo* studies investigating the effects of inhibition of dual-specificity tyrosine phosphorylation regulated kinase 1A (DYRK1A) in patients with Down's syndrome.[15,16]

In recent years scientists have attempted to develop data-driven resources that evaluate the quality of chemical probes so that the community has confidence in their selection and use. Such platforms include the Probe Miner (http://probeminer.icr.ac.uk) and the Chemical Probes Portal (http://chemicalprobes.org).

1.2.3. De-risking the Drug Discovery Process through Industrial-academic Collaboration

The number of newly approved chemical entities, which generate financial returns for pharmaceutical companies, has not kept pace with increases in R&D expenditure.[17] This has resulted in the restructuring of the international Pharmaceutical and Biotechnology (Biopharma) sector and shift of focus towards low-risk targets that are profitable enough to ensure survival.[17]

A positive outcome of the changing landscape of the pharmaceutical industry has been the opportunity for closer collaboration between industry and academia with a move towards a more open model of drug discovery. Early stage fundamental research considered too high risk and costly for industry can be carried out by academia until target confidence is achieved.[18] Orphan and neglected diseases whose patient base do not generate enough of a commercial return to compensate for the cost of R&D can be investigated by academic groups that are funded through charitable donations and university funding.[18]

An open source collaboration between GlaxoSmithKline (GSK), the Structural Genomics Consortium (SGC) and Nanosyn led to a publication in which 367 kinase inhibitors donated by

GSK were screened against 260 human kinases.[19] The full kinase profiling dataset was published and deposited in an open source database, ChEMBLdb.[20] The 367 kinase inhibitors donated by GSK became known as the Published Kinase Inhibitor Set (PKIS). Subsequently, the PKIS (and later the PKIS2) sets were screened by the SGC against a panel of 400 human kinases in the DiscoveRx KINOMEscan® platform and the results were deposited in ChEMBLdb.[21]

A major component of the SGC's work is to improve and expand the quality of the chemical probes contained within the PKIS and PKIS2 sets with the ultimate goal of developing a high quality Kinase Chemogenomics Set (KCGS).[21] In the context of this thesis, the DYRK1A project was carried out as a collaboration between the Sussex Drug Discovery Centre (SDDC) and SGC in an effort to deliver a higher quality chemical probe for DYRK1A. This probe would be freely available to the scientific community and would enable mechanistic and validation studies of DYRK1A as a target for disease.

1.3. Descriptors and Metrics Used to Assess the Quality of Ligands

1.3.1. Ligand Descriptors and Metrics

In recent years more attention has been given to the molecular properties of ligands during H2L and LO as oppose to solely increasing affinity for the target of interest. The recognition that physicochemical properties drive all aspects of compound quality including target affinity and ADMET is becoming more widespread.[22, 23] Selecting an optimal probe at the start of a project with the right balance of physicochemical properties will give the best chance of avoiding attrition at later and more costly stages in the drug discovery process due to compound-related failures.

Although there are many physicochemical properties that can be used to describe a molecule, in terms of compound quality, descriptors of critical importance are molecular weight (Mwt), lipophilicity (log P and log $D_{7.4}$), propensity of the molecule to ionise (pK_a), solubility and hydrogen bonding parameters (HBA and HBD).[23] These descriptors are summarised in Table 1.

Table 1. Critical Physicochemical Descriptors that Govern Compound Quality

Descriptor	Synonym	Definition
Molecular weight	Mwt	Mass of a molecule (and relative size)
Partition Coefficient	cLog P	Partition coefficient of a molecule observed in water-*n*-octanol system. A measure of lipophilicity
Distribution Coefficient	Log $D_{7.4}$	Partition coefficient of a molecule observed in a buffer of known pH (i.e. 7.4) and *n*-octanol system. A measure of lipophilicity at a known pH (i.e. 7.4)
Hydrogen-bond acceptor	HBA	The atom, ion, or molecule component of a hydrogen bond which does not supply the bridging (shared) hydrogen atom
Hydrogen-bond donor	HBD	A bond or molecule that supplies the hydrogen atom to form a hydrogen bond
Topological polar surface area	TPSA	Surface sum over all polar atoms or molecules, primarily oxygen and nitrogen, also including their attached hydrogen atoms
Ionisable constant	pK_a	pK_a is defined as the negative log of the dissociation constant. The pK_a is the pH at which the compound in solution is 50% ionised

In a seminal publication by Lipinski *et al*. the 'rule of 5' was formulated, which proposed a set of guidelines to predict the likelihood of a compound displaying good absorption following oral administration based on its physicochemical properties.[24] Although not all bioactive molecules fit into the 'rule of 5', approximately 80% of marketed oral drugs pass all four rules and < 5% of marketed oral drugs fail on two or more rules.[23] Notable exceptions to the 'rule of 5' include natural products and transporter substrates.

During H2L and LO medicinal chemists have traditionally focussed on increasing the potency of molecules towards the target.[25] However, this has often resulted in the inappropriate use of lipophilicity to build potency into molecules ('molecular obesity')[26] as a chemotype is progressed through H2L and LO. Increased lipophilicity has been linked to promiscuity, higher propensity for hERG inhibition as well as poor solubility.[22] To prevent inflation of molecular properties a number of metrics have been proposed to guide design.[27]

Ligand efficiency (LE) is the average binding energy per atom in a molecule.[28,29] The lipophilic ligand efficiency (LLE or LipE) is an estimate of the specificity of a molecule in binding to a target relative to partitioning into 1-octanol. LE and LLE are calculated as shown in Figure 3.

$$\mathbf{LE = (-2.303\ (RT/HA))\ x\ log\ K_d}$$

$$\mathbf{LLE = pIC_{50} - clog\ P}$$

Figure 3. Equations for Ligand efficiency (LE) and lipophilic ligand efficiency (LLE or LipE). R is the ideal gas constant (1.987 x 10^{-3} kcal / K/ mol), T is temperature in Kelvin (K), K_d is the dissociation constant, HA denotes the number of non-hydrogen atoms, pIC_{50} is the negative logarithmic value of the half-maximal inhibitory concentration, log P is the Partition coefficient.

It has been suggested that LE > 0.3 kcal per mole per heavy atom and LLE > 5 should be achieved for drug candidates that have a K_d < 10 nM when Mwt is 500 Da and cLog P < 3.[23]

1.3.2. Tracking Compound Quality During the DYRK1A Project

In the context of the DYRK1A project, compound optimisation was tracked by calculating the physicochemical properties of molecules prior to synthesis. Once biological data was acquired the LE and LipE were calculated so that inhibitors were progressed based on these metrics rather than on potency alone. LipE plots (Figure 4) were used to monitor compound quality and for decision making throughout the project.

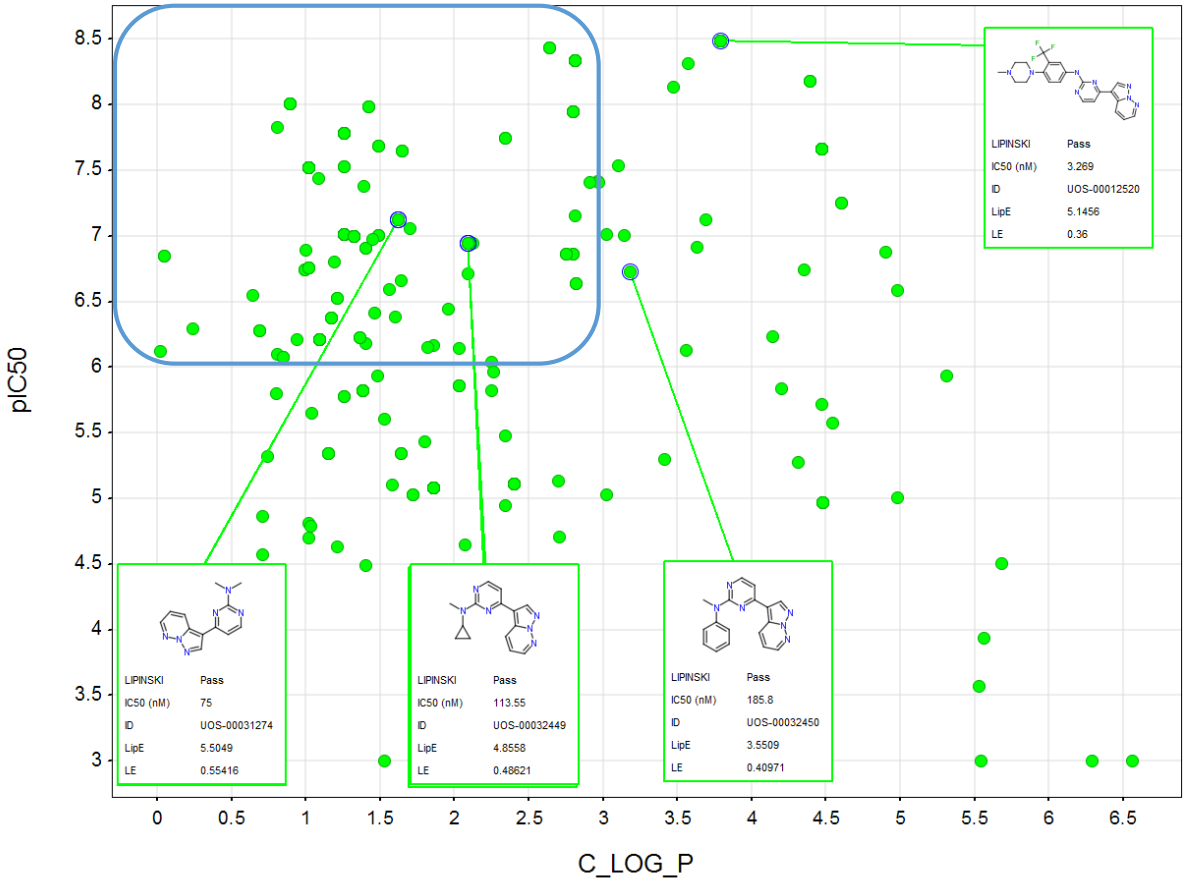

Figure 4. Example of a LipE Plot – tracking inhibitor development during the DYRK1A project using Dotmatics Vortex software. Desirable affinity and lipophilicity is in the space demarcated by the blue box.

An additional metric that was closely monitored during the DYRK1A project, as DYRK1A is a kinase expressed in the CNS, was the CNS Multiparameter Optimisation (MPO) score. The CNS MPO score developed by Wager *et al.*[30] is an algorithm that predicts whether a molecule has a high or low probability of being able to penetrate the blood-brain-barrier (BBB) in order to engage a target in the CNS. Six physicochemical descriptors were correlated to give an overall MPO Score ((1) cLog P, (2) cLog $D_{7.4}$, (3) Mwt, (4) TPSA, (5) HBD and (5) pK_a) and showed that 74% of marketed CNS drugs have CNS MPO scores $\geq$ 4. Furthermore, it was proposed that higher values of TPSA, HBD and Mwt correlate with enhanced P-glycoprotein (P-gp) mediated efflux.[30] A recent review by Heffron highlights clear differences in the physicochemical property space that FDA-approved kinase inhibitors and CNS drugs traditionally occupy.[31] In addition to being substantially more lipophilic, kinase inhibitors also exhibit elevated levels of the three properties that correlate with a molecule's propensity to be a P-gp substrate.

Table 2. Approved CNS Kinase Inhibitors and CNS drugs[31]

Median Property Value	Approved Kinase Inhibitors (n = 34)[a]	CNS drugs (n = 119)[a]
cLog P	4.2	2.8
cLog $D_{7.4}$	3.6	1.7
TPSA (Å)	91	45
HBD	2	1
Mwt	483	305
pK_a	7.0	8.4

[a]Values obtained from reference [31].

Whilst investigating CNS penetrant inhibitors of Phosphoinositide 3-kinase (PI3K), Heffron *et al*. established a minimum set of physicochemical property requirements for molecules predicted to exhibit high brain exposure. The minimum requirements included low hydrogen-bond donor count, high MPO score and low lipophilicity (HBD < 2, CNS MPO > 4.5, cLog P < 2.5).[32] During the DYRK1A project plots of CNS MPO score v cLog P were used in an attempt to try and synthesise molecules with the greatest chance of brain exposure. One such plot can be seen in Figure 5 for the pyrazolo[1,5-*b*]pyridazine series.

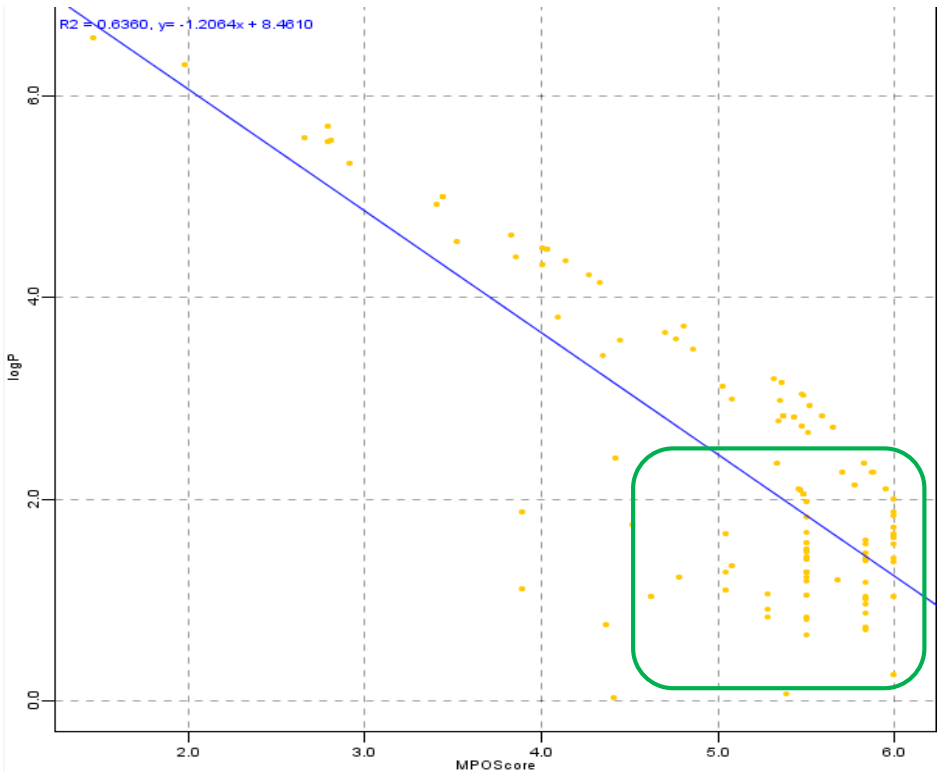

Figure 5. Plot of CNS MPO score v cLog P produced in KNIME® to track compound quality. Green box – desirable CNS kinase space.

The Konstanz Information Miner (KNIME®, version 2.12) is a business analytics tool and open source program that allows for the creation and sharing of applications (workflows) to mine and manipulate data.[33] To ensure compound quality a number of KNIME® chemoinformatic workflows were used throughout the DYRK1A project. The ChemAxon workflow (Figure 6) was used to filter prospective inhibitors based on their predicted physicochemical properties. This and other workflows were used after library enumeration and docking to filter and deprioritise molecules that did not meet probe selection criteria.

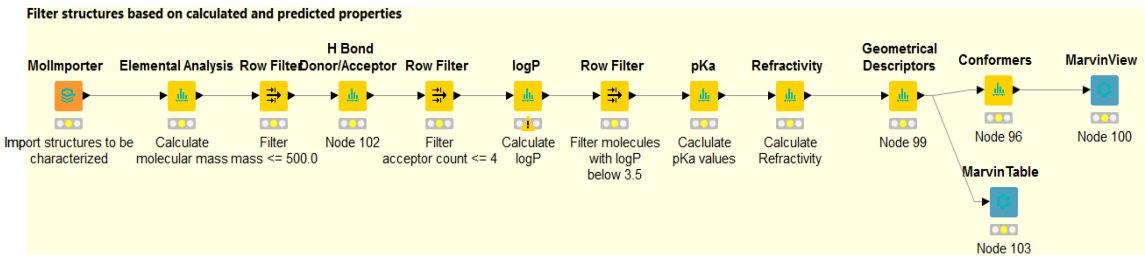

Figure 6. ChemAxon Physicochemical Property Prediction workflow prosecuted in KNIME®.

1.3.3. Predicting *In Vitro* PK during the DYRK1A Project

Prospective inhibitors were subject to KNIME® workflows that predict the *in vitro* pharmacokinetics of molecules based on their physicochemical properties. Molecules that were designed *in silico* to have improved solubility were processed through a KNIME® workflow that calculates Solubility Forecast Index (SFI). Compounds with SFI < 5 are believed to have a higher probability of achieving good physical properties.[34] The workflow, which has been condensed into a metanode, and the calculation used to determine SFI are depicted in Figure 7.

SFI = clog $D_{7.4}$ + #Ar

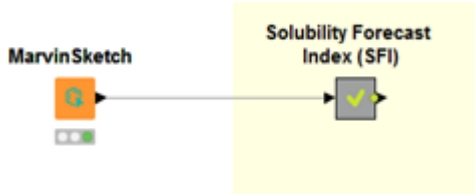

Figure 7. Community KNIME® SFI workflow used to predict solubility of inhibitors. # Ar denotes the number of aromatic rings.

A CNS MPO score workflow was written by Dr Ben Wahab at the SDDC. This workflow is derived from the original research article by Wager *et al*. and was used to estimate the likelihood of a molecule being CNS penetrant.[30] In addition the BBB and PGP Predictor workflows were used to predict and assess a molecule's suitability as a CNS molecular probe (Figure 8). The Blood Brain Barrier (BBB) node is based on work by Norinder and Haerberlein in which computational approaches were analysed that predict BBB distribution for molecules.[35] The first rule states if N + O $\leq$ 5 there is a high chance of the molecule entering the brain. The second rule states if Log P – (N + O) is positive then log BB is positive. Molecules with log BB > 0.3 are likely to cross the BBB, whilst those with log BB < -1 are poorly distributed in the brain.[36] The third aspect of the node is based on TPSA, TPSA should not be greater than 80 $Å^2$ for a CNS penetrant compound.[30] The P-gp Predictor Node estimates the likelihood of a particular molecule being a P-gp substrate.[37]

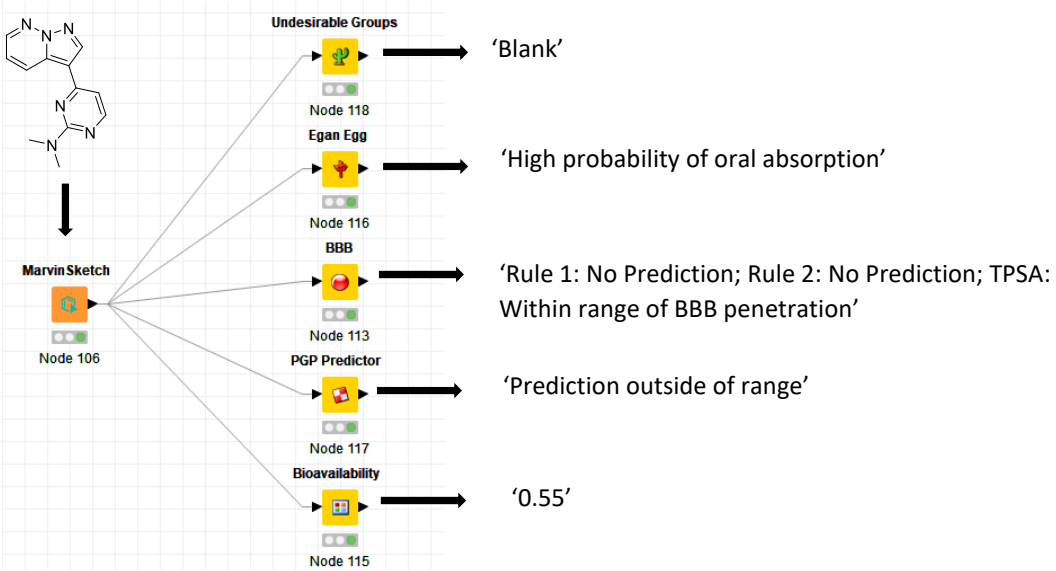

Figure 8. Prediction of oral bioavailability and CNS penetration for compounds. Example pyrazolo[1,5-*b*]pyridazine **96**.

A number of other *in vitro* PK nodes depicted in Figure 8 were used to assess the suitability of a prospective compound for use as a probe and for compound progression. The 'Undesirable Groups' node highlights functional groups within a molecule that are known to be reactive or toxic and includes PAINS.[14] This node is based on a list developed by workers at Evotec. The Egan Egg is a Vertex estimation tool that correlates oral absorption with lipophilicity and polar surface area. A result inside the egg indicates a high probability of oral absorption.[38] The Bioavailability node gives a Bioavailability Score (ABS) based on the probability of a molecule being bioavailable in rat or displaying measurable caco-2 permeability. ABS is governed by the Polar Surface Area (PSA) of a molecule; if PSA > 150 $Å^2$ for an anion ABS is 0.11, if PSA < 150 $Å^2$ and PSA > 75 $Å^2$ then ABS is 0.56, if PSA < 75 $Å^2$ then ABS is 0.85. For compounds outside of these parameters if the molecule passes the Lipinski rule-of-five (ROF) ABS is 0.55, and 0.17 if the compound fails the Lipinski ROF. A low ABS correlates with poor bioavailability.[39]

1.3.4. Prediciting Selectivity

KNIME® can also be used to mine the ChEMBL database (ChEMBLdb).[40] The ChEMBLdb is an open source database of drugs, drug-like molecules and biological targets, holding information on more than 1.4 million compounds and over 12 million records of their effects on biological systems.

Included within the ChEMBLdb is a large amount of kinase profiling data. This data was mined to predict the polypharmacology of a chemotype using the 'NN Activity Pairs' workflow developed by Dr George Papadatos at ChEMBL-EBI.

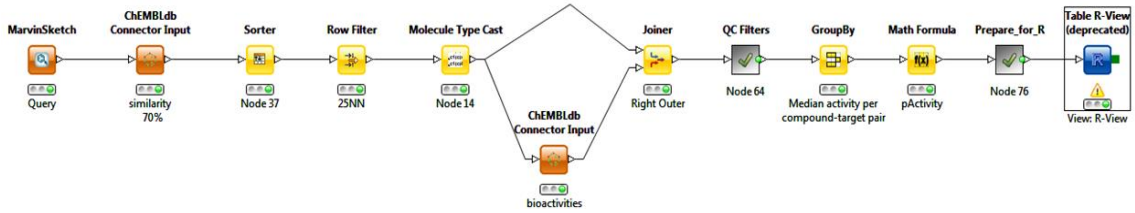

Figure 9. 'NN Activity Pairs' KNIME® community workflow used to mine kinase profiling data stored in ChEMBLdb.

Another method used to interpret the kinase profiling data available in the public domain was to visualise it graphically as described by Metz *et al*.[41] For the chemotype of interest, p(activity) data for the target kinase was plotted against p(activity) data of kinase off-targets. The resulting plots were analysed to identify activity cliffs for matched molecular pairs (MMPs) to guide synthesis of more selective inhibitors. During the DYRK1A project, the PKIS and PKIS2 datasets were analysed in this way for the chemotypes of interest.

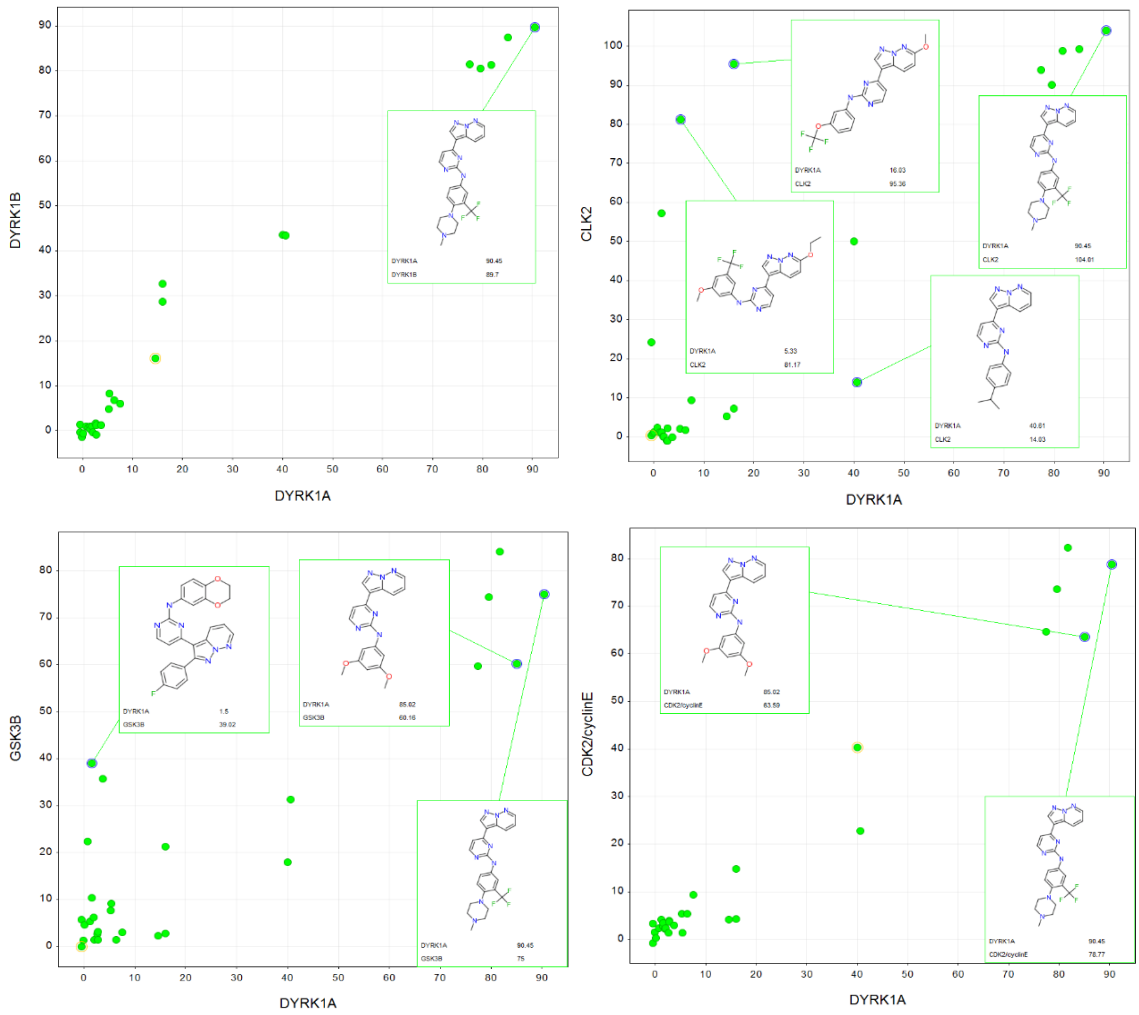

Figure 10. Activity cliff searching in Vortex from Dotmatics. Profiling Data for the pyrazolo[1,5-*b*]pyridazine series was imported into Vortex. X axis is % inhibition at 1 µM for DYRK1A. Y axis is % inhibition at 1 µM for off-target (DYRK1B, CLK2, GSK3β, CDK2). Kinase % inhibition data from reference [19].

A number of patents were mined during this work. A Servier-Vernalis Patent possessed the names of imidazo[4,5-*b*]pyridine analogues that were disclosed as dual DYRK1A-CLK1 inhibitors.[42] The imidazo[4,5-*b*]pyridines were closely related to the imidazo[1,2-*b*]pyridazine series being investigated for DYRK1A inhibition in-house. Contained within the patent was the binding data of the imidazo[4,5-*b*]pyridines series acquired from cellular FRET assays for DYRK1A, DYRK1B, CLK1 and CDK9. This data was mined to look for functional groups within the imidazo[4,5-*b*]pyridine series that afforded DYRK1A selectivity. As the patent contained only names and not structures, the names of the molecules were typed into a Microsoft Excel spreadsheet. The bioactivity data described in the patent was entered into the same spreadsheet against the correct name. The names of the molecules were converted to molecular structures using JChem extensions in Excel. The data could then be interrogated for activity cliffs of key off-targets with the hope that selectivity could be translated to the imidazo[1,2-*b*]pyridazine series.

			Assay Results (μM)			
Number	Compound Name	Compound Structure	D1A Fret	D1B Fret	CLK1 Fret	CDK9 Fret
49	4-[2-methyl-3-(tetrahydro-2H-pyran-4-yl)-3H-imidazo[4,5-b]pyridin-5-yl]pyridine-2,6-diamine	#NAME?	0.003	0.017	0.017	0.979
24	N-(4-{2[5-(2,6-diaminopyridin-4-yl)-2-methyl-3H-imidazo{4,5-b}pyridin-3-yl]ethyl}phenyl)acetamide	#NAME?	0.005	0.015		3.538
29	4-{2-methyl-3-[2-(thiophen-3-yl)ethyl]-3H-imidazo[4,5-b]pyridin-5-yl}pyridine-2,6-diamine	#NAME?	0.004	0.011		3.435
47	4-[3-(2-chlorobenzyl)-2-methyl-3H-imidazo[4,5-b]pyridin-5-yl]pyridine-2,6-diamine	#NAME?	0.003	0.046		0.728

Figure 11. Patent Mining during DYRK1A project. Data from patent entered into Microsoft Excel. ChemAxon JChem Extensions used to convert Name to Structure. Kinase assay data from reference [42].

1.4. Emerging Synthetic Technologies – Photoredox Catalysis in Medicinal Chemistry

In chemistry a radical is an atom, molecule or ion with an unpaired valence electron.[43] The reactivity of radical intermediates is often difficult or impossible to replicate *via* any other means.[44] Traditional methods to generate radical intermediates have relied on hazardous radical initiators (e.g. azobisisobutyronitrile), toxic reagents (e.g. tributyltin hydride) and harsh conditions (high temperatures and high-energy UV irradiation).[43] In the past the outcome of radical reactions was assumed to be less predictable than conventional polar, two-electron chemistry, probably as a result of the reaction conditions employed.[45] This has led to radical chemistry in organic synthesis being underexploited despite the unique reactivity of radicals.

Over the past decade radical chemistry has had a resurgence in popularity owing largely to the rapidly expanding field of photoredox catalysis whereby low energy visible light (380 nm – 750 nm) is used to drive the generation of reactive radical intermediates. The major advantage of generating radicals *via* photoredox catalysis is that the reaction conditions employed are remarkably mild compared to traditional generation of radicals.[46] Ruthenium and iridium polypyridyl complexes are the most common photocatalysts used because they strongly absorb visible light and can be excited specifically with respect to the substrate. Their excited states are formed extremely efficiently and the excited states persist long enough to react with the substrate.[47] Iridium polypyridyl photocatalysts were used exclusively in this thesis.

Commercial photoreactor set-ups have been developed to standardise reaction protocols and improve reproducibility of experiments. These include the EvoluChem™ PhotoRedOx Box used throughout this thesis, and the MacMillan-Merck M1 Photoreactor.[48] Scale-up issues have been overcome in some cases with the use of continuous flow processing. Beatty *et al*. reported photoredox catalysed trifluoromethylation of aryl and heteroaromatic compounds and performed the reaction in flow on kilogram scale.[49]

A number of recent reviews have detailed the application of photoredox catalysis in organic chemistry and medicinal chemistry.[50,51] Photoredox catalysis has been used to achieve the late-stage functionalization (LSF) of heteroarenes.[52] In this thesis the trifluoromethylation of the pyrimidine motif of a late-stage analogue of the pyrazolo[1,5-*b*]pyridazine series was attempted.

1.5. Aim

The overall aim of this thesis was to generate suitable molecular probes for (i) Serine Racemase (SR) and (ii) Dual-specificity Tyrosine Regulated Kinase 1A (DYRK1A) that would enable the roles of each of these enzymes to be delineated in an *in vivo* model of disease. Literature inhibitors of these enzymes were not suitable molecular probes as they did not possess the right balance of properties (affinity, selectivity and ADMET) to engage the targets *in vivo*.

Chapter 2. Serine Racemase and Published Small-Molecule Inhibitors

Chapter 2 details the entirety of the work undertaken on the Serine Racemase project. An overview of the target is provided followed by an up-to-date review of published small molecule inhibitors. Attempts to furnish a suitable molecular probe for Serine Racemase are presented thereafter.

2.1. Serine Racemase: An Attractive Target for *N*-methyl-*D*-aspartate Receptor (NMDA-R) Modulation

Glutamate-mediated synaptic transmission is essential for normal functioning of the nervous system.[53] NMDA-Rs are ionotropic glutamate receptors responsible for excitatory neurotransmission in the CNS. Overstimulation of the NMDA-Rs resulting in excessive Ca^{2+} influx is associated with neuronal toxicity and cell death. Excitotoxicity is implicated in many neurodegenerative diseases such as Alzheimer's disease (AD), Huntington's disease (HD), Parkinson's disease (PD), stroke, amyloid lateral sclerosis (ALS), as well as other neurological and psychiatric indications such as epilepsy, neuropathic pain, cerebral ischemia, schizophrenia and depression.[54, 55]

The therapeutic benefit of treating patients with current NMDA-R antagonists (Figure 12) is severely limited. Administration of antagonists such as Ketamine (**1**) or Phencyclidine (**2**) (PCP or Angel Dust) causes undesirable side effects. Ketamine causes drowsiness so much so that it can be used as an anaesthetic and PCP (**2**) causes patients to hallucinate. Memantine (**3**) is a weak NMDA-R antagonist that is generally well tolerated, with adverse effects such as occasional restlessness present in only 1% of the population. Currently, **3** is on the market as a therapy for AD.[56,57] Unfortunately, in mild to moderate cases of AD, a beneficial effect on cognition is not clinically detectable and ultimately this method of treatment does not halt disease progression.[58]

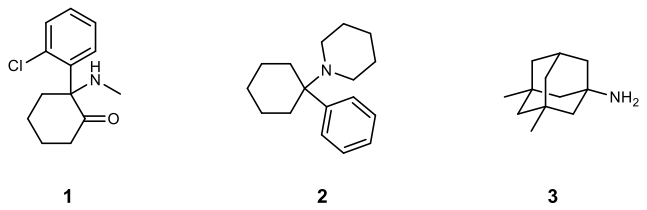

Figure 12. NMDA-R antagonists; 1 – ketamine, 2 – phencyclidine, 3 – memantine.

NMDA-Rs are activated only when the endogenous agonist, glutamate, and a co-agonist, glycine or *D*-serine are bound to the receptor.[59] Serine Racemase (SR) is the enzyme that catalyses the racemisation of endogenous *L*-serine to *D*-serine.[60] Recent works have implicated the metabolism of the NMDA-R co-agonist, *D*-serine, in the progression of certain diseases. SR knock-out (KO) mice with abnormal glutamatergic neurotransmission display schizophrenic like phenotypes.[61,62] SR KO-mice are protected against β-amyloid (Aβ) peptide induced neurotoxicity and cerebral ischemia, giving credence to the theory that the inhibition of SR could be a viable treatment for AD.[63,64] Elevated levels of *D*-serine coincide with the proliferation of ALS in mouse models.[65]

Proof of concept clinical trials using *D*-serine for the treatment of schizophrenia, PD, depression and anxiety have reportedly demonstrated clinically relevant effects. However, the use of *D*-serine as a stand-alone treatment may not be desirable due to possible nephrotoxicity resulting from gram level doses of *D*-serine required.[66]

One approach to mitigate the activity of the NMDA-Rs is to limit the amount of the co-agonist, *D*-serine, available for activation through inhibition of SR. Indirect antagonism through inhibition of SR may be better tolerated than conventional NMDA-R antagonists.

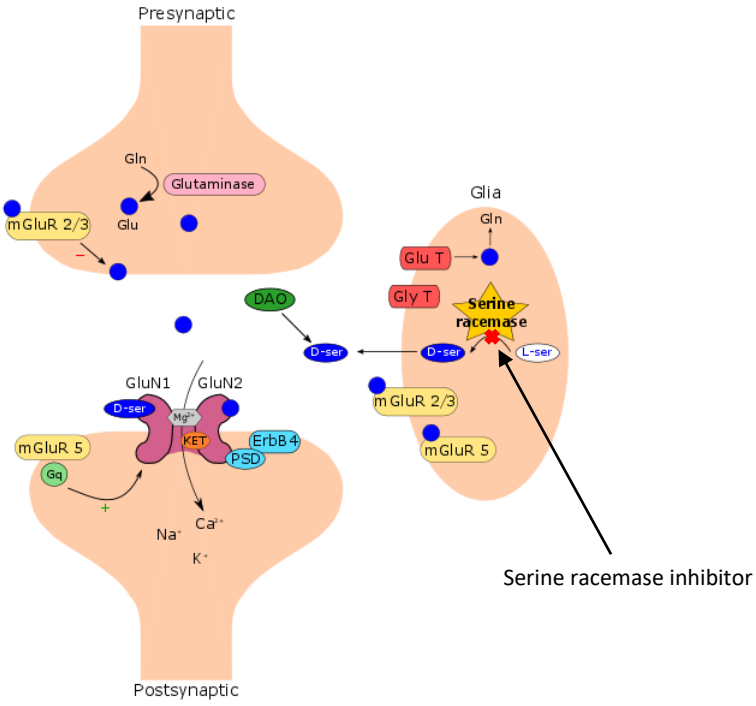

Figure 13. The Glutamate Synapse. Glutaminase converts glutamine (Gln) to glutamate (Glu; blue circles). Glutamate binds to metabotropic type 2/3 ($mGlu_{2/3}$) and type 5 ($mGlu_5$) receptors to modulate glutamate neurotransmission, and to ionotropic *N*-methyl-*D*-aspartate (NMDA) receptors (NMDA-Rs; pink, post-synaptic membrane) at the GluN2 subunit. Once coagonist *D*-serine binds at GluN1 subunit and a depolarising current relieves Mg^{2+}-dependent block, the channel opens and cations (Ca^{2+}, Na^{+}, K^{+}) can diffuse into the post-synaptic terminal. *D*-serine is produced from *L*-serine in glial cells by serine racemase, transported into the synaptic cleft, then eventually degraded by D-amino acid oxidase (DAO). Glutamate and glycine are removed from the synaptic cleft by glutamate transporters (Glu T; encoded by the EAAT1–5 genes) and glycine transporters (Gly T) respectively. A serine racemase inhibitor would stop the production of co-agonist *D*-serine, required for activation of NMDA-Rs. Image and caption modified and reproduced with permission from the Doctoral Thesis of Dr Chloe Koulouris – Identification and Characterisation of a Novel Inhibitor of Serine Racemase through a Fragment-based Drug Discovery Strategy.

2.2. Serine Racemase

2.2.1. Distribution, Localisation and Function

Examples of SR enzymes have been identified and characterised throughout all of the biological kingdoms.[67] The mammalian orthologue of SR exists as a dimeric protein residing in the cytosol and has molecular weight of 37 kDa per monomer.[68]

The distribution of SR in the CNS coincides with the abundance of *D*-serine present; SR has been found in the cortical regions of the brain, hippocampus and amygdala.[68,69] Studies have detected SR in glial cells,[70] neurons,[71] protoplasmic astrocytes, pyramidal neurons of the hippocampus and cortex, Purkinje cells and Bergmann glia of the cerebellum.[72,73] SR has also been identified in cells of the peripheral nervous system (PNS) such as Müller cells and astrocytes of the retina,

Schwann cells and epineural fibroblasts of the sciatic spinal nerve.[74, 75] Outside of the nervous systems, SR has been detected in liver, kidney and heart tissue.[76]

The major role of SR in the CNS is believed to be as a biological catalyst to promote the synthesis of the neurotransmitter *D*-serine for NMDA-R modulation. However, SR is also capable of degrading *D*-serine by catalysing the deamination of *D*-serine to afford pyruvate and ammonia. Comparisons of the catalytic efficiencies (k_{cat}) of racemisation and β-elimination amongst homologues appears to indicate that elimination activity is a residual function of human SR.[68] SR is also present in the placenta, and the transport of *D*-serine to the foetus appears to be crucial for synaptogenesis, implicating SR in early brain development.[77] It remains unclear as to the role of SR outside of the CNS, but it is speculated that it performs a similar role in supplying peripheral NMDA-Rs with *D*-serine.[68]

2.2.2. Serine Racemase and *D*-Serine Synthesis

SR is one of many pyridoxal-5'-phosphate (PLP) dependent enzymes. PLP-dependent enzymes are involved in amino acid synthesis and metabolism, requiring them to have a wide range of distinct catalytic functions.[78]

The initial mechanistic steps are uniform for all PLP-dependent enzymes and the mechanism for *D*-serine synthesis is shown in Figure 14. Initially, PLP is bound covalently to the ε-amino group of an active site lysine residue – the Schiff base formed is called the internal aldimine (**A**). PLP exchanges the lysine ε-amino group for the α-amino group of a substrate (i.e. *L*-serine) which enters the active site, resulting in the formation of an external aldimine (**B**). The specific architecture of the enzyme's active site determines the fate of the external aldimine. Cleavage of the α-carbon bond perpendicular to the plane of the pyridoxal ring affords **C**, the Dunathan intermediate (Figure 14).[79]

In the case of SR, once **B** is formed the α-hydrogen of *L*-serine lies perpendicular to the ring plane, resulting in cleavage of the C-H bond.[67,68,80] Proton donation to the α-carbon from the opposite side of the ring plane by a serine residue (S82) in the active site of SR completes the isomerisation of *L*-serine to *D*-serine. Covalently bound *D*-serine is then displaced by a lysine residue (K56) in a transaldimination reaction to regenerate the internal aldimine, **A**.[81]

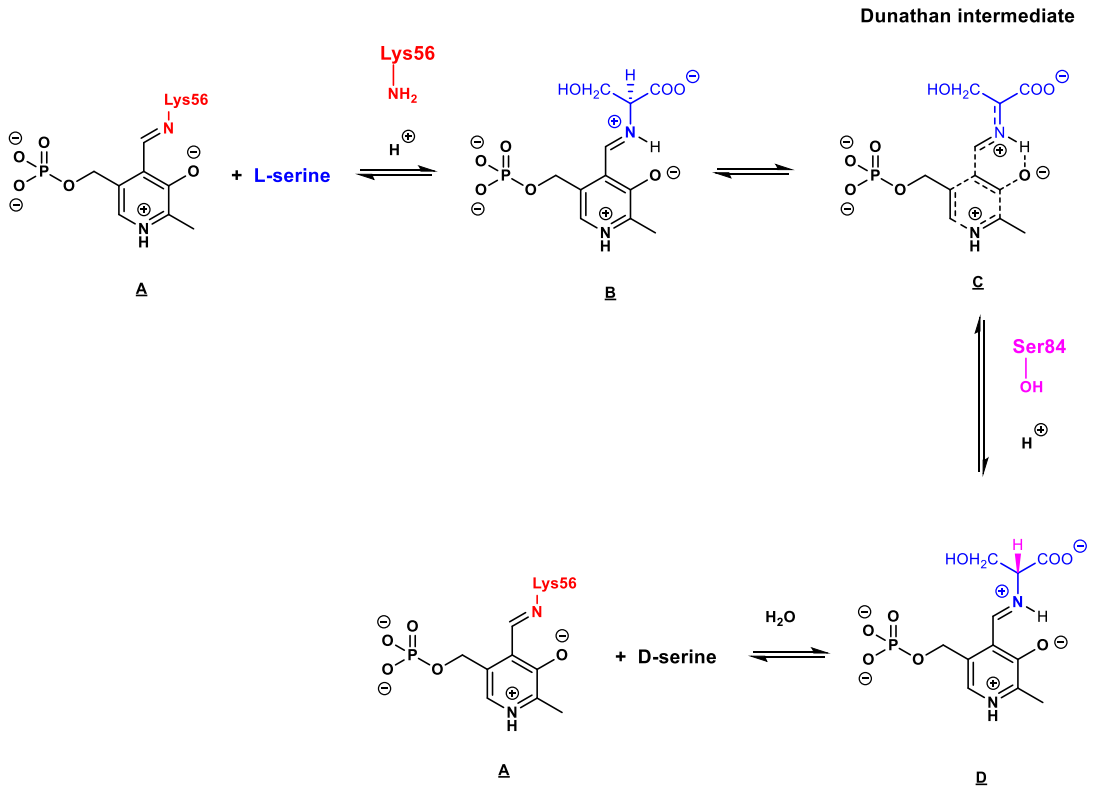

Figure 14. Mechanism of racemisation of *L*-serine to *D*-serine.[81]

2.2.3. Structure of Serine Racemase and the Interaction of Inhibitors with the Target

In 2019 there are over ten x-ray crystal structures of SR available in the Protein Data Bank (PDB), with examples from S. Pombe (PDB 1WTC, 1V71, 2ZR8, 2ZPU), rat (PDB 3L6C, 3HMK), and three human (PDB 3L6R, 3L6B, 5X2L) in different conformations. Vancomycin resistance SR from VanTg (PDB 4ECL) and maize SR (PDB 5CVC) are also represented. The amino acid sequence of the orthosteric sites are highly conserved between species and overall homology of SR varies from 35-91%.[82,83]

The SR enzymes have an overall fold characteristic of the β-family of PLP-dependent enzymes, which includes the closest known homologue of SR, serine dehydratase (SDH) (PDB 1PWH, 1PWE, 1P5J). SDH shares 23% sequence identity and is 90% similar in structure to SR.[68] SDH is also able to catalyse β-elimination of *L*-serine to pyruvate and ammonia, however, only SR can perform racemisation of *L*-serine to *D*-serine.[68]

Eukaryotic SR exists as a dimer, stabilised by hydrophobic interactions, with each monomer containing a small and large domain connected by a flexible loop.[68,84] The large domain contains the PLP cofactor with a core of seven-stranded twisted β-sheets surrounded by ten helices. The small domain consists of four central parallel β-sheets and three α-helices in a twisted α/β-

architecture. The large and small domains are joined by a flexible loop which contains the catalytically active serine residue (S84).[68] All literature structures show the presence of a divalent metal cation (Mg^{2+} or Mn^{2+}) bound in a position adjacent to the orthosteric site and contacting three conserved residues (E210, A214 and D216).[68]

Comparison of crystal structures appears to show that a 'closed' conformation is adopted when an orthosteric ligand, such as malonate is bound (Figure 15), whereas the apo-protein appears to exist in a more 'open' conformation that facilitates the binding of *L*-serine.[68]

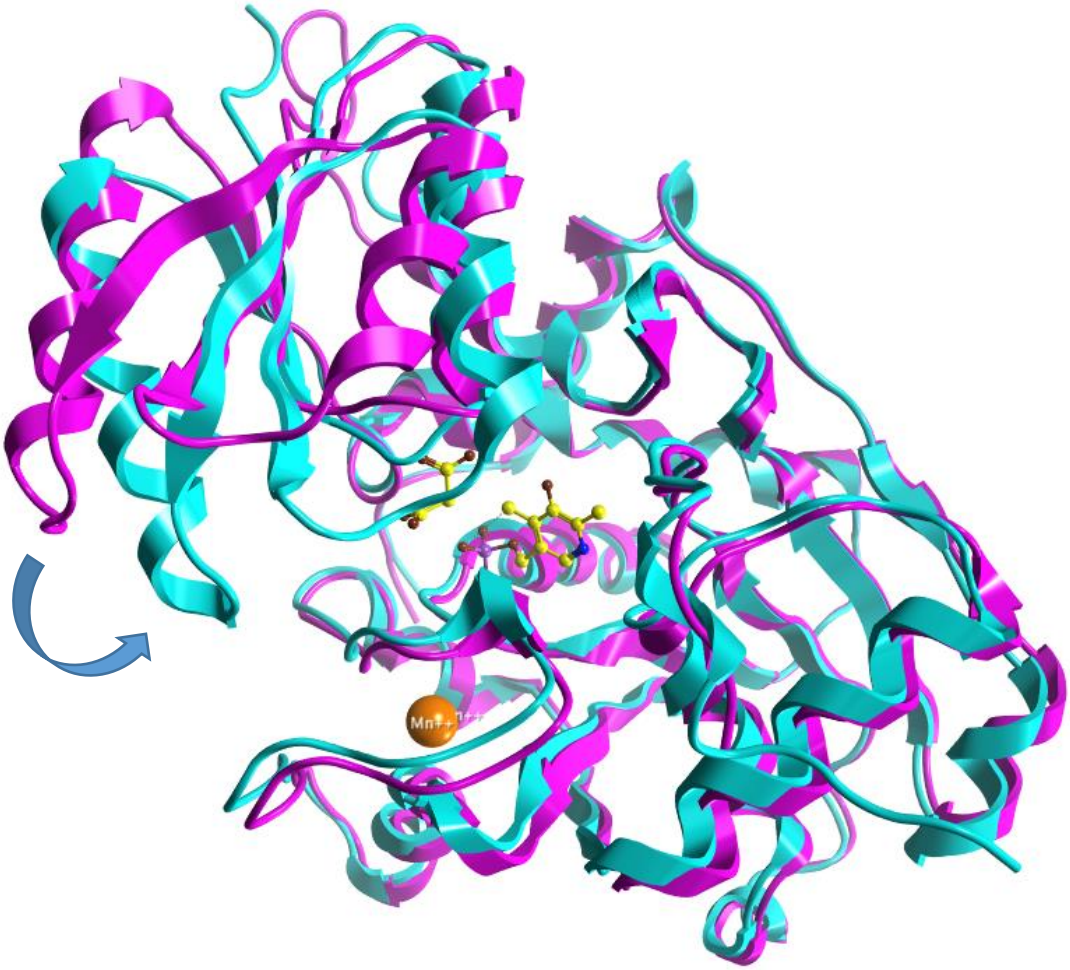

Figure 15. Overlay of rat holo 'open' (magneta) and human protein-malonate complex 'closed' SR (cyan). malonate (yellow) and PLP-cofactor (yellow) and magnesium ion (orange) all present.[68] Image produced in MOE 2016, CCG from crystal structures PDB 3HMK and PDB 3L6B.[68] using Amber10:EHT force field.

The crystal structure of S.Pombe SR (PDB 1WTC) is unique in that it shows an adenosine triphosphate (ATP) analogue, phosphomethylphosphonic acid adenylate ester (AMP-PCP), bound at the dimer interface. ATP binding is thought to increase the catalytic activity of SR in a cooperative fashion by affecting both relative racemisation and β-elimination rates.[85,86,87]

Although available mammalian SR structures do not contain an ATP analogue bound at the dimer interface, docking studies suggest that ATP could be accommodated at the dimer interface. The proposed binding pocket of human SR resembles other ATP-binding proteins.[68, 88]

2.3. Published Small Molecule Inhibitors of Serine Racemase

A decade of research has not furnished a single sub-micromolar inhibitor of SR. The most potent inhibitors of SR are small, non-drug-like molecules related to malonate. SR inhibitors can be classified as dicarbonyl inhibitors, peptidic inhibitors and molecules discovered by structure-based drug-design (SBDD). A prominent review of the subject details a more extensive list of all molecules that have shown detectable inhibition against SR.[67]

Malonate, **4**, (Table 3) remains the only inhibitor to have been co-crystallised with human SR. Although **4** is reported to be promiscuous, it still represents one of the most potent inhibitors of SR (IC_{50} = 67 µM).[89] Malonic acid analogues with small polar groups (**5**, **6** and **7**) on the α-carbon are tolerated well compared to those with bulky, more hydrophobic motifs.[90]

L-erythro-3-hydroxyaspartate (LEHA, **8**) is a potent competitive inhibitor of SR (K_i = 40 µM). Interestingly, the enantiomer, *D-erythro*-3-hydroxyaspartate exhibits no inhibition of SR. Similar to *L*-serine and *D*-serine, hydroxyaspartate can also serve as a substrate for β-elimination by SR. Docking studies suggest that **8** occupies the orthosteric site and forms hydrogen-bonds to active site residues in a similar fashion to **4**.[67,91] Combined treatment of **8** with an NMDA-R anatagonist reportedly supressed long-term potentiation (LTP) in a neurophysiology study in astrocytes.[92]

Compounds **9** and **10** represent two of the more potent analogues from a series of hydroxamic acid derivatives of malonate.[93] Inhibitory activity of **9** and **10** in the presence of excess magnesium was maintained, indicating that metal chelation did not affect inhibition. However, due to the reputation of hydroxamic acids as metal chelating agents, **9** and **10** do not represent attractive starting points for inhibitor design.

Table 3: Dicarbonyl Inhibitors of SR

Compound Number	Chemical structure	SR IC_{50} (μM)	SR K_i (μM)	Ref.
4	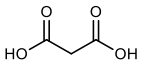	67	-	a
5	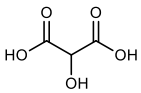	94	-	a
6	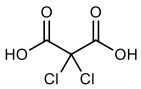	57	-	a
7	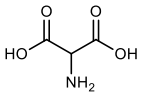	400	-	a
8	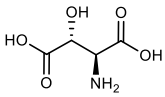	-	43	b
9	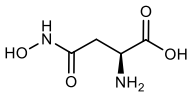	-	97	c
10	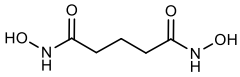	-	170	c

[a]Data from reference [90]; [b]Data from reference [91]; [c]Data from reference [93]. IC_{50} and K_i derived from SR enzymatic activity assay.

Peptide inhibitors **11** and **12** were generated *via* a one-bead one-compound combinatorial library approach (Table 4).[94] The majority of the most potent inhibitors identified from this source incorporated the 3-phenylpropionic acid moiety and the histidine motif, indicating a structural bias for the pocket. Peptides **11** and **12** were found to be competitive with *L*-serine, indicating that the binding mode must obstruct *L*-serine binding.[94] However it is difficult to conceive that **11** and **12** are able to bind to the orthosteric site of SR in the 'closed' form due to their size. In general, peptides are not desirable drugs because they are readily metabolised by peptidases and proteases *in vivo*. Permeability of the blood-brain barrier (BBB) is also an issue due to the hydrogen-bonding ability of the peptidic backbone and often the presence of polar residues.[95]

Table 4: Peptidic Inhibitors of SR

Compound Number	Chemical structure	SR K_i (μM)[a]
11	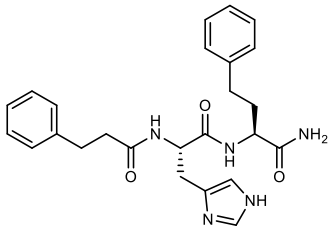	320 ± 70
12	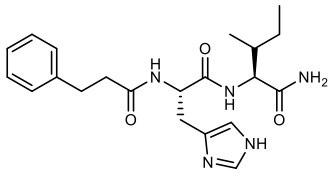	610 ± 120

[a]Data from reference [94]. K_i derived from SR enzymatic activity assay.

Compound **13** exhibited millimolar inhibition of SR and was the first example of a SR inhibitor designed by virtual screening (Table 5). The *in silico* method employed by Mori *et al.* involved pharmacophoric similarity searches using **11** as a template scaffold.[96] Glide docking was then used to rationalise the binding of **13** into the orthosteric site of SR. A small library of peptidomimetics were designed and the most potent example was **14** (IC_{50} = 520 μM) (Table 5).[96] The library was synthesised to explore the existence and probe for interactions with a small lipophilic sub pocket of SR, adjacent to the orthosteric site. This work led to the publication of a patent with further examples of inhibitors.[96, 97]

A recent attempt at an *in silico* screening campaign of the ZINC library failed to furnish any sub-millimolar inhibitors of SR.[98] The resulting millimolar inhibitors of SR, **15** and **16**, are structurally diverse from other reported inhibitors (Table 5). **15** and **16** were docked into the 'open' conformation of SR and adopted similar poses with both inhibitors reportedly contacting serine residue (S83).[99]

More recently, in 2017, the Mori group published further inhibitors derived from their previous virtual screening work. **17**, **18** and **19** were all reported to be more potent than malonate using the same assay format. **19** apparently demonstrated an inhibitory effect on hyperactivation of the NMDA-Rs in an *in vivo* model.[100] **20** is the most recent SR inhibitor published by the Mori group and inhibits SR approximately 2 fold more than **13**.[101]

Table 5: Inhibitors of SR derived from SBDD

Compound Number	Chemical structure	SR IC_{50} (µM)	Ref
13	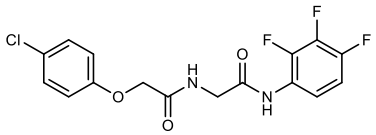	1300	a
14	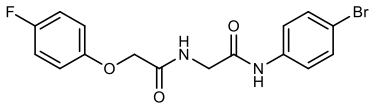	520	a
15	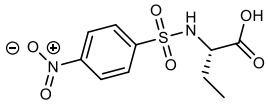	1500	b
16	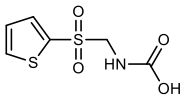	1500	b
17	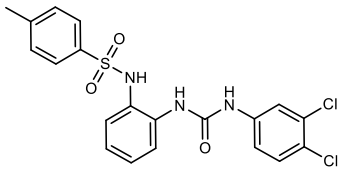	280	c
18	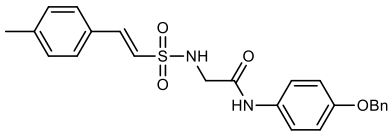	270	c
19	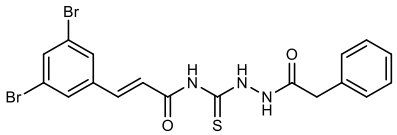	140	c
20	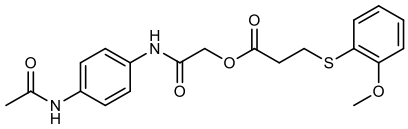	836	d

[a]Data from reference [96]; [b]Data from reference [99]; [c]Data from reference [100]; [d]Data from reference [101]. IC_{50} derived from SR enzymatic activity assay.

2.4. Summary

Serine Racemase represents an exciting pharmacological target owing to its role in the synthesis of *D*-serine, an essential co-agonist of the NMDA-R. Animal models support the hypothesis that inhibition of SR could be a potential treatment for a variety of neurological diseases for which there are few treatments currently available.

Recent contributions to the field of SR inhibitors have been reviewed. Over a decade of research has failed to furnish any potent, sub-micromolar inhibitors of SR. None of the published inhibitors have been optimised for CNS drug delivery, and in fact due to low potency, very few have progressed to *in vivo* studies. Thus, there is a compelling need to discover potent and selective chemical tools that can be used to decipher the roles of *D*-serine and SR *in vivo*.

2.5. Development of Small Molecules as Potential Chemical Probes for Serine Racemase

2.5.1. Project Aims and Rationale

The aim of the work undertaken was to synthesise an inhibitor of the human SR enzyme with the purpose of defining the role of *D*-serine and SR in CNS diseases. Desirable properties of the inhibitor included sub-micromolar potency against SR, high selectivity for SR over similar enzymes including SDH and favourable pharmacological properties for use as an *in vivo* tool.

A decade ago, Evotec terminated a Serine Racemase Inhibitor project at a stage of Hit-to-Lead Optimisation. The data generated during that project formed the basis of the current project. Fragment **21** (IC_{50} = 33 µM Evotec), which resembled the endogenous co-factor PLP, was viewed as a potential starting point for the project given the lack of potent inhibitors reported in the literature. Hit confirmation followed by hit expansion would determine whether the fragment warranted further investigation.

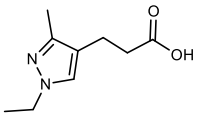

21

Figure 16. Fragment 21 identified by Evotec.

2.5.2. Serine Racemase Screening Cascade and Compound Prioritisation

The primary assay for the SR project was an enzyme-coupled biochemical assay. The inhibition constants (IC_{50}) of compounds were determined by measuring *D*-serine formation by means of a chemiluminescent assay that detected *D*-serine specifically. Racemase activity was measured in the presence of the co-factor PLP, and the endogenous substrate, *L*-serine. After incubation for a set period of time the reaction was terminated. The level of *D*-serine was determined by incubation with *D*-amino acid oxidase (DAO), which specifically degrades *D*-amino acids generating an α-keto acid, ammonia and hydrogen peroxide. The production of hydrogen

peroxide was quantified by the use of hydrogen peroxidase and luminol. Specifically, luminol is oxidised by hydrogen peroxide to a cyclic peroxide that liberates a molecule of nitrogen gas to form an excited intermediate. The relaxation of the excited intermediate back to the ground state coincides with the production of energy (photons) that is detectable (Figure 17). The concentration of *D*-serine in each sample was calculated by comparing with standard curves with a defined maximum and minimum.

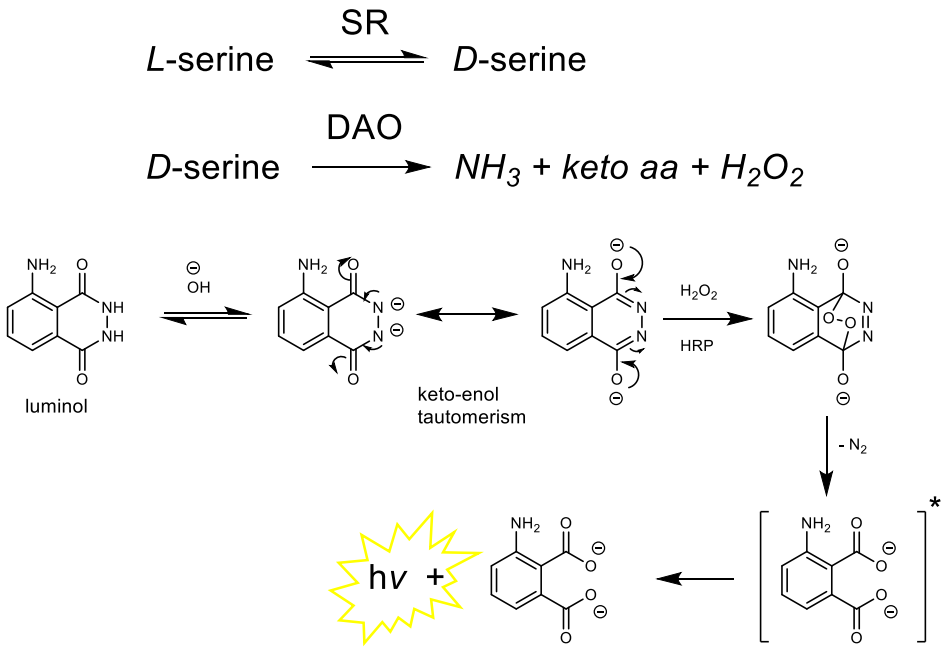

Figure 17. Concept of biochemical luminescence assay for *D*-serine detection to measure SR activity. SR = serine racemase; DAO = *D*-amino acid oxidase.

An orthogonal thermal shift assay was also in place, which quantified the change in thermal denaturation of SR in the presence and absence of suspected chemical inhibitors. The formation of a protein-ligand complex can increase thermal stability relative to the uncomplexed protein.[102] The thermofluor or thermal shift assay employs a fluorescent dye that binds non-specifically to hydrophobic surfaces and is quenched by water. The protein unfolds when heated exposing hydrophobic residues that have dye bound. Simultaneously water is expelled causing an increase in fluorescence. Continual heating will cause the protein to aggregate and the dye to dissociate. Fluorescence is measured at each temperature increment. A graph can be plotted for the protein-ligand complex and the uncomplexed protein to determine its melting temperature (T_m) and relative stabilities. The assay is depicted in Figure 18.

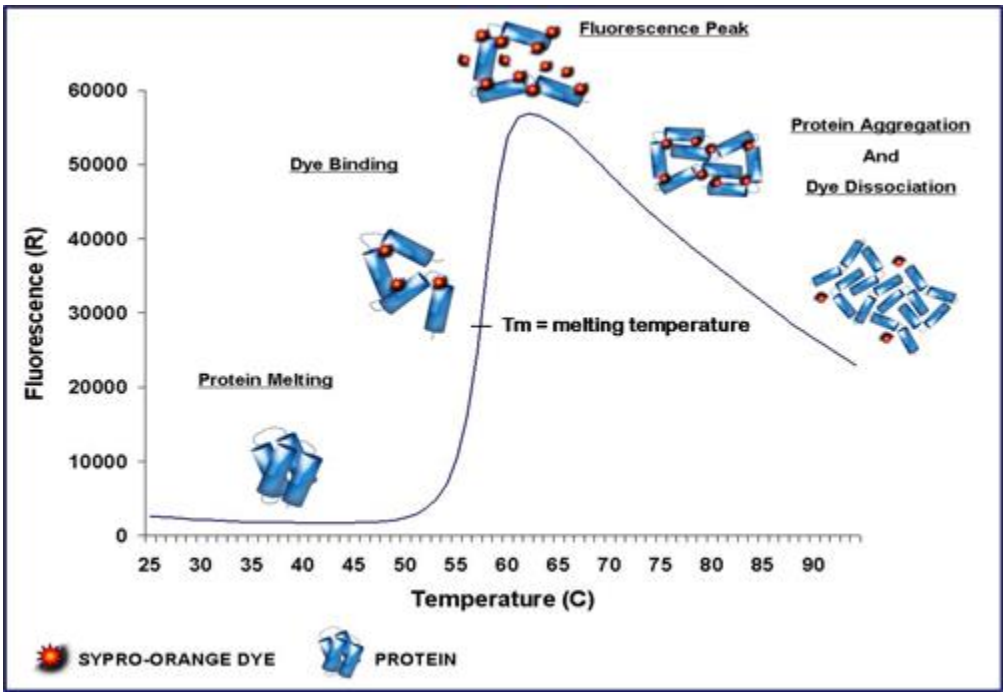

Figure 18. Fluorescent thermal shift assay. Image not protected by copyright; replicated without alteration. Original author Argonne National Laboratory.

The thermal shift assay had historically been used as a filter to determine which inhibitors were false positives due to inhibition of the enzyme through chemical denaturation. The usefulness of the thermal shift assay should be scrutinised as SR is known to be a flexible enzyme, existing in multiple states and so inhibitors of 'open' and 'closed' conformations are likely to stabilise SR to differing extents depending on which conformation the inhibitor binds to the enzyme.

2.6. The Evotec Pyrazole Fragment Series

2.6.1. Rationale

A decade ago, Evotec screened a 35 thousand fragment library against human SR and identified **21** as a potent inhibitor (SR IC_{50} = 33 µM) with an impressive ligand efficiency (LE = 0.5). **21** was the only reversible inhibitor identified in the screen and was shown to be competitive with a known orthosteric site inhibitor of SR, LEHA. Interestingly, flexible alignment with the orthosteric co-factor PLP revealed that **21** had the potential to occupy the position of PLP, which is required for racemisation (Figure 19). Support for this hypothesis was derived from historical data in which small alterations to the core of **21**, in the form of a methyl scan, had abolished inhibitory activity of the series. Thus, the position of **21** within the active site seemed highly restricted consistent with the highly restricted position of PLP.

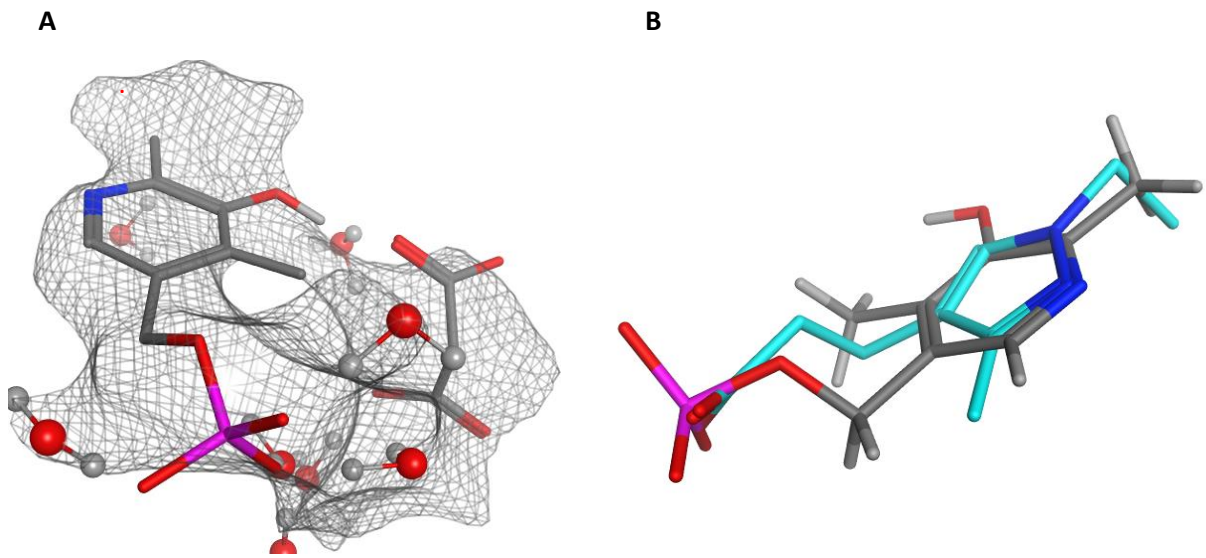

Figure 19: A – Crystal structure PDB: 3L6R.[68] Structure, prepared and energy minimised using Amber10:EHT force field, MOE 2015, CCG. Interaction surface of PLP within SR orthosteric site appearing highly constrained in the 'closed' SR conformation, unlikely to tolerate substitution to pyridine core. B – Flexible alignment using Amber10:EHT force field, MOE 2015, CCG of **21** (cyan) with the PLP cofactor showing promising overlap with pharmacophoric features.

Work concerning **21** initially involved resynthesis of the hit. Additionally, a small number of very close analogues were synthesised in parallel to establish any preliminary SAR. The hit would then be confirmed in the primary biochemical assay. Once potency was confirmed, the strategy was to proceed to hit expansion with the aim of retaining LE whilst building the fragment, bearing in mind the need for optimisation of the fragment for CNS drug properties (Mwt ≤ 400, Log D ≤ 3.5, ≥ 1.5, PSA < 75 Å > 40 Å). In parallel to this attempts were made to develop co-crystallisation conditions to determine the binding mode of **21** and give insights into the mechanism of inhibition to further aid SBDD and confirm binding.

2.6.2. Synthesis of Pyrazole Fragments

Retrosynthetic analysis revealed that synthesis of **21** should be possible in a three-step procedure from the commercially available pyrazole **22**. *N*-alkylation of **22**, followed by a C-C bond forming Heck reaction and subsequent hydrogenation was envisaged to furnish **21** (Scheme 1).

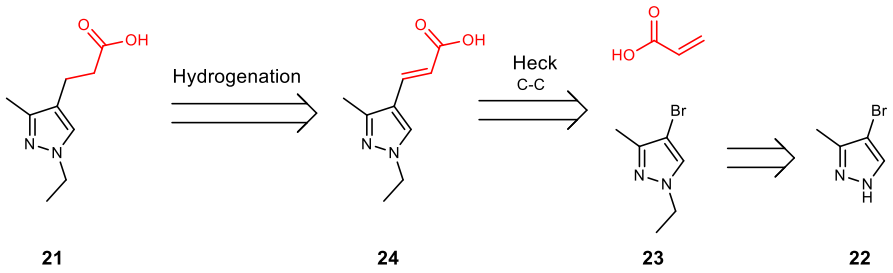

Scheme 1. Retrosynthetic analysis of **21.**

Selective *N*-alkylation of **22** with ethyl iodide was low yielding and resulted in the generation of regioisomers **23a** and **23b** (Scheme 2).

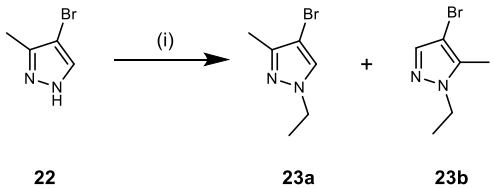

Scheme 2. *Reagents and conditions:* (i) iodoethane, sodium hydride, DMF, rt, 16 h, 14%.

The regioisomers were present in a 1:1.4 mixture, evidenced by the ^{1}H NMR spectrum of the isolated product. Doubling of signals with the same multiplicity - as expected for these regioisomers – is visible in Figure 20.

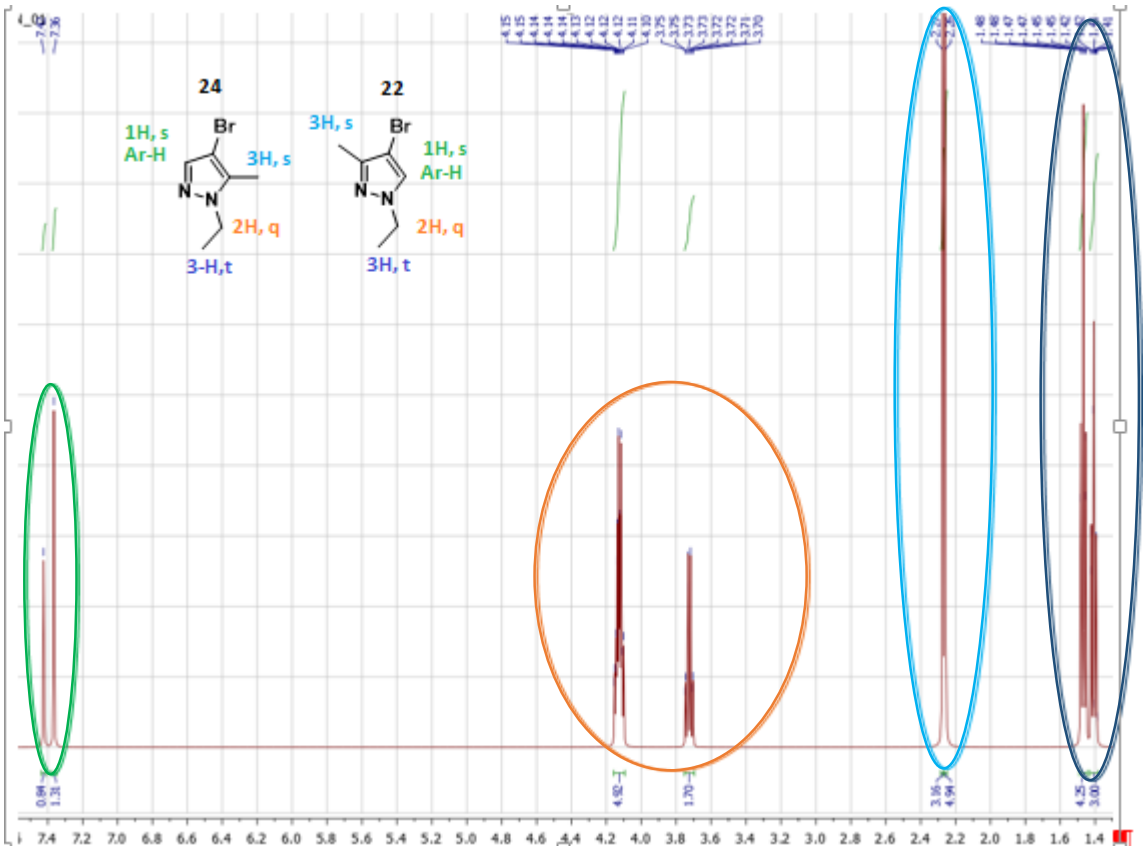

Figure 20. ^{1}H NMR of isolated product showing the presence of a mixture of regioisomers.

Attempts to make the reaction more regioselective failed. Temperature control (e.g. reaction carried out at room temperature) and use of alternative base (e.g. potassium hydroxide) were unsuccessful. To compound the challenge further the regioisomers appeared to be inseparable by conventional chromatography. Regioisomers **23a** and **23b** were carried forward into the subsequent Heck coupling in the hope that the products would be separable (Scheme 3). It was envisaged that this sequence would also afford another interesting isomer of **21** to test for SR inhibition. However, separation of isomers **24a** and **24b** did not appear possible by conventional chromatography (Figure 21).

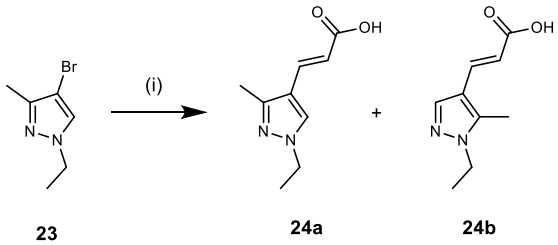

Scheme 3. *Reagents and conditions*: (i) acrylic acid, $Pd(OAc)_2$, tri(O-tolyl)phosphine, DIPEA, DMF, 150 °C, 1 h, µwave, 26%.

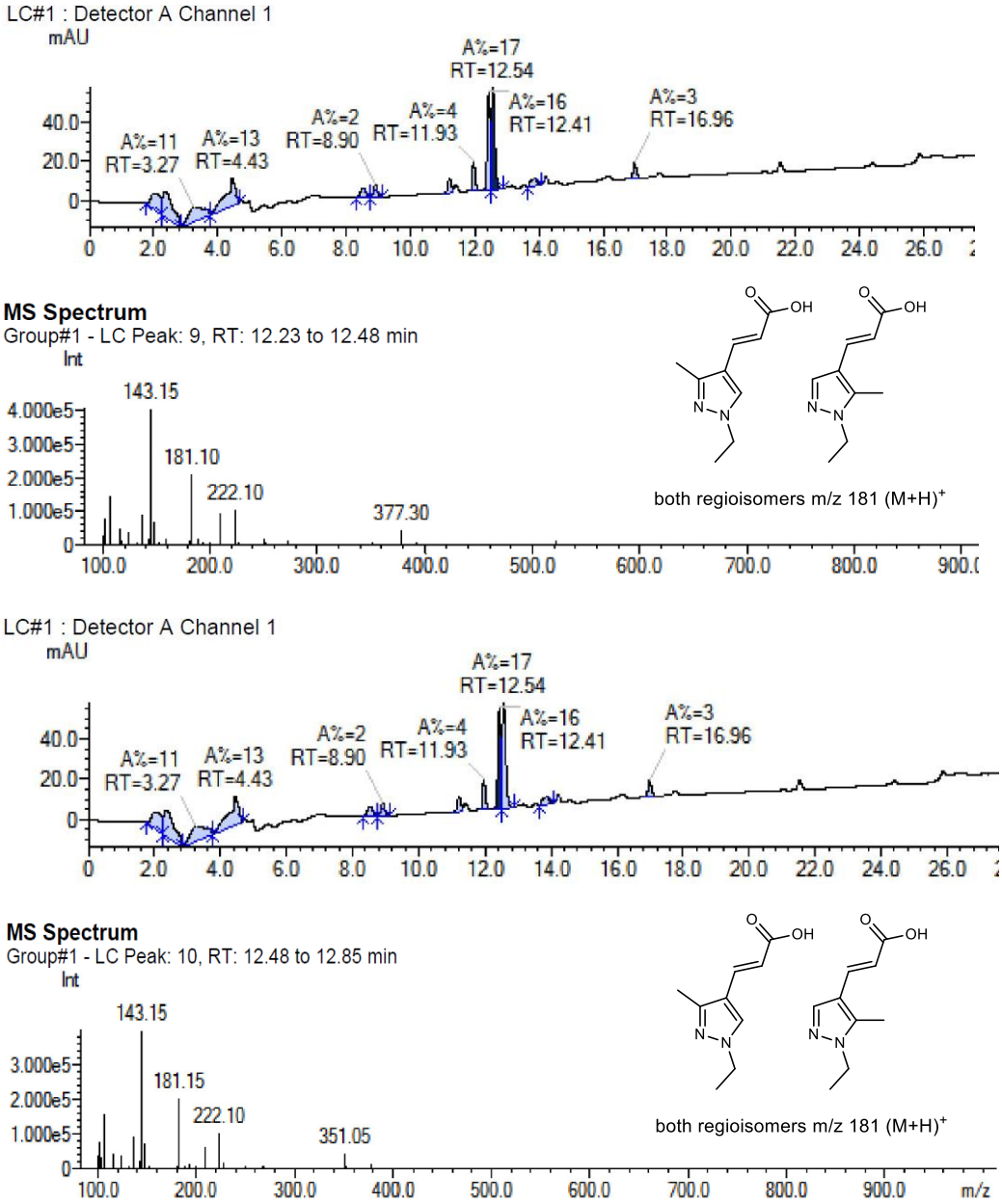

Figure 21. Chromatogram of reaction mixture of **24a** and **24b** - appears to show two co-running components that have the expected m/z of **24a** and its regioisomer **24b**.

At this time an alternative strategy had been identified from the literature that was employed on a similar substrate.[103] Using an analogous route, the synthesis of **24a** was achieved in one step. Aldehyde **25** was subjected to a Doebner-modified Knoevenagel condensation in which condensation and decarboxylation occur in the same step (Figure 22). The key advantage of this route was that it avoided the possibility of generating regioisomers as **25** was regioisomerically pure and was commercially available.

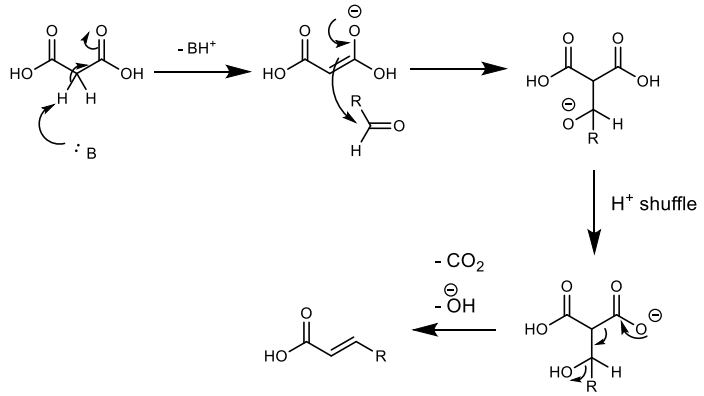

Figure 22. Doebner-modified Knoevenagel condensation.

Subsequent hydrogenation of **24a** in the presence of hydrogen gas over palladium-on-carbon afforded **21** in 90% yield over two steps (Scheme 4).

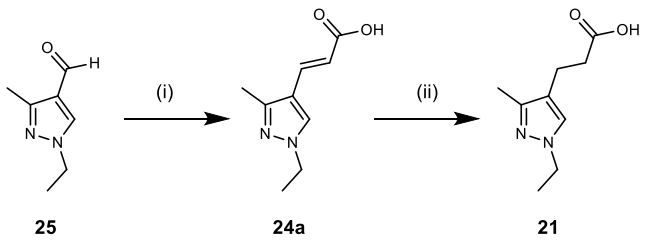

Scheme 4. *Reagents and conditions*: (i) malonic acid, piperidine, pyridine, 116 °C, 16 h; 91%; (ii) hydrogen gas, palladium on carbon (10% wetted with water), EtOH, rt, 16 h, 99%.

In parallel to the synthesis of **21** a small number of carboxylic acid derivatives were synthesised to probe for binding interactions and to make the series more drug-like and able to permeate the Blood-Brain Barrier (BBB). Readily accessible from the carboxylic acid **21** are the methyl ester **26** and the primary amide **27** in one step reactions. Acid catalysed esterification of **21** afforded methyl ester **26** in good yield (Scheme 5).

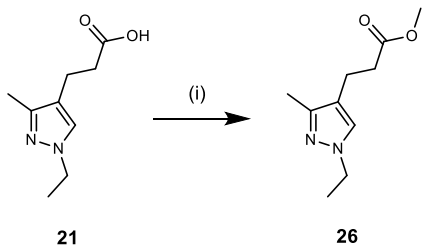

Scheme 5. *Reagents and conditions*: (i) sulfuric acid, MeOH, 70 °C, 4 h; 67%.

Stirring **21** in ammonium hydroxide at room temperature for three days furnished the primary amide **27** in good yield with minimal work up required (Scheme 6).

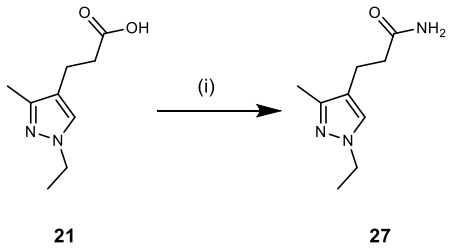

Scheme 6. *Reagents and conditions*: (i) 28% w/w ammonia in water, rt, 96 h; 74%.

After resynthesis **21** was not reconfirmed as an inhibitor in the primary biochemical assay. Another batch of **21** was also obtained from a commercial vendor but this also failed to inhibit SR in the primary assay. Analogues **26** and **27** were also tested in primary biochemical assay and did not inhibit SR.

In the absence of a robust orthogonal assay, counter assay, co-crystal structure of **21** or analogue of **21** to prove binding, hit expansion of **21** was halted until evidence emerged that it was a genuine hit.

2.7. A Literature derived Peptidomimetic Inhibitor Series

2.7.1. Rationale

In the absence of a renewed screening campaign and being in possession of historical data that was failing to reconfirm, a literature-based drug design approach seemed the most rational. The lack of sub-millimolar and drug-like SR inhibitors in the literature complicated the task.

Recently, peptidomimetics **28**-**30** (Figure 23) were reported to have greater potency than malonate as SR inhibitors.[96] However, it is noteworthy that malonate (IC_{50} = 1.21 mM) was much less potent in this study, which the authors attribute to a reduction in the purity of the SR protein used for assay.[96] Thus, the actual potency of these inhibitors could be micromolar or sub-micromolar. The peptidomimetics were reported as probable orthosteric inhibitors and a small-scale SAR study had indicated that potency may be increased by targeting a small lipophilic subpocket of SR.[96]

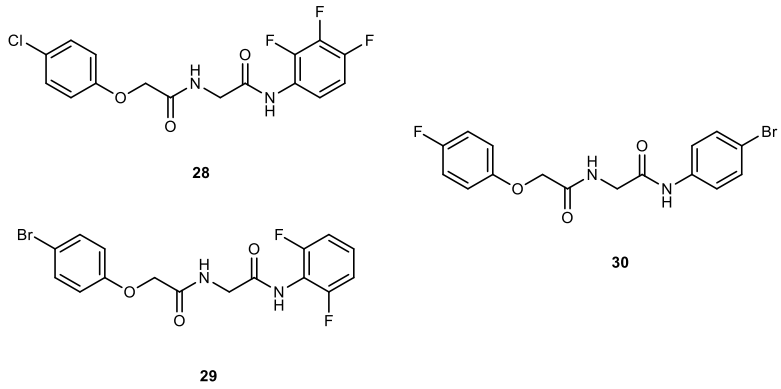

Figure 23. Reported Peptidomimetic Inhibitors of SR.[96]

To confirm whether the peptidomimetics warranted further investigation, synthesis followed by biochemical assay was necessary to determine the true potency of these compounds. Once activity was confirmed the series could represent one of the most potent inhibitors to date on which to base the design of further analogues.

2.7.2. Synthesis of Peptidomimetic Series

A synthetic route that permitted synthesis of **28**-**30**, and which also facilitated library design to probe the reported subpocket, was desired. It was envisaged that utilising a key intermediate acid and installing a diverse set of anilines through standard amide coupling could probe the subpocket effectively (Scheme 7).

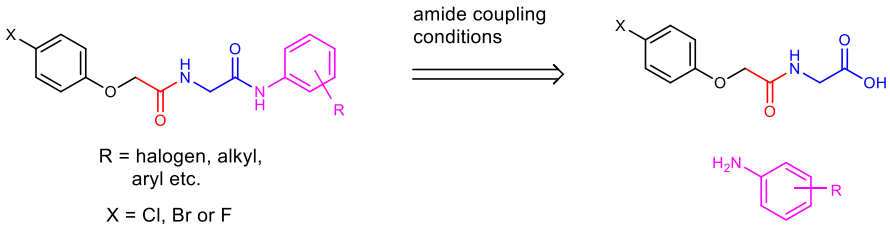

Scheme 7. Synthetic route design to peptidomimetics.

The synthetic route to **28** began with the readily available phenol **31**. Deprotonation of **31** with potassium hydroxide followed by subsequent alkylation was completed in high yield. Basic hydrolysis of the resulting methyl ester **32** to acid **33** was also high yielding and rapid. Installation of the glycine subunit *via* amide coupling conditions was completed in below average yield. Later amide couplings with 4-bromo- and 4-fluoro- phenols were higher yielding under the same conditions. Therefore, the lower recovery of **34** was likely due to isolation procedure.

Deprotection of the glycine subunit under the same basic conditions as those employed in a previous step afforded **35** in low yield. As a result of the low yield observed in the amide coupling of **33** to form **34**, it was thought that a change in coupling conditions should be attempted. The T3P® mediated amide coupling of **35** with desired aniline afforded **28** in fine yield (Scheme 8).

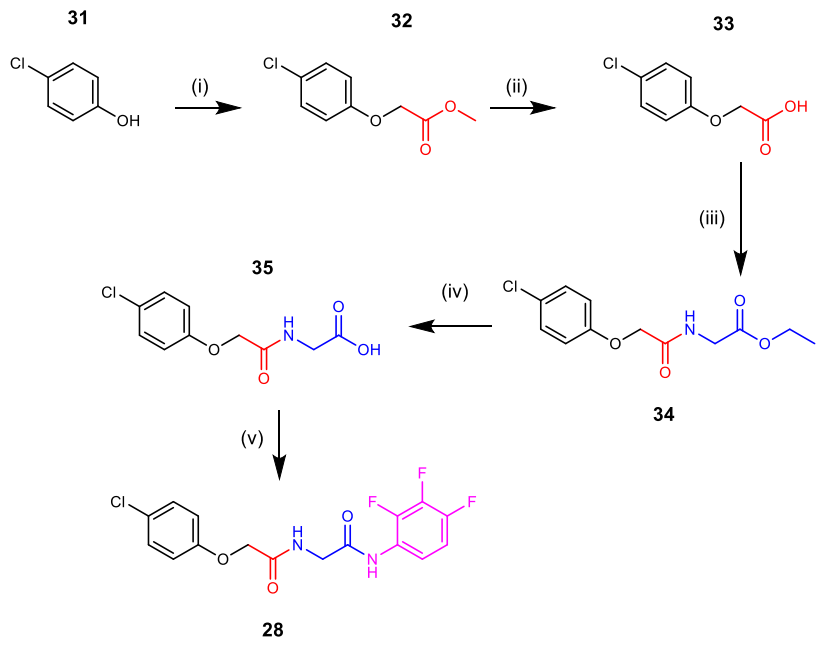

Scheme 8. *Reagents and conditions*: (i) methyl bromoacetate, KOH, DMF, 85 °C, 16 h; 91%; (ii) KOH, MeOH, 35 °C, 2 h; 93%; (iii) glycine ethyl ester hydrochloride, HOBt.H_2O, EDC.HCl, DIPEA, DMF, rt, 16 h, 43%; (iv) KOH, MeOH, 35 °C, 2 h; 19%; (v) 2,3,4-trifluoroaniline, T3P® (50 wt.% in EtOAc), TEA, THF, rt, 3 h, 87%.

2.7.3. Optimisation of Synthesis of Peptidomimetic Inhibitors

Investigation into route improvement was important so that late-stage intermediate **35** could be made on large scale. This would permit a library of analogues to be made to probe the reported subpocket of SR.

^{1}H NMR of the material isolated en route to **35** appeared to show that under basic conditions and slightly elevated temperature, the amide **34** had hydrolysed (Figure 24). The central spectrum of Figure 24 clearly shows a mixture of desired product **35** and the amide hydrolysis product **33**. Trituration of the mixture was successful in obtaining enough pure intermediate **35** to complete the synthesis of **28**. Hydrolysis of the amide in **34** persisted even when more dilute and mild hydrolysis conditions were trialled.

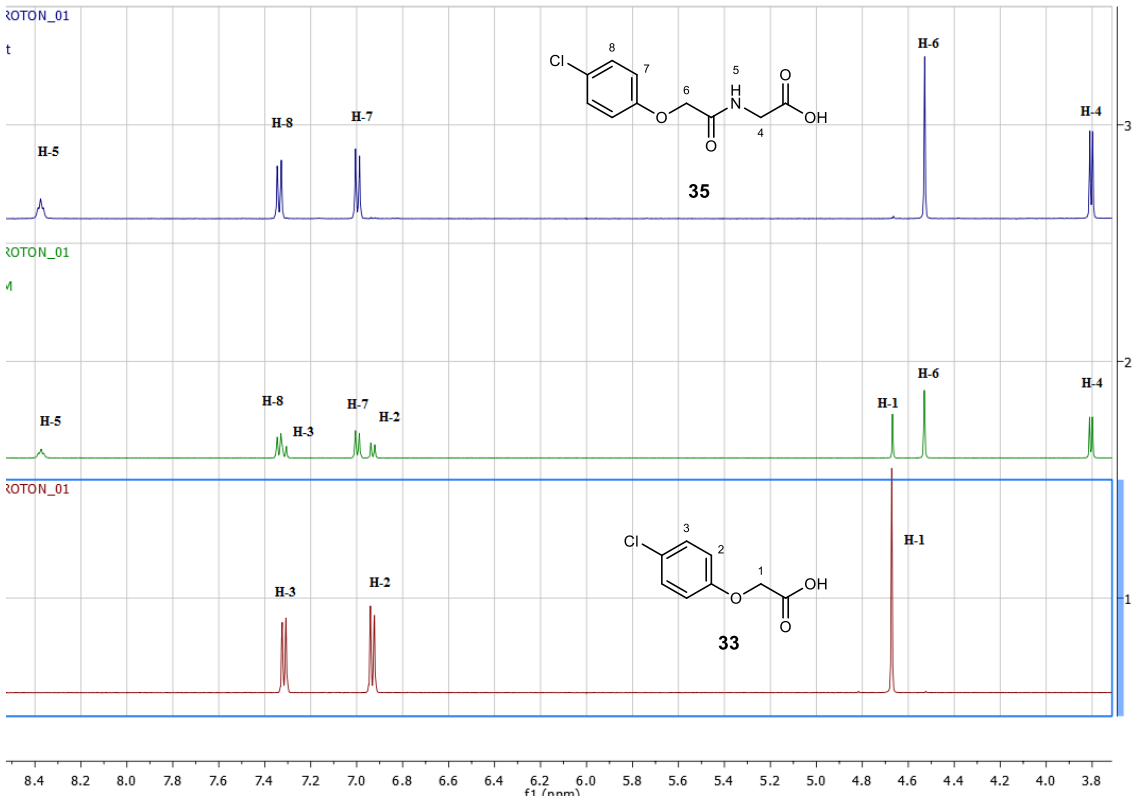

Figure 24. ^{1}H NMR of the product of the ester hydrolysis of **34**, resulting in the isolation of **35** and **33** as a mixture (central spectrum).

In theory, the issue of basic amide hydrolysis may have been circumvented by installing the benzyl ester of glycine rather than glycine ethyl ester hydrochloride. The benzyl ester would have required hydrogenation conditions to cleave and would hopefully have left the amide of **34** intact. An alternative route was developed in the short term to allow rapid access to **28**-**30** and close analogues. The stepwise synthesis of **28** could be optimised later if inhibitory activity of **28**-**30** was confirmed.

Optimisation of the synthesis reported by Mori *et al.*[96] started with earlier installation of the aniline subunit *via* an amide coupling of Boc-Gly-OH with the desired aniline. Removal of the acid-labile Boc group with 4 M HCl in 1,4-dioxane afforded the corresponding 2-amino-*N*-phenylacetamide as a hydrochloride salt. Employing T3P® amide coupling conditions to form the central amide bond of the peptidomimetic scaffold furnished the desired intermediate in high yield. Scheme 9 shows the synthesis of SR inhibitor **29** which was accessed in 79% yield over three steps.

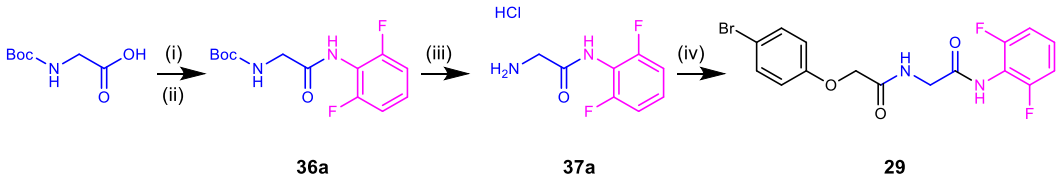

Scheme 9: *Reagents and conditions*: (i) CDI, CH_2Cl_2, rt, 16 h, 92%; (ii) 2,6-difluoroaniline, rt, 16 h, 92%; (iii) 4 M HCl in dioxane, rt, 16 h, 99%; (iv) 4-bromophenoxyacetic acid, T3P® (50 wt.% in EtOAc), TEA, THF, rt, 3 h, 78%.

Using the same procedure as outlined above a small library of peptidomimetics was synthesised in order to probe for optimal anilino and phenolic cross-products to interact with the reported subpocket.[96] Syntheses of all analogues was completed in respectable yield over 3 steps by following the same procedure but altering the aniline and phenoxyacetic acid employed (Table 6).

Table 6: Peptidomimetic Cross Products

Compound Number	Chemical structure	SR IC_{50} (µM)[a]	Yield over 3 steps (%)
28	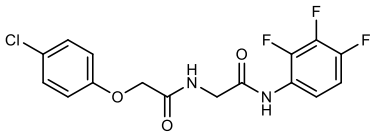	1210	6 (over 5 steps)
38	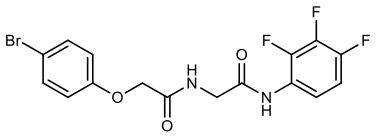	-	69
39	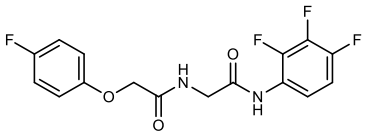	-	70
40	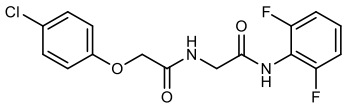	-	90
29	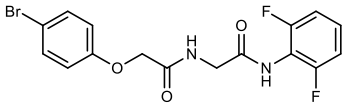	630	71
41	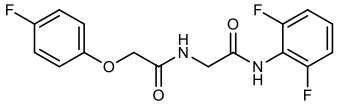	-	90
42	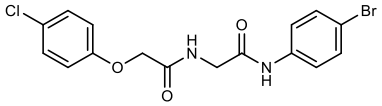	-	84
43	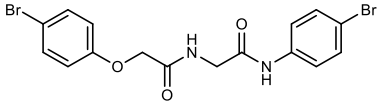	-	83
30	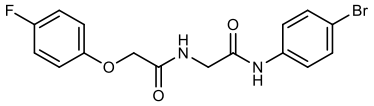	520	81

[a]Data from reference [96]; IC_{50} derived from SR enzymatic activity assay.

28-**43** were determined to be inactive in the primary SR biochemical assay despite **28**-**30** being reported as potent SR inhibitors in the literature.[96,97]

2.8. Summary

In the attempt to identify tool compounds for use in the biological validation studies of SR a two-pronged approach was employed. A fragment-based approach was initiated using data from a discontinued Evotec SR inhibitor project. The aim was to confirm the potent inhibitory activity of the fragment and co-crystallise the fragment in the binding site of SR so as to determine the binding mode. A mechanism of action could then be theorised and the fragment would then be evolved into a potent and selective SR inhibitor with the right physicochemical properties for target engagement *in vivo*. Despite successfully synthesising the fragment and also purchasing the fragment from a commercial vendor, it failed to reconfirm inhibitory activity in the primary assay.

A class of peptidomimetics reported as potent SR inhibitors[96] were resynthesised in an effort to validate the in-house assay and to use as internal controls for the assay in the future. The peptidomimetics also represented a possible starting point for drug discovery as they were reported to be more potent than SR inhibitor malonate. The synthesis of a small library of peptidomimetics was completed successfully including a number of analogues that have been reported as SR inhibitors in the literature.[96,97] Surprisingly, all of the analogues tested in the primary biochemical assay did not show signs of inhibiting SR.

There are a number of factors that can contribute to discrepancies observed between the data generated in-house and that which has been published in the literature. The SR assay format used was different to that used by Evotec and Mori *et al*.[96] Enzyme coupled-assay formats are composed of multiple steps that contain complex reaction mixtures. The data generated from the in-house SR biochemical enzyme coupled assay should be viewed with a number of caveats in mind. The assay format assumes that hydrogen peroxide production is in stoichiometry with *D*-serine production and that all of the *D*-serine produced is converted by DAO to hydrogen peroxide. The resulting hydrogen peroxide is then assumed to react only with HRP in preference to any other component in the reaction mixture. All of these assumptions, and associated errors, can contribute to discrepancies between the effects of inhibitors. Coupled-assay formats are at risk of compounds inhibiting one or more of the auxiliary enzymes rather than, or as well as, the primary enzyme under investigation. For the SR assay, the auxiliary enzyme is DAO, inhibition of DAO by a test compound would result in a false positive reading. To rule out false positive compounds that inhibit DAO (or some other component of the chemiluminescence reaction) the same SR coupled-assay format should be used in the absence of SR, the substrate used should be *D*-serine and a validated inhibitor of DAO should be available as a control. To further validate compound binding to SR, secondary assays should be used to support the results

of the coupled biochemical assay. A complimentary biophysical method such as isothermal titration calorimetry (ITC), which measures the heat released or absorbed as a ligand binds to a protein, is considered the gold standard for quantitative measurements of biomolecular interactions. Additionally, a structural technique such as x-ray crystallography would prove that a prospective inhibitor is binding to the protein of interest.

The fact that inhibitors reported by Evotec and inhibitors reported in the literature were not inhibiting SR in the primary assay jeopardised the future of the project. Disconcertingly, the internal standard for the biochemical enzyme coupled assay, malonate, inhibited SR in line with the literature. In the absence of a reliable orthogonal assay or any data to suggest that the inhibitors were genuine, the decision was taken to stop synthesis on the SR project until (i) another screening strategy was employed and / or (ii) new starting points were identified.

Chapter 3: Small Molecule Kinase Inhibitors, Tool Compounds for DYRK1A Kinase and the DYRK1A Project

Chapter 3 introduces protein kinases as a target class and provides an overview of the current state of FDA-approved kinase inhibitors. The biological rationale for selection of DYRK1A as a potential target, warranting further investigation for the treatment of human disease, is put forth. Published inhibitors of DYRK1A that have been described and used as tool compounds in the literature are reviewed. To conclude, an overview of the DYRK1A project, objectives and screening sequence are provided, complementing all subsequent chapters.

3.1. Protein Kinases

Kinases are enzymes that mediate the transfer of the γ-phosphate group from an adenosine-5-triphosphate (ATP) molecule to the hydroxyl group of a serine (S), threonine (T) or tyrosine (Y) residue borne by a range of substrates involved in essential biological processes.[104,105] As arbitrators of essential biological functions such as transcription, cell signalling, cell cycle progress, cell movement, cell differentiation and apoptosis, kinases have been studied extensively.[104-106] Aberrant functioning of kinases results in the disruption of normal biological processes and may lead to a variety of diseases. Analysis of the human genome has led to the identification of over 500 human kinases collectively referred to as the human kinome. Kinases are categorised into two major divisions by the residues that they phosphorylate - S and T residues or Y residues. The kinome is further subdivided into seven superfamilies based on the sequence similarity of the kinase domain.[106]

The first crystal structure of the kinase catalytic domain, which consists of approximately 290 amino acid residues, was produced nearly three decades ago.[107] Since then, there have been over 6000 structures of kinases deposited in the Protein Data Bank (PDB) showing that the secondary structure of the kinase domain is conserved. The bi-lobed core of the catalytic domain is made up of twelve folded subdomains. Five β-strands and the αC-helix comprise the smaller *N*-terminal lobe. The activation loop that connects the DFG motif and APE motif is part of the larger C-terminal lobe, which is α-helical in character.[104-106] The two sub-domains are connected by the hinge of the kinase. The pocket formed is the active site, which under normal conditions is the site that ATP binds to begin the process of phosphotransfer.[104-106]

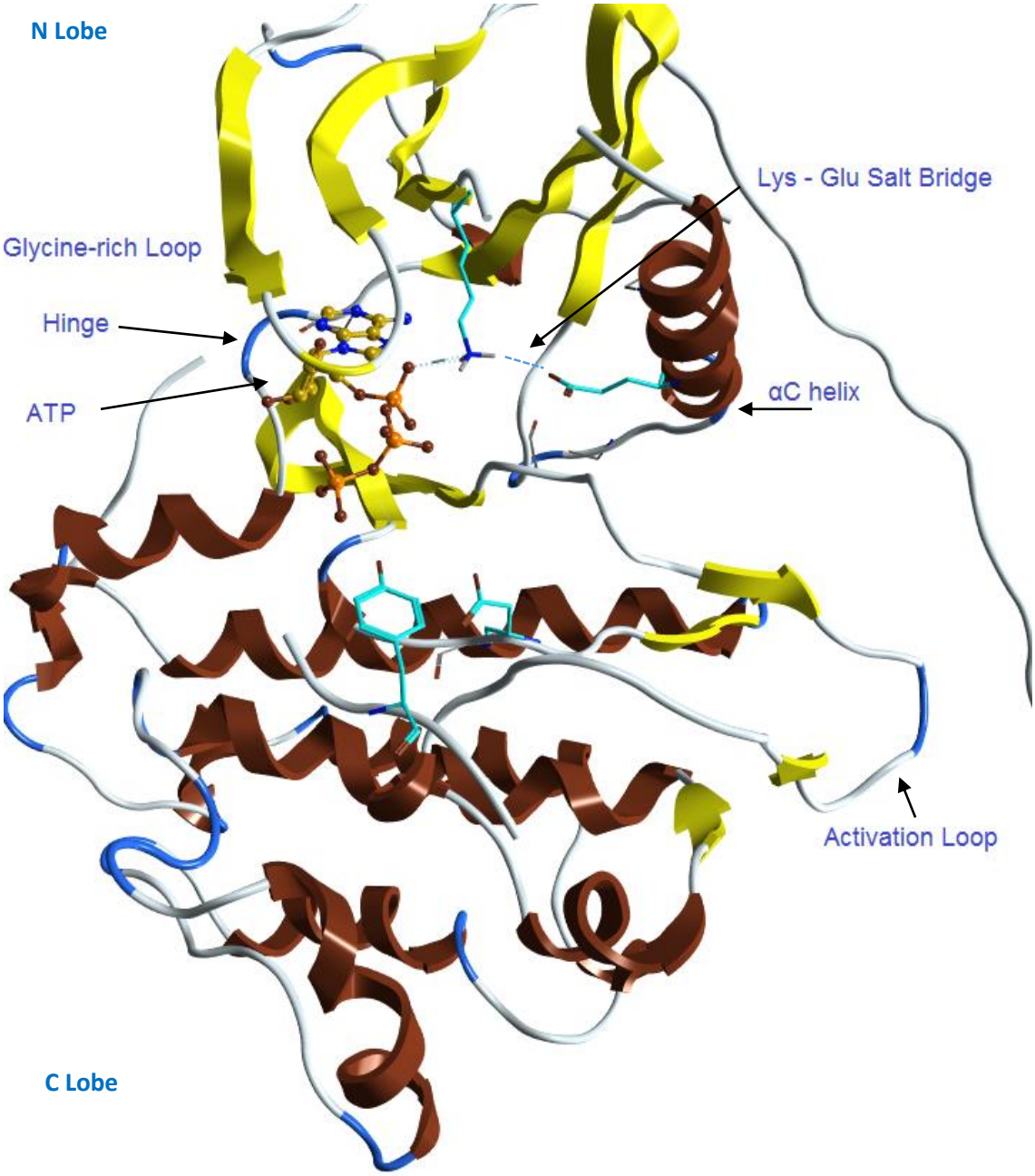

Figure 25. Labelled ATP binding site of a protein kinase (EGFR). Key residues that are likely to take part in phosphotransfer are visible. Image prepared from crystal structure PDB 2GS6 in MOE 2016, CCG with Amber10:EHT force field.

Kinases are capable of adopting an inactive and active form that are structurally different.[108] When the kinase is in an inactive state, the activation loop obstructs the ATP binding site by occupying it. The inactive kinase is usually activated by phosphorylation at a site on the activation loop.

The binding mode of ATP is for the most part conserved across the kinome. Hydrogen bonding interactions are established between the adenine heterocycle of ATP and the backbone of the

hinge region. Binding is strengthened by additional Van der Waals interactions between the heterocycle and aliphatic residues in the pocket. The triphosphate group is orientated towards the solvent-exposed region and the incoming substrate. The α- and β-phosphate groups form ionic contacts with polar residues and secondary interactions are reinforced by a magnesium cofactor that mediates phosphotransfer.[109]

Biological events and cellular processes are often orchestrated by a network of kinases, which coordinate downstream actions through phosphorylation and autophosphorylation events. Abnormal functioning of kinases, which can result in aberrant signalling is thought to be involved in the progression of many diseases. The development of phosphoproteomics has accelerated the identification of disease-promoting kinase targets and has enabled more comprehensive mapping of genes associated with major diseases. Kinases involved in these pathways and disease states may afford novel therapeutic opportunities.[110]

3.2. FDA-approved Small Molecule Kinase Inhibitors

It is estimated that 20-33% of global drug discovery efforts are aimed at delivering molecules that target protein kinases. Over the past 20 years kinases have become one of the most important drug targets.[111,112] As of April 2019 there were 50 FDA-approved small molecule kinase inhibitors that target about 20 different kinases.[113] Janssen's Balversa (erdfitinib) was the most recent small molecule kinase inhibitor granted accelerated approval for the treatment of "adult patients with locally advanced or metastatic bladder cancer that has a type of susceptible genetic alteration known as FGFR3 or FGFR2, and that has progressed during or following platinum-containing chemotherapy".[114] Currently, there are over two hundred molecules that have entered clinical trials and that target an additional 15-20 kinases.[115,116] A summary of FDA-approved small molecule kinase inhibitors are detailed in Table 7.

Approximately half of the approved kinase inhibitors are antagonists of receptor protein tyrosine kinases, nearly a fifth inhibit non-receptor protein tyrosine kinases and over a fifth inhibit protein serine/threonine protein kinases. Over 90% of kinase inhibitors target malignancies (solid tumours and non-solid tumours) and half of the FDA-approved kinase inhibitors possess multi-kinase activity. This can lead to a poor understanding of how effectively multiple signalling pathways are inhibited on the cellular level. Despite polypharmacology in some cases resulting in therapeutic benefits, the lack of basic understanding of disease mechanism can limit further clinical development and the discovery of new targets to alleviate symptoms.[117] The promiscuity of early kinase inhibitors all too often led to toxicity, reducing the

benefit and quality of life for the patient, limiting tolerated dose and the ability of the drug to inhibit its intended target.[118]

In the last decade the rate of FDA-approvals for kinase inhibitors that target non-malignancies has steadily increased. FDA-approved kinase inhibitors now exist for inflammatory diseases such as rheumatoid arthritis and psoriatic arthritis (Table 7). Although currently there are no FDA-approved small molecule kinase inhibitors for kinases in the CNS, Fasudil is a potent Rho-kinase inhibitor that is used clinically in China and Japan for the treatment of cerebral vasospasm and cognitive decline in stroke patients.[119]

Table 7. FDA-approved Small Molecule Kinase Inhibitors, their Primary Target and Therapeutic Indication

Drug	Year approved	Primary Target	Therapeutic Indications
Abemaciclib	2017	CDK4/6	Combination therapy and monotherapy for breast cancers
Acalabrutinib	2017	BTK	Mantle cell lymphoma
Afatinib	2013	EGFR	NSCLC
Alectinib	2015	ALK	ALK-positive NSLCL
Axitinib	2012	VEGFR	Advance renal cell carcinomas
Baricitinib	2018	JAK1/2/3 and Tyk	Rheumatoid arthritis
Binimetinib	2018	MEK1/2	Melanomas
Bosutinib	2012	BCR-Abl	Chronic myelogenous leukaemias
Brigatinib	2017	ALK	ALK-positive NSCLC
Cabozantinib	2012	RET	Advanced medullary thyroid cancers
Ceritinib	2014	ALK	ALK-positive NSCLC resistant to crizotinib
Cobimetinib	2015	MEK1/2	BRAF mutation-positive melanomas in combination with vemurafenib
Crizotinib	2011	ALK	ALK or ROS1-postive NSCLC
Dabrafenib	2013	B-Raf	BRAF mutation-positive melanomas and NSCLC
Dacomitinib	2018	EGFR	EGFR-mutant NSCLC
Dasatinib	2006	BCR-Abl	Chronic myelogenous leukaemias
Encorafenib	2018	B-Raf	Combination therapy for $BRAF^{V600E/K}$ melanomas
Erdafitinib	2019	FGFR	metastatic urothelial carcinoma with FGFR3/FGFR2 mutation
Erlotinib	2004	EGFR	NSCLC, pancreatic cancers
Everolimus	2009	FKBP12/mTOR	ER2-negative breast cancers, pancreatic neuroendocrine tumours, renal cell carcinomas,

			angiomyolipomas, subependymal giant cell astrocytomas
Fostamatinib	2018	Syk	Chronic immune thrombocytopenia
Gefitinib	2003	EGFR	NSCLC
Gilteritinib	2018	Flt3	Acute myelogenous leukaemias
Ibrutinib	2013	BTK	Chronic lymphocytic leukaemias, mantle cell lymphomas, marginal zone lymphomas, graft vs. host disease
Imatinib	2001	BCR-Abl	Philadelphia chromosome-positive CML or ALL, aggressive systemic mastocytosis, chronic eosinophilic leukaemias, dermatofibrosarcoma protuberans, hypereosinophilic syndrome, gastrointestinal stromaltumours, myelodysplastic/myeloproliferative disease
Lapatinib	2007	EGFR	HER2-positive breast cancers
Larotrectinib	2018	TRK	Solid tumours with NTRK fusion proteins
Lenvatinib	2015	VEGFR, RET	Differentiated thyroid cancers
Lorlatinib	2018	ALK	ALK-positive NSCLC
Midostaurin	2017	Flt3	Acute myelogenous leukaemias, mastocytosis, mast cell leukaemias
Neratinib	2017	ErbB2	HER2-positive breast cancers
Netarsudil	2018	ROCK1/2	Glaucoma
Nilotinib	2007	BCR-Abl	Philadelphia chromosome-positive CML
Nintedanib	2014	FGFR	Idiopathic pulmonary fibrosis
Osimertinib	2015	EGFR	NSCLC
Palbociclib	2015	CDK4/6	Oestrogen receptor- and HER2-positive breast cancers
Pazopanib	2009	VEGFR	Renal cell carcinomas, soft tissue sarcomas
Ponatinib	2012	BCR-Abl	Philadelphia chromosome-positive CML or ALL
Regorafenib	2012	VEGFR	Colorectal cancers
R406	2018	Syk	Chronic immune thrombocytopenia
Ribociclib	2017	CDK4/6	Combination therapy for breast cancers
Ruxolitinib	2011	JAK1/2/3 and Tyk2	Myelofibrosis, polycythemia vera
Sirolimus	1999	FKBP12/mTOR	kidney transplant, lymphangioleiomyomatosis
Sorafenib	2005	VEGFR	Hepatocellular carcinomas, renal cell carcinomas, thyroid cancers (differentiated)
Sunitinib	2006	VEGFR	Gastrointestinal stromal tumours, pancreatic neuroendocrine tumours, renal cell carcinomas

Temsirolimus	2007	FKBP12/mTOR	Advanced renal cell carcinomas
Tofacitinib	2012	JAK1/2/3 and Tyk2	Rheumatoid arthritis
Trametinib	2013	MEK1/2	Melanomas
Vandetanib	2011	VEGFR	Medullary thyroid cancers
Vemurafenib	2011	B-Raf	$BRAF^{V600E}$ mutant melanomas

Table updated and adapted from reference [113].

Over the past 10 years the number of FDA-approved kinase inhibitors has nearly quadrupled, bucking the general trend of declining approvals for new chemical entities for other disease targets. Undoubtedly, the extensive knowledge accumulated in kinase structural biology and medicinal chemistry since the discovery of Imatinib has aided in the development of more recent kinase inhibitors. The highly conserved and well-characterised nature of the ATP binding site of kinases has brought about fundamental changes in the way hits and leads are selected and developed. Knowledge-based approaches and structure-based approaches are particularly well suited to kinase inhibitor drug discovery.[120] Many kinase inhibitors contain privileged heterocyclic motifs and are the result of kinase inhibitor repurposing from previously approved drugs. Initial concerns over achieving target selectivity and reducing the side effects exhibited by early kinase inhibitors have largely been overcome by the development of kinome-wide and proteome-wide screening panels. Routine selectivity profiling has enabled the development of more selective and potent inhibitors of therapeutically validated targets.[120] Another reason for the growth in kinase inhibitors is the emergence of resistance to those inhibitors used in the field of oncology. This has led to the design of resistance-mutant specific inhibitors for the same validated kinase targets and has resulted in second and third generation kinase inhibitors.[120]

3.3. Classification of Kinase Inhibitors

Kinase inhibitors are categorised according to the state of the kinase they inhibit (active or inactive) and their binding mode. Type I inhibitors bind to the active form of the kinase in and around the adenine pocket. Type II inhibitors bind to an inactive form of the kinase - the DFG-D_{out}. Type III inhibitors bind to an allosteric site away from the ATP site.[121] Type $I^{1/2}$ inhibitors have been described that bind to an inactive form of the kinase with DFG-D_{in}.[122] Type $I^{1/2}$ inhibitors and Type II inhibitors can be further separated into A and B subtypes depending on whether the binding mode of the molecule extends beyond the gatekeeper residue into the back of the pocket (Type A) or not (Type B).[123]

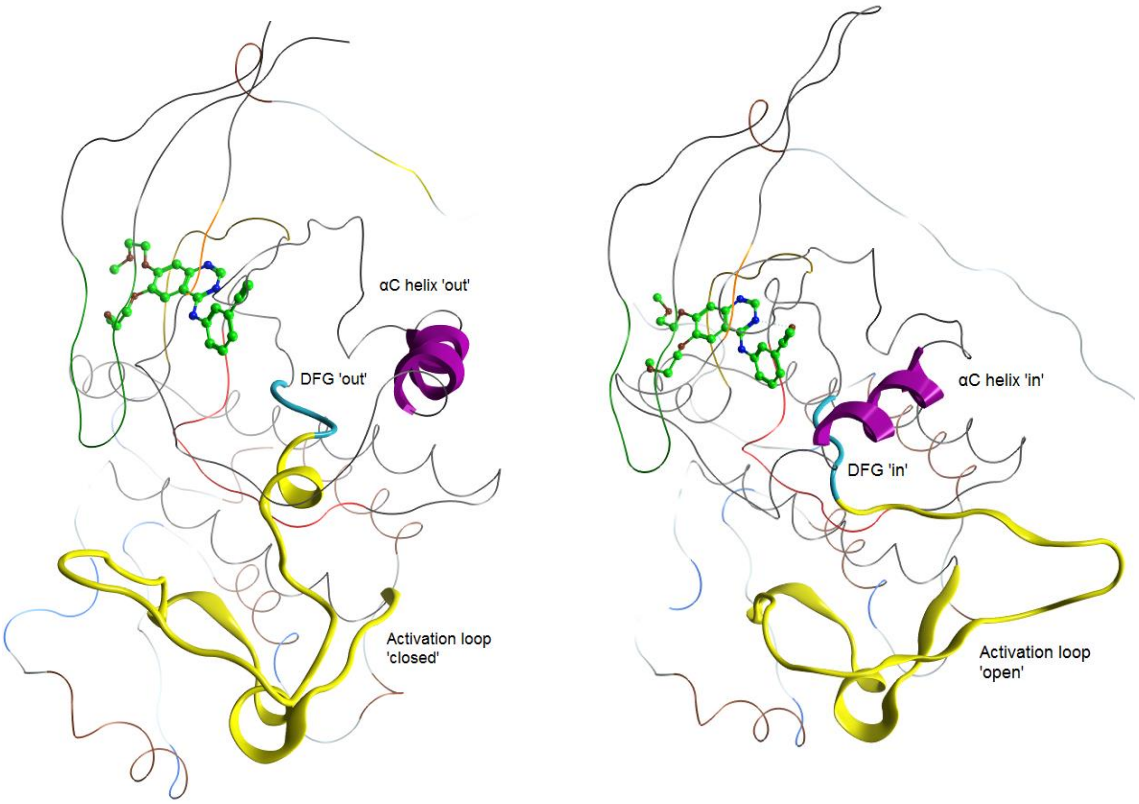

Figure 26. Comparison of a kinase (EGFR) in an inactive and active state. LHS – EGFR kinase in an inactive state (PDB 4HJO). In the inactive state of EGFR the αC helix (magneta) is 'out', activation loop (yellow) is 'closed' and DFG motif (cyan) is 'out'. RHS – EGFR kinase in an active state (PDB 1M17). In the active state of EGFR the αC helix (magneta) is 'in', activation loop (yellow) is 'open' and DFG motif (cyan) is 'in'. Figure prepared with MOE 2016, CCG with Amber10:EHT force field.

Allosteric inhibitors can be further divided into Type III or Type IV inhibitors.[124] Whereas a Type III allosteric inhibitor binds adjacent to the ATP site and between the lobes, a Type IV inhibitor does not bind in the cleft formed between the two lobes. Type V inhibitors have been described as molecules that are able to bind to two different regions of the kinase simultaneously and cause inhibition.[125]

In recent years covalent inhibitors of kinases have had a resurgence in popularity, leading to the approval of the first irreversible covalent kinase inhibitor drug, afatinib, in 2013. Covalent targeting of ATP site cysteine residues may provide a selectivity handle over kinases that do not possess such a cysteine.[123] Another possible advantage of irreversible covalent inhibitors is that covalent bond formation between an inhibitor and the kinase may ensure prolonged target occupancy, which may translate into improved clinical efficacy.[126]

There are multiple binding modes that molecules can adopt when binding to a kinase and causing inhibition. In terms of inhibitor selectivity, it has not been definitively proven that Type I inhibitors are the least selective.[127,128,129] It is likely that due to the increased variation in kinases

away from the ATP pocket that allosteric Type III inhibitors may be capable of delivering more selective inhibitors than Type I-II inhibitors. However, the allosteric site may be more susceptible to point mutations and resistance as there is less selection pressure to maintain the remote allosteric pocket than the physiologically relevant ATP binding site.

3.4. General Outlook for Kinase Inhibitors

The field of kinase drug discovery has made great strides over the past 20 years with initial fears of target selectivity and inhibitor promiscuity being largely overcome. The majority of small molecule FDA-approved kinase inhibitors were developed for the treatment of cancer with an increasing number of molecules being approved for inflammatory diseases.

It is evident that FDA-approved small molecule kinase inhibitor drugs only target a very small percentage of the human kinome (less than 5%), whilst over half of the human kinome (>250 kinases) has been linked to disease loci for cancer. Furthermore, an array of kinases are over-expressed or mutated in many cancers[130] as well as other diseases. It follows that research into the remaining 95% the kinome should furnish new treatments for a whole host of diseases and that the development of selective chemical probes to investigate and validate the uncovered kinome will play a significant role in delivering effective treatments to patients.

The dual-specificity tyrosine phosphorylation-regulated kinase 1A (DYRK1A) is a kinase of therapeutic interest and is part of the 95% described above. The following chapters will detail the work undertaken to provide the scientific community with a DYRK1A specific tool compound to delineate the role of DYRK1A in human disease.

3.5. Dual-Specificity Tyrosine Phosphorylation-Regulated Kinase 1A (DYRK1A)

3.5.1. DYRK Kinases Distribution, Structure and General Function

Dual-specificity tyrosine phosphorylation-regulated kinases (DYRKs) are a family of eukaryotic kinases that consist of at least six mammalian subtypes, categorised into two classes, Class 1 (DYRK 1A and 1B) and Class 2 (DYRK 2, 3, 4A and 4B).[131] DYRKs are part of the CMGC super family of kinases that includes glycogen synthase kinases (GSKs), cyclin dependent kinases (CDKs), mitogen-activated protein kinases (MAPKs), and CDK-like kinases (CLKs) (Figure 27).[133]

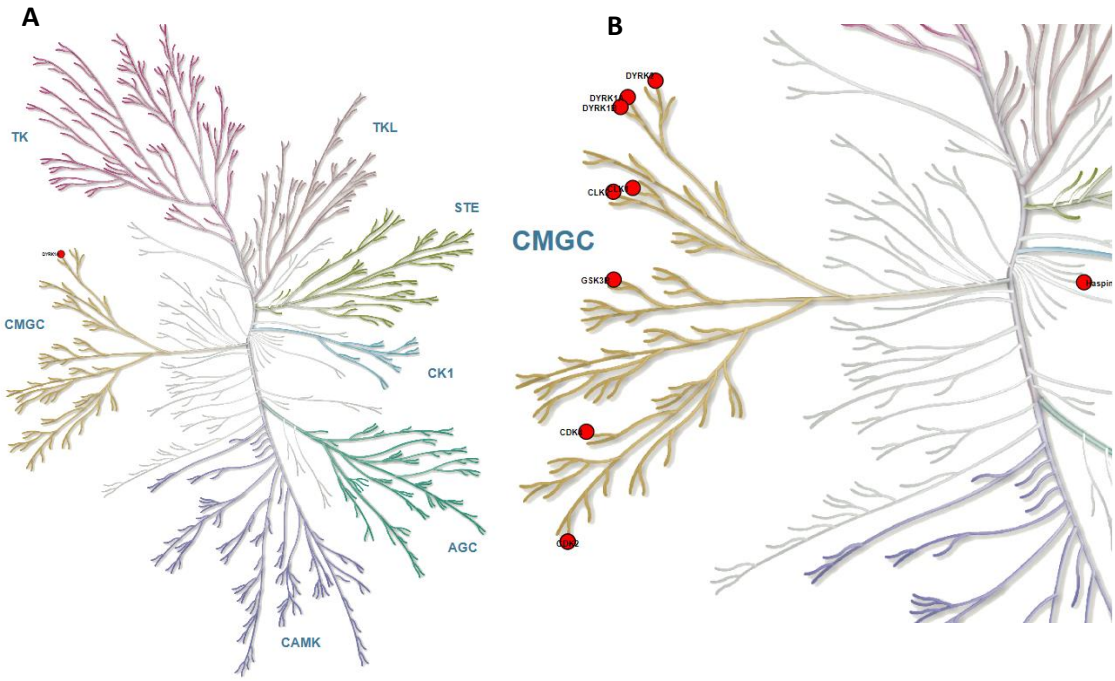

Figure 27. A – The human kinome; position of DYRK1A highlighted as red dot. B – The CMGC super family and common off-targets relevant to this thesis highlighted as red dots. Images created at www.kinhub.org.

Unique amongst DYRK family members, the DYRK1A gene is located on the DSCR (Down's syndrome critical region) of chromosome 21.[132,133] DYRK1A is expressed ubiquitously throughout the body and brain. DYRK1A is present at higher levels in the cerebellum, hippocampus and olfactory bulb, especially during early development.[134]

DYRK family kinases possess a highly conserved catalytic domain across species - the human orthologue of DYRK1A shares over 99% sequence identity with that of the rat and mouse. Class 1 DYRKs also share similar DYRK homology box, nuclear localisation signal and a motif rich in proline, glutamic acid, serine, and threonine residues.[131] Outwith the kinase domain there are major differences between Class 1 and Class 2 DYRKs. Notably, Class 1 DYRKs lack a *N*-terminal autophosphorylation accessory region .[135] The hinge region of DYRK1A and DYRK1B differ only by one amino acid residue - DYRK1A possesses a methionine (Met240) in the same position along the hinge that DYRK1B bears a leucine residue.

DYRK1A self-activates through autophosphorylation of Y321 on the activation loop of the catalytic domain during protein synthesis.[136] Substitution of Y321 with phenylalanine (F), glutamine (Q) or histidine (H) decreases the activity of DYRK1A.[137] Once activated, DYRK1A phosphorylates S and T residues of substrates including factors involved in transcription (CREB, NFAT, STAT3, Gli1), translation (eIF2B) and splicing (cyclin L2, SF2, SF3). DYRK1A also

phosphorylates synaptic proteins (dynamin I, ampiphysin I, synaptojanin I) and those involved in protein production, apoptosis and cell signalling (glycogen synthase, caspase-9, Notch).[138,139,140] Although DYRK1A is heavily implicated in both cell death and cell proliferation, the signalling pathways of DYRKs are relatively unknown compared with other members of the CMGC super family such as CDKs and MAPKs. Recent work by de la Luna *et al*. has identified E3 ubiquitin ligase RNF169 as well as other novel interaction partners. This work suggests that DYRK1A also plays a central role in cellular responses to DNA damage.[141] The activity and function of DYRK1A appears to be regulated by alterations in kinase expression level i.e. the activity of DYRK1A can be directly related to the amount of DYRK1A protein present.[142]

3.6. Inhibition of DYRK1A as a Potential Treatment for Human Disease

DYRK1A has received considerable attention from the pharmaceutical industry and academia owing to its potential as a therapeutic target in both oncology and neurodegenerative diseases. DYRK1A phosphorylates many proteins including other kinases, as well as splicing, transcription and translation factors involved in the regulation of numerous cellular pathways and functions. Thus, aberrant functioning of DYRK1A is expected to produce a signalling cascade that ultimately results in cognitive dysfunction and neurodegeneration (Alzheimer's disease (AD), Down's syndrome, Parkinson's disease (PD),[143] Huntington's disease (HD) and Pick's disease (PID))[144] or cancer in patients.

3.6.1. Alzheimer's Disease

The two physical disease-defining parameters of AD are the presence of cerebral plaques and neurofibrillary tangles (NFTs) in certain brain regions. The extracellular plaques are composed of a dense core of amyloid-beta peptide (Aβ) surrounded by a collection of destroyed or damaged neurons which form amorphous extracellular deposits. Helical filaments of abnormally β-folded and irregularly phosphorylated protein, called tau, aggregate to form neurophil threads and intraneuronal NFTs.[145] It is widely accepted that the accumulation of Aβ peptide as a result of altered processing of amyloid protein from its precursor (APP) causes a pathogenic cascade that ultimately gives rise to the clinical manifestations associated with AD (β-amyloid hypothesis of AD).[146,147] Thus reduction and inhibition of Aβ peptide accumulation is an attractive target in the treatment of AD. Compounds which are grouped into this category include secretase inhibitors and modulators.

Multiple neurotransmitter systems are affected during the progression of AD. Traditionally, therapies have focussed on maintaining the levels of the neurotransmitter acetylcholine in the

brain by inhibiting the action of acetylcholinesterase enzymes with drugs such as donepezil and tacrine. The cause of neurodegeneration is not fully understood and there are multiple forms of dementia. Existing treatments are not preventative and do not stop the progression of AD. There has been an increased interest in finding novel therapies for AD due to the undesirable side effect profile and lack of efficacy of the existing drugs. Cognitive function does not only rely on cholinergic transmission, therefore, it has been postulated that inhibition of enzymes involved in Aβ peptide production and modulation of other neurotransmitter systems involved in signalling pathways between neurons may improve cognition without the side effects associated with targeting the cholinergic system.

3.6.2. DYRK1A Inhibition as a Potential Therapy for AD

DYRK1A plays a central role in tau hyper-phosphorylation and aggregation by directly phosphorylating tau protein at sites commonly observed in NFTs and tau aggregates present in the brains of Down's syndrome and AD patients. Furthermore, DYRK1A acts as a GSK3-priming kinase promoting further tau phosphorylation and stimulating the assembly of NFTs.[148] Phosphorylation of amyloid precursor protein (APP) by DYRK1A promotes its cleavage by β- and γ-secretases, which in turn encourages the formation of Aβ40 and Aβ42 peptide plaques. Additionally, a subunit of γ-secretase, presenilin 1 (PS1), is phosphorylated by DYRK1A, enhancing the proteolytic activity of γ-secretase and producing additional Aβ peptide.[149] The presence of Aβ peptide in neuroblastoma cells induced the expression of DYRK1A mRNA resulting in increased levels of tau phosphorylation, implicating DYRK1A in the production of NFTs and Aβ peptide formation.[150] Alternative splicing factor (ASF) functions normally to maintain the balance of tau proteins in the brain. DYRK1A phosphorylates ASF and renders it inactive causing tau splicing to continue unregulated aiding aggregation.[151,152] The regulator of calcineurin-1 (RCAN1) is phosphorylated by DYRK1A, which in turn improves the ability of RCAN1 to inhibit calcineurin (CALN) and increases the levels of tau protein.[153]

The brains of Down's syndrome patients are characterized by the accumulation of Aβ plaques and hyperphosphorylated tau protein resembling AD. As DYRK1A is located on the Down's syndrome critical region (DSCR) of chromosome 21 and is consequently over-expressed in individuals with Down's syndrome, there is a plausible link between Down's syndrome and AD. Over-expression of DYRK1A could account for the prevalence of early onset of AD in the Down's syndrome population.

3.6.3. Down's syndrome and DYRK1A

Down's syndrome is a genetic condition which is the consequence of complete trisomy 21. The Down's syndrome phenotype can also be caused by partial or complete duplication of the Down's syndrome critical region (DSCR) (mosaicism) of chromosome 21q22.[154] Down's syndrome causes a variety of clinical phenotypes including physical dysmorphism (hypotonia, facial features, hand and foot features), developmental delay and health problems such as early on-set AD.[154]

The DYRK1A gene is located on the DSCR and results in a 1.5 fold increase in DYRK1A mRNA and protein levels for Down's syndrome patients.[155] Trisomic murine models of Down's syndrome (Ts65Dn, Ts1Cje and Ts1Rhr25) contain the gene for DYRK1A in the trisomic region and exhibit both the physical and developmental indications of Down's syndrome.[156,157,158,159,160] Transgenic mouse models bearing additional copies of genes in the DSCR, including DYRK1A, display brain abnormalities and impaired learning ability.[161,162,163] When the DYRK1A gene was absent from an analogous transgenic mouse model, cognitive impairment was not exhibited. Furthermore, transgenic mouse models that specifically overexpress DYRK1A exhibit Down's syndrome phenotypes, underlining the relationship of DYRK1A and the Down's syndrome phenotype.[164] In 2018 Schnabel *et al*. reported the first patient, a five-year old boy, with a Down's syndrome phenotype resulting from a microduplication of chromosome 21q, which only included the DYRK1A gene and no other Down's syndrome candidate gene (APP, DSCR1 (RCAN1), DSCAM).[165] This case supports the hypothesis that elevated levels of DYRK1A can contribute to the Down's syndrome phenotype. It follows that modulation of DYRK1A activity could provide therapeutic benefits for patients with cognitive impairment in Down's syndrome and mosaicism.[165]

3.6.4. Oncology and DYRK1A

The observation that certain types of cancer (except testicular cancers and leukaemia) are less prevalent in populations of Down's syndrome patients has led researchers to speculate that Trisomy 21, in particular, overexpression of DYRK1A, may suppress the development of certain tumours.[166] The Ts65Dn mouse model supressed the growth of Lewis lung carcinoma and B16F10 melanoma through the increased activity of DYRK1A inhibiting calcineurin.[167] DYRK1A also inhibits other oncogenic proteins such as the nuclear factor of activated T-cells (NFAT) and cyclin D1. DYRK1A has been shown to have an anti-proliferative effect on acute myeloid leukaemia (AML) cell lines.[168]

The presumption that Down's syndrome affords protection against certain cancers has been contested due to the fact that Down's syndrome patients have a less than average life

expectancy and that onsets of certain types of cancers are in advanced age.[169] Recent evidence has suggested that DYRK1A may have an oncogenic role; immortalised HPV16 keratinocytes that overexpress DYRK1A were shown to have an increased rate of cell survival.[170] In addition, the levels of DYRK1A are increased in malignant cervical lesions compared to normal tissue indicating that DYRK1A could play a role in carcinogenesis.[156] It is speculated that DYRK1A promotes the development of megakaryoblastic tumours through the inhibition of NFAT. Elevated expression of NFAT cytosplasmic 1 induced expression of DYRK1A, suggesting a negative feedback loop and promoting tumourigenesis. Also, the prevalence of acute megakaryoblastic leukaemia (AMKL) and acute lymphoblastic leukaemia (ALL) in children with Down's syndrome has been attributed to DYRK1A's role in promoting the overexpression of cytokines in AMKL.[156]

DYRK1A has been shown to be overexpressed in glioblastoma cells.[171] DYRK1A mediated hyperphosphorylation of sprouty2 can block EGFR degradation. However, DYRK1A can also stimulate EGFR degradation in glioblastoma cells by promoting endocytosis and lysosomal degradation. Thus it has been proposed that EGFR-dependent glioblastomas could be attenuated by DYRK1A inhibition.[156, 172]

DYRK1A increases the activity of transcriptional factors that potentiate hedgehog signalling, tumourigenesis, cell proliferation, cell cycle progress and apoptosis such as glioma-associated oncogene homologue 1 (Gli1) and signal transducers and activators of transcription (STAT3).[173,174,175,176] Cellular quiescence blocks cell differentiation and affords cancer cells some resistance to chemotherapeutics.[177] The cellular mechanisms required to arrest the cell cycle in a stage of quiescence are not fully understood. During quiescence, the DREAM (DP, RB, E2F, and MuvB) complex suppresses genes involved in the cell cycle thus promoting quiescence.[178] DYRK1A mediates the assembly of the DREAM complex in gastrointestinal stromal tumours (GIST), affording protection against imatinib induced apoptosis.[179] DYRK1A further prevents apoptosis by attenuation of Notch signalling and inactivation of caspase-9 through direct phosphorylation.[180,181] Approximately 10% of cancer patients survive their metastases that exhibit resistance to pro-apoptotic therapies.[182] Due to its central role in cancer cell survival, the inhibition of DYRK1A could be a means of improving the prognosis of cancers that are resistant to pro-apoptotic resistant therapies.

3.6.5. DYRK1A as a Therapeutic Target for other Diseases

The role of DYRK1A in the advancement of Huntington's disease (HD) is not well understood. DYRK1A has been shown to selectively bind to and phosphorylate Huntingtin-interacting protein

1 (Hip-1). Phosphorylation of Hip-1 by DYRK1A is alleged to play a key role in the regulation of cell death and neuronal differentiation.[183]

The progression of the movement disorder, Parkinson's disease (PD), has been linked to the activity of DYRK1A.[184] Phosphorylation of α-synuclein, the main component of Lewy bodies and a hallmark of PD, at Ser-87, has been attributed to DYRK1A. Enhanced α-synuclein aggregate formation as a result of DYRK1A phosphorylation could lead to enhanced neurotoxicity and the progression of PD. DYRK1A also phosphorylates parkin, the protein product of a gene responsible for autosomal recessive familial PD. DYRK1A phosphorylates parkin at Ser131, negatively regulating its E3 ubiquitin ligase activity.[185]

There is mounting evidence to suggest that DYRK1A deficiencies, *de novo* pathogenic variants or chromosomal mutations involving DYRK1A, alter brain development and function. Patients with DYRK1A haploinsufficiency syndrome (MDR7) display microcephaly, autism spectrum disorder (ASD) and intrauterine growth retardation.[186,187] Heterozygous disruption of DYRK1A results in patients exhibiting a typical clinical syndrome with mild to severe ID (intelligence quotient (IQ) below 70), microcephaly, intrauterine growth retardation, facial dimorphisms, behavioural issues and compromised motor functions.[188]

Abnormal insulin release by pancreatic islets as a result of aberrant β-cell activity and population size is a hallmark of all forms of diabetes.[189] Chemical agents that enhance β-cell proliferation have been proposed as an alternative to insulin injections that many patients require to prevent hyperglycaemia 10-15 years after diagnosis.[190,191] DYRK1A inhibitors have been shown to promote NFATc-dependent β-cell proliferation in human pancreatic cells, leading to the hypothesis that inhibitors of DYRK1A could be used for the treatment of diabetes.[192]

3.7. Existing Pharmacological Tools of DYRK1A

DYRK1A is the most studied kinase in the DYRK family. Numerous compounds are documented in the literature with DYRK1A inhibitory activity. For the most part these are (i) derived from natural products and their derivatives or (ii) synthetic inhibitors. The majority of DYRK1A antagonists are Type I kinase inhibitors and are essentially nitrogen-containing heterocycles. Descriptions of DYRK1A inhibitors that have been used most widely as pharmacological tools are outlined below. This is not intended to be a list of all compounds in the literature and patent literature that display DYRK1A inhibitory activity. This subject has been reviewed extensively.[193,194,195,196]

3.7.1. DYRK1A Tools derived from Natural Products and their Analogues

3.7.1.1. Epigallocatechin Gallate (EGCG)

The green tea extract, Epigallocatechin Gallate (EGCG, **43**), was the first allosteric inhibitor of DYRK1A discovered.[197,198]

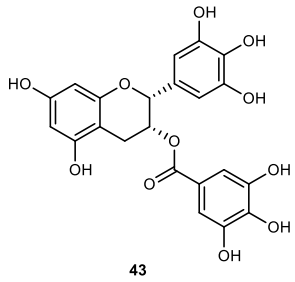

Figure 28. Published DYRK1A inhibitor EGCG.

43 is a fairly potent DYRK1A inhibitor (IC_{50} = 330 nM). DYRK1A-overexpressing transgenic mice displaying a Down's syndrome phenotype that were fed on a green tea diet, exhibited improved cognition and enhancements in long-term and short-term memory.[199] In a double-blind, randomised, placebo-controlled, phase-2-trial with 87 Down's syndrome participants, a combined regimen of daily treatment (9 mg/kg per day) with **43** and cognitive training for 12 months afforded significant improvements in visual recognition memory, inhibitory control and adaptive behaviour compared to the placebo group.[200]

Despite the promising results from a number of clinical and pre-clinical studies, **43** suffers from poor bioavailability and is metabolised to produce reactive metabolites. As a result **43** is likely to have poor brain exposure and target engagement *in vivo*.[201] The robustness of the clinical trials have also been questioned due to lack of consistency in results and few controls used.[202] Studies have used different EGCG-containing supplements, which contain varying levels of EGCG and other polyphenols, as a source of EGCG. This has allowed some to question whether the observed improvements in Down's syndrome phenotype are a result of other components in the supplement and not as a result of specific DYRK1A inhibition by **43**.[202,203]

Another complication with using **43** as a tool compound is that it has been categorised as a promiscuous pan-assay interference compound (PAINS) due to its known interference in biological assays.[14,204] The bis-catechol (pyrogallol) and catechol moieties are readily oxidised to a reactive species able to covalently bind proteins and chelate metals. Pyrogallols in particular are responsible for non-specific membrane perturbation and promiscuous protein binding.[205] All of these unwanted characteristics can lead to false positives in biological assays. Despite **43**'s

inadequacy as a tool compound, it still continues to be used as an *in vitro* and *in vivo* probe within the DYRK community. Most recently, Avanti Biosciences released a patent in 2018 with details of DYRK1A negative allosteric modulators (NAMs) derived from **43** that they claim can be used to treat cognitive and behavioural impairments in Down's syndrome patients. The most potent DYRK1A inhibitor from that patent, **44**, is depicted in Figure 29.[206] Worryingly, the molecule retains the PAINS motifs.

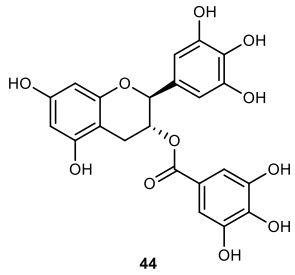

Figure 29. Avanti Biosciences Ltd published DYRK1A NAM.[206]

3.7.1.2. Harmine

Harmine, **45**, a β-carboline originally isolated from the South American vine *Banisteriopsis caapi*, was identified as a potent and orally bioavailable DYRK1A inhibitor (IC_{50} = 80 nM) with good selectivity against a panel of 69 other kinases.[207]

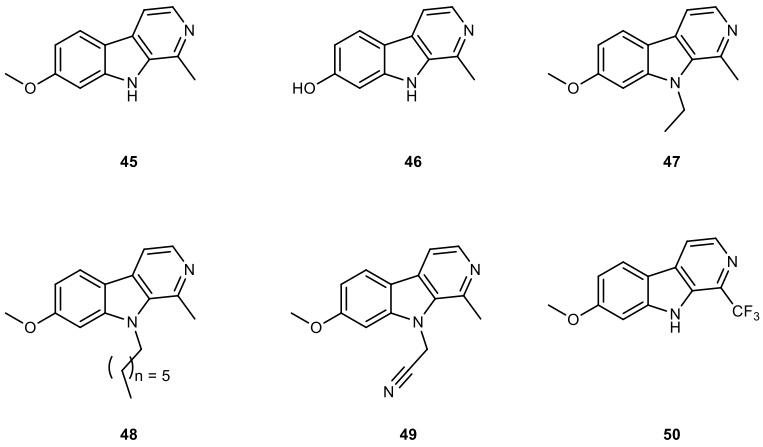

Figure 30. Published harmine analogues

Harmala alkaloids are used in traditional spiritual medicines by the peoples of the Amazon basin. The psychoactive substance Ayahuasca contains harmine and other harmala alkaloids. *In vitro* experiments have shown that **45** has the potential to stimulate neural stem cell proliferation, migration, and differentiation into adult neurons.[208] **45** has also been shown to be cyctotoxic against cancer cells [209,210] and possess antidiabetic activity.[211,212]

Although **45** appears to be a good tool compound as it is potent, selective, orally bioavailable and most likely brain penetrant, it possesses potent inhibitory activity of monoamine oxidase (MAO-A). As MAO-A regulates the concentration of monoamine neurotransmitters in the nervous system, any inhibition may cause an imbalance that in the most extreme cases can be fatal. In the past MAO-A were used as drugs for severe depression, however, most of these have been withdrawn from clinical practice due to side effects such as high toxicity, fatal hypertensive crisis, drug-food interactions, drug-drug interactions, serotonin syndrome and withdrawal syndrome.[213] Another complication with using **45** as a DYRK1A specific tool is that it also potently inhibits other isoforms of DYRK, with some reports suggesting **45** is a more potent inhibitor of DYRK1B (IC_{50} = 260 nM) than DYRK1A (IC_{50} = 350 nM).[214]

The production of the co-crystal structure of **45** bound to DYRK1A (PDB 3ANR) provides insights into the binding mode and potential mechanism of action of inhibition.[214] **45** occupies the ATP site, binding in a Type I fashion, to competitively inhibit DYRK1A. The structure shows important hinge binding interactions with Lys188, and paved the way for SBDD efforts to remove MAO-A activity and enhance DYRK1A selectivity.

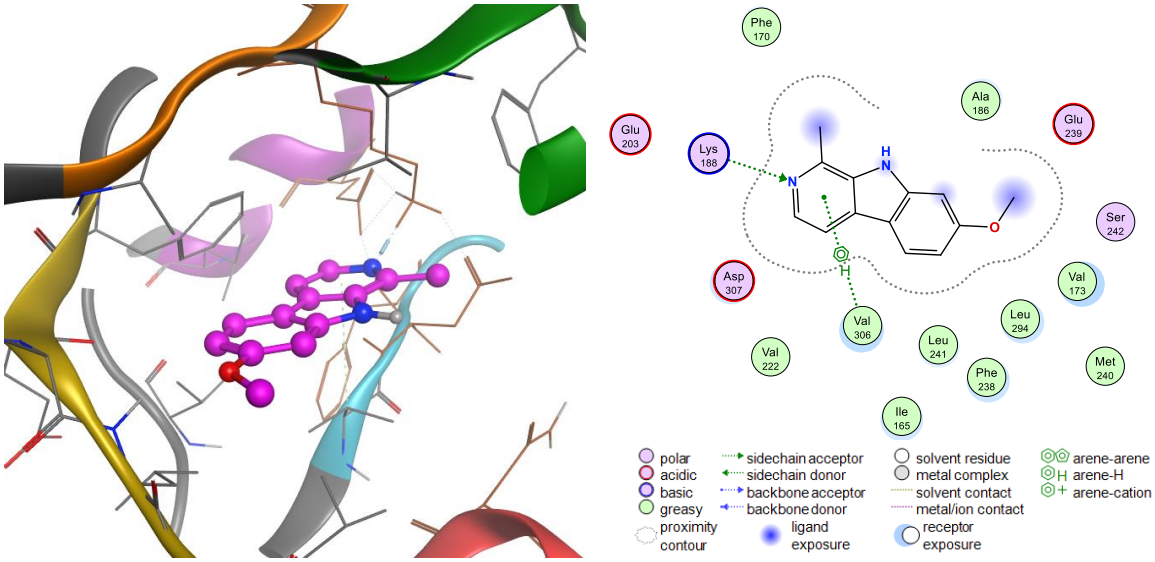

Figure 31. Co-crystal structure of harmine bound to DYRK1A from Ogawa *et al*. PDB 3ANR.[214] Structure prepared in MOE 2016, CCG with Amber10:EHT force field.

Becker *et al*. describe the use of *N*-alkylation to afford selectivity against MAO-A whilst maintaining DYRK1A inhibitory activity in a series of β-carbolines.[215] Work by Balint *et al*. supported this hypothesis and also discovered that functionalization of the 1-position, with hydroxymethyl or trifluoromethyl, of the β-carboline skeleton, afforded selectivity against MAO-A.[216] The complete kinome selectivity profiles of these harmine derivatives were not disclosed,

which makes it difficult to comment on the suitability of these derivatives as DYRK1A tools. Kumar *et al*. profiled **46**, the same hydroxyl analogue as was identified by Balint *et al*., in a 468 kinome panel before profiling the compound in an *in vitro* assay for β-cell proliferation.[217] Preliminary results indicated that selectivity vs DYRK1B was achieved, however, follow up studies were not repeated to confirm this. Other CMGC kinases including CLK1, CLK2 and DYRK2 were also identified as potent off-targets. **46** represents the most promising harmine analogue (DYRK1A IC_{50} = 106 nM) to date, with apparent selectivity against DYRK1B and MAO-A, and the ability to induce similar levels of β-cell proliferation as **45**. As yet no pharmacokinetic data has been disclosed and no *in vivo* research has been presented. For an inhibitor derived from **45** it would be important to rule out reactive and psychoactive metabolites prior to use as an *in vivo* tool compound.

3.7.1.3. Leucettine L41

Isolated from the marine sponge *Leucetta microraphis*, leucettamine B, **51**, was found to be a fairly potent inhibitor of DYRK1A (IC_{50} = 420 nM).[218] **51** exhibited good kinome-wide selectivity but was also potent against other CMGC kinases DYRK2 (IC_{50} = 490 nM), CLK1 (IC_{50} = 100 nM), CLK2 (IC_{50} = 910 nM) and CLK4 (IC_{50} = 120 nM).[219] Although isoform-selective inhibition of the CLKs has been proposed as a target for improving cognition in autism spectrum disorder (ASD) and Phelan-McDermid syndrome,[220] a pan-inhibitor of the CLKs is likely to cause genotoxicity issues.[221]

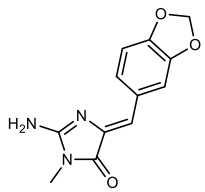

51

Figure 32. Leucettamine B

Interested in discovering compounds that target multiple kinases involved in the progression of AD, Meijer *et al*. have focussed their research efforts on producing dual CLK1/DYRK1A inhibitors rather than a selective tool compound. A library of 450 analogues derived from leucettamine B was synthesised with the aim of increasing potency at both CLK1 and DYRK1A.[222,223] A compound from this library, Leucettine L41, **52**, exhibited 10 fold improvement in inhibition of DYRK1A compared to **51** and was selected for further profiling.[224]

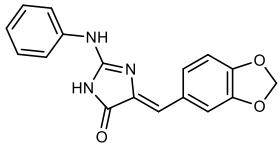

52

Figure 33. Leucettine L41.

The co-crystal structure of **52** bound to DYRK1A revealed the compound to be an ATP-competitive Type I inhibitor. The structure shows important hinge binding interactions established with Leu241 and Lys188, and can be compared to those observed in the harmine co-crystal structure.

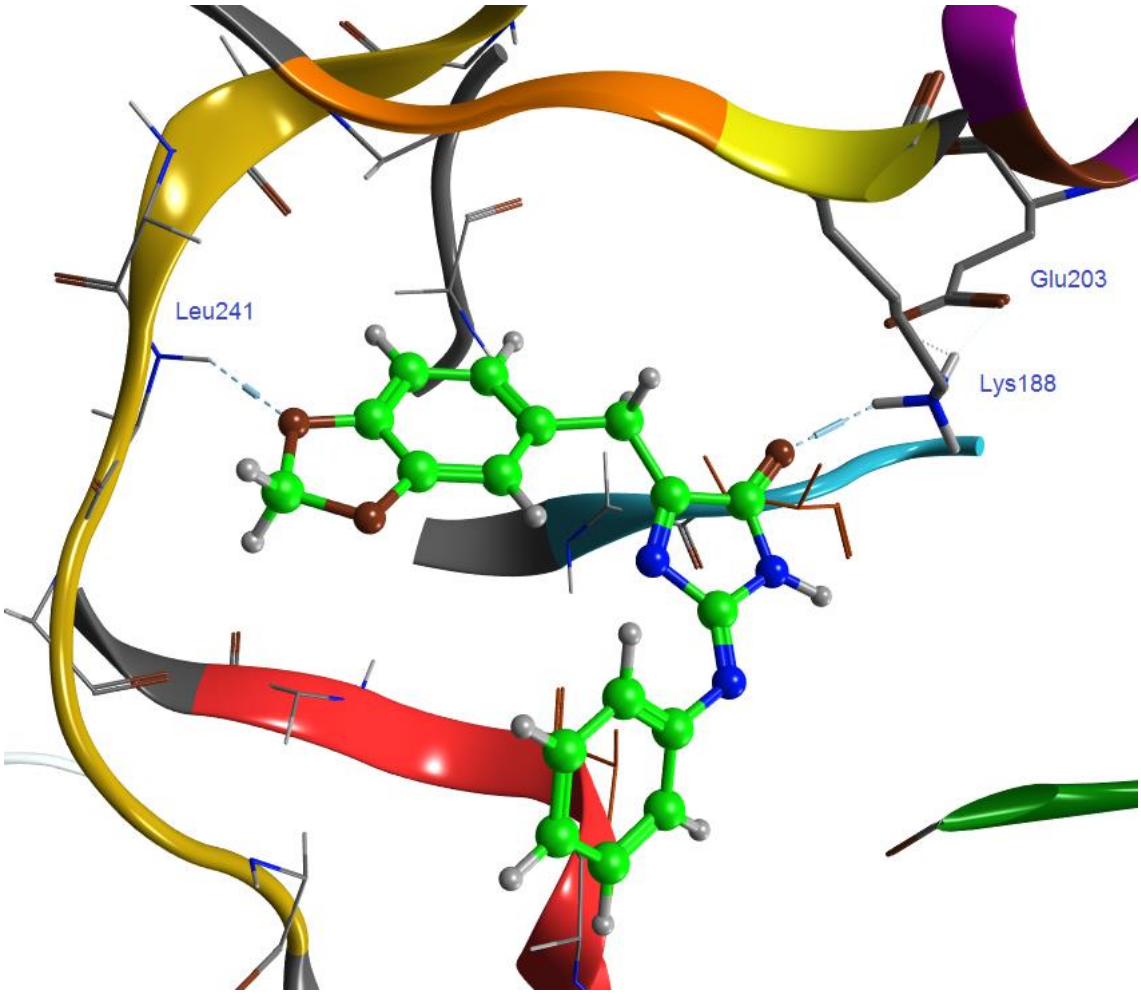

Figure 34. Crystal structure of L41 (**52**) bound to DYRK1A from Tahtouh *et al*. PDB 4AZE.[224] Structure prepared in MOE 2016, CCG with Amber10:EHT force field.

The kinome-wide selectivity profile of **52** is similar to that of **51**.[225] However, with **52**, pan-CLK inhibition is more of an issue (IC_{50} CLK1 = 39 nM, IC_{50} CLK2 = 210 nM, IC_{50} CLK3 = 2400 nM, IC_{50} CLK4 = 31 nM) and in addition GSK3β (IC_{50} = 410 nM) was identified as an off-target. DYRK1A serves as a priming kinase for GSK3β in signalling pathways involved in AD and diabetes. Therefore mechanistic studies using a DYRK1A inhibitor that also inhibits GSK3β may deliver erroneous conclusions when testing biological hypotheses.[225]

Another issue with both **51** and **52**, is that like EGCG, their molecular scaffold is a recognised PAINS pharmacophore. The unsaturated enone in both **51** and **52** could in theory act *in vivo* as a Michael acceptor, binding covalently with the protein and the cell, interfering with biological assays. Despite these concerns, **52** is still one of the most common DYRK1A tools used in *in vitro* assays. Recent experiments have seen **52** used as an *in vivo* tool where it has been reported to rescue cognitive deficits in Down's syndrome murine models and also play a neuroprotective role when co-administered with Aβ peptide. This has been attributed to **52**'s inhibition of DYRK1A rather than the CLKs or GSK3β, and has been used as evidence that **52** is able to cross the blood brain barrier and exert an on-target effect *in vivo*.[226,227,228]

3.7.1.4. Meridianins, meriolins and variolins

Naturally occurring meridianins, isolated from the South Atlantic tunicate *Aplidium meridianum*, and their synthetic analogues, were initially investigated for their anticancer properties as they exhibited potent inhibition of the CDKs.[229] The meridianins inhibited CDK kinases as well as a number of other CMGC kinases (DYRK1A, CK1, GSK3β and CLK1).[230] The 7-bromo meridianin, **55**, is equipotent at DYRK1A (IC_{50} = 68 nM) and CLK1 (IC_{50} = 65 nM).[231] The structurally similar Variolin B, **56**, isolated from the Antarctic sponge *Kirkpatrickia variolosa*, was also initially investigated for anti-cancer properties. **56** was determined to be a potent inhibitor of both DYRK1A (IC_{50} = 68 nM) and CK1 (IC_{50} = 5 nM),[231] and possessed antitumour and cytotoxic activity towards human cancer cells.[232,233] A complex pharmacokinetic profile and poor aqueous solubility of **56** has precluded its advancement into clinical trials.[234]

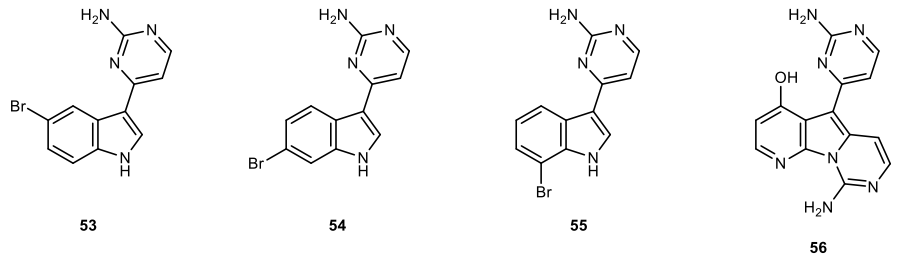

Figure 35. Published inhibitors of DYRK1A – the meridianins (**53**-**55**) and Variolin B (**56**).

Meridianins and variolins were combined to afford a daughter compound with increased potency and improved selectivity for CDK2 and CDK9 than either parent class. The meriolins were shown to prevent phosphorylation of neuroblastoma cell lines at known CDK phosphorylation sites and initiated degradation of survival factors. Tumour growth in two mouse xenograft models was inhibited by the meriolins.[235] Recently, DYRK1A (IC_{50} = 29 nM) has been identified as a potent off-target of the meriolins.[148]

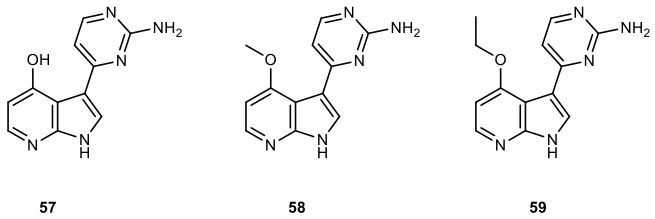

Figure 36. Published inhibitors of DYRK1A – Chimeric meriolins.[235]

3.7.2. DYRK1A Tools derived from Synthetic Inhibitors

3.7.2.1. INDY

The CLK inhibitors Tg003 (CLK2 IC_{50} = 20 nM, **62**) and INDY (CLK2 IC_{50} = 78 nM, **60**) were first patented as CLK2 inhibitors.[236,237] Later, Ogawa *et al*. published a study detailing the development of **60** as a selective DYRK1A inhibitor (IC_{50} = 240 nM).[214] **60** was established as a Type I inhibitor that also inhibited DYRK1B with equal potency (DYRK1B IC_{50} = 220 nM). Compared to harmine, **60** displayed similar DYRK1A activity but did not inhibit MAO-A.[214]

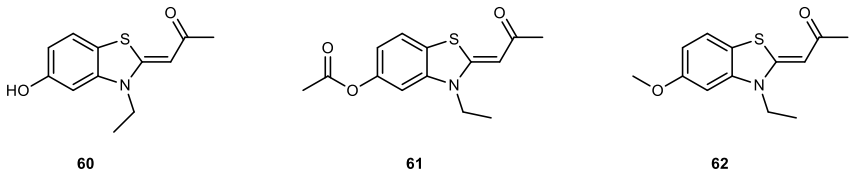

Figure 37. Published DYRK1A inhibitors – INDY, ProINDY and TG003.

The binding mode of **60** in DYRK1A occupies the ATP site, binding in a Type I fashion, to competitively inhibit DYRK1A. The structure shows that **60** maintains the same hydrogen-bonding interaction to Lys188 as harmine, but forms an addition CH-O bond with the carbonyl of Leu241.

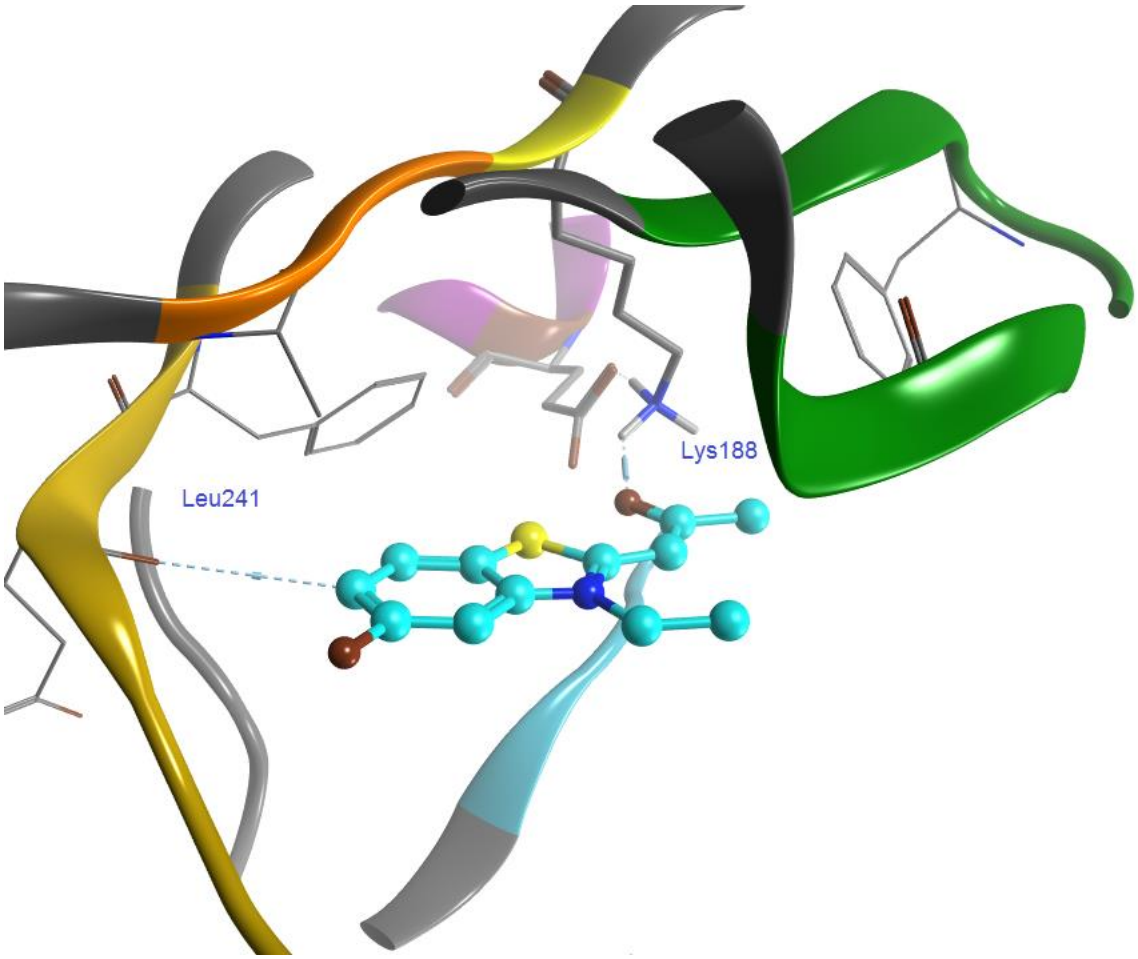

Figure 38. Crystal structure of **60** bound to DYRK1A from Ogawa et al. PDB 3ANQ.[214] Structure prepared in MOE 2016, CCG with Amber10:EHT force field.

In vitro experiments showed that **60** reversed irregular tau-phosphorylation and restored supressed NFAT signalling brought on by DYRK1A overexpression. DYRK1A was overexpressed in *Xenopus laevis* tadpoles which resulted in head malformation.[214] Incubation with the pro-drug of INDY, **61**, appeared to completely reverse this physical deformity.[214]

62, **60** and **61** all contain the same Michael acceptor motif as L41. Hence, the same concerns over false positive assay results must also be applied to these compounds.

3.7.2.2. EHTs

A library of novel thiazolo[5,4-*f*]quinazolines, inspired by the marine alkaloids dercitines and kuanoniamines, were developed by Diaxonhit (formerly Exonhit SA) and tested for DYRK1A and DYRK1B inhibitory activity.[238,239] Five of these compounds displayed single-digit and sub-nanomolar DYRK1 inhibitory activity,[240,241] representing some of the most potent DYRK1 inhibitors disclosed.[242] The binding mode of the EHTs has been rationalised with *in silico* docking models as the compounds have not been successfully co-crystallised with DYRK1A.

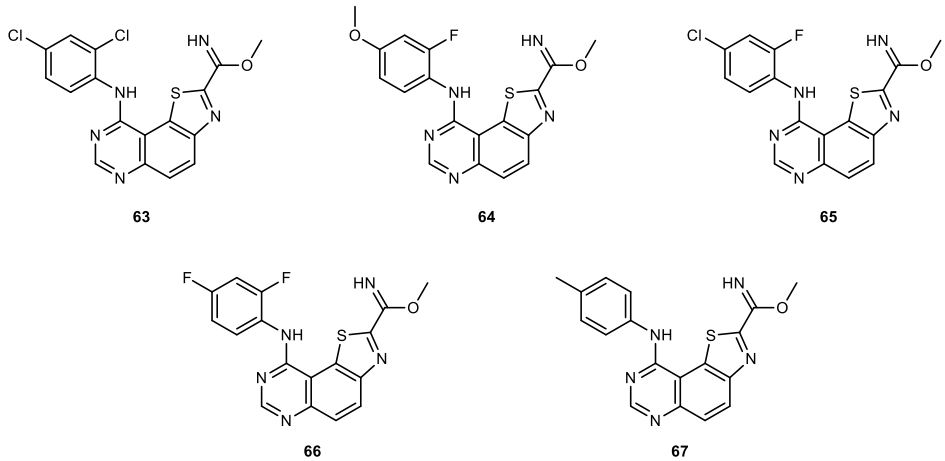

Figure 39. Published DYRK1A inhibitors – EHT series.[240-241]

Recent work has claimed that **63** inhibits DYRK1A-mediated tau phosphorylation at multiple AD-relevant sites on tau. In addition the study claimed that **63** rescued Aβ-mediated tau hyperphosphorylation and Aβ production, as well as tau aggregation.[243] **63** is one of the most potent DYRK1A inhibitors (IC_{50} = 0.22 nM) described in the literature with a high degree of kinome-wide selectivity out of 339 kinases.

63 also potently inhibited DYRK1B (IC_{50} = 0.28 nM), DYRK2 (IC_{50} = 10.8 nM), DYRK3 (IC_{50} = 93.2 nM), GSK3α (IC_{50} = 7.4 nM), CLK1 (IC_{50} = 22.8 nM), CLK2 (IC_{50} = 88.8 nM) and CLK4 (IC_{50} = 59 nM),[241] limiting its use as a specific DYRK1A probe. Another issue with the EHTs is poor aqueous solubility that is likely to obstruct *in vivo* experiments. Furthermore, although the imidate functionality is not a known PAINS motif, it is conceivable that the sp^2 carbon could be susceptible to nucleophilic attack.

3.8. Summary

In summary, the most widely used tool compounds of DYRK1A have been reviewed. After a decade of research, DYRK1A still remains an attractive target for both neurological diseases and cancer modulation. There has been much action over the past five years in terms of publication output and patent applications filed. However, much of the information provided by these is limited. Many of the molecules from the literature appear to have sub-optimal physicochemical properties for use as an *in vivo* CNS tool compound and are not selective for the DYRK1A isoform. Often in the patent literature there is no mention of selectivity against key off-targets or mention of *in vitro* or *in vivo* pharmacokinetics. Worryingly, many of the current tools contain known PAINS motifs. Using these tools may hinder research efforts in the long run.

Ultimately, an optimal balance of DYRK1A potency and selectivity is yet to be found. The reported DYRK1A inhibitors appear not to have been optimised for BBB penetration and target engagement and so are unlikely to modulate DYRK1A *in vivo.* Thus there remains a need to further optimise DYRK1A inhibitors and discover other drug-like scaffolds that will inhibit DYRK1A *in vivo* and determine whether the inhibition of DYRK1A in humans would provide a therapeutic benefit.

3.9. DYRK1A Inhibitor Project

3.9.1. DYRK1A Project Aims

The primary objective of the project is to identify a selective and drug like inhibitor of DYRK1A that has a high chance of being centrally penetrant to give the best chance of target engagement for future *in vivo* studies. A tool compound of this quality would be used to unequivocally test the therapeutic potential of DYRK1A inhibition for the treatment of diseases such as early on-set AD, cancer and diabetes.

To achieve the primary objective, two major obstacles must be overcome (i) identification of lead like starting points with the potential to deliver a compound with the desired target profile and (ii) subsequent design of selective and high affinity ligands of DYRK1A with a likelihood of high central penetration.

A recent publication co-authored by the project's collaborator, Dr Jonathan Elkins, SGC Oxford, describes the screening of a set of drug-like kinase inhibitors (PKIS) and the identification of several new DYRK1A inhibitor templates within that set.[19] It was envisaged that these drug-like starting points could be repurposed for selective DYRK1A inhibition.

Selectivity within the DYRK1A family was foreseen to be a major challenge given the literature data. It is often observed that other CMGC kinases (DYRK1B, CLKs, CDKs, GSK3s, CKs) are co-inhibited with DYRK1A inhibitors. The ligand-binding site of DYRK1A and DYRK1B for instance differ only by one amino acid residue on the hinge region. A secondary aim of the project is to determine whether greater specificity between the DYRK1A and 1B isoforms can be achieved, in addition to selectivity between DYRK1A and CLKs.

The other major challenge is to design a CNS penetrant kinase inhibitor. Currently there are no FDA-approved CNS kinase inhibitors.[244] However, there are at least five small molecule kinase inhibitors in clinical trials for neurodegenerative diseases,[245] giving some hope that it is possible to design a CNS penetrant kinase inhibitor. Recent reviews have suggested that careful

modulation of physicochemical properties can lead to molecules with a higher chance of success.[244,246]

If all objectives were achieved during this work it would be expected that further financial support could be obtained to fund further *in vitro* and *in vivo* optimisation studies focussed on the identification of a DYRK1A lead.

3.9.2. DYRK Tool Compound Criteria

The desired criteria identified by the SDDC for an orally available DYRK1A inhibitor with a high chance of CNS penetration is outlined in Table 8.

Table 8. Desirable Criteria for Tool Compound of DYRK1A

Category	Parameter	DYRK1A probe
Physicochemical properties	Molecular weight (Mwt)	< 400
	Clog $D_{7.4}$	≤ 3.5, ≥ 1.5
	TPSA (A^2)	< 75 > 40
	H bond donors	< 2
	CNS MPO	> 4.5
***In vitro* pharmacology**	Enzymatic DYRK1A IC_{50} (nM)	< 100
	Ligand efficiency (LE)	> 0.3
	Selectivity	> 50-fold
	Cellular DYRK1A IC_{50} (nM)	< 1000 (< 10-fold enzymatic)
In vitro ADME	Rat liver microsomal (RLM) clearance (µL/min/mg)	< 200
	Human liver microsomal (HLM) clearance (µL/min/mg)	< 200
	Thermodynamic solubility [mg/mL]	> 0.1

In addition to those properties outlined above in Table 8, the inhibitor should also be non-cytotoxic, should have a good chance of brain penetration and be orally bioavailable. If the criteria above were met then the compound would also be considered as a chemical probe as defined by the Structural Genomics Consortium (SGC).[10] The criteria of SGC chemical probes is presented in Table 9.

Table 9. SGC Chemical Probes Criteria

Category	Parameter	DYRK1A probe
In vitro pharmacology	Enzymatic IC_{50} (nM)	< 100
	Selectivity	> 30-fold proteins in same family
	Cellular IC_{50} (nM)	< 1000

3.9.3. DYRK Screening Platform and Infrastructure of the DYRK1A Project

Given the issues with the published DYRK1A probes, particular focus was placed on compound quality and the physicochemical properties of DYRK1A ligands throughout the project. Prior to synthesis prospective compounds were generated *in silico* through reaction enumeration. Compounds were prioritised for synthesis based on their calculated physicochemical properites, CNS MPO scores and filtered for known toxicophores. In many cases molecules were docked into the active form of DYRK1A to predict their binding modes.

Once a compound had been synthesised, the screening sequence began with the generation of the enzymatic IC_{50} for DYRK1A using a ligand-binding displacement assay that measured the ability of inhibitors to displace a fluorescent tracer compound from the ATP binding site of the kinase domain.

Compounds with primary DYRK1A binding affinity that met the criteria (IC_{50} < 100 nM) were progressed to selectivity testing and *in vitro* pharmacokinetic profiling (rat liver microsomes (RLM), human liver microsomes (HLM) and solubility). The pharmacokinetic profiles of the molecules were not considered to be critical for selection of a compound for selectivity profiling at this stage.

The selectivity profiles of ligands were assessed in one of three ways: (i) ligands were assayed using a radiometric protein kinase assay to measure the kinase activity of a small panel of selected CMGC kinases (DYRK1A, CDK2 and GSK3β) in the presence of ligand. This industry-standard assay provided by ProQinase GMBH served as a reliable secondary assay to the ligand-binding displacement assay; (ii) in some cases ligands were progressed to a 48-kinase panel differential scanning fluorimetry (DSF) assay. The melting points of protein kinases were measured in the absence and presence of ligand. The difference in thermal shifts could be compared for each kinase to give a rough indication of compound binding; (iii) ligands for which there was a high confidence of kinome-wide selectivity, based on molecular modelling and assay derived data, were screened in a 468-kinase panel competition binding assay provided by DiscoveRx.

Complimentary techniques are required when estimating the kinase selectivity profiles of prospective inhibitors. Interpretation and comparison of kinase selectivity profiles for ATP competitive inhibitors can be complex; a ligand's potency (IC_{50}) for a kinase is determined by the ligand's intrinsic binding affinity (K_i) for the kinase and the degree of competition from the co-factor ATP. The degree of competition from ATP is determined by the affinity of the kinase for ATP ($K_{m,ATP}$) and the concentration of ATP ([ATP]),[247] as described by the Cheng-Prusoff equation:[248]

$$\mathbf{IC_{50} = K_i\ (1 + [ATP] / K_{m,ATP})}$$

As a result most kinase selectivity assays are conducted with the [ATP] equal to the approximate $K_{m,ATP}$ of each kinase, and so IC_{50} approximates K_i. In a cellular setting, the [ATP] is much higher (approximately 1-5 mM) than $K_{m,ATP}$,[249] therefore under cellular conditions differences in $K_{m,ATP}$ between kinases can have a greater effect in determining inhibitor affinity.[247] For this reason observed cellular selectivity is not always in agreement with the biochemical selectivity profiles of inhibitors derived from *in vitro* kinase assays.

Ligands that were both selective and exibited high affinity for DYRK1A were then profiled in a cellular assay, the NanoBRET target engagement assay. The NanoBRET assay gave an indication of cellular activity of the DYRK1A inhibitor and also determined whether the compound was cell-permeable and showed any cytotoxicity. A select few inhibitors that met most or all of the selection criteria were profiled in a MDCK-MDR1 assay provided by Cyprotex. This assay provided an indication as to whether a compound was capable of permeating the BBB and whether the compound was likely to undergo P-gp mediated efflux.

In parallel to the biochemical assays and cell-based assays, inhibitors were co-crystallised in DYRK1A to provide information on binding mode and rationalise gains in selectivity and binding affinity. These structures provided a model for SBDD. An overview of the screening cascade is shown in Figure 40.

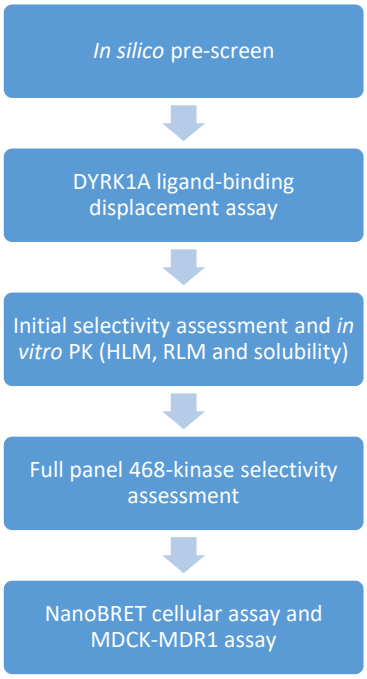

Figure 40. Multiparametric screening sequence to afford DYRK1A tool compounds.

CHAPTER 4. Rationale Design of Pyrazolo[1,5-*b*]pyridazines for Selective Inhibition of DYRK1A

Chapter 4 describes the selection and hit confirmation of a series of pyrazolo[1,5-*b*]pyridazines as high affinity ligands of DYRK1A. In the absence of a co-crystal structure and whilst biological assays and crystallisation conditions were established, a chemoinformatics approach was taken to guide inhibitor design. Series off-targets for which the pyrazolo[1,5-*b*]pyridazine series was originally designed to inhibit, were successfully dialled-out to afford a selective DYRK1A inhibitor with good overall properties.

4.1. Identification and Selection of the Pyrazolo[1,5-*b*]pyridazine Series

Prior to this work, GSK and its legacy companies made a collection of 376 drug-like kinase inhibitors available to external groups for screening, called the PKIS. A seminal paper by Elkins *et al*. describes the screening of the PKIS set against a panel of 224 kinases, including the DYRK family.[19] Several clusters of compounds, including the pyrazolo[1,5-*b*]pyridazine series, previously unreported as DYRK1A inhibitors, exhibited potent inhibition of DYRK1A at 1 µM. 5 compounds of the 28 members of the pyrazolo[1,5-*b*]pyridazine series inhibited DYRK1A > 75% at 1 µM. The series displayed potent off-target activity at other CMGC kinases (CDKs, CLKs, GSK3β and DYRKs), but otherwise had good kinome-wide selectivity. **68** showed more unspecific activity than the other pyrazolo[1,5-*b*]pyridazine analogues, however, it was the most potent DYRK1A inhibitor described in the original publication (Table 10).[19]

Table 10. DYRK1A Percentage Inhibition Data at 1 µM for Compounds from the PKIS set

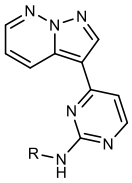

Compound	R	DYRK1A % inhibition[a]
68	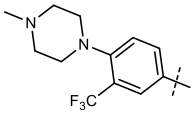	90
69	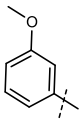	85
70	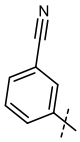	81
71	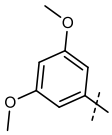	85
72	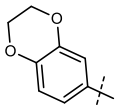	80

[a]DYRK1A inhibition at 1µM in DiscoveRx KINOMEscan® experiment[19]

To validate the series, four of the analogues in Table 10 were re-synthesised and assayed for IC_{50} determination in the DYRK1A ligand-binding displacement assay.

All compounds re-synthesised exhibited strong binding affinity for DYRK1A (IC_{50} < 15 nM), with **68** exhibiting the strongest DYRK1A binding affinity (IC_{50} of 3 nM). An overview of the selectivity profile and physicochemical properties of **68** is displayed in Figure 41.

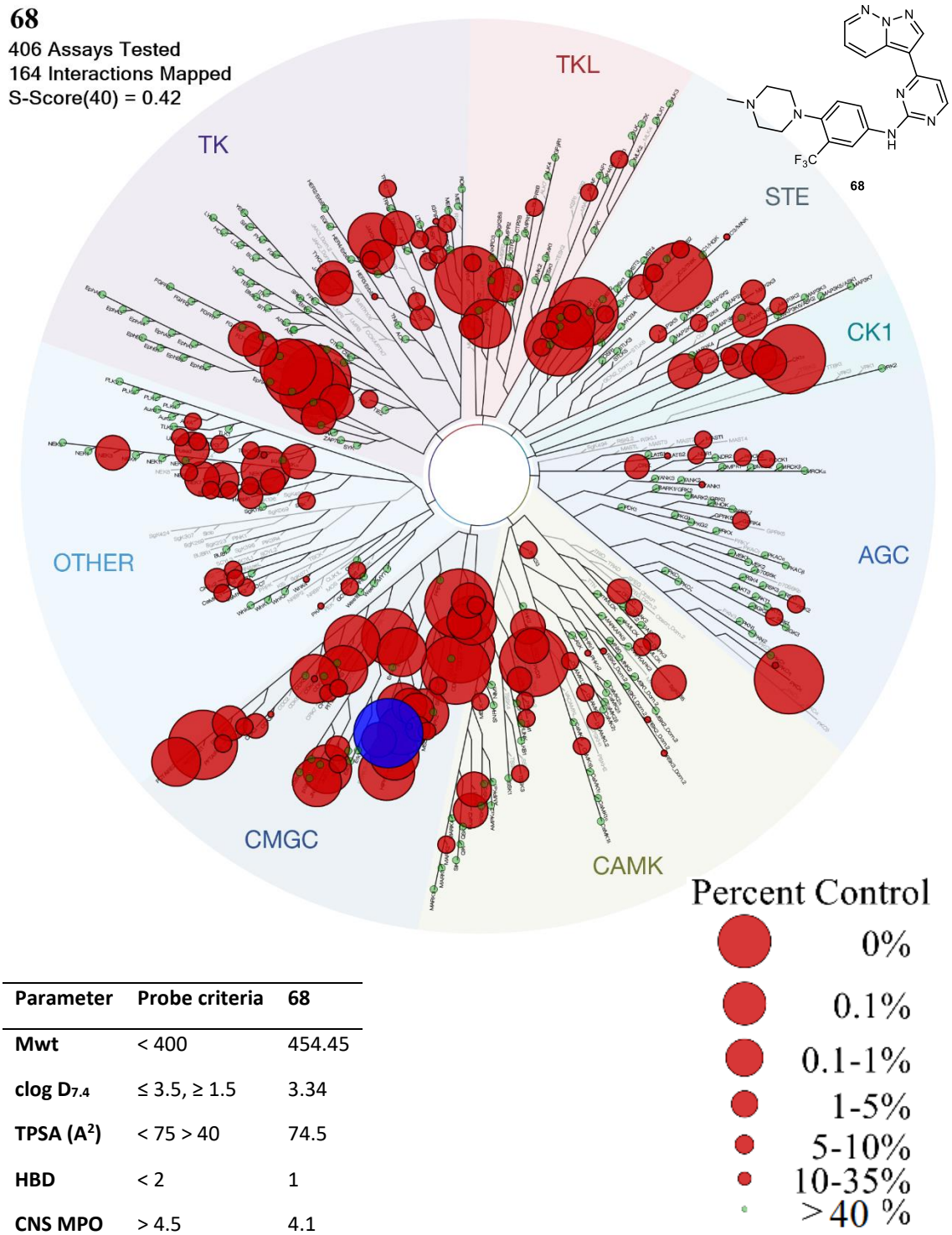

Parameter	Probe criteria	68
Mwt	< 400	454.45
clog $D_{7.4}$	≤ 3.5, ≥ 1.5	3.34
TPSA (A^2)	< 75 > 40	74.5
HBD	< 2	1
CNS MPO	> 4.5	4.1

Figure 41. Profile of **68** and KINOMEscan® results of **68** at 1 µM depicted as Treespot™ diagram. DYRK1A is highlighted in blue. Image generated using TREEspot™ Software Tool and reprinted with permission from KINOMEscan®, a division of DiscoveRx Corporation, © DISCOVERX CORPORATION 2010. Selectivity data from reference [21].

In terms of physicochemical properties, the pyrazolo[1,5-*b*]pyridazine series had the highest molecular weight and lipophilicty of all of the series selected for optimisation. The series had been previously developed by GSK as "selective" inhibitors of CDK2/CDK4[250] and GSK3β[251] for the treatment of cancer and diabetes.

Removal of CDK2/4 and GSK3β inhibition, in addition to modulation of lipophilicity, molecular weight, solubility and microsomal stability, would all be required for the series to be repurposed into a specific molecular probe of DYRK1A.

4.2. Preliminary SAR of Pyrazolo[1,5-*b*]pyridazine Series

Analysis of the kinase profiling data generated by Elkins *et al.*,[19,21] allowed for the identification of functional groups that appeared to be key for DYRK1A binding affinity. Positions where additional substituents caused detrimental effects on DYRK1A binding affinity were also identified. An overview of the SAR of the pyrazolo[1,5-*b*]pyridazine series is summarised in Figure 42.

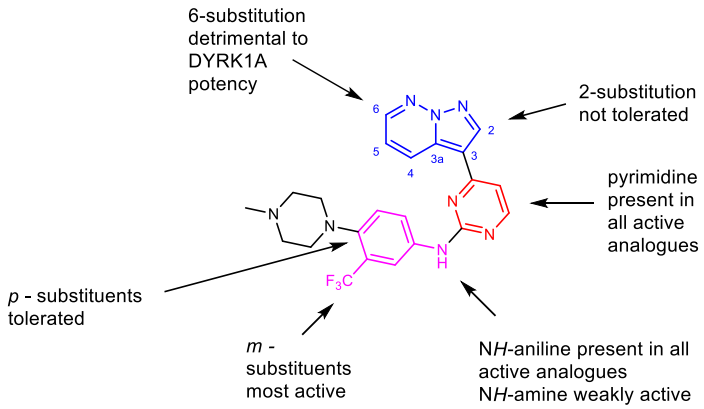

Figure 42. Summary of key SAR for pyrazolo[1,5-*b*]pyridazine series with respect to DYRK1A Inhibition

The N-*H*-aniline (pink) and the pyrimidine nitrogens (red) were present in all active compounds within the cluster. It was postulated that these motifs would be required to form the classic HBD-HBA bidentate interaction with the hinge of DYRK1A. This would coincide with placement of the aniline aryl group along the hinge and the piperazine motif projecting into the solvent-exposed region.

Substituents that were added to the 2-position of the pyrazolo[1,5-*b*]pyridazine head (blue) were not tolerated. 2-Methyl and 2-phenyl derivatives showed no measurable DYRK1A binding affinity, suggesting that substituents borne in this position would clash in some way with the

active site residues of DYRK1A. A methoxy group was tolerated to some extent at the 6-position. However, methyl, ethyl, phenyl and morpholine groups all appeared not to be tolerated at the 6-position of the pyrazolo[1,5-*b*]pyridazine.

A diverse array of functionality and electronics (electron withdrawing and electron donating substituents) were permitted at the *m*-position of the aniline ring. The piperazine (black) present on **68** was not essential for strong DYRK1A binding affinity but was likely to have a significant effect on solubility and judging by the selectivity profile may have caused unspecific binding. Isopropyl was tolerated in the para position albeit with lower activity than previous analogues. A few examples of primary amines rather than anilines were present in the set, such as the cyclopropyl analogue. All of these analogues showed weaker DYRK1A binding affinity than the aniline derivatives.

4.3. Synthesis of the Pyrazolo[1,5-*b*]pyridazine Series

A further advantage of using the PKIS set for screening is that information regarding synthetic routes already exists in the public domain. Following the literature procedure;[251] the aminated pyridazine **74** was formed in excellent yield after reaction of pyridazine **73** with hydroxylamine-*O*-sulfonic acid (HOSA). Subsequent [3+2] cycloaddition between **74** and butyne-2-one afforded the pyrazolo[1,5-*b*]pyridazine **75** in average yield. DMF/DMA condensation furnished the corresponding enamine **76** in excellent yield. Conversion of **76** to the corresponding pyrimidine was sluggish under conventional heating at elevated temperatures, taking up to 48 hours for the formation of desired product to occur (Scheme 10).

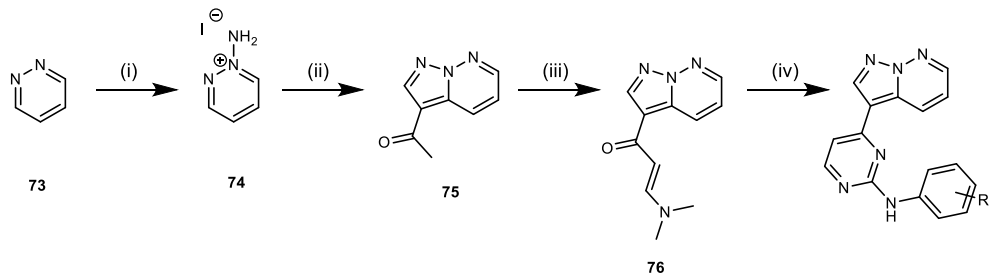

Scheme 10. *Reagents and conditions:* (i) Hydroxylamine-*O*-sulfonic acid, $KHCO_3$, KI, H_2O, 70°C, 1.5 h, 94%; (ii) butyne-2-one, KOH, CH_2Cl_2, rt, 16 h, 60%; (iii) DMF-DMA, 100°C, 16 h, 91%; (iv) phenyl guanidines, 2-methoxyethanol, 110 °C, 16-48 h, 13-37%.

One disadvantage of the literature synthesis was that the preparation of each analogue required the respective phenyl guanidine to be synthesised first. In most cases the synthesis of the phenyl

guanidine was low yielding. Phenyl guanidines were prepared using concentrated nitric acid and cyanamide from the corresponding aniline (Scheme 11).

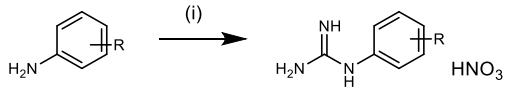

Scheme 11. *Reagents and conditions:* (i) cyanamide (50 wt.% in H_2O), HNO_3, EtOH, 100 °C, 16-48 h, 35-62%.

In an effort to improve the versatility of the synthesis, the chloropyrimidine intermediate, **77**, was prepared. Nucleophilic aromatic substitution with a range of nucleophiles was then possible. Scale-up of the **77** was completed in high yield from **76** (Scheme 12).

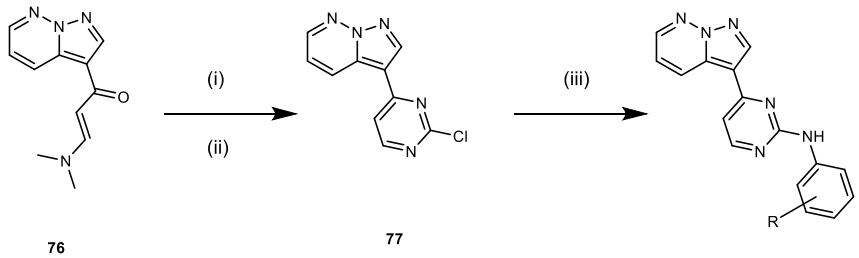

Scheme 12. *Reagents and conditions:* (i) urea, sodium, 140 °C, 10 min, 91%; (ii) phosphorus(V)oxychloride, 110 °C, 3 h, 92%; (iii) conditions A: anilines, 2-propanol, 150 °C, 2-16 h, 4-44%; conditions B: anilines, 2-propanol, 150 °C, 15-20 min, µwave, 43-60%.

4.4. SARs and Biological Evaluation of Pyrazolo[1,5-*b*]pyridazine Series

The DYRK1A binding affinity data for pyrazolo[1,5-*b*]pyridazines **68**-**86** are presented in Table 11. The ligand-binding displacement data for the compounds reported in the PKIS is presented, in addition to those synthesised during hit expansion.

The majority of the compounds possessed high affinity binding for DYRK1A, consistent with what had been reported by Elkins *et al*.[19,21]

Table 11. DYRK1A Binding Affinity of 'Anilines'

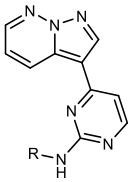

Compound	R	DYRK1A IC_{50}[a]
68	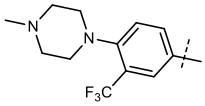	3
78	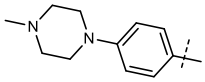	40
79		38
80		64
69	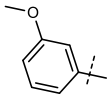	12
71	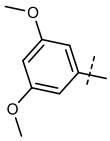	4
70	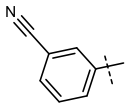	5
81	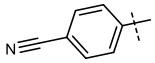	103
82		7
83	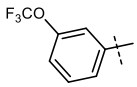	7
84	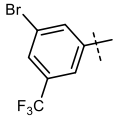	24
85	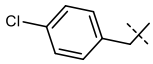	218

86	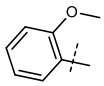	137

[a]IC_{50} (nM) in TR-FRET-based ligand-binding displacement assay (n = 1)

Consistent with the PKIS dataset,[19,21] clear preference is shown for *meta* substituents - *meta* substituted **70** exhibits 20 fold stronger affinity than *para* substituted **81**, whilst *meta* substituted **82** displays 9 fold higher affinity than *ortho* analogue **80**. This trend is also observed for *ortho* analogue **86**, which exhibits approximately 11 fold weaker affinity than *meta* analogue **69**.

Taking into account electronics, it seems that there is no clear preference for either electron withdrawing or electron donating substituents on the aniline ring. There are examples of both that are very high affinity ligands: **70** bearing a nitrile (electron withdrawing) substituent is as strong a binder as **82** bearing a methyl (electron donating) substituent. 3,5-Disubstituted analogues **71** and **84** are both high affinity ligands of DYRK1A (IC_{50} = 4 nM and 24 nM respectively). These results suggest that moderation of the pK_a of the aminopyrimidine motif does not impact binding affinity. Insertion of a carbon between the pyrimidine and the aryl substituent, as in **85**, has resulted in a drop in affinity, although this could also be due to the presence of a *para* chloro substituent.

68-**71** were highlighted as potential drug-like DYRK1A inhibitors in a recent publication.[19] Resynthesis and small scale hit expansion resulted in a number of very high affinity ligands of DYRK1A. It was almost certain that most of these ligands also inhibited CDK2 and GSK3β, the original targets for which the pyrazolo[1,5-*b*]pyridazine series was first developed.[250,251]

Subsequently, this thesis will focus on how this series of inhibitors was modified to remove unwanted GSK3β and CDK2 inhibitory activity, whilst retaining DYRK1A inhibitory activity. The different strategies employed to repurpose this series of kinase inhibitors into a selective and potent DYRK1A molecular probe will be presented in full.

4.5. Chemoinformatics-led Design of Selective DYRK1A Inhibitors

4.5.1. Rationale

At the beginning of the project, in 2016, there were multiple DYRK1A crystal structures in the public domain. However, there were no co-crystal structures of the pyrazolo[1,5-*b*]pyridazine series in DYRK1A. Although analogues of the pyrazolo[1,5-*b*]pyridazine series had been co-crystallised in CDK2 (PDB 3EJ1) it was not wholly assumed that the binding mode was identical

in both kinases as they share no more than 35% homology. Additionally, the analogue bound in the CDK2 co-crystal structure has a cyclopropylamine substituent rather than an aniline substituent.

In parallel to the production of an *in silico* binding model, a ligand-based approach was initiated to identify activity cliffs for the series off-targets, CDK2 and GSK3β. The polypharmacology profile of the pyrazolo[1,5-*b*]pyridazine scaffold was assessed using the business analytics tool, KNIME®, to mine the ChEMBL database for existing kinase bioactivity data of compounds with the pyrazolo[1,5-*b*]pyridazine substructure. Similarity searching was used to identify molecules that were similar to the pyrazolo[1,5-*b*]pyridazine series with reduced off-target activity. In this fashion it was possible to identify compounds in the same series that were inactive at GSK3β and CDK2. The strategy was to prioritise synthesis of compounds that were shown to be inactive against the off-targets with the hope that they may retain activity at DYRK1A due to differences in the kinase domain.

The specific KNIME® workflow used was adapted from the ChEMBL web services community workflow, 'NN-activity pairs', originally designed at ChEMBL-EBI by Dr George Papadatos and donated to the KNIME® community for the prediction of polypharmacology of kinase inhibitors (Figure 43).

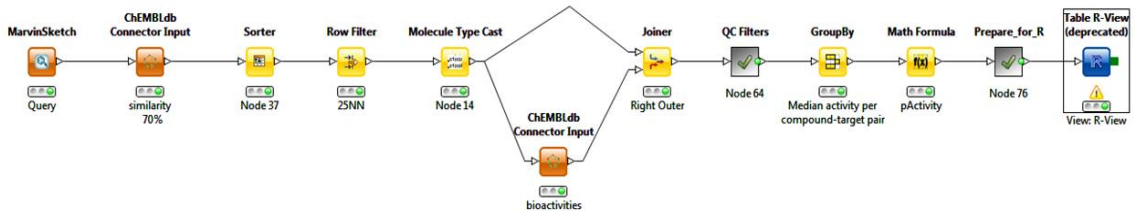

Figure 43. Chemoinformatic mining of the data within the ChEMBLdb for compounds with the pyrazolo[1,5-*b*]pyridazine substructure using the 'NN Activity Pairs' workflow in KNIME®.

Briefly, the substructure of the pyrazolo[1,5-*b*]pyridazine series was first drawn in the MarvinSketch node. Execution of the node facilitated a search for the pyrazolo[1,5-*b*]pyridazine substructure in the ChEMBLdb and retrieved molecules with 70% string similarity. On a separate occasion compounds were searched for in the ChEMBLdb using a 100% substructure search rather than a similarity search. Analogues were then sorted (Sorter node) in order of similarity and the 25 nearest neighbours were identified and then filtered (Row Filter node). The kinase bioactivity data of each of the 25 nearest neighbours, based on similarity, was retrieved from ChEMBL database (ChEMBLdb Connector Input node). A number of Quality Control (QC) filters

(QC Filter metanode) were performed on the data; only *Homo sapiens* data was collected, bioactivity data was permitted to include IC_{50}, EC_{50} and K_i, and units were kept to nM. Bioactivity data was only retrieved for kinases. The median activity per compound-target pair was then used to determine the pIC_{50} of each compound for each kinase using a math formula node. The results were then produced in the form of a Kinase Activity Profile (Figure 44), which displays the pIC_{50}s for these 25 nearest neighbour molecules in a traffic light style histogram (green = $pIC_{50} > 7$; orange = pIC_{50} 6-7; red = $pIC_{50} < 6$) against a number of kinases for which data exists, and could be extracted from the ChEMBL database.

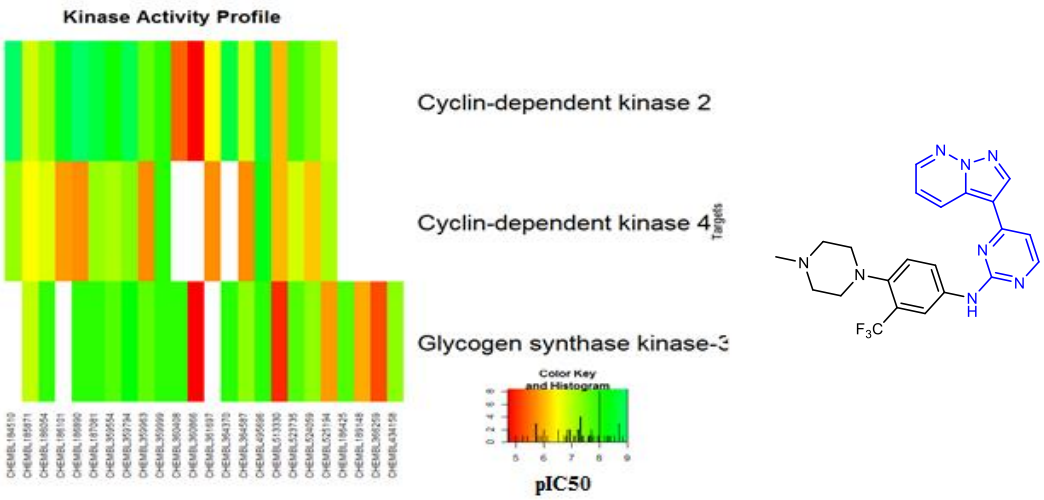

Figure 44. Kinase activity profile of pyrazolo[1,5-*b*]pyridazine series. Blue substructure searched for and similarity search was performed with respect to the whole of molecule **68**.

This chemoinformatics approach and interpretation of the resulting Kinase Activity Profile allowed for rapid classification of analogues as being active or inactive against the key off-targets GSK3β and CDK2. The chemical structures of the inactive and active compounds could be easily interrogated to find activity cliffs as the compounds were all matched-molecular pairs.[252] Analogues that were identified as inactive against CDK2 and GSK3β using this approach were of great interest as DYRK1A inhibitors. A number of activity cliffs with respect to the off-targets were identified, the most significant have been summarised in Figure 45.

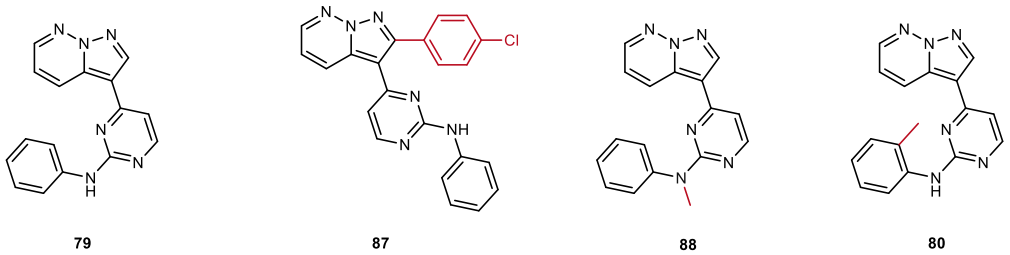

Figure 45. Activity cliffs (red) identified rapidly from chemoinformatics approach.

88 (ChEMBL360866) and **79** (ChEMBL359554) were the first set of matched-pairs identified. It was evident that alkylation of the amino pyrimidine N-*H* of the series abolished CDK2 and GSK3β binding affinity. Inspection of the original work revealed that the introduction of a methyl group onto the amino pyrimidine N-*H* resulted in a 1000 fold loss in CDK2 and GSK3β activity.[251] 2-substitution with alkyl and aryl groups of the pyrazolo[1,5-*b*]pyridazine core was already known to cause a decrease in DYRK1A activity from the PKIS data,[19] thus the synthesis of **87** (ChEMBL189148) was not pursued. **80** (ChEMBL366259), by chance, had already been synthesised during the first synthetic round and was available for further biological evaluation.

4.5.2. Synthesis

Investigation of the *N*-alkyl selectivity handle was attractive as it was quick and easy to test. Nucleophilic aromatic substitution of chloride **77** was carried out with *N*-methylbenzylamine to furnish **88** in 44% yield. Methylation of **82** and **69** afforded access to desired *N*-methylated products **89** and **90** (Scheme 12).

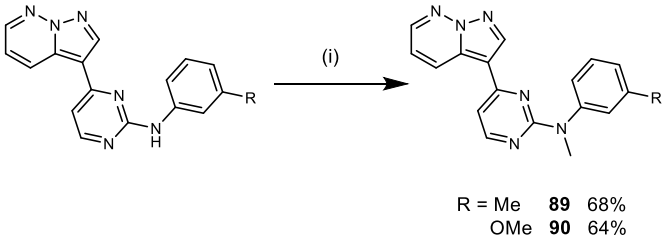

Scheme 12. *Reagents and conditions:* (i) sodium hydride, iodomethane, DMF, rt, 2 h.

4.5.3. SARs and Biological Evaluation of *N*-methyl Derivatives

The DYRK1A binding affinity of **79**, **82** and **69** and their methylated matched-pairs (**88**, **89** and **90**) are displayed in Table 12. The majority of methylated analogues maintained binding affinity for DYRK1A, albeit with an approximate 10 fold loss in activity observed across the board. This

loss of DYRK1A binding affinity would be deemed acceptable if an improvement in selectivity against CDK2 and GSK3β was also achieved.

Table 12. DYRK1A Binding Affinity of *N*-alkylated Analogues

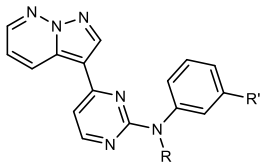

Compound	R	R'	DYRK1A IC_{50}[a]
79	H	H	38
88	Me	H	186
82	H	Me	7
89	Me	Me	76
69	H	OMe	12
90	Me	OMe	97

[a]IC_{50} (nM) in TR-FRET-based ligand-binding displacement assay (n = 1)

To test that the inclusion of the methyl group resulted in an improvement in selectivity against CDK2 and GSK3β, **79** and its alkylated analogue, **88**, were assayed for % inhibition at single concentration (1 µM) in an activity assay provided by ProQinase GMBH. The DYRK1A, GSK3β and CDK2 inhibitory activity of **79** and **88** are presented in Table 13. The results corroborate what was hypothesised from the chemoinformatics approach, indicating that the inclusion of a methyl group on the aminopyrimidine N-*H* afforded selectivity over CDK2 and GSK3β.

Table 13. CMGC Selectivity Profiles of 79 and 88

Compound	DYRK1A[a]	GSK3β[a]	CDK2[a]
79	97	76	98
88	79	13	33

[a] % inhibition in radiometric kinase assay (^{33}PanQinase® Activity Assay) at 1 µM inhibitor concentration provided by ProQinase GmbH (n = 1).

Although **88** appeared to be selective against the two off-targets, DYRK1A binding affinity did not fit the criteria (IC_{50} < 100 nM) to warrant further selectivity profiling. Fortunately, **89** and **90** exhibited high enough DYRK1A affinity and bore the *N*-methyl substituent that afforded selectivity against CDK2 and GSK3β. **88** was not progressed further due to its reduced DYRK1A binding affinity.

The selectivity profiles of **89** and **90** were assessed in a 48-kinase panel using a DSF assay. The results of this assay appeared to show that relative to the control staurosporine, **89** and **90** had good selectivity profiles, stabilising few proteins other than DYRK1A.

89 and **90** were profiled in a 468 kinase panel to assess their kinome-wide selectivity profiles. The compounds were assayed in the KINOMEscan® platform provided by DiscoveRx, a proprietary active-site directed competition binding assay. The results of the selectivity panels for **89** and **90** are displayed as TREEspot™ diagrams in Figure 46. DYRK1A is highlighted as a blue spot.

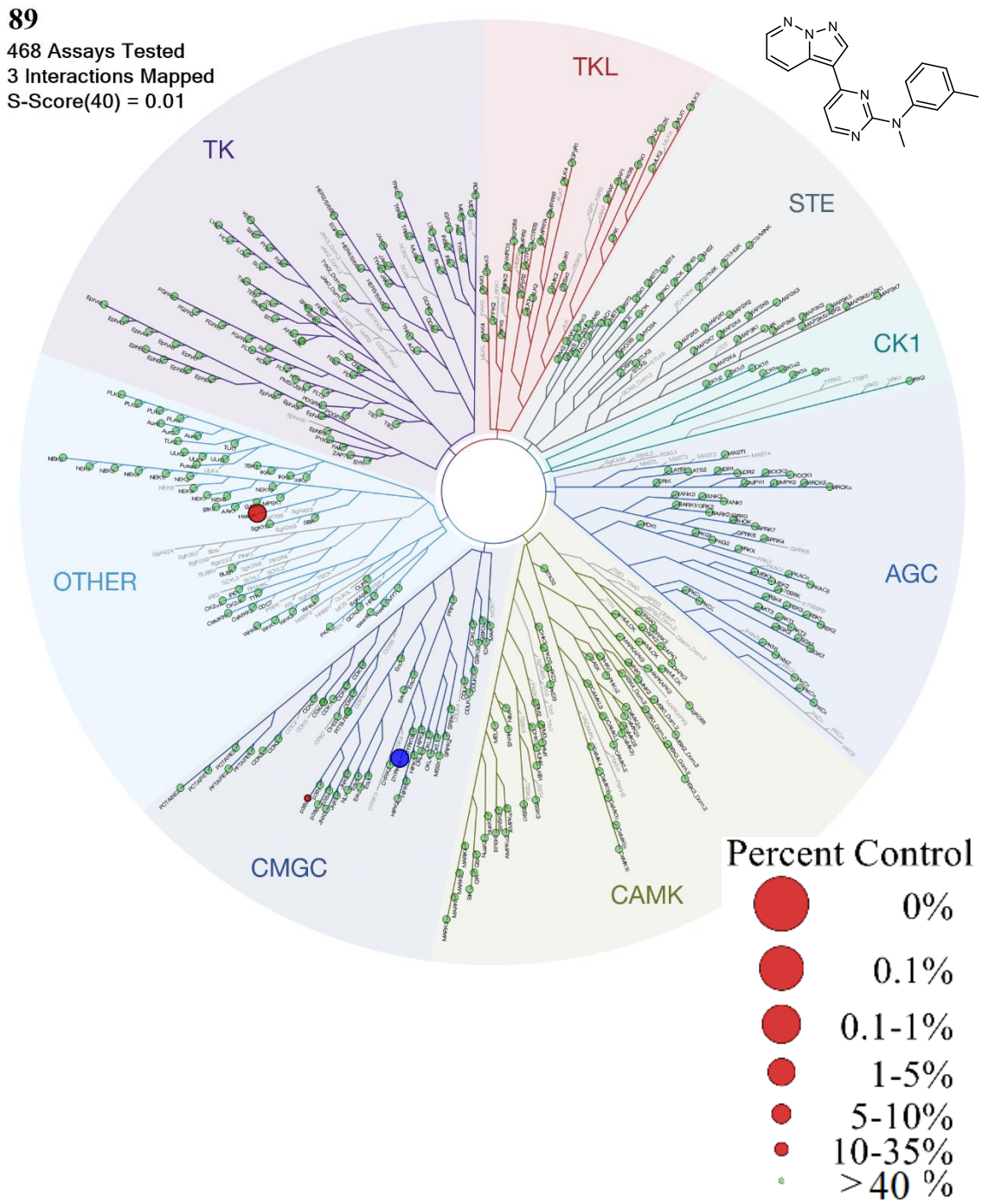

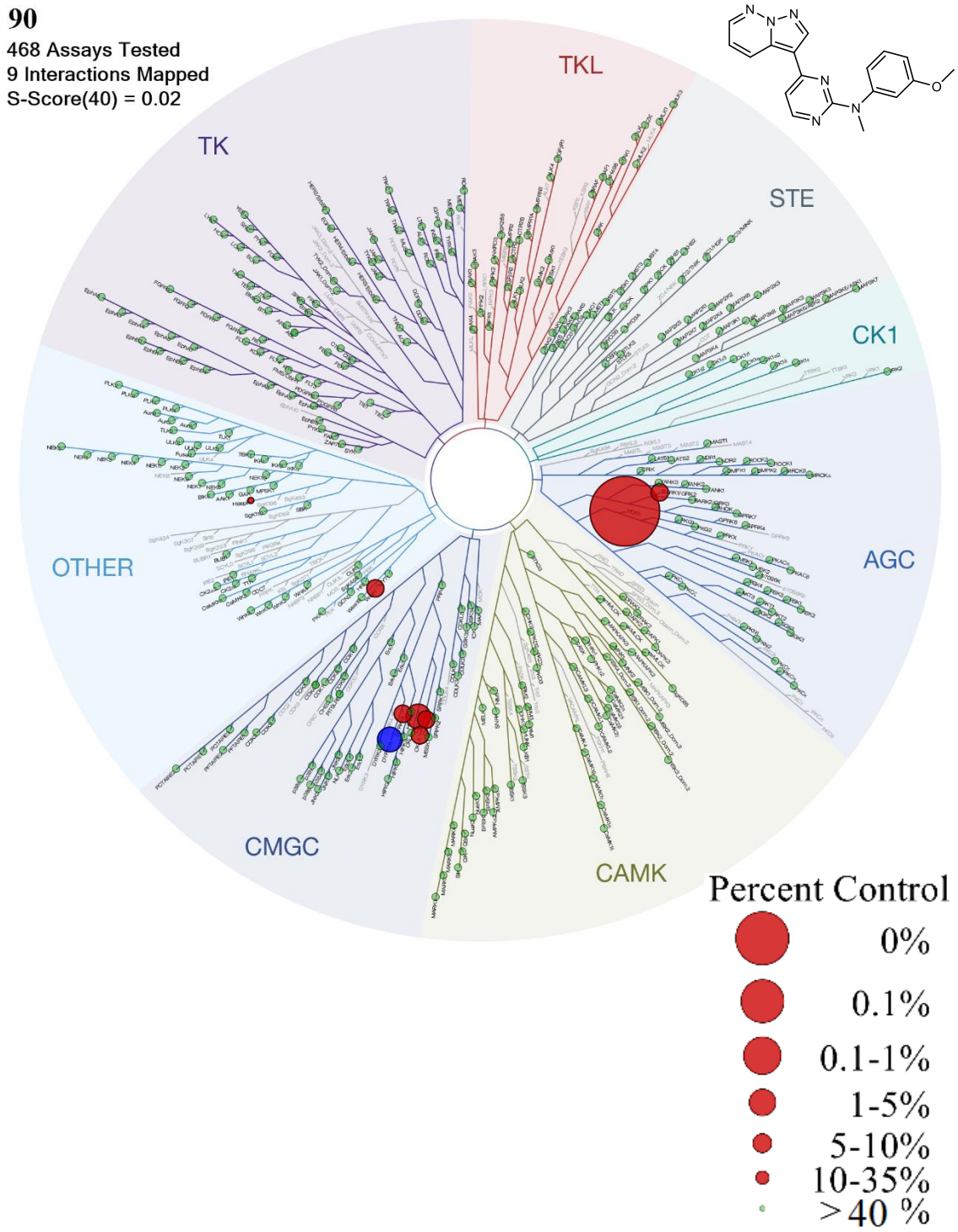

Figure 46. KINOMEscan® Treespot™ maps for compounds **89** (top) and **90** (bottom). DYRK1A is highlighted in blue. Image generated using TREEspot™ Software Tool and reprinted with permission from KINOMEscan®, a division of DiscoveRx Corporation, © DISCOVERX CORPORATION 2010.

Both **89** and **90** exhibited high levels of kinome-wide selectivity in the KINOMEscan® panel and showed no inhibition of the original off-targets, CDK2 and GSK3β (Figure 46 and Table 14). **90** appears to display high affinity for two AGC kinases. It may be that these kinases are false-positives and at the time of writing follow-up selectivity profiling is underway to confirm this.

89 and **90** represent a set of matched-pairs, differing only in the substituent borne on the *m*-position of the aniline ring. It appears that the smaller methyl group of **89** is more detrimental to DYRK1B and CLK activity than the larger and more electron rich methoxy group of **90**. At the outset of the project it was thought that selectivity between the 1A and 1B isoforms of DYRK would be difficult to achieve due to the high levels of homology in the ATP site. However, this data suggests that a methyl group may be key to delivering selectivity between the two isoforms.

Table 14. Overview of Kinome Selectivity Profiles of **89** and **90**

Compound	Percent kinases inhibited > 75%[a]	Percent kinases inhibited > 50%[a]	Kinases most potently inhibited
89	0	1.9	Haspin, p38-gamma
90	1.5	2.6	CLKs, DYRK1B, PDPK1, Haspin, WEE1

[a] % Inhibition as determined by DiscoveRx KINOMEscan® experiment.

As **89** and **90** were very selective (Table 14) and exhibited high binding affinity for DYRK1A, they were profiled for metabolic stability (HLM, RLM) and thermodynamic solubility. These results are displayed in Table 15.

Table 15: Metabolic Stability of *N*-methyl analogues

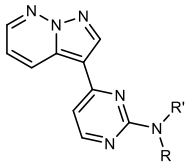

Compound	R	R'	HLM (µL/min/mg)	RLM (µL /min/mg)	Solubility (mg/mL)
68	H	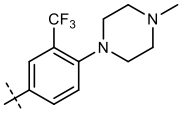	57.2 +/- 4.9	240.1 +/- 8.1	0.01
89	Me	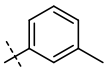	75 +/- 4.5	783.7 +/- 30.6	0.01
90	Me	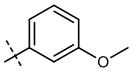	258 +/- 3.5	902.7 +/- 58.3	0.08

HLM and RLM Determinations mean of n =2 +/- standard deviation (unless otherwise stated). HLM = human liver microsomes; RLM = rat liver microsomes; thermodynamic solubility data derived from single experiment at pH 6.8.

89 and **90** did not meet the tool compound criteria based on poor solubility and high rates of *in vitro* metabolism. However, given the high levels of selectivity and strong binding affinity of **89**, it was decided to profile **89** in a MDCK-MDR1 assay to assess whether there were any P-gp or permeability liabilities with the series.

Table 16. MDCK-MDR1 permeability of **89**

Compound	CNS MPO[a] score	Direction = A2B Mean P_{app} (10^{-6} cms^{-1})[b]	Direction = B2A	Efflux Ratio (Mean P_{app} B2A / Mean P_{app} A2B)[b]
89	4.8	20.9 +/- 0.10	20.1 +/- 0.90	0.96

[a]CNS MPO score calculated using CNS MPO KNIME® workflow with ChemAxon nodes. [b]Data generated by Cyprotex in MDCK-MDR1 assay. Permeability coefficient (P_{app}) calculated across cells in direction: A2B (Apical to Basolateral) and B2A (Basolateral to Apical). Determinations +/- standard deviation (mean of n =2 unless otherwise stated).

The high CNS MPO score of **89** correlated with good levels of permeability and low P-gp efflux.

4.6. *Ortho* Substitution Inspired by a Chemoinformatics and Literature-based Approach to Afford More Selective DYRK1A inhibitors

4.6.1. Rationale

Another potential starting point for the discovery of DYRK1A inhibitors could be to begin with selective DYRK1B inhibitors and to attempt to selectively dial-out DYRK1B inhibition through making very subtle changes to the molecular scaffold. A recent publication by AstraZeneca (AZ) describes molecules similar in structure to **68** as selective DYRK1B inhibitors that are drug-like and have been accepted by the community as quality tool compounds (chemicalprobes.org).[253] Selective DYRK1B probe AZ191 (**91**) is depicted in Figure 47.

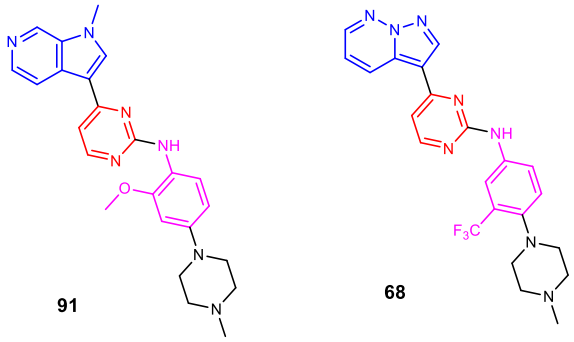

Figure 47. AZ191 (**91**) a published selective DYRK1B inhibitor; **68** a potent DYRK1A inhibitor.

It was assumed that **91** would also be a potent DYRK1A inhibitor due to the similarity between the ATP site of both DYRK 1 isoforms. Interestingly, AZ had detailed how they had overcome the CDK2 liability of the 6-azaindole series and it was hoped that the CDK2 liability in the pyrazolo[1,5-*b*]pyridazine series could be overcome using a similar strategy. Flexible alignment of **91** and **68** provided some confidence that the same strategy could be used to good effect as

the suspected pyrimidine hinge binding units overlaid well (Figure 48). Furthermore, **91** was reported to possess good cellular potency and *in vitro* PK properties so it was envisaged that a chimera of the pyrazolo[1,5-*b*]pyridazine series and **91** may afford a DYRK1A/1B inhibitor with improved *in vitro* PK properties for a tool compound.

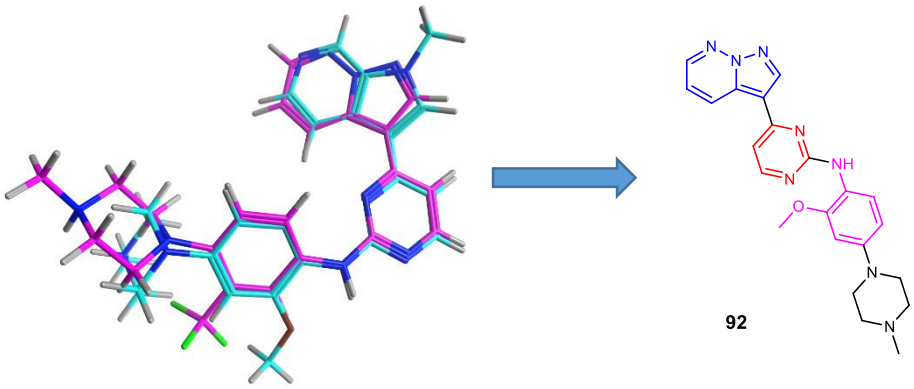

Figure 48. Flexible alignment of 68 (magneta) and 91 (cyan), which resulted in the design of 92. Flexible alignment performed in MOE 2016, CCG with Amber10:EHT force field.

The key to DYRK1B selectivity appeared from the publication to be the addition of an *ortho*-substituent, specifically an *ortho*-methoxy substituent in the case of **91**.[253] The chemoinformatics approach added weight to the hypothesis that *ortho* substitution removed CDK2 and GSK3β liability; the *ortho*-methyl analogue **80** possessed less CDK2 and GSK3β inhibitory activity than the unsubstituted analogue **79**, whilst maintaining strong binding affinity for DYRK1A (IC_{50} = 64 nM) (Figure 45).

4.6.2. Synthesis of an AZ191 Inspired Pyrazolo[1,5-*b*]pyridazine

Attempts to synthesise **92** from **77** with the corresponding aniline resulted in no conversion to the desired product.

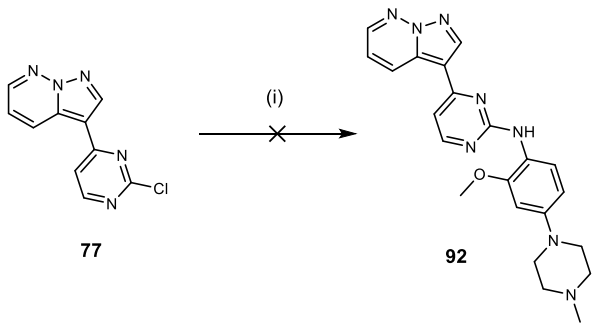

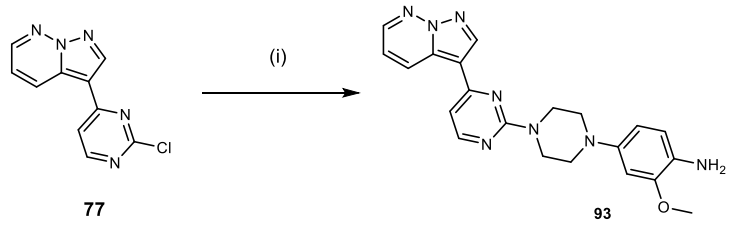

Scheme 13. *Reagents and conditions:* (i) aniline, 2-propanol, 150 °C, 20 min, µwave, **93** not isolated.

Analysis of the reaction mixture showed that the starting material was fully consumed and a single major product was furnished with m/z 403.2 $(M+H)^+$. This is consistent with the piperazine nitrogen acting as the nucleophile in preference to the aniline nitrogen to afford **93**. **92** was synthesised in the same manner as described in Section 4.3 from the corresponding guanidine and intermediate **76** in 37% yield.

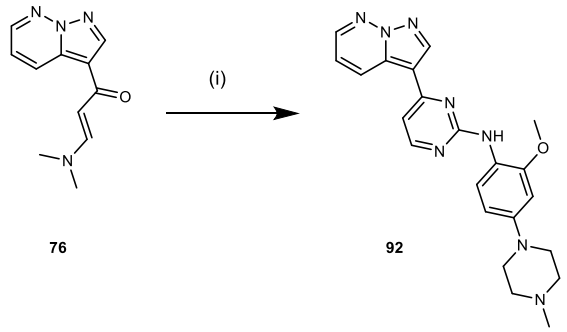

Scheme 14. *Reagents and conditions:* 1-[2-methoxy-4-(4-methylpiperazin-1-yl)phenyl]guanidine; nitric acid, DMF, 110 °C, 16 h, 37%.

4.6.3. SARs and Biological Evaluation of 92

91, a commercially available tool compound for DYRK1B, was purchased from Tocris. The DYRK1A inhibitory activity of **91** was not disclosed in the initial publication,[253] so we thought that it would be a good idea to determine the DYRK1A binding affinity and see how selective a DYRK1B tool **91** is for comparative studies.

91 exhibited high affinity for DYRK1A in the ligand-binding displacement assay. The pyrazolo[1,5-*b*]pyridazine matched pair, **92**, retains a high level of binding affinity for DYRK1A, but is approximately 4 fold weaker than **91** (Table 17). It is surprising that **92** is a weaker binder for DYRK1A than **91**, which may indicate that **91** and **92** have different binding modes. As there are no DYRK1B crystal structures available in the public domain, the binding modes of these compounds in DYRK1B can only be predicted using *in silico* modelling. The inclusion of the piperazine motif afforded **92** a high level of solubility, which previously had been difficult to

achieve in the pyrazolo[1,5-*b*]pyridazine series. Furthermore, metabolic stability had been improved relative to **89** and **90**.

Table 17. DYRK1A Binding Affinity, Solubility and Metabolic Stability of 91 and 92

Compound	DYRK1A IC_{50} [a]	HLM (µL/min/mg)	RLM (µL /min/mg)	Solubility (mg/mL)
91	31	-	-	-
92	136	198.0 +/- 61.3	104.3 +/- 0.1	0.43

[a]IC_{50} (nM) in TR-FRET-based ligand-binding displacement assay (n = 1); HLM and RLM Determinations mean of n =2 +/- standard deviation (unless otherwise stated). HLM = human liver microsomes; RLM = rat liver microsomes; thermodynamic solubility data derived from single experiment at pH 6.8.

Although **92** did not meet the initial criteria for DYRK1A binding affinity, we were interested to assess whether the selectivity gains expected with the introduction of the *ortho* substituent outweighed the loss in DYRK1A affinity.

To assess the effect of *meta* and *ortho* substitution on selectivity, **68**, **78** and **92** were profiled in the ProQinase activity assay at 1 µM against DYRK1A, GSK3β and CDK2 (Table 18). The results suggest that **68**, although possessing the strongest binding affinity for DYRK1A, may also be the least selective in part due to non-specific binding caused by the inclusion of a lipophilic trifluoromethyl group. In contrast, addition of an *ortho* methoxy substituent in analogue **92** serves to remove GSK3β inhibition and is detrimental to CDK2 inhibition whilst maintaining DYRK1A inhibitory activity.

Table 18. CMGC Selectivity Profiles of 92, 68 and 78

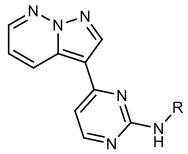

Compound	R	DYRK1A[a]	GSK3β[a]	CDK2[a]
92	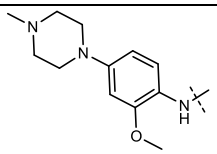	64	11	34
68	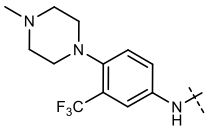	100	95	98
78	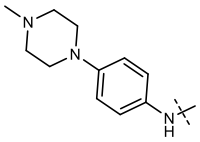	95	42	97

[a] % inhibition in radiometric kinase assay (^{33}PanQinase® Activity Assay) at 1 µM inhibitor concentration provided by ProQinase GmbH (n = 1).

The selectivity profile of **92** was assessed in a 48-kinase panel using a DSF assay. The results of this assay appeared to show that relative to the control staurosporine, **92** had a good selectivity profile comparable to previous compounds **89** and **90**, stabilising few proteins other than DYRK1A.

Due to the favourable selectivity window over CDK2 and GSK3β exhibited by **92**, the decision was taken to profile **92** in a 468 kinase panel to assess its kinome-wide selectivity. **92** was assayed in the KINOMEscan® platform provided by DiscoveRx, a proprietary active-site directed competition binding assay. The results of the selectivity panel are displayed as a TREEspot™ diagram in Figure 49.

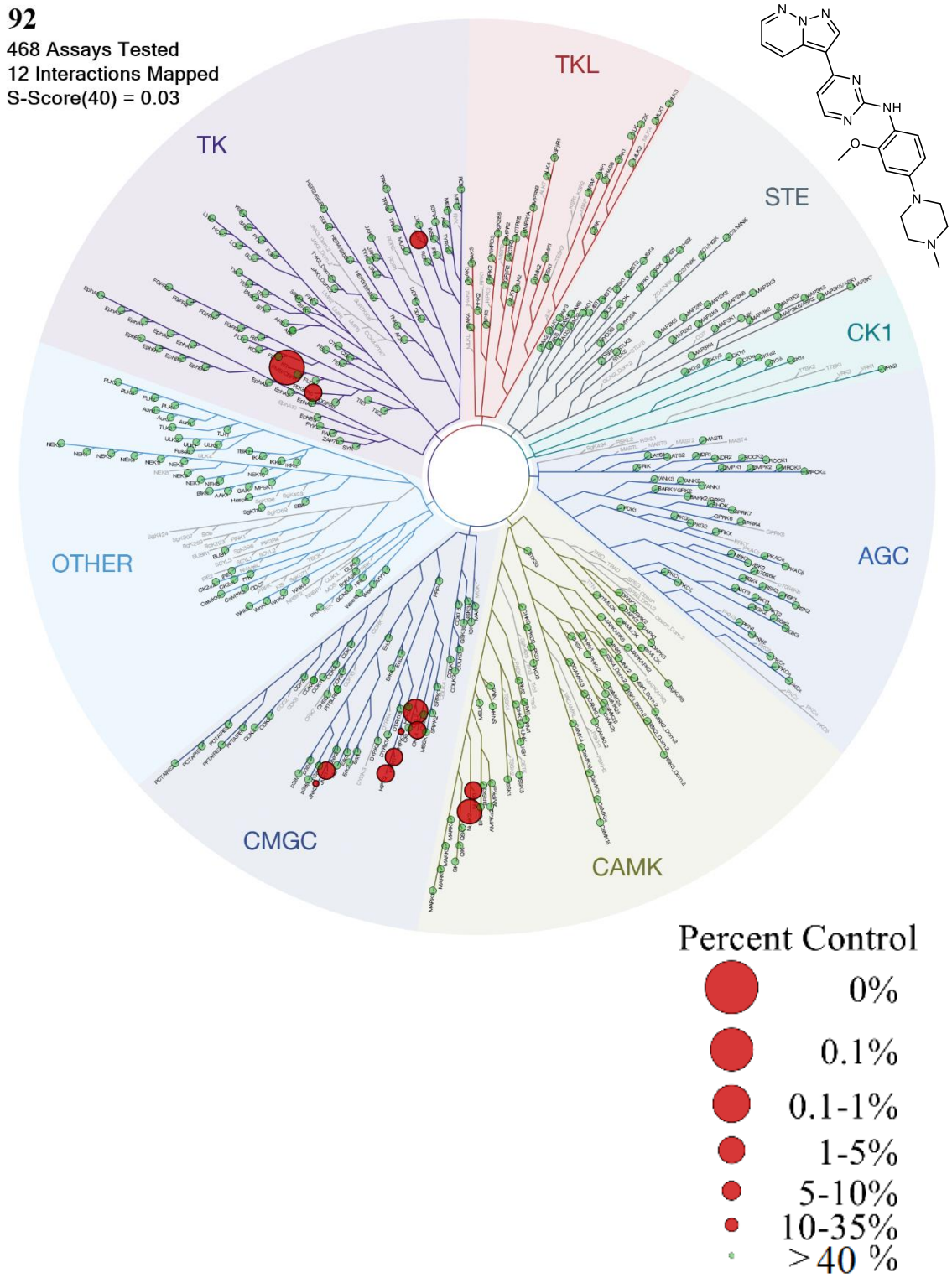

Figure 49. KINOMEscan® Treespot™ map for **92**. Image generated using TREEspot™ Software Tool and reprinted with permission from KINOMEscan®, a division of DiscoveRx Corporation, © DISCOVERX CORPORATION 2010.

92 exhibited high levels of kinome-wide selectivity in the KINOMEscan® panel and showed no inhibition of the original off-targets, CDK2 and GSK3β. This data suggests that **92** would be better described as a CLK2 inhibitor. **92** is > 7 fold more selective for CLK2 than DYRK1A and > 3

fold more selective for CLK2 than CLK4. An overview of **92**'s kinase selectivity profile is presented in Table 19.

Table 19. Overview of Kinome Selectivity Profiles of **92**

Compound	Percent kinases inhibited > 75%[a]	Percent kinases inhibited > 50%[a]	Kinases most potently inhibited
92	2.4	5.1	CLKs, DYRK1B, KIT, PDGFRB, SNARK

[a] % Inhibition as determined by DiscoveRx KINOMEscan® experiment.

92 displays less kinome-wide selectivity than **89** and **90**. Perhaps the incorporation of the larger piperazine motif has caused **92** to exhibit more unspecific binding to other kinases. One advantage of **92** being larger is that haspin, an off-target of **89** and **90**, has been removed as a liability.

It would be interesting to make the methyl analogues depicted in Figure 50. Perhaps combining the selectivity profiles of **89** and **92** would afford a DYRK1A inhibitor with selectivity against DYRK1B, CLKs and haspin. Inclusion of the piperazine ring may lead to lower metabolic turnover and higher solubility for the series.

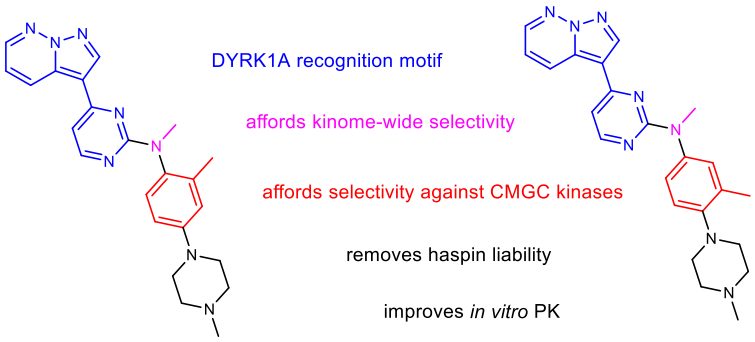

Figure 50. Proposed structure of more selective inhibitors with better *in vitro* PK

4.7. Structural Studies and Rationalisation of Selectivity of 79 and 88

One hypothesis for the observed difference in selectivity between **79** and **88** could be that the introduction of a methyl group onto the amino pyrimidine N-*H*, which when unsubstituted is likely to form a hydrogen bond with the hinge, causes a change in binding mode that is tolerated in DYRK1A but not in CDK2 and GSK3β. This could result in a completely different kinome-wide selectivity profile as opposed to an improved selectivity profile with the selective removal of CDK2 and GSK3β activity.

As mentioned previously a co-crystal structure of the pyrazolo[1,5-*b*]pyridazine series bound to DYRK1A was not available at the outset of the project. *In silico* docking of **79** and **88** into a publically available crystal structure of DYRK1A (PDB 2WO6) was performed with Glide docking in Schrodinger 2016 using OPLS3 force field. Docking suggested that both **79** and **88** were capable of binding to DYRK1A. In both models at least two hydrogen bonding interactions are established between sp^2-type nitrogen atoms of the ligands, a leucine (Leu241) located on the hinge and the catalytic lysine (Lys188). This is consistent with the binding modes of published DYRK1A inhibitors, harmine and L41. A key difference between the two models is that the alkylated compound, **88**, appeared to have an alternate binding mode to **79**. This result provided an alternative hypothesis and may account for a change in selectivity profile observed. The docking models were then overlaid with available PDB structures of GSK3β and CDK2 in an attempt to account for the difference in off-target activity for **79** and **88**.

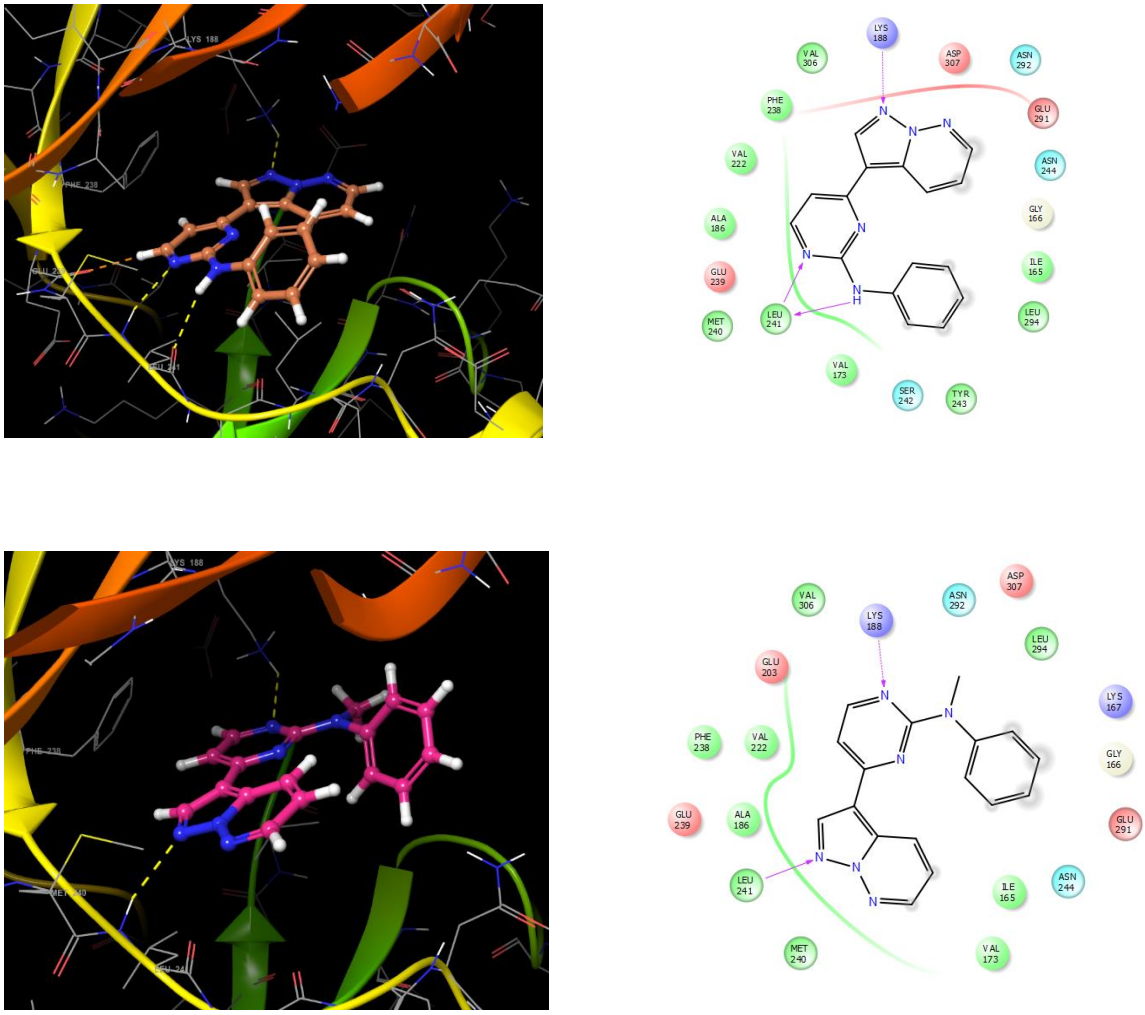

Figure 51. Schrodinger Glide docking of **79** and **88** in DYRK1A (PDB 2WO6) showing a potential change in binding mode that could lead to different observed selectivity. Structure prepared in Schrodinger Maestro 11 with OPLS3 force field.

The co-crystal structure of an analogue of the pyrazolo[1,5-*b*]pyridazine series was available in CDK2 (PDB 3EJ1). Molecular modelling using the Builder tool in MOE to replace the cyclopropyl with a phenyl group, followed by energy minimisation using Amber10:EHT force field allowed for a predicted binding mode of **79** in CDK2. Although the analogue in PDB 3EJ1 did not have a phenyl substituent but rather had a cyclopropylamine substituent, previous docking campaigns by Tavares *et al*. and our own docking had shown that **79** had a high likelihood of binding in a bidentate fashion.[251] This was thought of as a rough estimation of binding mode in CDK2 and could be compared to the docking studies carried out in Schrodinger. The model of **79** bound to CDK2 was aligned with the publically available crystal structures of DYRK1A (PDB 2WO6) and GSK3β (PDB 109U) based on sequence and structure. The three structures were then superimposed based on alignment of the catalytic subunits of each kinase to afford a model of **79** bound to the primary target, DYRK1A and off-targets CDK2 and GSK3β. The model showed a good alignment with RMSD = 0.305 Å.

The CDK2 and GSK3β receptors and solvent could then be inactivated (hidden) to leave only the DYRK1A receptor with **79** bound. The model was minimised using Amber10:EHT force field. This model was compared to the *in silico* docking models produced in Schrodinger Maestro 11 (Figure 51). Both were in agreement, providing confidence for the probable binding mode of **79** in DYRK1A.

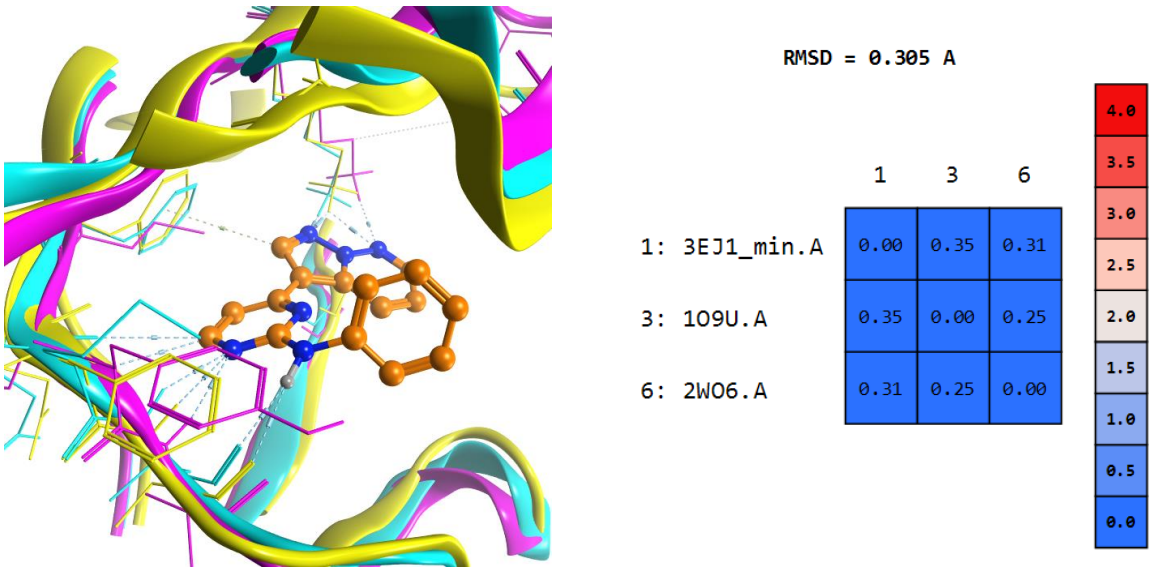

Figure 52. Crystal structure of pyrazolo[1,5-*b*]pyridazine analogue bound to CDK2 (yellow) modified with MOE Builder tool to show proposed binding mode of **79** in CDK2 (yellow) (PDB 3EJI). CDK2 model overlaid with crystal structures of DYRK1A (cyan) (PDB 2WO6) and GSK3β (magneta) (PDB 109U). Structure prepared in MOE, CCG, 2016 with Amber10:EHT force field.

The DYRK1A model generated in MOE could then be further modified with the MOE Builder tool to add a methyl group onto the N-*H* of **79** to furnish **88**. After energy minimisation, the postulated binding mode of **88** could be compared to the model for **79**. These diagrams are shown in Figure 53.

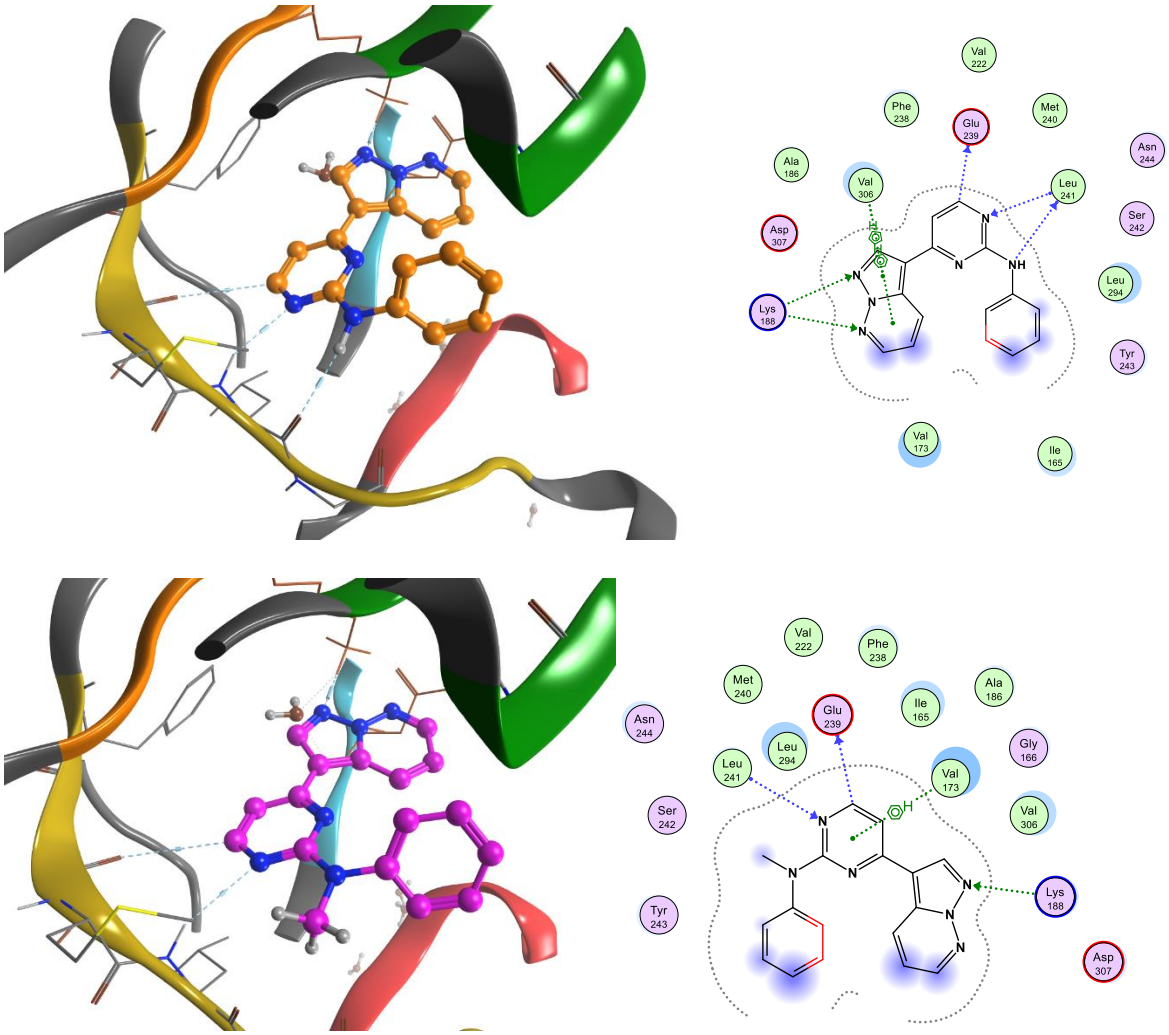

Figure 53. **79** and **88** modelled into the ATP site of DYRK1A. *N*-methyl group of **88** added with MOE Builder tool to model of **79** in DYRK1A and energy minimised. 2-D ligand interaction diagram shows similar contacts made between the ligand and DYRK1A as is observed in published crystal structures of DYRK1A inhibitors. Structure prepared in MOE 2016, CCG with Amber10:EHT force field.

Interestingly, the two *in-silico* models generated on two different platforms, Schrodinger and MOE, did not agree with each other. The model developed in MOE appears to show that the binding mode of **79** and **88** is essentially the same in DYRK1A, and that an additional methyl group may not invoke a change in binding mode in DYRK1A. Overlays with GSK3β and CDK2 appeared to show clashes between the kinase hinges and **88** in the same model. Although there was some ambiguity in the binding mode of **88**, both models were used simultaneously until the co-crystal structure of **88** was produced.

4.8. Summary

A series of kinase inhibitors that were originally published as CDK2 and GSK3β inhibitors have been repurposed into selective DYRK1A inhibitors through the use of an innovative chemoinformatics approach. A KNIME® workflow was used to mine publically available kinase profiling data stored in ChEMBLdb in order to identify activity cliffs for the series of interest. Once potential activity cliffs and off-target liabilities were identified, a small number of hypothesis-testing analogues were synthesised and assayed for DYRK1A binding affinity, selectivity, metabolic stability and solubility. Using this approach the kinome-wide selectivity of the series was achieved in very few steps and with very little resource to afford selective and high affinity molecular probes of DYRK1A.

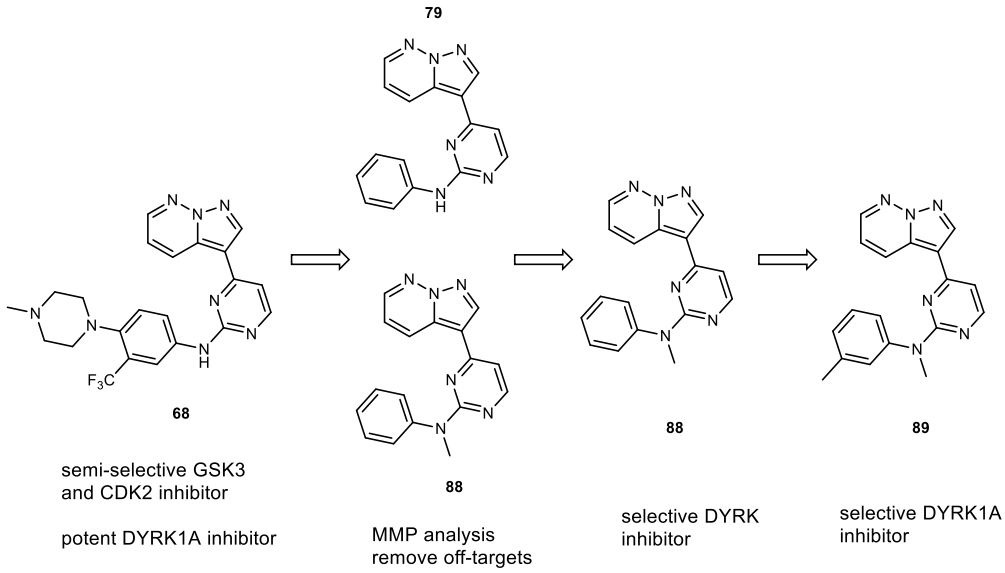

Figure 54. Summary of scaffold evolution for selective DYRK1A inhibitors.

Although the well documented inclusion of an *ortho*-methoxy substituent close to the kinase hinge resulted in abolishment of CDK2 and GSK3β activity, it was alkylation of the conventional N-*H* hinge binder that afforded kinome-wide selectivity. Furthermore, the chemoinformatics approach identified that *ortho* methyl analogues are selective vs GSK3β and CDK2. Hence it may be that both of these kinases are easily dialled out by any *ortho* substituent. This strategy of methyl scanning at the *ortho* position and onto the N-*H* hinge binder should be added to a repertoire of methods to gain selectivity against these kinases (and the majority of the kinome).

As this was the initial round of hit expansion, selectivity rather than physicochemical properties was afforded the most attention. **89** represents one of the finest DYRK1A inhibitors discovered to date, with more optimal kinase selectivity than most other published inhibitors and

documented metabolic stability and solubility data. **89** exhibited low P-gp efflux and good permeability in the MDCK-MDR1 assay, consistent with a molecule able to cross the BBB. Issues identified with **89** include low solubility (0.01 mg/mL) and high microsomal turnover in rat (784 µL/min/mg). Microsomal turnover in human is much more attractive (75 µL/min/mg) and as a compound to develop further, a LE of 0.42 is very promising.

Based on the results of this chapter, further structural modification of the pyrazolo[1,5-*b*]pyridazine series is required. This thesis will now focus on the work undertaken to improve compound quality through a combination of SBDD and close control of ligand efficiency metrics. Kinome-wide selectivity will be maintained using the knowledge acquired during this period of initial SAR exploration. With the production of the first co-crystal structure of the series bound to DYRK1A, the following chapter will make use of this to guide rational design. Maintenance of the hinge binding motif and Lys188 binding motif of the molecule (blue), and retention of the alkylated hinge binder (red), will retain selectivity. Metabolic stability and solubility will be improved through a concerted effort to lower lipophilicity and reduce the number of aromatic rings (Figure 55).

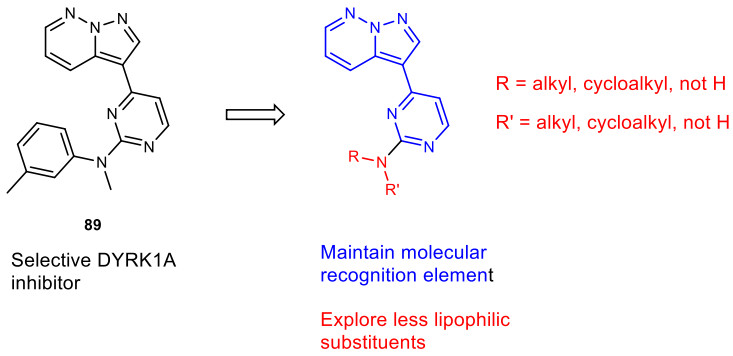

Figure 55. Further exploration of pyrazolo[1,5-*b*]pyridazine series.

CHAPTER 5. Structure-enabled Design of DYRK-selective Pyrazolo[1,5-*b*]pyridazines: Part I

Chapter 5 describes the focussed hit expansion of a series of pyrazolo[1,5-*b*]pyridazines in an effort to discover selective and high affinity molecular probes of DYRK1A. Concentrating on improving metabolic stability and solubility, the lipophilicity and number of aromatic rings of the series. In parallel the *N*-methyl selectivity handle hypothesis is probed further to furnish a number of DYRK1A molecular probes with high levels of selectivity, improved binding affinity, superior metabolic stability and better solubility than **89**.

5.1. Structure-guided Design of the Pyrazolo[1,5-*b*]pyridazine Series

Approximately 15 months into the DYRK1A project, the first in a series of high resolution co-crystal structures of the pyrazolo[1,5-*b*]pyridazine series bound to DYRK1A was elucidated. The co-crystal structure of **88** bound to DYRK1A proved conclusively that the series adopted the same binding mode in DYRK1A regardless of whether the N-*H* hinge binder was capped with a methyl or not, supporting the *in silico* prediction generated in MOE (Figure 56).

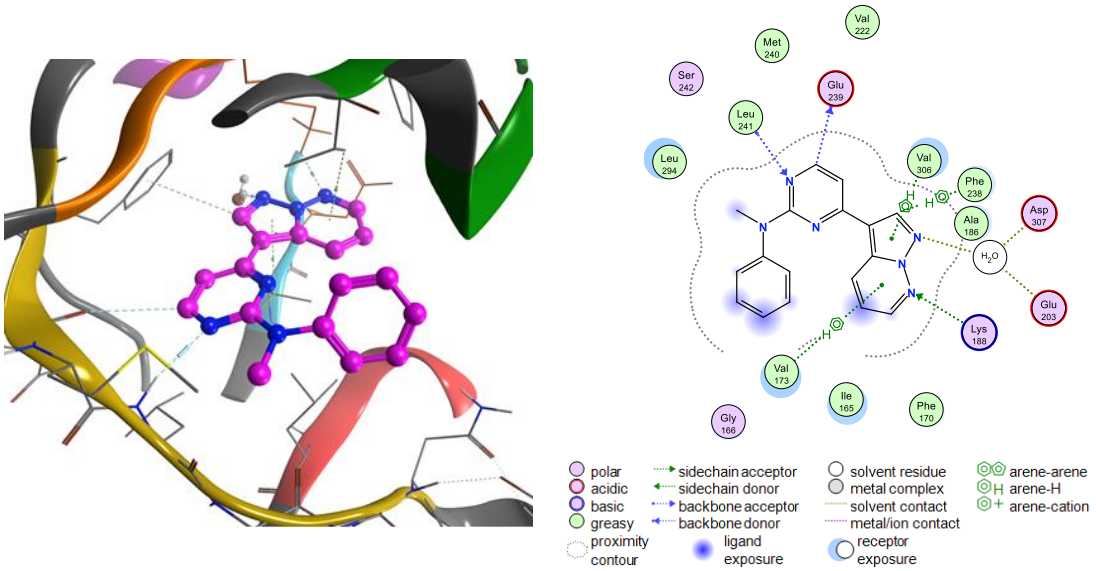

Figure 56. Co-crystal structure of **88** bound in Type I fashion to DYRK1A as predicted with in silico model generated in MOE. Structure prepared and minimised with MOE 2016, CCG with Amber10:EHT force field.

When bound to DYRK1A, **88** adopts a pseudo-monodentate binding mode. Interestingly, the C-*H* at the 6-position of the pyrimidine serves as a surrogate hydrogen bond donor, making a CH-

O interaction with Glu239 of the hinge. This type of informal hydrogen bond, whereby an aromatic C-*H* group acts as a HBD has been observed for other kinase inhibitors and has been postulated to provide a degree of selectivity.[254,255,256] Further π-interactions between **88** and the gatekeeper (Phe238), the glycine rich loop (Val173) (green) and the DFG-loop (Val306) (cyan) are observed. The pyridine-type nitrogen of the pyrazolo portion of the pyrazolo[1,5-*b*]pyridazine head supports a long-range water network that is connected *via* a conserved water molecule at the back of the kinase pocket. Hydrogen bonds are formed between this water molecule, Asp307 and Glu203, the latter which forms a salt bridge with the catalytic lysine (Lys188). The non-bridging nitrogen belonging to the pyridazine portion of the head serves as a hydrogen bond acceptor to the catalytic lysine (Lys188), further stabilizing the inhibitor in the pocket.

5.2. Reducing Lipophilicity and Aromatic Ring Count through Replacement of the Anilino Substituent

5.2.1. Rationale

The established binding mode of **88**, combined with the available ligand data in the ChEMBLdb provided confidence that the methyl cap was the key to affording wider kinome selectivity for the series. The ligands discovered in Chapter 4 had room for improvement. Although selectivity had been significantly improved for **89** and **90** compared to **68**, the DYRK1A binding affinity and physicochemical properties of the series remained sub-optimal in terms of compound quality. The series had a high aromatic ring count (4), low sp^3 character and moderate-to-high lipophilicity (clog P > 3 - 3.7). These attributes are all commensurate with problems in development.[257,258]

An effort was undertaken to reduce lipophilicity whilst maintaining the selectivity profile and increasing DYRK1A affinity achieved thus far. Inspection of the receptor-ligand surface representation of **88** bound to DYRK1A (Figure 57) led to the theory that replacement or removal of the phenyl group would be beneficial in terms of reducing lipophilicity and would probably improve solubility and metabolic stability. The phenyl group does not appear to be making any formal interactions that are required for the stabilisation of the protein-ligand complex.

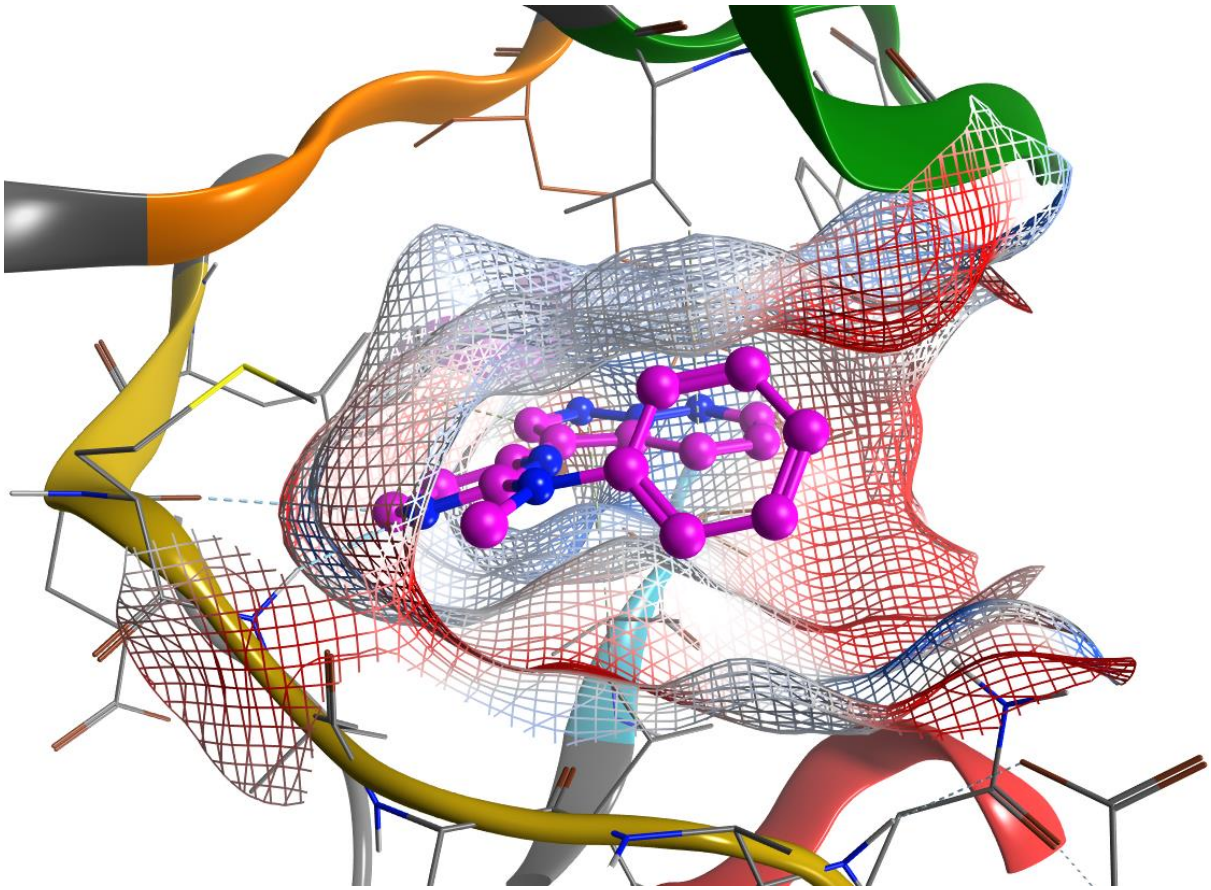

Figure 57. 'Open' solvent exposed region and electrostatic representation of receptor surface of DYRK1A - a potential for series expansion and modulation of solubility and microsomal stability whilst retaining the 'hinge + Lys188' recognition motif. Crystal structure generated in-house with **88** bound to DYRK1A. Structure preparation in MOE 2016, CCG with Amber10:EHT force field.

The molecule was deconstructed in order to reduce lipophilicity and reduce aromatic ring count. The free amino pyrimidine **94** exhibited approximately 3 fold weaker binding affinity for DYRK1A than **88**. However, the LE (0.55) and LipE (5.6) of **94** were far superior. **94** could be the minimally active pharmacophore, on which to develop the series further. Addition of a single methyl group (**95**) resulted in an ligand that was equipotent to **88** but possessed a superior LipE and LE. The dimethyl analogue **96**, designed with selectivity in mind, exhibits DYRK1A IC_{50} < 100 nM without a reduction in LE or LipE and represents a good starting point for further elaboration.

Table 20. DYRK1A Binding Affinity of **88** and **94-96**

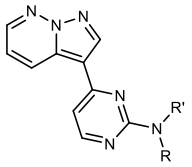

Compound	R	R'	DYRK1A IC_{50}[a]	LE, LipE
88	Me	Ph	186	0.41, 3.6
94	H	H	521	0.55, 5.6
95	Me	H	181	0.56, 5.8
96	Me	Me	75	0.56, 5.5

[a]IC_{50} (nM) in TR-FRET-based ligand-binding displacement assay (n = 1). LE = 1.4(pIC_{50})/non-hydrogen atoms; LipE = pIC_{50} – clog P.

5.2.2. Synthesis of *N*-methyl Analogues

The synthesis of the *N*-alkylated analogues followed the same synthetic procedure as previously detailed in Chapter 4. However, the nucleophilic aromatic substitution to afford the desired product was performed with an amine rather than an aniline (Scheme 15). Nucleophilic aromatic substitution was found to be more facile with amines and consequently the reactions did not require the use of microwave heating. This was useful as multiple final products could be accessed using parallel synthesis on one heating block. For unhindered amines reactions were generally complete within 2h and at a lower temperature than for sterically hindered secondary amines. If the secondary amine was not commercially available, intermediate **77** was first reacted with the primary amine and the product was then treated with sodium hydride and iodomethane at room temperature to afford the desired analogue.

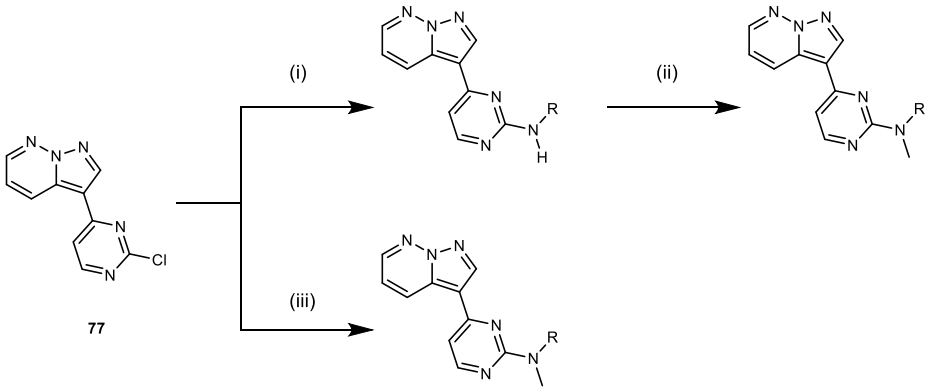

Scheme 15. *Reagents and conditions*: (i) amine, 2-propanol, 110 °C - 140 °C, 2 - 16 h. (ii) sodium hydride, iodomethane, DMF, rt, 2 h. (iii) *N*-methylated amine, 2-propanol, 110 °C - 140 °C, 2 - 16 h.

5.2.3. SARs and Biological Evaluation of *N*-methyl Analogues

DYRK1A binding affinity, ligand efficiency (LE) and lipophilic ligand efficiency (LipE) for **94**-**104** are presented in Table 21. **88** has been added to Table 21 for easy comparison of data.

The cyclopropyl analogue **97**, and its methylated analogue, **98**, display similar affinity to **95** and **96** with similar LE and LipE. Short chain ether **100** and the methylated analogue **101** exhibit modest improvements in DYRK1A binding affinity relative to **88** with retention of LipE. Longer aliphatic chains bearing lipophilic substituents designed to interact more favourably with the P-loop (**103** and **104**) show improved DYRK1A affinity relative to **88**, but exhibit weakened LipE and LE, suggesting that longer and more lipophilic alkyl chains do not provide as much 'bang for your buck' as first appears.

Interestingly, adding a methyl group onto the N-*H* of analogues bearing an aryl substituent causes a reduction in DYRK1A binding affinity, whereas for analogues bearing an alkyl substituent the introduction of a methyl group on the N-*H* results in an increase in DYRK1A affinity; **79** (DYRK1A IC_{50} = 38 nM) is approximately 5 fold stronger than **88** (DYRK1A IC_{50} = 186 nM), whereas **95** (DYRK1A IC_{50} = 181 nM) is approximately 2.5 fold weaker than **96** (DYRK1A IC_{50} = 75 nM).

The series was expanded to include a more diverse set of *N*-methyl derivatives. Synthesis was carried out as previously described. DYRK1A binding affinity of *N*-methyl derivatives is displayed in Table 21.

Table 21. DYRK1A Binding Affinity of N*H* and *N*-methylated Matched-pairs

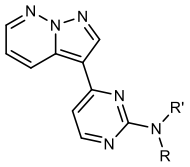

Compound	R	R'	DYRK1A IC_{50}	LE, LipE
88	Me	Ph	186	0.41, 3.6
94	H	H	521	0.55, 5.6
95	Me	H	181	0.56, 5.8
96	Me	Me	75	0.56, 5.5
97		H	107	0.51, 5.5
98		Me	114	0.49, 4.9
99	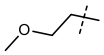	H	612	0.43, 5.3
100	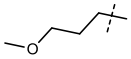	H	128	0.46, 5.9
101	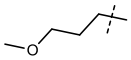	Me	218	0.42, 5.0
102	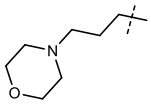	H	844	0.34, 5.3
103	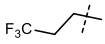	Me	230	0.40, 3.8
104	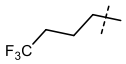	Me	100	0.41, 3.9

[a]IC_{50} (nM) in TR-FRET-based ligand-binding displacement assay (n = 1). LE = 1.4(pIC_{50})/non-hydrogen atoms; LipE = pIC_{50} – clog P.

96 and **98** possessed DYRK1A binding affinity around IC_{50} = 100 nM, hence they were profiled in a three-kinase panel to assess whether selectivity over CDK2 and GSK3β was maintained for compounds bearing alkyl motifs. **96** and **98** showed a similar selectivity window over GSK3β and CDK2 as compounds with aromatic substituents, suggesting that the binding mode of these smaller, more fragment like molecules had been maintained.

Table 22. CMGC Selectivity Profiles of 96 and 98

Compound	DYRK1A[a]	GSK3β[a]	CDK2[a]
96	61	5	3
98	57	7	5

[a] % inhibition in radiometric kinase assay (^{33}PanQinase® Activity Assay) at 1 µM inhibitor concentration provided by ProQinase GmbH (n = 1).

The selectivity profiles of **96** and **98** were assessed in a 48-kinase panel using a DSF assay. The results of this assay appeared to show that relative to the control staurosporine, **96** and **98** had good selectivity profiles, exhibiting similar selectivity profiles to selective analogues **89** and **90**.

96 and **98** were profiled in a 468 kinase panel to assess their kinome-wide selectivity. The compounds were assayed in the KINOMEscan® platform provided by DiscoveRx, a proprietary active-site directed competition binding assay. The results of the selectivity panel are displayed as TREEspot™ diagrams in Figure 58.

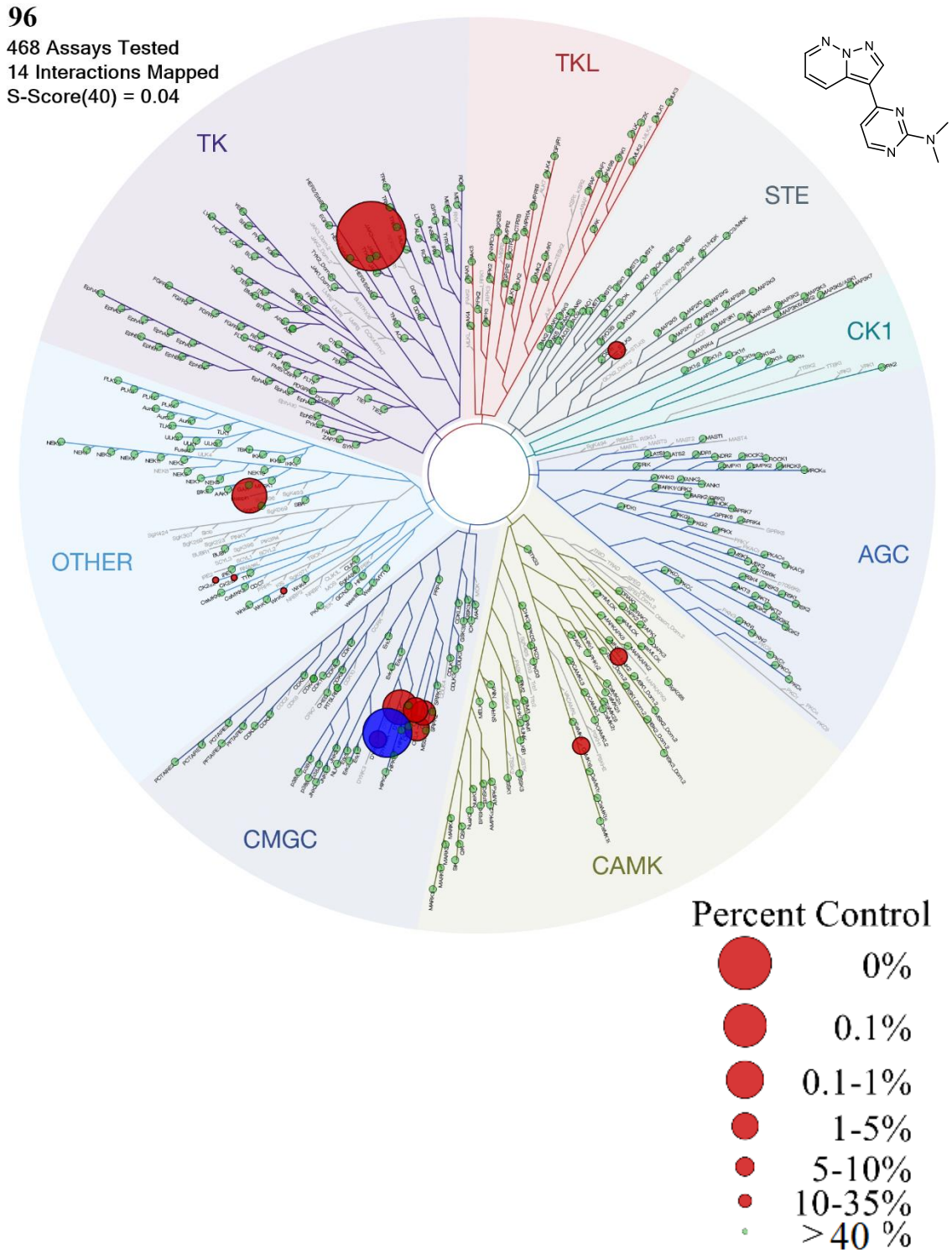

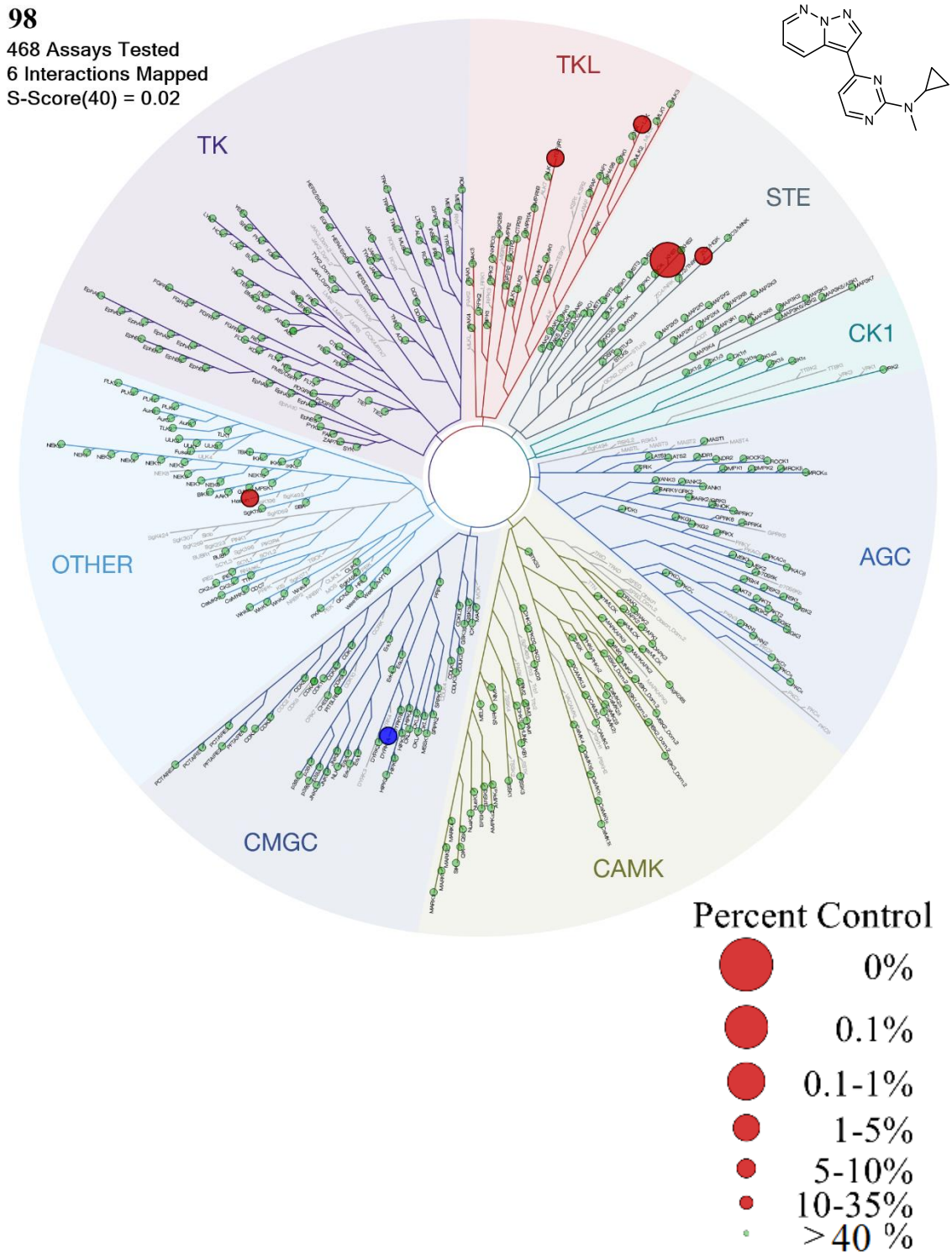

Figure 58. KINOMEscan® Treespot™ maps for **96** (top) and **98** (bottom). DYRK1A is highlighted in blue. Image generated using TREEspot™ Software Tool and reprinted with permission from KINOMEscan®, a division of DiscoveRx Corporation, © DISCOVERX CORPORATION 2010.

Both **96** and **98** showed good kinome-wide selectivity profiles. **96** and **98** support the hypothesis that there is a 'magic methyl' selectivity handle for the pyrazolo[1,5-*b*]pyridazine series and for DYRK1A. **98** appeared to be the most selective DYRK1A inhibitor with < 1% of the human kinome

inhibited over 75% (Table 23). As with the majority of published DYRK1A inhibitors, the mitotic kinase haspin is inhibited by both **96** and **98**. Other members of the DYRK family and the closely related CLK kinases are also inhibited to some extent (Table 23).

Table 23. Overview of Kinome Selectivity Profiles of Compounds 96 and 98

Compound	Percentage kinases inhibited > 75%[a]	Percentage kinases inhibited > 50%[a]	Kinases most potently inhibited
96	1.7	3.8	JAK3, haspin, DYRK1B, CLK4
98	0.9	1.7	MAP4K5, MAP4K4, LZK, haspin

[a] % Inhibition as determined by DiscoveRx KINOMEscan® experiment.

96 was the highest affinity binder (DYRK1A IC_{50} = 75 nM) and was further profiled for suitability as a molecular probe. The binding affinity of **96** was determined more accurately at a range of concentrations (K_D) for DYRK1A and the kinase off-targets identified in the KINOMEscan experiment. The selectivity profile of **96** is outlined in Table 24. The selectivity profile of **96** appears to be better than initially thought as JAK3 was shown to be a false positive. **96** exhibits good selectivity for DYRK1A (IC_{50} = 3 nM) vs the closely related DYRK1B (IC_{50} = 56 nM) with around 20 fold selectivity. Similarly, CLK1 (IC_{50} = 70 nM) and CLK4 (IC_{50} = 61 nM) are strongly inhibited by **96**, but again the compound exhibits approximately 20 fold higher affinity for DYRK1A than either of these commonly inhibited kinases. **96** displays around 5 fold weaker affinity for haspin (IC_{50} = 15 nM) than DYRK1A.

In parallel **96** was also profiled against a smaller subset of kinases in a radiometric activity assay provided by ProQinase. Under the different assay format **96** was not as selective for DYRK1A, in fact **96** most potently inhibited CLK4 (IC_{50} = 83 nM) followed by DYRK1B (IC_{50} = 120 nM). The only consistent result of both the DiscoveRx assay and the ProQinase assay was that JAK3 was confirmed as a false positive in the intial KINOMEscan®. Prior to any *in vivo* studies it would be wise to determine the cellular selectivity profiles (e.g. NanoBRET assay, Promega) of this series of small molecule kinase inhibitors.

Table 24. Selectivity Profiling of **96**

Kinase	K_D [a]	IC_{50} [b]
CAMK1B	10000	-
CLK1	70	180
CLK2	220	-
CLK4	61	83
DYRK1A	3	220
DYRK1B	56	120
DYRK2	360	2900
Haspin	15	-
HIPK2	1200	-
JAK3 (JH1domain-catalytic)	10000	> 10000
MKNK2	1800	-
STK39	10000	-
WNK2	10000	-

[a]K_D (nM) determined in competition binding assay (DiscoveRx, n = 2).[b]IC_{50} (nM) determined in radiometric kinase activity assay ^{33}PanQinase® Activity Assay (ProQinase, n = 1).

96 and **98** were profiled for metabolic stability (HLM, RLM) and thermodynamic solubility. The results are shown in Table 25. In comparison to **89**, both compounds exhibit improved solubility for use as molecular probes. **96** and **98** also exhibit reduced metabolic turnover in rat, which could be beneficial for in the future for progression to *in vivo* experiments in rodent.

Table 25. Metabolic Stability and Solubility of 96 and 98

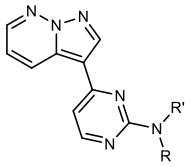

Compound	R	R'	HLM (µL/min/mg)	RLM (µL/min/mg)	Solubility (mg/mL)
89	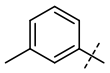	Me	75 +/- 4.5	783.7 +/- 30.6	0.01
96	Me	Me	241.8[a] +/- 31.7	230.1[a] +/- 30.8	0.1
98		Me	71.2 +/- 1.8	433.5 +/- 58.1	0.06

HLM and RLM Determinations mean of n =2 +/- standard deviation (unless otherwise stated).[a] Mean of n = 4 +/- standard deviation. HLM = human liver microsomes; RLM = rat liver microsomes; thermodynamic solubility data derived from single experiment at pH 6.8.

The overall profile of **96** was very close to meeting the tool compound criteria established at the beginning of the project. A measure of cellular activity was now required with the aim of achieving cellular potency within 10 fold of DYRK1A enzymatic binding affinity and inhibitory activity. Cellular DYRK1A activity was assessed using a NanoBRET assay (Figure 59).

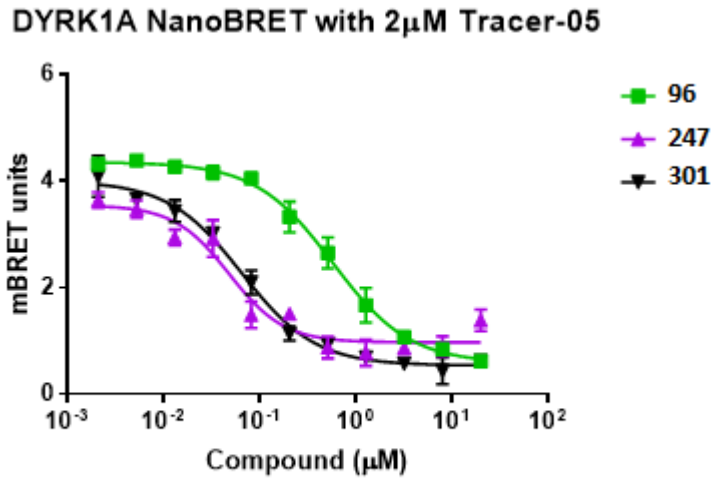

	96	247	301
IC50	0.5762	0.04814	0.06543

Figure 59. NanoBRET cellular activity of 96 (green curve). IC_{50} reported in µM.

Cellular DYRK1A potency was found to be within 10 fold of DYRK1A enzymatic binding affinity and inhibitory activity, and crucially **96** displayed significant on-target activity below 1 µM concentration. Thus fulfilling the requirement for an SGC chemical probe for DYRK1A.

To assess whether **96** was capable of probing a CNS target, such as DYRK1A, the permeability and P-gp mediated efflux of **96** was assessed in a MDCK-MDR1 assay provided by Cyprotex.

Table 26. MDCK-MDR1 permeability of **96**

Compound	CNS MPO[a] score	Direction = A2B Mean P_{app} (10^{-6} cms^{-1})[b]	Direction = B2A	Efflux Ratio (Mean P_{app} B2A / Mean P_{app} A2B)[b]
96	6	71.4 +/- 0.65	58.7 +/- 1.45	0.822

[a]CNS MPO score calculated using CNS MPO KNIME® workflow with ChemAxon nodes. [b]Data generated by Cyprotex in MDCK-MDR1 assay. Permeability coefficient (P_{app}) calculated across cells in direction: A2B (Apical to Basolateral) and B2A (Basolateral to Apical). Determinations +/- standard deviation (mean of n =2 unless otherwise stated).

The high CNS MPO score of **96** correlated with good levels of permeability and low P-gp efflux, suggesting that **96** may be capable of being developed as a CNS molecular probe.

5.2.4. Binding Mode of 96 and 98

Due to the smaller size of **96** and **98** there was concern that the ligands may be capable of adopting multiple binding modes in the pocket of DYRK1A, providing an alternative explanation for the observed selectivity profiles. To rule that possibility out and to enable subsequent rational drug design, **96** and **98** were co-crystallised in DYRK1A. Both inhibitors maintained the same binding mode as had been observed for **88** (Figure 60). This result suggested that the binding mode of the series would be maintained as long as the pyrazolo[1,5-*b*]pyridazine motif and pyrimidine moiety were retained, effectively as DYRK1A 'hinge-Lys188' recognition elements.

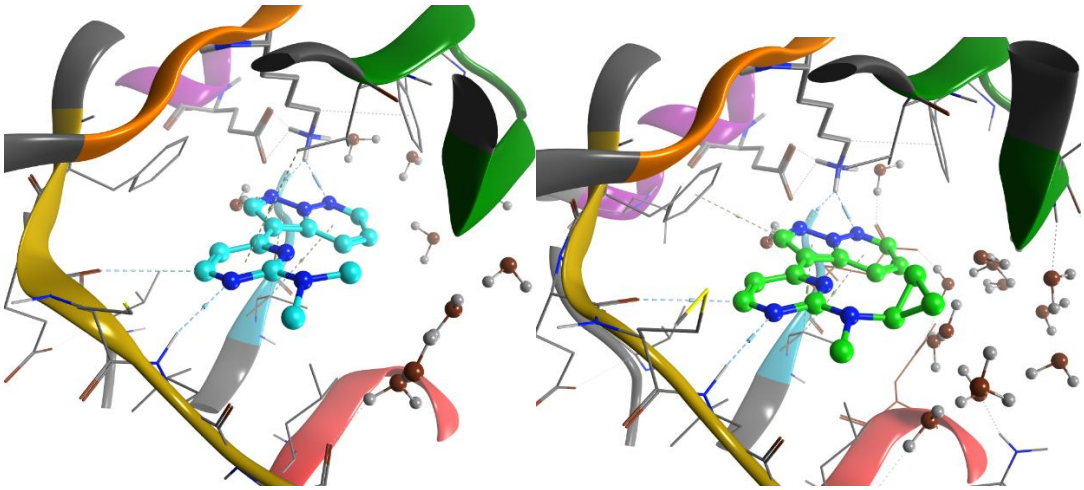

Figure 60. Binding modes of **96** and **98** in DYRK1A show very similar pose. Crystal structures generated in-house. Structures prepared in MOE 2016, CCG with Amber10:EHT force field.

96 represents one of the most selective DYRK1A inhibitors to date with the most complete profile reported. The cellular activity of **96** was reduced in comparison to the inhibitory activity on the isolated protein, however, the levels of activity are acceptable for a tool compound. The

physicochemical properties of **96** are in general very good, especially for a kinase inhibitor. High LE (0.55), LipE (5.5) and a CNS MPO score of 6/6 are indicative of a high quality compound. The solubility of **96** is also attractive, and is in contrast to other published DYRK1A inhibitors that are often reported to be insoluble, limiting their utility as *in vivo* probes. **96** exhibited low P-gp efflux and good levels of permeability in a MDCK-MDR1 assay suggesting that **96** is capable of becoming a molecular probe for a CNS target.

5.3. Probing the DYRK1A Selectivity Pocket; Substituting the *N*-methyl for Something Larger and Less Metabolically Labile

5.3.1. Rationale

It had been established that adding a methyl group onto the N-*H* of the amino pyrimidine was tolerated in DYRK1A and afforded kinome-wide selectivity (Chapters 4 and 5). We were now interested to assess whether larger alkyl groups were tolerated in this position in an attempt to further improve selectivity and metabolic stability. Metabolic clearance data indicated that *N*-dealkylation was a probable cause of instability (Table 27) as compounds with methyl groups were rapidly turned over compared to their unmethylated matched pairs. This was observed for both aniline and amine derivatives.

Table 27. Metabolic Stability of *N*-methyl Analogues

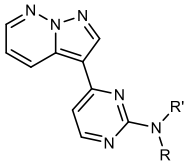

Compound	R	R'	HLM (µL/min/mg)	RLM (µL/min/mg)
94	H	H	22.1 +/- 15.6	48.5[a]
95	Me	H	74.7 +/- 15.3	45.7 +/- 6.5
96	Me	Me	241.8[b] +/- 31.7	230.1[b] +/- 30.8
98		Me	71.2 +/- 1.8	433.5 +/- 58.1
69	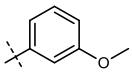	H	117 +/- 20.6	122.6 +/- 24.1
90	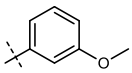	Me	258 +/- 3.5	902.7 +/- 58.3

HLM and RLM Determinations mean of n =2 +/- standard deviation (unless otherwise stated). [a]Data derived from singlicate experiment. [b]Data is mean of n = 4 +/- standard deviation. HLM = human liver microsomes; RLM = rat liver microsomes.

The *N*-methyl group had afforded kinome-wide selectivity probably by causing clashes with hinge residues in other kinases. It follows that larger alkyl moieties close to the hinge may invoke more energetic clashes with more kinase hinges and so give better selectivity for DYRK1A.

5.3.2. Synthesis of *N*-alkyl analogues

Due to the sterically hindered nature of the secondary amines required, the nucleophilic aromatic substitutions required a longer reaction time and were carried out at a higher temperature in a sealed tube. The yields were also lower with more unconsumed starting material present in the reaction mixture after 96 h in some cases.

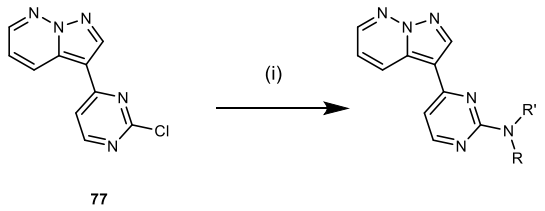

Scheme 16. *Reagents and conditions:* (i) secondary amine, 2-propanol, 140 °C, 16-96 h.

In cases where the secondary amine was not commercially available, **77** was first reacted with the primary amine or aniline and the product was then treated with sodium hydride and iodoalkane at room temperature.

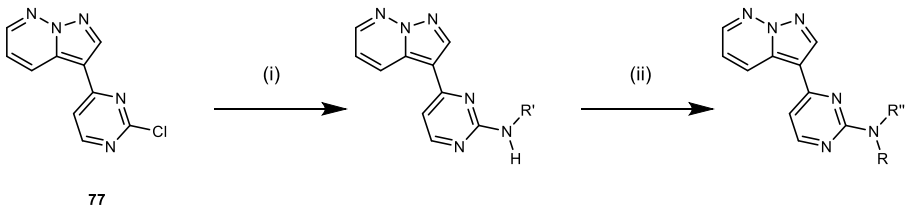

Scheme 17. *Reagents and conditions:* (i) amine, 2-propanol, 110 °C – 140 °C, 2-16 h. (ii) sodium hydride, haloalkane, DMF, rt, 5 h.

5.3.3. SARs and Biological Evaluation of *N*-alkylated Compounds

DYRK1A binding affinity, ligand efficiency (LE) and lipophilic ligand efficiency (LipE) for *N*-alkylated compounds are presented in Table 28. Data for *N*-methylated compounds has been added to Table 28 for easy comparison of data.

Adding a larger group than methyl to the amino pyrimidine N-*H* results in a decrease in DYRK1A binding affinity. This is most likely due to increased steric repulsion from the hinge of the kinase

that could result in a less favourable binding mode being adopted by the ligand. Adding a larger N-*H* capping group than methyl such as ethyl (**89** vs **106**) or isopropyl (**88** vs **105** and **98** vs **108**) significantly reduced DYRK1A binding affinity. These results suggest that the pocket or cleft into which this methyl or alkyl substituent is directed must be relatively small and only able to accommodate a substituent about the size of a methyl group.

Table 28. DYRK1A Binding Affinity of N-*H* and *N*-alkylated Analogues

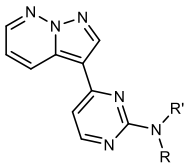

Compound	R	R'	DYRK1A IC_{50}[a]	LE, LipE
79	H	Ph	38	0.47, 4.5
88	Me	Ph	186	0.41, 3.6
105		Ph	2283	0.32, 1.7
82	H	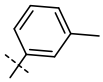	7	0.5, 4.7
89	Me	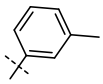	76	0.42, 3.4
106	Et	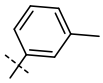	297	0.37, 2.5
94	H	H	521	0.55, 5.6
95	Me	H	181	0.56, 5.8
96	Me	Me	75	0.56, 5.5
107	Pr		752	0.39, 2.8
97	H		107	0.51, 5.5
98	Me		114	0.49, 4.9
108			1196	0.38, 3.1
99	H	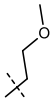	612	0.43, 5.3
109	Pr	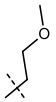	317	0.4, 4.0

[a]IC_{50} (nM) in TR-FRET-based ligand-binding displacement assay (n = 1). LE = 1.4(pIC_{50})/non-hydrogen atoms; LipE = pIC_{50} – clog P.

96 and **98** possessed the best balance of properties so far for a DYRK1A molecular probe. However, the high clearance of compound **96** may require improvement if the series is to be

used as an *in vivo* tool. Intrinsic clearance data appears to show that *N*-dealkylation is a potential source of metabolism. Attempts to modulate *N*-dealkylation by capping the amino pyrimidine N-*H* with alkyl groups other than a methyl was detrimental to DYRK1A binding affinity. Thus another strategy was needed to maintain selectivity but improve the metabolic stability and solubility of the series.

5.4. Probing the DYRK1A Selectivity Pocket; Substituting the *N*-methyl for Cyclic Amines

5.4.1. Rationale

Gaining selectivity and affinity from further exploration of the solvent-exposed region seemed likely as **96** was already very selective. It was envisaged that selectivity within the DYRK and CLK families could be fine-tuned by targeting specific residues along the hinge through *in silico* design. It seemed that a dead-end had been reached with appending larger substituents to the N-*H* amino pyrimidine. The 'selectivity' pocket of DYRK1A seemed to be quite shallow, about the size of a methyl.

Analysis of the hinge regions of DYRK1A, DYRK1B and CLK1 showed key differences in the 'gatekeeper + 2' residue. DYRK1A possesses a methionine (Met240) residue in the 'gatekeeper + 2' position, whereas CLK1 and DYRK1B possess a leucine residue in the same position. Exploiting this difference in residues could lead to selectivity over both DYRK1B and CLK1.

Currently a crystal structure of DYRK1B does not exist in the public domain. To compensate for this a homology model was produced of DYRK1B from its primary amino acid sequence. The structures of DYRK1A, DYRK1B homology model and CLK1 were aligned by sequence and then overlaid based on the active site of the kinases. The receptor surfaces were modelled to look for regions that were sufficiently different to target. It can be seen in Figure 61 that there are differences in the hinge regions of the three kinases that had the potential to be exploited. The cyclopropyl group of **98** appears to clash with the pocket of CLK1 (orange surface) and DYRK1B (purple surface). The experimentally derived selectivity profile of **98** supports this model to some extent as **98** showed improved selectivity against the CLK kinases and DYRK1B.

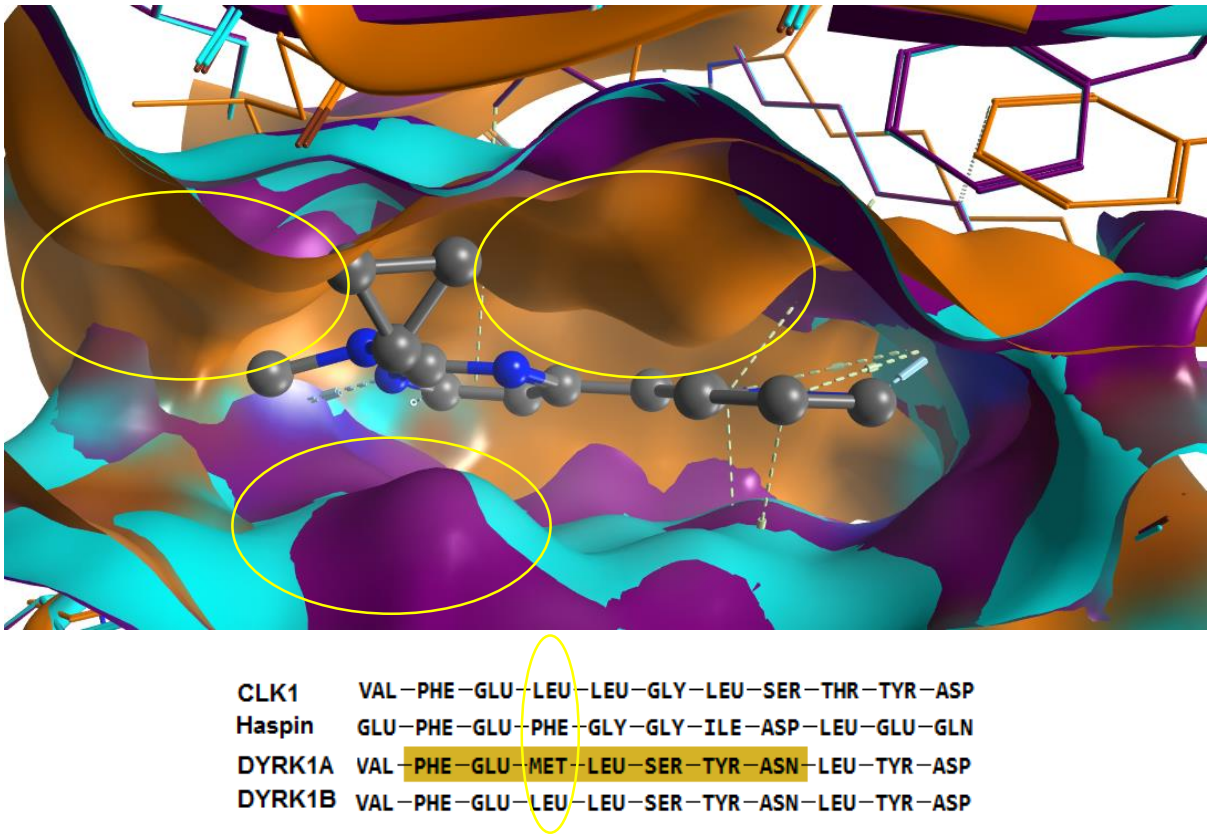

Figure 61. Overlay of surface representations of DYRK1A (cyan), DYRK1B homology model (purple) and CLK1 (orange); potential areas for directing substituents to cause steric clashes with off-targets circled in yellow. Crystal structure of CLK1 (PDB 5J1V). In-house crystal structure of DYRK1A. Homology model built using DYRK1B primary amino acid sequence and homology Builder in MOE 2016, CCG with Amber10:EHT force field.

As Met240 represented a potential selectivity handle for DYRK1A, the nature of the residue and the types of ligands that are preferred in close proximity to methionine residues became of interest. The Protein Data Bank (PDB) and Cambridge Structural Database (CSD) were searched with CSD-CrossMiner for all ligands that were orientated no more than 3 Å away from a methionine residue. All of the resulting protein-ligand structures were then inspected for reoccurring functional groups and motifs directed towards methionine residues. Broadly, it appeared that lipophilic groups were favoured close to methionine. C*H*-arene and CH_2-methylene interactions with methionine residues were well represented. A recent review summarises all of the interactions that methionine residues are believed to make in protein-ligand complexes.[259] It was envisaged that incorporation of a cyclic amine onto the pyrazolo[1,5-*b*]pyridazine series would orientate a CH_2-methylene close to Met240. The cyclic group may circumvent both the size issue and metabolic stability issues observed in previous analogues, as *N*-dealkylation may be less prevalent.

The ligand in the co-crystal structure of **96** bound to DYRK1A was modified using MOE Builder and minimised using Amber10:EHT force field. This gave a prediction of binding mode prior to synthesis. Cyclobutyl, cyclopentyl and cyclohexyl analogues were considered first. No change in binding mode was observed. All cyclic analogues appeared as though they would be accommodated within the binding site of DYRK1A. The angle and orientation of the C*H*$_2$-methylene functionality appeared to be most similar to that of the dimethyl group in the cyclopentyl and cyclohexyl analogues.

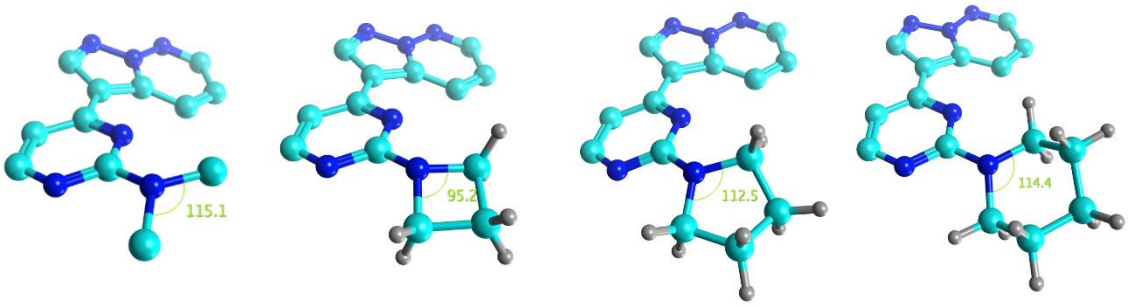

Figure 62. Cyclic amine analogues were modelled into the DYRK1A ATP site using the Builder tool in MOE and minimised. Bond angles calculated using MOE 2016, CCG with Amber10:EHT force field.

5.4.2. Synthesis of Small Cyclic Analogues

Small cyclic amines were easily installed using the same chemistry as developed previously (Chapter 4 and 5). Beginning from **77**, the desired product was rapidly furnished *via* nucleophilic aromatic substitution with appropriate cyclic amine.

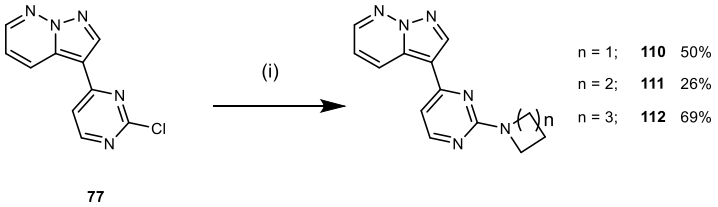

Scheme 18. *Reagents and conditions:* (i) cycloalkyl amine, 2-propanol, 140 °C, 5 h or 22 min, 140 °C, µwave.

5.4.3. SARs and Biological Evaluation of 110 – 112

DYRK1A binding affinity, LE and LipE are displayed in Table 29. **96** is included for convenient comparison. Solubility and metabolic stability was also determined to assess whether cyclic amine analogues overcame the issues exhibited by **96** and **98**.

Installation of a cyclic amine coincided with a reduction in DYRK1A binding affinity. Surprisingly, the cyclopentylamine analogue, **111**, appeared to be most detrimental despite being in between

the size of **110** and **112**. This decline in affinity could have been due to the insolubility of the compound. It could not be explained with molecular modelling why **110** and **112** inhibited DYRK1A, but **111** did not. However, **111** showed a marked improvement in metabolic stability data for both HLM and RLM compared to **96**. This result served as evidence that metabolic stability could be positively modulated by appending cyclic amines to the pyrimidine of the series. It followed that if DYRK1A binding affinity and solubility could be improved then the current strategy may afford improved DYRK1A molecular probes compared to **96**.

Table 29. DYRK1A Binding Affinity of 110-112

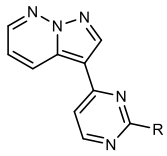

Compound	R	DYRK1A IC_{50}	LE, LipE	HLM (µL/min/mg)	RLM (µL/min/mg)	Solubility (mg/mL)
96		75[a]	0.56, 5.5	241.8[b] +/- 31.7	230.1[b] +/- 30.8	0.1
110		461[a]	0.47, 4.8	224.1[b] +/- 2.2	84.1 +/- 3.4	0.02
111		1377[a]	0.41, 3.8	61.7[b] +/- 13.4	37.1 +/- 16.1	0
112		478[a]	0.42, 3.9	245.8[b] +/- 7.9	904.7 +/- 75.5	0.02

[a]IC_{50} (nM) in TR-FRET-based ligand-binding displacement assay (n = 1). LE = 1.4(pIC_{50})/non-hydrogen atoms; LipE = pIC_{50} – clog P. HLM and RLM Determinations mean of n =2 +/- standard deviation (unless otherwise stated).[b]Mean of n = 4 +/- standard deviation. HLM = human liver microsomes; RLM = rat liver microsomes; thermodynamic solubility data derived from single experiment at pH 6.8.

It was envisaged that additional heteroatoms in the cyclic rings of the substituents may modulate the metabolic stability and solubility.

5.4.4. Synthesis of 113-115

Small cyclic amines were installed using the same chemistry as described previously. It was found that microwave heating facilitated rapid nucelophilic aromatic substitution. A number of cyclic amines (i.e. piperidine) were installed rapidly (22 min) and in high yield.

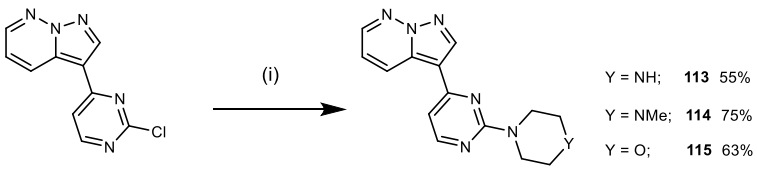

77

Scheme 19. *Reagents and conditions:* (i) cycloalkyl amine, 2-propanol, 140 °C, 5 h or 22 min, 140 °C, µwave

5.4.5. SARs and Biological Evaluation of 113 – 115

DYRK1A binding affinity, LE and LipE for **113**-**115** is are presented in Table 30. **112** is included for comparison.

Evaluation of the solubility and metabolic stability data of **112** with that of **113** - **115** showed that both of these properties were improved when a heteroatom was added to the cyclic ring. DYRK1A binding affinity for **113** was improved relative to **112**, however **113** was too weak a ligand to be considered as a DYRK1A molecular probe, and so was not progressed further.

Table 30. DYRK1A Binding Affinity of 113-115

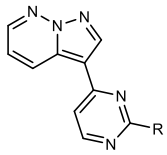

Compound	R	DYRK1A IC_{50}	LE, LipE	HLM (µL/min/mg)	RLM (µL/min/mg)	Solubility (mg/mL)
112		478[a]	0.42, 3.9	245.8[b] +/- 7.9	904.7 +/- 75.5	0.02
113		312[a]	0.43, 5.1	74.7[b] +/- 6.7	51.8 +/- 2.3	0.08
114	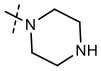	594[a]	0.42, 6.4	1.5 +/- 0.5	30 +/- 7.9	1.28
115	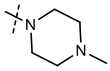	962[a]	0.38, 4.9	11.4[b] +/- 7.1	236.8 +/- 7.4	1.20

[a]IC_{50} (nM) in TR-FRET-based ligand-binding displacement assay (n = 1). LE = 1.4(pIC_{50})/non-hydrogen atoms; LipE = pIC_{50} – clog P. HLM and RLM Determinations mean of n =2 +/- standard deviation (unless otherwise stated).[b]Mean of n = 4 +/- standard deviation. HLM = human liver microsomes; RLM = rat liver microsomes; thermodynamic solubility data derived from single experiment at pH 6.8.

Limited exploration of the substituent appended to the pyrimidine and directed towards the solvent-exposed region afforded DYRK1A ligands with improved solubility and metabolic stability compared to those previously synthesised. However, the ligands synthesised did not possess high enough binding affinity for DYRK1A to be further investigated as molecular probes. Additional exploration of the substituent directed towards the solvent-exposed region was still thought to be a valid route to furnish higher affinity and selective DYRK1A ligands with improved solubility and metabolic stability.

5.5. Structure-based Design of Selective and High Affinity Binders of DYRK1A

5.5.1. Rationale

At this stage in the project multiple co-crystal structures of the pyrazolo[1,5-*b*]pyridazine series had been produced. Rational design rather than a combinatorial approach was taken in the hope of utilising the structural information whilst streamlining the number of compounds needed to be made.

Nucleophilic aromatic substitution was carried out between 300 cyclic amines from an in-house library and intermediate **77** *in silico* using MOE library enumeration. The enumerated virtual library was subjected to KNIME® medicinal chemistry workflows designed to remove compounds that (i) were not 'rule of 5' compliant; (ii) possessed toxicophores; (iii) were predicted to have poor solubility (clogS) and; (iv) had CNS MPO score < 4. Compounds that passed through the workflows were docked into an in-house crystal structure of DYRK1A. Induced-fit docking in MOE with Amber10:EHT force field was used to bias the results towards compounds that were predicted to bind to DYRK1A in the same fashion as **96**. Compounds that docked successfully were synthesised and tested for biological activity. The docking models generated were superimposed with the crystal structures of off-target kinases. This allowed for the manual inspection of prospective inhibitors to indicate compounds that may be more selective. An overview of the method is depicted in Figure 63.

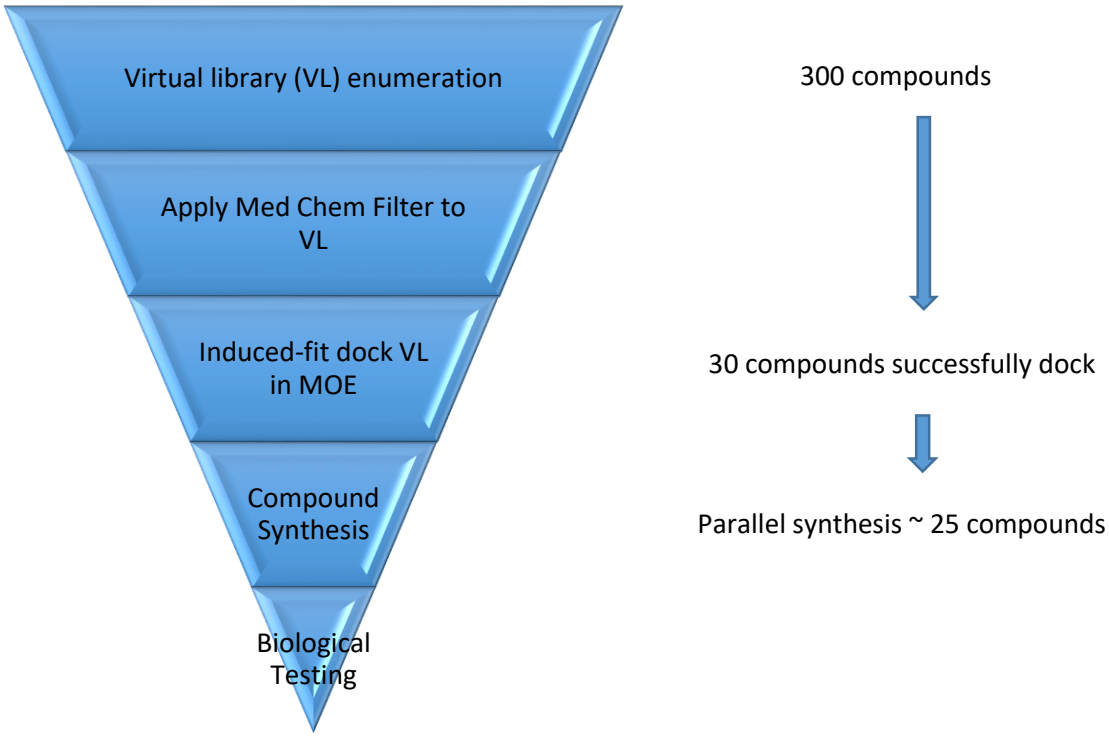

Figure 63. Overview of *in silico* method used to design DYRK1A kinase inhibitors. VL enumeration with library enumeration tool and induced-fit docking performed in MOE 2016, CCG with Amber10:EHT force field. KNIME® Med Chem filters used ChemAxon nodes and are described in more detail in Chapter 1.3.

Molecules that were high affinity ligands of DYRK1A in the primary biological assay were processed through another KNIME® workflow that was used to predict oral bioavailability and CNS penetration.

5.5.2. Synthesis of Enumerated and Docked Virtual Library

Synthesis of intermediate **120** followed the literature procedure.[251] In short, the treatment of **116** with hydroiodic acid afforded **117**. Sonogashira coupling of **117** with TMS-acetylene followed by desilylation with potassium fluoride furnished **118**. Base mediated 1,3-dipolar cycloaddition upon treatment of **118** with 1-aminopyridazinium iodide (**74**) provided **119**. *m*-CPBA oxidation of **119** yielded the corresponding sulfone **120**. An additional batch of **120** was synthesised *via* an alternative route, whereby **76** was reacted first with thiourea and then sodium methoxide to furnish **119**. Usual *m*-CPBA oxidation then afforded **120**.

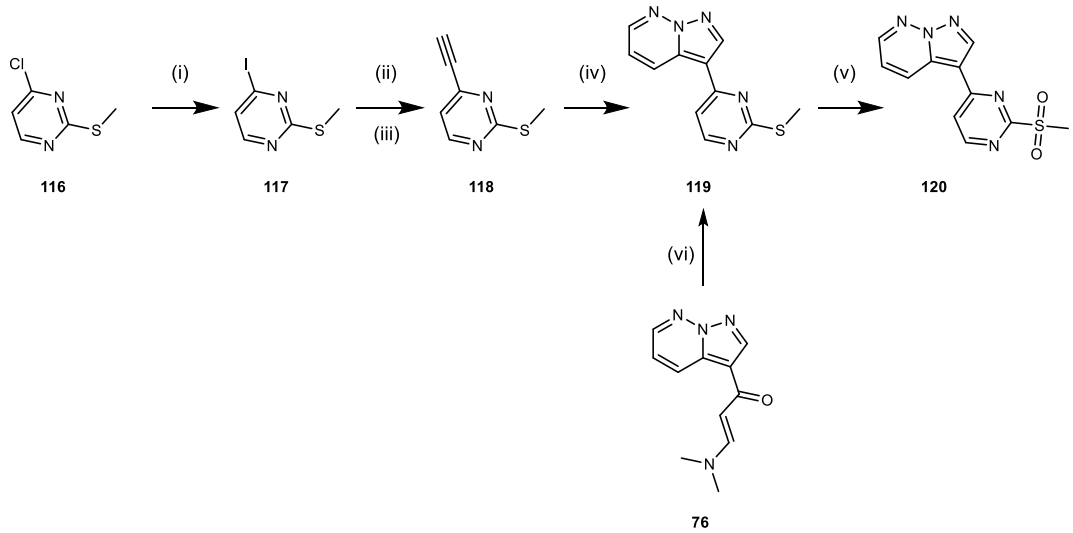

Scheme 20. *Reagents and conditions:* (i) HI, rt, 24 h, 94%; (ii) (trimethylsilyl)acetylene, bis(triphenylphosphine)palladium(II) dichloride, copper iodide, THF, TEA, 50 °C, 1 h; (iii) potassium fluoride, rt, 1 h, 29%; (iv) 1-aminopyridazinium iodide, KOH, CH_2Cl_2, rt, 14 h, 51%; (v) *m*-CPBA, CH_2Cl_2, 67%; (vi) thiourea, sodium methoxide, 1-butanol, 90 °C, 16 h then iodomethane, 30 °C, 4h, 27%.

Utilising either **120** or **77** as intermediates in the final step, cyclic amines were installed using the same nucleophilic aromatic substitution as developed previously (Chapters 4 and 5) to furnish the desired products rapidly.

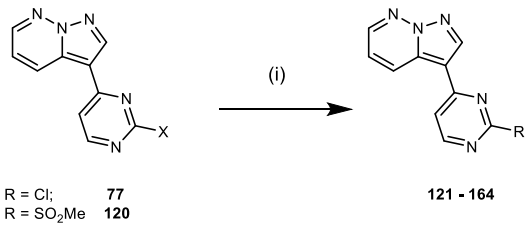

Scheme 21. *Reagents and conditions:* (i) cycloalkyl amine, 2-propanol, 140 °C, 16-96 h.

5.5.3. SARs and Biological Evaluation of Enumerated Library

DYRK1A binding affinity, LE and LipE of **121** - **164** are presented in Table 31.

As a result of using the predictive medicinal chemistry filters mentioned previously, all compounds are in the right physicochemical space for CNS penetration, exhibiting CNS MPO scores > 4.5. All molecules possess Mwt < 500 and are 'rule of 5' compliant.

In general molecules bearing substituents with smaller ring sizes (4 or 5 carbon atoms) showed greater DYRK1A binding affinity than larger rings (> 5 carbon atoms). There are DYRK1A inhibitors presented in Table 31 with more molecular complexity than the dimethyl lead, **96**.

Hence it is possible that selectivity for these analogues may be improved, in addition to metabolic stability and solubility.

Table 31. DYRK1A Binding Affinity of 121 - 164

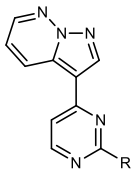

Compound	R	DYRK1A IC_{50}[a]	LE, LipE	Mwt	CNS MPO score[b]
121		370	0.43, 4.4	284.29	6.0
122		510	0.4, 5.2	294.31	6.0
123		80	0.45, 5.8	294.31	6.0
124	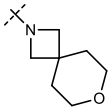	1299	0.34, 4.2	322.36	6.0
125		110	0.46, 4.5	280.33	5.8
126		190	0.43, 4	294.35	5.6
127	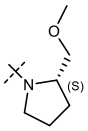	384	0.39, 4.4	310.35	6.0
128	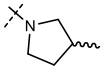	206	0.45, 4.3	280.33	5.8
129	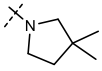	425	0.41, 3.6	294.35	5.6
130	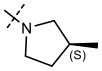	114	0.46, 4.6	280.33	5.8
131	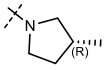	149	0.46, 4.4	280.33	5.8
132	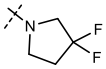	259	0.42, 4.2	302.28	5.8
133	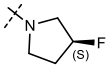	185	0.45, 5	284.29	6.0
134	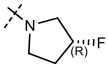	66	0.48, 5.4	284.29	6.0
135	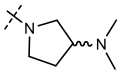	244	0.4, 6.6	309.37	5.5
136	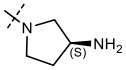	134	0.46, 8.4	281.32	4.9

137	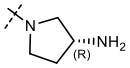	72	0.48, 8.7	281.32	4.9
138	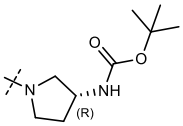	282	0.33, 4.3	381.43	5.3
139		797	0.43, 4.6	268.27	6.0
140		310	0.43, 4.7	278.32	6.0
141	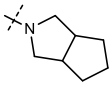	1236	0.36, 3.2	306.37	5.6
142	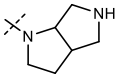	1655	0.35, 7.3	307.35	4.8
143	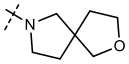	270	0.38, 4.9	322.36	6.0
144		2846	0.35, 4.1	294.31	6.0
145	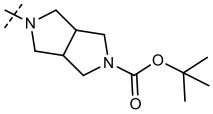	3087	0.26, 3.4	407.47	5.6
146	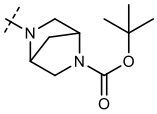	2506	0.27, 3.2	393.44	5.6
147	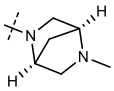	6144	0.32, 4.2	307.35	6.0
148	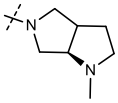	2063	0.33, 5.5	321.38	5.6
149	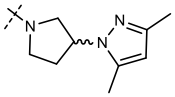	2765	0.29, 3.4	360.42	5.9
150	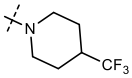	475	0.35, 3.3	348.33	5.5
151	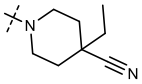	645	0.35, 3.4	333.39	5.6
152	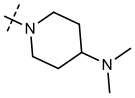	634	0.36, 6.9	323.4	5.1
153	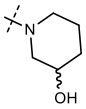	310	0.41, 5.1	296.33	5.8
154	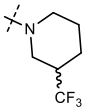	394	0.36, 3.2	348.33	5.3
155	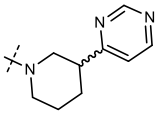	301	0.34, 4.3	358.4	5.9

156	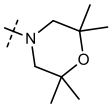	1944	0.32, 2.9	338.41	5.6
157	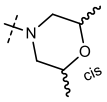	279	0.4, 4.3	310.35	5.9
158	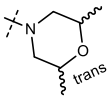	508	0.38, 4.1	310.35	5.9
159	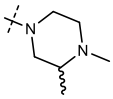	1352	0.36, 4.5	309.37	6.0
160	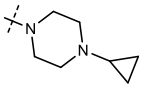	668	0.36, 4.6	321.38	6.0
161	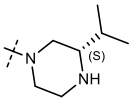	631	0.36, 5.5	323.4	5.3
162	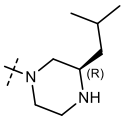	307	0.36, 5.2	337.42	5.4
163	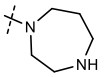	1300	0.38, 6.8	295.34	5.1
164		3363	0.33, 3.5	308.34	6.0

[a]IC_{50} (nM) in TR-FRET-based ligand-binding displacement assay (n = 1). LE = 1.4(pIC_{50})/non-hydrogen atoms; LipE = pIC_{50} – clog P.[b]CNS MPO score calculate with KNIME® workflow with ChemAxon nodes.

123 and single enantiomers **134** and **137** were the only inhibitors with DYRK1A IC_{50} < 100 nM. Inhibitors with LE > 0.45 (**123**, **125**, **128**, **130**, **131**, **133**, **134**, **136** and **137**) were selected for further profiling. The majority of these compounds bore a decorated cyclopentylamine moeity.

The metabolic stability and solubility of compounds with LE > 0.45 are displayed in Table 32. Lead compound **96** has been included for reference.

Solubility and microsomal stability (HLM, RLM) exhibited by primary amines **136** and **137** is superior to **96**. *R*-enantiomer **137** exhibits stronger binding affinity, improved metabolic stability and is 2 fold more soluble than the *S*-enantiomer **136**. Oxetane **123** displays a good balance of microsomal stability (HLM, RLM) and solubility. Taking an overview of the data in Table 32, it appears as though molecules with polar motifs are better tolerated in terms of microsomal stability and solubility. Inhibitors that bear a lipophilic moiety (**130**, **131, 133** and **134**) tend to be metabolised more rapidly and exhibit reduced solubility.

Table 32. Compounds with highest binding affinity for DYRK1A from Library Enumeration

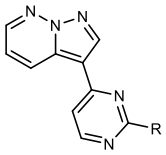

Compound	R	DYRK1A IC_{50}[a]	LE, LipE	HLM (µL/min/mg)	RLM (µL/min/mg)	Solubility (mg/mL)
96		75	0.55, 5.5	241.8[b] +/- 31.7	230.1[b] +/- 30.8	0.1
123		80	0.45, 5.8	125.6 +/- 9.3	118.6 +/- 5.5	0.06
125		110	0.46, 4.5	328.1 +/- 25.2	928.9 +/- 116.0	0.01
136	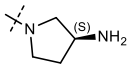	134[a]	0.46, 8.4	199.1[c]	48.2 +/- 22.8	1.92
137	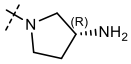	72[a]	0.48, 8.7	40[c]	65.5 +/- 24.4	4.37
130	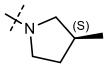	114	0.46, 4.6	378.1 +/- 66.0	448.1 +/- 19.9	0.02
131	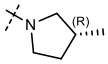	149	0.46, 4.4	389 +/- 23.3	184 +/- 18.0	0.05
133	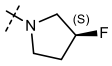	185	0.45, 5	320.5 +/- 10.7	251.2 +/- 6.1	0.04
134	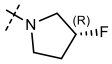	66	0.48, 5.4	295.7 +/- 14.0	129.7 +/- 16.7	0.04

[a]IC_{50} (nM) in TR-FRET-based ligand-binding displacement assay (n = 1). LE = 1.4(pIC_{50})/non-hydrogen atoms; LipE = pIC_{50} – clog P. HLM and RLM Determinations mean of n =2 +/- standard deviation (unless otherwise stated).[b]Mean of n = 4 +/- standard deviation. [c]Data derived from single experiment. HLM = human liver microsomes; RLM = rat liver microsomes; thermodynamic solubility data derived from single experiment at pH 6.8.

Compounds with DYRK1A IC_{50} < 100 nM were profiled in a 468 kinase panel to assess kinome-wide selectivity. **123**, **125**, **130**, **131**, **134**, **136** and **137** were assayed in the KINOMEscan® platform provided by DiscoveRx, a proprietary active-site directed competition binding assay. The results that were returned at the time of writing are displayed as TREEspot™ diagrams in Figure 64.

125

468 Assays Tested
2 Interactions Mapped
S-Score(40) = 0.01

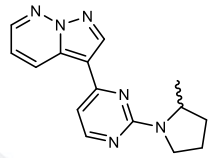

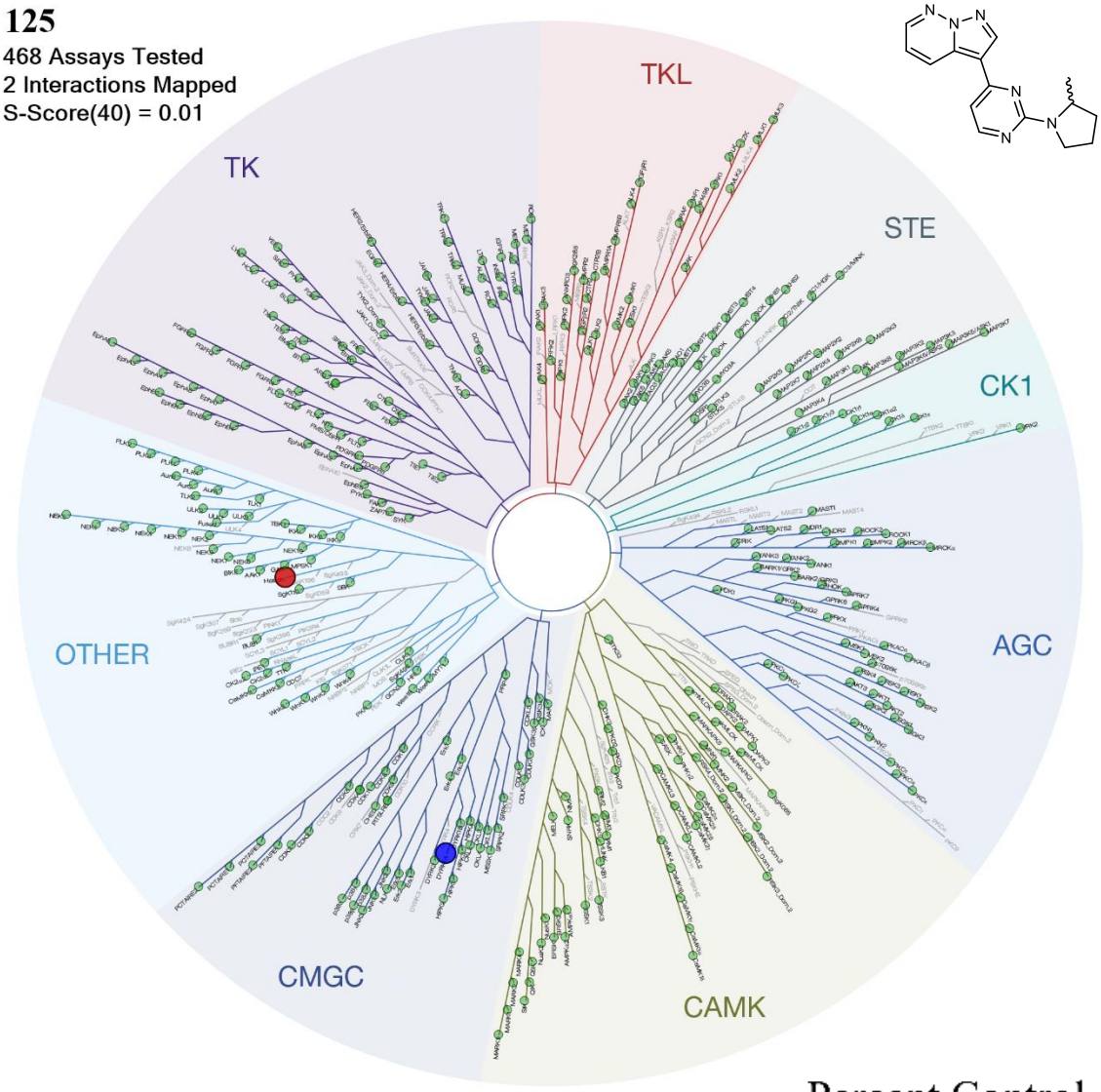

Percent Control

- 0%
- 0.1%
- 0.1-1%
- 1-5%
- 5-10%
- 10-35%
- >40 %

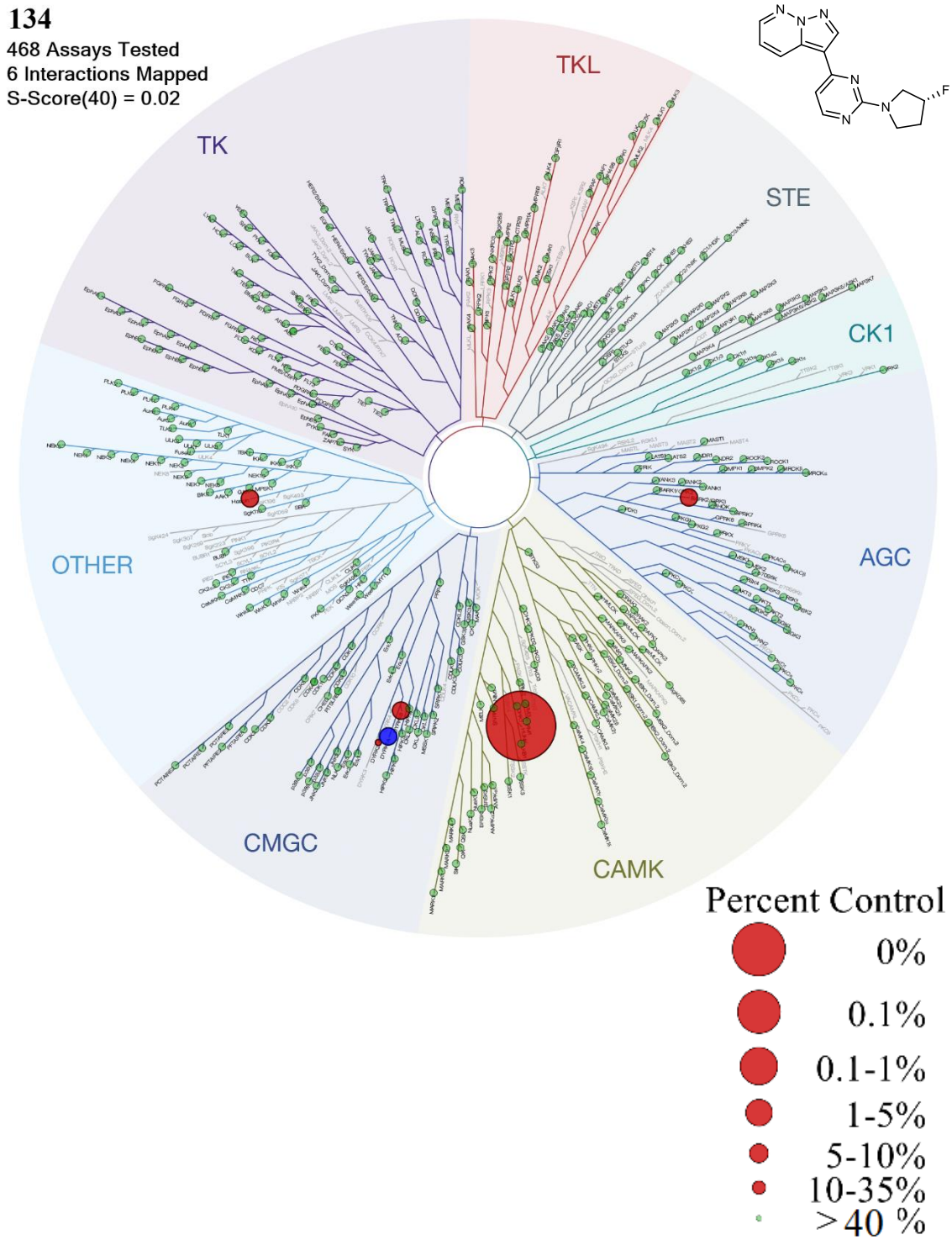

Figure 64. KINOMEscan® Treespot™ maps for **125** (top) and **134** (bottom). DYRK1A is highlighted in blue. Image generated using TREEspot™ Software Tool and reprinted with permission from KINOMEscan®, a division of DiscoveRx Corporation, © DISCOVERX CORPORATION 2010.

125 and **134** maintained the high levels of kinome-wide selectivity, comparable to that of **96**. Selectivity data showed that cyclopentyl analogues **125** and **134** exhibited higher affinity for

DYRKs than CLKs. The *ortho*-methyl group of **125** afforded selectivity over DYRK1B and the CLKs, whereas the *meta*-fluoride substituent (**134**) did not afford selectivity over DYRK1B. **125** and **134** also possess high binding affinity for haspin, consistent with most other exemplars in the pyrazolo[1,5-*b*]pyridazine series.

Table 33. Overview of kinome selectivity profiles of 125 and 134

Compound	Percentage kinases inhibited > 75%[a]	Percentage kinases inhibited > 50%[a]	Kinases most potently inhibited
125	0.2	1.5	Haspin, PI3K, ALK, TAOK3
134	0.9	1.5	Haspin, DYRK1B, HUNK, GRK3, DYRK2

[a] % Inhibition as determined by DiscoveRx KINOMEscan® experiment.

125 represents one of the most selective DYRK1A ligands discovered to date, with comparable selectivity to **89**, **96** and **98**.

5.6. Summary

The physicochemical properties, solubility and metabolic stability of **89** and **90** were sub-optimal for use as *in vivo* tool compounds (Chapter 4). Multiparametric optimisation of this class of pyrazolo[1,5-*b*]pyridazines was pursued. The binding mode of the pyrazolo[1,5-*b*]pyridazine series was elucidated with the production of the first co-crystal structure of **88** bound to DYRK1A. The co-crystal structure provided a platform for SBDD. Reduction in aromatic ring count and clog P were attempted whilst the selectivity and DYRK1A affinity profiles of inhibitors **89** and **90** were improved. This resulted in a number of potential candidates, **96** and **98**, which may be used as a molecular probe of DYRK1A. **96** fulfilled most of the criteria set out at the start of the DYRK1A project for use as a molecular probe. Due to the slightly higher rate of metabolism exhibited by **96** it was decided that further optimisation should be undertaken. Further inhibitors were designed and modelled *in silico* prior to synthesis to ensure that the correct chemical space for a CNS kinase molecular probe was being explored. A number of molecules inhibited DYRK1A with IC_{50} < 100 nM, exhibited good selectivity and had metabolic stability, that on balance, were superior to **96**. The full set of selectivity results for **123**, **130**, **131**, **136** and **137** are still being awaited, but given the promising selectivity profiles of **125** and **134**, it is likely that this class of DYRK1A ligands will all be very selective.

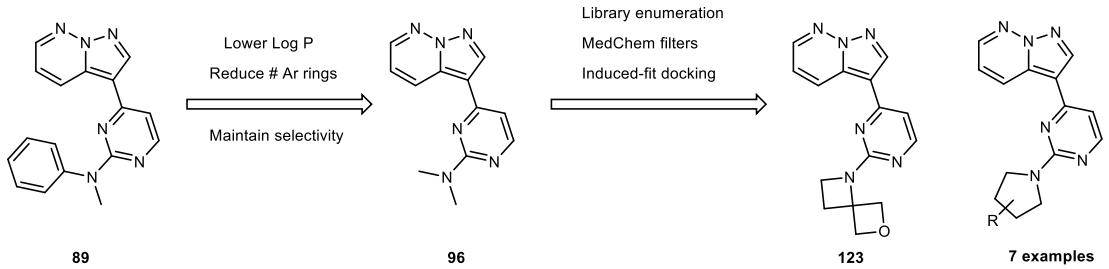

Figure 65. Overview of DYRK1A Inhibitor Development.

Thus far, only the solvent-exposed region of DYRK1A had been explored for gains in selectivity. Gains in kinome-wide selectivity had already been achieved, the only other kinases inhibited by the series were the CLKs and other DYRKs. Perhaps small changes to the pyrimidine or pyrazolo[1,5-*b*]pyridazine head would lead to improved selectivity and potency for DYRK1A. These small changes may also lead to less metabolism if metabolic 'soft-spots' could be identified and blocked.

CHAPTER 6. Structure-enabled Design of DYRK-selective Pyrazolo[1,5-*b*]pyridazines: Part II

Chapter 6 describes the focussed exploration around the pyrimidine motif of the pyrazolo[1,5-*b*]pyridazine series. Specific hypotheses are tested; lipophilic- and halogen-π interactions with the phenylalanine gatekeeper of DYRK1A are investigated with 5-substituted pyrimidines. Scaffold hopping from the pyrimidine to the corresponding pyridine and triazine heterocycles is investigated as a means of delivering a higher affinity, selective and soluble pyrazolo[1,5-*b*]pyridazine analogue with improved metabolic stability.

6.1. Investigation of 5-substituted Pyrimidine Analogues

6.1.1. Rationale

Investigating the kinetics of inhibitor binding and the concept of achieving kinetic selectivity for targets with similar binding constants is becoming a hot topic in kinase drug discovery.[260,261] Kinetic selectivity is when an inhibitor has a prolonged residence time at the target of interest, caused by stabilising interactions, and has rapid dissociation at off-targets.[262] Recently it was shown that residence time of an inhibitor can be significantly increased through halogen-aromatic π interactions established between an aromatic gatekeeper residue and the halogen atom of an inhibitor.[263] As DYRK1A possesses a phenylalanine gatekeeper and the binding site environment must be subtly different from the series' off-targets given the subtle differences already observed in selectivity for inhibitors in the pyrazolo[1,5-*b*]pyridazine series, it was envisaged that adding a range of halogen atoms to the 5-position of the pyrimidine ring may establish halogen-aromatic π interactions that could translate into improved binding affinity and kinetic selectivity.

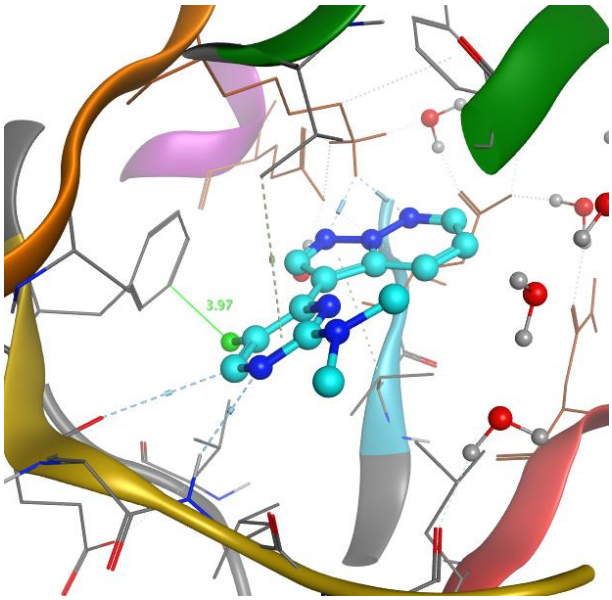

Figure 66. Speculative Halogen-aromatic π interaction modelled in DYRK1A in-house crystal structure. Structure modelled with Builder tool in MOE 2016, CCG with Amber10:EHT force field.

It had been established that a number of analogues in the pyrazolo[1,5-*b*]pyridazine series suffered from sub-optimal metabolic clearance. The 3A4 P450 Site of Metabolism workflow in Schrodinger Maestro 11 combines induced-fit docking to determine whether the molecule can access the reactive heme centre of the P450 enzyme and a rule-based approach to intrinsic reactivity. Atomic reactivity is predicted with a linear free energy approach based on the Hammett and Taft scheme where reactivity of a given atom is the sum of a baseline reactivity rate and a series of perturbations determined by connectivity. Using the workflow, the 5-position of the pyrimidine, in addition to the dimethyl motif, was identified as being susceptible to attack by P450 enzymes. It was envisaged that positioning a fluorine or a trifluoromethyl motif at the 5-position may block metabolism.

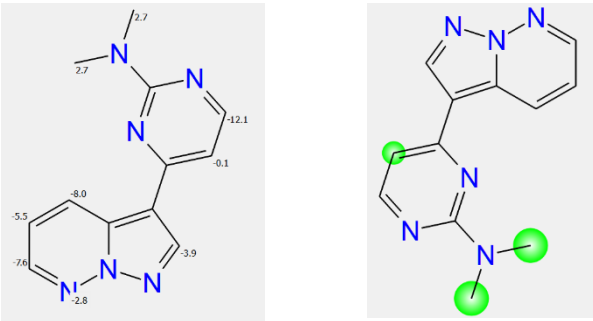

Figure 67. P450 Site of Metabolism calculation in Schrodinger Maestro 11 – (LHS) Intrinsic reactivity; (RHS) Overall SOM (Site of Metabolism) Score using OPLS3 force field.

All of the co-crystal structures produced with the pyrazolo[1,5-*b*]pyridazine series bound to DYRK1A appeared to show the presence of an aromatic CH-O hydrogen bond to the kinase hinge from the proton at the 6-position of the pyrimidine. It was theorised that by making this interaction stronger by increasing the acidity of the C-*H*, potency for DYRK1A may be increased. Thus, appending electron-withdrawing substituents onto the 5-position of the pyrimidine may lead to a more acidic C-*H* bond donor.

Molecular pre-organisation prior to binding, and subtle differences in inhibitor orientation can translate to large increases in binding affinity and improved *in vitro* PK. Small molecule x-ray crystal structures of exemplars from the pyrazolo[1,5-*b*]pyridazine series and all of the inhibitors co-crystallised with DYRK1A had the same overall conformation and orientation, suggesting that there was an intrinsic preference for inhibitor orientation. Adding a fluorine to the 5-position of the pyrimidine may establish an intramolecular interaction between the pyrazolo[1,5-*b*]pyridazine and pyrimidine, which could cause an alteration in the relative orientation of the heterocycles with respect to each other. These subtle differences may bring about unforeseen improvements in potency, selectivity and *in vitro* PK.

6.1.2. Synthesis of 5-substituted Pyrimidine Analogues

It was envisaged that the shortest synthetic route to access 5-substituted pyrimidine analogues was to form a carbon-carbon bond between a boronic acid or ester of the pyrazolo[1,5-*b*]pyridazine and the corresponding 5-substituted halopyrimidine *via* a Suzuki cross-coupling reaction.

The first challenge was to construct the pyrazolo[1,5-*b*]pyridazine boronate building block as there was no literature procedure for its preparation. 1,3-dipolar cycloaddition was carried out with methyl propiolate and intermediate **74** to afford the methyl ester of the pyrazolo[1,5-*b*]pyridazine **165** in low yield.

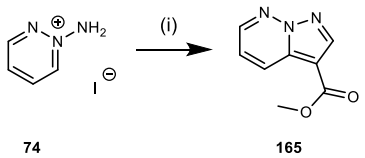

Scheme 22. *Reagents and conditions:* (i) methyl propiolate, potassium carbonate, CH_2Cl_2, rt, 16 h, 36%.

An interesting observation was made during attempts to optimise the 1,3-dipolar cycloaddition. High yields were difficult to achieve and impossible to repeat. The strength of base, reaction time and reaction solvent all affected the yield obtained. One reason for the low yields obtained

was encountered during the work-up procedure; liquid-liquid extraction consistently produced a dichloromethane-potassium hydroxide emulsion that was difficult to separate. Work-up with ethyl acetate also produced an emulsion. Yields were improved by washing the reaction mixture through with dichloromethane rather than shaking with organic solvent.

LCMS of the reaction mixture often showed a major component with m/z 178 $(M+H)^+$, consistent with the desired product. However, other significant components were also present with m/z 180 and m/z 291. The crude ^{1}H NMR of the reaction mixture appeared to show consumption of the aminated pyridazine **74** (signals present in Figure 68 - A) and appearance of desired product **165** (signals present in Figure 68 - C) plus at least one other component.

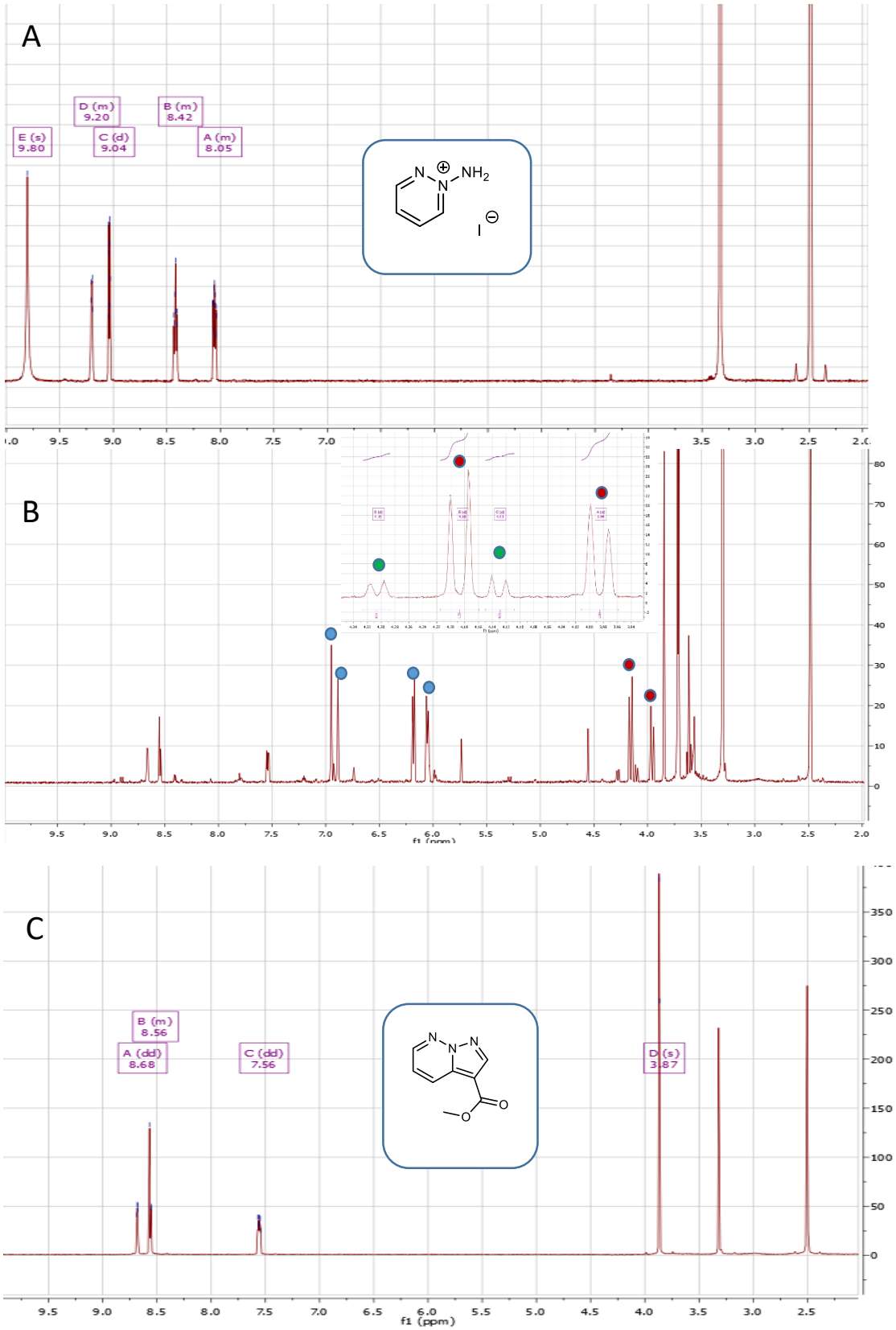

Figure 68. A – ^{1}H NMR of **74;** B – ^{1}H NMR of Crude Reaction Mixture; C – ^{1}H NMR of Methyl Ester Product **165**.

Inspection of the ^{1}H NMR of the crude reaction mixture (Figure 68 - B) shows that the starting material **74** (Figure 68 – A) has been fully consumed. One possibility is that deamination of **74** has occurred under the reaction conditions to regenerate pyridazine.

A second possibility is that the cycloaddition, rather than being a one-step concerted process, is a two-step cycloaddition that has stalled at the first addition intermediate. The four protons (blue dots) between δH 7.00 – 6.00 ppm are likely to correspond to pyridazine-type protons and the two protons (red dots) at δH 4.35 – 3.95 ppm are consistent with an alkene functional group. It is possible that these protons (blue and red dots) belong to one species. Closer inspection of the doublet at δH 3.99 ppm (d, *J* = 15.6 Hz) and doublet at δH 4.18 ppm (d, *J* = 15.6 Hz) are consistent with a pair of *trans* alkene protons (Figure 68 – B). There is also another set of doublets (green dots) at δH 4.31 ppm (d, *J* = 12.0 Hz) and δH 4.13 ppm (d, *J* = 12.0 Hz) which are consistent with *cis* alkene protons. If what has been proposed is correct, the ratio of *trans*:*cis* addition products is 5:1, suggesting that the *trans* addition product is the major species remaining in the reaction mixture. The crude ^{1}H NMR combined with the LCMS data suggests that this 1,3-dipolar cycloaddition is a two-step process with a formal intermediate. Every attempt to isolate the intermediate or side product was unsuccessful. Two-step 1,3-dipolar cycloadditions have been postulated in the past,[264,265] and more recently with the advent of applied quantum chemistry.[266] It is interesting to speculate that the 1,3-dipolar cycloaddition here is a two-step mechanism that may rely on *trans* → *cis* isomerism before ring closure occurs. This would explain the unreacted *trans* isomer being the major component remaining in the reaction mixture.

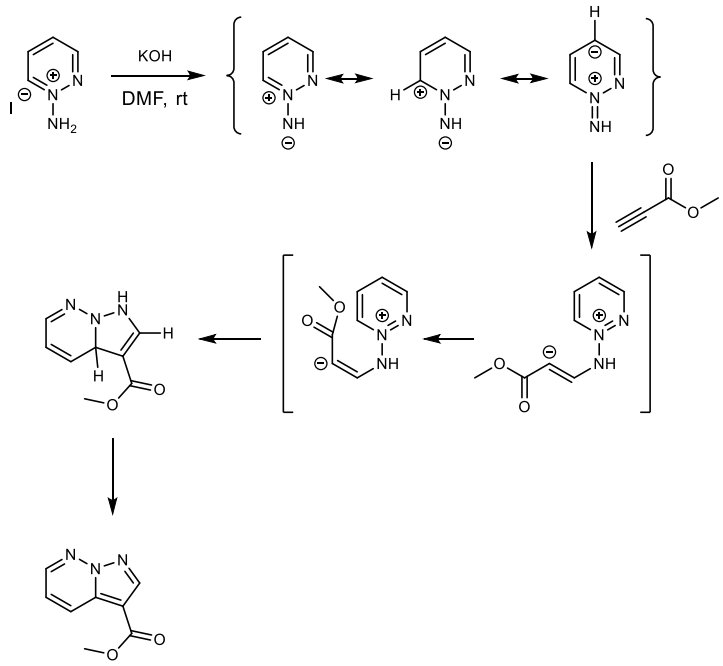

Figure 69. Proposed pathway of two-step 1,3-dipolar cycloaddition.

The synthesis of the boronate intermediate was continued with basic ester hydrolysis of **165** to afford the carboxylic acid derivative **166**. Decarboxylative bromination with *N*-bromosuccinimide furnished bromide **167** in one-step. This facile and greener alternative to the Hunsdiecker-Borodin reaction led to a publication in which the same methodology was extended to a range of other haloheteroarenes.[267] Small molecule x-ray crystallography confirmed beyond all doubt the regioselectivity of the decarboxylative bromination reaction.

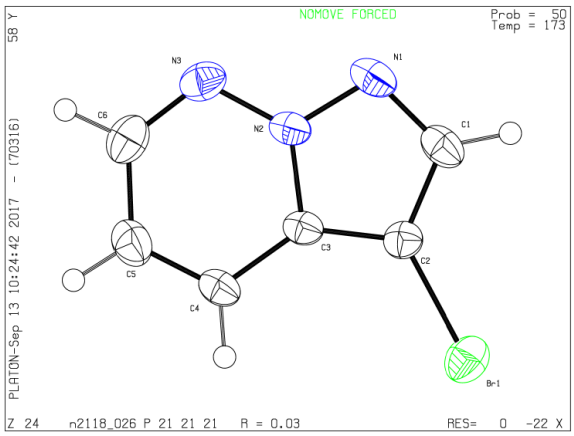

Figure 70. Small molecule x-ray crystallography of **167**.

167 underwent Miyaura borylation to provide the boronic ester **168,** which was used in subsequent C-C cross-couplings *in situ* and without further purification.

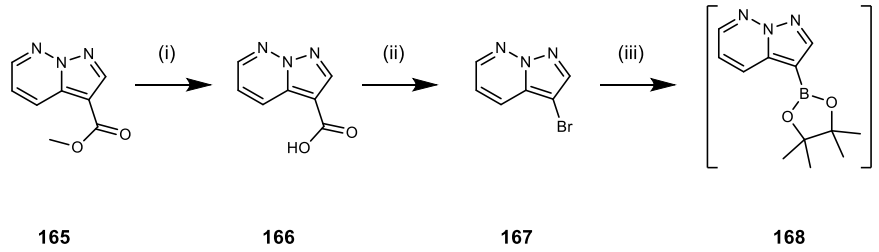

Scheme 23. *Reagents and conditions:* (i) lithium hydroxide, MeOH, rt, 16 h then 1 M HCl, rt, 30 min, 74%; (ii) *N*-bromosuccinimide, DMF, rt, 3h, 78%; (iii) bis(pinacolato)diboron, [1,1′-bis(diphenylphosphino)ferrocene]dichloropalladium(II), complex with CH_2Cl_2, potassium acetate, 1,4-dioxane, 90 °C, 16 h.

Dimethylation of 5-substituted aminopyrimidines was carried out with sodium hydride and excess iodomethane at room temperature to afford pyrimidines **169** and **171**. The resulting halides were reacted with **168** under Suzuki conditions to afford the desired products **170** and **172** in low yield.

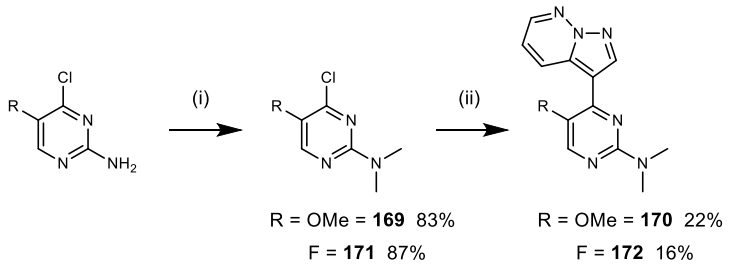

Scheme 24. *Reagents and conditions:* (i) sodium hydride, iodomethane, DMF, rt, 16 h; (ii) **168**, bis[2-(di-*tert*-butylphosphanyl)cyclopenta-2,4-dien-1-yl]iron; dichloropalladium, sodium carbonate, acetonitrile:water (10:1), 140 °C overnight.

Synthesis of analogues **174**, **176** and **178** was carried out in reverse order to that outlined above. The first step was the Suzuki reaction between the boronic ester **168** and required the appropriate 2,4-dichloropyrimidine to afford intermediates **173**, **175** and **177**. Nucleophilic aromatic substitution with dimethylamine furnished the desired products.

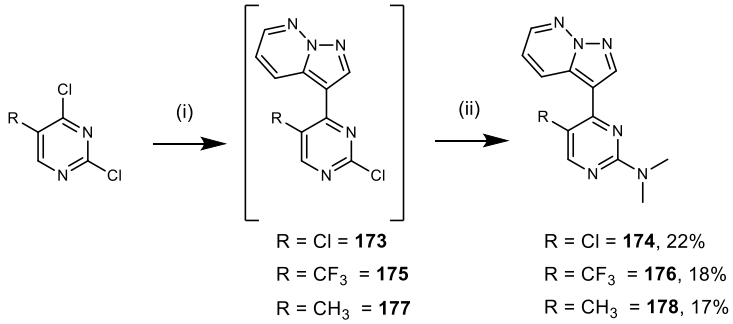

Scheme 25. *Reagents and conditions:* (i) 168, bis[2-(di-*tert*-butylphosphanyl)cyclopenta-2,4-dien-1-yl]iron; dichloropalladium, potassium carbonate, DMF, 60 °C, 1.5 h; (ii) 2 M dimethylamine in THF, 100 °C, 2 h.

An issue with the synthetic procedure described above was that regioselectivity of the Suzuki reaction was not optimal, which was a contributing factor to the low yields observed. During the syntheses of **174**, **176** and **178** regioisomers were formed. Co-elution of regioisomers during reaction purification made it challenging to isolate the desired regioisomer in sufficient purity for biological testing.

Small molecule x-ray crystallography supported ^{1}H NMR experiments to confirm the correct identity of regioisomers. Figure 71 shows the x-ray crystal structure of **174**, proving that the desired regioisomer was isolated.

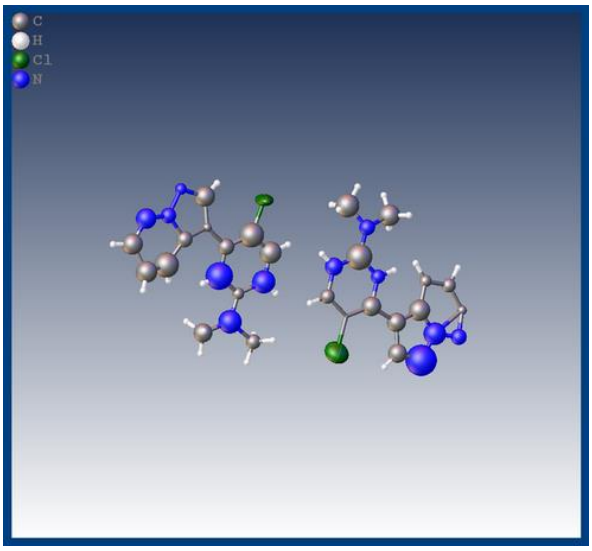

Figure 71. Small molecule x-ray crystallography of 174.

The regioisomer of **178** was isolated and the structure elucidated with ^{1}H NMR and small molecule x-ray crystallography.

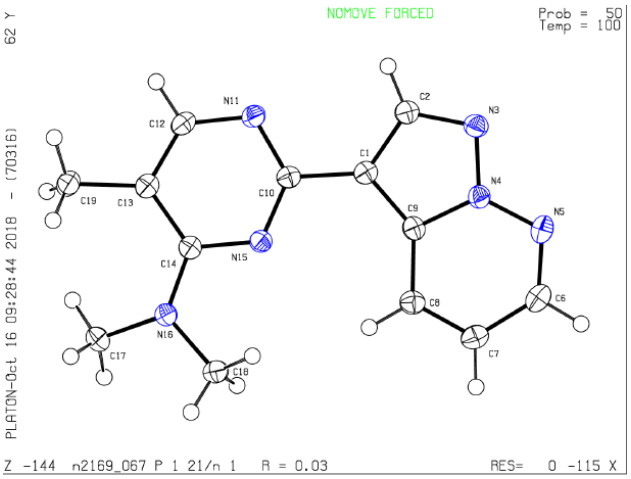

Figure 72. Small molecule x-ray crystallography of regioisomer isolated from synthesis of **178**.

To avoid regioselectivity issues during the Suzuki reaction, electrophilic halogenation on a late-stage 'intermediate' was attempted. **174**, **181** and **183** were all accessed from the same pyrazolo[1,5-*b*]pyridazine **94**. Electrophilic halogenation with *N*-chlorosuccinimide, *N*-bromosuccinimide and *N*-iodosuccinimide at the 5-position, followed by dimethylation of the amino functionality with sodium hydride and iodomethane afforded the desired products.

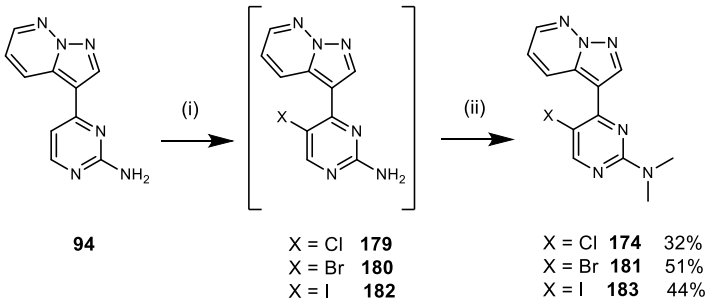

Scheme 26. *Reagents and conditions:* (i) NXS, acetonitrile, rt, 2h; (ii) sodium hydride, iodomethane, THF, rt, overnight.

Electrophilic halogenation of chloride (**77**), methyl sulfone (**120**) and thioether (**119**) late stage intermediates did not afford the desired product under the same reaction conditions.

A more versatile synthetic route was developed that allowed the installation of amines other than dimethylamine to the pyrimidine scaffold. The route is the first example to our knowledge of an organic base promoted 1,3-dipolar cycloaddition with this particular 1,3-dipole, **74**. Utilisation of the organic base DBU and acetonitrile as the reaction solvent allowed for the reaction mixture to be heated to an elevated temperature and permitted a simpler work-up procedure that avoided the formation of a dichloromethane-potassium hydroxide emulsion during liquid-liquid extraction. Installation of the alkyne at the 4-position of the pyrimidine was completed using Sonogashira protocol. Cycloaddition between 1,3-dipolarphile **184** and 1,3-dipole **74** afforded intermediate **185**. Interestingly, **184** underwent silyl deprotection and cycloaddition simultaneously. Subsequent nucleophilic aromatic substitution furnished the desired product, **172**.

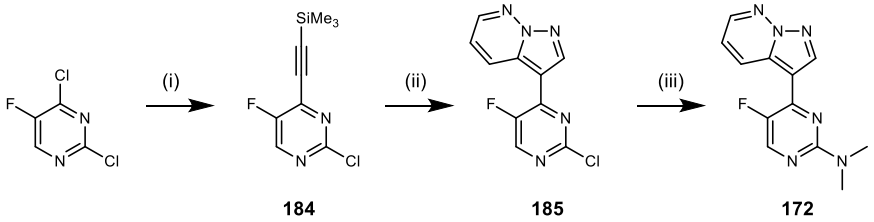

Scheme 27. *Reagents and conditions:* (i) bis(triphenylphosphine)palladium(II) dichloride, copper iodide, TEA, (trimethylsilyl)acetylene, THF, rt, overnight, 42%; (ii) DBU, 1-aminopyridinium iodide, 50 °C, 1 h, 42%; (iii) 2 M dimethylamine in THF, 110 °C, 2 h, 57%.

Other synthetic routes were investigated in an attempt to optimise the synthetic procedure. One approach considered was to form the pyrazolo[1,5-*b*]pyridazine boronate in one step from **74**. A small number of publications have described 1,3-dipolar cycloadditions that employ either ethynyl trifluoroborate[268] or alkynylboronate[269,270] as the dipolarphile. Attempting to replicate the literature procedures but substituting the dipole for **74** did not furnish the pyrazolo[1,5-*b*]pyridazine boronate. Unsuccessful attempts were made to promote the cycloaddition with (i) DBU and acetonitrile and (ii) potassium hydroxide and dichloromethane.

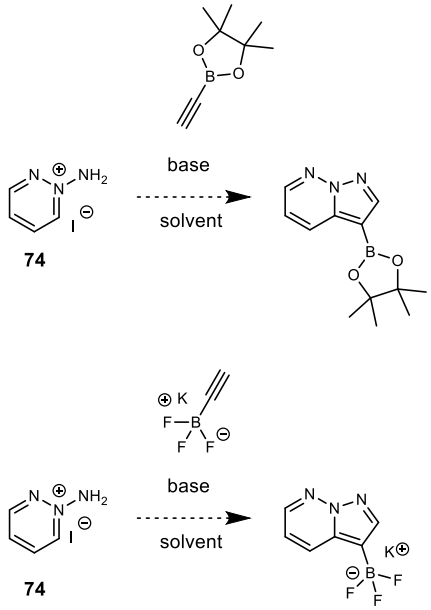

Scheme 28. Synthetic attempts to furnish key intermediate **168** and trifluoroborate analogue in one step.

The postulated mechanism of the 1,3-dipolar cycloaddition involves loss of aromatic mesomerism upon addition to the azomethine imine (Figure 69). There are a limited number of known cycloaddition partners of **74**, those that are known are activated dipolarphiles such as methyl propiolate.[271] Alkynyl boronic esters are electron-deficient dienophiles. Their reactivity is poor and the few literature examples of 3+2 cycloadditions with alkynyl boronic esters require reactive dienes and harsh reaction conditions.[272]

Decarboxylative cross-coupling was also trialled as a means of forming the C-C bond between the pyrimidine and pyrazolo[1,5-*b*]pyridazine motifs. It had been established that carboxylic acid **166** was susceptible to decarboxylation under the right conditions as decarboxylative halogenation had proved facile. A number of recent publications describe blue-light promoted decarboxylative couplings using photoredox catalysis.[273,274,275] Literature procedures adapted to using substrate **166** were trialled using a commercially designed photoreactor, the EvoluChem™ PhotoRedOx Box. A number of reaction conditions were screened but were unsuccessful in furnishing the desired product.

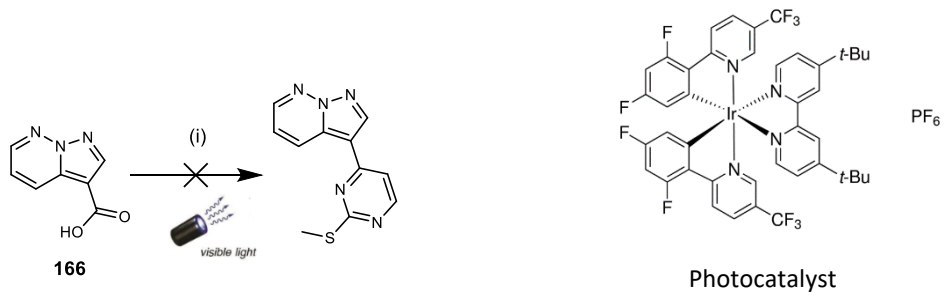

Scheme 29. *Reagents and conditions:* (i) 4-iodo-2-methylsulfanyl-pyrimidine, nickel(II) chloride ethylene glycol dimethyl ether complex, 4,4'-di-*tert*-butyl-2,2'-bipyridyl, $(Ir[dF(CF_3)ppy]_2(dtbpy))PF_6$, DMSO, rt, 16 h. Base = 2-*tert*-butyl-1,1,3,3-tetramethylguanidine or potassium phosphate tribasic or DBU or cesium carbonate. 40W Kessil A 160WE LED lamp.

The major component in all of the reaction mixtures was unreacted **166**. Due to the difficulties in promoting the decarboxylative coupling under the current conditions investigated, the procedure was abandoned at this stage of the project. Blue-light promoted late-stage trifluoromethylations were also explored as a means of installing a trifluoromethyl moiety at the 5-position of the pyrimidine. Late-stage functionalization of final compounds was an interesting concept as it would provide an opportunity for parallel library synthesis and matched-pair analysis, saving time that would have been required for *de novo* compound synthesis. Similar reaction conditions were employed as Macmillan had previously described for the trifluoromethylation of electron deficient heteroarenes.[276]

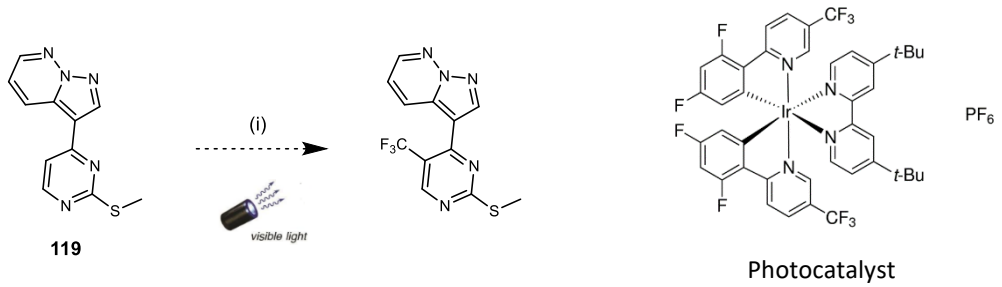

Scheme 30. *Reagents and conditions:* (i) Tris[2-(4,6-difluorophenyl)pyridinato-C2,N]iridium(III), trifluoromethanesulfonyl chloride, dipotassium phosphate, acetonitrile, 40W Kessil A 160WE LED lamp, rt, 16 h.

Approximately 80% of the reaction mixture after 16 h appeared to be unconsumed starting material **119**. However, trifluoromethylation had occurred. Inspection of the LCMS chromatogram showed a minor component with the correct mass for the desired product at Rt 1.17 min with m/z 312.0 $(M+H)^+$. Upon isolation of the minor component it became apparent that two species in a ratio of 2:1 were present. The two species were not separable by conventional chromatography. ^1H NMR of the mixture appeared to show that trifluoromethylation had occurred at two positions. The major product possessed a

trifluoromethyl group on the pyrimidine ring and the minor species had incorporated a trifluoromethyl group onto the pyrazolo[1,5-*b*]pyridazine head. The major component was tentatively assigned as 3-[2-methylsulfanyl-5-(trifluoromethyl)pyrimidin-4-yl]pyrazolo[1,5-*b*]pyridazine (Figure 73, A). The lack of doublet signals characteristic of the pyrimidine protons and instead the existence of a singlet proton was indicative that trifluoromethylation had occurred on the pyrimidine ring. With the available analytical data it cannot be ruled out that trifluoromethylation did not occur in the 6-position. The minor component was tentatively assigned as 2-(methylsulfanyl)-4-[5-(trifluoromethyl)pyrazolo[1,5-*b*]pyridazin-3-yl]pyrimidine. Inspection of the multiplicity and coupling constants of protons C (d, J = 5.3 Hz, 1H) and D (d, J = 5.3 Hz, 1H) (Figure 73, B) are consistent with pyrimidine protons that are adjacent to each other. The multiplicity and coupling constants of protons, F (d, J = 2.4 Hz, 1H) and A (d, J = 2.4 Hz, 1H), appear to be consistent with protons at the 4 and 6 position of the pyrazolo[1,5-*b*]pyridazine heterocycle. If the protons were adjacent to one another the coupling constant is likely to be larger than that observed.

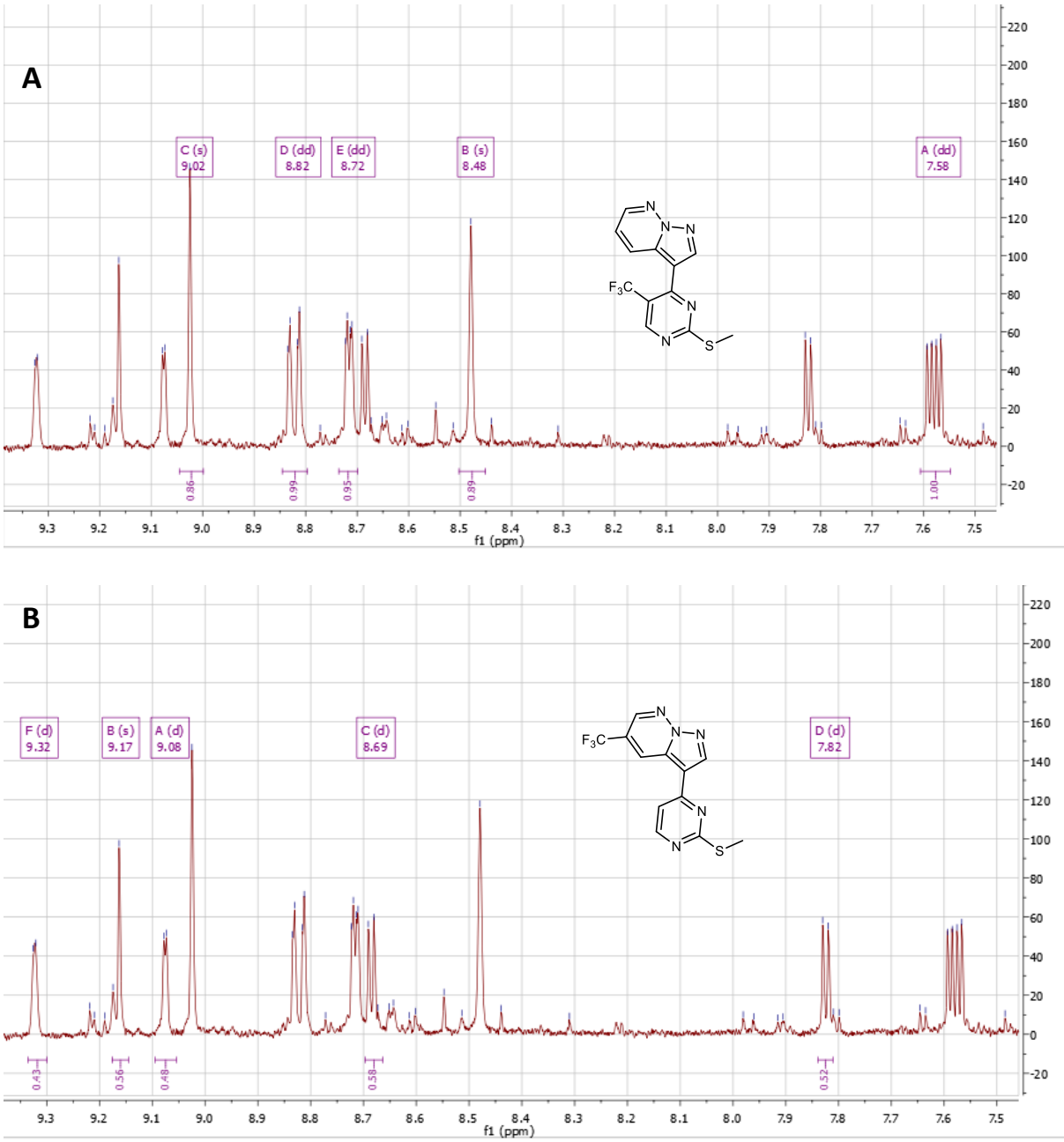

Figure 73. A – ^{1}H NMR Aromatic Region of Major Species present in Minor Component; B – ^{1}H NMR Aromatic Region of Minor Species present in Minor Component

Due to the difficulty in separating the two regioisomers, this late-stage trifluoromethylation strategy was abandoned. After optimisation this procedure could be an important way to promote 5-derivatisation of the pyrazolo[1,5-*b*]pyridazine heterocycle.

6.1.3. SARs and Biological Evaluation of 5-substituted Pyrimidines

The DYRK1A binding affinity of 5-substituted pyrimidines are presented in Table 34. The unsubstituted compound **96** is included for reference.

The majority of compounds exhibit severely diminished DYRK1A binding affinity. The 5-fluoro analogue **172** is the only exemplar that displayed comparable affinity to **96**.

Table 34. DYRK1A Binding Affinity of 5-substituted Pyrimidines

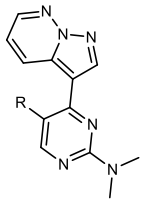

Compound	R	DYRK1A IC_{50}[a]
96	H	75
172	F	57
174	Cl	330
181	Br	1587
183	I	1607
176	CF_3	12784
178	Me	2847
170	OMe	1185

[a]IC_{50} (nM) in TR-FRET-based ligand-binding displacement assay (n = 1)

Of the compounds only the 5-fluoro analogue **172** exhibited higher DYRK1A binding affinity than **96**. All other analogues exhibited reduced DYRK1A binding affinity. Increasing the size of the halogen (F → Cl → Br → I) was more detrimental to DYRK1A binding affinity for the series. This suggests that when the pyrazolo[1,5-*b*]pyridazine series binds to DYRK1A, the space around the phenylalanine gatekeeper is very restricted, limiting the size of substituent that can be placed favourably in the 5-position. As the majority of the halogen analogues were not accommodated in the DYRK1A binding pocket, their residence time was not assessed and so kinetic selectivity not determined.

172 was profiled for metabolic stability and thermodynamic solubility. These results are displayed in Table 35. **96** has been included for comparison.

Table 35. Metabolic Stability and Solubility of 172

Compound	HLM (µL/min/mg)	RLM (µL/min/mg)	Solubility (mg/mL)
96	241.8[a] +/- 31.7	230.1[a] +/- 30.8	0.10
172	696.5 +/- 49.9	983.1 +/- 38.7	0.03

HLM and RLM Determinations mean of n =2 +/- standard deviation (unless otherwise stated).[a]Mean of n = 4 +/- standard deviation. HLM = human liver microsomes; RLM = rat liver microsomes; thermodynamic solubility data derived from single experiment at pH 6.8..

Counterintuitively, installation of a fluorine at the 5-position of the pyrimidine (**172**) did not block metabolism but in fact increased *in vitro* metabolic clearance. Perhaps the inclusion of the fluorine affected the electronics of the pyrimidine ring, making the methyl groups more susceptible to *N*-dealkylation. Analogues with different amine substituents would need to be made to test that theory. The solubility of **172** was substantially lower than **96**. This observation could be as a result of the increased lipophilicity of **172** due to the addition of a fluorine substituent. Another possibility is that the fluorine is promoting an intramolecular interaction between the two heteroaromatic rings, causing them to adopt a more co-planar orientation. This could increase π-π stacking between molecules and lower solubility.

In terms of metabolic stability and solubility, **172** was inferior to **96**. However, **172** was amongst the highest affinity binders of DYRK1A in the pyrazolo[1,5-*b*]pyridazine series. Thus the kinome-wide selectivity profile of **172** was determined as the additional fluorine may afford some benefits in terms of selectivity. **172** was assayed in the KINOMEscan® platform at DiscoveRx, a proprietary active-site directed competition binding assay. The results of the selectivity panel are displayed as a TREEspot™ diagram in Figure 74.

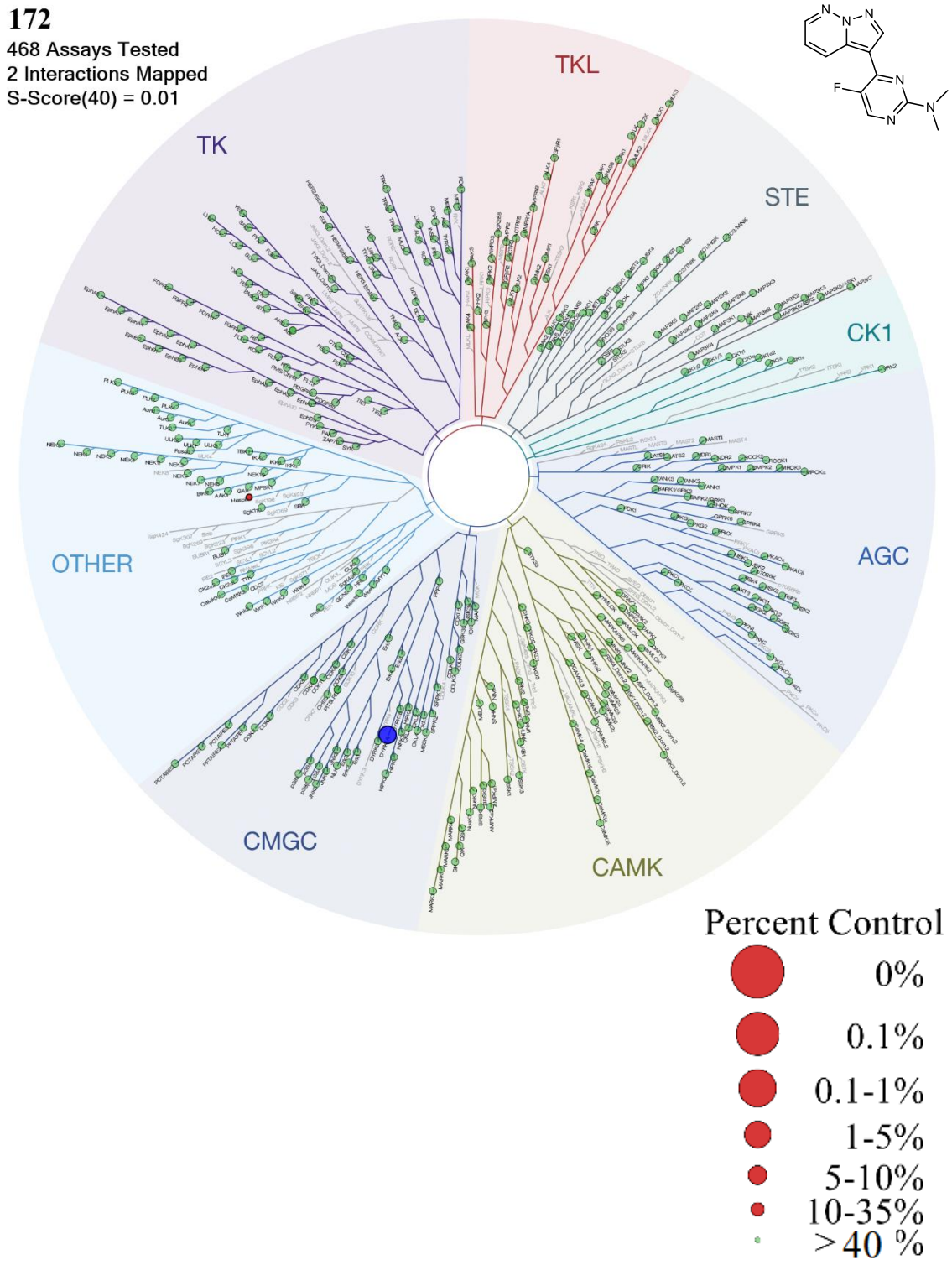

Figure 74. KINOMEscan® Treespot™ map for **172**. DYRK1A is highlighted in blue. Image generated using TREEspot™ Software Tool and reprinted with permission from KINOMEscan®, a division of DiscoveRx Corporation, © DISCOVERX CORPORATION 2010.

172 maintained a high levels of kinome-wide selectivity. Preliminary selectivity data shows that the 5-fluoro analogue has superior selectivity over DYRK1B and shows promising selectivity against the CLKs. After DYRK1A, the mitotic kinase haspin is inhibited most by **172**, but again, the 5-fluoride appears to afford some selectivity over haspin, making **172** the most selective ligand discovered thus far.

Table 36. Overview of Kinome Selectivity Profiles of Inhibitor 172

Compound	Percentage kinases inhibited > 75%[a]	Percentage kinases inhibited > 50%[a]	Kinases most potently inhibited
172	0.2	1.5	Haspin

a % Inhibition as determined by DiscoveRx KINOMEscan® experiment.

To assess whether **172** was capable of becoming a molecular probe for a CNS target such as DYRK1A, the permeability and P-gp mediated efflux of **172** was assessed in a MDCK-MDR1 assay provided by Cyprotex.

Table 37. MDCK-MDR1 permeability of 172

Compound	CNS MPO[a] score	Direction = A2B Mean P_{app} (10^{-6} cms^{-1})[b]	Direction = B2A	Efflux Ratio (Mean P_{app} B2A / Mean P_{app} A2B)[b]
172	6	54.9 +/- 3.60	57.6 +/- 0.32	1.05

[a]CNS MPO score calculated using CNS MPO KNIME® workflow with ChemAxon nodes. [b]Data generated by Cyprotex in MDCK-MDR1 assay. Permeability coefficient (P_{app}) calculated across cells in direction: A2B (Apical to Basolateral) and B2A (Basolateral to Apical). Determinations +/- standard deviation (mean of n =2 unless otherwise stated).

The high CNS MPO score of **172** correlated with good levels of permeability and low P-gp efflux, suggesting that **172** may be capable of being developed as a CNS molecular probe.

6.2. Investigation of 6-substituted Pyrimidine Analogues

6.2.1. Rationale

The close proximity of the 6-position of the pyrimidine to the hinge of DYRK1A made it likely that substituents added to this position would result in steric clashes with the hinge. However, if a substituent was tolerated in DYRK1A and not in other kinases, a selective DYRK1A tool may be furnished.

Multiple ligand-DYRK1A co-crystal structures have shown that DYRK1A is able to accommodate ligands that bind in a monodentate fashion.[277] The pyrazolo[1,5-*b*]pyridazine series bound in an interesting fashion, utilising a C-*H* bond donor from the 6-position of the pyrimidine. Installation of a substituent at this position may determine whether that interaction could be removed.

6.2.2. Synthesis of 6-substituted Pyrimidine Analogues

6-substituted pyrimidine analogues (**187**, **189**, **191** and **193**) were synthesised following the same general 'alkylation-Suzuki' procedure. The appropriate aminopyrimidine was dimethylated with sodium hydride and iodomethane. The desired products were furnished *via* subsequent Suzuki cross-coupling reaction using boronic ester **168**.

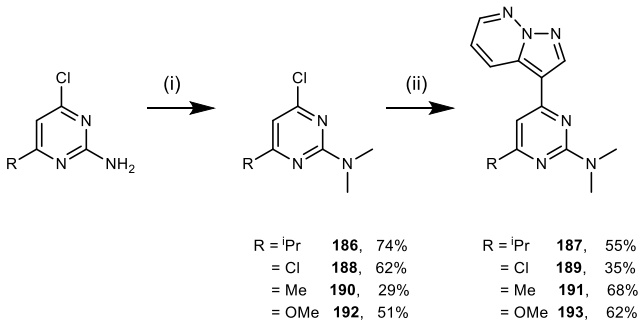

Scheme 31. *Reagents and conditions:* (i) sodium hydride, iodomethane, rt, 16 h; (ii) 168, bis[2-(di-*tert*-butylphosphanyl)cyclopenta-2,4-dien-1-yl]iron; dichloropalladium, potassium carbonate, 1,4-dioxane, 70 °C, 2 h.

The synthesis of analogue **195** involved initial Suzuki reaction to install the pyrazolo[1,5-*b*]pyridazine head onto the commercially available dichloropyrimidine. Subsequent nucleophilic aromatic substitution with dimethylamine afforded **195**.

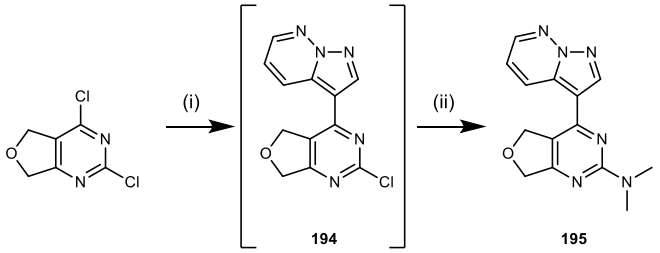

Scheme 32. *Reagents and conditions:* (i) **168**, bis[2-(di-*tert*-butylphosphanyl)cyclopenta-2,4-dien-1-yl]iron; dichloropalladium, 2 M potassium carbonate, 1,4-dioxane, 110 °C, 4 h; (ii) 2 M dimethylamine in THF, 110 °C, overnight, 25%.

6.2.3. SARs and Biological Evaluation of 6-substituted Pyrimidine Analogues

The DYRK1A binding affinity for 6-substituted pyrimidine analogues is displayed in Table 38. The unsubstituted compound **96** is included for reference.

All 6-substituted pyrimidine analogues exhibit a severe decline in DYRK1A binding affinity.

Table 38. DYRK1A Binding Affinity of 6-substituted Pyrimidine Analogues

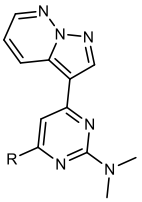

Compound	R	DYRK1A IC_{50}[a]
96	H	75
189	Cl	1354
191	Me	11675
193	OMe	**
187		19013
195		7455

[a]IC_{50} (nM) in TR-FRET-based ligand-binding displacement assay (n = 1). **Data could not be fitted to a curve.

Substituents added to the 6-position of the pyrimidine were not tolerated probably as a result of unfavourable clashes between the ligand and the amino acid residues on the hinge region of DYRK1A. These compounds were not progressed to microsomal stability or solubility testing, and were not advanced to selectivity assessment as they could not be considered as DYRK1A ligands due to their lack of affinity.

6.3. Scaffold Hopping Between Pyrimidine, Pyridine and Triazine Analogues

6.3.1 Rationale

Bioisosteric replacement and 'scaffold hopping' between heterocycles provides a way of modulating solubility and metabolic stability, as well as establishing extra interactions to improve potency and selectivity of inhibitors.[278] It was envisaged that substituting the pyrimidine for a triazine or pyridine may modulate some of the undesirable features of the current series such as rapid metabolism and low solubility. Reduction in topological polar surface area would also be achieved through removal of a nitrogen atom from the pyrimidine ring.

It would be interesting to see whether removal of the nitrogen atom responsible for a hydrogen-bond to the hinge region of DYRK1A was tolerated without a change in binding mode. Also it would be interesting to investigate whether the removal of the nitrogen atom at the 3-position of the pyrimidine had any effect on potency, solubility and metabolic stability. In theory, removal of the nitrogen atom from the 3-position may lead to a molecule with less restricted rotation about the C-C bond that connects the pyrimidine to the pyrazolo[1,5-*b*]pyridazine. Any of these changes could unexpectedly lead to a molecular probe with a better overall profile than the current leads.

6.3.2. Synthesis of Pyridine and Triazine Analogues

Each heterocyclic analogue required a bespoke synthetic route. **197** was accessed in two steps. 2,6-dibromopyridine was reacted with dimethylamine to afford intermediate **196**. The pyrazolo[1,5-*b*]pyridazine motif was subsequently installed *via* a Suzuki reaction using the required boronic ester **168**.

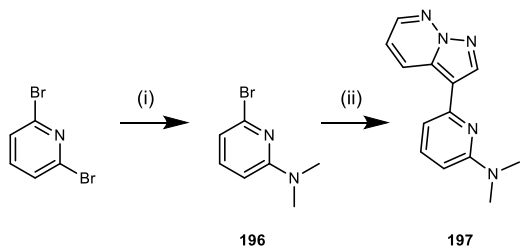

Scheme 33. *Reagents and conditions:* (i) dimethylamine 2M in THF, THF, 80 °C, overnight, 93%; (ii) **168**, bis[2-(di-*tert*-butylphosphanyl)cyclopenta-2,4-dien-1-yl]iron; dichloropalladium, sodium carbonate, acetonitrile:water (6:1), 140 °C, overnight, 36%.

Pyridine analogue **199** was furnished in a two-step procedure. The aminopyridine was dimethylated with sodium hydride and methyl iodide to access intermediate **198**. Subsequent Suzuki reaction with **168** installed the pyrazolo[1,5-*b*]pyridazine heterocycle.

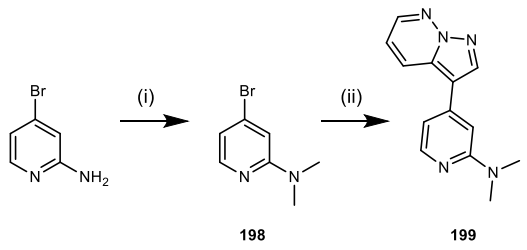

Scheme 34. *Reagents and conditions:* (i) dimethylamine 2M in THF, THF, 80 °C, overnight, 83%; (ii) **168**, bis[2-(di-*tert*-butylphosphanyl)cyclopenta-2,4-dien-1-yl]iron; dichloropalladium, sodium carbonate, acetonitrile:water (6:1), 140 °C, 20 min, µwave, 32%.

The triazine analogue **201** was again synthesised in a two-step procedure. 2,4-dichloro-1,3,5-triazine was treated with dimethylamine hydrochloride at room temperature to furnish intermediate **200**, which was used crude and reacted under Suzuki conditions to afford the desired product **201** in low yield.

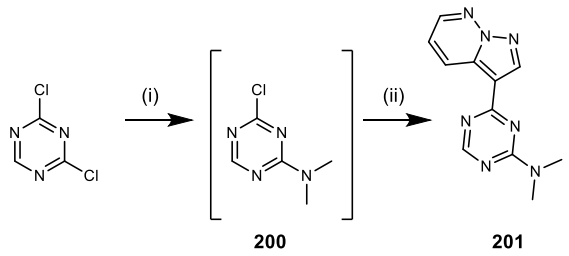

Scheme 35. *Reagents and conditions:* (i) dimethylamine hydrochloride, *N*,*N*-diisopropylethylamine, THF, rt, 3 h; (ii) **168**, bis[2-(di-*tert*-butylphosphanyl)cyclopenta-2,4-dien-1-yl]iron; dichloropalladium, 2 M potassium carbonate, 1,4-dioxane, 80 °C, 16 h, 4%.

6.3.3. SARs and Biological Evaluation of Pyridine and Triazine Analogues

The DYRK1A binding affinity of pyridine and triazine analogues is displayed in Table 39. The pyrimidine analogue **96** is included for reference.

All heterocyclic analogues showed diminished DYRK1A binding affinity compared to **96**.

Table 39. DYRK1A Binding Affinity of Pyridine and Triazine Analogues

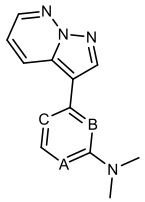

Compound	A	B	C	DYRK1A IC_{50}	LE, LipE
96	N	N	C	75	0.55, 5.5
199	N	C	C	680	0.48, 4.3
197	C	N	C	916	0.47, 3.8
201	N	N	N	184	0.52, 4.9

[a]IC_{50} (nM) in TR-FRET-based ligand-binding displacement assay (n = 1). LE = 1.4(pIC_{50})/non-hydrogen atoms; LipE = pIC_{50} – clog P.

Removal of the nitrogen atom that forms a hydrogen bond to the hinge region of DYRK1A has led to approximately a 10 fold reduction in binding affinity for **197**. Likewise, removal of the nitrogen atom from the 3-position of the pyrimidine and replacement with C-*H* has resulted in a 10 fold loss in DYRK1A binding affinity for **199**. Removal of the nitrogen atom in **199** may cause there to be more freedom of movement around the two heterocycles and less molecular preorganisation. The additional C-*H* proton in **199** may interact with the proton of the 4-position of the pyrazolo[1,5-*b*]pyridazine causing repulsion so that **199** adopts an unfavourable binding conformation in DYRK1A.[279]

Although triazine **201** exhibits > 2 fold weaker affinity than pyrimidine **96**, the LE is still representative of a good quality ligand. If potency could be improved elsewhere in the molecule, the triazine may lead to a molecular probe for DYRK1A. Thus, **201** was profiled for solubility and metabolic stability. The results for thermodynamic solubility and microsomal clearance of **201** are presented in Table 40. Data for **96** is included for comparison.

Introduction of a nitrogen at the 5-position to afford the triazine **201** gave a > 2 fold improvement in metabolic stability in both human and rat liver microsomes. Solubility was reduced compared to **96**.

Table 40. Solubility and Metabolic stability of 96 and 201

Compound	HLM (µL/min/mg)	RLM (µL/min/mg)	Solubility (mg/mL)
96	241.8[a] +/- 31.7	230.1[a] +/- 30.8	0.10
201	93.6 +/- 0.14	105.3 +/- 7.0	0.05

HLM and RLM Determinations mean of n =2 +/- standard deviation (unless otherwise stated).[a]Mean of n = 4 +/- standard deviation. HLM = human liver microsomes; RLM = rat liver microsomes; thermodynamic solubility data derived from single experiment at pH 6.8.

At this stage of the project **201** was not profiled further for selectivity due to the sub-optimal levels of DYRK1A affinity observed.

6.4. Summary

The 5-position of the pyrimidine of the pyrazolo[1,5-*b*]pyridazine series was explored extensively. Initial efforts to increase DYRK1A affinity and exploit 'kinetic selectivity' through π-aromatic gatekeeper interactions proved unsuccessful. The size of substituent in the 5-position of the pyrimidine was limited to the size of a hydride or fluoride atom. Any larger substituent in the 5-position led to a marked decrease in DYRK1A affinity.

The 5-fluoro analogue, **172**, exhibited marginal improvements in DYRK1A binding affinity and selectivity over kinase off-targets. The minor increase in activity could be due to positive lipophilic interactions or F-π interactions[280] between the fluorine and the phenylalanine gatekeeper. It would be interesting to compare the residence times of **172** and **96** to assess whether there was any F-π interaction and potential for kinetic selectivity. The observed increase in DYRK1A affinity and selectivity could be due to a more favourable entropy upon **172** binding as a result of molecule preorganisation and intramolecular bonding. **172** exhibited good permeability and low P-gp efflux, indicating that **172** could be capable of being a CNS penetrant kinase inhibitor probe. The addition of a fluoride to the 5-position of the pyrimidine did not have a positive impact on metabolic stability as first theorised. The inhibitor also possessed lower solubility than **96**.

Exploration of the 6-position of the pyrimidine revealed that substituents other than a proton were unlikely to be tolerated. This is likely to be a result of steric clashes between the substituent in the 6-position with amino acid residues that constitute the hinge region of DYRK1A.

Scaffold hopping to the triazine analogue **201** afforded an inhibitor with improved metabolic stability compared to pyrimidine **96**, however, DYRK1A binding affinity was reduced by approximately 2 fold.

Potentially, a chimeric molecule that incorporate 5-fluoropyrimidine but possesses a more solubilising and less metabolically labile amine substituent may provide access to the optimal DYRK1A inhibitor tool. Alternatively, a triazine analogue that bears an amine substituent able to increase DYRK1A binding affinity could provide a novel molecular probe with a superior profile.

The following chapter is dedicated to structure-aided design of heterocyclic analogues of the pyrazolo[1,5-*b*]pyridazine motif with the intent to discover a molecule with the perfect balance of DYRK1A affinity, selectivity, solubility and metabolic stability.

CHAPTER 7. Structure-enabled Design of DYRK-selective Pyrazolo[1,5-*b*]pyridazines: Part III

Chapter 7 describes the replacement and decoration of the pyrazolo[1,5-*b*]pyridazine motif. Literature-based approaches and *in silico* design methods are used to generate molecules in the desired chemical space with a high likelihood of target engagement that test specific hypotheses. Active site waters are assessed and hydrogen-bonding networks are targeted. Ligand growth into the back-pocket residues of the ATP site is attempted to furnish the first DYRK1A Type 1.5 kinase inhibitor. Scaffold hopping and bioisosteric replacement is used to modulate solubility and metabolic stability. Finally, chimeric molecules that combine all of the knowledge generated thus far are investigated in an attempt to provide the community with a suitable DYRK1A molecular probe.

7.1. Modification of the Pyrazolo[1,5-*b*]pyridazine Scaffold

7.1.1. Rationale

Previous work had shown that pyrimidine modification did not lead to major improvements in DYRK1A binding affinity, solubility or metabolic stability (Chapter 6). Although substituents directed towards the solvent-exposed region had brought about more selective and higher affinity binders (Chapters 4 and 5), there was still an opportunity to improve the DYRK1A binding affinity, selectivity, solubility and metabolic stability of the series. So far adding substituents to the pyrazolo[1,5-*b*]pyridazine motif had not been investigated.

At the 2018 8th RSC/SCI symposium on kinase inhibitor design in Cambridge, UK, it was disclosed that researchers at the SGC (University of North Carolina) were investigating the pyrazolo[1,5-*b*]pyridazine series in an effort to discover selective CLK probes. This work was documented on an online open-source platform, openlabnotebooks.org.[281] The work appeared to show that CLK inhibition could be dialled-out by adding substituents to the 6-position of the pyrazolo[1,5-*b*]pyridazine core. Review of the kinase profiling data available in the public domain revealed that substituents in the 6-position of the pyrazolo[1,5-*b*]pyridazine series were tolerated to some extent in DYRK1A - CHEMBL496162 was reported to inhibit DYRK1A by 60% at 1 µM.[19,21] Taking this data into account (Figure 75), exploration of the 6-position appeared to be a valid approach to removing CLK off-target activity for the series.

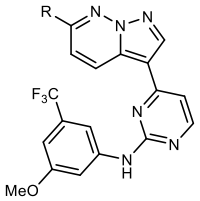

Compound	R	% Remaining Activity			IC_{50} / nM		
		CLK1	CLK2	CLK3	CLK1	CLK2	CLK3
CAF048	H	15	11	93	24	48	-
CAF170	OCH_3	10	11	104	46	35	-
CAF022	OCH_2CH_3	26	20	103	-	160	-
CAF018	$OCH(CH_3)_2$	62	69	106	-	-	-
CAF091	OCH_2CF_3	79	71	100	-	-	-

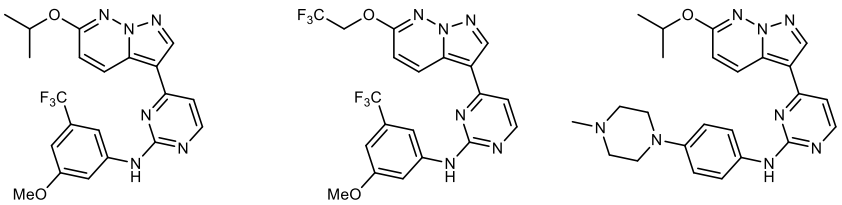

CAF018 CAF091 CHEMBL496162

Figure 75. 6-substituted pyrazolo[1,5-*b*]pyridazines; CAF018 and CAF091 appear to lose activity against the CLKs. Figure modified from source.[281]

In general, analogues of the pyrazolo[1,5-*b*]pyridazine series with substituents in the 2 position exhibited poor DYRK1A binding affinity.[19,21] Despite this, the 2-methyl analogue was a compound of interest for two reasons: (i) if inactive the compound could serve as an anti-tool i.e. a compound that exhibits no activity against DYRK1A and that can be used in parallel to an active analogue to dissect the biology of DYRK1A; (ii) with the additional methyl cap on the aniline or amine N-*H*, the series may now be sufficiently different to allow incorporation of a small substituent at the 2-position.

Analogues with substituents in the 4- and 5-position of the pyrazolo[1,5-*b*]pyridazine were not well documented. Molecular modelling suggested that substituents borne by the 4- and 5-positions would be orientated beneath the glycine rich loop. In other DYRK1A series that were being investigated in parallel, it had been observed that placement of substituents, especially lipophilic substituents, under the glycine rich loop had improved DYRK1A affinity.

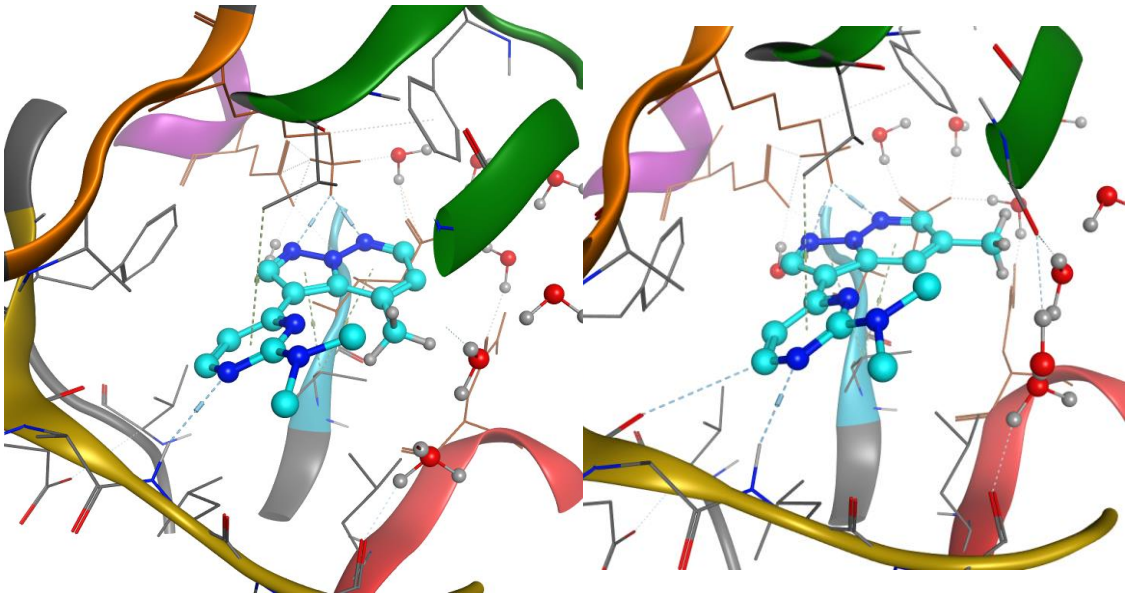

Figure 76. Molecular Modelling of 4- and 5-methyl substituted analogues in DYRK1A in-house crystal structure. Hydrogen bonding interactions with hinge, back-pocket water and Lys188 are predicted to be maintained. Structure modelled with Builder tool in MOE 2016, CCG with Amber10:EHT force field.

7.1.2. Synthesis of Substituted Pyrazolo[1,5-*b*]pyridazines

It was envisaged that 4-, 5- and 6- substituted pyrazolo[1,5-*b*]pyridazines could all be accessed from the same general route as previously established but using the appropriately substituted pyridazine, following closely the literature procedure described for similar analogues.[251]

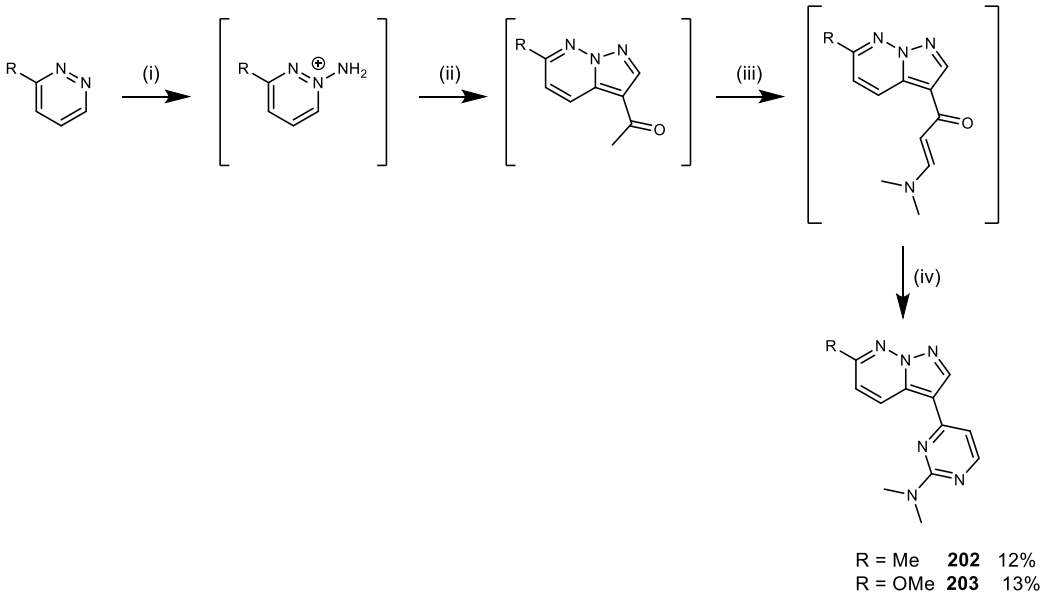

Scheme 36. *Reagents and conditions*: (i) hydroxylamine-*O*-sulfonic acid, $KHCO_3$, KI, H_2O, 70°C, 2 h; (ii) butyne-2-one, KOH, CH_2Cl_2, rt, overnight; (iii) DMF-DMA, 75°C, 16 h; (iv) 1,1-dimethylguanidine sulfate salt, 2-methoxyethanol, 125 °C, overnight.

6-Substituted analogues **202** and **203** were furnished successfully following the steps documented in the literature.[251] In contrast to the general procedure, no intermediate purification steps were carried out, and the intermediates were taken forward crude after the reaction solvent from the preceding step was removed. By telescoping intermediates into the next step of the reaction, unnecessary losses during purification steps were avoided.

The 5-methyl-substituted and 4-methyl-substituted analogues were isolated from the same reaction mixture, albeit in low yields, using the same strategy. The 4-methoxy analogue was furnished using this sequence, however the 5-methoxy analogue was not isolated. Perhaps *N*-amination of the 4-methoxypyridazine, which is required for the synthesis of the 4- and 5-subsituted analogues, is more biased towards amination at N2 rather than N1. It is likely that this observation is the result of an electronic effect. Under the acidic reaction conditions the more pronounced electron donating nature of the *para* methoxy group could be causing N1 to be less susceptible to *N*-amination.

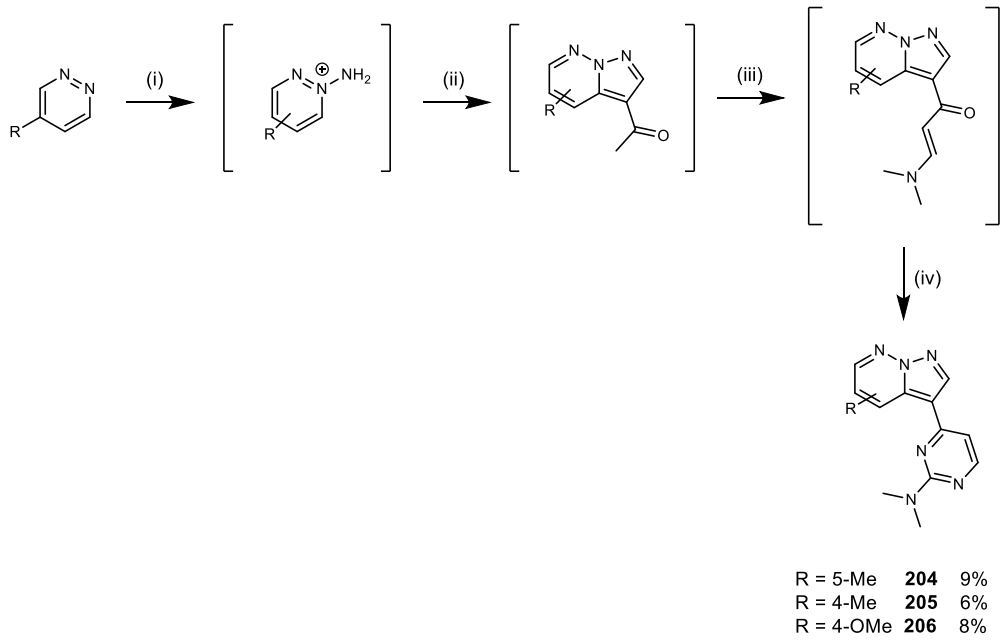

Scheme 37. *Reagents and conditions*: (i) hydroxylamine-*O*-sulfonic acid, $KHCO_3$, KI, H_2O, 70°C, 2 h; (ii) butyne-2-one, KOH, CH_2Cl_2, rt, overnight; (iii) DMF-DMA, 75°C, 16 h; (iv) 1,1-dimethylguanidine sulfate salt, 2-methoxyethanol, 125 °C, overnight.

Small molecule x-ray crystallography supported the ^{1}H NMR experiments in elucidating the correct identity of regioisomers isolated. Figure 78 depicts the 5-methyl analogue **204**.

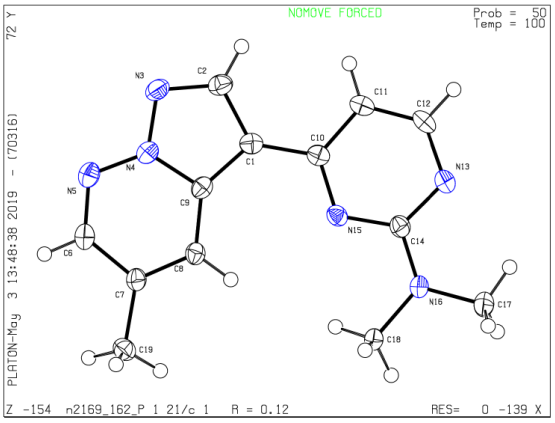

Figure 78. Small molecule x-ray crystal structure of **204**.

The small molecule x-ray structure of **206** showed that the molecule adopted a different conformation. Although this may not be the case in the presence of the protein, it may be possible that the molecule is no longer able to adopt the preferred active conformation that has been observed for the pyrazolo[1,5-*b*]pyridazine series.

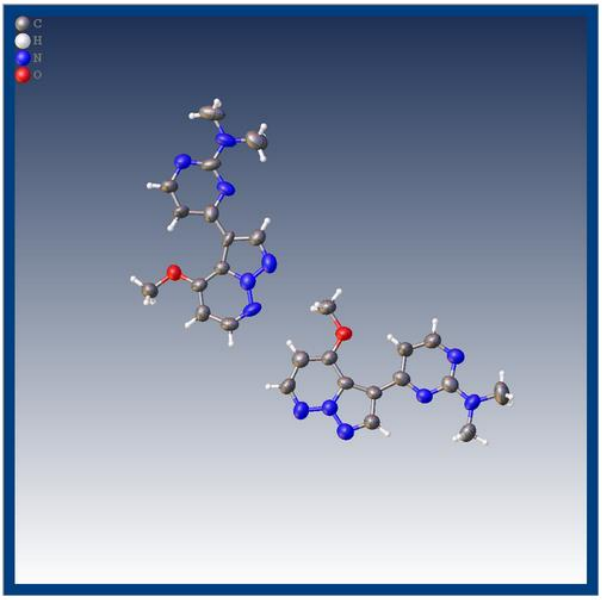

Figure 79. Small molecule x-ray crystal structure of **206**.

Although multiple attempts to synthesise the 5-methoxy analogue were made it was never isolated. There are very few methods documented for *N*-amination of heterocycles.[282] Given the interesting biological activity of this class of the pyrazolo[1,5-*b*]pyridazine and others formed via *N*-amination, an interesting future study would be to investigate the regioselectivity of *N*-amination reactions and the discovery of novel ammonia transfer reagents.

The 2-methyl analogue **210** was synthesised using a more bespoke route. Insertion of propyne onto intermediate **117** using Sonogashira conditions furnished the desired dipolarphile **207**. Subsequent 1,3-dipolar cycloaddition with **74** afforded intermediate **208**. *m*-CPBA oxidation to furnish the sulfone, **209**, followed by nucleophilic aromatic substitution with dimethylamine afforded the desired 2-substituted product, **210**.

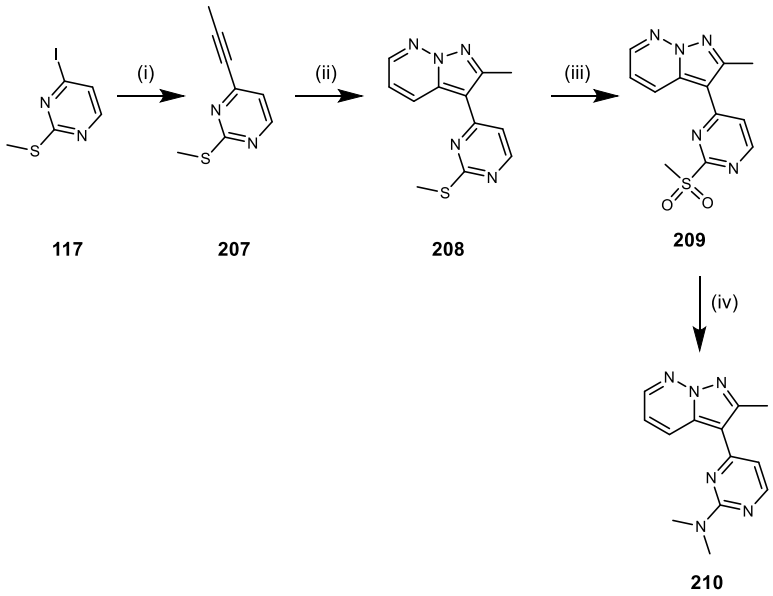

Scheme 38. *Reagents and conditions*: (i) bis(triphenylphosphine)palladium(II) dichloride, copper iodide, TEA, propyne (ca. 5% in THF, ca. 1 mol/L), THF, rt, overnight, 87%; (ii) pyridazin-1-ium-1-amine iodide, DBU, acetonitrile, 50 °C, 16 h, 73%; (iii) *m*-CPBA, CH_2Cl_2, rt, overnight, 80%; (iv) 2 M dimethylamine in THF, 110 °C, 2 h, 74%.

7.1.3. SARs and Biological Evaluation of Substituted Pyrazolo[1,5-*b*]pyridazines

The DYRK1A binding affinity for substituted pyrazolo[1,5-*b*]pyridazine analogues are displayed in Table 41. Included for comparison is **96**.

All analogues that bear an additional substituent on the pyrazolo[1,5-*b*]pyridazine motif exhibit diminished DYRK1A binding affinity relative to **96**.

Table 41. DYRK1A Binding Affinity of Pyrazolo[1,5-*b*]pyridazine Analogues

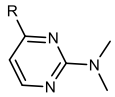

Compound	R	DYRK1A IC_{50}[a]	LE
96	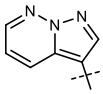	75	0.55
202	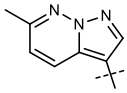	880	0.45
204	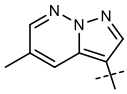	116	0.51
205	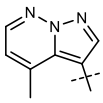	732	0.45
203	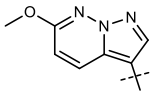	2619	0.39
206	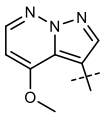	137	0.48

[a]IC_{50} (nM) in TR-FRET-based ligand-binding displacement assay (n = 1). LE = 1.4(pIC_{50})/non-hydrogen atoms.

Substitution in the 6-position has led to > 10 fold drop in DYRK1A binding affinity for **202** and **203**. This is likely due to unfavourable clashes between the molecules and the DYRK1A protein surface close to the catalytic lysine. **205**, bearing a methyl substituent at the 4-position, also exhibits an approximate 10 fold loss in DYRK1A binding affinity. The methyl group may disrupt the pyrazolo[1,5-*b*]pyridazine series from taking its optimal inhibitory conformation. The 4-methoxy analogue **206** exhibits approximately a 2 fold reduction in DYRK1A binding affinity, despite the potential change in orientation. A methyl substituent in the 5-position (**204**) appears to be well tolerated under the glycine rich loop.

At the time of writing selectivity assessment of **204** and **206** is underway. **204** and **206** are being profiled in a 468 kinase panel to assess kinome-wide selectivity, provided by DiscoveRx.

204 and **206** were profiled for solubility and metabolic stability. The results are shown in Table 42. The data for **96** is included for comparison.

Table 42. Solubility and Metabolic Stability of **204** and **206**

Compound	HLM (µL/min/mg)	RLM (µL/min/mg)	Solubility (mg/mL)
96	241.8[a] +/- 31.7	230.1[a] +/- 30.8	0.10
204	159.5 +/- 66.2	164.2[b]	0.01
206	89.3 +/- 10.9	77.2 +/- 16.8	0.07

HLM and RLM Determinations mean of n =2 +/- standard deviation (unless otherwise stated).[a]Mean of n = 4 +/- standard deviation. [b]Data from single experiment. HLM = human liver microsomes; RLM = rat liver microsomes; thermodynamic solubility data derived from single experiment at pH 6.8.

Both analogues **204** and **206** exhibited improvements over **96** in terms of metabolic stability, indicating that positions on the pyrazolo[1,5-*b*]pyridazine ring may be sites of metabolism. **204** and **206** are less soluble than **96**. On balance, **206** appears to possess a more attractive profile than **96**. The knowledge that specific substituents at particular locations on the pyrazolo[1,5-*b*]pyridazine motif can lead to improvements in metabolic stability and solubility may be useful for future inhibitor design.

7.2. Scaffold Hopping using the Pyrazolo[1,5-*b*]pyridazine as a Template

7.2.1. Rationale

7.2.2. Scaffold Hopping

Thus far alterations to the pyrazolo[1,5-*b*]pyridazine core had not led to a vastly superior tool in terms of DYRK1A binding affinity, selectivity, metabolic stability and solubility. Previous work had not identified which of the atoms within the 5,6-heterocyclic core were essential pharmacophoric features to maintain. Furthermore, the pyrazolo[1,5-*b*]pyridazine core although not prevalent in the literature, is not novel, and as mentioned was being explored by others for CLK inhibition.[281] Scaffold hopping seemed like a sensible approach to determine the essential features of the series, move into novel chemical space and as a means of improving DYRK1A affinity, selectivity, solubility and metabolic stability.[283]

A series of high-resolution co-crystal structures of the pyrazolo[1,5-*b*]pyridazine series had been produced that showed the series to be relatively rigid, adopting the same general conformation and orientation. The conformation of the pyrazolo[1,5-*b*]pyridazine was used as a template to search for other chemotypes that could serve as bioisosteric replacements. The scaffold hopping software, Spark™ from Cresset, was used to predict biologically equivalent replacements for the pyrazolo[1,5-*b*]pyridazine. The physicochemical properties of bioisosteric replacement analogues were also calculated in Spark™ to ensure that the correct physicochemical space was being sampled (Figure 80).

Rank	Structure	BIF%	Score	Field Score	Shape Score	MW	#Atoms	SlogP	TPSA	#RB	Rof5	Radial Plot
1	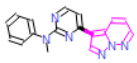	99	0.991	0.988	0.995	302	23	3	59	3	0	0.800 
3	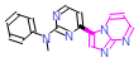	95	0.96	0.928	0.991	302	23	3	59	3	0	0.800 
2	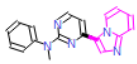	95	0.962	0.936	0.988	301	23	3.6	46	3	0	0.727 

Figure 80. Bioisosteric replacement using Cresset Spark™ with XED force field. BIF% = Bioisostere Factor; Score = combined Field and Shaped score, Field score = field similarity of generated molecule with respect to reference molecule; Shape score = shape similarity of generated molecule with respect to reference molecule; Mw = molecular weight; #Atoms = number of atoms; SlogP = Wildman-Crippen Log P; TPSA = topological polar surface area; #RB = number of rotatable bonds; Ro5 = rule of five violations.

Computationally generated analogues were then modelled in DYRK1A using Flare™ from Cresset and minimised using the XED force field to visually assess the electrostatic fields and binding mode of the proposed bioisosteric replacement. Figure 81 highlights the differences in electrostatic fields generated for specific bioisosteric replacements.

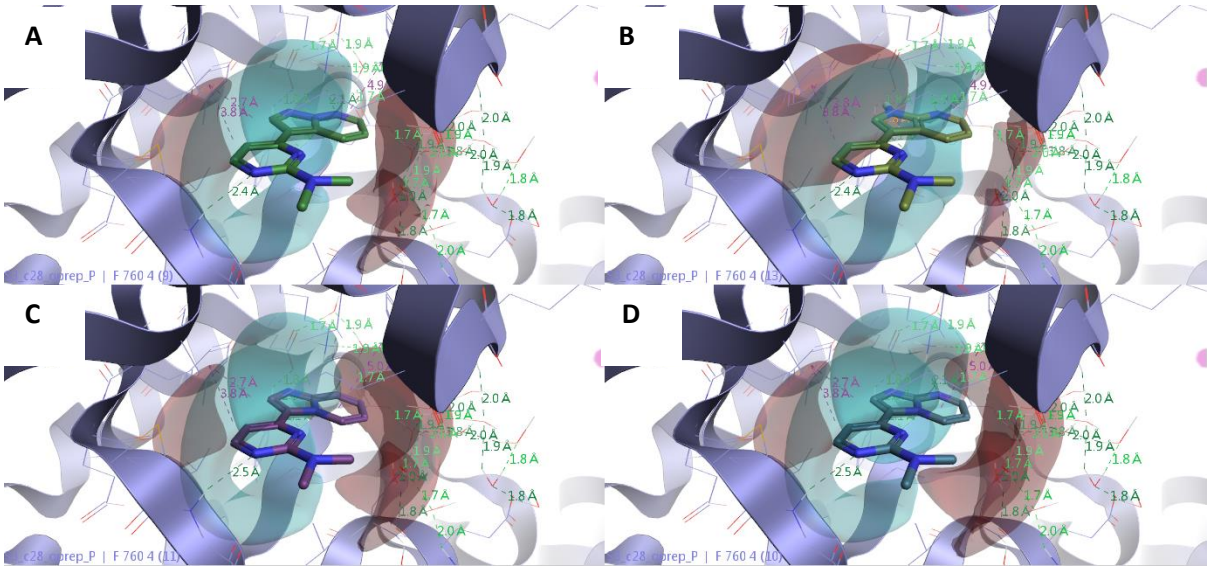

Figure 81. Visualisation of Spark™ generated bioisosteric replacements for the pyrazolo[1,5-*b*]pyridazine core in Flare™. A – 96 bound to DYRK1A in-house crystal structure. B – Core suggestion with low BIF% score and field score. C and D – Core suggestions with high BIF% score and field score. An in-house crystal structure was modified to possess the proposed core, energy minimisation was then performed in Flare™ with the XED force field.

7.2.3. Interactions with Active Site Water Molecules

Close inspection of all of the in-house pyrazolo[1,5-*b*]pyridazine co-crystal structures generated revealed the existence of a water molecule located towards the back of the DYRK1A binding site. This particular consensus water mediated a hydrogen-bonding network between the pyrazolo[1,5-*b*]pyridazine motif, the catalytic lysine (K188) and glutamate of DYRK1A. A recent review details the importance of understanding the role of active site waters and the potential of exploiting them in drug discovery.[284] We were interested to investigate (i) whether the active site water could be displaced or replaced, and if this would result in a gain in entropy or selectivity; (ii) if the water-mediated hydrogen bonding interactions could be strengthened; (iii) whether displacement of the active site water and access to the back-pocket of DYRK1A was possible, so as to form a Type I.5 inhibitor, potentially bringing gains in selectivity versus key off-targets.

The hydration free energies of the active site waters were estimated to identify energetically unfavourable waters to displace. To this end a statistical mechanical model known as the 3D-RISM (Reference Interaction Site Model) method was implemented in MOE. Figure 82 shows the predicted occupancy of water oxygen atoms. Growing the ligand into these spaces may displace or replace a water molecule.

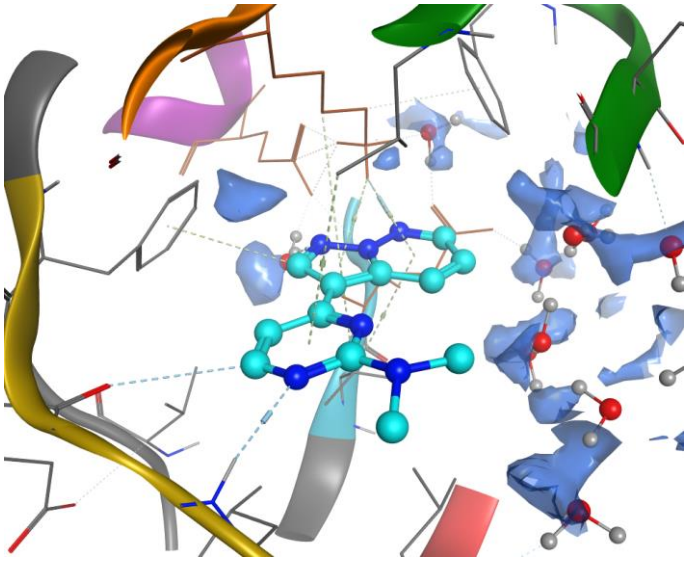

Figure 82. Active site waters in DYRK1A. In-house crystal structure of **96** bound to DYRK1A. 3D-RISM calculation and predicted occupancy of water oxygen atoms in the ligand-protein complex. Structure preparation and calculations performed in MOE 2016, CCG with Amber10:EHT force field

The results of the 3D-RISM calculation did not identify any of the waters in the active site of DYRK1A to be particularly high in energy or 'unhappy'. Thus, focus was centred on displacing

and replacing the consensus water at the back-pocket of DYRK1A. Molecules capable of displacing the consensus water were designed *in silico*. Compounds were modelled directly into an in-house pyrazolo[1,5-*b*]pyridazine co-crystal structure using MOE Builder to design molecules by eye that could potentially displace the water. Energy minimisation using Amber10:EHT force field gave of an indication of whether the molecule would be accommodated in the pocket.

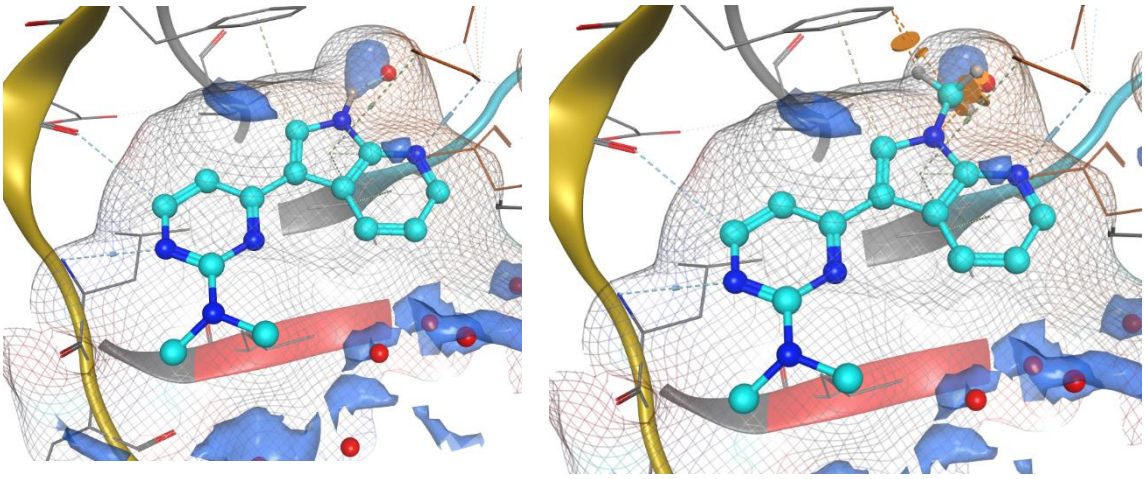

Figure 83. Design of core replacements that displace the consensus water in the back pocket of DYRK1A. Core replacements were modelled into the active site of DYRK1A using in-house crystal structure of **96** bound to DYRK1A and then using Builder tool to modify core. Energy minimisation and structure preparation was carried out in MOE 2016, CCG using Amber10:EHT force field.

7.2.4. Synthesis of Heterocyclic Analogues of the Pyrazolo[1,5-*b*]pyridazine Series

It was envisaged that most analogues would be accessed from the appropriate boronic acid or ester and common intermediate **211** under Suzuki conditions. Analogues **212**-**215** were accessed from the same general route.

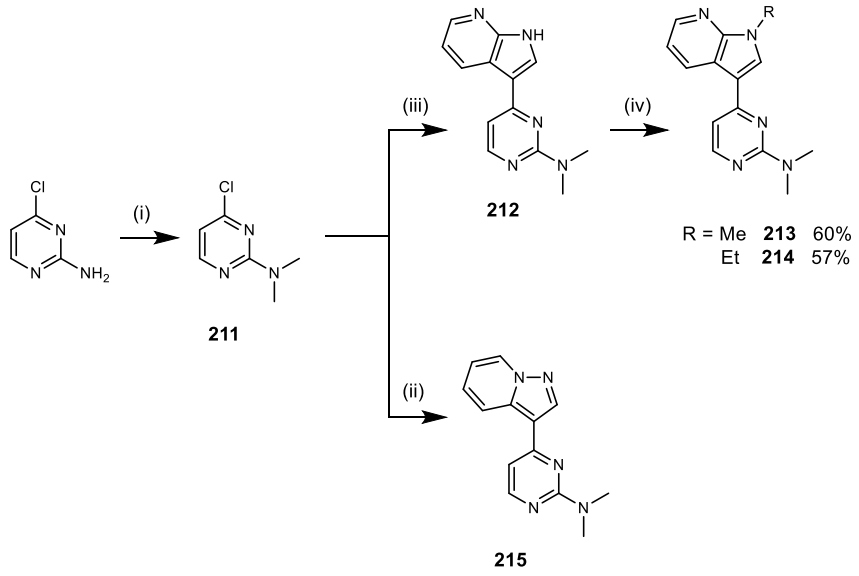

Scheme 39. *Reagents and conditions*: (i) sodium hydride, iodomethane, THF, rt, 16 h, 89%; (ii) bis[2-(di-*tert*-butylphosphanyl)cyclopenta-2,4-dien-1-yl]iron; dichloropalladium, 3-(4,4,5,5-tetramethyl-1,3,2-dioxaborolan-2-yl)pyrazolo[1,5-*a*]pyridine, 2 M potassium carbonate, 1,4-dioxane, 70 °C, 16 h, 83%; (iii) 2-Methyl-2-propanyl 3-(4,4,5,5-tetramethyl-1,3,2-dioxaborolan-2-yl)-1*H*-pyrrolo[2,3-*b*]pyridine-1-carboxylate, tris(dibenzylideneacetone)dipalladium(0), potassium fluoride, tri-*tert*-butylphosphonium tetrafluoroborate, 120 °C, 20 min, µwave then 4 N HCl in 1,4 dioxane, rt, 2 h, 91%; (iv) sodium hydride, haloalkane, DMF, rt, 1 h.

Boronic ester **218** was synthesised in-house. Following a literature procedure, 1*H*-pyrrolo[2,3-*C*]pyridine was tosyl protected. Selective monohalogenation with *N*-bromosuccinimide afforded intermediate **217**. Miyaura borylation of the bromide afforded the desired boronic ester **218**, which was used in subsequent Suzuki reactions crude and without further purification.[285]

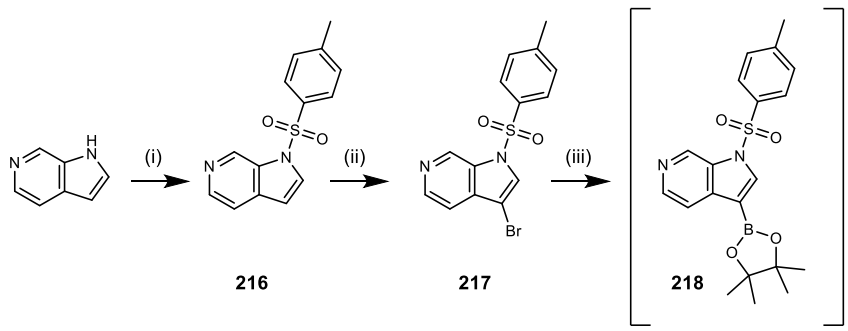

Scheme 40. *Reagents and conditions*: (i) tetrabutylammonium hydrogensulfate, 33% sodium hydroxide, *p*-toluenesulfonyl chloride, toluene, rt, overnight, 92%; (ii) *N*-bromosuccinimide, DMF, rt, overnight, 14%; (iii) bis(pinacolato)diboron, bis(triphenylphosphine)palladium(II) dichloride, potassium acetate, 1,4-dioxane, 100 °C, 2 h, 85%.

The synthesis of **219** was then completed using the same Suzuki protocol as described above.

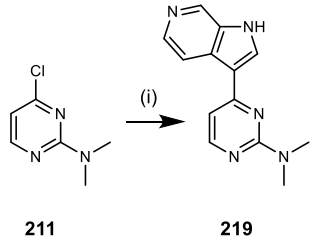

Scheme 41. *Reagents and conditions*: (i) 1-(*p*-tolylsulfonyl)-3-(4,4,5,5-tetramethyl-1,3,2-dioxaborolan-2-yl)pyrrolo[2,3-*c*]pyridine, potassium fluoride, tris(dibenzylideneacetone)dipalladium(0), tri-*tert*-butylphosphonium tetrafluoroborate, acetonitrile:water (4:1), 120 °C, 5 h then 1 M sodium hydroxide, 100 °C, 1 h, µwave, 12%.

Synthesis of the *N*-methyl analogue of **220** turned out to be more difficult than experienced in other templates. Methylation of **220** under conventional conditions using sodium hydride and iodomethane resulted in *N*-methylation of the 6 position in addition to methylation of the indole N-*H*. Performing the alkylation for 30 min afforded the desired *N*-methyl product **220** in sufficient yield and purity to test for DYRK1A binding affinity. The dimethylated compound **221** was also isolated as the major component.

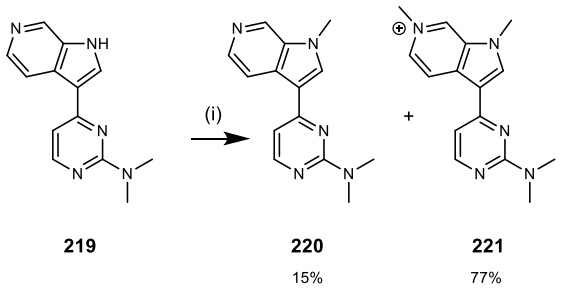

Scheme 42. *Reagents and conditions*: (i) sodium hydride, iodomethane, DMF, rt, 30 min.

Initially it was envisaged that the remaining heterocyclic analogues could be accessed via a two-step approach. The commercially available haloheteroarene would be converted to the boronate via Miyaura reaction. Subsequently the C-C bond would be constructed between pyrimidine **211** and appropriate boronate via Suzuki reaction. This approach proved unreliable and low yielding for a number of analogues.

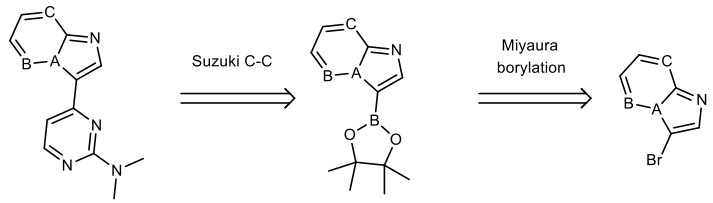

Scheme 43. Route Envisaged to Heterocyclic Analogues.

Another approach considered was to switch the reactivity of the coupling partners. Many of the haloheteroarenes were commercially available. Reaction of the appropriate haloheteroarene with 2-(methylsulfanyl)-4-(tributylstannyl)pyrimidine under Stille conditions was attempted but again proved sluggish, low yielding and difficult to remove traces of stannane. As both of the Suzuki and Stille routes were not optimal, an analogous route to that employed for the synthesis of the pyrazolo[1,5-*b*]pyridazine series was developed. All remaining analogues were synthesised via this route.

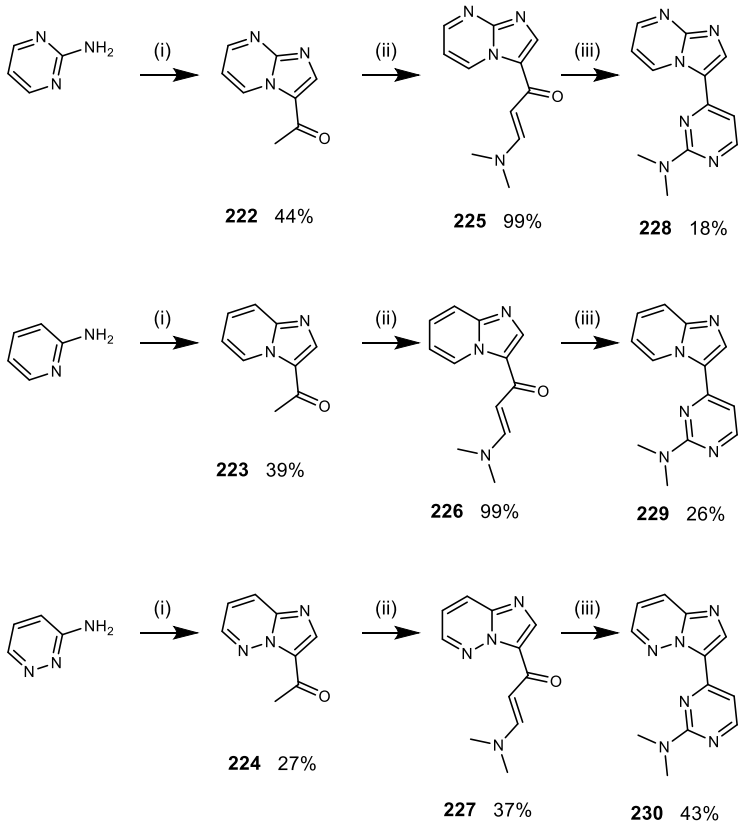

Scheme 44. *Reagents and conditions*: (i) DMF-DMA, toluene, 90 °C, 2 h – overnight then chloroacetone, EtOH, reflux, overnight; (ii) DMF-DMA, 75 °C, 16 h; (iii) 2-methoxyethanol, potassium carbonate, 1,1-dimethylguanidine sulfate salt, 125 °C, overnight.

During the synthesis of **228** a second molecule, **231**, was isolated with the same Mwt and a similar structure by ^{1}H NMR. **231** was the major product and was formed in approximately 2:1 ratio with **228**. Small molecule x-ray crystallography confirmed suspicions that the major product isolated was a regioisomer of the intended product (Figure 84). It is likely that the regioisomer was formed under the basic reaction conditions *via* a Dimroth rearrangement (Figure 85).

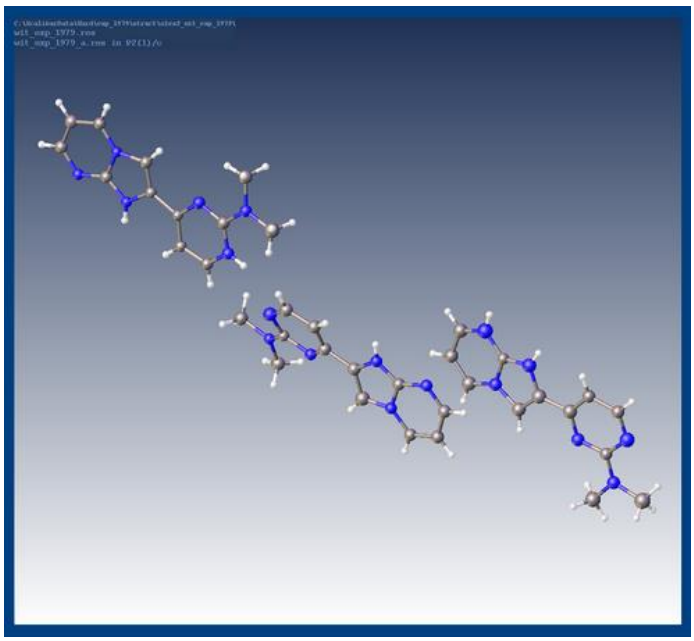

Figure 84. Small molecule x-ray crystal structure of **231**. The structure was elucidated as the regioisomer of **228**.

Imidazo[1,2-*a*]pyrimidines are known to undergo this type of rearrangement and have in the past been mis-assigned in the literature.[286]

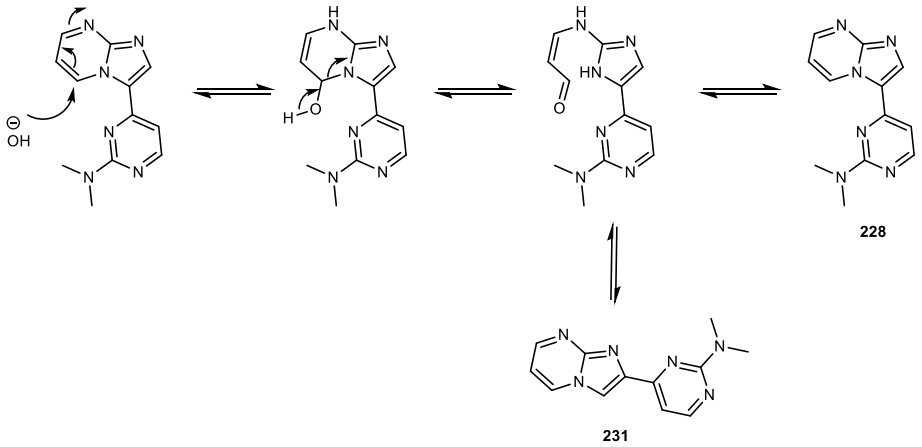

Figure 85. Proposed mechanism for the Dimroth rearrangement of **228** to **231**.

7.2.5. SARs and Biological Evaluation of Heterocyclic Analogues

The DYRK1A inhibitory activities of the heterocyclic analogues are displayed in Table 43. Included for comparison is pyrazolo[1,5-*b*]pyridazine **96**.

Of all of the molecules synthesised only **212** and **228** possess strong DYRK1A binding affinity and maintain excellent LE.

Table 43. DYRK1A Binding Affinity of Heterocyclic Analogues

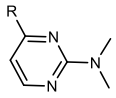

Compound	R	DYRK1A IC_{50}[a]	LE
96	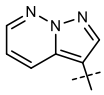	75	0.55
215	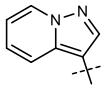	893	0.47
228	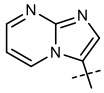	158	0.53
229	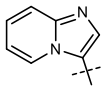	695	0.48
230	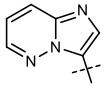	54445	0.33
212	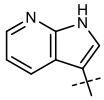	134	0.54
213	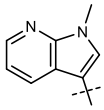	11880	0.36
214	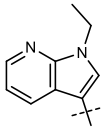	7725	0.36
219	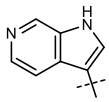	1012	0.47
220	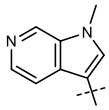	968	0.44
221	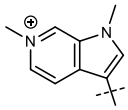	30193	0.32

[a]IC_{50} (nM) in TR-FRET-based ligand-binding displacement assay (n = 1). LE = 1.4(pIC_{50})/non-hydrogen atoms;

An interesting observation is that **215** exhibits >10 fold reduction in DYRK1A binding affinity compared to **96**, suggesting that the N8 is important for activity. Comparing **228** to molecule **229**, again the removal of N8, results in a 4 fold reduction in DYRK1A binding affinity. The importance of N8 to DYRK1A binding affinity is further supported by the reduction in DYRK1A inhibitory activities observed in analogues **219**-**221** and **229**-**230**. This is consistent with the binding mode of the series as N8 forms a hydrogen-bond with Lys188.

228 is capable of maintaining both hydrogen-bonds formed between the ligand and the consensus water, and the ligand and the catalytic lysine residue, thus **228** maintains binding affinity at DYRK1A. This is also true for **212**. **230** exhibits approximately 80 fold reduction in DYRK1A binding affinity compared to **229**, suggesting that the inclusion of N5 has caused this decline in activity. It could be that the N5 of the imidazo[1,2-*b*]pyridazine heterocycle is making an unfavourable interaction with a nitrogen from the pyrimidine motif, N3', obstructing the active conformation of the ligands (Figure 86). This phenomenon, the necessary nitrogen atom, has been reviewed recently.[276]

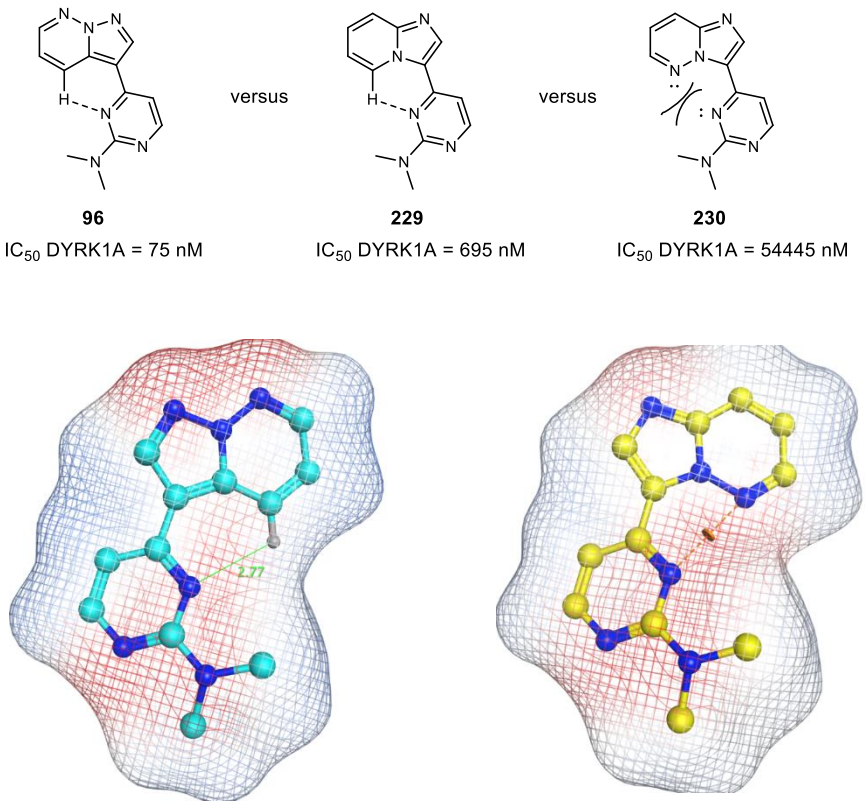

Figure 86. Electrostatic surfaces of **96** and **230** in active bound conformation. Electrostatic and lone pair repulsion (orange) between nitrogens of imidazo[1,2-*b*]pyridazine ring and pyrimidine could result in lower affinity observed for **230** compared to **96**. [276, 287] LHS - In-house crystal structure of **96** bound to DYRK1A. RHS – core of **230** modelled into DYRK1A using Builder tool to modify existing structure. Structure preparation carried out in MOE 2016, CCG with Amber10:EHT force field.

All of compounds designed to interact or displace the consensus water (**213**, **214** and **220**) exhibited diminished DYRK1A binding affinity. Potentially, the major issue here could be that the phenylalanine gatekeeper is preventing access to the back-pocket. To our knowledge there are currently no Type 1.5 inhibitors for kinases that possess phenylalanine gatekeepers. This is likely due to the high energy cost associated with rearrangement of the residue to accommodate the ligand in the back-pocket.[122]

212 and **228** were further profiled for selectivity. Initially the selectivity profile of **212** was assessed in a 48-kinase panel using a DSF assay. The results of this assay appeared to show that relative to the control staurosporine, **212** had promising selectivity profile. However, **212** had a substantially worse selectivity profile than other all pyrazolo[1,5-*b*]pyridazine analogues tested. It was suspected that a change in binding mode had occurred for **212** due to the additional N-*H* present, capable of hydrogen-bond donation to the hinge. The co-crystal structure of **212** bound to DYRK1A was elucidated and showed that scaffold hopping to the pyrrolo[2,3-*b*]pyridine resulted in a flipped binding mode with respect to the pyrazolo[1,5-*b*]pyridazine series, resulting in a significantly poorer selectivity profile.

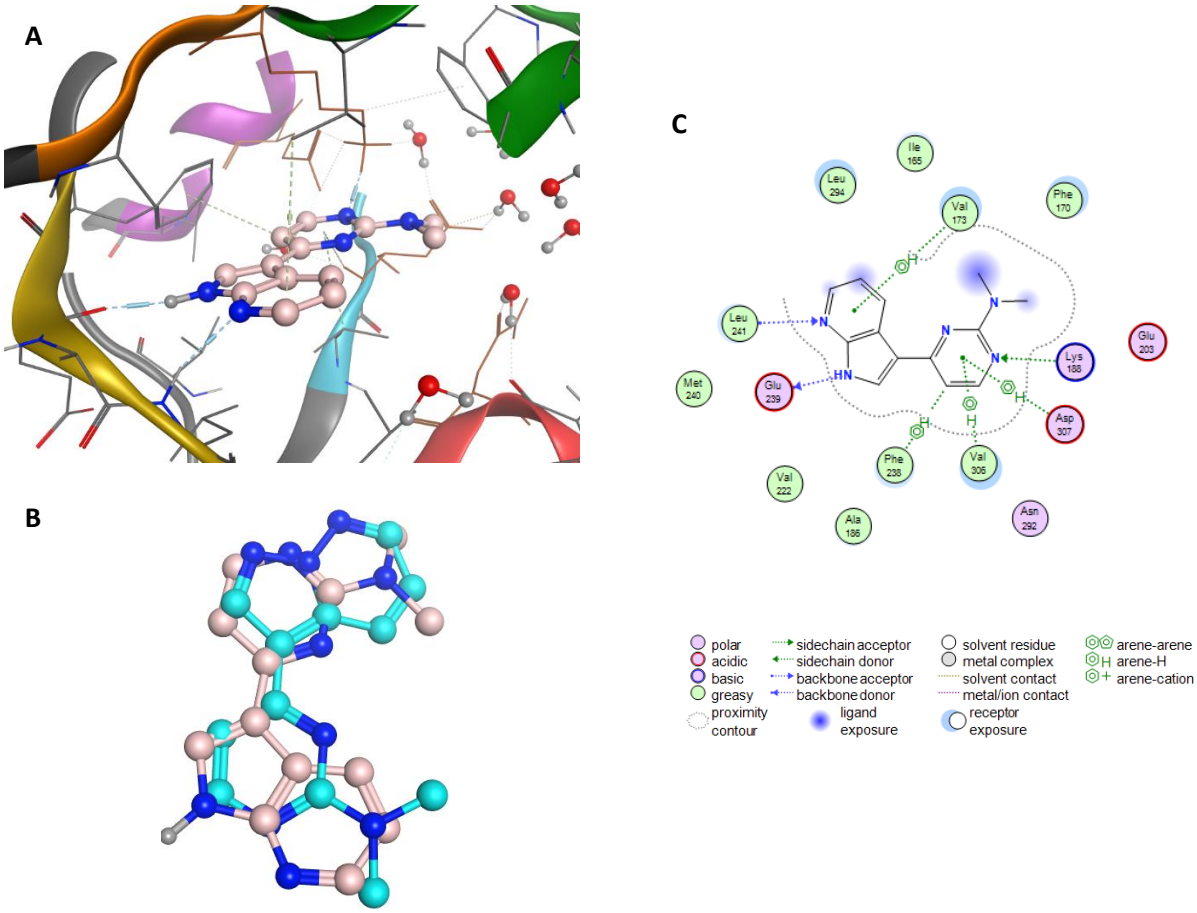

Figure 87. A - Crystal structure of 212 in DYRK1A exhibiting flipped binding mode. B – Overlay of active conformations of 212 and 96. C – 2D ligand interaction diagram of 212 showing hydrogen-bonding interactions with Leu241, Glu239 and Lys188. Structure preparation carried out in MOE 2016, CCG with Amber10:EHT force field.

As **212** possesses a different binding mode and selectivity profile to the pyrazolo[1,5-*b*]pyridazine series, it represents the first analogue in a new series of DYRK1A inhibitors based on the pyrrolo[2,3-*b*]pyridine template. At the time of writing selectivity assessment of **228** is underway. **228** is being profiled in a 468 kinase panel to assess kinome-wide selectivity, provided by DiscoveRx.

212 and **228** were profiled for metabolic stability and thermodynamic solubility. The results are displayed in Table 44. The data for **96** is included for comparison.

Table 44. Metabolic Stability and Solubility of 212 and 228

Compound	Human (µL/min/mg)	Rat (µL/min/mg)	Solubility (mg/mL)
96	241.8[a] +/- 31.7	230.1[a] +/- 30.8	0.1
212	153.9[a] +/- 38.8	234.2 +/- 16.5	0
228	154.3 +/- 6.3	95.5 +/- 24.5	0.47

HLM and RLM Determinations mean of n =2 +/- standard deviation (unless otherwise stated). [a]Mean of n = 4 +/- standard deviation. HLM = human liver microsomes; RLM = rat liver microsomes; thermodynamic solubility data derived from single experiment at pH 6.8.

212 does not exhibit substantial improvements in solubility or metabolic stability when compared to **96**. On the other hand, **228** exhibits superior metabolic clearance and solubility data compared to **96**. These results suggest that scaffold hopping from the pyrazolo[1,5-*b*]pyridazine core to the imidazo[1,2-*a*]pyrimidine heterocycle could be a good strategy for improving metabolic stability and solubility in the future. The DYRK1A binding affinity of the imidazo[1,2-*a*]pyrimidine analogue is lower than that of the pyrazolo[1,5-*b*]pyridazine tool, thus potency would have to be increased elsewhere in the molecule to afford a superior tool compound.

7.3. Library Enumeration and Structure-guided Substitution of the Pyrazolo[1,5-*b*]pyridazine Heterocycle

7.3.1. Rationale

The previous Chapters 4-6 reported significant gains in kinome-wide selectivity through the incorporation of the *N,N*-dimethylaminopyrimidine subunit onto the pyrazolo[1,5-*b*]pyridazine head. So far scaffold hopping to similar 5,6-heterocycles had not furnished a DYRK1A inhibitor with greater on-target potency than the pyrazolo[1,5-*b*]pyridazine analogue **96**. A more diverse exploration of head groups could potentially furnish higher affinity binders of DYRK1A with better solubility and metabolic stability, which retained kinome-wide selectivity afforded by the *N,N*-dimethylaminopyrimidine tail.

A similar structure-based design approach was used to that detailed in Chapter 5. However, the virtual library enumerated was populated with all of the available heterocyclic boronic acids and esters in-house. The enumerated library was triaged using the same KNIME® workflows as before. Potential inhibitors were docked into an in-house co-crystal structure of DYRK1A using induced-fit docking in MOE with Amber10:EHT force field. Compounds that docked successfully were synthesised and tested for biological activity.

7.3.2. Synthesis of Enumerated Library

The enumerated library was synthesised using parallel chemistry. In the first step 4-chloro-2-aminopyrimidine was dimethylated using sodium hydride and iodomethane at room temperature to afford **211**. The C-C bond was constructed between **211** and commercially available boronic acids *via* Suzuki cross-coupling chemistry.

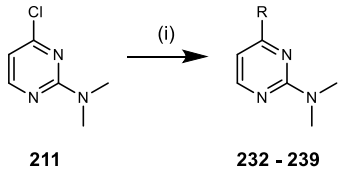

Scheme 45. *Reagents and conditions*: (i) bis[2-(di-*tert*-butylphosphanyl)cyclopenta-2,4-dien-1-yl]iron; dichloropalladium, 2 M potassium carbonate, 1,4-dioxane, 80 °C, 16 h, 4 – 94%.

7.3.3. SARs and Biological Evaluation of Enumerated Library

The DYRK1A binding affinity of the synthesised library is displayed in Table 45. **96** has been included for reference.

All alterations to the pyrazolo[1,5-*b*]pyridazine scaffold resulted in severely diminished DYRK1A binding affinity.

Table 45. DYRK1A Binding Affinity of Enumerated Library

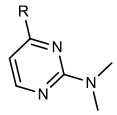

Compound	R	DYRK1A IC_{50}[a]	LE
96	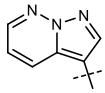	75	0.55
232	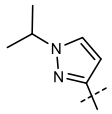	**	-
233	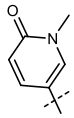	8069	0.42
234	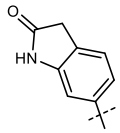	16237	0.35
235	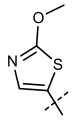	3557	0.48
236	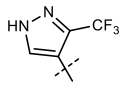	8018	0.4
237	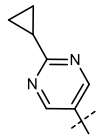	**	-
238	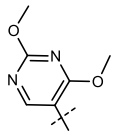	**	-
239	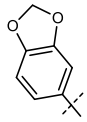	1382	0.46

[a]IC_{50} (nM) in TR-FRET-based ligand-binding displacement assay (n = 1). LE = 1.4(pIC_{50})/non-hydrogen atoms. ** Data could not be fitted to curve.

232 - **239** all exhibited much weaker binding affinity than **96** and were not progressed as DYRK1A ligands. **232**, **237** and **238** had no measurable DYRK1A binding affinity. This small-scale exploration shows that diverging too far away from the pyrazolo[1,5-*b*]pyridazine core may not to be the best method of discovering new DYRK1A inhibitors. A more rational approach, retaining the 'hinge + Lys188' recognition motif and iteratively adding substituents may yet yield an analogue with a better overall profile.

7.4. Is SAR Additive with Chimeric Pyrazolo[1,5-*b*]pyridazines and Imidazo[1,2-*a*]pyrimidines?

7.4.1. Rationale

A small selection of chimeric molecules (Figure 88) were designed with the aim of furnishing DYRK1A inhibitors that balanced DYRK1A affinity and selectivity with desirable solubility and metabolic stability.

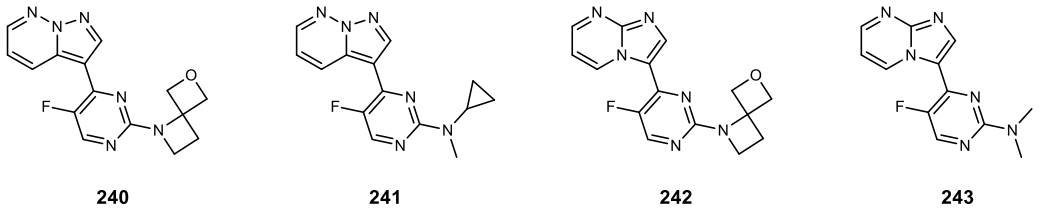

Figure 88. SAR summary of the pyrazolo[1,5-*b*]pyridazine series and chimeric molecules designed.

7.4.2. Synthesis of Chimeric Analogues 240 - 243

240 and **241** were accessed via the same procedure established for the synthesis of **172**. The alkyne was installed via Sonogashira reaction to afford 1,3-dipolarphile **184**. Subsequent DBU-promoted 1,3-dipolar cycloaddition with intermediate **74** rapidly constructed the pyrazolo[1,5-*b*]pyridazine motif to give **185**. Nucleophilic aromatic substitution with appropriate amine afforded the desired products **240** and **241**.

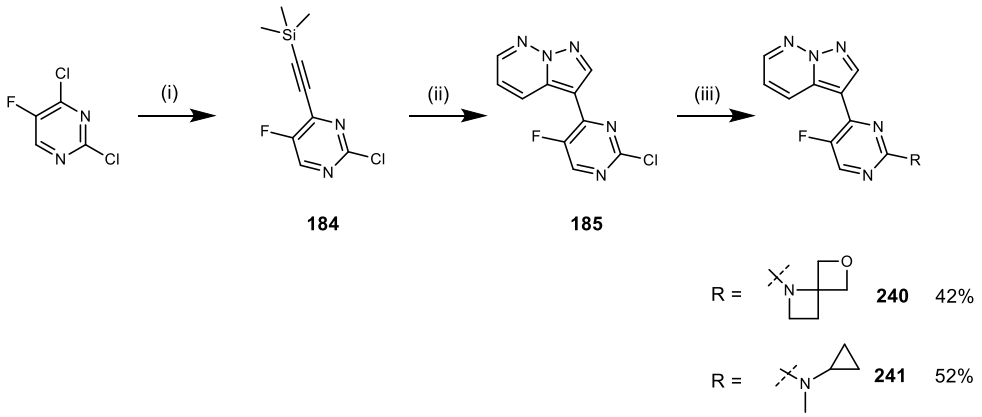

Scheme 46. *Reagents and conditions:* (i) bis(triphenylphosphine)palladium(II) dichloride, copper iodide, TEA, (trimethylsilyl)acetylene, THF, rt, overnight, 42%; (ii) DBU, 1-aminopyridinium iodide, 50 °C, 1 h, 42%; (iii) secondary amine, 120 °C, 16 h.

242 and **243** were furnished in an alternative 3 step procedure from the same 2,4-dichloro-5-fluoropyrimidine starting material. Vinyl ether **244** was accessed via Heck cross-coupling reaction. Subsequent 1,3-dipolar cycloaddition with 2-aminopyrimidine afforded the

imidazo[1,2-*a*]pyrimidine intermediate **245**. Nucleophilic aromatic substitution with the appropriate amine afforded the desired products **242** and **243**.

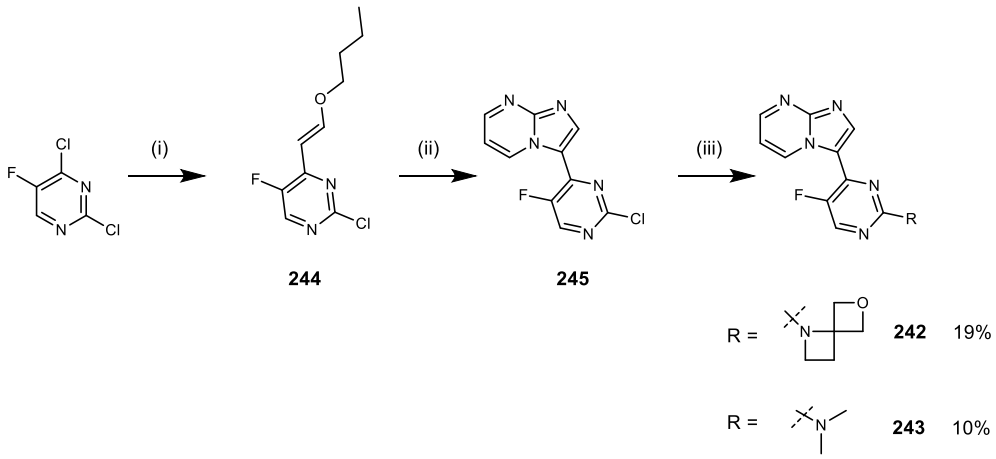

Scheme 47. *Reagents and conditions*: (i) butoxyethene, palladium(II) acetate, TEA, polyethylene glycol 500, 80 °C, overnight, 55%; (ii) *N*-bromosuccinimide, 1,4-dioxane:water (3:1), rt, 1 h then pyrimidin-2-amine, 85 °C, 2 h, 83%; (iii) secondary amine, 120 °C, 2 - 16 h.

At the time of writing, **240** - **243** had been submitted for DYRK1A binding displacement assay and the results are being awaited. No further profiling was carried out.

7.5. Summary

The *N*,*N*-dimethylaminopyrimidine hinge-binding motif was maintained whilst the pyrazolo[1,5-*b*]pyridazine heterocycle was substituted as a means of increasing DYRK1A binding affinity whilst improving selectivity, solubility and metabolic stability for the series.

Performing a methyl scan on the pyrazolo[1,5-*b*]pyridazine motif revealed that the metabolic stability of the series could be improved by adding a methyl substituent to the 5-position (**204**) of the core without significantly weakening DYRK1A binding affinity. Installing a methyl group onto any of the other positions on the pyrazolo[1,5-*b*]pyridazine scaffold resulted in diminished DYRK1A binding affinity. Interestingly, substituting a methoxy group onto the 4-position of the pyrazolo[1,5-*b*]pyridazine core resulted in a molecule (**206**) with strong DYRK1A binding affinity and a much-improved solubility and metabolic stability profile.

In silico scaffold hopping using Cresset Spark™ identified a number of 5,6-heterocycles as potential bioisosteric replacements for the pyrazolo[1,5-*b*]pyridazine motif. The imidazo[1,2-*a*]pyrimidine **228** exhibited a slight decrease in DYRK1A affinity but enhanced solubility and metabolic stability compared to the pyrazolo[1,5-*b*]pyridazine matched-pair **96**. The synthetic route employed to furnish **228** afforded two molecules with the same molecular weight and

similar ^{1}H NMR, indicating that regioisomers had been formed. The identity of **231** was proved with x-ray crystallography. It is speculated that **231** was formed via a Dimroth rearrangement of **228** under the basic reaction conditions employed.

Scaffold hopping to the pyrrolo[2,3-*b*]pyridine scaffold afforded **212**, which possessed strong binding affinity for DYRK1A. However, **212** exhibited a flipped binding mode with respect to the pyrazolo[1,5-*b*]pyridazine series, which resulted in a poorer selectivity profile. The co-crystal structure of **212** could be used to design a back-up series of DYRK1A inhibitors based on the pyrrolo[2,3-*b*]pyridine core in the future.

Chimeras of the most promising DYRK1A inhibitors identified throughout Chapters 4-7, **240**-**243**, were synthesised successfully and were submitted for DYRK1A binding-displacement assay. Follow up studies will be undertaken if any exemplar exhibits IC_{50} < 100 nM.

The following two chapters document the work carried out in parallel on two back-up series of DYRK1A inhibitors.

CHAPTER 8. Investigation of a Series of Imidazo[1,2-*b*]pyridazines as Inhibitors of DYRK1A

In addition to the pyrazolo[1,5-*b*]pyridazine series a number of other heterocyclic scaffolds were being investigated in parallel for DYRK1A inhibition. Chapter 8 describes the investigation of a series of imidazo[1,2-*b*]pyridazines as DYRK1A inhibitors. After identifying the key stabilising interactions of the series with DYRK1A, optimisation of the solubility and metabolic stability of the series is attempted. To achieve this the number of aromatic rings and lipophilicity of the series is reduced. SBDD and patent analyses are used in an attempt to furnish stronger affinity ligands of DYRK1A that are more selective.

8.1.1. Identification and Selection of the Imidazo[1,2-*b*]pyridazine Series

In 2017 Bendjeddou *et al*. reported a series of imidazo[1,2-*b*]pyridazines, represented by **246**, which potently and selectively inhibited DYRK1A (IC_{50} = 33 nM) with off-target activity at CLKs and CDKs.[288]

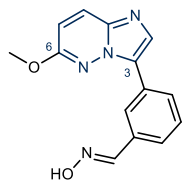

246

Figure 89. Published imidazo[1,2-*b*]pyridazine DYRK1A inhibitor **246**.[288]

In the same year, a series of imidazo[1,2-*a*]pyridines and benzimidazoles, with the same 3,6-substitution pattern, were disclosed as DYRK1A inhibitors in a patent filed by the University of Arizona Board of Reagents.[289]

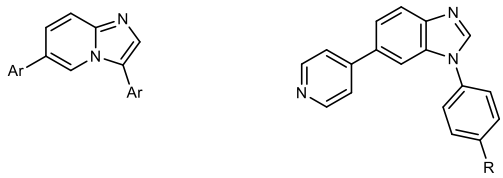

R = CN, SO_2Me, ether, amine, acid, ester, amide

Figure 90. Imidazo[1,2-*a*]pyridines and benzimidazoles disclosed as DYRK1A inhibitors.[289]

A collection of imidazo[1,2-*b*]pyridazines that were of interest to another in-house kinase project were screened in the KINOMEscan® platform provided by DiscoveRx against 468 kinases at 1 µM concentration. The results of the screening identified **247** as a relatively selective DYRK1A inhibitor.

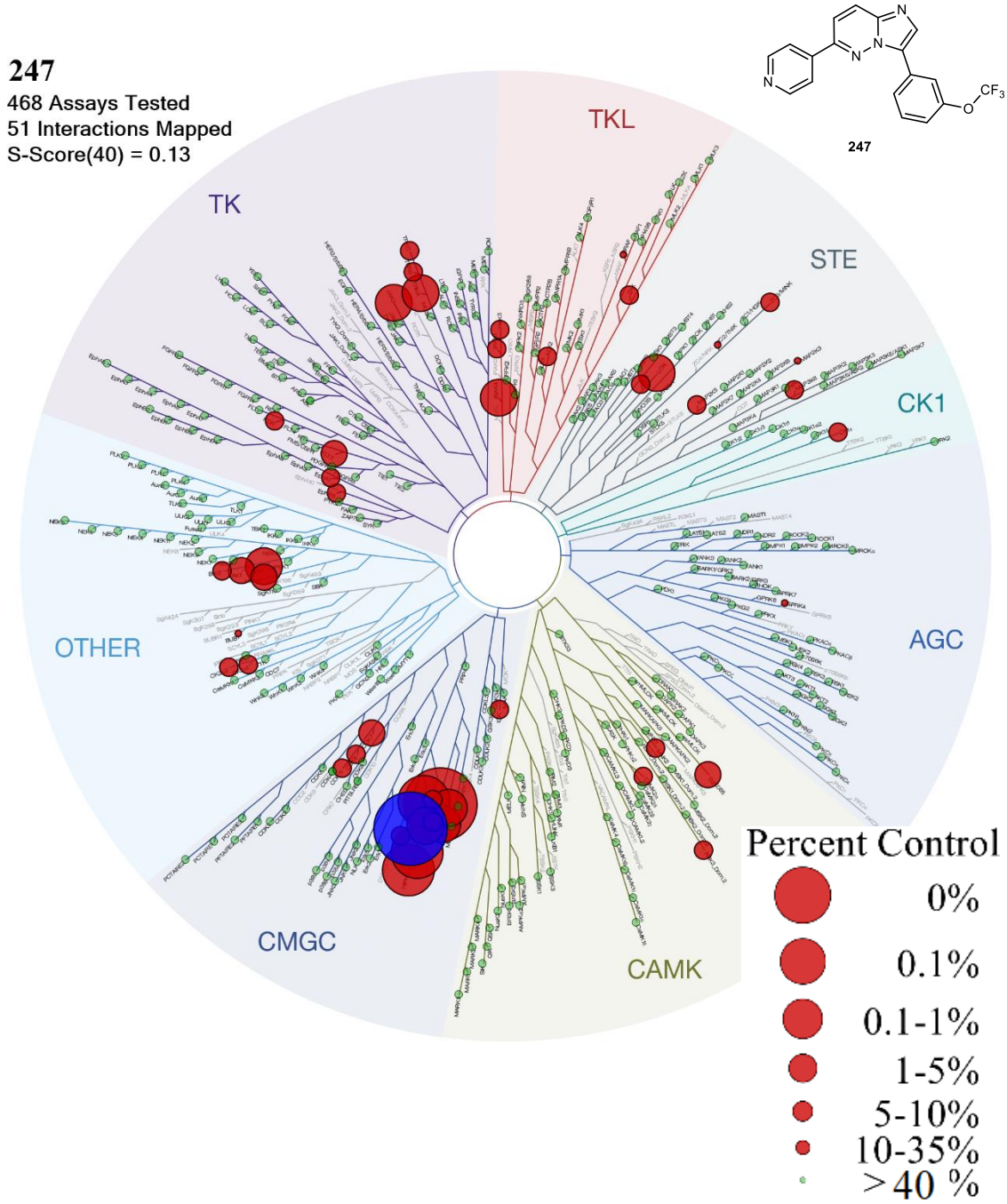

Figure 91. Structure of imidazo[1,2-*b*]pyridazine **247** and good selectivity evidenced by KINOMEscan® results. DYRK1A is highlighted in blue. Image generated using TREEspot™ Software Tool and reprinted with permission from KINOMEscan®, a division of DiscoveRx Corporation, © DISCOVERX CORPORATION 2010.

247 inhibited approximately 11% of the human kinome over 75%. The kinome-wide selectivity profile of **247** was superior to **68**, the starting point in the pyrazolo[1,5-*b*]pyridazine series.

Table 46. Overview of Kinome Selectivity Profiles of Compounds 247

Compound	Percentage kinases inhibited > 75%[a]	Percentage kinases inhibited > 50%[a]	Kinases most potently inhibited
247	11	23	CLKs, HIPKs, DYRK1B, PI3K, FLT3

[a] % Inhibition as determined by DiscoveRx KINOMEscan® experiment.

In addition to the attractive kinome-wide selectivity profile exhibited by **247**, the presence of a 3,6-biaryl substitution pattern common to other DYRK1A inhibitors, provided confidence that the imidazo[1,2-*b*]pyridazine series warranted further investigation. DYRK1A affinity was measured for a small cluster of imidazo[1,2-*b*]pyridazines using the DYRK1A ligand-binding displacement assay to confirm binding.

Table 47. DYRK1A Binding Affinity for Imidazo[1,2-*b*]pyridazines

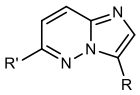

Compound	R'	R	DYRK1A IC_{50}	LE, LipE
247		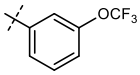	22	0.41, 3.2
248	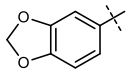	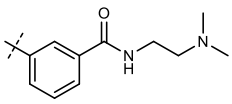	39	0.32, 5.6
249	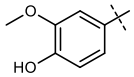		5	0.51, 4.7
250	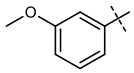	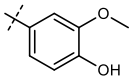	122	0.37, 3.3

[a]IC_{50} (nM) in TR-FRET-based ligand-binding displacement assay (n = 1). LE = 1.4(pIC_{50})/non-hydrogen atoms; LipE = pIC_{50} – clog P.

All imidazo[1,2-*b*]pyridazines re-confirmed as high affinity ligands of DYRK1A with good LE and LipE. Although **247** possessed the worst LipE of the compounds assayed, inspection of the selectivity data suggested that **247** possessed the highest level of kinome-wide selectivity.

The increased DYRK1A affinity of **247** compared to any of the advanced analogues discovered in the pyrazolo[1,5-*b*]pyridazine series made it an attractive starting point. Another positive feature of **247** was that it possessed no HBDs to begin with, which is advantageous for

compounds that need to penetrate the BBB. A CNS MPO score of 4.3 for **247** is already close to desirable space for a CNS penetrant compound. The only weaknesses of **247** were its high lipophilicity (clog P = 4.5), high aromatic ring count (4) and high sp^2 character, which are commensurate with poor *in vitro* PK properties.[22,23] The solubility and metabolic stability of **247** were determined in-house, the results are displayed in Table 48.

Table 48. Metabolic Stability and Solubility of **247**

Compound	HLM (µL/min/mg)	RLM (µL/min/mg)	Solubility (mg/mL)
247	173.4 +/- 20.9	104.8 +/- 14.7	0

HLM and RLM Determinations mean of n =2 +/- standard deviation (unless otherwise stated). HLM = human liver microsomes; RLM = rat liver microsomes; thermodynamic solubility data derived from single experiment at pH 6.8.

The metabolic stability of **247** was within the limits set out at the beginning of the project for a molecular probe. However, the solubility of **247** was extremely low, with no measurable solubility recorded.

As **247** represented one of the highest affinity DYRK1A ligands with good selectivity, in-cell DYRK1A target engagement was assessed using a NanoBRET assay. **247** maintained a potent level of DYRK1A inhibition in cell and was over 10 fold more potent than **96**, showing no signs of cytotoxicity.

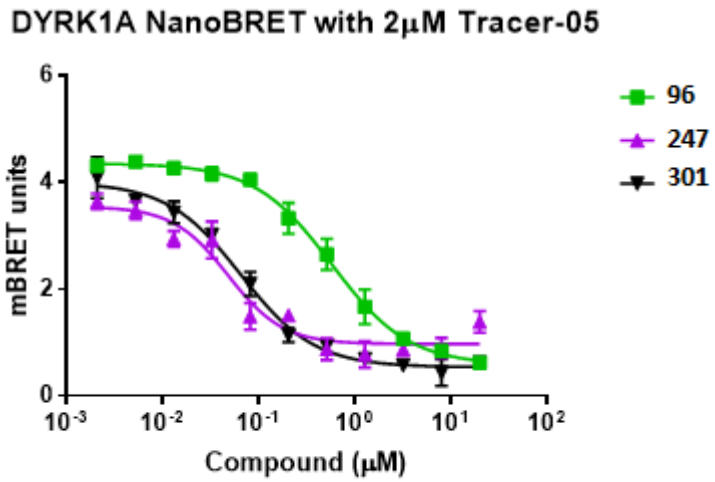

	96	247	301
IC50	0.5762	0.04814	0.06543

Figure 92. NanoBRET cellular activity of **247** (magneta curve). IC_{50} reported in µM.

It was essential to determine which features of **247** were responsible for its attractive selectivity profile. It was also desirable to know the reason for the higher levels of DYRK1A binding affinity exhibited by **247**, compared to analogues of the pyrazolo[1,5-*b*]pyridazine series. The aim of the work undertaken on the imidazo[1,2-*b*]pyridazine series was to improve DYRK1A binding affinity and selectivity, whilst improving solubility and metabolic stability.

8.1.2. Synthesis of the Imidazo[1,2-*b*]pyridazine Series

It was envisaged that a library of 3,6-derivatised imidazo[1,2-*b*]pyridazines could be rapidly accessed from commercially available **251** via two successive C-C bond forming reactions. The first Suzuki cross-coupling, carried out at 110 °C, installed the required aryl group selectively at the 3-position with only a minor amount of regioisomer being produced. Recrystallisation in petroleum ether, followed by washing with petroleum ether furnished the desired isomer, **252**, in good yield and purity. The second Suzuki cross-coupling to install the 4-pyridyl subunit was prosecuted with microwave heating at 140 °C to afford the products **247**-**265** rapidly.

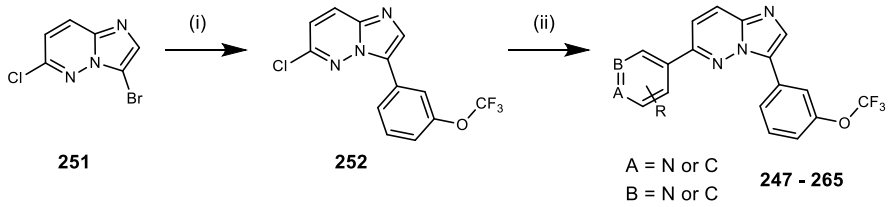

Scheme 48. *Reagents and Conditions*; (i) [3-(trifluoromethoxy)phenyl]boronic acid, [1,1'-bis(diphenylphosphino)ferrocene]dichloropalladium(II), cesium carbonate, water:1,4-dioxane (1:6), 110 °C, 5 h, 56%; (ii) boronic acid, bis(triphenylphosphine)palladium(II) dichloride, sodium carbonate, water:acetonitrile (1:5), 140 - 150 °C, 15 – 20 min.

8.1.3. SARs and Biological Evaluation of Imidazo[1,2-*b*]pyridazines

The DYRK1A binding affinity data for imidazo[1,2-*b*]pyridazine analogues is presented in Table 49. The data for **247** is included for reference.

Small scale exploration around the 6-postion appeared to show that the 4-pyridyl was important for activity when the 3-position was occupied by the 3-(trifluoromethoxy)phenyl substituent. Comparing analogues **247** and **253** demonstrates the importance of the pyridine nitrogen, likely a point of contact to Leu241 (hinge) or Lys188 (catalytic lysine).

Table 49. DYRK1A Binding Affinity of Imidazo[1,2-*b*]pyridazines

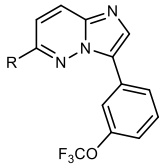

Compound	R	DYRK1A IC_{50}[a]
247		22
253		53375
254	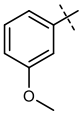	536310
255	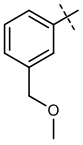	506605
256	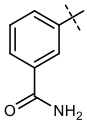	2647
257	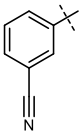	1000000
258	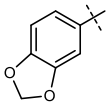	1349
259	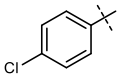	1000000
260	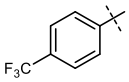	1000000

[a]IC_{50} (nM) in TR-FRET-based ligand-binding displacement assay (n = 1)

The relationship between the 4-pyridyl subunit and DYRK1A binding affinity was investigated further. Substituents were added to the 4-pyridyl motif in an effort to aid solubility. It was theorised that by adding substituents to the *ortho* position of the pyridyl that the ring may twist out of the plane of the imidazo[1,2-*b*]pyridazine motif, potentially disrupting any π-π stacking between molecules. The position of the nitrogen on the pyridyl ring was also explored to determine the optimal position of the nitrogen atom for stabilising any protein-ligand interaction.

Table 50: DYRK1A Binding Affinity of Pyridyl Analogues

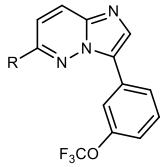

Compound	R	DYRK1A IC_{50}[a]	LE, LipE
247		22	0.41, 3.2
261		1911	0.31, 1.2
262	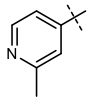	64	0.37, 2.7
263		259	0.34, 1.6
264	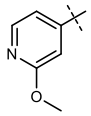	133	0.34, 2.0
265	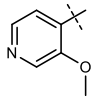	19270	0.26, 1.0

[a]IC_{50} (nM) in TR-FRET-based ligand-binding displacement assay (n = 1). LE = 1.4(pIC_{50})/non-hydrogen atoms; LipE = pIC_{50} – clog P.

Substitution of the 4-pyridyl (**247**) for the 3-pyridyl (**261**) moiety resulted in approximately 100 fold loss in DYRK1A affinity, indicating the importance of the position of the nitrogen atom in the pyridyl ring. Flanking the 4-pyridyl nitrogen with a methyl (**262**) was well tolerated, whereas the larger, more electron rich methoxy (**264**) substituent exhibited a 6 fold loss in potency. Incorporation of substituents *meta* to the 4-pyridyl nitrogen was detrimental in all cases to DYRK1A binding affinity. Again, the smaller methyl (**263**) group was better tolerated with approximately 12 fold loss in potency, compared to the methoxy (**265**) group, which exhibited around 875 fold loss in potency. **262** represented one of the highest affinity binders of DYRK1A and met the potency criteria set out at the beginning of the project. However, although LE was acceptable, LipE was low.

262 was profiled for solubility and metabolic stability to assess whether the additional methyl substituent gave any benefit relative to **247**. The results are displayed in Table 51. Data for **247** is included for reference.

Table 51. Metabolic Stability and Solubility of **262**

Compound	HLM (µL/min/mg)	RLM (µL/min/mg)	Solubility (mg/mL)
247	173.4 +/- 20.9	104.8 +/- 14.7	0
262	71 +/- 3.3	128.8 +/- 3.8	0

HLM and RLM Determinations mean of n =2 +/- standard deviation (unless otherwise stated). HLM = human liver microsomes; RLM = rat liver microsomes; thermodynamic solubility data derived from single experiment at pH 6.8.

The solubility of **262** was not improved compared to **247**. **247** and **262** were profiled further for selectivity. Initially the selectivity profiles of **247** and **262** were assessed against a panel of 48 kinases using a DSF assay. The results of the assay appeared to show that relative to staurosporine, both **247** and **262** selectively inhibited DYRK1A.

8.1.4. Binding Mode of the Imidazo[1,2-*b*]pyridazine Series

The co-crystal structure of **247** bound to DYRK1A was elucidated and gave an insight into the binding mode of the imidazo[1,2-*b*]pyridazine series. Important structural elements that were making interactions in the ATP site of DYRK1A were identified. The co-crystal structure is presented in Figure 93.

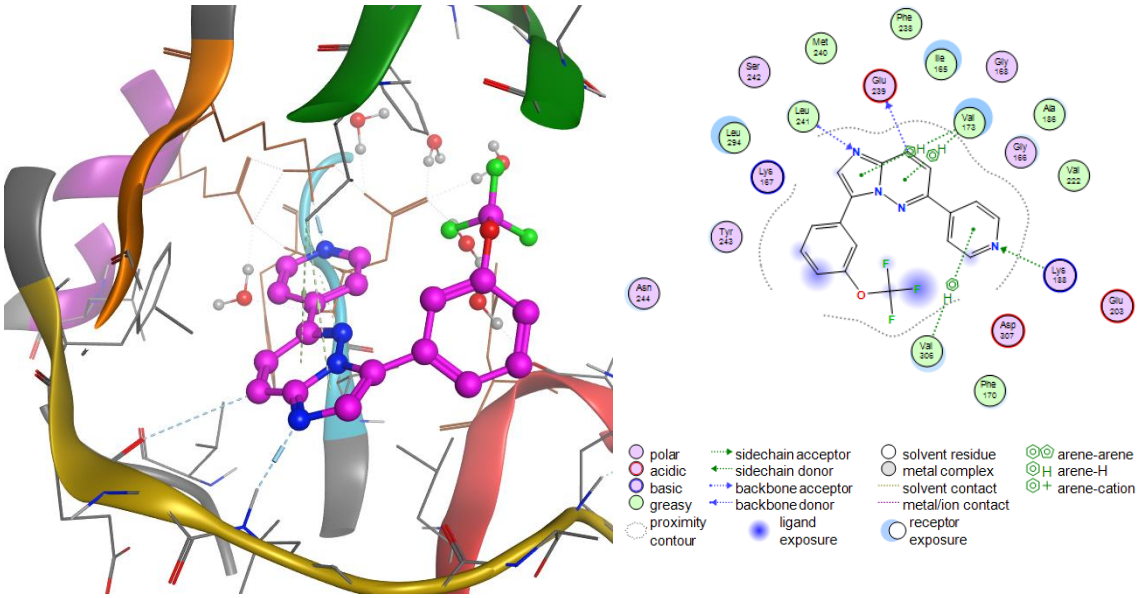

Figure 93. Co-crystal structure of **247** Bound to DYRK1A ATP site in Type I fashion, making hydrogen bonding interactions with Leu241, Glu239 and Lys188. Green – Glycine-rich loop; Gold – Hinge; Pale Blue – DFG motif. Structure prepared and minimised with MOE 2016, CCG with Amber10:EHT force field.

Inspection of the co-crystal structure revealed that **247** binds in Type I fashion to the ATP site of DYRK1A. A hydrogen-bond established between the 4-pyridyl *N* atom and the catalytic Lys188 is clearly present, revealing why the 4-pyridyl was so essential, as analogues incapable of forming this hydrogen bond (**253**-**260**) did not inhibit DYRK1A. A hydrogen bond is formed

between the imidazo *N* and a hinge Leu241 residue. A non-classical hydrogen-bond is formed between the aromatic C-*H* of the imidazo[1,2-*b*]pyridazine and the carbonyl of Glu239 in the hinge of DYRK1A, similar to that formed in the pyrazolo[1,5-*b*]pyridazine series. The lipophilic trifluoromethoxyphenyl motif sits beneath the glycine rich loop. In contrast to the pyrazolo[1,5-*b*]pyridazine series, no interaction between the ligand and the phenylalanine gatekeeper appear to have been made and no interaction between the ligand and the consensus water are made. This suggests that these interactions are not essential for gaining DYRK1A affinity as **247** exhibits stronger DYRK1A binding affinity than many of the ligands from the pyrazolo[1,5-*b*]pyridazine series.

Affinity, selectivity and metabolic stability were comparatively good for **247**, however, the solubility of **247** was sub-optimal and due to the high lipophilicity of **247**, LipE was comparatively low. The poor solubility of the imidazo[1,2-*b*]pyridazine series required optimisation if the series was to progress to furnish a DYRK1A molecular probe. It was envisaged that reducing lipophilicity, planarity and aromatic ring count could lead to an inhibitor of DYRK1A with a better overall profile. With the production of the co-crystal structure of **247** bound to DYRK1A, SBDD could ensue.

8.2. 'Escaping from Flatland', Reducing Aromatic Ring Count and Installation of Solubilising Motifs

8.2.1. Rationale

Aqueous solubility is essential for the development of drug candidates and poor solubility profiles has halted the progression of many molecules through the clinic.[290] Molecules with low aqueous solubility are likely to exhibit poor absorption. The risk assessments for insoluble compounds are often incomplete as accurate levels of exposure are difficult to ascertain. There are also risks that the compound crystallises *in vivo* leading to acute toxicity.[291]

Solubility is inversely proportional to lipophilicity.[292] Aromatic ring count, even when lipophilicity is constant, also affects aqueous solubility. This is due to increased molecular rigidity, melting point phenomena and π-π stacking.[293] Taking these points together, reducing lipophilicity by reducing the number of aromatic rings, should provide analogues with improved solubility. Alongside this strategy, the solubility of prospective compounds was predicted using *in silico* tools. The ChemAxon predictor for intrinsic solubility (log S), based on work by Hou *et al*.[294], was used to estimate the solubility of prospective ligands. In addition, the Property

Forecast Index (PFI) for hydrophobicity (log $D_{7.4}$ (or log P) + #Ar) was calculated prior to synthesis for all molecules.[295]

Other strategies to increase solubility in molecules, such as adding hydrophilic substituents to the scaffold, or disrupting molecular planarity and symmetry have also been effective in increasing solubility and lowering melting point.[292] The imidazo[1,2-*b*]pyridazine series was deconstructed to determine the minimally active pharmacophore. The DYRK1A binding affinity of the constitutive parts of **247**, fragments **266** and **267**, are presented in Table 52. **247** is included for comparison.

Table 52. DYRK1A Binding Affinity of 247, 266 and 267

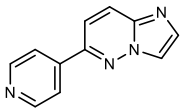

266

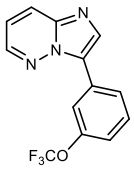

267

Compound	DYRK1A IC_{50}[a]	LE, LipE
247	22	0.41, 3.2
266	1019	0.56, 4.5
267	18060	0.33, 1.1

[a]IC_{50} (nM) in TR-FRET-based ligand-binding displacement assay (n = 1). LE = 1.4(pIC_{50})/non-hydrogen atoms; LipE = pIC_{50} – clog P.

The majority of DYRK1A binding affinity appeared to be derived from the 'hinge + Lys188' binding motif (**266** vs **267**). However, the addition of the aryl group boosted DYRK1A binding affinity by 50 fold (**247** vs **266**). Thus, it appears that the combination of both the recognition motif to bind to the hinge and back-pocket ('hinge + Lys188' recognition motif), plus the lipophilic subunit under the glycine-rich loop in **247** led to an extremely high affinity binder of DYRK1A.

It was envisaged that maintaining both of these interactions whilst reducing aromatic ring count and lipophilicity would be difficult. One strategy employed was to substitute both of the aromatic groups at the 3- and 6-positions with non-aromatic solubilising groups such as tetrahydropyran or morpholine, which may be capable of making similar and additional interactions.

8.2.2. Synthesis of Analogues with Less Aromatic Character

Fragment **266** was constructed via a Suzuki reaction between commercially available 6-chloroimidazo[1,2-*b*]pyridazine and pyridine-4-boronic acid hydrate. Suzuki reactions that

involved the pyridine-4-boronic acid hydrate required ongoing optimisation as yields were seldom above 50%. A representative table of conditions trialled is presented below.

Table 53. Installation of the Pyridine-4-boronic acid hydrate under Suzuki Conditions

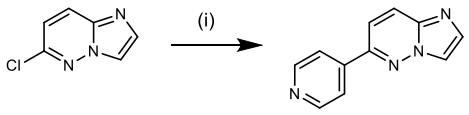

266

Base	Catalyst	Solvent	Temperature (°C)	Reaction Time (h)	Isolated Yield (%)
Na_2CO_3 (2 eq)	$Pd(PPh_3)_4$ (0.03)	toluene:water (3:1)	120	16	0
Na_2CO_3 (2 eq)	Pd-118 (0.05)	acetonitrile:water 5:1	80	16	70 (500 mg scale)
Na_2CO_3 (2 eq)	Pd-118 (0.05)	acetonitrile:water 5:1	80	16	30 (1 g scale)
K_2CO_3 (3 eq)	Pd-118 (0.1)	1,4-dioxane:water (10:1)	45	16	0

Electrophilic bromination of the 3-position of **266** with *N*-bromosuccinimide furnished intermediate **268**, which now had a handle for diversification of the 3-position. Suzuki cross-coupling with 3,6-dihydro-2*H*-pyran-4-boronic acid afforded **269**, an analogue with reduced aromaticity that was submitted for assay.

After unsuccessful attempts to reduce the alkene in **269** with triethylsilane, and then with hydrogen in the presence of palladium on carbon, catalytic hydrogenation transfer with ammonium formate at elevated temperature furnished the tetrahydropyran analogue **270**.

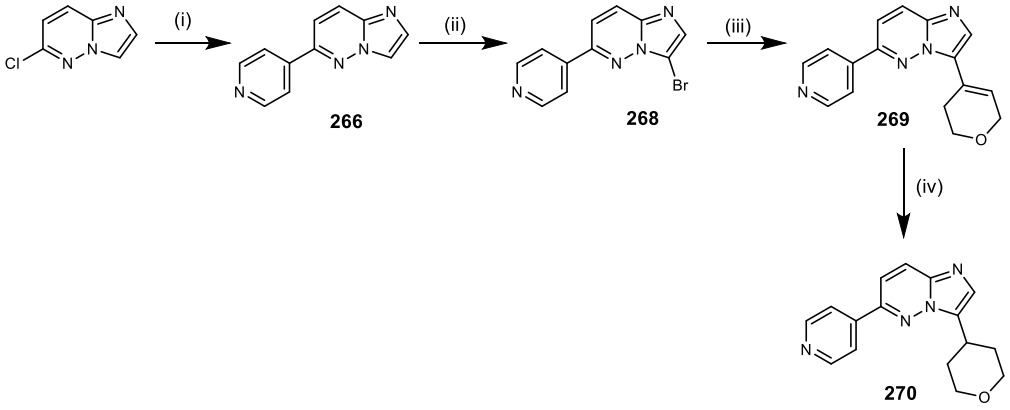

Scheme 49. *Reagents and Conditions;* (i) pyridine-4-boronic acid hydrate, bis[2-(di-*tert*-butylphosphanyl)cyclopenta-2,4-dien-1-yl]iron; dichloropalladium, sodium carbonate, acetonitrile:water (20:1), 80 °C, overnight, 30%; (ii) *N*-bromosuccinimide, chloroform, rt, overnight, 51%; (iii) 3,6-dihydro-2*H*-pyran-4-boronic acid pinacol ester, bis[2-(di-*tert*-butylphosphanyl)cyclopenta-2,4-dien-1-yl]iron; dichloropalladium, potassium carbonate, water:acetonitrile (1:6), 140 °C, 25 min, µwave, 41%; (iv) ammonium formate, 10% palladium on carbon, ethanol, 75 °C, 32 h, 22%.

Installation of the tetrahydropyran motif in place of the pyridine, as a non-aromatic bioisosteric replacement, was completed in two steps from intermediate **252**. 3,6-dihydro-2*H*-pyran-4-boronic acid pinacol ester was installed at the 6-position of the imidazo[1,2-*b*]pyridazine core via Suzuki reaction. Hydrogenation of the resulting alkene in **271** was completed at room temperature to afford tetrahydropyran analogue **272**.

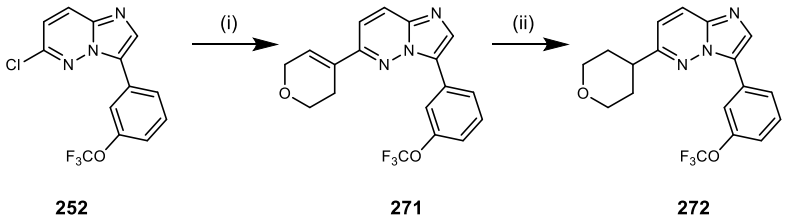

Scheme 50. *Reagents and Conditions;* (i) 3,6-dihydro-2*H*-pyran-4-boronic acid pinacol ester, bis[2-(di-*tert*-butylphosphanyl)cyclopenta-2,4-dien-1-yl]iron; dichloropalladium, potassium carbonate, water:acetonitrile (1:6), 140 °C, 25 min, µwave, 62%; (ii) hydrogen gas, 10% palladium on carbon, ethanol, rt, 24 h, 94%.

The morpholine analogue, **273**, was successfully synthesised from **252** under Buchwald-Hartwig conditions.

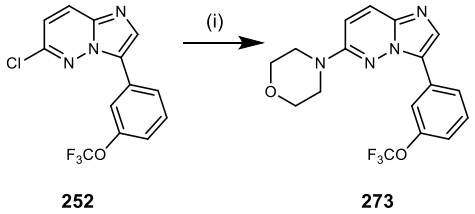

Scheme 51. *Reagents and Conditions;* (i) morpholine, 2-dicyclohexylphosphino-2′,4′,6′-triisopropylbiphenyl, palladium (II) acetate, sodium hydroxide, 1,4-dioxane, 90 °C, 72 h, 25%.

8.2.3. SARs and Biological Evaluation of Tetrahydropyran and Morpholine Analogues

The DYRK1A binding affinity data for analogues **269** - **273** are presented in Table 54. The data for **247** is included for comparison.

Few compounds designed to lower lipophilicity, reduce aromatic ring count, increase sp^3 character and increase solubility also maintained binding affinity for DYRK1A.

Table 54. DYRK1A Binding Affinity of Tetrahydropyran and Morpholine Analogues

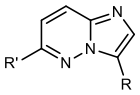

Compound	R'	R	DYRK1A IC_{50}	LE, LipE
247		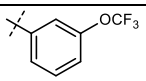	22	0.41, 3.2
269			88	0.47, 5.4
270			815	0.41, 4.4
271		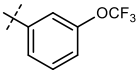	180	0.36, 2.4
272		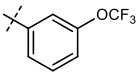	1450	0.31, 1.6
273		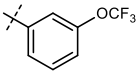	579	0.34, 2.1

[a]IC_{50} (nM) in TR-FRET-based ligand-binding displacement assay (n = 1). LE = 1.4(pIC_{50})/non-hydrogen atoms; LipE = pIC_{50} – clog P.

All attempts to make **247** more soluble resulted in reduced DYRK1A binding affinity. Both fully saturated tetrahydropyrans were inactive (**270** and **272**) suggesting that a tetrahydropyran is not an appropriate bioisostere for a pyridine motif. Unsaturated alkenes **269** and **271** were high affinity ligands, with **269** meeting the criteria set for a DYRK1A tool compound in terms of binding affinity. It appears that altering the orientation of the lone pair of electrons from that

adopted by the pyridyl resulted in diminished activity. Presumably, the lone pair of the oxygen atom in the more rigid structure of **269** was able to form a weaker hydrogen bond to Lys188. Inspection of LipE shows that the 3-(trifluoromethoxy)phenyl substituent, although good for DYRK1A affinity, is not good for efficiency.

Although the binding affinity of this set of analogues was reduced compared to **247**, it was important to assess the solubility of **269** - **273**. The results are displayed in Table 55. Inhibitor **247** is included for reference.

Table 55. Aqueous Solubility of Inhibitors 269 - 273

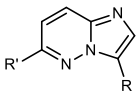

Compound	R'	R	Solubility (mg/mL)
247		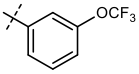	0
269			0.02
271		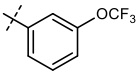	0
272		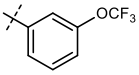	0.03
273		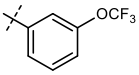	0

Thermodynamic solubility data derived from single experiment at pH 6.8.

All of the analogues suffered from low solubility. Only analogues **269** and **272** exhibited any measurable solubility. These results suggested that another strategy was required to improve the solubility of the series.

8.3. Exploration of the 2-position of the Imidazo[1,2-*b*]pyridazine Series

8.3.1. Rationale

Work on the pyrazolo[1,5-*b*]pyridazine series (Chapters 4-7) had revealed that placement of a methyl or methylene group near to the hinge residue, Met240 of DYRK1A, afforded kinome-wide selectivity. It was desirable to translate this selectivity into the imidazo[1,2-*b*]pyridazine series. The co-crystal structures of pyrazolo[1,5-*b*]pyridazine **96** and imidazo[1,2-*b*]pyridazine **247** bound to DYRK1A were aligned by sequence and superimposed in MOE. MOE Builder was

then used to model the addition of a methyl substituent onto analogue **247** at the 2-position of the imidazo[1,2-*b*]pyridazine core. Minimisation appeared to show that the 2-methylated analogue would be tolerated in the pocket of DYRK1A.

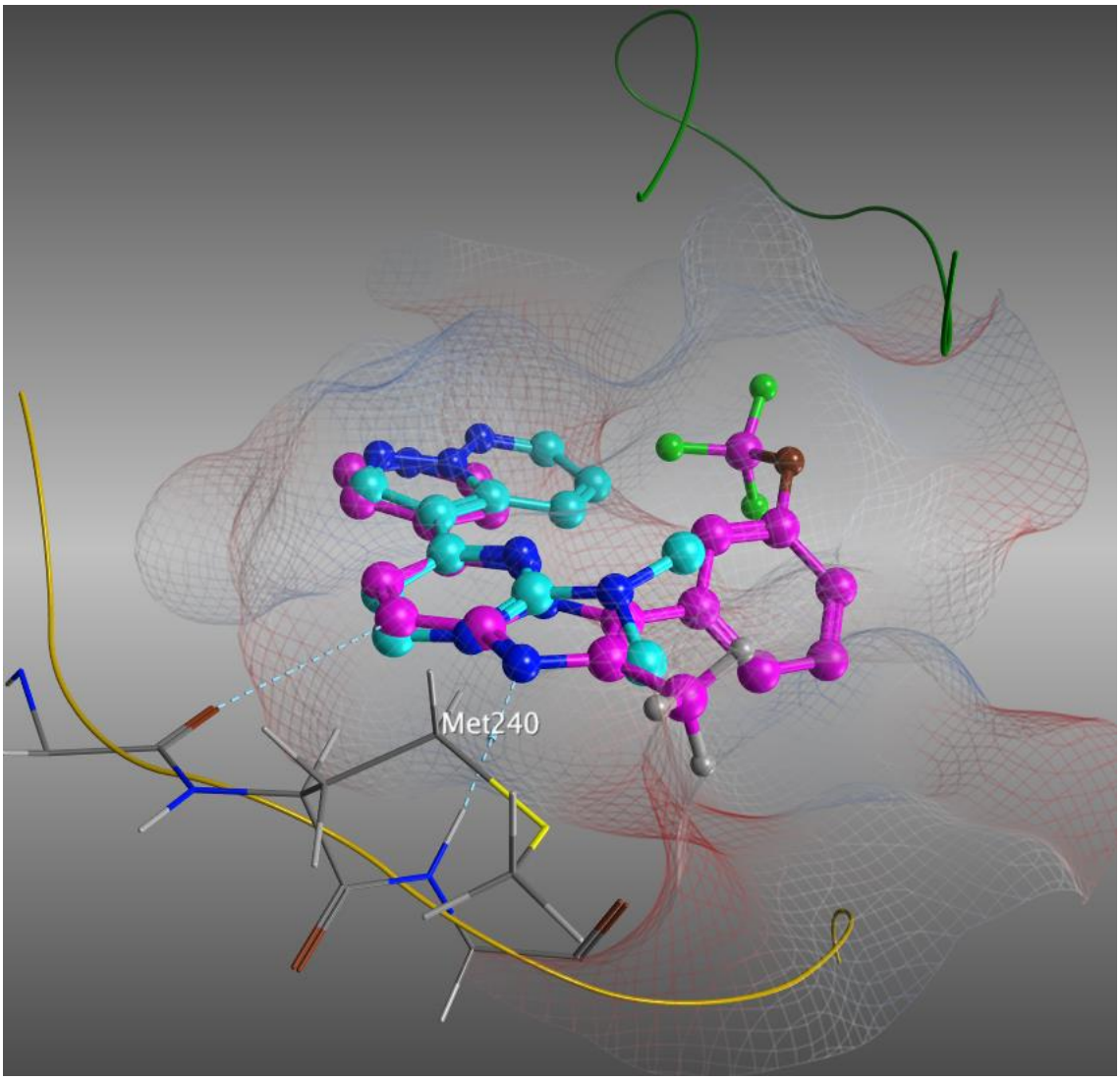

Figure 94. Alignment and superimposition of **96** (cyan) and **247** (magneta) in the in-house crystal structure of **247** in DYRK1A. Builder tool used to add 2-methyl substituent onto **247**. Minimisation shows growth from the 2-position may be tolerated, whilst lipophilic aryl group under glycine-rich loop. Hinge (gold) and glycine-rich loop (green), electrostatic receptor surface also shown. Structure prepared and minimised with MOE 2016, CCG with Amber10:EHT force field.

Funnell *et al*. described a sub-nanomolar CLK inhibitor, **T3**, with favourable selectivity, cell permeability and stability, which blocked cancer cell proliferation.[296] DYRK1A is reported as an off-target of **T3**. Although the inhibitor is reportedly 200 fold more potent for CLK1, **T3** inhibits DYRK1A with IC_{50} = 260 nM in a LANCE Ultra kinase assay system. Interestingly, the structure of **T3** closely resembles the imidazo[1,2-*b*]pyridazine 'hinge + Lys188' recognition motif (highlighted red in Figure 95).

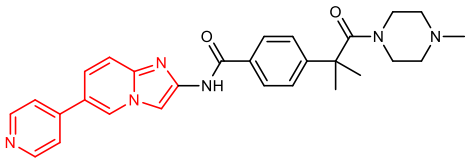

IC_{50} (nM)	T3
CLK1	0.67
CLK2	15
CLK3	110
DYRK1A	260
DYRK1B	230

Figure 95. CLK inhibitor **T3** inhibits DYRK1A IC_{50} = 260 nM. Suspected 'hinge + Lys188' recognition motif shown in red. Data from ref [296].

At the time of writing (April 2019), two crystal structures of **T3** analogues were deposited in the PDB, one bound to CLK1 (PDB 6RAA) and the other bound to CLK3 (PDB 6RCT). These crystal structures were overlaid with the co-crystal structure of **247** bound to DYRK1A (Figure 96) to assess whether substitution in the 2-position was likely to be tolerated.

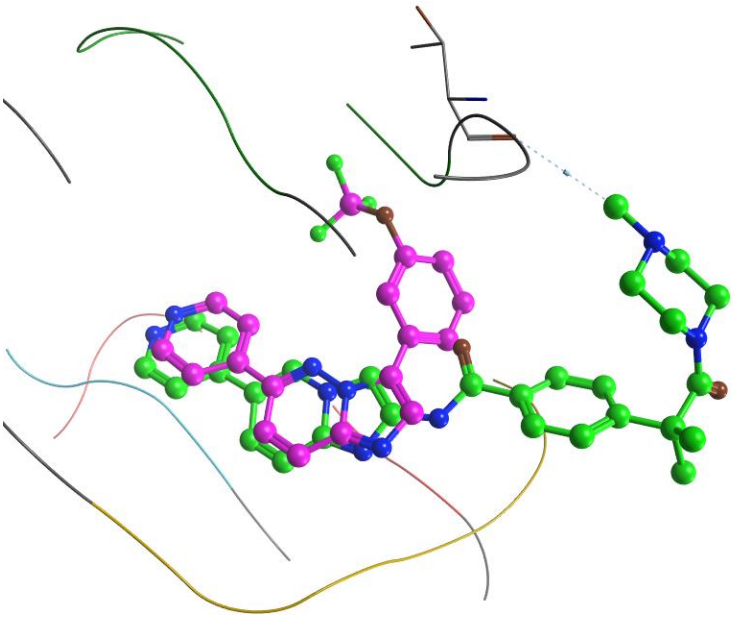

Figure 96. Overlay of **T3** (green) (PDB 6RAA) and **247** (magneta). Substitution of the 2-position of **247** appears likely to be tolerated given the binding mode of **T3**. **T3** forms a hydrogen-bond with Thr166 close to the glycine-rich loop. Hinge (gold) glycine-rich loop (green), DFG motif (cyan) all shown. Structure prepared and minimised with MOE 2016, CCG with Amber10:EHT force field.

It was evident from the overlay of **T3** and **247** (Figure 96) that substitution at the 2-position of **247** was likely to be tolerated in DYRK1A. A small array of analogues with substituents to probe the 2-position were synthesised.

8.3.1. Synthesis of Analogues with Substituents in the 2-position

The 2-substituted imidazo[1,2-*b*]pyridazine core was constructed by heating 6-chloropyridazin-3-amine in the appropriate α-haloketone in the presence of TEA. Installation of the 4-pyridyl motif was achieved with Suzuki conditions. These fragment-like analogues were tested for biological activity as it was theorised that there would be no reason to install the 3-(trifluoromethoxy)phenyl substituent if the constituent fragment was not accommodated by DYRK1A.

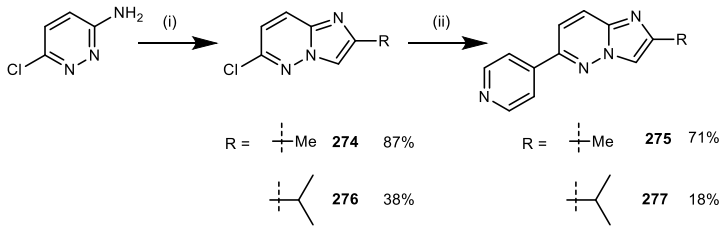

Scheme 52. *Reagents and Conditions;* (i) α-haloketone, TEA, 150 °C, 1 h; (ii) Pyridine-4-boronic acid hydrate, bis[2-(di-*tert*-butylphosphanyl)cyclopenta-2,4-dien-1-yl]iron; dichloropalladium, sodium carbonate, acetonitrile:water (9:1), 80 °C, 16 h.

Reversal of the synthetic steps was also attempted to furnish 2-substituted analogues. The 4-pyridyl motif was installed through Suzuki conditions.[297] The core and 2-substituent were then built in one step through heating 6-(4-pyridyl)pyridazin-3-amine (**278**) with appropriate α-haloketone. In this way **279** and **280** were accessed.

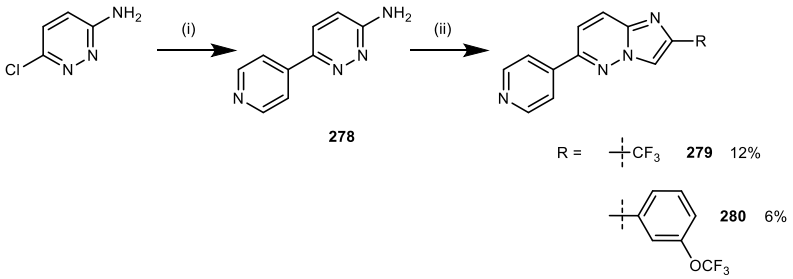

Scheme 53. *Reagents and Conditions;* (i) pyridine-4-boronic acid hydrate, bis(triphenylphosphine)palladium(II)dichloride, potassium phosphate tribasic, 1-butanol:water (6:1), 130 °C, 16 h, 14%; (ii) α-haloketone, TEA, ethanol, 150 °C, 4 h - overnight;

The synthetic sequence was continued for analogues that were found to have high affinity for DYRK1A. Electrophilic bromination of the 3-position of the imidazo[1,2-*b*]pyridazine was achieved selectively with *N*-bromosuccinimide. Subsequent Suzuki reaction was sluggish but eventually installed the required 3-(trifluoromethoxy)phenyl substituent to afford **282** and **284** separately.

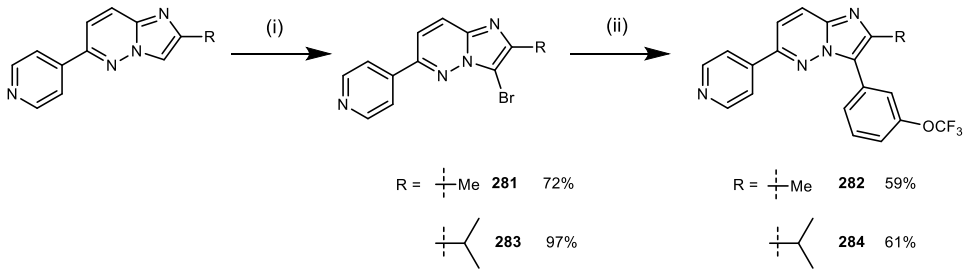

Scheme 54. *Reagents and Conditions;* (i) *N*-bromosuccinimide, DMF, rt, 16 h. (ii) [3-(trifluoromethoxy)phenyl]boronic acid, bis[2-(di-*tert*-butylphosphanyl)cyclopenta-2,4-dien-1-yl]iron; dichloropalladium, cesium carbonate, acetonitrile:water (8:1), 110 °C, 48 h.

8.3.2. SARs and Biological Evaluation of 2-Substituted Analogues 266 - 280

The DYRK1A binding affinity data for **266** - **280** are presented in Table 56. The data for **247** and **266** is included for comparison.

Table 56. DYRK1A Binding Affinity of 266-280

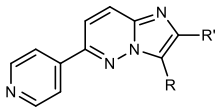

Compound	R'	R	DYRK1A IC_{50}	LE, LipE
266	H	H	1019	0.56, 4.5
275	Me	H	419	0.56, 4.8
277		H	294	0.51, 3.7
279	CF_3	H	**	-
280	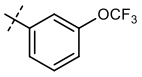	H	28296	-
247	H	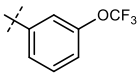	22	0.41, 3.2

[a]IC_{50} (nM) in TR-FRET-based ligand-binding displacement assay (n = 1). LE = 1.4(pIC_{50})/non-hydrogen atoms; LipE = pIC_{50} – clog P. **Data did not fit a curve.

Fragments **275** and **277** exhibit significantly stronger binding affinity for DYRK1A than unsubstituted fragment **266**. **275** possesses improved LLE versus **241**, suggesting that the additional methyl is an efficient substitution. **279** does not exhibit any binding affinity for DYRK1A and neither does **280**, the regioisomer of **247**. This is probably due to increased steric

clashes with the hinge region of DYRK1A. At the time of writing **282** and **284** were submitted for DYRK1A ligand-binding displacement assay and the results were being awaited before further profiling.

275 was profiled further for metabolic stability and solubility. The results are displayed in Table 57. Data for **266** is included for comparison.

Table 57. Metabolic Stability and Solubility of 275

Compound	HLM (µL/min/mg)	RLM (µL/min/mg)	Solubility (mg/mL)
266	11.9 +/- 1.8	114.1 +/- 1.3	0.59
275	27.8 +/- 1.1	106.7 +/- 6.6	0.54

HLM and RLM Determinations mean of n =2 +/- standard deviation (unless otherwise stated). HLM = human liver microsomes; RLM = rat liver microsomes; thermodynamic solubility data derived from single experiment at pH 6.8.

Comparing **275** to **266**, the additional methyl substituent at the 2-position did not dramatically affect microsomal stability or solubility. If the additional methyl group provides a better selectivity profile for the imidazo[1,2-*b*]pyridazine series, fragment **275** would represent a good starting point for fragment-based drug design.

8.4. Patent Inspired Design of Imidazo[1,2-*b*]pyridazine Series

8.4.1. Rationale

In 2017 Servier-Vernalis released two patents that described selective DYRK1 and CLK1 inhibitors.[42] The Markush structure of one of the chemotypes disclosed in the patent, the imidazo[4,5-*b*]pyridine derivatives, were of particular interest and are depicted in Figure 97.

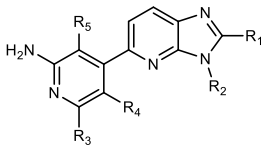

Figure 97. Series of imidazo[4,5-*b*]pyridines as DYRK1/CLK1 inhibitors disclosed by Servier-Vernalis.[42]

Flexible alignment of **247** and analogues from the imidazo[4,5-*b*]pyridines was convincing in showing that the two series had the potential to bind in a similar fashion, as pharmacophoric features overlaid well.

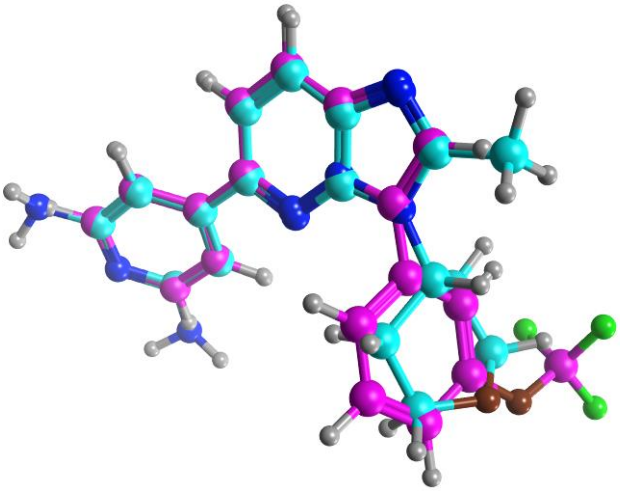

Figure 98. Flexible alignment of an exemplar (cyan) of the imidazo[4,5-*b*]pyridine series and **247**. Good alignment of atoms, suspected to be involved in hydrogen-bond formation in DYRK1A, is observed between **247** and a molecule from the Servier-Vernalis patent. Structure prepared and minimised with MOE 2016, CCG with Amber10:EHT force field.

Servier-Vernalis had profiled a number of compounds against DYRK1A, DYRK1B, CLK1 and CDK9.[42] The selectivity data within this patent was interrogated and the inhibitors modelled in the active site of DYRK1A in an effort to reveal areas of the molecule that may afford selectivity versus CLK1 and DYRK1B. The data appeared to suggest that incorporation of aliphatic and aromatic groups at the 3-position of the imidazo[1,2-*b*]pyridazine series would modulate selectivity. The methyl group of the imidazo[4,5-*b*]pyridine series appeared to occupy the same position as the methyl group in **275**, perhaps affording good selectivity for both series. A selection of analogues from the patent and their selectivity data is shown in Figure 99.

			Assay Results (µM)			
Number	Compound Name	Compound Structure	D1A Fret	D1B Fret	CLK1 Fret	CDK9 Fret
49	4-[2-methyl-3-(tetrahydro-2H-pyran-4-yl)-3H-imidazo[4,5-b]pyridin-5-yl]pyridine-2,6-diamine	#NAME?	0.003	0.017	0.017	0.979
24	N-(4-{2[5-(2,6-diaminopyridin-4-yl)-2-methyl-3H-imidazo{4,5-b}pyridin-3-yl]ethyl}phenyl)acetamide	#NAME?	0.005	0.015		3.538
29	4-{2-methyl-3-[2-(thiophen-3-yl)ethyl]-3H-imidazo[4,5-b]pyridin-5-yl}pyridine-2,6-diamine	#NAME?	0.004	0.011		3.435
47	4-[3-(2-chlorobenzyl)-2-methyl-3H-imidazo[4,5-b]pyridin-5-yl]pyridine-2,6-diamine	#NAME?	0.003	0.046		0.728

Figure 99. Patent analysis to search for selectivity handles. JChem Excel extensions were used to convert the names of compounds from the patent into structure. D1A = DYRK1A, D1B = DYRK1B. Data is IC_{50} (µM) derived from a DYRK1A cellular FRET assay described in reference [42].

A key advantage of the imidazo[1,2-*b*]pyridazine series was that it lacked any HBDs, whereas the Servier-Vernalis compounds had > 2. This could limit their use as tool compounds for a CNS target such as DYRK1A. Inspired by the Servier-Vernalis patent, the 3-position was explored.

8.4.1. Synthesis of Servier-Vernalis Inspired Analogues

It was envisaged that solubilising groups and motifs similar to those present in the Servier-Vernalis patent could be appended to the 3-position of the imidazo[1,2-*b*]pyridazine scaffold via a Mannich reaction on **274**. Subsequent installation of the 4-pyridyl moiety under Suzuki conditions would furnish the final products. This type of Mannich reaction on an imidazo[1,2-*b*]pyridazine substrate is not widely known. A single research article from Lombardino at Pfizer, published in 1968, describes a similar Mannich reaction using more simple amines and 6-methoxyimidazo[1,2-*b*]pyridazine.[298] We wished to expand the substrate scope of this reaction, whilst using it to access analogues that were less aromatic, more soluble and able to direct substituents under the glycine-rich loop of DYRK1A.

Preliminary investigation revealed that the reaction did not proceed in the absence of acetic acid. Thus, the acid-catalysed Mannich reaction was used to append a range of cyclic and solubilising moieties to the 3-position of the imidazo[1,2-*b*]pyridazine scaffold.

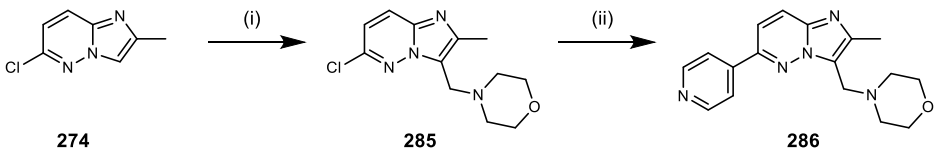

Scheme 55. *Reagents and Conditions;* (i) morpholine, formaldehyde solution, acetic acid, methanol, 65 °C, 4 h, 90%; (ii) Pyridine-4-boronic acid hydrate, bis[2-(di-*tert*-butylphosphanyl)cyclopenta-2,4-dien-1-yl]iron; dichloropalladium, potassium carbonate, acetonitrile (3.2:0.8), 120 °C, 21 min, µwave, 41%.

The Mannich reaction was also successfully carried out on a later stage analogue, fragment **275**, showing its utility for late-stage diversification of the imidazo[1,2-*b*]pyridazine scaffold. Using this method a small library of Mannich products were rapidly synthesised. Establishment of the two synthetic routes would facilitate future expansion and exploration of the 3- and 6- positions of the imidazo[1,2-b]pyridazine series if required.

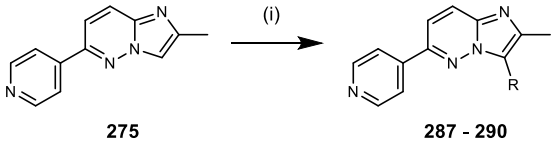

Scheme 56. *Reagents and Conditions;* (i) secondary amine, formaldehyde solution, acetic acid, methanol, 65 °C, 4 h.

8.4.2. SARs and Biological Evaluation of Servier-Vernalis inspired Analogues

The DYRK1A binding affinity data for Servier-Vernalis inspired analogues is presented in Table 58.

Table 58. DYRK1A Binding Affinity of Servier-Vernalis inspired Analogues

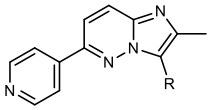

Compound	R	DYRK1A IC_{50}[a]
286	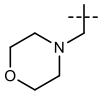	5370
287	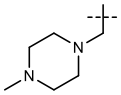	33878
288	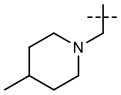	28291
289		6811
290		39514

[a]IC_{50} (nM) in TR-FRET-based ligand-binding displacement assay (n = 1).

All analogues exhibited diminished DYRK1A binding affinity compared to **247**. **286** - **290** were not advanced to solubility or metabolic stability studies as the losses in DYRK1A affinity were unacceptable.

At this point in the project, it appeared very challenging to predict where gains in solubility could be made without abolishing DYRK1A binding affinity and selectivity. Molecular modelling had not foreseen that analogues **286** - **290** would not be accommodated in the binding site of DYRK1A.

With few options left, it was decided to profile the pocket further, determine which vectors of the imidazo[1,2-*b*]pyridazine core could be grown out of, and if any stabilising interactions were possible. It was envisaged that a fragment-based approach starting with one of the fragments identified above (**266** or **275**), which possessed good LE and LipE may, after optimisation, provide a more appropriate tool compound.

8.5. Groundwork for Future Fragment Design

8.5.1. Rationale

In terms of fragments, **266** and **275** were already established as relatively high affinity ligands of DYRK1A with good LE and LipE, representing good starting points for fragment-based drug

design. **266** and **275** possessed promising metabolic stability and solubility. Additionally, molecular modelling could provide some rationale of how the fragments bound to the ATP site of DYRK1A.

A

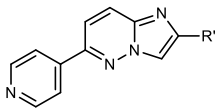

Compound	R'	DYRK1A IC_{50}	LE, LipE	HLM (µL/min/mg)	RLM (µL/min/mg)	Solubility (mg/mL)
266	H	1019	0.56, 4.5	11.9 +/- 1.8	114.1 +/- 1.3	0.59
275	Me	419	0.56, 4.8	27.8 +/- 1.1	106.7 +/- 6.6	0.54

[a]IC_{50} (nM) in TR-FRET-based ligand-binding displacement assay (n = 1). LE = 1.4(pIC_{50})/non-hydrogen atoms; LipE = pIC_{50} – clog P. HLM and RLM Determinations mean of n =2 +/- standard deviation (unless otherwise stated). HLM = human liver microsomes; RLM = rat liver microsomes; thermodynamic solubility data derived from single experiment at pH 6.8.

B **C**

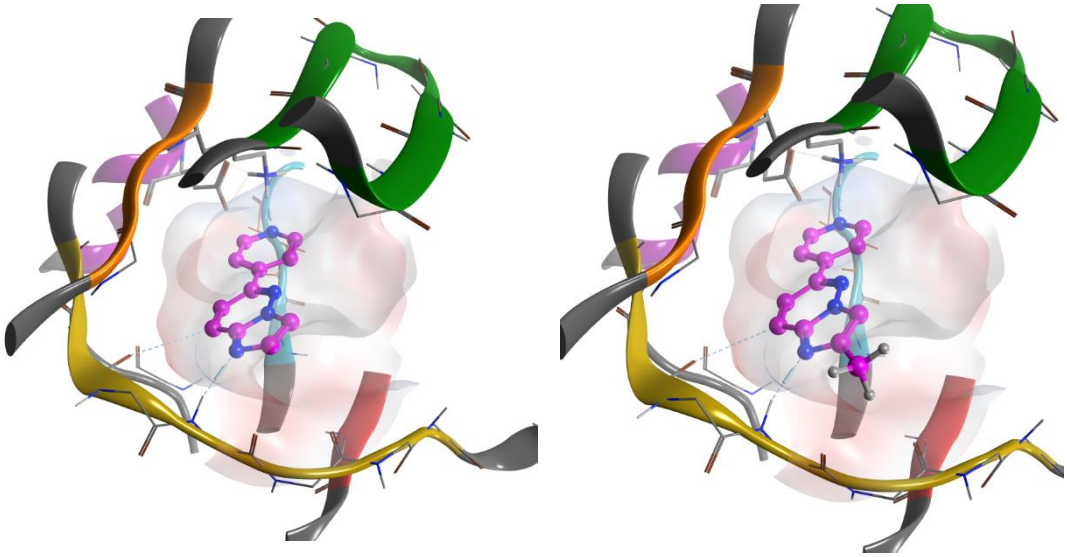

Figure 100. Overview of Fragments 266 and 275. A – DYRK1A affinity, ligand efficiency metrics, metabolic stability and solubility all promising for fragments 266 and 275. In-house crystal structure of 247 modified with Builder tool to display 266 and 275 for subsequent fragment-based design. Structure prepared and minimised with MOE 2016, CCG with Amber10:EHT force field.

The 2-, 3- and 6-positions of the imidazo[1,2-*b*]pyridazine series had been explored in an effort to make more soluble inhibitors whilst maintaining the key binding motifs identified from the co-crystal structure of **247** bound to DYRK1A. The 7- and 8- position of the imidazo[1,2-*b*]pyridazine had not been investigated at all. Methyl groups are commonly installed on

molecules in an effort to enhance their biological activity, selectivity and physical properties. In some cases the seemingly innocuous change from a C-H to a C-Me translates to > 100 fold improvement in IC_{50}, this is known colloquially as the 'magic methyl effect'.[299] Already in the current series adding a methyl to the 2-position appeared to boost DYRK1A affinity by > 2 fold. To complete the methyl-scan in the imidazo[1,2-*b*]pyridazine series the 7- and 8-methyl analogues were prioritised for synthesis.

In addition to the methyl scan, the nature of the heterocyclic core was also of interest. It was envisaged that scaffold hopping may help to further define features on the molecule that were essential to keep, and whether additional interactions were possible between the heterocyclic core and the receptor. Scaffold hopping in the pyrazolo[1,5-*b*]pyridazine series (Chapter 7) had already been proven successful in improving the metabolic stability and solubility of the series. Cresset Spark™ software was again utilised to predict suitable bioisosteric replacements for the imidazo[1,2-*b*]pyridazine heterocycle.

8.5.2. Synthesis of Heterocyclic Fragments

The remaining methyl-substituted analogues required construction of the haloheteroarene precursors. Both 7- and 8- methyl haloheteroarenes **291** and **292** were furnished in a two-step one-pot reaction. Nucleophilic displacement with aminoacetaldehyde, followed by cyclisation in sulfuric acid afforded both 7- and 8-methyl regioisomers, which were found to be separable by conventional chromatography. Intermediates **291** and **292** were furnished in a 2:1 ratio.

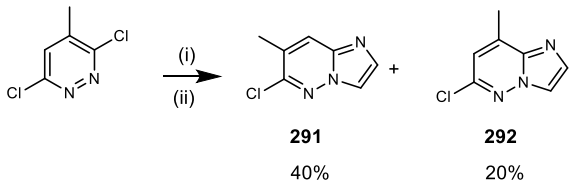

Scheme 57. *Reagents and Conditions;* (i) aminoacetaldehyde dimethylacetal, 100 °C, 4 h; (ii) sulfuric acid, 100 °C, 1 h.

Subsequent Suzuki reaction was then performed in parallel to afford fragments **293** and **294**.

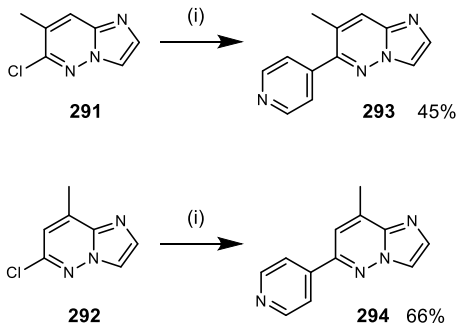

Scheme 58. *Reagents and Conditions;* (i) pyridine-4-boronic acid hydrate, bis[2-(di-*tert*-butylphosphanyl)cyclopenta-2,4-dien-1-yl]iron; dichloropalladium, potassium carbonate, ethanol:water (1.6:0.4), 120 °C, 21 min, µwave.

The heterocyclic core of triazolo analogue **297** was synthesised in three steps. Taking advantage of failed attempts to synthesise 6-chloro-4-methyl-pyridazin-3-amine as a precursor for the synthesis of **293** and **294**. Initially 3,6-dichloro-4-methylpyridazine was subjected to nucleophilic attack with hydrazine hydrate. The intention was to reduce **295** to the corresponding primary amine. However, multiple attempts at this failed. With the remaining hydrazine intermediate **295** it was decided to make another analogue. **295** was cyclised with formic acid by boiling in a sealed tube for 6 h. Subsequent Suzuki reaction furnished the desired triazolo[4,3-*b*]pyridazine fragment.

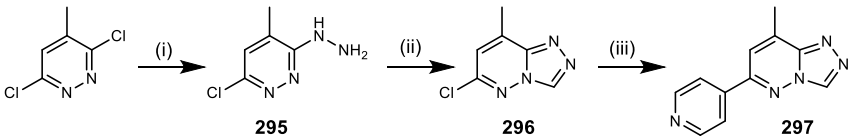

Scheme 59. *Reagents and Conditions;* (i) hydrazine hydrate, 80 °C, 16 h, 39%; (ii) formic acid, 100 °C, 6 h, 80%; (iii) pyridine-4-boronic acid hydrate, bis[2-(di-*tert*-butylphosphanyl)cyclopenta-2,4-dien-1-yl]iron; dichloropalladium, potassium carbonate, 120 °C, 60 min, µwave, 11%.

The heterocyclic analogues **298-300** were accessed from the commercially available haloheteroarene precursors and pyridine-4-boronic acid hydrate using Suzuki conditions.

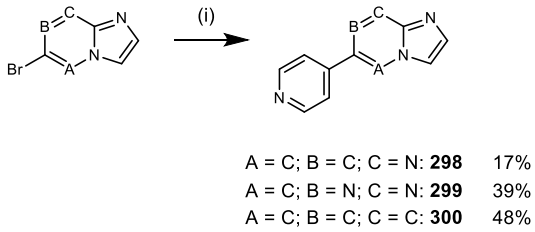

Scheme 60. *Reagents and Conditions;* (i) pyridine-4-boronic acid hydrate, bis[2-(di-*tert*-butylphosphanyl)cyclopenta-2,4-dien-1-yl]iron; dichloropalladium, cesium carbonate, acetonitrile:water (10:1), 140 °C, 25 min, µwave.

8.5.3. SARs and Biological Evaluation of Fragments

The DYRK1A binding affinity data for the fragment analogues is presented in Table 59. The data for **266** and **275** is included for comparison.

Table 59: DYRK1A Binding Affinity of Fragments

Compound	R	DYRK1A IC_{50}[a]	LE/LipE
266	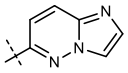	1019	0.56, 4.5
298	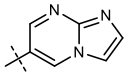	513	0.59, 6.1
299	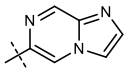	19748	0.44, 4.3
300	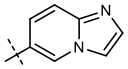	160	0.63, 5.6
275	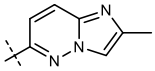	419	0.56, 4.8
294	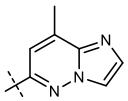	81645	-
293	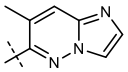	**	-
297	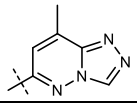	16165	-

[a]IC_{50} (nM) in TR-FRET-based ligand-binding displacement assay (n = 1). LE = 1.4(pIC_{50})/non-hydrogen atoms; LipE = pIC_{50} – clog P. **Data did not fit a curve.

Appending a methyl to either the 7- or 8- position of the 5,6-heterocycle appears to be detrimental to the DYRK1A binding affinity of the series (**293**, **294** and **297**). The only position of the 5,6-heterocycle that appears not to tolerate a nitrogen atom is the 7-position of the core (**299**). Removal of a nitrogen from the 4-position of the series appears to improve the DYRK1A

binding affinity of the core as **300** exhibits approximately 6 fold higher binding affinity for DYRK1A than **266**. Scaffold hopping to the imidazo[1,2-*a*]pyrimidine, **298**, appears to have brought about a 2 fold improvement in DYRK1A binding affinity. Thus in terms of DYRK1A binding affinity, the imidazo[1,2-*b*]pyridazine scaffold appears not to be an optimal core for the series.

300 was profiled for solubility and metabolic stability. The results are shown in Table 60. **266** and **275** are included for comparison.

Table 60: Metabolic Stability and Solubility of 300

Compound	HLM (µL/min/mg)	RLM (µL/min/mg)	Solubility (mg/mL)
266	11.9 +/- 1.8	114.1 +/- 1.3	0.59
275	27.8 +/- 1.1	106.7 +/- 6.6	0.54
300	18.7 +/- 0.7	120.7 +/- 3.3	0.38

HLM and RLM Determinations mean of n =2 +/- standard deviation (unless otherwise stated). HLM = human liver microsomes; RLM = rat liver microsomes; thermodynamic solubility data derived from single experiment at pH 6.8.

The solubility and microsomal clearance of **300** are good for a starting point on which to begin fragment-based drug design and discover molecular probes of DYRK1A. It would be interesting to synthesise and test the 2-methyl substituted analogue of **300** and **298**, to assess whether binding affinity for DYRK1A is increased as had been observed for the imidazo[1,2-*b*]pyridazine scaffold.

8.6. Summary

247 was identified as a high affinity binder of DYRK1A. Small scale SAR exploration followed by the elucidation of a co-crystal structure of **247** bound to DYRK1A enabled the rational design of DYRK1A inhibitors. **247** was a high affinity binder of the isolated DYRK1A protein and also exhibited good activity in the NanoBRET cellular assay. **247** was relatively selective for DYRK1A against the rest of the kinome and exhibited acceptable levels of metabolic clearance. The major issue with **247** was that it possessed very low levels of solubility. **247** also lacked selectivity within the DYRK and CLK families.

More soluble compounds were designed *in silico* prior to synthesis. Strategies such as reducing lipophilicity and planarity, adding hydrophilic substituents and increasing sp^3 character were all explored. Further analogue design was influenced by contemporary patent literature in an attempt to translate selectivity into the imidazo[1,2-*b*]pyridazine series.

Despite these efforts, it was challenging to improve solubility and clearance whilst maintaining binding affinity for DYRK1A and improving selectivity. As exploratory space became limited the imidazo[1,2-*b*]pyridazine series was reduced to its minimally active pharmacophore. Scaffold hopping to other similar heterocycles such as the imidazo[1,2-*a*]pyridine provided ligands that exhibited stronger binding affinity for DYRK1A. The resulting fragments **266**, **275** and **300** represent good starting points in terms of metabolic stability, solubility, LE and LipE for Fragment-based drug design. A number of iterative cycles would be needed before an appropriate DYRK1A tool was discovered in the imidazo[1,2-*b*]pyridazine series. However, the available substitution vectors have been identified limiting the amount of work needed.

CHAPTER 9. Investigation of a Series of Pyrazolo[3,4-*c*]pyridazines as DYRK1A Inhibitors

In addition to the pyrazolo[1,5-*b*]pyridazine series and imidazo[1,2-*b*]pyridazine series a number of other heterocyclic scaffolds were being investigated in parallel for DYRK1A inhibition. Chapter 9 describes the investigation of a series of pyrazolo[3,4-*c*]pyridazines as DYRK1A inhibitors. After identifying the key stabilising interactions of the series with DYRK1A, optimisation of the solubility and selectivity of the series is attempted. To achieve this scaffold hopping around the heterocyclic core is investigated. A literature-based approach is used in an attempt to remove off-target liabilities in order to afford a selective and high affinity binder of DYRK1A with good physicochemical properties for use as a molecular probe.

9.1. Investigation of the Pyrazolo[3,4-*c*]pyridazine Series

The pyrazolo[3,4-*c*]pyridazine series was identified from the PKIS dataset as potent inhibitors of DYRK1A.[19] From the PKIS set there were 4 members of the pyrazolo[3,4-*c*]pyridazine cluster,[300] of which 1 compound inhibited DYRK1A > 75% at 1 µM. In general, the series displayed potent off-target activity at other CMGC kinases (CDKs, CLKs, GSK3β and other DYRKs), but otherwise had excellent kinome-wide selectivity. Representative analogue **301** was the most potent and selective DYRK1A inhibitor in the pyrazolo[3,4-*c*]pyridazine series. A combination of low molecular weight and good physicochemical properties made **301** an attractive starting point for development. The series had previously been investigated by GSK as potent GSK3β inhibitors.[300] Compounds from the same pyrazolo[3,4-*c*]pyridazine chemotype had been disclosed as a class of potent CDK1/cyclin B inhibitors, identified through a high-throughput screen by BASF Bioresearch Corp. (Worcester, MA). This set of pyrazolo[3,4-*c*]pyridazines were developed by Braña *et al*. as potent and selective CDK1 inhibitors and possessed antitumour activity.[301]

Table 61. DYRK1A Percentage Inhibition Data at 1 µM for Compounds from the PKIS Set[19]

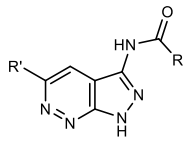

Compound	R'	R	DYRK1A % inhibition[a]
302	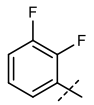	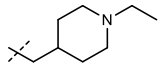	53
303		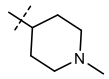	34
304	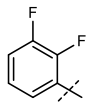	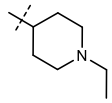	61
301			93

[a]DYRK1A inhibition at 1µM in DiscoveRx KINOMEscan® experiment.[19]

To validate the pyrazolo[3,4-*c*]pyridazine series, the first task was to resynthesize **301** so that it could be tested for DYRK1A affinity in the primary ligand-binding displacement assay. As the pyrazolo[3,4-*c*]pyridazine cluster of active compounds was small, it was desirable to establish a synthetic route that allowed diversification of both the 5-position of the heterocyclic core and the amide. This would enable rapid hit expansion and a more thorough analysis of SAR for the pyrazolo[3,4-*c*]pyridazine series.

9.2. Synthesis of the Pyrazolo[3,4-*c*]pyridazine Series

9.2.1. Attempts to Make the Synthetic Route more Amenable to Library Synthesis

Witherington *et al*. reported a high-yielding, 4-step synthesis of similar pyrazolo[3,4-*c*]pyridazines starting from a commercially available ethyl ester and converting it to the primary amide. The nitrile, formed from dehydration of the amide with phosphorus(V)oxychloride, was cyclized with hydrazine to form the desired pyrazolo[3,4-*c*]pyridazine scaffold. Selective acylation of the primary amine furnished the desired GSK-3β inhibitor in high yield.[300]

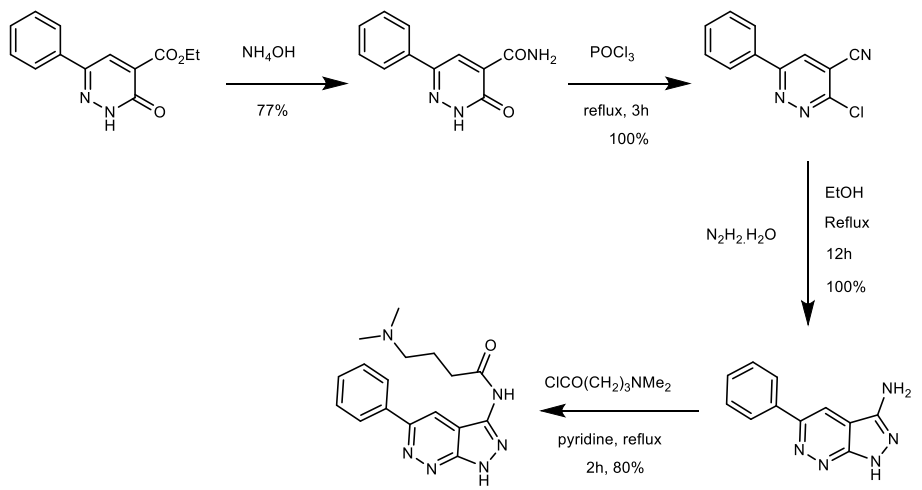

Scheme 61. Literature Procedure for the Preparation of Pyrazolo[3,4-*c*]pyridazines.[300]

The route was attractive due to high yields reported in each step, however, its success relied on the starting ethyl ester being commercially available, which proved not to be the case for the 3-pyridyl analogue required for the synthesis of **301**. The Witherington route[300] is less amenable to library synthesis as installation of the phenyl substituent at the 5-position is carried out in the first step. A superior synthesis would allow diversification of a late stage intermediate, in which the 5-position aryl and 3-position acyl moieties could be explored at will (Figure 101). Retrosynthetic analysis of the pyrazolo[3,4-*c*]pyridazine chemotype provided an idea for the late stage intermediate, **305**, with two points of diversification – the primary amine for acylation and the aryl halide suitable for C-C or C-X cross couplings. **305** was reported in the literature,[302] so the real focus would be to determine the optimal order and conditions of the acylation and C-C cross couplings to afford the desired product.

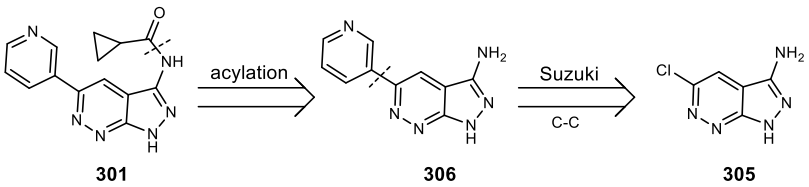

Figure 101. Retrosynthetic analysis of the pyrazolo[3,4-*c*]pyridazine chemotype.

9.2.2. Synthesis of 305

The commercially available 3,6-dichloropyridazine-4-carboxylic acid was converted to primary amide **307** via the corresponding acid chloride in high yield over 2 steps. When this reaction was repeated on larger scale the yield could not be replicated. Refluxing the carboxylic acid in neat

thionyl chloride followed by addition of ammonium hydroxide furnished **307** in good yield and in a shorter time frame (Figure 102).

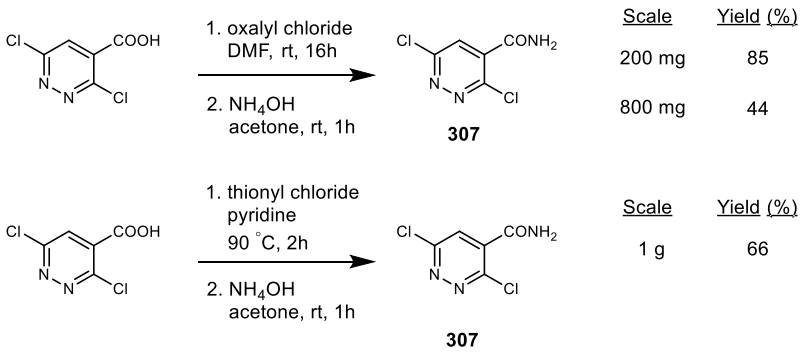

Figure 102. Overview of conditions trialled for synthesis of **307**.

Primary amide dehydration to form nitrile **308** followed by cyclisation with hydrazine furnished **305** in good yield (Scheme 62).

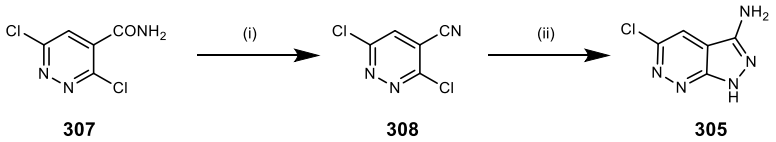

Scheme 62. *Reagents and Conditions*: (i) phosphorus(V)oxychloride, 90 °C, 2.5 h, 62%; (ii) hydrazine hydrate, 60 °C, 3 h, 84%.

Selective mono-acylation of **305** proved difficult using conditions outlined by Witherington *et al*.[300] with bi- and tri-acylated material isolated upon work-up. Reducing the temperature of the reaction and using strictly 1:1 equivalents of acid chloride:**305** failed to furnish the desired mono-acylated product in satisfactory yield. Amide coupling conditions with cyclopropanecarboxylic acid and T3P® also failed to afford **309**.

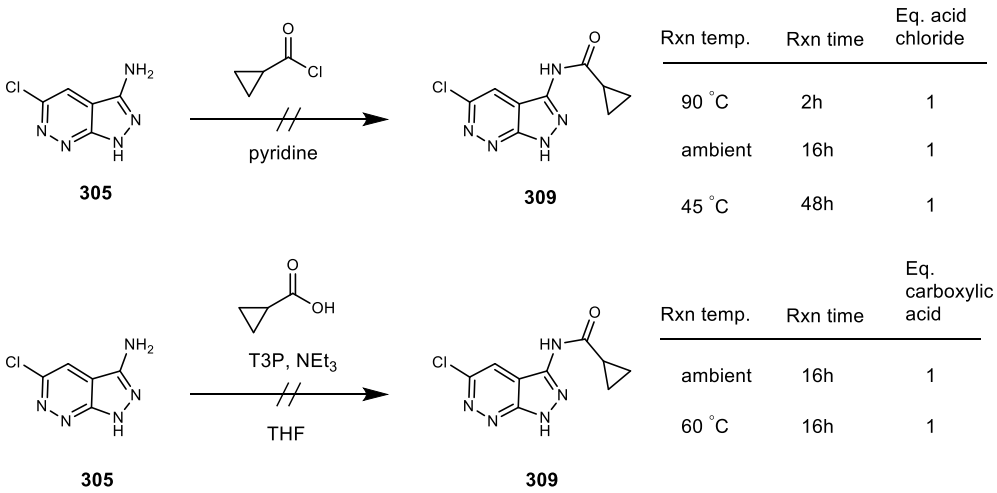

Figure 103. Synthetic attempts to selectively mono-acylate intermediate 309.

Due to the difficulties encountered with selective acylation of intermediate **305**, the steps were reversed. Efforts turned to installation of the 5-aryl group through a Suzuki cross-coupling prior to acylation. Under the Suzuki conditions displayed in Scheme 63, the desired product was not furnished. Inspection of the reaction mixture appeared to show that unreacted **305** remained with no evidence to suggest that **310** had formed. The Suzuki cross coupling mechanism has been well studied and requires 2 equivalents of base.[303] It is possible that the pyrrole N-*H* was deprotonated, using up equivalents of base and thus preventing the desired reaction.

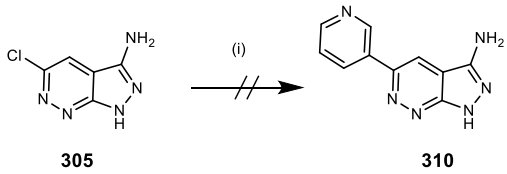

Scheme 63. *Reagents and conditions*: (i) [1,1′-bis(diphenylphosphino)ferrocene]dichloropalladium(II), cesium carbonate, pyridine-3-boronic acid, 1,4-dioxane, 80 °C.

The Suzuki cross coupling was also attempted on an earlier intermediate, **307**. The reaction was performed under microwave irradiation at 140 °C for 15 min and gave a mixture of regioisomers.

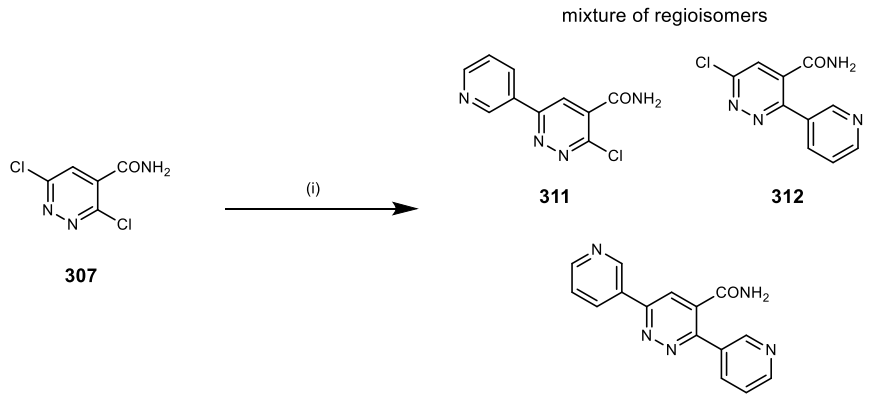

Scheme 64. *Reagents and conditions*: bis(triphenylphosphine)palladium(II) dichloride, sodium carbonate, pyridine-3-boronic acid, acetonitrile:water 5:1, 140 °C, 15 min, µwave.

The mixture of regioisomers **311** and **312** were formed – evident by the doubling of signals in the ^{1}H NMR spectrum. The biaryl product was also produced but in much lower yield and was not isolated from the reaction mixture.

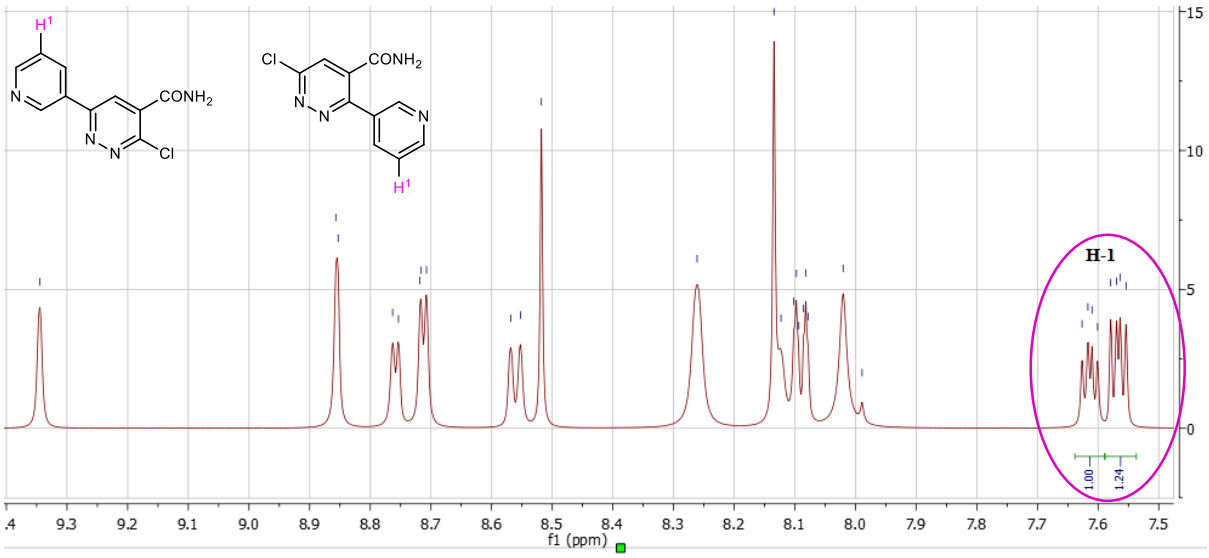

Figure 104. Doubling of pyridine proton signals in ^{1}H NMR of isolated material indicating presence of regioisomers **311** and **312**.

Separation of **311** and **312** by conventional chromatography proved difficult and the LCMS-MDAP spectrum appeared to show a major peak with the expected mass-to-charge ratio of **311** and **312** with a shouldering peak.

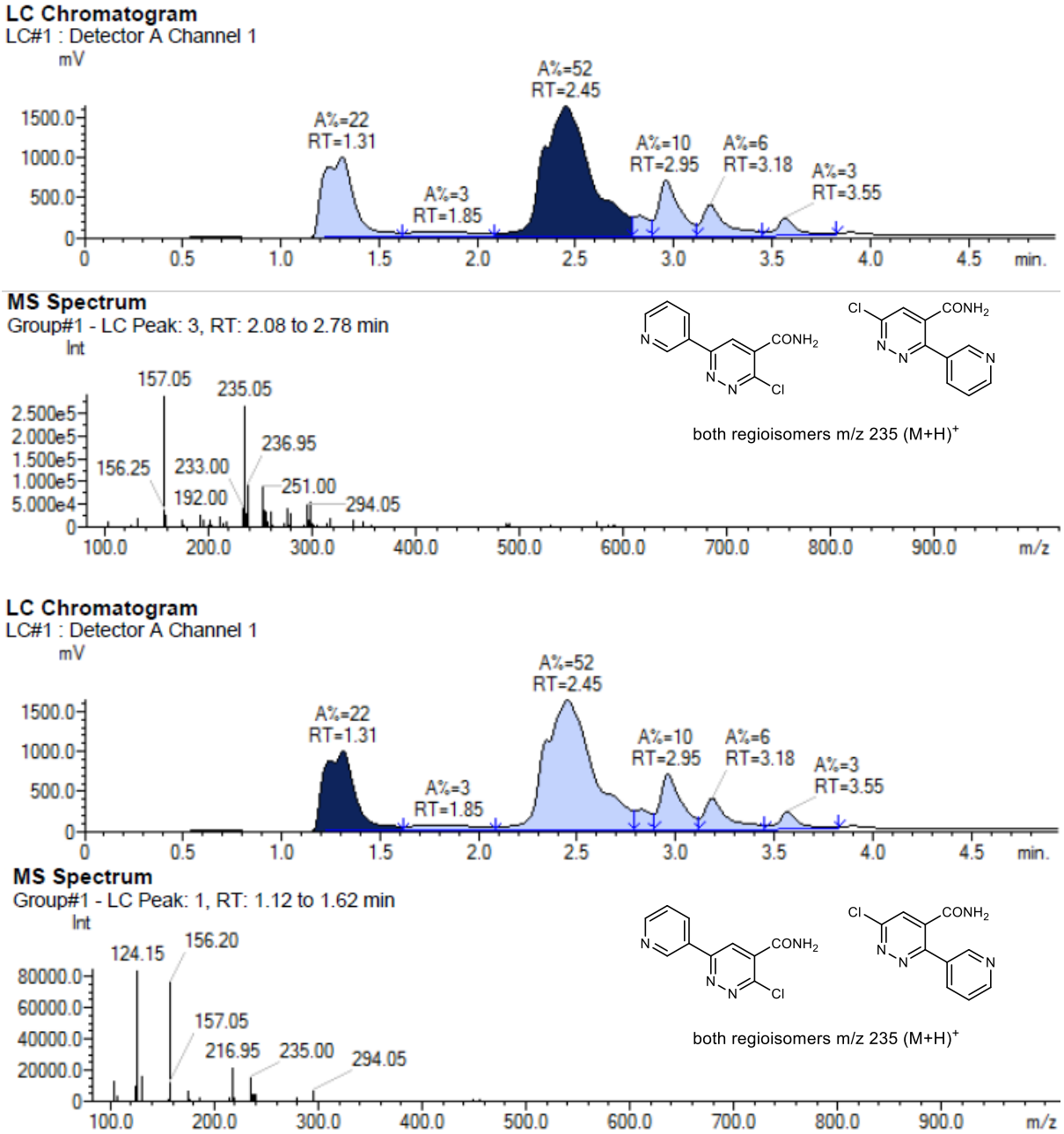

Figure 105. LCMS-MDAP indicates presence of regioisomers 311 and 312

Due to the perceived amount of time required to optimise selective acylation and C-C bond formation procedures, it was decided that the more robust literature procedure should be followed. Once **301** was successfully synthesised and confirmed as a DYRK1A inhibitor, route optimisation could take place.

9.2.3. Following the Published Procedure to Synthesise 301

Aldol condensation between 3-acetylpyridine **313** and diethyl ketomalonate was low yielding. This was not perceived as a major problem due to the ready availability of the starting materials. Subsequent cyclisation of **314** with hydrazine proceeded in respectable yield to afford **315**.

Primary amide formation followed by dehydration to form the nitrile **316** proceeded in acceptable yield. Cyclisation of **316** with hydrazine afforded the key intermediate **310** in poor yield. Uncontrolled acylation of **310** with cyclopropylcarbonyl chloride and subsequent deacylation with piperidine afforded the target compound **301** in acceptable yield.

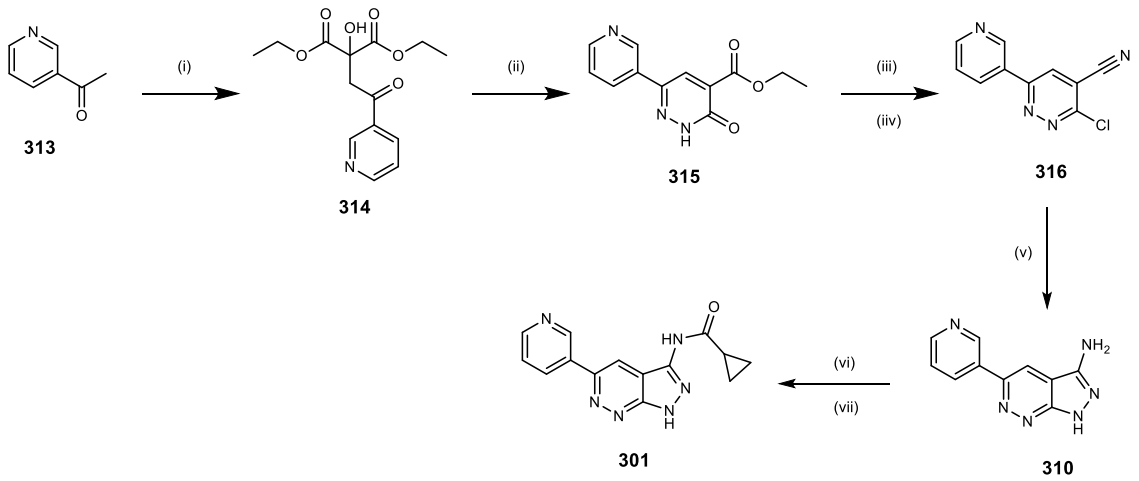

Scheme 65. *Reagents and Conditions*: (i)diethyl kethyl ketomalonate, pyridine, 125 °C, overnight, 34%; (ii) hydrazine, EtOH, reflux, overnight, 50%; (iii) 28% v/v ammonium hydroxide solution, rt, 16 h; (iv) phosphorus(V)oxychloride, 2 h, reflux, 40%; (v) hydrazine hydrate, 80 °C, 16 h, 18%; (vi) cyclopropanecarbonyl chloride, TEA, 1,4-dioxane, reflux, 30 min; (vii) piperidine, rt, overnight, 48%.

9.2.4. SAR and Biological Activity of 301

The DYRK1A binding affinity, metabolic stability and solubility profile of **301** is presented in Table 62.

Table 62. DYRK1A Binding Affinity, Metabolic Stability and Solubility of 301

Compound	DYRK1A IC_{50}[a]	LE, LipE	HLM (µL / min / mg)	RLM (µL / min / mg)	Solubility (mg/mL)
301	10	0.53, 7.1	28.9 +/- 15.3	60.2 +/- 25.7	0

[a]IC_{50} (nM) in TR-FRET-based ligand-binding displacement assay (n = 1). LE = 1.4(pIC_{50})/non-hydrogen atoms; LipE = pIC_{50} – clog P. HLM and RLM Determinations mean of n =2 +/- standard deviation (unless otherwise stated). HLM = human liver microsomes; RLM = rat liver microsomes; thermodynamic solubility data derived from single experiment at pH 6.8.

Upon re-synthesis **301** exhibited DYRK1A IC_{50} = 10 nM. In terms of compound quality, the pyrazolo[3,4-*c*]pyridazine series had the lowest molecular weight and lipophilicity of all of the series selected for optimisation. Consequently, the LE = 0.53 and LipE = 7.1 were superior to all other series being investigated. Although **301** possessed two HBDs, the CNS MPO score was 5.3, which again was the most attractive starting point of any of the series being investigated. The metabolic stability of **301** was promising given the low level of microsomal turnover in both HLM

= 28.9 µL/min/mg and RLM = 60.2 µL/min/mg. The thermodynamic solubility of the pyrazolo[3,4-*c*]pyridazine series was extremely poor and would need optimisation.

From the original PKIS dataset[19] it was apparent that **301** was a relatively selective inhibitor of DYRK1A. The selectivity profile of **301** was assessed in a 48-kinase panel using a DSF assay. The results of this assay confirmed that relative to the control staurosporine, **301** had a good selectivity profile, stabilising few other proteins than DYRK1A.

301 was profiled in a panel of 468 kinases to assess its kinome-wide selectivity profile. **301** was assayed in the KINOMEscan® platform provided by DiscoveRx, a proprietary active-site directed competition binding assay. The results of the selectivity profiling are displayed as a TREEspot™ diagram in Figure 106.

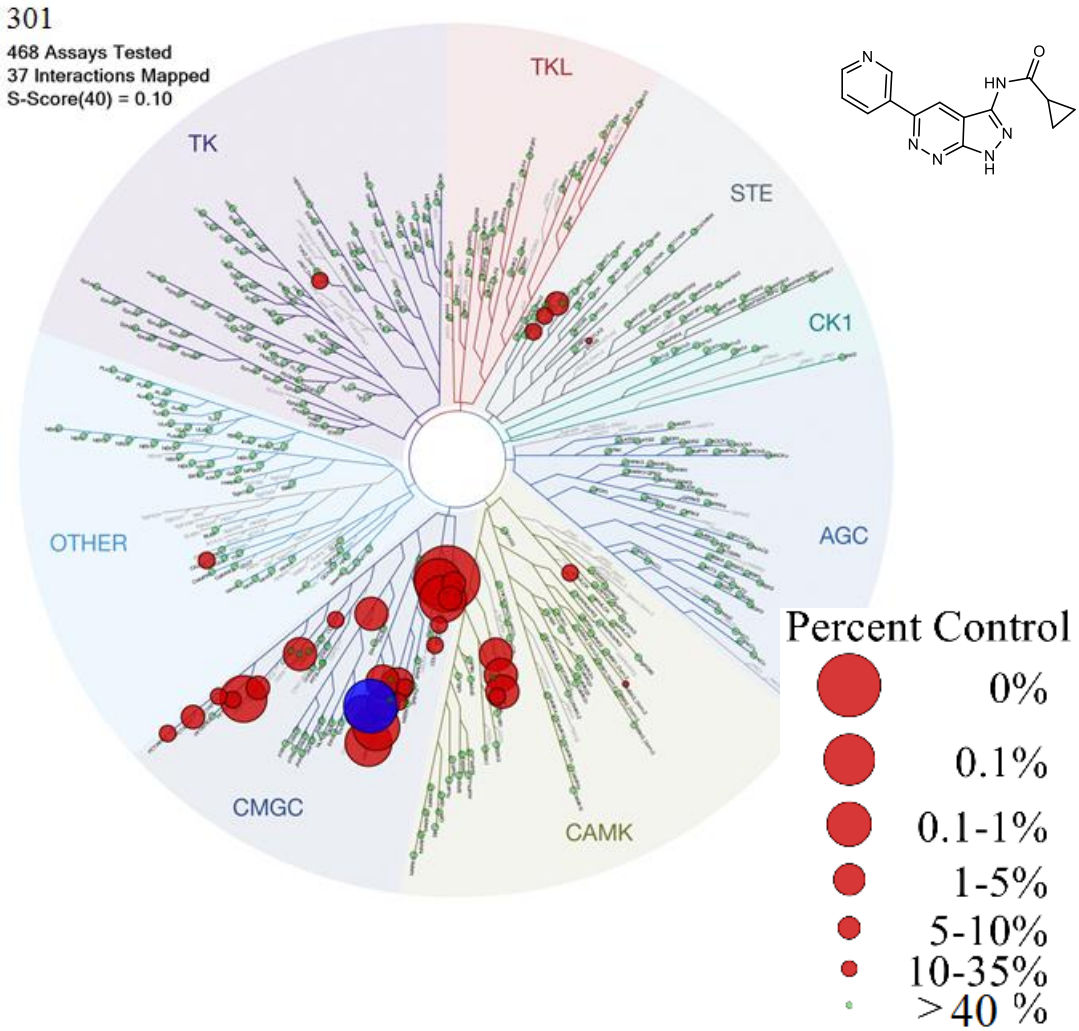

Figure 106. Selectivity profile of **301** evidenced by KINOMEscan® results. DYRK1A is highlighted in blue. Image generated using TREEspot™ Software Tool and reprinted with permission from KINOMEscan®, a division of DiscoveRx Corporation, © DISCOVERX CORPORATION 2010.

301 exhibited very good kinome-wide selectivity. The KINOMEscan data suggests that under 6% of the kinome is strongly inhibited by **301** at 1 µM (Table 63). The kinome-wide selectivity profile of **301** was superior to the starting points in both of the other series under investigation and seemed to show a strong bias towards binding to the CMGC family. Hence, the majority of off-targets in the pyrazolo[3,4-*c*]pyridazine series were the same off-targets that had been successfully removed in the pyrazolo[1,5-*b*]pyridazine series, giving confidence that **301** was a good starting point for the design of a selective inhibitor of DYRK1A.

Table 63. Overview of Kinome Selectivity Profiles of **301**

Compound	Percent kinases inhibited > 75%[a]	Percent kinases inhibited > 50%[a]	Kinases most potently inhibited
301	5.8%	9.6%	GSK3s, HIPKs, CDKs, DYRKs, CLKs

[a] % Inhibition as determined by DiscoveRx KINOMEscan® experiment.

As **301** possessed very strong binding affinity for DYRK1A, and was very selective, in-cell DYRK1A target engagement was assessed using a NanoBRET assay. **301** maintained a potent level of DYRK1A inhibition in cell and was just under 10 fold more potent than the pyrazolo[1,5-*b*]pyridazine **96**, showing no signs of cytotoxicity.

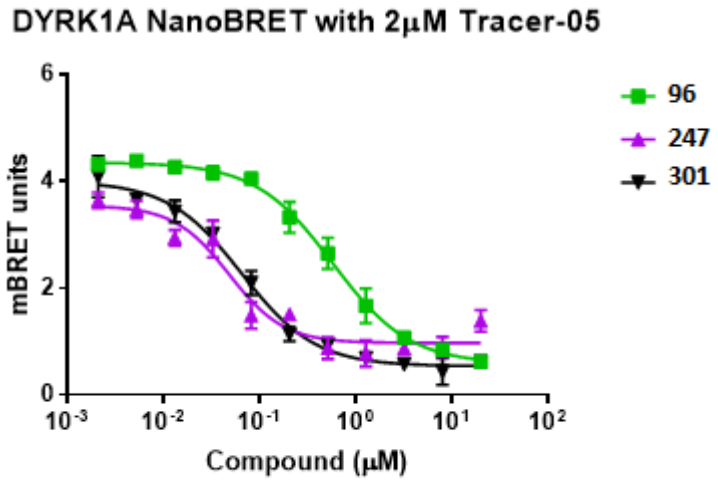

	96	247	301
IC50	0.5762	0.04814	0.06543

Figure 107. NanoBRET cellular activity of **301** (black curve). IC_{50} reported in µM.

Given the promising overall profile of **301**, it represented an interesting starting point towards a DYRK1A molecular probe. It was essential to determine which features of **301** were responsible for its DYRK1A binding affinity and good selectivity profile as these would need to

be maintained. Removal of off-target CMGC kinases whilst improving the solubility of the series would be required to repurpose this series of GSK3β/CDK inhibitors into a specific molecular probe for DYRK1A.

9.3. Initial Investigation of the Pyrazolo[3,4-*c*]pyridazine Series

9.3.1. Rationale.

All efforts to obtain a co-crystal structure of the pyrazolo[3,4-*c*]pyridazine series bound to DYRK1A failed. As a result, the co-crystal of a the imidazo[1,2-*b*]pyridazine series was used to create a pharmacophore model, which **301** was docked onto using induced-fit docking. Both the pyrazolo[1,5-*b*]pyridazine series and the imidazo[1,2-*b*]pyridazine series share common pharmacophoric features. In both series pyridyl type nitrogens form hydrogen-bond acceptors with Leu241 and Lys188. It is likely that **301** would also form hydrogen-bonds with Leu241 and Lys188. The *in silico* binding model is depicted in Figure 108.

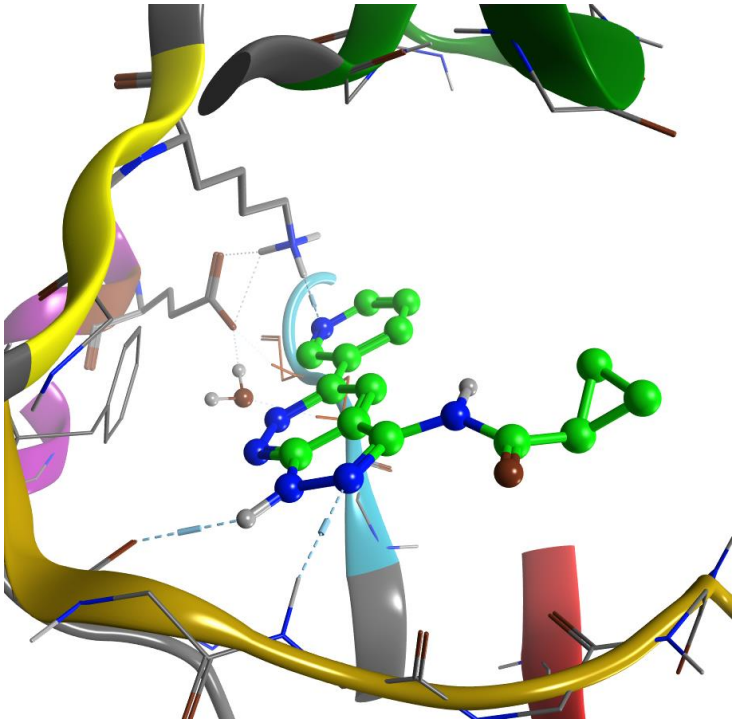

Figure 108. *In silico* binding model of **301** bound to DYRK1A based on pyrazolo[3,4-*c*]pyridazine crystal structure described by Witherington *et al.*[300] **301** docked with induced-fit docking onto pharmacophore of in-house crystal structure of **247** bound to DYRK1A where hydrogen-bond acceptor to Leu241 and hydrogen-bond acceptor to Lys188 are designated as pharmacophoric features. Structure prepared and minimised with MOE 2016, CCG with Amber10:EHT force field.

The docking model shows that **301** is capable of forming hydrogen-bonds to Leu241 and Lys188. Another hydrogen-bond is also established between the indazole N-*H* and Glu239, replacing the

CH-O interaction that has been observed in the pyrazolo[1,5-*b*]pyridazine series and the imidazo[1,2-*b*]pyridazine series. The high number of potential hinge binding motifs in the pyrazolo[3,4-*c*]pyridazine series made the binding mode prediction challenging and by no means definitive.

As the binding mode of the series was not certain, a ligand-based or knowledge-based approach was preferred. Ligand data for the pyrazolo[3,4-*c*]pyridazine series available in the public domain was studied to guide analogue design. It appeared from the literature that alterations to the pyrazolo[3,4-*c*]pyridazine core heavily influenced the GSK3β activity of the series.[300] Movement of the nitrogen to the 4-position, between the amide and the aryl group, was reported to deliver selectivity against GSK3β.[300] The authors suggested that electron repulsion between the N4 and the amide nitrogen caused an unfavourable conformation of the molecule to be adopted in GSK3β (Figure 109).[300] Due to differences in the hinge region of DYRK1A and GSK3β, it was hoped that this scaffold hop would not be detrimental to DYRK1A inhibitory activity and would afford selectivity against GSK3β.

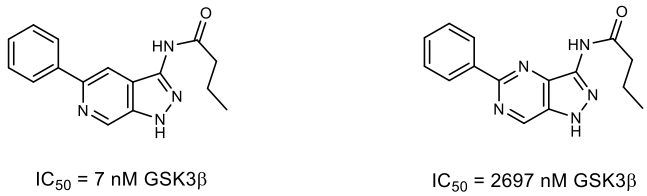

Figure 109. Position of Nitrogen in 5,6-system appears to affect GSK3β Activity.[300]

The PKIS2 dataset included a number of heterocyclic analogues of the pyrazolo[3,4-c]pyridazine series that were reported to be inhibitors of DYRK1A.[21] The data suggested that the position of the nitrogens in the heterocyclic core can be changed without abolition of DYRK1A inhibitory activity.

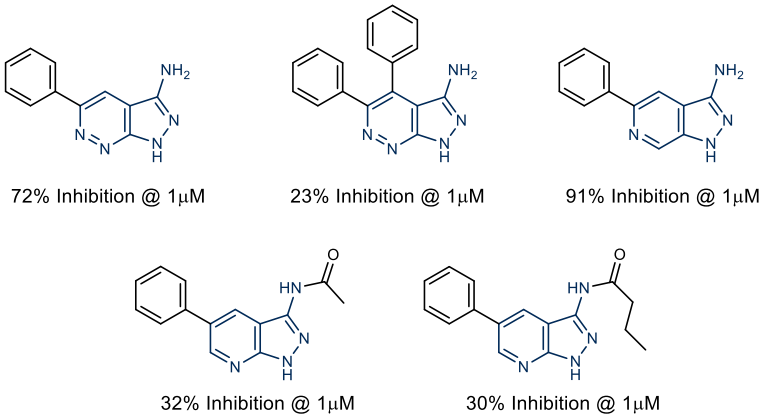

Figure 110. Similar scaffolds disclosed in PKIS2 that inhibit DYRK1A. Percentage Inhibition of DYRK1A at 1 μM, data from referece [21].

Patents released in 2013 and 2018 filed by Samumed LLC suggested that not all of the core nitrogens were necessary for DYRK1A inhibitory activity.[304,305] The patents describe a series of 5-substituted indazole-3-carboxamides with the Markush formula shown in Figure 111. A major claim of the patents are that the compounds have the propensity to inhibit DYRK1A. The Samumed series is extremely similar to **301**.

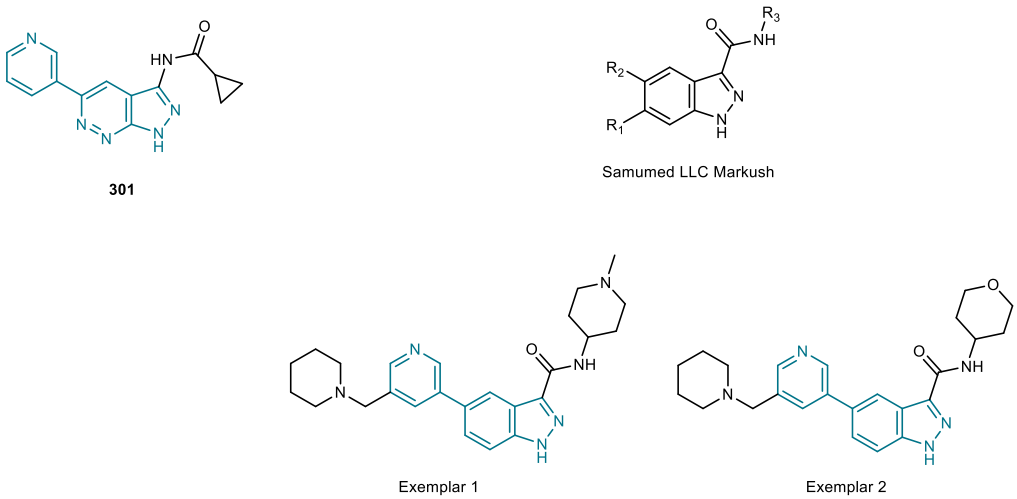

Figure 111. Comparison of **301** with DYRK1A inhibitors disclosed by Samumed LLC. Suspected 'hinge + Lys188' recognition motif of **301** and two exemplars from patent highlighted in cyan.

The available literature appeared to show that alteration of the pyrazolo[3,4-*c*]pyridazine core could lead to improvements in selectivity. In addition, scaffold hopping to other heterocyclic cores may have the potential to provide more soluble analogues of **301** without diminishing DYRK1A affinity or selectivity as long as key ligand-protein binding motifs are maintained.

9.3.2. Synthesis of Heterocyclic Analogues

The original synthesis of **301** had been problematic. Fortunately, advanced precursors were commercially available that made the synthesis of heterocyclic analogues much simpler. It was found that performing multiple steps without purification or isolation of intermediates improved the overall yield of reactions. In general, the 3-pyridyl motif was installed successfully under Suzuki conditions. After removal of solvent under reduced pressure, the crude intermediate was over-acylated (**317**, **319** and **321**) under harsh reaction conditions. The reaction solvent was removed under reduced pressure and the over-acylated intermediates were stirred in piperidine to remove all but one acyl group to access the target compounds **318**, **320** and **322**.

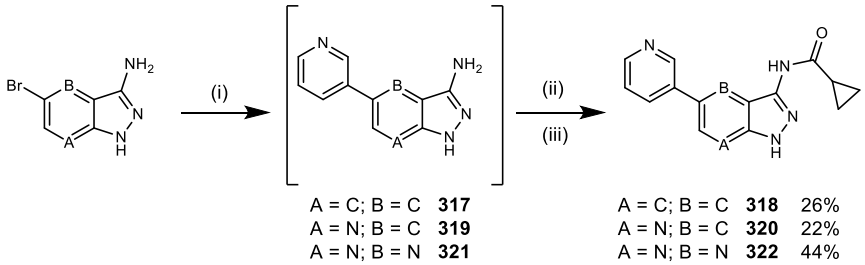

Scheme 66. *Reagents and conditions*: (i) tetrakis(triphenylphosphine)palladium(0), pyridine-3-boronic acid, sodium carbonate, acetonitrile:water (2:1), 150 °C, µwave, 20 - 40 min; (ii) cyclopropanecarbonyl chloride chloride, TEA, 1,4-dioxane, 80 °C, 5 h; (iii) piperidine, rt, overnight.

The synthesis of **324** required a longer synthetic sequence as the heterocycle **323** required prior construction. After cyclisation of the commercially available nitrile with hydrazine to afford **323**, the same route was followed as outlined for **318**, **320** and **322**. Reaction solvent was removed between addition of reagents, affording the desired product with only one final purification step.

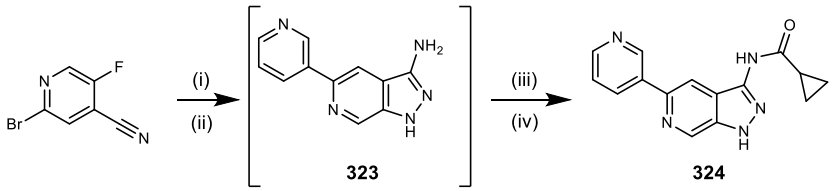

Scheme 67. *Reagents and Conditions*: (i) hydrazine hydrate, DMSO, 120 °C, 3 h; (ii) pyridine-3-boronic acid, bis[2-(di-*tert*-butylphosphanyl)cyclopenta-2,4-dien-1-yl]iron; dichloropalladium, sodium carbonate, acetonitrile:water (8:2), 100 °C, overnight; (iii) cyclopropanecarbonyl chloride, TEA, 80°C, 3 h; (iv) piperidine, rt, overnight, 19%.

9.3.3. SAR and Biological Activity of Heterocyclic Analogues

The DYRK1A binding affinity of the heterocyclic analogues is presented in Table 64. **301** is included for comparison.

In general, most changes to the heterocyclic core were well tolerated, resulting in high affinity ligands of DYRK1A. At the time of writing **324** had been submitted for ligand-binding displacement assay and the results were being awaited.

Table 64. DYRK1A Binding Affinity of Heterocyclic Analogues

Compound	DYRK1A IC_{50}[a]	LE, LipE
301	10	0.53, 7.1
318	18	0.52, 5.4
320	20	0.51, 6.2
322	2246	0.38, 4.6

[a]IC_{50} (nM) in TR-FRET-based ligand-binding displacement assay (n = 1). LE = 1.4(pIC_{50})/non-hydrogen atoms; LipE = pIC_{50} – clog P.

With the exception of **322**, all other compounds have similar affinity to **301**. Hence it appears that the presence of the nitrogen atoms of the pyridazine portion of the pyrazolo[3,4-*c*]pyridazine core do not contribute significantly to the binding affinity for DYRK1A.

Although predicted to be a potential way of improving selectivity against GSK3β, adding a nitrogen to the 4-position of the core (**322**) was also detrimental to DYRK1A binding affinity, equating to an approximate 100-200 fold loss in DYRK1A binding affinity. Gaining selectivity against GSK3β in the pyrazolo[3,4-*c*]series may involve more than scaffold hopping to other heterocyclic analogues.

As solubility had been identified as a major issue with **301**, high affinity ligands **318** and **320** were further profiled for metabolic stability and solubility. This data is exhibited in Table 65. Data for **301** is included for comparison.

Table 65. Metabolic Stability and Solubility 318 and 320

Compound	HLM (µL/min/mg)	RLM (µL/min/mg)	Solubility (mg/mL)
301	28.9 +/- 15.3	60.2 +/- 25.7	0
318	9.5[a] +/- 3.8	31.5[b] +/- 12.5	0.03
320	8.5 +/- 2.1	16.5[a] +/- 2.8	0.04

HLM and RLM Determinations mean of n =2 +/- standard deviation (unless otherwise stated). [a]Mean of n =4 +/- standard deviation. [b]Mean of n =3 +/- standard deviationHLM = human liver microsomes; RLM = rat liver microsomes; thermodynamic solubility data derived from single experiment at pH 6.8.

The metabolic stability of **318** and **320** was superior to that of **301**. The thermodynamic solubility of both **318** and **320** was improved compared to **301**. Taking together the metabolic stability data, solubility and DYRK1A binding affinity data it appears that removal of one or both of the nitrogens from the pyridazine portion of the pyrazolo[3,4-*c*]pyridazine core is having a positive effect on the series. It is important to note that **318** and **320** were also much easier to synthesise as advanced building blocks were commercially available.

318 and **320** were profiled for selectivity in a 48 kinase panel DSF assay. The results of the assay showed that **318** and **320** were relatively selective compared to the control staurosporine, stabilising few proteins apart from DYRK1A. Furthermore, the profiles of **318** and **320** shared a strong resemblance to the profile of **301**, indicating that the kinome-wide profiles of **318** and **320** were very good. The decision was taken not to profile **318** or **320** in the DiscoveRx full panel assay as it was strongly believed that the two inhibitors would still inhibit the same CMGC kinases as **301** given the literature and DSF data.

9.4. *N*-methylation of the Pyrazolo N-*H*

9.4.1. Rationale

As the pyridazine portion of the series appeared to have no impact on binding affinity, the aminopyrazole portion of the core was likely to contribute to binding, in line with the *in silico* binding model of **301** bound to DYRK1A (Figure 108). As a quick test of the binding model, it was rationalised that methylation of the pyrazole N-*H* would remove a hydrogen bond to the hinge and probably cause a clash with hinge residues. If this was true and the binding model correct, the *N*-methyl analogue would be inactive.

9.4.2. Synthesis of *N*-[1-methyl-5-(3-pyridyl)pyrazolo[3,4-*c*]pyridazin-3-yl]cyclopropanecarboxamide

Copper-catalysed cyclisation with methyl hydrazine and **316** afforded **325**. Usual over-acylation with cyclopropanecarbonyl chloride followed by selective deprotection with piperidine afforded the desired analogue **326**.

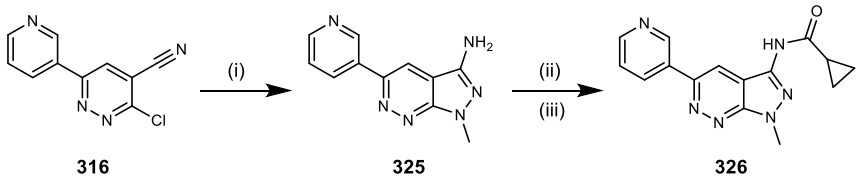

Scheme 68: *Reagents and Conditions*: (i) copper iodide, cesium carbonate, 1,10-phenanthroline, methylhydrazine, DMF, 60 °C, overnight, 69%; (ii) cyclopropanecarbonyl chloride, TEA, 1,4-dioxane, 60 °C, 30 min; (iii) piperidine, rt, overnight, 55%.

9.4.3. SAR and Biological Activity of 326

The DYRK1A binding affinity of *N*-methyl analogue **326** is presented in Table 66. Details for **301** are included for reference.

Table 66. DYRK1A Binding Affinity of **326**

Compound	DYRK1A IC_{50}[a]
301	10
326	19860

[a]IC_{50} (nM) in TR-FRET-based ligand-binding displacement assay (n = 1).

The methylated analogue **326** was inactive, indicating that the pyrazole N-*H* was involved in binding, probably to the hinge region as depicted in the *in silico* binding model (Figure 108).

9.5. Modifications to the 3-pyridyl Motif to Determine Importance for Binding Affinity

9.5.1. Rationale

As the two pyridazine nitrogen atoms were not contributing to binding, the synthetically more tractable indazole core was used to determine the necessity of the 3-pyridyl motif.

The *in silico* binding model (Figure 108) suggested that the majority of interactions were taking place at the hinge of the kinase with the aminopyrazole motif. The pyridine subunit was directed towards the back-pocket of DYRK1A, likely forming a hydrogen-bond with Lys188.

9.5.2. Synthesis of Pyridyl Replacements

328 and **330** were synthesised in a one-pot three step procedure without purification or isolation of intermediates. Removal of reaction solvent between each step followed by addition of the next set of reagents afforded a crude mixture containing the desired product. Conventional chromatography in the final step afforded **328** and **330** in sufficient purity for biological assay.

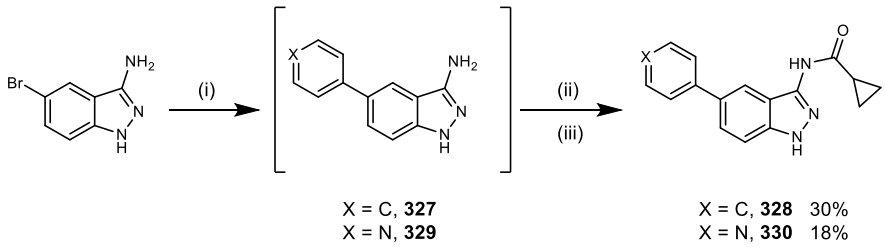

Scheme 69. *Reagents and conditions*: (i) tetrakis(triphenylphosphine)palladium(0), pyridine-3-boronic acid, sodium carbonate, acetonitrile:water (6:1), 150 °C, µwave, 20 - 40 min; (ii) cyclopropanecarbonyl chloride chloride, TEA, 1,4-dioxane, 60 - 80 °C, 1 - 5 h; (iii) piperidine, rt, overnight.

9.5.3. SAR and Biological Activity of 328 and 330

The DYRK1A binding affinity of **328** and **330** is presented in Table 67. **301** is included for comparison.

In general, all indazole analogues that lacked the 3-pyridyl motif exhibited diminished DYRK1A binding affinity.

Table 67. DYRK1A Binding Affinity of 328 and 330

Compound	DYRK1A IC_{50}[a]
301	18
330	737
328	3349

[a]IC_{50} (nM) in TR-FRET-based ligand-binding displacement assay (n = 1).

Transposition of the nitrogen atom from the 3-pyridyl (**301**) to form the 4-pyridyl analogue (**330**) resulted in over 30 fold reduction in DYRK1A binding affinity. This result suggests that the 3-pyridyl nitrogen is stabilising the protein-ligand interaction, supporting the binding model. In the absence of a co-crystal structure it is difficult to determine conclusively, but the 4-pyridyl nitrogen could be too far displaced to form these stabilising interactions. Complete removal of the pyridyl nitrogen abolishes DYRK1A binding affinity in the pyrazolo[3,4-*c*]pyridazine series, again suggesting that the 3-pyridyl motif is orientated in an optimal orientation to form stabilising interactions with receptor.

9.6. Summary

The pyrazolo[3,4-*c*]pyridazine series was identified from the PKIS set as a potent GSK3β inhibitor with off-target activity at other CMGC kinases including DYRK1A. From the outset, solubility and selectivity against GSK3β and the CDKs were the major obstacles to overcome. A co-crystal structure of the pyrazolo[3,4-*c*]pyridazine series did not materialise, despite multiple attempts. Due to the nature of the chemotype, its small structure and capability to form several hydrogen-bonding interactions, prediction of the binding mode was more of a challenge than in other series. To complicate things further the pyrazolo[3,4-*c*]pyridazine core was synthetically challenging to construct compared to other series that were being worked on in parallel. Focussed SAR around the pyrazolo[3,4-*c*]pyridazine core and pyridyl motif helped to formulate a binding model hypothesis of the series in DYRK1A. Efforts to improve the metabolic stability of the series were successful without losses in DYRK1A binding affinity. Selectivity against GSK3β

and CDKs had not been improved relative to the starting pyrazolo[3,4-*c*]pyridazine hit **301**. Consequently, work on this series was suspended whilst efforts were focussed on the pyrazolo[1,5-*b*]pyridazine and imidazo[1,2-*b*]pyridazine series.

In 2017 Nakano-Kobayashi *et al*. reported the fragment ALGERNON as a potent DYRK1A inhibitor.[306] The structure of ALGERNON is depicted in Figure 112. It is a substructure of **318**, and is derived from the same indazole core that Samumed LLC investigated as DYRK1A inhibitors. The complete selectivity profile of the molecule was not mentioned in the publication and it would be surprising if the molecule was selective for DYRK1A.[306] A literature search reveals a more complete selectivity profile of ALGERNON and analogues of ALGERNON disclosed in 2011 by workers at Abbott Laboratories in their seminal paper 'Navigating the Kinome'.[41] ALGERNON represents the centre-point in 'Cluster 5' and does not appear selective for DYRK1A.

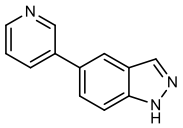

Figure 112. ALGERNON.[306]

Nakano-Kobayashi's study reports that treatment of pregnant dams with ALGERNON rescued aberrant cortical formation in Down's syndrome mouse embryos and that these offspring exhibited normal cognitive behaviour.[306] Given the potency of ALGERNON, the amide substituent of the pyrazolo[3,4-*c*]pyridazine series appears not to be significantly contributing to DYRK1A inhibitory activity. If selectivity is a problem for ALGERNON, the *in silico* model and the knowledge gained during this work could be used to furnish more selective inhibitors derived from ALGERNON.

CHAPTER 10. Conclusions and Future Directions

10.1. Design of Tool Compounds to Probe the Role of Serine Racemase and *D*-Serine in Diseases of the CNS

The NMDA-R co-agonist *D*-Serine, and the enzyme responsible for its synthesis, SR, represent attractive therapeutic targets for indirect modulation of the NMDA-Rs as a means of treating disorders associated with NMDA-R dysfunction. The aim of the SR project was to identify suitable chemical probes for use in *in vivo* experiments so as to delineate the role of SR and *D*-serine in diseases of the CNS. The SR project was reopened after an intermission of 10 years following Evotec's decision to terminate the original project. The few literature inhibitors of SR that do exist, such as malonate and synthetic amino acids, are not drug-like and are not suitable for use as *in vivo* tools.

In an attempt to identify novel and more drug-like tool compounds, with the prospect of target engagement *in vivo*, a number of strategies were employed. Legacy data from Evotec's terminated project, which included fragment screening data and HTS data, was studied for potential starting points. Hits identified from these sources were resynthesised to be validated in an in-house biochemical assay before attempts were made to co-crystallise confirmed inhibitors with SR. If successful, SBDD efforts would then ensue. In parallel, literature inhibitors were investigated as a back-up series and to validate the in-house assay. Literature inhibitors confirmed as active would then be co-crystallised with SR to begin a period of rational based design.

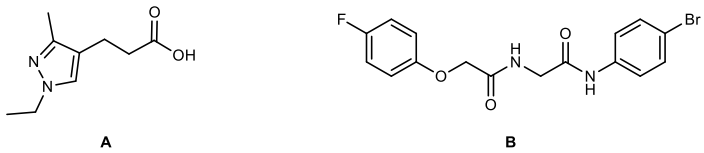

Figure 113. A - Evotec fragment and B – Mori peptidomimetic; Both reported as SR inhibitors.

The results of the primary assay data generated for the Evotec fragments and literature inhibitors raised questions over the validity of the in-house assay and the legitimacy of the hits identified. Evotec and literature peptidomimetics exhibited no inhibition of SR, consequently the SR project was halted until further hit identification and validation work was completed. Medicinal chemistry efforts would only resume once a genuine hit had been identified.

A major challenge with the SR project was the uncertainty surrounding the validity of historical data generated by Evotec that ultimately led to the termination of the original SR project. Another concern was that inhibitors identified in the literature also failed to repeat in the primary assay. In the future the SR project must establish a robust screening protocol with suitable orthogonal assays. Some consideration should also be given to obtaining selectivity against closely related PLP-dependent enzymes such as SDH.

10.2. Design of Tool Compounds to Probe the Role of DYRK1A in Diseases of the CNS

Publically available kinase profiling data was used to identify hits for DYRK1A. The hits were already in drug-like space and a large volume of data already existed for these molecules, which enabled inhibitor repurposing. Three distinct series were worked on in parallel before one series, the pyrazolo[1,5-*b*]pyridazine series, was optimised and profiled more extensively.

10.2.1. The Pyrazolo[1,5-*b*]pyridazine Series

The pyrazolo[1,5-*b*]pyridazine series (Chapter 4-7) was repurposed from a selective GSK3β/CDK2 kinase inhibitor through targeted removal of GSK3β/CDK2 activity using a chemoinformatics approach. Matched-molecular pairs and nearest neighbours within the pyrazolo[1,5-*b*]pyridazine series were identified, activity cliffs for GSK3β/CDK2 were highlighted and subsequently exploited.

Although a number of activity cliffs were identified, installation of a methyl group onto the aminopyrimidine N-*H* was predicted, and then experimentally proven, to result in complete abolishment of GSK3β/CDK2 inhibitory activity. The additional methyl group caused a 5 fold reduction in DYRK1A binding affinity, resulting in a DYRK1A inhibitor, **88**, with IC_{50} = 186 nM.

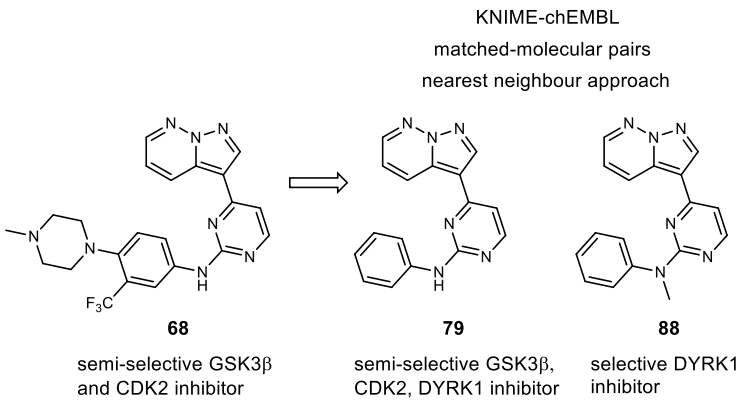

Figure 114. Chemoinformatic approach for removal of GSK3β/CDK2 ihibitory activity.

Matched-pair analysis of *N*-methyl analogues furnished two inhibitors with IC_{50} < 100 nM, one of which was **89**, exhibiting DYRK1A affinity IC_{50} = 76 nM, with unprecedented levels of selectivity over DYRK1B and the CLKs.

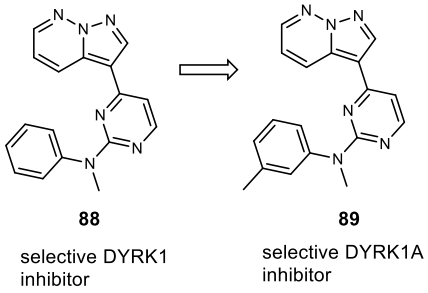

Figure 115. Matched-pair analysis afforded a DYRK1A selective inhibitor through addition of another methyl group.

The addition of a second methyl group had resulted in a DYRK1A ligand with IC_{50} < 100 nM and unprecedented levels of kinome-wide selectivity. **89** also possesses high permeability and low P-gp efflux as determined in an MDCK-MDR1 assay. **89** exhibits high metabolic turnover and low aqueous solubility in line with most other published DYRK1A inhibitors.

The elucidation and inspection of the first DYRK1A co-crystal structure with **88** bound, supported *in silico* modelling, and led to the hypothesis that selectivity for DYRK1A was being driven by the positioning of the *N*-methyl group at the solvent-exposed region, close to the gatekeeper+2 residue of the hinge, Met240. Small lipophilic substituents such as methyl or methylene moeities appeared to be accommodated at this position in DYRK1A better than in the majority of other kinases. This finding should help others to discover more selective inhibitors of DYRK1A through SBDD.

Focussed optimisation of the series in terms of DYRK1A binding affinity, metabolic stability (HLM and RLM) and solubility, whilst maintaining the good selectivity profile afforded by the *N*-methyl group, was prosecuted. Ligand optimisation was driven by improving physicochemical properties and metrics that govern compound quality such as LE, LipE and CNS MPO score. Reducing clog P and the number of aromatic rings led to **96**, which displayed improved binding affinity for DYRK1A, vastly improved solubility and maintained a high level of selectivity for DYRK1A. **96** displayed high levels of metabolic clearance, probably as a result of *N*-dealkylation of the *N,N*-dimethylaminopyrimidine motif. **98** possessed slightly better metabolic stability than **96** overall with comparable selectivity and DYRK1A binding affinity.

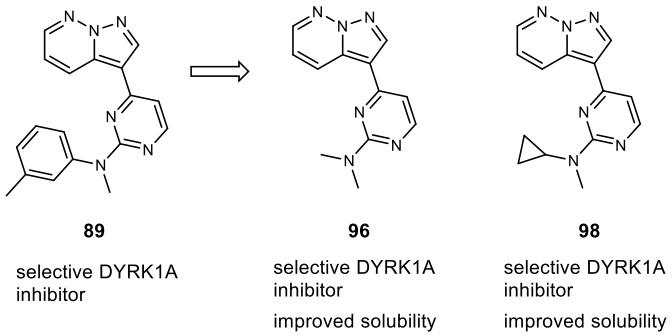

Figure 116. Optimisation through reduction of lipophilicity and aromatic ring count.

In-house DYRK1A co-crystal structures of **96** and **98** were used to guide the *in silico* design of a range of diverse substituents that were directed towards Met240 and the solvent-exposed region of DYRK1A with the aim of further increasing DYRK1A affinity, selectivity, metabolic stability and solubility. An *in silico* library was enumerated, filtered through KNIME® workflows and docked (Induced-Fit Docking) into DYRK1A before molecules that were predicted to bind in an active conformation were synthesised. In this way a number of analogues that exhibited strong binding affinity for DYRK1A were produced. On balance of binding affinity, solubility and metabolic stability, **123** appeared to have the best chance of becoming a molecular probe, however, full selectivity profiling of **123** is still underway. The KINOMEscan® selectivity data generated for **125** and **134** has been very promising. The compounds are both selective for DYRK1A; **125** has a selectivity score (S-score) (40) = 0.01 and **134** has an S-score (40) = 0.02, indicative of very selective kinase inhibitors.[307] It is likely that the other analogues displayed in Figure 117 are also very selective.

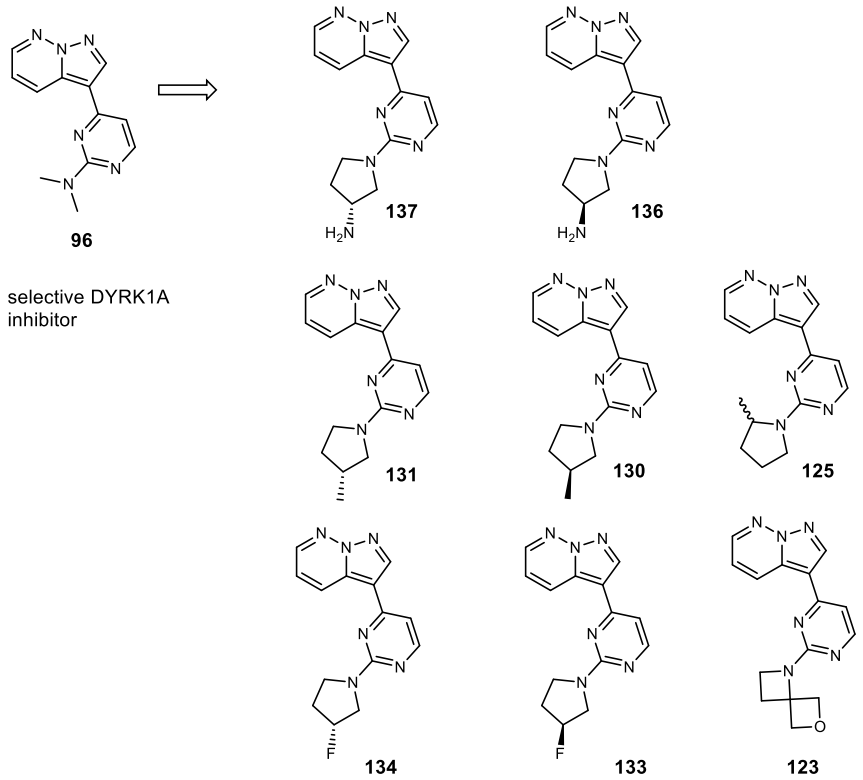

Figure 117. Rational design of a pyrazolo[1,5-*b*]pyridazine library.

Although **123** had a good overall profile as a DYRK1A tool compound, the metabolic stability of the pyrazolo[1,5-*b*]pyridazine series in general could be improved and required further investigation. Scaffold hopping and diversification of the pyrimidine motif afforded only two analogues that were high affinity ligands of DYRK1A, triazine **201** and 5-fluoro analogue **172**.

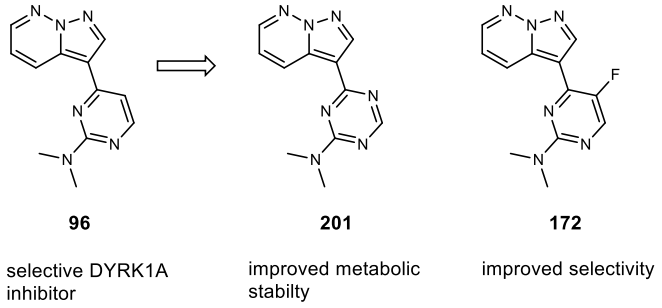

Figure 118. Investigation of the pyrimidine motif.

172 represented one of the highest affinity DYRK1A tools discovered IC_{50} = 57 nM, the 5-fluoride also appeared to afford a better level of selectivity over DYRK1B and the CLKs (S-score (40) = 0.01). **172** showed excellent permeability in the MDCK-MDR1 assay and exhibited no P-gp efflux. The metabolic stability of **172** was very poor, potentially limiting its use as an *in vivo* molecular probe.

Another area of exploration was the pyrazolo[1,5-*b*]pyridazine moiety itself. Scaffold hopping and diversification of the pyrazolo[1,5-*b*]pyridazine moiety led to a number of interesting analogues that possessed strong binding affinity for DYRK1A and had reduced rates of metabolic turnover. The full selectivity profiles of **204**, **206** and **228** are still being acquired.

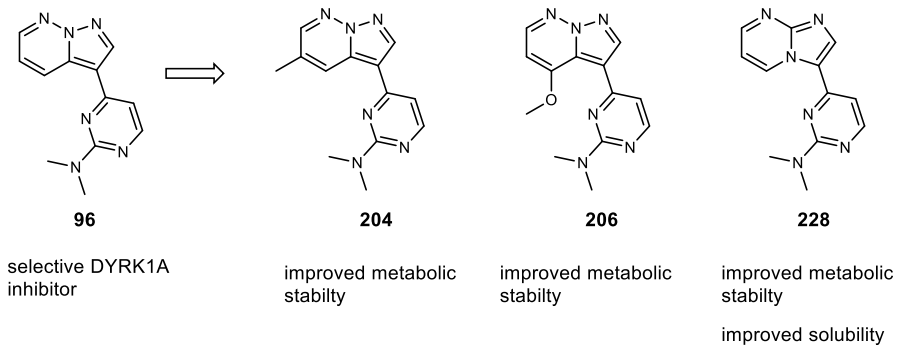

Figure 119. Investigation of the pyrazolo[1,5-*b*]pyridazine motif.

Chimeric molecules were designed in an attempt to combine improvements gained for parent molecules in binding affinity, selectivity, metabolic stability and solubility. All chimeric molecules were successfully synthesised and have been submitted for ligand-binding displacement assay before further profiling takes place.

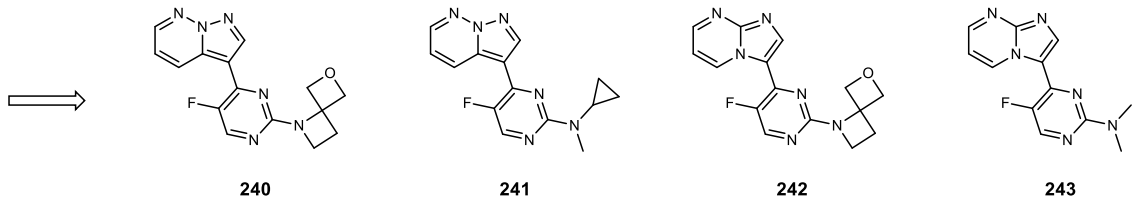

Figure 120. Chimeras of selective and high affinity ligands of DYRK1A with desirable metabolic stability and solubility.

If **240** - **243** possess improved binding affinity for DYRK1A, the selectivity profiles, metabolic stability, solubility and cellular activity will be assessed. Co-crystallography experiments to determine the binding mode of these chimeras would also be of interest. Future work in this series should involve the parallel exploration of the imidazo[1,2-*a*]pyrimidine scaffold and the pyrazolo[1,5-*b*]pyridazine scaffold. Substitutions to the 5- and 4-positions of both cores should also be explored.

The limits of the pyrazolo[1,5-*b*]pyridazine series are depicted by the key SAR summaries in Figure 121.

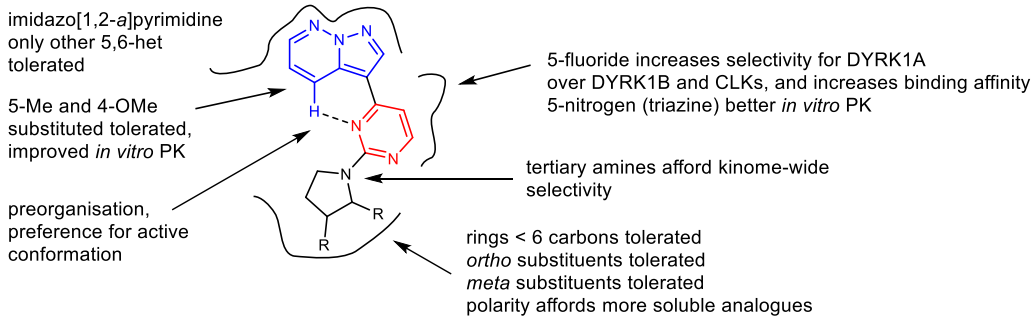

Figure 121. Summary of SARs for pyrazolo[1,5-*b*]pyridazine series.

In terms of synthetic achievement during this work a number of chemical methodologies were developed, notably the mild and selective halodecarboxylation of heteroarene carboxylic acids, which led to a peer-reviewed publication.[267] The study and development of reagents for electrophilic *N*-amination of heterocycles could be a future area of interest. The mechanism of the Huisgen 1,3-dipolar cycloaddition of azomethine ylides warrants further investigation and would benefit from modern methods of in-reaction monitoring and computational techniques. Enhancing understanding may lead to improved yields and scope of the reaction.

10.2.2. The Imidazo[1,2-*b*]pyridazine Series

Imidazo[1,2-*b*]pyridazine **247** was discovered as a relatively selective and high affinity binder of DYRK1A. It was challenging to modulate the metabolic stability and solubility of the imidazo[1,2-*b*]pyridazine series without diminishing DYRK1A binding affinity. SBDD was used in an attempt to transfer selectivity established in the pyrazolo[1,5-*b*]pyridazine series over to the imidazo[1,2-*b*]pyridazine series. Future development of the imidazo[1,2-*b*]pyridazine series would involve starting from soluble and high affinity fragments, such as **266**, **275**, **298** and **300**, and optimising them for DYRK1A selectivity and affinity using a structure-based approach.

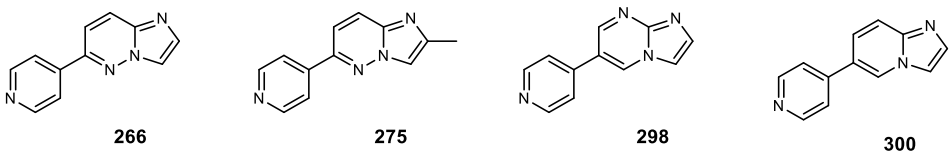

Figure 122. Fragments to optimise for DYRK1A selectivity and affinity.

The limits of the imidazo[1,2-*b*]pyridazine series are depicted by the key SAR summaries in Figure 123.

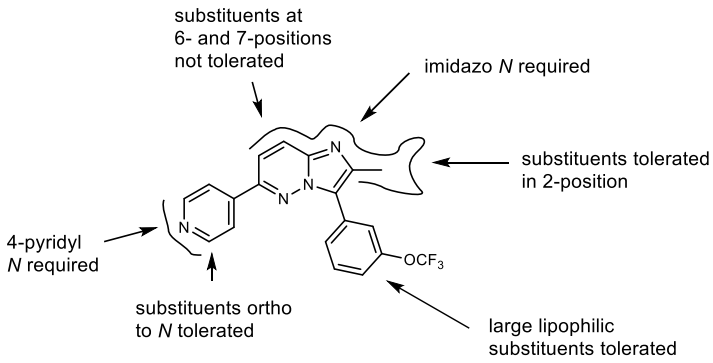

Figure 123. Summary of SARs for imidazo[1,2-*b*]pyridazine series.

10.2.3. The Pyrazolo[3,4-*c*]pyridazine Series

Pyrazolo[3,4-*c*]pyridazine **301** was identified as a selective and high affinity binder of DYRK1A. It was challenging to modulate the metabolic stability and solubility of the pyrazolo[3,4-*c*]pyridazine series without diminishing DYRK1A binding affinity. Through a small-scale SAR evaluation the binding mode of the series was rationalised for future analogue optimisation. The limits of the pyrazolo[3,4-*c*]pyridazine series are depicted by the key SAR summaries in Figure 124.

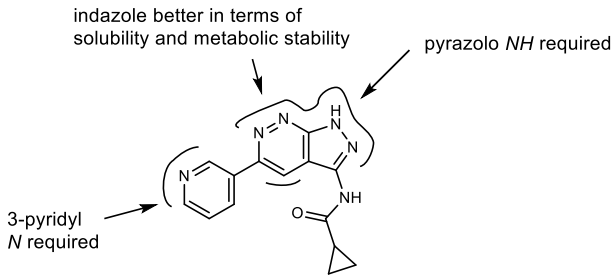

Figure 124. Summary of SARs for pyrazolo[3,4-c]pyridazine series.

Future development of the pyrazolo[3,4-*c*]series will focus on exploration of the 3-position as the binding motif has now been proposed. It may be possible to compare the binding modes of all three series and develop an inhibitor with a better overall profile. Potentially the selectivity trends established in the pyrazolo[1,5-*b*]pyridazine series could be transferred to both back-up series affording more selective and higher affinity DYRK1A ligands.

10.3. Future Direction to take with Inhibitors Identified in this Thesis

Table 68 summarises the most advanced ligands within each chemotype investigated as DYRK1A inhibitors at the time of writing. The leads from each of the series investigated have attractive attributes that warrant further investigation.

Table 68. Overview of Most Advanced Compounds within each DYRK1A Series

Parameter	DYRK1A probe	96	247	301
		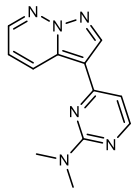	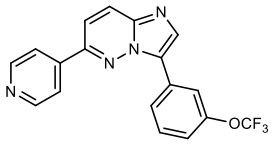	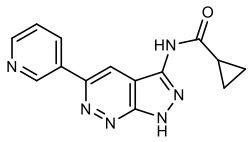
Molecular weight (Mwt)	**< 400**	240.3	356.3	280.3
Clog $D_{7.4}$	**≤ 3.5, ≥ 1.5**	1.6	4.5	0.9
TPSA (A^2)	**< 75 > 40**	59	52	96
HBD	**< 2**	0	0	2
CNS MPO	**> 4.5**	6.0	4.3	5.3
Enzymatic DYRK1A IC_{50}[a]	**< 100**	75	23	10
Ligand efficiency (LE)	**> 0.30**	0.56	0.41	0.53
Selectivity	**> 50-fold**	5 fold > Haspin; 20 fold > DYRK1B, CLK1, CLK4	>50% inh @ 1µM CDK2, DYRK3, VEG-FR, Aurora B; >75% CLK2	>50% inh @ 1µM CDK2, DYRK1B >75% GSK3β
Cellular DYRK1A IC_{50} (nM)	**< 1000 (< 10-fold enzymatic)**	576	48	65
RLM (µL/min/mg)	**< 200**	230.1[b] +/- 30.8	104.8 +/- 14.7	60.2 +/- 25.7
HLM (µL/min/mg)	**< 200**	241.8[b] +/- 31.7	173.4 +/- 20.9	28.9 +/- 15.3
Thermodynamic solubility [mg/mL]	**> 0.1**	0.1	0	0

[a]IC50 (nM) in TR-FRET-based ligand-binding displacement assay (n = 1). HLM and RLM Determinations mean of n =2 +/- standard deviation (unless otherwise stated). [b]Mean of n = 4 +/- standard deviation. HLM = human liver microsomes; RLM = rat liver microsomes; thermodynamic solubility data derived from single experiment at pH 6.8.

Based on the data presented in Table 68, **96** should be considered the most suitable compound for progressing as a molecular probe of DYRK1A. Although **96** exhibits the weakest binding affinity for both the enzymatic and cellular assays, the kinome-wide selectivity and isoform selectivity of **96** far surpasses the kinase selectivity profiles exhibited by **247** and **301**. For use

as a molecular probe of DYRK1A, selectivity is a crucial factor. **96** is an attractive starting point to develop further due to its small size (fragement-like), solubility and optimal CNS MPO score, which correlated experimentally with low P-gp efflux and good permeability. All of these properties provide a level of confidence that warrants further investigation of **96**. More advanced derivatives **96** have been synthesised and are being profiled for selectivity. One of these compounds may possess better microsomal turnover, higher levels of selectivity and cellular potency than **96**. These are the three aspects of **96** that should be optimised in future to provide superior molecular probes of DYRK1A.

The high volume of quality DYRK1A ligands based on the pyrazolo[1,5-*b*]pyridazine core, disclosed in this thesis, will allow for further profiling of the lead series to give confidence for use as *in vivo* tools. The series is more selective than any published DYRK1A inhibitor and therefore warrant use as *in vivo* probes until improved inhibitors are discovered.

The establishment of synthetic procedures, primary, orthogonal biological assays and conditions for co-crystallisation of the pyrazolo[1,5-*b*]pyridazine series means that subsequent DYRK1A inhibitor exploration should be rapid and relatively easy. Future work should incorporate a streamlined assay protocol, whereby in addition to DYRK1A IC_{50}, single point inhibition data should be generated for the CLKs, DYRKs and haspin for all inhibitors with DYRK1A IC_{50} < 200 nM. In this way isoform selectivity has a better chance of success. Once a number of candidate tool compounds are identified they should be profiled in *in vitro* assays designed to understand the suitability of the compounds for use as a CNS tool, such as the MDR1-MDCK permeability assay. Further *in vitro* and *in vivo* assays would then be sought. Funding from the Jerome Lejeune Foundation or Down Syndrome Research Foundation UK should be pursued to establish collaborations with appropriate partners who have access to *in vivo* models of Down's syndrome and AD.

Further possibilities to furnish more selective and potent inhibitors of DYRK1A may involve exploiting the hypothesis that there is a preference for pre-organisation in the pyrazolo[1,5-*b*]pyridazine series. To this end the molecules could be tethered in a preferred conformation in the form of a macrocycle. Another area of interest for kinase inhibitors is the exploration of covalent inhibitors. Although DYRK1A does not appear to have an active site cysteine residue suitable for targeting, there are amino acid residues in the ATP binding site of DYRK1A that could be suitable for targeting. Tyrosine, lysine and serine, present in the DYRK1A ATP site, may be able to form covalent bonds with the SuFEx moiety. A Type II or Type III inhibitor may be worth pursuing, however, this would require further screening campaigns, and this work has shown

that selectivity can be achieved with a Type I inhibitor. In recent years proteolysis-targeting chimeric molecules (PROTACs) have received significant interest as an emerging technique in drug discovery. Protein function is inhibited by hijacking a ubiquitin E3 ligase for protein degradation. The PROTACs consist of a ligand that recruits the E3 ligase, a linker, and a ligand that binds to the protein of interest. PROTACs that target protein kinases have already been investigated.[308] Due to the high degree of selectivity of **96** for the DYRK1A ATP binding site, **96** has potential to act as the DYRK1A binding element, that could be linked to an E3 ligase binding element, to furnish the first DYRK1A PROTAC.

10.4. Further Opportunites as a Result of this Work

During this project a number of molecules were discovered with high levels of kinome-wide selectivity and preferential selectivity for the CLKs and haspin over the DYRKs. **92** appears to bind to CLK2 with at least 7 fold stronger binding affinity than DYRK1A and 3 fold higher affinity than any of the other CLK isoforms. With optimisation, **92** may lead to an isoform selective CLK2 probe. The data generated on the pyrazolo[1,5-*b*]pyridazine series could lead to future projects that focus on inhibitors of the CLKs, other DYRKs and haspin.

The chemoinformatics approach used in this thesis has applicability in public domain drug design for other kinase targets and will be of interest to other academic groups who do not possess the resource to initiate screening campaigns. The strategy taken to target an unusual region of the kinase, namely the gatekeeper+2 residue for selectivity, was also profitable and gives hope that Type I inhibitors can still be found that are extremely selective. It would be interesting to survey the identity of the gatekeeper+2 residue throughout the kinome to see how conserved that particular residue is, and whether it could be targeted more often.

10.5. Final Considerations Regarding DYRK1A

Although it is imperative that the right tool compound is discovered for DYRK1A, there are a number of questions that remain around the target. It is known that the levels of DYRK1A fluctuate throughout neuronal and foetal development, thus it is important to establish if stages of development exist when a DYRK1A inhibitor could be used as a pharmacological intervention to produce long-lasting effects in patients. Otherwise, a DYRK1A inhibitor may be required as a chronic treatment. If this is the case the downstream targets and regulation pathways of DYRK1A need to be further characterised to assess the potential for toxicity. Thus there needs to be more investigation into the levels of DYRK1A present at different stages in the *in vivo* models used to assess the activity of DYRK1A inhibitors. High quality molecular probes, such as those described in this thesis, will help to delineate the role of DYRK1A in disease and will

ultimately determine whether the attenuation of DYRK1A will be suitable as a treatment for AD and Down's syndrome.

CHAPTER 11. Experimental

Computational Chemistry

Models were built using the latest version (2015 and 2016) of Molecular Operating Environment (MOE) software from the Chemical Computing Group (CCG). Files were downloaded as PDB files and energy minimisation performed using LigX or LigPrep function prior to calculation. Calculations involving Ligand-Protein Interactions and small molecules were completed using AMBER10:EHT force field.

Models were built using the latest version (Maestro 11) of Schrodinger software. Files were downloaded as PDB files and energy minimisation performed using Protein Preparation Wizard prior to calculation. Calculations involving Ligand-Protein Interactions and small molecules were completed using OPLS3 force field.

Models were built using the latest version (Spark™ and Flare™) of Cresset software. Files were downloaded as PDB files and energy minimisation performed using Protein Preparation Wizard prior to calculation. Calculations involving Ligand-Protein Interactions and small molecules were completed using XED force field.

Chemoinformatics was conducted with KNIME® 2.12. Community workflows were used and adapted that contained ChemAxon Infocom nodes and ChEMBL-EBI nodes.

Synthetic Organic Chemistry

All commercial reagents were purchased from Sigma-Aldrich, Alfa Aesar, Apollo Scientific, Fluorochem or Tokyo Chemical Industry and of the highest available purity. Unless otherwise stated, chemicals were used as supplied without further purification. Anhydrous solvents were purchased from Acros (AcroSeal™) or Sigma-Aldrich (SureSeal™) and were stored under nitrogen. Petrol ether refers to the fraction with a boiling point between 40 °C and 60 °C. Anhydrous solvents and reagents were used as purchased.

All reactions were conducted under an atmosphere of nitrogen unless otherwise stated. Reactions were magnetically stirred and monitored by LCMS or thin layer chromatography (TLC) using glass plates pre-coated with Merck silica gel 60 F254.

TLC was performed on glass plates pre-coated with Merck silica gel 60 F_{254}. Visualisation was achieved with U.V. florescence (254 nm) or by staining with a potassium permanganate dip or phosphomolybdic acid dip.

Flash column chromatography was carried out using commercial pre-packed columns from Biotage, Isco, Grace or filled with Merck silica gel 60 (40-63 µm) or C18 silica on an ISCO Combiflash Rf or a Biotage Isolera Prime.

All microwave reactions were conducted using a Biotage Initiator 8+ microwave reactor.

Melting point measurements are recorded on MPA100 OptiMelt apparatus.

HPLC data and purification was performed on an Agilent 1100 series HPLC spectrometer, using a Phenomenex Luna 10 µ C18 150 mm × 15 mm column, eluted using water and acetonitrile at 15 ml/min and detected at 254 nm. The gradient employed was:

Time (minutes)	% Water	% MeCN
0	95	5
20	0	100
24	0	100
25	95	5
27	95	5

Proton nuclear magnetic resonance spectra were recorded at 500 MHz on a Varian VNMRS 500 MHz spectrometer (at 30 ºC), using residual isotopic solvent ($CHCl_3$, δ_H = 7.27 ppm, DMSO δ_H = 2.50 ppm, MeOH δ_H = 3.31 ppm) as an internal reference. Chemical shifts are quoted on the δ scale in parts per million (ppm) relative to either TMS (δ 0.0), chloroform (δ 7.26), DMSO (δ 2.50) or acetone (δ 2.05) for 1H NMR, and either chloroform (δ 77.16), DMSO (δ 39.52) or acetone (δ 29.84).

Coupling constants (*J*) are recorded in Hertz (Hz), and resonances are characterised as singlet (s), doublet (d), doublet of doublets (dd), triplet (t), broad singlet (br. s), multiplet (m) and aromatic (Ar).

Carbon nuclear magnetic resonance spectra were recorded at 125 MHz on a Varian 500 MHz spectrometer and are proton decoupled, using residual isotopic solvent ($CHCl_3$, δ_C = 77.00 ppm, DMSO δ_C = 39.52 ppm, MeOH δ_C = 49.00 ppm) as an internal reference. Proton and carbon spectra assignments are supported by DEPT editing. Chemical shifts are quoted on the δ scale in ppm.

Specific Optical Rotations were measured using Schmidt and Haensch UniPol L polarimeter, in cells with a path length of 5 cm. The light source was maintained at 589 nm. The concentration

(*c*) is expressed in g/100 mL (equivalent to g/0.1 dm^3). Specific rotations are denoted $[\alpha]_D^T$ and are given in implied units of 10^{-1} deg cm^2 g^{-1} (T = ambient temperature in °C).

All reported yields refer to chromatographically and spectroscopically pure compounds, unless otherwise specified.

Infrared spectra were recorded on a Perkin Elmer FT-IR spectrometer as either an evaporated film or liquid film or as a solid. Absorption maxima are reported in wave numbers (cm^{-1}). Only significant absorptions are presented in the data, with key stretches identified in brackets.

LCMS data was recorded on a Waters 2695 HPLC using a Waters 2487 UV detector and a Thermo LCQ ESI-MS. Samples were eluted through a Phenomenex Lunar 3µ C18 50 mm × 4.6 mm column, using water and acetonitrile acidified by 0.1% formic acid at 1.5 ml/min and detected at 254 nm. The gradient employed was:

Method 1: 4 minute method

Time (minutes)	% Water + 0.1% formic acid	% MeCN + 0.1% formic acid
0.0	65	35
5.0	10	90
6.0	10	90
6.5	65	35

Method 2: 7 minute method

Time (minutes)	% Water + 0.1% formic acid	% MeCN + 0.1% formic acid
0.0	70	30
5.0	10	90
6.0	10	90
6.5	70	30
7.0	70	30

LCMS data was recorded on a Shimadzu Prominence Series coupled to a LCMS-2020 ESi and APCI mass spectrometer. Samples were eluted through a Phenomenex Gemini 5µ C18 110A 250 mm × 4.6 mm column, using water and acetonitrile acidified by 0.1% formic acid at 1 ml/min and detected at 254 nm. The gradient employed was:

Method 3: Analytical 5-95

Time (minutes)	% Water + 0.1% formic acid	% MeCN + 0.1% formic acid
0.0	95	5
1.0	95	5
21.0	5	95
25.0	5	95
30.0	70	30

Method 4: Analytical 30-90

Time (minutes)	% Water + 0.1% formic acid	% MeCN + 0.1% formic acid
0.0	70	30
1.0	70	30
21.0	10	90
25.0	10	90
30.0	70	30

Method 5: Analytical 5-95 (8 minute method)

Time (minutes)	% Water + 0.1% formic acid	% MeCN + 0.1% formic acid
0.0	95	5
6.0	95	5
7.0	5	95
7.5	5	95
8.0	70	30

LCMS purification by Mass Directed fraction collection was performed on a Shimadzu Prominence Series coupled to a LCMS-2020 ESI and APCI mass spectrometer using a Phenomenex Luna 10 µ C18 150 mm × 15 mm column, eluted using water and acetonitrile at 15 ml/min and detected at 254 nm.

Low resolution mass spectrometry data (EI) were recorded on Fission Instrument VG autospec at 70eV. High resolution mass spectrometry data (ESI) were recorded on Bruker Daltonics, Apex III, ESI source: Apollo ESI with methanol as spray solvent. Only molecular ions, fractions from molecular ions and other major peaks are reported as mass/charge (*m/z*) ratios..

4-Bromo-1-ethyl-3-methyl-pyrazole and 4-bromo-1-ethyl-5-methyl-pyrazole **23a and 23b**

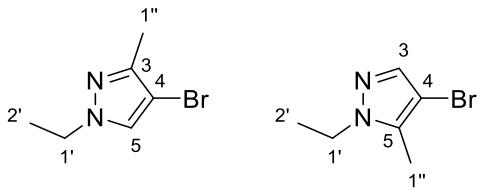

To a cooled solution of 4-bromo-3-methyl-1*H*-pyrazole (500 mg, 3.11 mmol) in DMF (5 mL) was added sodium hydride (143 mg, 3.73 mmol) and the reaction mixture stirred at 0 °C for 20 min. Iodoethane (0.37 mL, 4.66 mmol) was added slowly to the reaction mixture which was then allowed to warm to rt and was stirred overnight. The reaction mixture was quenched with water and then concentrated under reduced pressure. The residue was partitioned between EtOAc (20 mL) and water (20 mL) and extracted. The aqueous layer was further extracted with EtOAc (2 x 20 mL). The combined organics were washed with water (2 x 40 mL) followed by brine (40 mL). The organics were dried over $MgSO_4$, filtered and concentrated under reduced pressure to afford the title compound, as approximately a 1:1 mixture of 4-bromo-1-ethyl-3-methyl-pyrazole and 4-bromo-1-ethyl-5-methyl-pyrazole, **23a** and **23b**, as a colourless oil (160 mg, 0.42 mmol, 14%). R_f 0.60 (EtOAc/petroleum ether 1:9); ^{1}H NMR (500 MHz, $CDCl_3$) δ_H 7.39 (1H, s, H-5), 7.33 (1H, s, H-5), 4.14 – 4.04 (4H, m, H-1'), 2.26 (3H, s, H-1''), 2.23 (3H, s, H-1''), 1.44 (t, *J* = 7.2 Hz, 3H, H-2'), 1.39 (t, *J* = 7.8 Hz, 3H, H-2'); LCMS (LCQ): Rt = 2.85 min (Method 1); *m/z* (ESI^+) 189.1 $[M]^+$ and 191.1 $[M+2]^+$.

(*E*)-3-(1-Ethyl-3-methyl-pyrazol-4-yl)prop-2-enoic acid **24a**

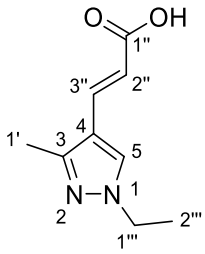

To a stirred suspension of 1-ethyl-3-methyl-*1H*-pyrazole-4-carbaldehyde (670 mg, 4.85 mmol) in pyridine (3.35 mL, 41.42 mmol) was added malonic acid (0.76 g, 7.27 mmol) followed by piperidine (0.67 mL, 6.78 mmol). The reaction mixture was stirred at 110 °C for 16 h. After cooling, water (5 mL) was added followed by ammonium hydroxide solution (2 mL, 28% w/w ammonia in water). The solution was acidified to pH 1 with 1 M hydrochloric acid and partitioned between CH_2Cl_2 (100 mL) and water (100 mL) and extracted. The aqueous layer was further extracted with CH_2Cl_2 (2 x 100 mL). The combined organics were washed with brine (20 mL), dried over $MgSO_4$, filtered and concentrated under reduced pressure to afford the title compound, (*E*)-3-(1-ethyl-3-methyl-pyrazol-4-yl)prop-2-enoic acid, **24a**, as an off-white solid (800 mg, 4.43 mmol, 91% yield). R_f 0.63 (EtOAc/petroleum ether 1:1); m.p. 158-160 °C; $\bar{\nu}_{max}$ (neat)/cm^{-1} 2974 (C-H, w), 2923 (C-H, w), 2492 (O-H, s, br), 1682 (C=O, s), 1646 (C=C, s), 1243 (C-O, s), 969 (*trans*-CH=CH-); ^{1}H NMR (500 MHz, DMSO-d$_6$) δ_H 11.99 (1H, s, COO*H*), 8.11 (1H, s, H-5), 7.39 (1H, d, *J*= 16.0 Hz, H-3''), 6.02 (1H, d, *J*= 16.0 Hz, H-2''), 4.02 (2H, q, *J*= 7.3 Hz, H-1'''), 2.21 (3H, s, H-1'), 1.32 (3H, t, *J* = 7.3 Hz, H-2'''); ^{13}C NMR (125 MHz, DMSO-d$_6$) δ_C 167.9 (C=O), 147.1 (C-2), 135.2 (C-3''), 130.3 (C-5), 117.2 (C-4), 114.9 (C-2''), 46.1 (C-1'''), 15.1 (C-2'''), 12.2 (C-1'); HRMS *m/z* (ESI) no ionisation observed with +ve or -ve ion mode LRMS only EI$^+$ 181 m/z; LCMS (LCQ): Rt = 0.8 min (Method 1); *m/z* (ESI$^+$) 181.2 [M+H]$^+$.

3-(1-Ethyl-3-methyl-1*H*-pyrazol-4-yl)propanoic acid **21**

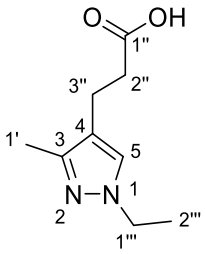

To a stirred solution of (*E*)-3-(1-ethyl-3-methyl-pyrazol-4-yl)prop-2-enoic acid (340 mg, 1.89 mmol) in EtOH (10 mL) was added palladium on carbon (wetted 10% with water) (60 mg, 0.63 mmol). The flask was evacuated and then back-filled three times with nitrogen gas before evacuating a final time and attaching a hydrogen balloon filled with hydrogen gas. A second balloon filled with hydrogen gas was added and the reaction mixture was stirred for 24 h at rt. The reaction mixture was filtered through celite with EtOH before being concentrated under reduced pressure to afford the title compound, 3-(1-ethyl-3-methyl-1*H*-pyrazol-4-yl)propanoic acid, **21**, as a cream solid (340 mg, 1.87 mmol, 99% yield). m.p. 86-87 °C; $\bar{\nu}_{max}$ (neat)/cm^{-1} 2974 (C-H, w), 2925(C-H, w), 2457 (O-H, s, br), 1677 (C=O, s), 1253 (C-O, s); ^{1}H NMR (500 MHz, DMSO-d$_6$) δ_H 7.35 (1H, s, H-5), 3.93 (2H, q, *J*= 7.3 Hz, H-1'''), 2.54 – 2.50 (2H, m, H-3''), 2.37 (2H, t, *J*= 7.6 Hz, H-2''), 2.04 (3H, s, H-1'), 1.27 (3H, t, *J*= 7.3 Hz, H-2'''); ^{13}C NMR (125 MHz, DMSO-d$_6$) δ_C 173.8 (C=O), 144.7 (C-3), 127.4 (C-5), 116.7 (C-4), 45.5 (C-1'''), 34.7 (C-2''), 18.8 (C-3''), 15.4 (C-2'''), 11.3 (C-1'); HRMS *m/z* (ESI$^+$) [Found: 183.1131., $C_9H_{14}N_2O_2$ requires [M+H]$^+$ 183.1128]; LCMS (LCQ): Rt = 0.8 min (Method 1); *m/z* (ESI$^+$) 183.1 [M+H]$^+$.

Methyl 3-(1-ethyl-3-methyl-pyrazol-4-yl)propanoate **26**

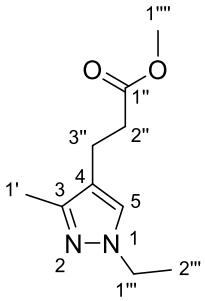

To a stirred suspension of 3-(1-ethyl-3-methyl-1*H*-pyrazol-4-yl)propanoic acid (200 mg, 1.1 mmol) in MeOH (10 mL) was added sulfuric acid (0.5 mL, 9.4 mmol). The reaction mixture was stirred at 70 °C for 4 h. After cooling, water (1 mL) was added, followed by careful addition of sodium hydroxide pellets. After neutralisation, the aqueous was partitioned between CH_2Cl_2 (100 mL) and water (100 mL) and was extracted. The aqueous layer was further extracted with CH_2Cl_2 (2 x 100 mL). The organic layer was washed with brine (100 mL), followed by saturated aqueous $NaHCO_3$ solution (100 mL). The combined organic components were dried over $MgSO_4$, filtered and concentrated under reduced pressure. The crude was purified by flash silica column chromatography on an Isco Combiflash system (12 g silica, elution with a 0-60% EtOAc / petroleum ether gradient) to afford the title compound, methyl 3-(1-ethyl-3-methyl-pyrazol-4-yl)propanoate, **26**, as a colourless oil (200 mg, 0.7 mmol, 67% yield). R_f 0.18 (EtOAc/petroleum ether 1:3); $\bar{\nu}_{max}$ (neat)/cm^{-1} 2992 (C-H, w), 2953 (C-H, w), 1734 (C=O, s), 1167 (C-O, s); ^{1}H NMR (500 MHz, $CDCl_3$) δ_H 7.13 (1H, s, H-5), 4.06 (2H, q, *J*= 7.3 Hz, H-1’’’), 3.67 (3H, s, H-1’’’’), 2.72 (2H, t, *J* = 7.7 Hz, H-3’’), 2.53 (2H, t, *J* = 7.9 Hz, H-2’’), 2.22 (3H, s, H-1’), 1.44 (3H, t, *J*= 7.3 Hz, H-2’’’); 13C NMR (125 MHz, $CDCl_3$) δ_C 173.4 (C=O), 146.2 (C-3), 127.1 (C-5), 117.1 (C-4), 51.5 (C-1’’’’), 46.5 (C-1’’’), 34.9 (C-2’’), 19.2 (C-3’’), 15.6 (C-2’’’), 11.6 (C-1’); HRMS *m/z* (ESI) no ionisation observed with +ve or -ve ion mode LRMS only EI$^+$ 197 m/z; LCMS (LCQ): Rt = 1.1 min (Method 1); *m/z* (ESI$^+$) 197.1 [M+H]$^+$.

3-(1-Ethyl-3-methyl-pyrazol-4-yl)propanamide **27**

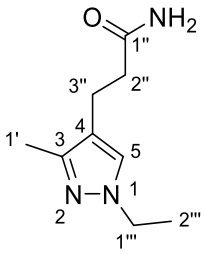

To 3-(1-ethyl-3-methyl-*1H*-pyrazol-4-yl)propanoic acid (30 mg, 0.13 mmol) was added ammonium hydroxide solution (2 mL, 28% w/w ammonia in water). The reaction mixture was stirred at rt for 4 days. The reaction mixture was concentrated under reduced pressure. The residue was partitioned between CH_2Cl_2 (20 mL) and water (20 mL), and extracted. The aqueous was further extracted with CH_2Cl_2 (2 x 20 mL). The organic layer was washed with water (1 x 20 mL) and brine (20 mL). The combined organic components were dried over $MgSO_4$, filtered and concentrated to dryness under reduced pressure to afford the title compound, 3-(1-ethyl-3-methyl-pyrazol-4-yl)propanamide, **27**, as an off-white solid (20 mg, 0.09 mmol, 74% yield). R_f 0.0 (EtOAc); m.p. 73-75 °C; $\bar{\nu}_{max}$ (neat)/cm^{-1} 3315 (N-H, m), 3246 (N-H, m), 2982 (C-H, w), 2962 (C-H, w) 1670 (C=O, s); ^{1}H NMR (500 MHz, DMSO-d$_6$) δ_H 7.30 (1H, s, H-5), 7.21 (1H, s, CONH), 6.68 (1H, s, CONH), 3.93 (2H, q, *J* = 7.2 Hz, H-1'''), 2.51 (2H, t, *J* = 7.7 Hz, H-3''), 2.21 (2H, t, *J* = 7.7 Hz, H-2''), 2.04 (3H, s, H-1'), 1.27 (3H, t, *J* = 7.2 Hz, H-2'''); ^{13}C NMR (125 MHz, DMSO-d$_6$) δ_C 173.6 (C=O), 144.7 (C-3), 127.3 (C-5), 117.4 (C-4), 45.5 (C-1'''), 35.9 (C-2''), 19.2 (C-3''), 15.4 (C-2'''), 11.4 (C-1');HRMS *m/z* (ESI$^+$) [Found: 182.1291., $C_9H_{15}N_3O$ requires $[M+H]^+$ 182.1288]; LCMS (LCQ): Rt = 2.2 min (Method 1); *m/z* (ESI$^+$) 182.1 $[M+H]^+$.

Methyl 2-(4-chlorophenoxy)acetate **32**

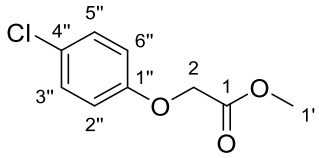

To a solution of 4-chlorophenol (1.0 g, 7.8 mmol) in DMF (10 mL) was added methyl bromoacetate (0.7 mL, 7.8 mmol) and potassium carbonate (1.6 g, 11.7 mmol). The reaction mixture was stirred at 85°C for 16 h. The reaction mixture was diluted with EtOAc (10 mL) and filtered through celite. The filtrate was concentrated under reduced pressure to afford a yellow oil. The yellow oil was purified by flash silica column chromatography on an Isco Combiflash system (12 g silica, elution with a 35-65% 10% acetone in petroleum ether / petroleum ether) to afford the title compound, methyl 2-(4-chlorophenoxy)acetate, **32**, as a colourless oil (1.4 g, 7.1 mmol, 91% yield). R_f 0.25 (acetone/petroleum ether: petroleum ether 1:50); ^{1}H NMR (500 MHz, DMSO-d_6) δ_H 7.35 – 7.28 (2H, app. m, H-3'' and 5''), 6.99 – 6.93 (2H, app. m, H-2''and 6''), 4.80 (2H, app. d, *J* = 2.4 Hz, H-2), 3.72 – 3.65 (3H, app. m, H-1'); LCMS (LCQ) no ionisation observed with +ve or -ve ion mode. The spectroscopic data are in good agreement with the literature values. Literature reference: WO2013/111798

2-(4-Chlorophenoxy)acetic acid **33**

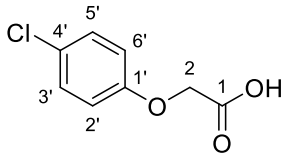

To a solution of methyl 2-(4-chlorophenoxy)acetate (1.17 g, 5.83 mmol) in MeOH (3 mL) was added potassium hydroxide (0.65 g, 11.66 mmol). The reaction mixture was stirred at 35°C for 2 h. The reaction was quenched by addition of water (10 mL). The reaction mixture was extracted with diethyl ether extraction (25 mL). The aqueous layer was acidified with 2 M hydrochloric acid. The resulting precipitate was filtered off and dried under vacuum to afford the title compound, 2-(4-chlorophenoxy)acetic acid, **33**, as a white crystalline solid (1.01 g, 5.44 mmol, 93% yield). R_f 0.65 (EtOAc/petroleum ether 1:1); ^{1}H NMR (500 MHz, DMSO-d_6) δ_H 13.00 (1H, s, COO*H*), 7.34 – 7.28 (2H, m, H-3' and 5'), 6.97 – 6.89 (2H, m, H-2' and 6'), 4.67 (2H, s, H-2); LCMS (LCQ) no ionisation observed with +ve or -ve ion mode. The spectroscopic data are in good agreement with the literature values. Literature reference: WO2013/111798

Ethyl 2-[[2-(4-chlorophenoxy)acetyl]amino]acetate **34**

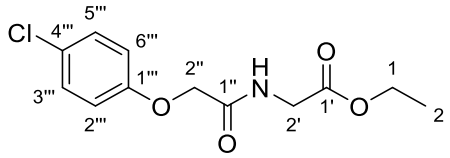

To a solution of 2-(4-chlorophenoxy)acetic acid (1.0 g, 5.4 mmol) in DMF (5 mL) was added 3-(ethyliminomethyleneammonio)propyl-dimethyl-ammonium chloride (1.9 g, 9.7 mmol), DIPEA (5.6 mL, 32.2 mmol), 1-hydroxybenzotriazole hydrate (1.2 g, 8.0 mmol) and glycine ethyl ester hydrochloride (0.8 g, 5.4 mmol). The reaction mixture was stirred at rt overnight. The reaction mixture was concentrated under reduced pressure to afford a yellow oil. The residue was taken up in EtOAc (50 ml) and the organics were washed with water (2 x 50 mL), brine (50 mL), followed by 1 M NaOH (2 x 50 mL). The combined organic components were dried over $MgSO_4$, filtered and concentrated to dryness under reduced pressure to afford the title compound, ethyl 2-[[2-(4-chlorophenoxy)acetyl]amino]acetate, **34**, as an off-white solid (0.7 g, 2.3 mmol, 43% yield). R_f 0.52 (EtOAc/petroleum ether 1:1); ^{1}H NMR (500 MHz, DMSO-d_6) δ_H 8.52 – 8.44 (1H, m, CONH), 7.37 – 7.32 (2H, m, H-3''' and 5'''), 7.02 – 6.95 (2H, m, H-2''' and 6'''), 4.54 (2H, s, H-2''), 4.09 (2H, q, *J* = 7.1, Hz, H-1), 3.88 (2H, d, *J* = 6.0 Hz, H-2'), 1.18 (3H, t, *J* = 7.1 Hz, H-2); LCMS (LCQ): Rt = 0.6 min (Method 1); *m/z* (ESI$^+$) 271.9 [M+H]$^+$; The spectroscopic data are in good agreement with the literature values. Literature Reference: Mahishi *et al*. Journal of the Indian Chemical Society, 1965, vol. 42, p. 67-71

2-[[2-(4-Chlorophenoxy)acetyl]amino]acetic acid **35**

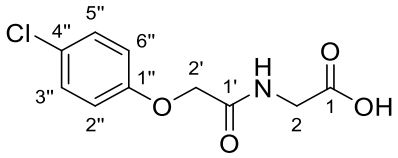

To a solution of ethyl 2-[[2-(4-chlorophenoxy)acetyl]amino]acetate (0.60 g, 2.21 mmol) in MeOH (1.5 mL) was added potassium hydroxide (0.25 g, 4.42 mmol) and the reaction was stirred at 35 °C for 2 h. The reaction was quenched by addition of water (10 mL). The reaction mixture was extracted with diethyl ether extraction (25 mL). The aqueous layer was acidified with 2 M hydrochloric acid. The resulting precipitate was filtered off and dried under vacuum. Trituration with EtOAc afforded the title compound 2-[[2-(4-chlorophenoxy)acetyl]amino]acetic acid, **35**, as an off-white solid (0.10 g, 0.62 mmol, 19% yield). R_f 0.25 (EtOAc/petroleum ether 1:1); ^{1}H NMR (500 MHz, DMSO-d_6) δ_H 8.42 – 8.31 (1H, m, CONH), 7.37 – 7.30 (2H, m, H-3'' and 5''), 7.03 – 6.96 (2H, m, H-2'' and 6''), 4.53 (2H, s, H-2'), 3.80 (2H, d, *J* = 5.9 Hz, H-2); LCMS (LCQ): Rt = 1.3 min (Method 1); *m/z* (ESI$^+$) 244.0 [M]$^+$ and 246.0 [M+2] $^+$; The spectroscopic data are in good agreement with the literature values. Literature reference: Irino *et al*. Chem Pharm Bull (Tokyo). 1972; 1, 47.

Tert-butyl *N*-[2-(2,6-difluoroanilino)-2-oxo-ethyl]carbamate **36a**

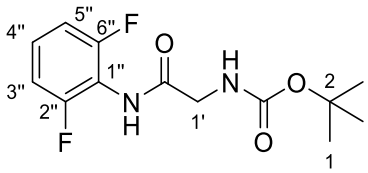

To a suspension of *N*-(*tert*-butoxycarbonyl)glycine (1.3 g, 7.4 mmol) in CH_2Cl_2 (10 mL) was added 1,1'-carbonyldiimidazole (1.4 g, 8.6 mmol). The reaction mixture was stirred at rt for 1 h. 2,6-difluoroaniline (0.8 mL, 7.4 mmol) was then added, and the reaction mixture was stirred overnight at rt. The reaction mixture was concentrated to dryness. The residue was taken up in EtOAc (100 mL) and was washed with water (2 x 100 mL), followed by brine (1x 100 mL), and saturated $NaHCO_3$ solution (2 x 100 mL). The organic components were dried over $MgSO_4$, filtered and concentrated to dryness under reduced pressure to afford a yellow oil. The oil was purified by flash silica column chromatography on an Isco Combiflash system (12 g silica, elution with a 25-65% acetone / petroleum ether gradient). Trituration with diethyl ether afforded the title compound, *tert*-butyl *N*-[2-(2,6-difluoroanilino)-2-oxo-ethyl]carbamate, **36a**, as a white solid (2.0 g, 6.8 mmol, 92% yield). R_f 0.61 (acetone/petroleum ether 4:6); m.p. 120-122 °C, $\bar{\nu}_{max}$ (neat)/cm^{-1} 3275 (N-H, m), 3238 (N-H, m), 2979 (C-H, w), 2939 (C-H, w), 1764 (C=O, -COO^{t}Bu, s), 1681 (C=O, -CONH, s); ^{1}H NMR (500 MHz DMSO-d$_6$) δ_H 9.61 (1H, s, CONH (amide)), 7.28-7.37 (1H, m, H-4''), 7.10-7.18 (2H, m, H-2'' and 5''), 7.06 (1H, br. s, CONH (carbamate)), 3.77 (2H, d, *J* = 6.2 Hz, H-1'), 1.38 (9H, s, H-1); ^{1}H NMR (600 MHz, $CDCl_3$) δ_H 8.07 (1H, s, CONH (amide)), 7.24 – 7.14 (1H, m, H-4''), 7.00 – 6.86 (2H, m, H-3'' and 5''), 5.45 – 5.30 (1H, m, br. s, CONH (carbamate)), 4.04 (2H, s, H-1'), 1.47 (9H, s, H-1); ^{13}C (125 MHz, $CDCl_3$) δ_C 168.5 (C=O (amide)), 157.9 (d, *J* = 251.5 Hz, C-2'' and 6''), 156.4 (C=O (carbamate)), 127.6 (C-4''), 113.5 (t, *J* = 15.7 Hz, C-1''), 111.6 (d, *J* = 23.3 Hz, C-3'' and 5''), 80.5 (C-2), 44.5 (C-1'), 28.2 (C-1); HRMS *m/z* (ESI$^+$) [Found: 309.1030, $C_{13}H_{16}F_2N_2NaO_3$ requires [M + Na]$^+$ 309.1021]; LCMS (LCQ): Rt = 0.5 min (Method 1); *m/z* (ESI$^+$) 287.2 [M+H]$^+$. The spectroscopic data are in good agreement with the literature values. Literature reference: WO2013/111798

Tert-butyl *N*-[2-oxo-2-(2,3,4-trifluoroanilino)ethyl]carbamate **36b**

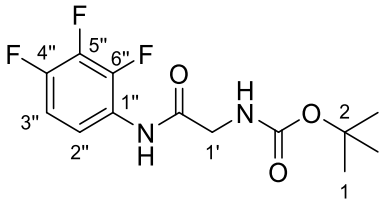

To a suspension of *N*-(*tert*-butoxycarbonyl)glycine (1.4 g, 11.4 mmol) in CH_2Cl_2 (10 mL) was added 1,1'-carbonyldiimidazole (1.4 g, 8.6 mmol). The reaction mixture was stirred at rt for 1 h. 2,3,4-trifluoroaniline (0.8 mL, 8.0 mmol) was added and the reaction was stirred overnight at rt. The reaction mixture was concentrated to dryness under reduced pressure. The residue was taken up in EtOAc (100 mL) and washed with water (2 x 100 mL), followed by brine (1x 100 mL), and saturated $NaHCO_3$ solution (2 x 100 mL). The organic components were dried over $MgSO_4$, filtered and concentrated to dryness under reduced pressure. Trituration with diethyl ether afforded the title compound, *tert*-butyl *N*-[2-oxo-2-(2,3,4-trifluoroanilino)ethyl]carbamate, **36b**, as a white solid (2.1 g, 6.9 mmol, 86% yield). R_f 0.71 (acetone/petroleum ether 2:3); m.p. 146-148 °C; $\bar{\nu}_{max}$ (neat)/cm^{-1} 3350 (N-H, m), 2995 (C-H, s), 1681 (C=O, -CONH, s); ^{1}H NMR (500 MHz, $CDCl_3$) δ_H 8.36 (1H,br. s, CONH (amide)), 8.04 – 7.96 (1H, m, H-2''), 7.01 – 6.90 (1H, m, H-3''), 5.16 (1H, br. s, CONH (carbamate)), 3.95 (2H, d, *J* = 6.1 Hz, H-1'), 1.50 (9H, s, H-1); ^{13}C NMR (150 MHz, $CDCl_3$) δ_C 168.1 (C=O (amide)), 156.4 (C=O (carbamate)), 148.4-146.6 (C-4''), 144.9-142.6 (C-6''), 138.8 (C-5''), 123.4 (C-1''), 115.7 (C-2''), 111.8 (C-3''), 81.7 (C-2), 45.9 (C-1'), 28.2 (C-1); HRMS *m/z* (ESI$^+$) [Found: 327.0934., $C_{13}H_{15}F_3N_2NaO_3$ requires [M + Na]$^+$ 327.0927]; LCMS (LCQ): Rt = 0.6 min (Method 1); *m/z* (ESI$^+$) 205.0 [M+H-Boc]$^+$.

Tert-butyl *N*-[2-(4-bromoanilino)-2-oxo-ethyl]carbamate **36c**

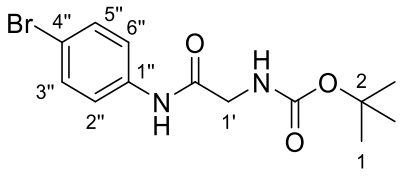

To a suspension of *N*-(*tert*-butoxycarbonyl)glycine (2.0 g, 11.4 mmol) in CH_2Cl_2 (10 mL) was sequentially added propylphosphonic anhydride solution, ≥50 wt. % in EtOAc (6.8 mL, 22.8 mmol), *N*,*N*-diethylethanamine (6.4 mL, 45.7 mmol) and 4-bromoaniline (4.9 mL, 34.3 mmol). The reaction mixture was stirred at rt for 3 h. The reaction mixture was concentrated to dryness. The residue was taken up in EtOAc (100 mL) and was washed with water (2 x 100 mL) followed by brine (1x 100 mL). The organic components were dried over $MgSO_4$, filtered and concentrated to dryness to afford a white solid. Trituration with diethyl ether afforded the title compound, *tert*-butyl *N*-[2-(4-bromoanilino)-2-oxo-ethyl]carbamate, **36c**, as a white solid (3.6 g, 10.8 mmol, 94% yield). m.p. 189-192 °C; $\bar{\nu}_{max}$ (neat)/cm^{-1} 3369 (N-H, m), 2989 (C-H, s) 1677 (-CO-NH, s); ^{1}H NMR (500 MHz, $CDCl_3$) δ_H 8.18 (1H, s, CONH (amide)), 748-7.38 (4H, m, H-2'', 3'', 5'', 6''), 5.18 (1H, br. s, CONH (carbamate)), 3.91 (2H, d, *J* = 6.1 Hz, H-1'), 1.49 (9H, s, H-1); HRMS *m/z* (ESI$^+$) [Found: 351.0326, $C_{13}H_{17}BrN_2NaO_3$ requires [M + Na]$^+$ 351.0315]; LCMS (LCQ): Rt = 2.2 min (Method 1); *m/z* (ESI$^+$) 228.9 [M-Boc]$^+$ and 231.0 [(M+2)-Boc]$^+$; The spectroscopic data are in good agreement with the literature values. Literature reference: WO2013/111798

General Procedure 1: Synthesis of 2-amino-*N*-phenylacetamide hydrochloride salts

4 M HCl in dioxane (20 mL) was added to *tert*-butyl *N*-[2-oxo-2-(anilino)ethyl]carbamate (3 mmol) and the reaction was stirred at rt for 5 h. The solvent was removed under reduced pressure to afford the title 2-amino-*N*-phenylacetamide hydrochloride.

2-Amino-*N*-(2,6-difluorophenyl)acetamide hydrochloride **37a**

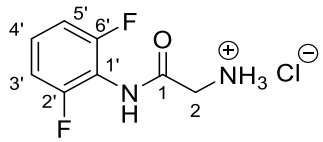

Following general procedure **1**, reaction of *tert*-butyl *N*-[2-(2,6-difluoroanilino)-2-oxo-ethyl]carbamate (0.87 g, 3.0 mmol) afforded the title compound, 2-amino-*N*-(2,6-difluorophenyl)acetamide hydrochloride, **37a**, as a white solid (0.67 g, 3.0 mmol, 99% yield). R_f 0.1 (acetone/petroleum ether 4:6); Decomposes 192-213 °C; $\bar{\nu}_{max}$ (neat)/cm^{-1} 3367 (N-H, m), 3125 (N-H, m), 2914 (C-H, s), 1687 (C=O, s); ^{1}H NMR (500 MHz, DMSO-d$_6$) δ_H 10.26 (1H, s, CONH), 8.15 (3H, s, NH), 7.42-7.34 (1H, m, H-4'), 7.25-7.13 (2H, m, H-3' and 5'), 3.87 (2H, d, *J* = 5.7 Hz, 2-CH); ^{13}C NMR (150 MHz, DMSO-d$_6$) δ_C 165.3, 157.5 (dd, *J* = 249.2, 5.2 Hz, C-2' and 6'), 128.4 (t, *J* = 9.8 Hz, C-4'), 113.4 (t, *J* = 17.0 Hz, C-1'), 112.0 (dd, *J* = 19.6, 4.0 Hz, C-3' and 5'), 40.3 (C-2); HRMS *m/z* (ESI$^+$) [Found: 187.0679., $C_8H_8F_2N_2O$ requires [M + H]$^+$ 187.0677]; LCMS (LCQ): Rt = 0.7 min (Method 1); *m/z* (ESI$^+$) 187.0 [M+H]$^+$; The spectroscopic data are in good agreement with the literature values. Literature reference: WO2013/111798.

2-Amino-*N*-(2,6-difluorophenyl)acetamide hydrochloride **37b**

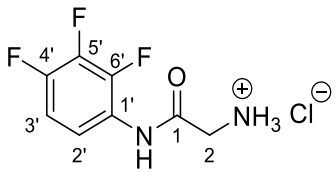

Following general procedure **1**, tert-butyl *N*-[2-oxo-2-(2,3,4-trifluoroanilino)ethyl]carbamate (1.0 g, 3.29 mmol) afforded the title compound, 2-amino-*N*-(2,6-difluorophenyl)acetamide hydrochloride **37b**, as a white solid (0.73 g, 3.03 mmol, 92% yield). R_f 0.1 (acetone/petroleum ether 4:6); Decomposes > 245 °C; $\bar{\nu}_{max}$ (neat)/cm^{-1} 3287 (N-H, m), 2948 (C-H, s), 2891 (C-H, s), 1692 (C=O, s); ^{1}H NMR (500 MHz, DMSO-d$_6$) δ_H 10.51 (1H, s, CONH); 8.17 (3H, s, NH), 7.69-7.54 (1H, m, 2'-H), 7.41-7.27 (1H, m, 3'-H), 3.85 (2H, s, 2-H); ^{13}C NMR (150 MHz, DMSO-d$_6$) δ_C 165.6 (C=O, C-1), 147.21 (dd, *J* = 245.0, 10.1 Hz), 143.41 (dd, *J* = 249.3, 11.0 Hz, C-6'), 140.3-138.2 (m, C-5'), 123.05 (dd, *J* = 9.4, 3.4 Hz, C-1'), 118.89 – 118.52 (m, C-2'), 112.0 (dd, J = 17.9, 3.7 Hz, C-3'), 40.7 (C-2); HRMS *m/z* (ESI$^+$) [Found: 205.0585., $C_8H_8F_3N_2O$ requires [M + H]$^+$ 205.0583]; LCMS (LCQ): Rt = 0.4 min (Method 1); *m/z* (ESI$^+$) 205.0 [M+H]$^+$.

2-Amino-*N*-(4-bromophenyl)acetamide hydrochloride **37c**

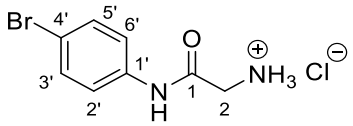

Following general procedure **1**, *tert*-butyl *N*-[2-(4-bromoanilino)-2-oxo-ethyl]carbamate (3.5 g, 10.6 mmol) afforded the title compound, 2-amino-*N*-(4-bromophenyl)acetamide hydrochloride, **37c**, as a white solid (2.8 g, 10.5 mmol, 99% yield). Decomposes at > 210 °C; $\bar{\nu}_{max}$ (neat)/cm^{-1} 3280 (N-H, m), 2963 (C-H, s), 1669 (C=O, s); ^{1}H NMR (500 MHz, DMSO-d$_6$) δ_H 10.70 (1H, s, CONH); 8.15 (3H, s, NH), 7.60-7.51 (4H, m, H-3', 2', 5' 6'), 3.77 (2H, s, H-2); ^{13}C NMR (150 MHz, DMSO-d$_6$) δ_C 165.0 (C=O, C-1), 137.8 (C-1'), 131.7 (C-3' and 5'), 121.0 (C-2' and 6'), 115.4 (C-4'), 41.0 (C-2); HRMS *m/z* (ESI$^+$) [Found: 230.9954., $C_8H_9BrN_2O$ requires [M + 2]$^+$ 230.9971]; LCMS (LCQ): Rt = 0.5 min (Method 1); *m/z* (ESI$^+$) 228.9 [M]$^+$ and 230.9 [M+2]$^+$; The spectroscopic data are in good agreement with the literature values. Literature reference: WO2013/111798

General Procedure 2: Synthesis of Substituted Acetamides

To a stirred solution of 4-halophenoxyacetic acid (1 eq.) in THF (2 mL) was sequentially added [2-(anilino)-2-oxo-ethyl]ammonium chloride (3 eq.), propylphosphonic anhydride solution, ≥50 wt. % in EtOAc (2 eq.) and TEA (4 eq.). The reaction mixture was stirred at rt for 2-3 h.

The reaction mixture was concentrated to dryness under reduced pressure. The residue was taken up in EtOAc (50 mL) and washed with water (2 x 50 mL) followed by saturated $NaHCO_3$ solution (50 mL). The organic components were dried over $MgSO_4$, filtered and concentrated to dryness under reduced pressure. Trituration with diethyl ether afforded the title acetamide as a white solid.

2-[[2-(4-Chlorophenoxy)acetyl]amino]-*N*-(2,3,4-trifluorophenyl)acetamide **28**

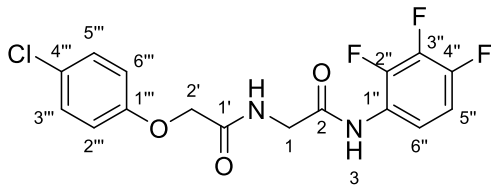

To a stirred solution of 2-[[2-(4-chlorophenoxy)acetyl]amino]acetic acid (100 mg, 0.12 mmol) in THF (2 mL) was added 2,3,4-trifluoroaniline (0.04 mL, 0.37 mmol), propylphosphonic anhydride solution, ≥50 wt. % in EtOAc (0.11 mL, 0.25 mmol) and TEA (0.05 mL, 0.37 mmol). The reaction mixture was stirred at rt for 3 h. The reaction mixture was concentrated under reduced pressure. The residue was taken up in EtOAc (50 mL) and the organic layer was washed with water (2 x 50 mL), followed by 1 M hydrochloric acid (2 x 50 mL). The organic components were dried over $MgSO_4$, filtered and concentrated to dryness under reduced pressure. The crude was purified by flash silica column chromatography on an Isco Combiflash system (12 g silica, elution with a 20-60% acetone / petroleum ether gradient) to afford the title compound, 2-[[2-(4-chlorophenoxy)acetyl]amino]-*N*-(2,3,4-trifluorophenyl)acetamide, **28**, as an off-white solid (40 mg, 0.11 mmol, 87% yield). R_f 0.16 (acetone/petroleum ether 1:3); m.p. 189-192 °C; $\bar{\nu}_{max}$ (neat)/cm^{-1} 3410 (N-H, m), 3278 (N-H, m), 1658 (C=O, s), 1626 (C=O, s); ^{1}H NMR (500 MHz, DMSO-d$_6$) δ_H 9.98 (1H, s, CONH-3), 8.42 (1H, s, CONH), 7.61-7.53 (1H, m, H-6''), 7.35 (2H, d, *J* = 8.9 Hz, H-3''' and 5'''), 7.32-7.25 (1H, m, H-5''), 7.01 (2H, d, *J* = 8.9 Hz, H-2''' and H-6'''), 4.56 (2H, s, H-2'), 4.01 (2H, d, *J* = 5.7 Hz, H-1); ^{13}C NMR (125 MHz, DMSO-d$_6$) δ_C 168.5 (C=O, C-1'), 168.4 (C=O, C-2), 157.1 (C-1'''), 148.3-146.1 (m, C-4''), 144.9-142.8 (m, C-2''), 140.9-138.4 (m, C-3''), 129.7 (C-3''' and C-5'''), 125.5 (C-4'''), 124.4 (C-1''), 119.4 (C-6''), 117.1 (C-2''' and C-6'''), 112.2 (dd, *J* = 17.5, 3.6 Hz, C-5''), 67.6 (C-2'), 42.5 (C-1); HRMS *m/z* (ESI$^+$) [Found: 395.0384., $C_{16}H_{12}ClF_3N_2NaO_3$ requires [M + Na]$^+$ 395.0381]; LCMS (MDAP): Rt = 19.2 min, >95% (Method 3); *m/z* (ESI$^+$) 373.1 [M+H]$^+$; The spectroscopic data are in good agreement with the literature values. Literature reference: H. Mori , R. Wada, J. Li, T. Ishimoto, M. Mizuguchi, T. Obita, H. Gouda, S. Hirono, N. Toyooka. *Bioorg. Med. Chem. Lett*., 2014, **24**, 3732.

2-[[2-(4-Bromophenoxy)acetyl]amino]-*N*-(2,6-difluorophenyl)acetamide **29**

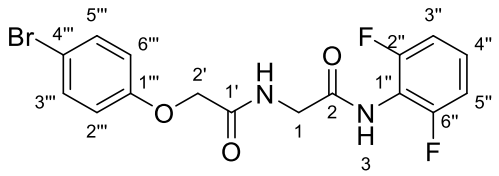

Following general procedure **2** with 4-bromophenoxyacetic acid (100 mg, 0.4 mmol) and [2-(2,6-difluoroanilino)-2-oxo-ethyl] ammonium chloride (300 mg, 1.3 mmol) afforded the title compound, 2-[[2-(4-bromophenoxy)acetyl]amino]-*N*-(2,6-difluorophenyl)acetamide, **29**, as a white solid (100 mg, 0.3 mmol, 78% yield). R_f 0.58 (acetone/petroleum ether 4:6); m.p. 177-179 °C; $\bar{\nu}_{max}$ (neat)/cm^{-1} 3262 (N-H, m), 1686 (C=O, s), 1658 (C=O, s); ^{1}H NMR (500 MHz, DMSO-d$_6$) δ_H 9.71 (1H, s, CONH-3), 8.46 (1H, s, CONH), 7.46 (2H, d, *J* = 9.0 Hz, H-3''' and 5'''), 7.39-7.30 (1H, m, H-4''), 7.19-7.11 (2H, m, H-3'' and 5''), 6.96 (2H, d, *J* = 9.0 Hz, H-2''' and 6'''), 4.56 (2H, s, H-2'), 4.00 (2H, d, *J* = 5.9 Hz, H-1'); ^{13}C NMR (150 MHz, DMSO-d$_6$) δ_C 167.9 (C=O, C-1'), 167.8 (C=O, C-2), 157.69 (dd, *J* = 248.9, 5.2 Hz, C-2'' and 6''), 157.0 (C-1'''), 132.1 (C-3''' and 5'''), 128.0 (t, *J* = 9.6 Hz, C-4''), 117.1 (C-2''' and 6'''), 114.7 (t, *J* = 16.8 Hz, C-1''), 112.6 (C-4'''), 111.8 (dd, *J* = 19.5, 4.2 Hz, C-3'' and 5''), 67.0 (C-2'), 41.5 (C-1); HRMS *m/z* (ESI$^+$) [Found: 420.9983., $C_{16}H_{13}BrF_2N_2NaO_3$ requires [M + Na]$^+$ 420.9970]; LCMS (LCQ): Rt = 0.5 min (Method 1); *m/z* (ESI$^+$) 398.7 [M]$^+$ and 400.7 [M+2]$^+$; LCMS (MDAP): Rt = 18.11 min, >95% (Method 3); *m/z* (ESI$^+$) 399.0 [M]$^+$, 401.0 [M+2]$^+$. The spectroscopic data are in good agreement with the literature values. Literature reference: WO2013/111798

N-(4-Bromophenyl)-2-[[2-(4-fluorophenoxy)acetyl]amino]acetamide **30**

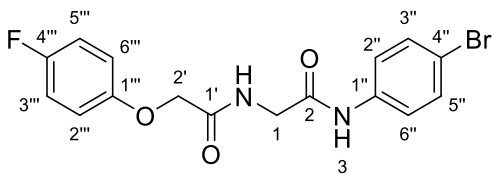

Following general procedure **2** with 4-fluorophenoxyacetic acid (50 mg, 0.29 mmol) and [2-(4-bromoanilino)-2-oxo-ethyl]ammonium chloride (160 mg, 0.59 mmol) afforded the title compound, *N*-(4-bromophenyl)-2-[[2-(4-fluorophenoxy)acetyl]amino]acetamide, **30**, as a white solid (100 mg, 0.26 mmol, 87% yield). R_f 0.25 (acetone/petroleum ether 3:7); m.p. 193-195 °C; $\bar{\nu}_{max}$ (neat)/cm^{-1} 3309 (N-H, m), 3262 (N-H, m), 2921 (C-H, s), 1686 (C=O, s), 1656 (C=O, s); ^{1}H NMR (500 MHz, DMSO-d$_6$) δ_H 10.11 (1H, s, CONH-3), 8.37 (1H, s, CONH), 7.55 (2H, d, *J* = 8.8 Hz, H-3'' and 5''), 7.49 (2H, d, *J* = 8.8 Hz, H-2'' and 6''), 7.17-7.09 (2H, m, H-3''' and 5'''), 7.04-6.98 (2H, m, H-2''' and 6'''), 4.53 (2H, s, H-2'), 3.95 (2H, d, *J* = 5.9 Hz, H-1); ^{13}C NMR (150 MHz, DMSO-d$_6$) δ_C 168.1 (C=O, C-1'), 167.6 (C=O, C-2), 157.9 (d, *J* = 236.5 Hz, C-4'''), 154.5 (d, *J* = 2.1 Hz, C-1'''), 138.2 (C-1''), 131.6 (C-3'' and 5''), 121.1 (C-2'' and 6''), 116.1 (d, *J* = 8.1 Hz, C-2''' and 6'''), 115.8 (d, *J* = 23.1 Hz, C-3''' and 6'''), 114.8 (C-4''), 67.4 (C-2'), 42.4 (C-1); HRMS *m/z* (ESI$^+$) [Found: 405.0056., $C_{16}H_{14}BrFN_2NaO_3$ requires [M + Na]$^+$ 403.0064]; LCMS (LCQ): Rt = 0.6 min (Method 1); *m/z* (ESI$^+$) 380.8 [M]$^+$ and 382.9 [M+2]$^+$; LCMS (MDAP): Rt = 19.0 min, >95% (Method 3); *m/z* (ESI$^+$) 381.1 [M]$^+$, 383.0 [M+2]$^+$. The spectroscopic data are in good agreement with the literature values. Literature reference: WO2013/111798

2-[[2-(4-Bromophenoxy)acetyl]amino]-*N*-(2,3,4-trifluorophenyl)acetamide **38**

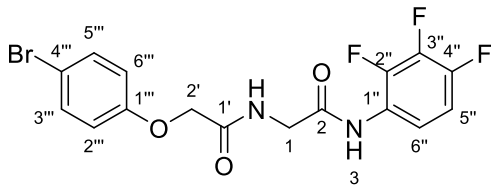

Following general procedure **2** with 4-bromophenoxyacetic acid (100 mg, 0.43 mmol) and [2-oxo-2-(2,3,4-trifluoroanilino)ethyl]ammonium chloride (310 mg, 1.30 mmol) afforded the title compound, 2-[[2-(4-bromophenoxy)acetyl]amino]-*N*-(2,3,4-trifluorophenyl)acetamide, **38**, as a white solid (140 mg, 0.34 mmol, 78% yield). R_f 0.70 (acetone/petroleum ether 4:6); m.p. 203-204 °C; $\bar{\nu}_{max}$ (neat)/cm^{-1} 3257 (N-H, m), 2934 (C-H, s), 1687 (C=O, s), 1656 (C=O, s); ^{1}H NMR (500 MHz, DMSO-d$_6$) δ_H 9.98 (1H, s, CONH-3), 8.42 (1H, s, CONH), 7.62-7.52 (1H, m, H-6''), 7.47 (2H, d, *J* = 9.0 Hz, H-3''' and 5'''), 7.33-7.24 (1H, m, H-5''), 6.96 (2H, d, *J* = 8.9 Hz, H-2''' and H-6'''), 4.56 (2H, s, H-2'), 4.01 (2H, d, *J* = 5.7 Hz, H-1); ^{13}C NMR (125 MHz, DMSO-d$_6$) δ_C 168.1 (C=O, C-1'), 168.0 (C=O, C-2), 157.0 (C-1'''), 147.9-145.9 (m, C-4''), 144.3-142.2 (m, C-2''), 140.2-138.1 (m, C-3''), 132. 1 (C-3''' and C-5'''), 123.7 (dd, *J* = 9.3, 3.4 Hz, C-1''), 119.13 – 118.45 (m, C-6''), 117.1 (C-2''' and 6'''), 112.7 (C-4'''), 111.8 (dd, *J* = 17.7, 3.7 Hz, C-5''), 67.0 (C-2'), 42.0 (C-1); HRMS *m/z* (ESI$^+$) [Found: 438.9894., $C_{16}H_{12}BrF_3N_2Na_1O_3$ requires [M + Na]$^+$ 438.9876]; LCMS (MDAP): Rt = 19.4 min, >95% (Method 3); *m/z* (ESI$^+$) 439.0 [M + Na]$^+$.

2-[[2-(4-Fluorophenoxy)acetyl]amino]-*N*-(2,3,4-trifluorophenyl)acetamide **39**

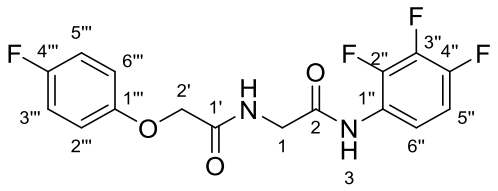

Following general procedure **2** with 4-fluorophenoxyacetic acid (100 mg, 0.59 mmol) and [2-oxo-2-(2,3,4-trifluoroanilino)ethyl]ammonium chloride (280 mg, 1.18 mmol) afforded the title compound, 2-[[2-(4-fluorophenoxy)acetyl]amino]-*N*-(2,3,4-trifluorophenyl)acetamide, **39**, as a white solid (190 mg, 0.52 mmol, 88% yield). R_f 0.30 (acetone/petroleum ether 3.5:6.5); m.p. 205-207 °C; $\bar{\nu}_{max}$ (neat)/cm^{-1} 3413 (N-H, m), 3241 (N-H, m), 1707.4 (C=O, s), 1658 (C=O, s), 1625 (N-H, m); ^{1}H NMR (500 MHz, DMSO-d$_6$) δ_H 9.99 (1H, s, CONH-3), 8.40 (1H, s, CONH), 7.61-7.52 (1H, m, H-6''), 7.33-7.24 (1H, m, H-5''), 7.16-7.09 (2H, m, H-2''' and 6'''), 7.04-6.95 (2H, m, H-3''' and 5'''), 4.53 (2H, s, H-2'), 4.02 (2H, d, *J* = 4.5 Hz, H-1); ^{13}C NMR (150 MHz, DMSO-d$_6$) δ_C 168.2 (C=O, C-1'), 168.1 (C=O, C-2), 156.9 (d, *J* = 236.4 Hz, C-4'''), 154.1 (d, *J* = 1.4 Hz, C-1'''), 148.3 – 145.5(m, C-4''), 144.4 – 142.2 (m, C-2''), 140.3 – 138.1 (m, C-3''), 124.7 (dd, *J* = 9.7 Hz, 2.8 Hz, C-1''), 119.0 – 118.6 (m, C-6''), 116.1 (d, *J* = 8.2 Hz, C-2''' and 6'''), 115.8 (d, *J* = 23.0 Hz, C-3'' and 5''), 111.8 (dd, *J* = 17.6, 3.7 Hz, C-5''), 67.4 (C-2'), 42.0 (C-1); HRMS *m/z* (ESI$^+$) [Found: 379.0689., $C_{16}H_{12}F_4N_2NaO_3$ requires [M + Na]$^+$ 379.0676]; LCMS (LCQ): Rt = 2.0 min (Method 1); *m/z* (ESI$^+$) 356.9 [M+H]$^+$; LCMS (MDAP): Rt = 18.2 min, >95% (Method 3); *m/z* (ESI$^+$) 379.0 [M+Na]$^+$;

2-[[2-(4-Chlorophenoxy)acetyl]amino]-*N*-(2,6-difluorophenyl)acetamide **40**

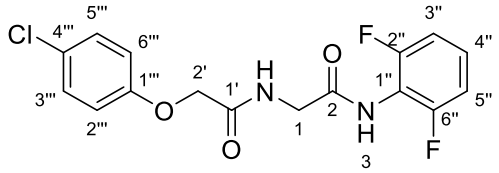

Following general procedure **2** with 4-chlorophenoxyacetic acid (70 mg, 0.38 mmol) and [2-(2,6-difluoroanilino)-2-oxo-ethyl] ammonium chloride (250 mg, 1.13 mmol) afforded the title compound, 2-[[2-(4-chlorophenoxy)acetyl]amino]-*N*-(2,6-difluorophenyl)acetamide, **40**, as a white solid (130 mg, 0.37 mmol, 99% yield). R_f 0.58 (acetone/petroleum ether 4:6); m.p. 182-184 °C; $\bar{\nu}_{max}$ (neat)/cm^{-1} 3262 (N-H, m), 2935 (C-H, s), 1687 (C=O, s), 1656 (C=O, s); ^{1}H NMR (500 MHz, DMSO-d$_6$) δ_H 9.71 (1H, s, CONH-3), 8.45 (1H, br. s, CONH), 7.40-7.31 (3H, m, H-3’’’, 5’’’ and 4’’), 7.19-7.12 (2H, m, H-3’’ and 5’’), 7.01 (2H, d, *J* = 8.7 Hz, H-2’’’ and 6’’’), 4.56 (2H, s, H-2’), 4.01 (2H, d, *J* = 5.7 Hz, H-1); ^{13}C NMR (150 MHz, DMSO-d$_6$) δ_C 167.9 (C=O, C-1’), 167.8 (C=O, C-2), 157.7 (d, *J* = 248.9 Hz, Hz, C-2’’ and 6’’), 156.6 (C-1’’’), 129.2 (C-3’’’ and 5’’’), 128.0 (C-4’’), 124.9 (C-4’’’), 116.6 (C-2’’’ and 6’’’), 114.2 (C-1’’), 111.98 – 111.63 (m, C-3’’ and 5’’), 67.1 (C-2’), 41.5 (C-1); HRMS *m/z* (ESI$^+$) [Found: 377.0485., $C_{16}H_{13}ClF_2N_2NaO_3$ requires [M + Na]$^+$ 377.0475]; LCMS (LCQ): Rt = 0.5 min (Method 1); *m/z* (ESI$^+$) 354.8 [M+H]$^+$; LCMS (MDAP): Rt = 17.8 min, >95% (Method 3); *m/z* (ESI$^+$) 355.1 [M+H]$^+$.

N-(2,6-Difluorophenyl)-2-[[2-(4-fluorophenoxy)acetyl]amino]acetamide **41**

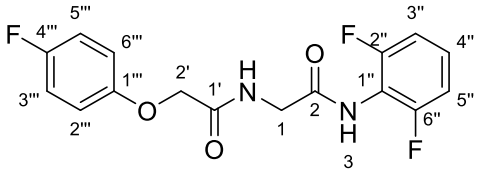

Following general procedure **2** with 4-fluorophenoxyacetic acid (50 mg, 0.29 mmol) and [2-(2,6-difluoroanilino)-2-oxo-ethyl] ammonium chloride (130 mg, 0.59 mmol) afforded the title compound, *N*-(2,6-difluorophenyl)-2-[[2-(4-fluorophenoxy)acetyl]amino]acetamide, **41**, as a white solid (80 mg, 0.24 mmol, 99% yield). R_f 0.50 (acetone/petroleum ether 4:6); m.p. 189-191 °C; $\bar{\nu}_{max}$ (neat)/cm^{-1} 3256 (N-H, m), 2934 (C-H, s), 1687 (C=O, s), 1656 (C=O, s); ^{1}H NMR (500 MHz, DMSO-d$_6$) δ_H 9.72 (1H, s, CONH-3), 8.42 (1H, br. s, CONH), 7.39-7.30 (1H, m, H-4''), 7.18-7.09 (4H, m, H-2''', 6''', 3'' and 5''), 7.03-6.97 (2H, m, H-3''' and H-5'''), 4.53 (2H, s, H-2'), 4.01 (2H, d, *J* = 5.7 Hz, H-1); ^{13}C NMR (150 MHz, DMSO-d$_6$) δ_C 168.6 (C=O, C-1'), 168.3 (C=O, C-2), 158.1 (d, *J* = 248.8, 5.1 Hz, C-2'' and C-6''), 157.3 (d, *J* = 236.4 Hz, C-4'''), 154.6 (d, *J* = 2.3 Hz, C-1''''), 128.5 (t, *J* = 9.5 Hz, C-4''), 116.6 (d, *J* = 8.1 Hz, C-2''' and 6'''), 116.3 (d, *J* = 23.0 Hz, C-3''' and 5'''), 114.6 (t, *J* = 16.9 Hz, C-1''), 112.3 (dd, *J* = 19.5, 4.1 Hz, C-3'' and 5''), 67.9 (s, C-2'), 42.0 (s, C-1); HRMS *m/z* (ESI$^+$) [Found: 361.0782., $C_{16}H_{13}F_3N_2NaO_3$ requires [M + Na]$^+$ 361.0770]; LCMS (LCQ): Rt = 0.5 min (Method 1); *m/z* (ESI$^+$) 338.8 [M+H]$^+$; LCMS (MDAP): Rt = 16.8 min, >95% (Method 3); *m/z* (ESI$^+$) 339.1 [M+H]$^+$, 361.1 [M+Na]$^+$. The spectroscopic data are in good agreement with the literature values. Literature reference: WO2013/111798

N-(4-Bromophenyl)-2-[[2-(4-chlorophenoxy)acetyl]amino]acetamide **42**

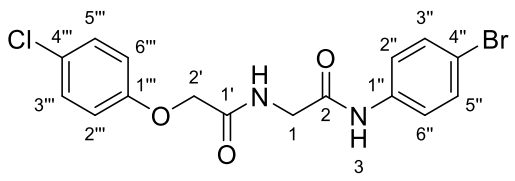

Following general procedure **2** with 4-chlorophenoxyacetic acid (550 mg, 0.29 mmol) and [2-(4-bromoanilino)-2-oxo-ethyl]ammonium chloride (160 mg, 0.59 mmol) afforded the title compound, **42**, as a white solid (110 mg, 0.59 mmol, 90% yield). R_f 0.43 (acetone/petroleum ether 4:6); m.p. 208-210 °C; $\bar{\nu}_{max}$ (neat)/cm^{-1} 3253 (N-H, m), 2939 (C-H, s), 1656 (C=O, s); ^{1}H NMR (500 MHz, DMSO-d$_6$) δ_H 10.10 (1H, s, CONH-3), 8.39 (1H, s, CONH), 7.55 (2H, d, *J* = 8.7 Hz, H-3'' and 5''), 7.48 (2H, d, *J* = 8.7 Hz, H-2'' and 6''), 7.35 (2H, d, *J* = 8.5 Hz, H-3''' and 5'''), 7.01 (2H, d, *J* = 9.0 Hz, H-2''' and 6'''), 4.56 (2H, s, H-2'), 3.95 (2H, d, *J* = 5.9 Hz, H-1); ^{13}C NMR (150 MHz, DMSO-d$_6$) δ_C 167.9 (C=O, C-1'), 167.5 (C=O, C-2), 156.5 (C-1'''), 138.2 (C-1''), 131.6 (C-3'' and 5''), 129.2 (C-3''' and 5'''), 124.9 (C-4'''), 121.1 (C-2'' and C-6''), 116.6 (C-4''), 114.8 (C-2''' and C-6'''), 67.1 (C-2'), 42.3 (C-1); HRMS *m/z* (ESI) no ionisation observed with +ve or -ve ion mode. LRMS only EI$^+$ 396 [M]$^+$ and 398 [M+2]$^+$ m/z; LCMS (LCQ): Rt = 0.6 min (Method 1); *m/z* (ESI$^+$) 396.8 [M]$^+$ and 398.8 [M+2]$^+$; LCMS (MDAP): Rt = 20.0 min, >95% (Method 3); *m/z* (ESI$^+$) 421 [M + Na]$^+$.

2-[[2-(4-Bromophenoxy)acetyl]amino]-*N*-(4-bromophenyl)acetamide **43**

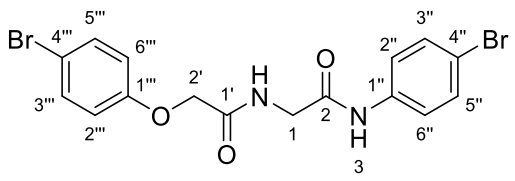

Following general procedure **2** with 4-bromophenoxyacetic acid (680 mg, 0.29 mmol) and [2-(4-bromoanilino)-2-oxo-ethyl]ammonium chloride (160 mg, 0.59 mmol) afforded the title compound, 2-[[2-(4-bromophenoxy)acetyl]amino]-*N*-(4-bromophenyl)acetamide, **43**, as a white solid (120 mg, 0.26 mmol, 89% yield). R_f 0.50 (acetone/petroleum ether 4:6); m.p. 220-222 °C; $\bar{\nu}_{max}$ (neat)/cm^{-1} 3253 (N-H, m), 2937 (C-H, s), 1656 (C=O, s); ^{1}H NMR (500 MHz, DMSO-d$_6$) δ_H 10.10 (1H, s, CONH-3), 8.39 (1H, s, CONH), 7.55 (2H, d, *J* = 8.8 Hz, H-3'' and 5''), 7.50-7.45 (4H, m, H-3''', 5''', 2'' and 6''), 6.97 (2H, d, *J* = 8.8 Hz, H-2''' and 6'''), 4.56 (2H, s, H-2'), 3.95 (2H, d, *J* = 5.8 Hz, H-1); ^{13}C NMR (150 MHz, DMSO-d$_6$) δ_C 167.9 (C=O, C-1'), 167.5 (C=O, C-2), 157.0 (C-1'''), 138.2 (C-1''), 132.1 (C-3''' and 5'''), 131.6 (C-3'' and 5''), 121.1 (C-2'' and 6''), 117.1 (C-2''' and 6'''), 114.8 (C-4''), 112.7 (C-4'''), 67.0 (C-2'), 42.4 (C-1); HRMS *m/z* (ESI$^+$) [Found: 464.9264., $C_{16}H_{14}Br_2N_2NaO_3$ requires [M + Na]$^+$ 464.9263]; LCMS (LCQ): Rt = 0.7 min (Method 1); *m/z* (ESI$^+$) 440.6 [M]$^+$ and 442.6 [M + 2]$^+$; LCMS (MDAP): Rt = 20.3 min, >95% (Method 3); *m/z* (ESI$^+$) 465.8 [M + Na]$^+$.

General Procedure for the Preparation of Guanidine Nitrates.

To a solution of aniline (0.9 mmol) in EtOH (4 mL) was added 0.09 mL (0.99 mmol) of conc nitric acid followed by a 50% aqueous solution of cyanamide (0.68 mL, 4.4 mmol). The reaction mixture was then heated under reflux for 16 - 48 h. The reaction was cooled to 0 °C followed by the addition of ether (10 mL). The contents were then refrigerated overnight, and the resulting solid was filtered, affording the product in 35-62% yield.

1-[4-(4-methylpiperazin-1-yl)-3-(trifluoromethyl)phenyl]guanidine.

This compd was prepared following the general procedure using 4-(4-Methyl-1-piperazinyl)-3-(trifluoromethyl)aniline. MS (ESI) $(M + H)^+$ 302

1-[2-methoxy-4-(4-methylpiperazin-1-yl)phenyl]guanidine.

This compd was prepared following the general procedure using 1-[2-methoxy-4-(4-methylpiperazin-1-yl)phenyl]aniline. MS (ESI) $(M + H)^+$ 417

1-[4-(4-methylpiperazin-1-yl)phenyl]guanidine.

This compd was prepared following the general procedure using 4-(4-methylpiperazin-1-yl)aniline. MS (ESI) $(M + H)^+$ 234.

1-(3-methoxyphenyl)guanidine.

This compd was prepared following the general procedure using *m*-anisidine. 1H NMR (500 MHz, DMSO-d^6) δ 9.48 (s, 1H), 7.37 – 7.19 (m, 5H), 6.89 – 6.85 (m, 1H), 6.81 – 6.77 (m, 2H), 3.76 (s, 3H). MS (ESI) $(M + H)^+$ 166.

1-(3-cyanophenyl)guanidine.

This compd was prepared following the general procedure using 3-aminobenzonitrile. 1H NMR (500 MHz, DMSO-d^6) δ 9.73 (s, 1H), 7.78 – 7.70 (m, 2H), 7.63 (t, J = 8.2 Hz, 1H), 7.57 – 7.54 (m, 1H), 7.53 – 7.45 (m, 4H). MS (ESI) $(M + H)^+$ 161.

The spectroscopic data are in good agreement with the literature values. Literature reference: F.X. Tavares, J.A. Boucheron, S.H. Dickerson, R.J. Griffin, F. Preugschat, S.A. Thomson, T.Y. Wang and H-Q Zhou. *J. Med. Chem*. 2004, **47**, 4716. WO 03/051886 PCT/US02/39672 p. 60

N-[4-(4-Methylpiperazin-1-yl)-3-(trifluoromethyl)phenyl]-4-pyrazolo[1,5-*b*]pyridazin-3-yl-pyrimidin-2-amine **68**

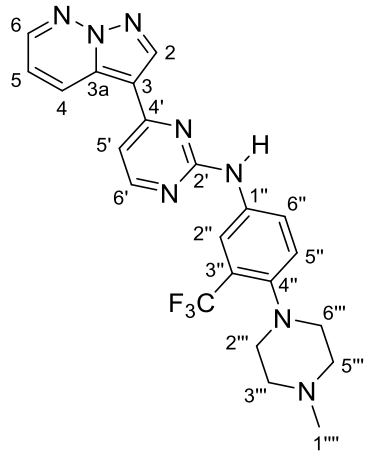

To a solution of (*E*)-3-(dimethylamino)-1-pyrazolo[1,5-*b*]pyridazin-3-yl-prop-2-en-1-one (80 mg, 0.37 mmol) in DMF (1 mL) in a sealed and degassed microwave vial was added 1-[4-(4-methylpiperazin-1-yl)-3-(trifluoromethyl)phenyl]guanidine; nitric acid (270 mg, 0.74 mmol), followed by potassium carbonate potassium carbonate (150 mg, 1.11 mmol). The reaction mixture was heated to 110 °C for 16 h. The reaction mixture was concentrated under reduced pressure. The residue was purified using flash reverse phase column chromatography on a Biotage system (12 g C-18, elution with 10-100% MeOH /water gradient). Desired fractions were combined and concentrated under reduced pressure to afford the title compound, *N*-[4-(4-methylpiperazin-1-yl)-3-(trifluoromethyl)phenyl]-4-pyrazolo[1,5-*b*]pyridazin-3-yl-pyrimidin-2-amine, **68**, as an off-white solid (30 mg, 0.06 mmol, 17% yield). R_f 0.11 (MeOH/ CH_2Cl_2 1:9); m.p. 218-220 °C; $\bar{\nu}_{max}$ (neat)/cm^{-1} 3263 (N-H, m), 3187 (N-H, m), 2854 (C-H, w), 2809 (C-H, s), 1626 (C=N, m); ^{1}H NMR (500 MHz, DMSO-d$_6$) δ_H 9.80 (1H, s, NH), 9.10 (1H, d, *J* = 9.2 Hz, H-4), 8.90 (1H, s, H-2), 8.61 (1H, dd, *J* = 4.5, 1.9 Hz, H-6), 8.49 (1H, d, *J* = 5.2 Hz, H-6'), 8.15 (1H, d, *J* = 2.6 Hz, H-2''), 7.94 (1H, dd, *J* = 8.8, 2.5 Hz, H-6''), 7.55 (1H, d, *J* = 8.7 Hz, H-5''), 7.45 – 7.42 (1H, m, H-5), 7.41 (1H, d, *J* = 5.2 Hz, H-5'), 2.84 (4H, t, *J* = 4.7 Hz, H-2''' and 6'''), 2.47 – 2.40 (4H, m, H-3''' and 5'''), 2.23 (3H, s, H-1''''); ^{13}C NMR (125 MHz, DMSO-d$_6$) δ_C 159.7 (C-2'), 159.4 (C-4'), 158.1 (C-6'), 145.7 (C-4''), 144.1 (C-6), 139.9 (C-2), 137.8 (C-1''), 132.5 (C-3a), 129.4 (C-4), 125.97 (d, *J* = 27.7 Hz, C-3''), 125.1 (C-5''), 123.6 (C-6''), 118.8 (C-5), 116.9 (C-2''), 109.9 (C-3), 108.2 (C-5'), 55.1 (C-3''' and 5'''), 53.1 (C-2''' and 6'''), 45.8 (C-1''''). Signals at 123.9 ppm with J_1 = 246.3 Hz consistent with trifluoromethyl group; HRMS *m/z* (ESI$^+$) [Found: 455.1912., $C_{22}H_{21}F_3N_8$ requires [M + H]$^+$ 455.1914]; LCMS (LCQ): Rt = 0.6 min (Method 1); *m/z* (ESI$^+$) 455.3 [M + H]$^+$; LCMS (MDAP): Rt = 11.4 min, >95% (Method 3); *m/z* (ESI$^+$) 455.2 [M + H]$^+$; The spectroscopic data are in good agreement with the literature values. Literature reference: Stevens, Kirk L.; Reno, Michael J.; Alberti, Jennifer B.; Price, Daniel J.; Kane-Carson, Laurie S.; Knick, Victoria B.;

Shewchuk, Lisa M.; Hassell, Anne M.; Veal, James M.; Davis, Stephen T.; Griffin, Robert J.; Peel, Michael R. Bioorganic and Medicinal Chemistry Letters, 2008 , vol. 18, # 21 p. 5758 – 5762. Patent: WO2004/35588 A1, 2004 ;

N-(3-Methoxyphenyl)-4-pyrazolo[1,5-*b*]pyridazin-3-yl-pyrimidin-2-amine **69**

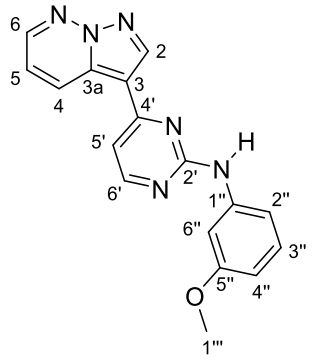

To a solution of (*E*)-3-(dimethylamino)-1-pyrazolo[1,5-*b*]pyridazin-3-yl-prop-2-en-1-one (150 mg, 0.69 mmol) in DMF (1 mL) in a sealed and degassed microwave vial was added 1-(3-methoxyphenyl)guanidine nitrate (320 mg, 1.39 mmol), followed by potassium carbonate (290 mg, 2.08 mmol). The reaction mixture was heated to 110 °C for 16 h. The reaction mixture was concentrated under reduced pressure. The crude was purified using flash silica column chromatography on an Isco Combiflash system (12 g silica, elution with 0-100% 10% MeOH in CH_2Cl_2 / CH_2Cl_2 gradient) to afford the title compound, *N*-(3-methoxyphenyl)-4-pyrazolo[1,5-*b*]pyridazin-3-yl-pyrimidin-2-amine, **69**, as a white solid (30 mg, 0.09 mmol, 13% yield). R_f 0.38 (MeOH/CH_2Cl_2 1:9); m.p. 206-208 °C; $\bar{\nu}_{max}$ (neat)/cm^{-1} 3267 (N-H, m), 3191 (N-H, m), 3075 (C-H, w), 1626 (C=N, w), 1568 (C=C, s), 1545 (C=C, s); ^{1}H NMR (500 MHz, DMSO-d$_6$) δ_H 9.56 (1H, s, NH), 9.21 (1H, d, *J* = 9.0 Hz, H-4), 8.90 (1H, s, H-2), 8.62 (1H, dd, *J* = 4.4, 1.8 Hz, H-6), 8.49 (1H, d, *J* = 5.2 Hz, H-6'), 7.50 – 7.42 (2H, m, H-5 and 6''), 7.39 (1H, d, *J* = 5.3 Hz, H-5'), 7.34 (1H, d, *J* = 7.9 Hz, H-4''), 7.25 (1H, t, *J* = 8.1 Hz, H-3''), 6.62 – 6.55 (1H, m, C-2''), 3.77 (3H, s, H-1'''); ^{13}C NMR (125 MHz, DMSO-d$_6$) δ_C 160.0 (C-2'), 159.7 (C-5''), 159.3 (C-4'), 158.1 (C-6'), 144.1 (C-6), 141.7 (C-1''), 139.8 (C-2), 132.5 (C-3a), 129.6 (C-4), 129.3 (C-3''), 118.8 (C-5), 111.8 (C-4''), 110.0 (C-3), 107.8 (C-5'), 106.8 (C-2''), 105.3 (C-6''), 55.0 (C-1'''); HRMS *m/z* (ESI$^+$) [Found: 319.1303., $C_{17}H_{14}N_6O$ requires [M + H]$^+$ 319.1302]; LCMS (LCQ): Rt = 3.0 min (Method 1); *m/z* (ESI$^+$) 319.3 [M + H]$^+$; LCMS (MDAP): Rt = 17.9 min, >95% (Method 3); *m/z* (ESI$^+$) 319.3 [M + H]$^+$; The spectroscopic data are in good agreement with the literature values. Literature reference: F.X. Tavares, J.A. Boucheron, S.H. Dickerson, R.J. Griffin, F. Preugschat, S.A. Thomson, T.Y. Wang and H-Q Zhou. *J. Med. Chem*. 2004, **47**, 4716

3-[(4-Pyrazolo[1,5-*b*]pyridazin-3-ylpyrimidin-2-yl)amino]benzonitrile **70**

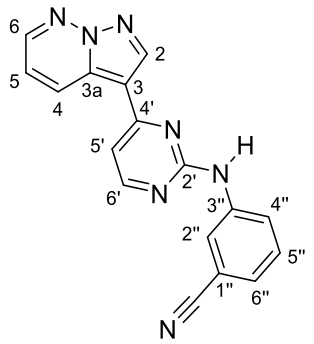

To a solution of (*E*)-3-(dimethylamino)-1-pyrazolo[1,5-*b*]pyridazin-3-yl-prop-2-en-1-one (150 mg, 0.69 mmol) in DMF (1 mL) in a sealed and degassed microwave vial was added 1-(3-cyanophenyl)guanidine nitrate (310 mg, 1.39 mmol), followed by potassium carbonate (290 mg, 2.08 mmol). The reaction mixture was heated to 110 °C for 16 h. The reaction was concentrated under reduced pressure. The crude was purified using flash silica column chromatography on an Isco Combiflash system (12 g silica, elution with 0-100% 10% MeOH in CH_2Cl_2 / CH_2Cl_2 gradient) to afford the title compound, 3-[(4-pyrazolo[1,5-*b*]pyridazin-3-ylpyrimidin-2-yl)amino]benzonitrile, **70**, as a yellow solid (30 mg, 0.09 mmol, 13% yield). R_f 0.78 (MeOH/ CH_2Cl_2 1:9); m.p. 282-283 °C; $\bar{\nu}_{max}$ (neat)/cm^{-1} 3266 (N-H, m), 3190 (N-H, m), 2223 (-$CN_{nitrile}$, s), 1627 (C=N, s), 1608 (C=C, s), 1568 (C=C, s), 1541 (C=C, s); ^{1}H NMR (500 MHz, DMSO-d_6) δ_H 9.93 (1H, s, NH), 9.14 (1H, d, *J* = 9.2 Hz, H-4), 8.92 (1H, s, H-2), 8.64 (1H, dd, *J* = 4.2, 1.9 Hz, H-6), 8.56 (1H, d, *J* = 5.2 Hz, H-6'), 8.40 – 8.34 (1H, m, H-2''), 7.97 (1H, d, *J* = 8.3 Hz, H-6''), 7.55 (1H, t, *J* = 7.8 Hz, H-5''), 7.52 – 7.45 (2H, m, H-5 and 5'), 7.43 (1H, d, *J* = 7.6 Hz, H-4''); ^{13}C NMR (125 MHz, DMSO-d_6) δ_C 159.5 (C-2'), 159.4 (C-4'), 158.1 (C-6'), 144.0 (C-6), 141.4 (C-6''), 139.9 (C-2), 132.5 (C-3a), 129.9 (C-5''), 129.2 (C-4), 124.7 (C-4''), 123.5 (C-3''), 121.3 (C-2''), 119.0 (CN), 118.9 (C-5), 111.4 (C-1''), 109.8 (C-3), 108.6 (C-5'); HRMS *m/z* (ESI$^+$) [Found: 314.1155., $C_{17}H_{11}N_7$ requires [M + H]$^+$ 314.1149]; LCMS (LCQ): Rt = 2.3 min (Method 1); *m/z* (ESI$^+$) 314.3 [M + H]$^+$; LCMS (MDAP): Rt = 18.7 min, >95% (Method 3); *m/z* (ESI$^+$) 314.1 [M + H]$^+$; The spectroscopic data are in good agreement with the literature values. Literature reference: F.X. Tavares, J.A. Boucheron, S.H. Dickerson, R.J. Griffin, F. Preugschat, S.A. Thomson, T.Y. Wang and H-Q Zhou. *J. Med. Chem*. 2004, **47**, 4716

N-(3,5-Dimethoxyphenyl)-4-pyrazolo[1,5-*b*]pyridazin-3-yl-pyrimidin-2-amine **71**

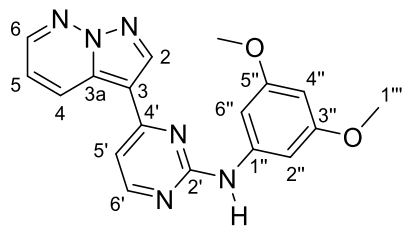

To a microwave vial containing 3-(2-chloropyrimidin-4-yl)pyrazolo[1,5-*b*]pyridazine (80 mg, 0.35 mmol) in 2-propanol (2 mL) was added 3,5-dimethoxyaniline (80 mg, 0.52 mmol) The vial was sealed and irradiated with microwaves at 150 °C for 20 min. The reaction mixture was concentrated under reduced pressure. The crude was purified using flash silica column chromatography on an Isco Combiflash system (12 g silica, elution with 0-100% 10% MeOH in CH_2Cl_2 / CH_2Cl_2 gradient) to afford the title compound, *N*-(3,5-dimethoxyphenyl)-4-pyrazolo[1,5-*b*]pyridazin-3-yl-pyrimidin-2-amine, **71**, as an off-white solid (50 mg, 0.15 mmol, 43% yield). m.p. 198-200 °C; $\bar{\nu}_{max}$ (neat)/cm^{-1} 3332 (N-H, m), 2993 (C-H, w), 2964 (C-H, w), 2840 (C-H, w), 1587 (C=C, m), 1538 (C=C, m); ^{1}H NMR (600 MHz, DMSO-d$_6$) δ_H 9.52 (1H, s, NH), 9.21 (1H, d, *J* = 9.0 Hz, H-4), 8.89 (1H, s, H-2), 8.61 (1H, dd, *J* = 4.4, 1.9 Hz, H-6), 8.48 (1H, d, *J* = 5.2 Hz, H-6'), 7.44 (1H, dd, *J* = 9.0, 4.4 Hz, H-5), 7.38 (1H, d, *J* = 5.2 Hz, H-5'), 7.05 (2H, d, *J* = 2.2 Hz, H-2'' and 6''), 6.20 – 6.13 (1H, m, H-4''), 3.74 (6H, s, H-1'''); ^{13}C NMR (150 MHz, DMSO-d$_6$) δ_C 161.0 (C-3'' and 5''), 160.4 (C-2'), 159.7 (C-4'), 158.5 (C-6'), 144.5 (C-6), 142.6 (C-1''), 140.2 (C-2), 132.9 (C-3a), 130.1 (C-4), 119.2 (C-5), 110.4 (C-3), 108.3 (C-5'), 98.1 (C-2'' and 6''), 93.9 (C-4''), 55.5 (C-1'''); HRMS *m/z* (ESI$^+$) [Found: 349.1412., $C_{18}H_{16}N_6O_2$ requires [M + H]$^+$ 349.1408]; LCMS (LCQ): Rt = 0.6 min (Method 1); *m/z* (ESI$^+$) 349.3 [M + H]$^+$; LCMS (MDAP): Rt = 18.1 min, >95% (Method 3); *m/z* (ESI$^+$) 349.1 [M + H]$^+$; The spectroscopic data are in good agreement with the literature values. Literature reference: F.X. Tavares, J.A. Boucheron, S.H. Dickerson, R.J. Griffin, F. Preugschat, S.A. Thomson, T.Y. Wang and H-Q Zhou. *J. Med. Chem*. 2004, **47**, 4716

Pyridazin-1-ium-1-amine iodide **74**

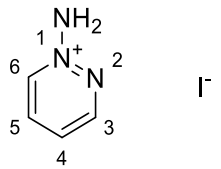

Aminosulfuric acid (13.10 g, 115.84 mmol) was dissolved in water (25 mL) and the reaction mixture was cooled to 10 °C in an icebath. 2.4 M potassium bicarbonate solution (48 mL, 115.2 mmol) was added to the reaction mixture until it was at pH 5. Pyridazine (5.62 mL, 77.4 mmol) was added in one portion and the reaction mixture was heated to 70 °C for 1.5 h. The pH was adjusted to pH 7 by addition of 2.4 M potassium bicarbonate solution (10.0 mL, 24 mmol). The reaction mixture was cooled to 40 °C and was stirred for 1 h. Potassium iodide (12.85 g, 77.41 mmol) in water (25 mL) was added to the reaction mixture and the reaction stirred for a further 1 h. The solvent was removed under reduced pressure. A solution of 5% MeOH in EtOH (100 mL) was then added to the residue. The resulting solids were collected by filtration and dried under reduced pressure to furnish the title compound, pyridazin-1-ium-1-amine iodide, **74**, as a yellow solid (17 g, 72.3 mmol, 94% yield). ^{1}H NMR (600 MHz, DMSO-d_6) δ_H 9.82 (2H, s, NH_2), 9.25 (1H, d, *J* = 5.1 Hz, H-3), 9.10 (1H, d, *J* = 6.3 Hz, H-6), 8.50 – 8.43 (1H, m, H-4), 8.14 – 8.08 (1H, m, H-5); The spectroscopic data are in good agreement with the literature values. Literature reference: F.X. Tavares, J.A. Boucheron, S.H. Dickerson, R.J. Griffin, F. Preugschat, S.A. Thomson, T.Y. Wang and H-Q Zhou. *J. Med. Chem*. 2004, **47**, 4716. WO 03/051886 PCT/US02/39672 p. 60

1-Pyrazolo[1,5-*b*]pyridazin-3-ylethanone **75**

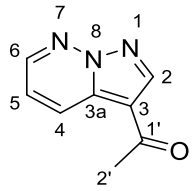

To a slurry of pyridazin-1-ium-1-amine iodide (16.0 g, 71.74 mmol) in CH_2Cl_2 (200 mL) was added 3-butyn-2-one (2.76 mL, 35.26 mmol). The reaction flask was cooled in an ice bath before adding a solution of potassium hydroxide (5.0 g, 89.11 mmol) in water (100 mL) in one portion. The reaction mixture was stirred at rt for 16 h. The organic layer was separated and the aqueous layer was extracted with CH_2Cl_2 (2 x 200 mL). The combined organic components were dried over $MgSO_4$, filtered and concentrated under reduced pressure to afford the title compound, 1-pyrazolo[1,5-*b*]pyridazin-3-ylethanone, **75**, as a red-black solid (3.43 g, 21.28 mmol, 60% yield). ^{1}H NMR (500 MHz, DMSO-d_6) δ_H 8.78 (1H, s, H-2), 8.72 – 8.63 (2H, m, H-4 and 6), 7.57 (1H, dd, *J* = 8.9, 4.6 Hz, H-5), 2.56 (3H, s, H-2'); LCMS (LCQ): Rt = 0.6 min (Method 1); *m/z* (ESI$^+$) 162.2 [M + H]$^+$; The spectroscopic data are in good agreement with the literature values. Literature reference: F.X. Tavares, J.A. Boucheron, S.H. Dickerson, R.J. Griffin, F. Preugschat, S.A. Thomson, T.Y. Wang and H-Q Zhou. *J. Med. Chem*. 2004, **47**, 4716

(*E*)-3-(Dimethylamino)-1-pyrazolo[1,5-*b*]pyridazin-3-yl-prop-2-en-1-one **76**

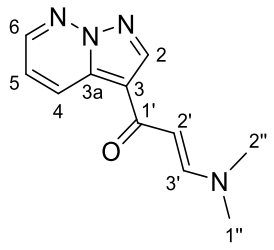

To a flask containing 1-pyrazolo[1,5-*b*]pyridazin-3-ylethanone (0.68 g, 4.22 mmol) was added DMF-DMA (3.78 mL, 28.44 mmol). The reaction mixture was heated to 100 °C for 16 h. The reaction mixture was concentrated under reduced pressure and triturated with diethyl ether to afford the title compound, (*E*)-3-(dimethylamino)-1-pyrazolo[1,5-*b*]pyridazin-3-yl-prop-2-en-1-one, **76**, as a black solid (0.87 g, 3.82 mmol, 91% yield). ^{1}H NMR (600 MHz, DMSO-d_6) δ_H 8.73 (1H, dd, *J* = 9.0, 2.0 Hz, 1H, H-4), 8.70 (1H, s, H-2), 8.57 (1H, dd, *J* = 4.4, 2.0 Hz, H-6), 7.68 (1H, d, *J* = 12.3 Hz, H-3'), 7.41 (1H, dd, *J* = 9.0, 4.4 Hz, H-5), 5.83 (1H, d, *J* = 12.3 Hz, H-2'), 3.20 – 2.80 (6H, m, H-1'' and H-2''); LCMS (LCQ): Rt = 0.6 min (Method 1); *m/z* (ESI$^+$) 217.0 [M + H]$^+$; The spectroscopic data are in good agreement with the literature values. Literature reference: F.X. Tavares, J.A. Boucheron, S.H. Dickerson, R.J. Griffin, F. Preugschat, S.A. Thomson, T.Y. Wang and H-Q Zhou. *J. Med. Chem*. 2004, **47**, 4716

4-Pyrazolo[1,5-*b*]pyridazin-3-ylpyrimidin-2-ol **77a**

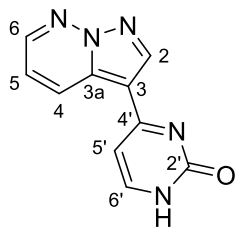

To (*E*)-3-(dimethylamino)-1-pyrazolo[1,5-*b*]pyridazin-3-yl-prop-2-en-1-one (2.5 g, 11.56 mmol) was added urea (15 g, 250 mmol) followed by sodium hydride (1.25 g, 31.25 mmol) and the reaction mixture was heated to 140 °C under nitrogen until melted fully. The melt was then maintained at this temperature for a further 5 min. Once the melt had cooled to rt, water (10 mL) was added slowly whilst stirring. The solution was made to pH 3 with 1 M HCl solution and stirred overnight at rt. The solid formed was filtered and triturated with ethanol to afford the title compound, 4-pyrazolo[1,5-*b*]pyridazin-3-ylpyrimidin-2-ol, **77a**, as a brown solid (2.3 g, 9.71 mmol, 84% yield). R_f 0.32 (MeOH/CH_2Cl_2 1:9); ^{1}H NMR (500 MHz, DMSO-d_6) δ_H 11.64 (1H, s, NH), 8.98 (1H, dd, *J*= 9.0, 2.0 Hz, H-4), 8.93 (1H, s, H-2), 8.65 (1H, dd, *J*= 4.5, 2.0 Hz, H-6), 7.94 (1H, d, *J*= 6.5 Hz, H-6'), 7.54 (1H, dd, *J*= 9.0, 4.5 Hz, H-5), 6.97 (1H, d, *J*= 6.5 Hz, H-5'); HRMS *m/z* (ESI$^+$) [Found: 214.0721., $C_{10}H_8N_5O$ requires [M + H]$^+$ 214.0723]; LCMS (LCQ): Rt = 0.6 min (Method 1); *m/z* (ESI$^+$) 214.3 [M + H]$^+$.

3-(2-Chloropyrimidin-4-yl)pyrazolo[1,5-*b*]pyridazine **77b**

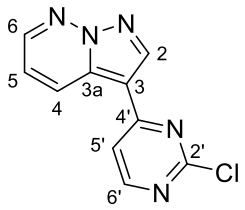

To a pressure vials was added 6-pyrazolo[1,5-*b*]pyridazin-3-yl-1*H*-pyrimidin-2-one (500 mg, 2.35 mmol) and phosphorus(V) oxychloride (2 mL, 21.46 mmol). The vial was sealed and heated to 110 °C for 6 h. The crude reaction mixture was added slowly to a water/ice mix and was stirred at rt for 1 h. The brown suspension that formed was filtered and washed with water to afford the title compound, 3-(2-chloropyrimidin-4-yl)pyrazolo[1,5-*b*]pyridazine, **77b**, as a brown solid (540 mg, 2.17 mmol, 92% yield). R_f 0.83 (MeOH/CH_2Cl_2 1:9); m.p. 293-295 °C; $\bar{\nu}_{max}$ (neat)/cm^{-1} 3103(C-H, m), 3035(C-H, w), 2930 (C-H, w), 2850 (C-H, w), 1620 (C=N, m), 1578 (C=C, m); ^{1}H NMR (500 MHz, DMSO-d_6) δ_H 8.96 (1H, s, H-2), 8.83 (1H, dd, *J*= 9.1, 1.9 Hz, H-4), 8.66 (1H, d, *J*= 5.3 Hz, H-6'), 8.62 (1H, dd, *J*= 4.5, 1.9 Hz, H-6), 7.99 (1H, d, *J*= 5.3 Hz, H-5'), 7.51 (1H, dd, *J*= 9.1, 4.5 Hz, H-5); LCMS (LCQ): Rt = 1.0 min (Method 1); *m/z* (ESI$^+$) 231.9 [M]$^+$ and 233.9 [M]$^+$; The spectroscopic data are in good agreement with the literature values. Literature reference: Schaenzer AJ, Wlodarchak N, Drewry DH, Zuercher WJ, Rose WE, Ferrer CA, Sauer JD, Striker R. ACS Infect Dis. 2018 Oct 12;4(10):1508-1518.

N-[4-(4-Methylpiperazin-1-yl)phenyl]-4-pyrazolo[1,5-*b*]pyridazin-3-yl-pyrimidin-2-amine **78**

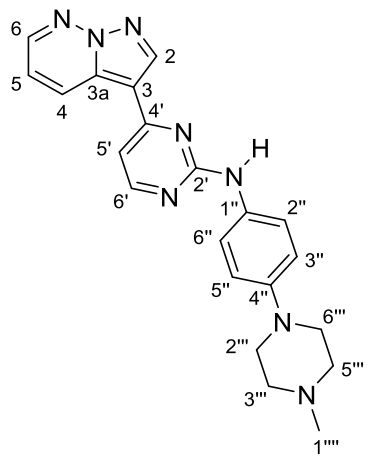

To a solution of (*E*)-3-(dimethylamino)-1-pyrazolo[1,5-*b*]pyridazin-3-yl-prop-2-en-1-one (150 mg, 0.69 mmol) in DMF (1 mL) in a sealed and degassed microwave vial was added 1-[4-(4-methylpiperazin-1-yl)phenyl]guanidine nitrate (410 mg, 1.39 mmol), followed by potassium carbonate (290 mg, 2.08 mmol). The reaction mixture was heated to 110 °C for 16 h. The reaction mixture was concentrated under reduced pressure. The crude was purified using flash silica column chromatography on an Isco Combiflash system (12 g silica, elution with 0-100% 10% MeOH in CH_2Cl_2 / CH_2Cl_2 gradient) to afford the title compound, *N*-[4-(4-methylpiperazin-1-yl)phenyl]-4-pyrazolo[1,5-*b*]pyridazin-3-yl-pyrimidin-2-amine, **78**, as a yellow solid (50 mg, 0.123 mmol, 18% yield). R_f 0.46 (MeOH/CH_2Cl_2 1:9); m.p. 261-264 °C; $\bar{\nu}_{max}$ (neat)/cm^{-1} 3255 (N-H, m); 3182 (N-H, m), 2938 (C-H, w), 2797 (C-H, w), 1626 (C=N, m), 1611 (C=N, m); ^{1}H NMR (500 MHz, $CDCl_3$) δ_H 8.83 (1H, d, *J* = 8.9 Hz, H-4), 8.48 (1H, s, H-2), 8.39 – 8.34 (2H, m, H-6 and 6''), 7.47 (2H, d, *J* = 8.5 Hz, H-2'' and 6''), 7.08 (1H, dd, *J* = 9.1, 4.5 Hz, H-5), 7.02 – 6.95 (3H, m, H-5'', 3'' and 5''), 6.90 (1H, s, NH), 3.27 – 3.19 (4H, m, H-2''' and 6'''), 2.69 – 2.56 (4H, m, H-3''' and 5'''), 2.39 (3H, s, H-1''''); ^{13}C NMR (125 MHz, DMSO-d6) δ_C 161.1 (C-2'), 160.0 (C-4'), 158.4 (C-6'), 148.2 (C-4''), 143.1 (C-6), 139.4 (C-2), 133.2 (C-3a), 131.9 (C-1''), 130.1 (C-4), 123.2 (C-2'' and 6''), 117.8 (C-5), 116.9 (C-3'' and 5''), 111.0 (C-3), 107.5 (C-5'), 55.3 (C-3''' and C-5'''), 49.9 (C-2''' and 6'''), 46.3 (C-1''''); HRMS *m/z* (ESI$^+$) [Found: 387.2039., $C_{21}H_{22}N_8$ requires [M + H]$^+$ 387.2040]; LCMS (LCQ): Rt = 0.5 min (Method 1); *m/z* (ESI$^+$) 387.3 [M + H]$^+$; LCMS (MDAP): Rt = 9.1 min, >95% (Method 3); *m/z* (ESI$^+$) 387.2 [M + H]$^+$; The spectroscopic data are in good agreement with the literature values. Literature reference: F.X Tavares, J.A. Boucheron, S.H. Dickerson, R.J. Griffin, F. Preugschat, S.A. Thomson, T.Y. Wang and H-Q Zhou. *J. Med. Chem*. 2004, **47**, 4716

N-Phenyl-4-pyrazolo[1,5-*b*]pyridazin-3-yl-pyrimidin-2-amine **79**

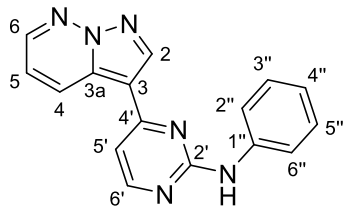

To a microwave vial containing 3-(2-chloropyrimidin-4-yl)pyrazolo[1,5-b]pyridazine (80 mg, 0.35 mmol) in 2-propanol (2 mL) was added aniline (0.06 mL, 0.69 mmol). The vial was sealed and heated conventionally at 110 °C for 2 h. The reaction mixture was concentrated under reduced pressure. The crude was purified using flash silica column chromatography on an Isco Combiflash system (12 g silica, elution with 0-50% 20% MeOH in CH2Cl2 / CH2Cl2 gradient). Desired fractions were combined and concentrated under reduced pressure to afford the title compound, N-phenyl-4-pyrazolo[1,5-b]pyridazin-3-yl-pyrimidin-2-amine, 79, as an off-white solid (45 mg, 0.15 mmol, 43% yield). m.p. 213-214 °C; ν̄max (neat)/cm-1 3247 (N-H, m); 2947 (C-H, w), 2848 (C-H, w), 1625 (C=N, m), 1572 (C=C, m), 1546 (C=C, s); ^{1}H NMR (500 MHz, DMSO-d_6) δ_H 9.59 (1H, s, NH), 9.18 (1H, d, *J* = 9.0 Hz, H-4), 8.90 (1H, s, H-2), 8.61 (1H, dd, *J* = 4.5, 1.9 Hz, H-6), 8.47 (1H, d, *J* = 5.2 Hz, H-6'), 7.75 (2H, d, *J* = 8.1 Hz, H-2'' and 6''), 7.46 (1H, dd, *J* = 9.0, 4.5 Hz, H-5), 7.38 (1H, d, *J* = 5.2 Hz, H-5'), 7.36 – 7.30 (2H, m, H-3'' and 5''), 6.99 (1H, app. t, *J* = 7.3 Hz, H-4''); ^{13}C NMR (125 MHz, DMSO-d_6) δ_C 160.0 (C-2'), 159.3 (C-4'), 158.1 (C-6'), 144.0 (C-6), 140.5 (C-1''), 139.8 (C-2), 132.5 (C-3a), 129.6 (C-4), 128.5 (C-3'' and 5''), 121.6 (C-4''), 119.4 (C-2'' and 6''), 118.8 (C-5), 110.0 (C-3), 107.7 (C-5'); HRMS m/z (ESI$^+$) [Found: 289.1189., $C_{16}H_{13}N_6$ requires [M + H]$^+$ 289.1196]; LCMS (LCQ): Rt = 0.5 min (Method 1); m/z (ESI$^+$) 289.30 [M + H]$^+$; LCMS (MDAP): Rt = 17.3 min, >95% (Method 3); m/z (ESI$^+$) 289.1 [M + H]$^+$; The spectroscopic data are in good agreement with the literature values. Literature reference: F.X. Tavares, J.A. Boucheron, S.H. Dickerson, R.J. Griffin, F. Preugschat, S.A. Thomson, T.Y. Wang and H-Q Zhou. J. Med. Chem. 2004, 47, 4716

N-(*o*-Tolyl)-4-pyrazolo[1,5-*b*]pyridazin-3-yl-pyrimidin-2-amine **80**

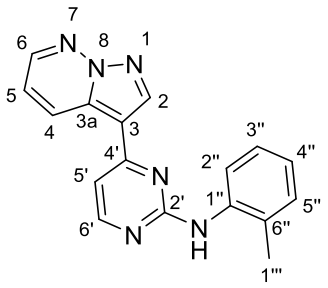

To a pressure vial containing 3-(2-chloropyrimidin-4-yl)pyrazolo[1,5-*b*]pyridazine (80 mg, 0.35 mmol) in 2-propanol (1.6 mL) was added *o*-toluidine (0.07 mL, 0.69 mmol). The vial was sealed and heated to 140 °C for 16 h. The reaction mixture was concentrated under reduced pressure. The crude was purified using flash silica column chromatography on an Isco Combiflash system (12 g silica, elution with 0-60% EtOAc / petroleum ether gradient). Desired fractions were combined and concentrated under reduced pressure. The crude was purified using flash reverse phase column chromatography on a Biotage system (12 g C-18, elution with 10-100% MeOH / water gradient). Desired fractions were combined and concentrated under reduced pressure to afford the desired product, *N*-(*o*-tolyl)-4-pyrazolo[1,5-*b*]pyridazin-3-yl-pyrimidin-2-amine, **80**, as a colourless solid (4 mg, 0.01 mmol, 4% yield). R_f 0.76(EtOAc/ petroleum ether 1:1); ^{1}H NMR (500 MHz, MeOD) δ_H 8.68 (1H, s, H-2), 8.59 (1H, d, *J* = 9.0 Hz, H-4), 8.44 (1H, dd, *J* = 4.5, 2.0 Hz, H-6), 8.31 (1H, d, *J* = 5.3 Hz, H-6'), 7.48 (1H, dd, *J* = 7.8, 1.3 Hz, H-2''), 7.35 (1H, d, *J* = 7.2 Hz, H-5''), 7.29 (1H, t, *J* = 7.6 Hz, H-3''), 7.25 – 7.20 (2H, m, H-4'' and 5'), 7.15 (1H, dd, J = 9.0, 4.5 Hz, 1H, CH-5), 2.31 (3H, s, H-1'''); ^{13}C NMR (150 MHz, MeOD) δ_C 162.8 (C-2'), 161.6 (C-4'), 159.1 (C-6'), 145.0 (C-6), 140.3 (C-2), 139.2 (C-1''), 135.4 (C-6''), 134.4 (C-3a), 131.7 (C-5''), 131.2 (C-4), 127.7 (C-2''), 127.5 (C-3''), 126.8 (C-4''), 119.6 (C-5), 111.9 (C-3), 107.6 (C-5'), 18.4 (C-1'''); HRMS *m/z* (ESI$^+$) [Found: 325.1170., $C_{17}H_{14}N_6Na$ requires [M + Na]$^+$ 325.1172]; LCMS (MDAP): Rt = 11.0 min, >95% (Method 3); *m/z* (ESI$^+$) 302.9 [M + H]$^+$; The spectroscopic data are in good agreement with the literature values. Literature reference: F.X. Tavares, J.A. Boucheron, S.H. Dickerson, R.J. Griffin, F. Preugschat, S.A. Thomson, T.Y. Wang and H-Q Zhou. *J. Med. Chem*. 2004, **47**, 4716

4-[(4-Pyrazolo[1,5-*b*]pyridazin-3-ylpyrimidin-2-yl)amino]benzonitrile **81**

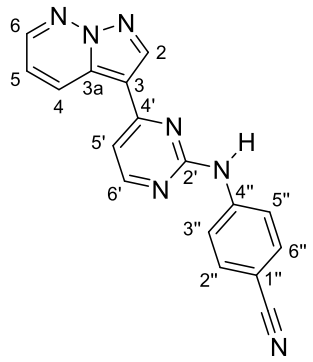

To a solution of (*E*)-3-(dimethylamino)-1-pyrazolo[1,5-*b*]pyridazin-3-yl-prop-2-en-1-one (50 mg, 0.23 mmol) in 2-methoxyethanol (1.17 mL, 14.86 mmol) in a sealed and degassed microwave vial was added 1-(4-cyanophenyl)guanidine (70 mg, 0.42 mmol) and potassium carbonate (40 mg, 0.28 mmol) and the vial was irradiated with microwaves for 15 min at 150 °C. The reaction mixture was concentrated under reduced pressure. The crude was purified using flash silica column chromatography on an Isco Combiflash system (12 g silica, elution with 0-100% 10% MeOH in CH_2Cl_2 / CH_2Cl_2 gradient) to afford the desired product, 4-[(4-pyrazolo[1,5-*b*]pyridazin-3-ylpyrimidin-2-yl)amino]benzonitrile, **81**, as a colourless solid (20 mg, 0.06 mmol, 28% yield). R_f 0.81 (MeOH/CH_2Cl_2 1:9); m.p. 309-311 °C; $\bar{\nu}_{max}$ (neat)/cm^{-1} 3261 (N-H, m), 3182 (N-H, m), 3004 (C-H, w), 2222 (-$CN_{nitrile}$, s), 1628 (C=N, w), 1578 (C=C, s), 1541 (C=C,s); ^{1}H NMR (500 MHz, DMSO-d_6) δ_H 10.14 (s, 1H, NH), 9.21 (1H, dd, *J* = 9.0, 1.9 Hz, H-4), 8.96 (1H, s, H-2), 8.67 (1H, dd, *J* = 4.5, 1.9 Hz, H-6), 8.60 (1H, d, *J* = 5.3 Hz, H-6'), 8.05 – 8.00 (2H, m, H-2'' and 6''), 7.84 – 7.76 (2H, m, H-3'' and 5''), 7.60 – 7.51 (2H, m, H-5 and 5'); HRMS *m/z* (ESI$^+$) [Found: 336.0958., $C_{17}H_{11}N_7Na$ requires [M + Na]$^+$ 336.0968]; LCMS (LCQ): Rt = 2.5 min (Method 1); *m/z* (ESI$^+$) 314.3 [M + H]$^+$; The spectroscopic data are in good agreement with the literature values; Literature reference: F.X Tavares, J.A. Boucheron, S.H. Dickerson, R.J. Griffin, F. Preugschat, S.A. Thomson, T.Y. Wang and H-Q Zhou. *J. Med. Chem*. 2004, **47**, 4716

N-(*m*-Tolyl)-4-pyrazolo[1,5-*b*]pyridazin-3-yl-pyrimidin-2-amine **82**

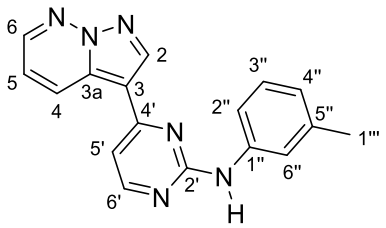

To a microwave vial containing 3-(2-chloropyrimidin-4-yl)pyrazolo[1,5-*b*]pyridazine (80 mg, 0.35 mmol) in 2-propanol (2 mL) was added *m*-toluidine (0.07 mL, 0.69 mmol). The vial was sealed and irradiated with microwaves at 150 °C for 20 min. The reaction mixture was concentrated under reduced pressure. The crude was purified using flash silica column chromatography on an Isco Combiflash system (12 g silica, elution with 0-100% 10% MeOH in CH_2Cl_2 / CH_2Cl_2 gradient) to afford the title compound, *N*-(*m*-tolyl)-4-pyrazolo[1,5-*b*]pyridazin-3-yl-pyrimidin-2-amine, **82**, as an off-white solid (70 mg, 0.21 mmol, 66% yield). m.p. 223-225 °C; $\bar{\nu}_{max}$ (neat)/cm^{-1} 3267 (N-H, m), 3194 (N-H, m), 3016 (C-H, w), 2951 (C-H, w), 1621 (C=N, m), 1572 (C=C, s), 1547 (C=C, s); ^{1}H NMR (500 MHz, DMSO-d$_6$) δ_H 9.46 (1H, s, NH), 9.11 (1H, d, *J* = 9.0 Hz, H-4), 8.84 (1H, app. d, *J* = 3.6 Hz, H-2), 8.56 (1H, s, H-6), 8.46 – 8.35 (1H, m, H-6’), 7.58 (1H, s, H-6’’), 7.49 – 7.37 (2H, m, H-5 and 2’’), 7.34 – 7.28 (1H, m, H-5’), 7.20 – 7.12 (1H, m, H-3’’), 6.81 – 6.74 (1H, m, H-4’’), 2.27 (3H, s, H-1’’’); ^{13}C NMR (125 MHz, DMSO-d$_6$) δ_C 160.1 (C-2’), 159.3 (C-4’), 158.1 (C-6’), 144.1 (C-6), 140.4 (C-1’’), 139.8 (C-2), 137.7 (C-5’’), 132.5 (C-3a), 129.5 (C-4), 128.4 (C-3’’), 122.5 (C-4’’), 110.9 (C-6’’), 118.8 (C-5), 116.7 (C-2’’), 110.1 (C-3), 107.6 (C-5’), 21.3 (C-1’’’); HRMS *m/z* (ESI$^+$) [Found: 303.1355., $C_{17}H_{14}N_6$ requires [M + H]$^+$ 303.1353]; LCMS (LCQ): Rt = 3.1 min (Method 1); *m/z* (ESI$^+$) 303.4 [M + H]$^+$; LCMS (MDAP): Rt = 18.2 min, >95% (Method 3); *m/z* (ESI$^+$) 303.1 [M + H]$^+$

4-Pyrazolo[1,5-*b*]pyridazin-3-yl-*N*-[3-(trifluoromethoxy)phenyl]pyrimidin-2-amine **83**

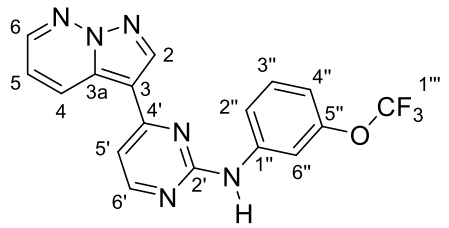

To a microwave vial containing 3-(2-chloropyrimidin-4-yl)pyrazolo[1,5-*b*]pyridazine (80 mg, 0.35 mmol) in 2-propanol (2 mL) was added 3-(trifluoromethoxy)aniline (0.07 mL, 0.52 mmol). The vial was sealed and irradiated with microwaves at 150 °C for 20 min. The reaction mixture was concentrated under reduced pressure. The crude was purified using flash silica column chromatography on an Isco Combiflash system (12 g silica, elution with 0-100% 10% MeOH in CH_2Cl_2 / CH_2Cl_2 gradient) to afford the title compound, 4-pyrazolo[1,5-*b*]pyridazin-3-yl-*N*-[3-(trifluoromethoxy)phenyl]pyrimidin-2-amine, **83**, as an off-white solid (60 mg, 0.15 mmol, 44% yield). m.p. 167-168 °C; $\bar{\nu}_{max}$ (neat)/cm^{-1} 3263 (N-H, m), 3197 (N-H, m), 3017 (C-H, w), 2951 (C-H, w), 1619 (C=N, w), 1572 (C=C, s), 1547 (C=C, s); ^{1}H NMR (500 MHz, DMSO-d$_6$) δ_H 9.85 (1H, s, NH), 9.13 (1H, d, *J* = 9.0 Hz, H-4), 8.87 (1H, s, H-2), 8.59 (1H, dd, *J* = 4.5, 1.9 Hz, H-6), 8.49 (1H, d, *J* = 5.3 Hz, H-6'), 7.94 (1H, s, H-6''), 7.68 (1H, d, *J* = 8.2 Hz, H-2''), 7.47 – 7.36 (3H, m, H-5, 5' and 3''), 6.90 (1H, d, *J* = 8.1 Hz, H-4''); ^{13}C NMR (125 MHz, DMSO-d$_6$) δ_C 159.6 (C-2'), 159.5 (C-4'), 158.1 (C-6'), 148.7 (C-5''), 144.1 (C-6), 142.4 (C-1''), 139.9 (C-2), 132.5 (C-3a), 130.2 (C-3''), 129.4 (C-4), 119.8 (q, *J* = 254.0 Hz, C-1'''), 118.9 (C-5), 117.4 (C-2''), 113.0 (C-4''), 110.7 (C-6''), 109.8 (C-3), 108.5 (C-5'); HRMS *m/z* (ESI$^+$) [Found: 373.1022., $C_{17}H_{11}F_3N_6O$ requires [M + H]$^+$ 373.1019]; LCMS (LCQ): Rt = 3.4 min (Method 1); *m/z* (ESI$^+$) 373.3 [M + H]$^+$; LCMS (MDAP): Rt = 21.9 min, >95% (Method 3); *m/z* (ESI$^+$) 373.1 [M + H]$^+$

N-[3-bromo-5-(trifluoromethyl)phenyl]-4-pyrazolo[1,5-*b*]pyridazin-3-yl-pyrimidin-2-amine **84**

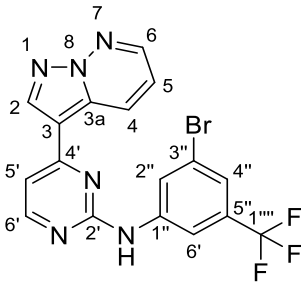

To a pressure vial containing 3-(2-chloropyrimidin-4-yl)pyrazolo[1,5-*b*]pyridazine (200 mg, 0.86 mmol) in 2-propanol (4 mL) was added 3-bromo-5-(trifluoromethyl)aniline (0.24 mL, 1.73 mmol). The vial was sealed and heated to 140 °C for 16 h. The reaction mixture was concentrated under reduced pressure. The crude was purified using flash silica column chromatography on an Isco Combiflash system (12 g silica, elution with 0-60% EtOAc / petroleum ether gradient). Desired fractions were combined and concentrated under reduced pressure. The crude was purified using flash reverse phase column chromatography on a Biotage system (12 g C-18, elution with 10-100% MeOH / water gradient). Desired fractions were combined and concentrated under reduced pressure to afford the desired product, *N*-[3-bromo-5-(trifluoromethyl)phenyl]-4-pyrazolo[1,5-*b*]pyridazin-3-yl-pyrimidin-2-amine, **84**, as a yellow solid (60 mg, 0.12 mmol, 14% yield). R_f 0.86 (EtOAc/ hexane 1/1); Decomposed > 258 °C; $\bar{\nu}_{max}$ (neat)/cm^{-1} 3283 (N-H, m); 3190 (N-H, m), 3040 (C-H, w), 1615 (C=N, m), 1564 (C=C, m), 1538 (C=C, m); ^{1}H NMR (500 MHz, DMSO-d$_6$) δ_H 10.14 (1H, s, NH), 9.11 (1H, d, *J* = 9.1 Hz, H-4), 8.95 (1H, s, H-2), 8.65 (1H, dd, *J* = 4.5, 1.9 Hz, H-6), 8.59 (1H, d, *J* = 5.3 Hz, H-6'), 8.41 (1H, s, H-2''), 8.16 (1H, s, H-6''), 7.54 – 7.46 (3H, m, H-5', 4'' and 5); ^{13}C NMR (125 MHz, DMSO-d$_6$) δ_C 159.5 (C-2'), 159.3 (C-4'), 158.2 (C-6'), 144.1 (C-6), 142.9 (C-1''), 140.0 (C-2), 132.5 (C-3a), 131.13 (q, J = 31.8 Hz, C-5'''), 129.2 (C-4), 126.2 - 121.8 (m, CF_3), 124.1 (C-2''), 122.3 (C-3''), 119.75 – 119.60 (m, C-4''), 119.1 (C-5), 113.74 – 113.58 (m, C-6''), 109.7 (C-3), 109.1 (C-5'); HRMS *m/z* (ESI$^+$) [Found: 437.0162., $C_{17}H_{11}BrF_3N_8$ requires [M + H]$^+$ 437.0175]; LCMS (MDAP): Rt = 23.6 min, >95% (Method 3); *m/z* (ESI$^+$) 435.0 [M]$^+$ and 437.0 [M+2]$^+$; The spectroscopic data are in good agreement with the literature values. Literature reference: F.X. Tavares, J.A. Boucheron, S.H. Dickerson, R.J. Griffin, F. Preugschat, S.A. Thomson, T.Y. Wang and H-Q Zhou. *J. Med. Chem*. 2004, **47**, 4716

N-[(4-Chlorophenyl)methyl]-4-pyrazolo[1,5-*b*]pyridazin-3-yl-pyrimidin-2-amine **85**

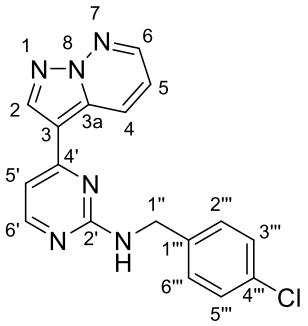

To a pressure vial containing 3-(2-chloropyrimidin-4-yl)pyrazolo[1,5-*b*]pyridazine (80 mg, 0.35 mmol) in 2-propanol (1.6mL) was added 4-chlorobenzylamine (0.08 mL, 0.69 mmol). The vial was sealed and heated to 140 °C for 16 h. The reaction mixture was concentrated under reduced pressure. The crude was purified using flash silica column chromatography on an Isco Combiflash system (12 g silica, elution with 0-70% EtOAc / petroleum ether gradient). Desired fractions were combined and concentrated under reduced pressure. The crude was purified using flash reverse phase column chromatography on a Biotage system (12 g C-18, elution with 10-100% MeOH / water gradient). Desired fractions were combined and concentrated under reduced pressure to afford the desired product, *N*-[(4-chlorophenyl)methyl]-4-pyrazolo[1,5-*b*]pyridazin-3-yl-pyrimidin-2-amine, **85**, as a pale yellow solid (19 mg, 0.05 mmol, 15% yield). R_f 0.50 (EtOAc/ hexane 1:1); m.p. 183-185 °C; $\bar{\nu}_{max}$ (neat)/cm^{-1} 3238 (N-H, m); 3074 (C-H, m), 3028 (C-H, w), 2969 (C-H, w), 2933 (C-H, w), 1619 (C=N, m), 1575 (C=C, m), 1546 (C=C, m); ^{1}H NMR (500 MHz, DMSO-d$_6$) δ_H 9.31 - 9.10 (1H, m, H-4), 8.81 (1H, s, H-2), 8.65 – 8.38 (2H, m, H-6 and 5), 8.30 (1H, d, *J*= 5.1 Hz, H-6'), 7.86 (1H, t, *J*= 6.1 Hz, NH), 7.48 – 7.34 (4H, m, H-2''', 3''', 5''', 6'''), 7.15 (1H, d, *J*= 5.1 Hz, H-5'), 4.57 (2H, s, H-1''); ^{13}C NMR (150 MHz, DMSO-d$_6$) δ_C 166.6 (C-2'), 161.8 (C-4'), 158.9 (C-6'), 145.2 (C-6), 140.7 (C-2), 134.5 (C-3a), 130.7 (C-4), 120.3 (C-5), 111.6 (C-3), 110.1 (C-5'), 68.8 (C-5''), 50.2 (C-3''), 28.9 (C-4''). Remaining carbon signals potentially under cluster of signals at 128 ppm; HRMS *m/z* (ESI$^+$) [Found: 359.0780., $C_{17}H_{13}ClN_6Na$ requires [M + Na]$^+$ 359.0782]; LCMS (MDAP): Rt = 11.0 min, >95% (Method 3); *m/z* (ESI$^+$) 336.9 [M]$^+$ and 338.9 [M+2]$^+$; The spectroscopic data are in good agreement with the literature values. Literature reference: Stevens KL, Reno MJ, Alberti JB, Price DJ, Kane-Carson LS, Knick VB, Shewchuk LM, Hassell AM, Veal JM, Davis ST, Griffin RJ, Peel MR. Bioorg Med Chem Lett (2008) 18:5758-5758

N-(2-Methoxyphenyl)-4-pyrazolo[1,5-*b*]pyridazin-3-yl-pyrimidin-2-amine **86**

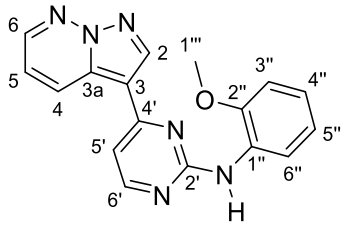

To a microwave vial containing 3-(2-chloropyrimidin-4-yl)pyrazolo[1,5-*b*]pyridazine (80 mg, 0.35 mmol) in 2-propanol (1 mL) was added *o*-anisidine (0.04 mL, 0.35 mmol). The vial was sealed and irradiated with microwaves at 150 °C for 20 min. The reaction mixture was concentrated under reduced pressure. The crude was purified using flash silica column chromatography on an Isco Combiflash system (12 g silica, elution with 0-100% 10% MeOH in CH_2Cl_2 / CH_2Cl_2 gradient). Desired fractions were combined and concentrated under reduced pressure to afford the title compound, *N*-(2-methoxyphenyl)-4-pyrazolo[1,5-*b*]pyridazin-3-yl-pyrimidin-2-amine, **86**, as an off-white solid (50 mg, 0.14 mmol, 40% yield). R_f 0.94 (MeOH/ CH_2Cl_2 1:9); m.p. 146-147 °C; $\bar{\nu}_{max}$ (neat)/cm^{-1} 3442 (N-H, m), 3111 (C-H, w), 2956 (C-H, w), 2934 (C-H, w), 1620 (C=N, w), 1560 (C=C, s), 1533 (C=C, s); ^{1}H NMR (500 MHz, DMSO-d$_6$) δ_H 8.99 (1H, d, *J* = 9.0 Hz, H-4), 8.87 (1H, s, H-2), 8.62 – 8.54 (1H, m, H-6), 8.42 (1H, d, *J* = 5.2 Hz, H-6'), 8.40 (1H, s, NH), 7.98 (1H, d, *J* = 7.8 Hz, H-6''), 7.38 (1H, dd, *J* = 9.0, 3.8 Hz, H-5), 7.35 (1H, d, *J* = 5.2 Hz, H-5'), 7.14 – 7.06 (2H, m, H-3'' and H-4''), 7.03 – 6.96 (1H, m, H-5''), 3.85 (3H, s, H-1'''); ^{13}C NMR (150 MHz, DMSO-d$_6$) δ_C 160.5 (C-2'), 159.8 (C-4'), 158.6 (C-6'), 150.9 (C-1''), 144.5 (C-6), 140.2 (C-2), 132.9 (C-3a), 130.0 (C-4), 126.8 (C-2''), 124.1 (C-4'') 123.0 (C-6''), 120.6 (C-5''), 119.1 (C-5), 111.6 (C-3''), 110.7 (C-3), 108.0 (C-5'), 56.1 (C-1'''); HRMS *m/z* (ESI$^+$) [Found: 319.1307., $C_{17}H_{14}N_6O$ requires [M + H]$^+$ 319.1302]; LCMS (LCQ): Rt = 1.7 min (Method 1); *m/z* (ESI$^+$) 319.2 [M + H]$^+$; LCMS (MDAP): Rt = 17.1 min, >95% (Method 3); *m/z* (ESI$^+$) 319.1 [M + H]$^+$

N-Methyl-*N*-phenyl-4-pyrazolo[1,5-*b*]pyridazin-3-yl-pyrimidin-2-amine **88**

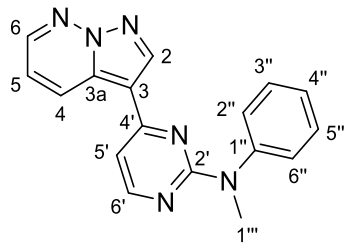

To a microwave vial containing 3-(2-chloropyrimidin-4-yl)pyrazolo[1,5-*b*]pyridazine (80 mg, 0.35 mmol) in 2-propanol (2 mL) was added *N*-methylbenzylamine (0.07 mL, 0.69 mmol). The vial was sealed and heated conventionally at 110 °C for 2 h. The reaction was concentrated under reduced pressure. The crude was purified using flash silica column chromatography on an Isco Combiflash system (12 g silica, elution with 0-50% 20% MeOH in CH_2Cl_2 / CH_2Cl_2 gradient). Desired fractions were combined and concentrated under reduced pressure to afford the title compound, *N*-methyl-*N*-phenyl-4-pyrazolo[1,5-*b*]pyridazin-3-yl-pyrimidin-2-amine, **88**, as an off-white solid (48 mg, 0.15 mmol, 44% yield). m.p. 157-159 °C; $\bar{\nu}_{max}$ (neat)/cm^{-1} 3098 (C-H, w), 2922 (C-H, w), 2856 (C-H, w), 1622 (C=N, m), 1563 (C=C, m), 1528 (C=C, m); ^{1}H NMR (500 MHz, DMSO-d$_6$) δ_H 8.84 (1H, s, H-2), 8.51 (1H, dd, *J* = 4.5, 2.0 Hz, H-6), 8.40 (1H, d, *J* = 5.2 Hz, H-6'), 8.26 – 8.19 (1H, m, H-4), 7.51 – 7.46 (2H, m, H-2'' and 6''), 7.43 – 7.39 (2H, m, H-3''and 5''), 7.33 (1H, t, *J* = 7.4 Hz, H-4''), 7.27 (1H, d, *J* = 5.2 Hz, H-5'), 7.16 (1H, dd, *J* = 9.0, 4.5 Hz, H-5), 3.54 (3H, s, H-1''); ^{13}C NMR (125 MHz, DMSO-d$_6$) δ_C 161.7 (C-2'), 158.8 (C-4'), 158.1 (C-6'), 145.7 (C-1''), 143.9 (C-6), 139.6 (C-2), 132.4 (C-3a), 129.10 (C-2'' and 6''), 129.08 (C-4), 127.2 (C-3'' and 5''), 125.7 (C-4''), 118.4 (C-5), 110.1 (C-3), 106.1 (C-5'), 38.1 (C-1'''); HRMS *m/z* (ESI$^+$) [Found: 303.1346., $C_{17}H_{15}N_6$ requires [M + H]$^+$ 303.1353]; LCMS (LCQ): Rt = 0.6 min (Method 1); *m/z* (ESI$^+$) 303.3 [M + H]$^+$; LCMS (MDAP): Rt = 16.3 min, >95% (Method 3); *m/z* (ESI$^+$) 303.1 [M + H]$^+$; The spectroscopic data are in good agreement with the literature values. Literature reference: F.X. Tavares, J.A. Boucheron, S.H. Dickerson, R.J. Griffin, F. Preugschat, S.A. Thomson, T.Y. Wang and H-Q Zhou. *J. Med. Chem*. 2004, **47**, 4716.

N-Methyl-*N*-(*m*-tolyl)-4-pyrazolo[1,5-*b*]pyridazin-3-yl-pyrimidin-2-amine **89**

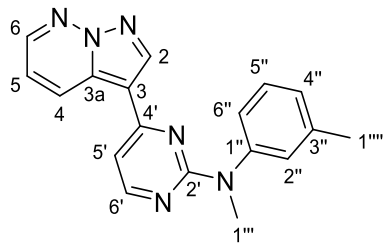

To a solution of *N*-(*m*-tolyl)-4-pyrazolo[1,5-*b*]pyridazin-3-yl-pyrimidin-2-amine (20 mg, 0.07 mmol) in DMF (2 mL) was added sodium hydride (5 mg, 0.22 mmol) followed by iodomethane (0.01 mL, 0.17 mmol). The reaction mixture was stirred under nitrogen for 2 h at rt. The reaction mixture was concentrated under reduced pressure. The crude was dissolved in EtOAc (10 mL) and washed with 0.1 M LiCl solution (20 mL). The aqueous was extracted two further times with EtOAc (2 x 10 mL). The combined organics were washed with brine (30 mL), dried over $MgSO_4$, filtered and concentrated under reduced pressure. The residue was triturated with diethyl ether to afford the desired product, *N*-methyl-*N*-(*m*-tolyl)-4-pyrazolo[1,5-*b*]pyridazin-3-yl-pyrimidin-2-amine, **89**, as an off-white solid (15 mg, 0.05 mmol, 68% yield). R_f 0.34 (EtOAc / hexane 1/1); m.p. 178-180 °C; $\bar{\nu}_{max}$ (neat)/cm^{-1} 3098 (C-H, w), 3045 (C-H, w), 2924 (C-H, w), 1624 (C=N, m), 1563 (C=C, m), 1527 (C=C, m); ^{1}H NMR (500 MHz, DMSO-d$_6$) δ_H 8.83 (1H, s, H-2), 8.50 (1H, dd, *J*= 4.5, 2.0 Hz, H-6), 8.39 (1H, d, *J*= 5.2 Hz, H-6'), 8.22 (1H, d, *J*= 9.0 Hz, H-4), 7.36 (1H, t, *J*= 7.7 Hz, H-5''), 7.25 (1H, d, *J*= 5.2 Hz, H-5'), 7.22 (1H, s, H-2''), 7.19 – 7.12 (3H, m, H-1'', 3'' and 5), 3.50 (3H, s, H-1'''), 2.33 (3H, s, H-1''''); ^{13}C NMR (125 MHz, DMSO-d$_6$) δ_C 161.7 (C-2'), 158.7 (C-4'), 158.1 (C-6'), 145.6 (C-1'''), 143.9 (C-6), 139.6 (C-2), 138.5 (C-3''), 132.4 (C-3a), 129.04 (C-4 or C-5''), 129.00 (C-4 or C-5''), 127.7 (C-2''), 126.3 (C-1'' or C-3''), 124.0 (C-1'' or C-3''), 118.4 (C-5), 110.1 (C-3), 106.1 (C-5'), 38.1 (C-1'''), 21.0 (C-1''''); HRMS *m/z* (ESI$^+$) [Found: 317.1509., $C_{18}H_{17}N_6$ requires [M + H]$^+$ 317.1509]; LCMS (MDAP): Rt = 17.4 min, >95% (Method 3); *m/z* (ESI$^+$) 317.1 [M + H]$^+$

N-(3-Methoxyphenyl)-*N*-methyl-4-pyrazolo[1,5-*b*]pyridazin-3-yl-pyrimidin-2-amine **90**

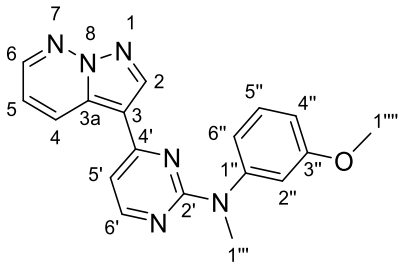

To a solution of *N*-(3-methoxyphenyl)-4-pyrazolo[1,5-*b*]pyridazin-3-yl-pyrimidin-2-amine (80 mg, 0.25 mmol) in DMF (8mL) was added sodium hydride (20 mg, 0.83 mmol) followed by iodomethane (0.04 mL, 0.64 mmol). The reaction was stirred under nitrogen for 2 h. The reaction was concentrated under reduced pressure. The crude was dissolved in EtOAc (10 mL) and washed with 0.1 M LiCl solution (20 mL). The aqueous was extracted two further times with EtOAc (2 x 10 mL). The combined organics were washed with brine (30 mL), then dried over $MgSO_4$, filtered and concentrated under reduced pressure. The residue was triturated with diethyl ether to afford the title compound, *N*-(3-methoxyphenyl)-*N*-methyl-4-pyrazolo[1,5-*b*]pyridazin-3-yl-pyrimidin-2-amine, **90**, as an off-white solid (56 mg, 0.16 mmol, 64% yield). R_f 0.70 (MeOH/ CH_2Cl_2 1:9); m.p. 184-186 °C; $\bar{\nu}_{max}$ (neat)/cm^{-1} 3099 (C-H, w), 3045 (C-H, w), 2924 (C-H, w), 1624 (C=N, m), 1563 (C=C, m), 1527 (C=C, m); ^{1}H NMR (500 MHz, DMSO-d$_6$) δ_H 8.85 (1H, s, H-2), 8.54 – 8.49 (1H, m, H-6), 8.41 (1H, d, *J*= 5.2 Hz, H-6'), 8.32 – 8.27 (1H, m, H-4), 7.40 (1H, t, *J*= 7.9 Hz, H-5''), 7.28 (1H, d, *J*= 5.2 Hz, H-5'), 7.18 (1H, dd, *J*= 9.1, 4.5 Hz, H-5), 7.01 – 6.96 (2H, m, H-2'' and 6''), 6.94 – 6.90 (1H, m, H-4''), 3.77 (3H, s, 1''''), 3.53 (3H, s, H-1'''); ^{13}C NMR (150 MHz, DMSO-d$_6$) δ_C 161.6 (C-2'), 159.9 (C-3''), 158.7 (C-4''), 158.0 (C-6'), 146.8 (C-1''), 143.8 (C-6), 139.6 (C-2), 132.34 (C-3a), 129.7 (C-5''), 129.1 (C-4), 119.2 (C2'' or C-6''), 118.3 (C-5), 113.1 (C2'' or C-6'') , 111.1 (C-4''), 110.1 (C-3), 106.2 (C-5'), 55.2 (C-1''''), 38.0 (C-1'''); HRMS *m/z* (ESI$^+$) [Found: 333.1454., $C_{18}H_{17}N_6O$ requires [M + H]$^+$ 333.1458]; LCMS (MDAP): Rt = 16.5 min, >95% (Method 3); *m/z* (ESI$^+$) 333.1 [M + H]$^+$

N-[2-Methoxy-4-(4-methylpiperazin-1-yl)phenyl]-4-pyrazolo[1,5-*b*]pyridazin-3-yl-pyrimidin-2-amine **92**

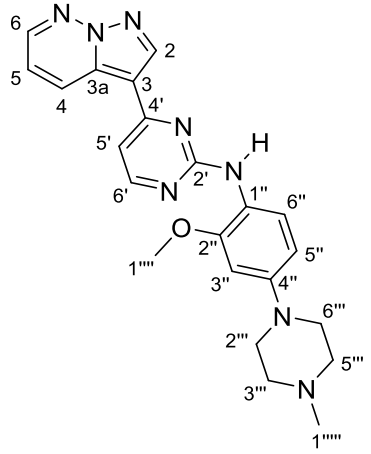

To a solution of (*E*)-3-(dimethylamino)-1-pyrazolo[1,5-*b*]pyridazin-3-yl-prop-2-en-1-one (80 mg, 0.37 mmol) in DMF (1 mL) in a sealed and degassed microwave vial was added 1-[2-methoxy-4-(4-methylpiperazin-1-yl)phenyl]guanidine; nitric acid (240 mg, 0.74 mmol), and potassium carbonate (150 mg, 1.11 mmol). The vial was heated to 110 °C for 16 h. The reaction mixture was concentrated under reduced pressure. The residue was purified using flash reverse phase column chromatography on a Biotage system (12 g C-18, elution with 10-100% acetonitrile / water gradient). Desired fractions were combined and concentrated under reduced pressure to afford the title compound, *N*-[2-methoxy-4-(4-methylpiperazin-1-yl)phenyl]-4-pyrazolo[1,5-*b*]pyridazin-3-yl-pyrimidin-2-amine, **92**, as a yellow solid (60 mg, 0.14 mmol, 37% yield). R_f 0.33 (MeOH/ CH_2Cl_2 1:9); m.p. 78-79 °C; $\bar{\nu}_{max}$ (neat)/cm^{-1} 3263 (N-H, m), 2941 (C-H, w), 2801 (C-H, w), 1619 (C=N, w), 1571 (C=C, s), 1545 (C=C, s), 1203 (C-O, s); ^{1}H NMR (500 MHz, DMSO-d$_6$) δ_H 8.82 (2H, m, H-2 and 4), 8.59 – 8.49 (1H, m, H-6), 8.32 (1H, d, *J* = 5.3 Hz, H-6'), 8.27 (1H, s, NH), 7.51 (1H, d, *J* = 8.6 Hz, H-5''), 7.33 – 7.26 (1H, m, H-5), 7.22 (1H, d, *J* = 5.2 Hz, H-5'), 6.66 (1H, s, H-3''), 6.53 (1H, d, *J* = 8.4 Hz, H-6''), 3.77 (3H, s, H-1''''), 3.16 (4H, t, *J* = 4.8 Hz, H-2''' and 6'''), 2.49 – 2.44 (4H, m, H-3''' and 5'''), 2.23 (3H, s, H-1'''''); ^{13}C NMR (125 MHz, DMSO-d$_6$) δ_C 161.3 (C-2'), 159.2 (C-4'), 158.2 (C-6'), 152.8 (C-2''), 149.2 (C-4''), 144.0 (C-6), 139.6 (C-2), 132.5 (C-3a), 129.8 (C-4), 125.5 (C-5''), 120.2 (C-1''), 118.5 (C-5), 110.2 (C-3), 106.8 (C-6''), 106.5 (C-5'), 100.2 (C-3''), 55.5 (C-1''''), 54.8 (C-3''' and 5'''), 48.8 (C-2''' and 6'''), 45.8 (C-1'''''); HRMS *m/z* (ESI$^+$) [Found: 417.2148., $C_{22}H_{24}N_8O$ requires [M + H]$^+$ 417.2146]; LCMS (LCQ): Rt = 0.5 min (Method 1); *m/z* (ESI$^+$) 417.3 [M + H]$^+$; LCMS (MDAP): Rt = 9.2 min, >95% (Method 3); *m/z* (ESI$^+$) 417.2 [M + H]$^+$.

4-Pyrazolo[1,5-*b*]pyridazin-3-ylpyrimidin-2-amine **94**

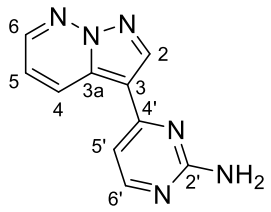

To a microwave vial containing 3-(2-chloropyrimidin-4-yl)pyrazolo[1,5-*b*]pyridazine (80 mg, 0.35 mmol) in 2-propanol (2 mL) was added ammonium hydroxide (2 mL, 29.59 mmol). The reaction mixture was irradiated with microwaves at 150 °C for 20 min. The reaction mixture was concentrated under reduced pressure. The residue was purified using flash silica column chromatography on an Isco Combiflash system (12 g silica, elution with 0-50% 20% MeOH in CH_2Cl_2 / CH_2Cl_2 gradient) to afford the title compound, 4-pyrazolo[1,5-*b*]pyridazin-3-ylpyrimidin-2-amine, **94**, as an off-white solid (50 mg, 0.2 mmol, 58% yield). m.p. 258-260°C; $\bar{\nu}_{max}$ (neat)/cm^{-1} 3350 (N-H, s), 3146 (N-H, s), 1624 (C=N, v), 1572 (C=C, s), 1562 (C=C, s); ^{1}H NMR (600 MHz, DMSO-d$_6$) δ_H 9.16 (1H, dd, *J* = 9.0, 2.0 Hz, H-4), 8.80 (1H, s, H-2), 8.59 (1H, dd, *J* = 4.4, 2.0 Hz, H-6), 8.25 (1H, d, *J* = 5.2 Hz, H-6'), 7.42 (1H, dd, *J* = 9.0, 4.4 Hz, H-5), 7.11 (1H, d, *J* = 5.2 Hz, H-5'), 6.66 (2H, s, NH_2); ^{13}C NMR (150 MHz, DMSO-d$_6$) δ_C 164.5 (C-2'), 159.3 (C-4'), 158.3 (C-6'), 143.9 (C-6), 139.4 (C-2), 132.4 (C-3a), 129.8 (C-4), 118.4 (C-5), 110.2 (C-3), 105.4 (C-5'); HRMS *m/z* (ESI$^+$) [Found: 213.0885., $C_{10}H_8N_6$ requires [M + H]$^+$ 213.0883]; LCMS (LCQ): Rt = 0.6 min (Method 1); *m/z* (ESI$^+$) 213.3 [M + H]$^+$; LCMS (MDAP): Rt = 8.2 min, >95% (Method 3); *m/z* (ESI$^+$) 213.1 [M + H]$^+$

N-Methyl-4-pyrazolo[1,5-*b*]pyridazin-3-yl-pyrimidin-2-amine **95**

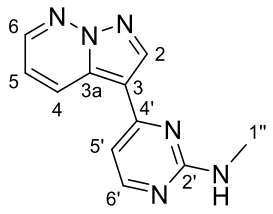

To a microwave vial containing 3-(2-chloropyrimidin-4-yl)pyrazolo[1,5-*b*]pyridazine (80 mg, 0.35 mmol) in 2-propanol (2 mL) was added methylamine (0.02 mL, 0.69 mmol). The reaction mixture was heated to 110 °C for 2 h. The reaction mixture was concentrated under reduced pressure. The residue was purified using flash silica column chromatography on an Isco Combiflash system (12 g silica, elution with 0-50% 20% MeOH in CH_2Cl_2 / CH_2Cl_2 gradient) to afford the title compound, **95**, as an off-white solid (60 mg, 0.24 mmol, 68% yield).m.p. 214-215 °C; $\bar{\nu}_{max}$ (neat)/cm^{-1} 3267 (N-H, m), 3099 (C-H, w), 1619 (C=N, w), 1573 (C=C, s), 1545 (C=C, s); ^{1}H NMR (500 MHz, DMSO-d$_6$) δ_H 8.99 (1H, s, 1H,H-4), 8.72 (1H, s, H-2), 8.49 (1H, dd, *J* = 4.5, 1.9 Hz, 1H, H-6), 8.22 – 8.14 (1H, m, H-6'), 7.35 (1H, dd, *J* = 9.1, 4.5 Hz, H-5), 7.12 – 6.93 (2H, m, H-5' and NH), 2.82 (3H, s, H-1''); ^{13}C NMR (125 MHz, DMSO-d$_6$) δ_C 162.8 (C-2'), 159.2 (C-4'), 158.2 (C-6'), 144.0 (C-6), 139.5 (C-2), 132.5 (C-3a), 129.6 (C-4), 118.8 (C-5), 110.5 (C-3), 105.1 (C-5'), 28.0 (C-1''); HRMS *m/z* (ESI$^+$) [Found: 227.1041., $C_{11}H_{10}N_6$ requires [M + H]$^+$ 227.1040]; LCMS (LCQ): Rt = 0.6 min (Method 1); *m/z* (ESI$^+$) 227.3 [M + H]$^+$; LCMS (MDAP): Rt = 3.1 min, >95% (Method 3); *m/z* (ESI$^+$) 227.1 [M + H]$^+$.

N,N-Dimethyl-4-pyrazolo[1,5-*b*]pyridazin-3-yl-pyrimidin-2-amine **96**

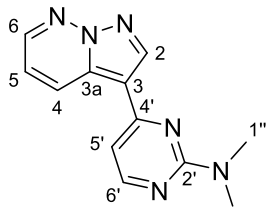

To a microwave vial containing 3-(2-chloropyrimidin-4-yl)pyrazolo[1,5-*b*]pyridazine (80 mg, 0.35 mmol) was added dimethylamine (0.03 mL, 0.69 mmol). The reaction mixture was heated at 110 °C for 2 h. The reaction mixture was concentrated under reduced pressure. The residue was purified using flash silica column chromatography on an Isco Combiflash system (12 g silica, elution with 0-50% 20% MeOH in CH_2Cl_2 / CH_2Cl_2 gradient) to afford the title compound, *N,N*-dimethyl-4-pyrazolo[1,5-*b*]pyridazin-3-yl-pyrimidin-2-amine, **96**, as an off-white solid (70 mg, 0.26 mmol, 77% yield). R_f 0.68 (MeOH/ CH_2Cl_2 1:9); m.p. 241 - 242 °C; $\bar{\nu}_{max}$ (neat)/cm^{-1} 2988 (C-H, w), 2928 (C-H, s), 2860 (C-H, w), 2790 (C-H, w), 1623 (C=N, w), 1566 (C=C, s), 1520 (C=C, m); ^{1}H NMR (500 MHz, DMSO-d$_6$) δ_H 8.95 (1H, dd, *J* = 9.0, 1.9 Hz, H-4), 8.83 (1H, s, H-2), 8.60 – 8.57 (1H, m, H-6), 8.35 (1H, d, *J* = 5.2 Hz, H-6'), 7.45 (1H, dd, *J* = 9.0, 4.4 Hz, H-5), 7.13 (1H, d, *J* = 5.2 Hz, H-5'), 3.21 (6H, s, H-1''); ^{13}C NMR (125 MHz, DMSO-d$_6$) δ_C 161.9 (C-2'), 159.9 (C-4'), 157.9 (C-6'), 143.9 (C-6), 139.7 (C-2), 132.3 (C-3a), 129.1 (C-4), 118.9 (C-5), 110.5 (C-3), 104.6 (C-5'), 37.0 (C-1''); HRMS *m/z* (ESI$^+$) [Found: 241.1197., $C_{12}H_{12}N_6$ requires [M + H]$^+$ 241.1196]; LCMS (LCQ): Rt = 0.6 min (Method 1); *m/z* (ESI$^+$) 241.3 [M + H]$^+$; LCMS (MDAP): Rt = 3.6 min, >95% (Method 3); *m/z* (ESI$^+$) 241.0 [M + H]$^+$

N-Cyclopropyl-4-pyrazolo[1,5-*b*]pyridazin-3-yl-pyrimidin-2-amine **97**

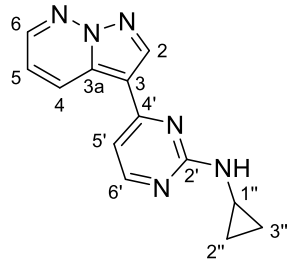

To a microwave vial containing 3-(2-chloropyrimidin-4-yl)pyrazolo[1,5-*b*]pyridazine (80 mg, 0.35 mmol) in 2-propanol (1 mL) was added cyclopropylamine (0.02 mL, 0.35 mmol). The vial was sealed and irradiated with microwaves at 150 °C for 20 min. The reaction mixture was concentrated under reduced pressure. The residue was purified using flash silica column chromatography on an Isco Combiflash system (12 g silica, elution with 0-100% 10% MeOH in CH_2Cl_2 / CH_2Cl_2 gradient) to afford the title compound, *N*-cyclopropyl-4-pyrazolo[1,5-*b*]pyridazin-3-yl-pyrimidin-2-amine, **97**, as an off-white solid (30 mg, 0.11 mmol, 30% yield). m.p. 210 -212 °C; $\bar{\nu}_{max}$ (neat)/cm^{-1} 3224 (N-H, m), 3170 (N-H, m), 3071 (C-H, w), 3035 (C-H, w), 2996 (C-H, w), 1624 (C=N, w); ^{1}H NMR (500 MHz, DMSO-d$_6$) δ_H 9.18 (1H, d, *J* = 9.1 Hz, H-4), 8.82 (1H, s, H-2), 8.61-8.53 (1H, m, H-6), 8.29 (1H, d, *J* = 5.1 Hz, H-6'), 7.43 (1H, dd, *J* = 9.1 Hz, 4.5 Hz, H-5), 7.40 (1H, s, NH), 7.15 (1H, d, *J* = 5.1 Hz, H-5'), 2.85-2.70 (1H, m, H-1''), 0.81 – 0.72 (2H, m, H-2'' and 3''), 0.55-0.49 (2H, m, H-2'' and 3''); ^{13}C NMR (150 MHz, DMSO-d$_6$) δ_C 163.3 (C-2'), 159.0 (C-4'), 158.1 (C-6'), 143.9 (C-6), 139.4 (C-2), 132.5 (C-3a), 129.7 (C-4), 118.6 (C-5), 110.2 (C-3), 105.5 (C-5'), 23.8 (C-1''), 6.5 (C-2'' and C-3''); HRMS *m/z* (ESI$^+$) [Found 253.1199., $C_{13}H_{12}N_6$ requires [M + H]$^+$ 253.1196]; LCMS (LCQ): Rt = 0.6 min (Method 1); *m/z* (ESI$^+$) 253.3 [M + H]$^+$; LCMS (MDAP): Rt = 9.5 min, >95% (Method 3); *m/z* (ESI$^+$) 253.1 [M + H]$^+$. The spectroscopic data are in good agreement with the literature values. Literature reference: Stevens, Kirk L.; Reno, Michael J.; Alberti, Jennifer B.; Price, Daniel J.; Kane-Carson, Laurie S.; Knick, Victoria B.; Shewchuk, Lisa M.; Hassell, Anne M.; Veal, James M.; Davis, Stephen T.; Griffin, Robert J.; Peel, Michael R. Bioorganic and Medicinal Chemistry Letters, 2008 , vol. 18, # 21 p. 5758 – 5762. WO2004/35588 A1, 2004 ;p 35

N-Cyclopropyl-*N*-methyl-4-pyrazolo[1,5-*b*]pyridazin-3-yl-pyrimidin-2-amine **98**

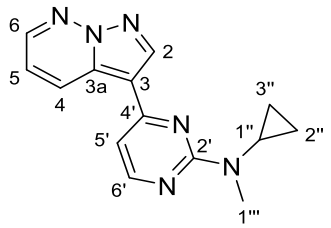

To a microwave vial containing 3-(2-chloropyrimidin-4-yl)pyrazolo[1,5-*b*]pyridazine (80 mg, 0.35 mmol) in 2-propanol (2 mL) was added *N*-cyclopropyl-methylamine hydrochloride (74 mg, 0.69 mmol). The vial was sealed and heated at 150 °C for 30 min under microwave irradiation. The reaction was concentrated under reduced pressure. The crude was purified using flash silica column chromatography on an Isco Combiflash system (12 g silica, elution with 0-50% 20% MeOH in CH_2Cl_2 / CH_2Cl_2 gradient) to afford the title compound, *N*-cyclopropyl-*N*-methyl-4-pyrazolo[1,5-*b*]pyridazin-3-yl-pyrimidin-2-amine, **98**, as an off-white solid (10 mg, 0.04 mmol, 10% yield). m.p. 162-164 °C; $\bar{\nu}_{max}$ (neat)/cm^{-1} 2982 (C-H, w), 2947 (C-H, w), 2852 (C-H, w), 1622 (C=N, m), 1563 (C=C, m), 1526 (C=C, m); ^{1}H NMR (500 MHz, DMSO-d$_6$) δ_H 9.11 (1H, d, *J* = 9.0 Hz, H-4), 8.86 (1H, s, H-2), 8.60 – 8.57 (1H, m, H-6), 8.38 (1H, d, *J* = 5.1 Hz, H-6'), 7.46 (1H, dd, *J* = 9.0, 4.4 Hz, H-5), 7.23 (1H, d, *J* = 5.1 Hz, H-5'), 3.15 (3H, s, H-1'''), 2.90 – 2.80 (1H, m, H-1''), 0.95 – 0.89 (2H, m, H-2'' and 3''), 0.67 (2H, p, *J* = 4.6 Hz, H-2'' and 3''); ^{13}C NMR (125 MHz, DMSO-d$_6$) δ_C 163.2 (C-2'), 158.8 (C-4'), 157.84 (C-6'), 144.0 (C-6), 139.7 (C-2), 132.5 (C-3a), 129.4 (C-4), 118.9 (C-5), 110.4 (C-3), 105.7 (C-5'), 35.72 (C-1'''), 31.56 (C-2'' and 3''), 8.29 (C-2'' and 3''); HRMS *m/z* (ESI$^+$) [Found: 267.1348., $C_{14}H_{15}N_6$ requires [M + H]$^+$ 267.1353]; LCMS (LCQ): Rt = 0.6 min (Method 1); *m/z* (ESI$^+$) 267.2 [M + H]$^+$; LCMS (MDAP): Rt = 9.93 min, >95% (Method 3); *m/z* (ESI$^+$) 267.1 [M + H]$^+$.

N-(2-Methoxyethyl)-4-pyrazolo[1,5-*b*]pyridazin-3-yl-pyrimidin-2-amine **99**

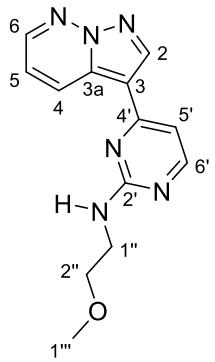

To a microwave vial containing 3-(2-chloropyrimidin-4-yl)pyrazolo[1,5-*b*]pyridazine (80 mg, 0.35 mmol) in 2-propanol (2 mL) was added 2-methoxyethanamine (0.04 mL, 0.41 mmol). The reaction mixture was heated to 110 °C for 4 h. The reaction mixture was concentrated *under reduced pressure*. The residue was purified using flash silica column chromatography on an Isco Combiflash system (12 g silica, elution with 0-50% 20% MeOH in CH_2Cl_2 / CH_2Cl_2 gradient) to afford the title compound, *N*-(2-methoxyethyl)-4-pyrazolo[1,5-*b*]pyridazin-3-yl-pyrimidin-2-amine, **99**, as an off-white solid (60 mg 0.21 mmol, 61% yield). m.p. 146-148 °C; $\bar{\nu}_{max}$ (neat)/cm^{-1} 3239 (N-H, m), 3226 (N-H, m), 3046 (C-H, w), 2988 (C-H, w), 2929 (C-H, s), 2902 (C-H, s), 1624 (C=N, v), 1571 (C=C, s), 1543 (C=C, s); ^{1}H NMR (500 MHz, MeOD) δ_H 9.07 (1H, d, *J* = 9.1 Hz, H-4), 8.63 (1H, s, H-2), 8.47 (1H, dd, *J* = 4.4, 2.0 Hz, H-6), 8.22 (1H, d, *J* = 5.3 Hz, H-6'), 7.35 (1H, dd, *J* = 9.1, 4.4 Hz, H-5), 7.07 (1H, d, *J* = 5.3 Hz, H-5'), 3.75 – 3.55 (4H, m, H-1'' and 2''), 3.41 (3H, s, H-1'''); ^{13}C NMR (125 MHz, MeOD) δ_C 163.7 (C-2'), 161.6 (C-4'), 158.8 (C-6'), 145.0 (C-6), 140.4 (C-2), 134.3 (C-3a), 130.9 (C-4), 119.8 (C-5), 112.1 (C-3), 106.8 (C-5'), 72.3 (C-2''), 59.1 (C-1'''), 42.1 (C-1''); HRMS *m/z* (ESI$^+$) [Found: 271.1304., $C_{13}H_{14}N_6O$ requires [M + H]$^+$ 271.1302]; LCMS (LCQ): Rt = 0.5 min (Method 1); *m/z* (ESI$^+$) 271.1 [M + H]$^+$; LCMS (MDAP): Rt = 3.5 min, >95% (Method 3); *m/z* (ESI$^+$) 271.1 [M + H]$^+$

N-(3-Methoxypropyl)-4-pyrazolo[1,5-*b*]pyridazin-3-yl-pyrimidin-2-amine **100**

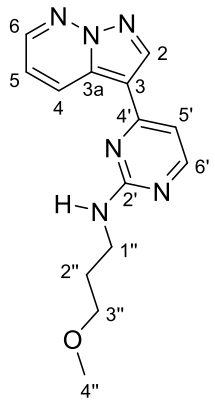

To a microwave vial containing 3-(2-chloropyrimidin-4-yl)pyrazolo[1,5-*b*]pyridazine (80 mg, 0.35 mmol) in 2-propanol (2 mL) was added methoxypropylamine (0.04 mL, 0.41 mmol). The reaction mixture was heated to 110 °C for 4 h. The reaction mixture was concentrated under reduced pressure. The residue was purified using flash silica column chromatography on an Isco Combiflash system (12 g silica, elution with 0-50% 20% MeOH in CH_2Cl_2 / CH_2Cl_2 gradient) to afford the title compound, *N*-(3-methoxypropyl)-4-pyrazolo[1,5-*b*]pyridazin-3-yl-pyrimidin-2-amine, **100**, as off-white solid (70 mg, 0.23 mmol, 68% yield). R_f 0.50 (MeOH/ CH_2Cl_2 1:9); m.p. 125-127 °C; $\bar{\nu}_{max}$ (neat)/cm^{-1} 3255 (N-H, m) 3156 (N-H, m), 3066 (C-H, w), 2927 (C-H, s), 2880 (C-H, s), 2815 (C-H, w), 1621 (C=N, m), 1570 (C=C, s), 1541 (C=C, s); ^{1}H NMR (500 MHz, MeOD) δ_H 9.13 (1H, d, *J* = 9.1 Hz, H-4), 8.64 (1H, s, H-2), 8.48 (1H, dd, *J* = 4.4, 1.9 Hz, H-6), 8.20 (1H, d, *J* = 5.3 Hz, H-6'), 7.35 (1H, dd, *J* = 9.1, 4.4 Hz, H-5), 7.06 (1H, d, *J* = 5.3 Hz, H-5'), 3.59 – 3.51 (4H, m, H-1''and 3''), 3.37 (3H, s, H-4''), 2.01 – 1.87 (2H, m, H-2''); ^{13}C NMR (125 MHz, MeOD) δ_C 163.7 (C-2'), 161.6 (C-4'), 158.8 (C-6'), 145.0 (C-6), 140.3 (C-2), 134.3 (C-3a), 131.1 (C-4), 119.8 (C-5), 112.2 (C-3), 106.4 (C-5'), 71.8 (C-3''), 59.0 (C-4''), 39.9 (C-1''), 30.7 (C-2''); HRMS *m/z* (ESI$^+$) [Found: 285.1462., $C_{11}H_9N_5$ requires [M + H]$^+$ 285.1458]; LCMS (LCQ): Rt = 0.5 min (Method 1); *m/z* (ESI$^+$) 285.2 [M + H]$^+$; LCMS (MDAP): Rt = 3.5 min, >95% (Method 3); *m/z* (ESI$^+$) 285.1 [M + H]$^+$

N-(3-Methoxypropyl)-*N*-methyl-4-pyrazolo[1,5-*b*]pyridazin-3-yl-pyrimidin-2-amine **101**

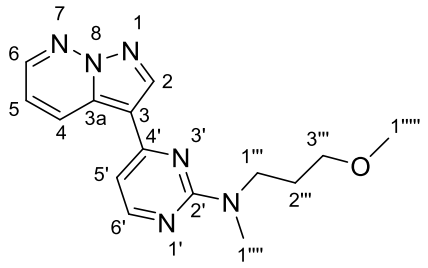

To a microwave vial containing 3-(2-methylsulfonylpyrimidin-4-yl)pyrazolo[1,5-*b*]pyridazine (80 mg, 0.26 mmol) in 2-propanol (3mL) was added 3-methoxypropylamine (0.05 mL, 0.52 mmol). The vial was sealed and was heated overnight at 140 °C. The reaction was concentrated under reduced pressure. The crude was purified using flash silica column chromatography on an Isco Combiflash system (12 g silica, elution with 0-50% 20% MeOH in CH_2Cl_2 / CH_2Cl_2 gradient). Desired fractions were combined and concentrated under reduced pressure. The crude was dissolved in THF (5 mL) and cooled in an ice bath. Sodium hydride (140 mg, 5.83 mmol) was added and the reaction mixture was stirred for 10 min before iodomethane (0.06 mL, 0.96 mmol) was added. The reaction was allowed to warm to rt and was stirred overnight. The reaction mixture was quenched with addition of water and then concentrated under reduced pressure. The crude was purified using flash silica column chromatography on an Isco Combiflash system (12 g silica, elution with 0-50% 20% MeOH in CH_2Cl_2 / CH_2Cl_2 gradient). Desired fractions were combined and concentrated under reduced pressure. The crude was purified using flash reverse phase column chromatography on a Biotage system (12 g C-18, elution with 10-100% MeOH / water gradient) to afford the title compound, *N*-(3-methoxypropyl)-*N*-methyl-4-pyrazolo[1,5-*b*]pyridazin-3-yl-pyrimidin-2-amine, **101**, as a pale yellow oil (6 mg, 0.02 mmol, 7% yield). R_f 0.51 (EtOAc); m.p. 174-176 °C; $\bar{\nu}_{max}$ (neat)/cm^{-1} 2968 (C-H, w), 2919 (C-H, w), 2856 (C-H, w), 1620 (C=N, m), 1563 (C=C, m), 1527 (C=C, m); ^{1}H NMR (600 MHz, MeOD) δ_H 8.97 (1H, dd, *J* = 9.0, 1.9 Hz, H-4), 8.58 (1H, s, H-2), 8.44 (1H, dd, *J* = 4.4, 1.9 Hz, H-6), 8.22 (1H, d, *J* = 5.3 Hz, H-6'), 7.28 (1H, dd, *J* = 9.0, 4.4 Hz, H-5), 6.96 (1H, d, *J* = 5.3 Hz, H-5'), 3.77 (2H, t, *J* = 7.4 Hz, H-1'''), 3.47 (2H, t, *J* = 5.9 Hz, H-3'''), 3.34 (3H, s, H-1'''''), 3.18 (3H, s, H-1''''), 1.95 – 1.88 (2H, m, H-2'''); ^{13}C NMR (150 MHz, MeOD) δ_C 162.9 (C-2'), 160.9 (C-4'), 158.6 (C-6'), 144.8 (C-6), 140.3 (C-2), 134.1 (C-3a), 130.9 (C-4), 119.7 (C-5), 112.4 (C-3), 105.6 (C-5'), 71.5 (C-3'''), 59.1 (C-1'''''), 48.1 (C-1'''), 36.3 (C-1''''), 28.6 (C-2'''); HRMS *m/z* (ESI$^+$) [Found: 321.1432., $C_{15}H_{18}N_6NaO$ requires [M + Na]$^+$ 321.1434]; LCMS (MDAP): Rt = 11.7 min, >95% (Method 3); *m/z* (ESI$^+$) 299.9 [M + H]$^+$

N-(3-Morpholinopropyl)-4-pyrazolo[1,5-*b*]pyridazin-3-yl-pyrimidin-2-amine **102**

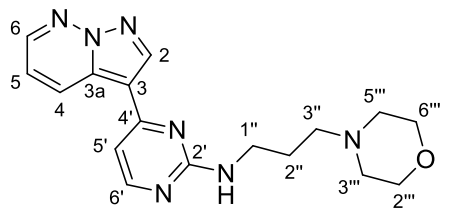

To a microwave vial containing 3-(2-chloropyrimidin-4-yl)pyrazolo[1,5-*b*]pyridazine (80 mg, 0.35 mmol) in 2-propanol (2 mL) was added 3-(morpholin-4-yl)propan-1-amine (0.1 mL, 0.69 mmol). The vial was sealed and heated at 110 °C for 2 h. The reaction mixture was concentrated under reduced pressure. The crude was purified using flash silica column chromatography on an Isco Combiflash system (12 g silica, elution with 0-50% 20% MeOH in CH_2Cl_2 / CH_2Cl_2 gradient) to afford the title compound, *N*-(3-morpholinopropyl)-4-pyrazolo[1,5-*b*]pyridazin-3-yl-pyrimidin-2-amine, **102**, as an off-white solid (70 mg, 0.20 mmol, 57% yield). m.p. 129.7-131.4 °C; $\bar{\nu}_{max}$ (neat)/cm^{-1} 3249 (N-H, m), 2947(C-H, w), 2849 (C-H, w), 2812 (C-H, w), 1622 (C=N, m), 1575 (C=C, m), 1548 (C=C, m); ^{1}H NMR (500 MHz, DMSO-d$_6$) δ_H 9.23 – 8.91 (1H, m, H-4), 8.81 (1H, s, H-2), 8.58 (1H, dd, *J*= 4.5, 1.9 Hz, H-6), 8.26 (1H, d, *J*= 5.1 Hz, H-6’), 7.48 – 7.38 (1H, m, H-5), 7.31 – 7.19 (1H, m, NH), 7.09 (1H, d, *J*= 5.1 Hz, H-5’), 3.62 – 3.47 (4H, m, H-2’’’ and 6’’’), 3.45 – 3.24 (2H, m, H-1’’), 2.36 (6H, d, *J*= 12.2 Hz, H-3’’, 3’’’ and 5’’’), 1.74 (2H, m, H-2’’); ^{13}C NMR (125 MHz, DMSO-d$_6$) δ_C 162.3 (C-2), 159.1 (C-4’), 158.3 (C-6’), 143.9 (C-6), 139.5 (C-2), 132.4 (C-3a), 118.6 (C-5), 109.3 (C-3), 105.1 (C-5’), 66.2 (C-2’’’ and 6’’’), 56.2 (C-3’’), 53.4 (C-3’’’ and 5’’’), 39.3 (C-1’’ under solvent peak), 25.9 (C-2’’); HRMS *m/z* (ESI$^+$) [Found: 340.1868., $C_{17}H_{21}N_7O$ requires [M + H]$^+$ 340.1880]; LCMS (LCQ): Rt = 0.4 min (Method 1); *m/z* (ESI$^+$) 340.1 [M + H]$^+$; LCMS (MDAP): Rt = 5.1 min, >95% (Method 3); *m/z* (ESI$^+$) 340.2 [M + H]$^+$

N-Methyl-4-pyrazolo[1,5-*b*]pyridazin-3-yl-N-(3,3,3-trifluoropropyl)pyrimidin-2-amine **103**

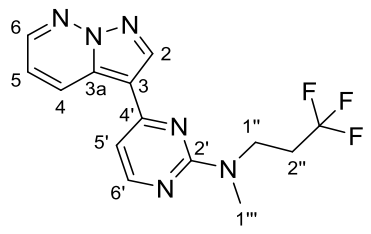

To a microwave vial containing 3-(2-chloropyrimidin-4-yl)pyrazolo[1,5-*b*]pyridazine (80 mg, 0.35 mmol) in 2-propanol (1 mL) was added 3,3,3-trifluoropropylamine (0.05 mL, 0.41 mmol). The vial was sealed and irradiated with microwaves at 140 °C for 35 min. The reaction was concentrated under reduced pressure. The crude was purified using flash silica column chromatography on an Isco Combiflash system (12 g silica, elution with 0-50% 20% MeOH in CH_2Cl_2 / CH_2Cl_2 gradient). Desired fractions were combined and concentrated under reduced pressure. The crude was dissolved in EtOAc (30 mL) and washed with sodium bicarbonate solution (2 x 30 mL). The organic layer was concentrated under reduced pressure. To the residue was added DMF (2 mL) followed by sodium hydride (25 mg, 1.03 mmol) and the mixture stirred in an ice bath for 10 min. Iodomethane (0.02 mL, 0.26 mmol) was added and the reaction mixture was stirred at rt for 2 h. The reaction was concentrated under reduced pressure. The crude was purified using flash silica column chromatography on an Isco Combiflash system (12 g silica, elution with 0-50% 20% MeOH in CH_2Cl_2 / CH_2Cl_2 gradient) to afford the title compound, *N*-methyl-4-pyrazolo[1,5-*b*]pyridazin-3-yl-*N*-(3,3,3-trifluoropropyl)pyrimidin-2-amine, **103**, as an off-white solid (50 mg, 0.15 mmol, 57% yield). R_f 0.63 (EtOAc / petroleum ether 1:1); m.p. 124-126 °C; $\bar{\nu}_{max}$ (neat)/cm^{-1} 3062 (C-H, w), 2979 (C-H, w), 2946 (C-H, w), 1623 (C=N, m), 1564 (C=C, s), 1511 (C=C, m); ^{1}H NMR (500 MHz, DMSO-d$_6$) δ_H 8.80 – 8.67 (2H, m, H-2 and 4), 8.51 – 8.45 (1H, m, H-6), 8.26 (1H, d, *J* = 5.0 Hz, H-6'), 7.35 – 7.22 (1H, m, H-5), 7.06 (1H, d, *J* = 5.0 Hz, H-5'), 3.88 – 3.70 (2H, m, H-1''), 3.10 (3H, s, H-1'''), 2.63 – 2.47 (2H, m, H-2''); ^{13}C NMR (125 MHz, DMSO-d$_6$) δ_C 161.0 (C-2'), 159.1 (C-4'), 158.0 (C-6'), 143.9 (C-6), 139.8 (C-2), 132.3 (C-3a), 128.9 (C-4), 127.0 (q, 276.8 Hz, CF_3), 118.8 (C-5), 110.3 (C-3), 105.2 (C-5'), 42.4 (C-1''), 35.3 (C-1'''), 30.39 (q, *J* = 28.4 Hz, C-2''); HRMS *m/z* (ESI$^+$) [Found: 323.1235., $C_{14}H_{14}F_3N_6$ requires [M + H]$^+$ 323.1227]; LCMS (MDAP): Rt = 18.5 min, >95% (Method 3); *m/z* (ESI$^+$) 323.0 [M + H]$^+$.

N-Methyl-4-{pyrazolo[1,5-*b*]pyridazin-3-yl}-*N*-(4,4,4-trifluorobutyl)pyrimidin-2-amine **104**

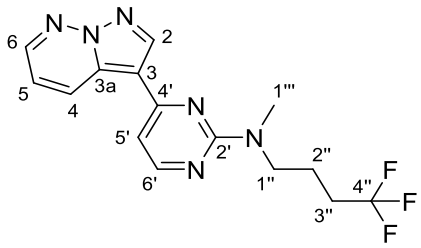

To a microwave vial containing 3-(2-chloropyrimidin-4-yl)pyrazolo[1,5-*b*]pyridazine (80 mg, 0.35 mmol) in 2-propanol (1 mL) was added 4,4,4-trifluorobutylamine (0.06 mL, 0.41 mmol). The vial was sealed and irradiated with microwaves at 140 °C for 35 min. The reaction was concentrated under reduced pressure. The crude was purified using flash silica column chromatography on an Isco Combiflash system (12 g silica, elution with 0-50% 20% MeOH in CH_2Cl_2 / CH_2Cl_2 gradient). Desired fractions were combined and concentrated under reduced pressure. The crude was dissolved in EtOAc (30 mL) and washed with sodium bicarbonate solution (2 x 30 mL). The organic layer was concentrated under reduced pressure. To the residue was added DMF (2 mL) followed by sodium hydride (25 mg, 1.03 mmol) and the mixture stirred in an ice bath for 10 min. Iodomethane (0.02 mL, 0.26 mmol) was added and the reaction mixture was stirred at rt for 2 h. The reaction was concentrated under reduced pressure. The crude was purified using flash silica column chromatography on an Isco Combiflash system (12 g silica, elution with 0-50% 20% MeOH in CH_2Cl_2 / CH_2Cl_2 gradient) to afford the title compound, *N*-methyl-4-pyrazolo[1,5-*b*]pyridazin-3-yl-*N*-(4,4,4-trifluorobutyl)pyrimidin-2-amine, **104**, as an off-white solid (50 mg, 0.14 mmol, 54% yield). R_f 0.63 (EtOAc / petroleum ether 1:1); m.p. 143-145 °C; $\bar{\nu}_{max}$ (neat)/cm^{-1} 3024 (C-H, w), 2979 (C-H, w), 2949 (C-H, w), 1623 (C=N, m), 1564 (C=C, m); ^{1}H NMR (500 MHz, DMSO-d$_6$) δ_H 8.95 – 8.88 (1H, m, H-4), 8.86 (1H, s, H-2), 8.62 – 8.57 (1H, m, H-6), 8.36 (1H, d, *J* = 5.0 Hz, H-6'), 7.45 (1H, dd, *J* = 9.0, 4.5 Hz, H-5), 7.17 (1H, d, *J* = 5.0 Hz, H-5'), 3.81 – 3.66 (2H, m, H-1''), 3.21 (3H, s, H-1'''), 2.40 – 2.24 (2H, m, H-3''), 1.90 – 1.76 (2H, m, H-2''); ^{13}C NMR (125 MHz, DMSO-d$_6$) δ_C 161.4 (C-2'), 159.0 (C-4'), 158.1 (C-6'), 143.9 (C-6), 139.8 (C-2), 132.3 (C-3a), 129.0 (C-4), 128.8 (d, J = 276.2 Hz, C4''), 118.9 (C-5), 110.4 (C-3), 104.9 (C-5'), 47.8 (C-1''), 35.4 (C-1'''), 30.28 (q, J = 27.8 Hz, C-3''), 19.6 (C-2''); HRMS *m/z* (ESI$^+$) [Found: 337.1393., $C_{15}H_{16}F_3N_6$ requires [M + H]$^+$ 337.1383]; LCMS (LCQ): Rt = 2.1 min (Method 1); *m/z* (ESI$^+$) 337.3 [M + H]$^+$; LCMS (MDAP): Rt = 17.4 min, >95% (Method 3); *m/z* (ESI$^+$) 337.0 [M + H]$^+$

N-Isopropyl-*N*-phenyl-4-pyrazolo[1,5-*b*]pyridazin-3-yl-pyrimidin-2-amine **105**

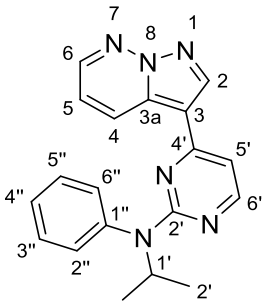

To a microwave vial containing a solution of *N*-phenyl-4-pyrazolo[1,5-*b*]pyridazin-3-yl-pyrimidin-2-amine (10 mg, 0.03 mmol) in DMF (1.75 mL) was added sodium hydride (2.5 mg, 0.10 mmol). The reaction mixture was stirred for 5 min at rt under nitrogen before 2-iodopropane (0.01 mL, 0.09 mmol) was added and the reaction mixture was stirred at rt for 5 h. The reaction mixture was concentrated under reduced pressure. The residue was partitioned between EtOAc (20 mL) and water (20 mL) and the layers separated. The aqueous layer was extracted with EtOAc (20 mL x 2). The combined organic layer was dried over $MgSO_4$, filtered and concentrated under reduced pressure. The crude was purified using flash silica column chromatography on an Isco Combiflash system (12 g silica, elution with 0-100% EtOAc / petroleum ether gradient) to afford a yellow oil. After trituration with petroleum ether the title compound, *N*-isopropyl-*N*-phenyl-4-pyrazolo[1,5-*b*]pyridazin-3-yl-pyrimidin-2-amine, **105**, was obtained as a white solid (11 mg, 0.03 mmol, 91% yield). R_f 0.63 (EtOAc/ petroleum ether 1:1); ^{1}H NMR (500 MHz, MeOD) δ_H 8.58 (1H, s, H-2), 8.36 (1H, dd, *J*= 4.5, 2.0 Hz, H-6), 8.32 (1H, d, *J*= 5.3 Hz, H-6'), 7.74 – 7.64 (1H, m, H-4), 7.61 – 7.55 (2H, m, H-5'' and 3''), 7.55 – 7.49 (1H, m, H-4''), 7.29 – 7.25 (2H, m, H-2'' and 6''), 7.08 (1H, d, *J*= 5.3 Hz, H-5'), 6.94 (1H, dd, *J*= 9.0, 4.5 Hz, H-5), 5.19 (1H, h, *J*= 6.8 Hz, H-1'), 1.25 (6H, d, *J*= 6.8 Hz, H-2'); ^{1}H NMR (600 MHz, DMSO-d_6) δ_H 8.74 (1H, s, H-2), 8.44 (1H, dd, *J* = 4.5, 1.9 Hz, H-6), 8.37 (1H, d, *J* = 5.2 Hz, H-6'), 7.61 – 7.52 (3H, m, H-4, 3'' and 5''), 7.51 – 7.45 (1H, m, H-4''), 7.24 (2H, d, *J* = 7.5 Hz, 2H, H-2''and 6''), 7.15 (1H, d, *J* = 5.2 Hz, H-5'), 7.00 – 6.95 (1H, m, H-5), 5.15 (1H, hept, *J* = 6.7 Hz, H-1'), 1.16 (6H, d, *J* = 6.7 Hz, H-2'); ^{13}C NMR (150 MHz, DMSO-d_6) δ_C 161.8 (C-2'), 158.8 (C-4'), 158.2 (C-6'), 143.9 (C-6), 140.6 (C-1''), 139.5 (C-2), 132.5 (C-3a), 131.4 (C-2'' and C-6''), 129.5 (C-5'' and C-3''), 129.2 (C-4), 127.1 (C-4''), 118.2 (C-5), 110.1 (C-3), 105.5 (C-5'), 46.5 (C-1'), 21.3 (C-2'); LCMS (MDAP): Rt = 14.7 min, >95% (Method 3); *m/z* (ESI$^+$) 331.0 $[M + H]^+$.

N-Ethyl-*N*-(*m*-tolyl)-4-pyrazolo[1,5-*b*]pyridazin-3-yl-pyrimidin-2-amine **106**

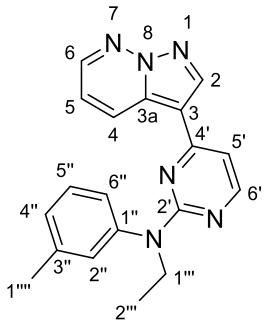

To a microwave vial containing a solution of *N*-(*m*-tolyl)-4-pyrazolo[1,5-*b*]pyridazin-3-yl-pyrimidin-2-amine (10 mg, 0.03 mmol) in DMF (1.66 mL) was added sodium hydride (3.97 mg, 0.10 mmol). The reaction mixture was stirred for 5 min at rt under nitrogen before iodoethane (0.01 mL, 0.08 mmol) was added and the reaction mixture was stirred at rt for 5 h. The reaction mixture was concentrated under reduced pressure. The residue was partitioned between EtOAc (20 mL) and water (20 mL) and the layers separated. The aqueous layer was extracted with EtOAc (20 mL x 2). The combined organic layer was dried over $MgSO_4$, filtered and concentrated under reduced pressure. The crude was purified using flash silica column chromatography on an Isco Combiflash system (12 g silica, elution with 0-100% EtOAc / petroleum ether gradient) to afford a yellow oil. After trituration with petroleum ether the title compound, *N*-ethyl-*N*-(*m*-tolyl)-4-pyrazolo[1,5-*b*]pyridazin-3-yl-pyrimidin-2-amine, **106**, was obtained as a white solid (10 mg, 0.03 mmol, 87% yield). R_f (EtOAc/ petroleum ether 1:1); ^{1}H NMR (500 MHz, MeOD) δ_H 8.59 (1H, s, H-2), 8.38 (1H, dd, *J* = 4.5, 2.0 Hz, H-6), 8.30 (1H, d, *J* = 5.3 Hz, H-6'), 8.05 (1H, d, *J* = 9.1 Hz, H-4), 7.42 (1H, t, *J* = 7.7 Hz, H-5''), 7.26 (1H, d, *J* = 7.6 Hz, H-4''), 7.17 (1H, s, H-2''), 7.13 (1H, d, *J* = 7.9 Hz, H-6''), 7.09 (1H, d, *J* = 5.3 Hz, H-5'), 7.01 (1H, dd, *J* = 9.1, 4.5 Hz, 1H, H-5), 4.07 (2H, q, *J* = 7.1 Hz, H-1'''), 2.41 (3H, s, H-1''''), 1.30 (3H, t, *J* = 7.1 Hz, H-2'''); ^{13}C NMR (150 MHz, MeOD) δ_C 163.0 (C-2'), 160.8 (C-4'), 158.8 (C-6'), 145.9 (C-1''), 144.9 (C-6), 140.8 (C-3''), 140.0 (C-2), 134.3 (C-3a), 131.0 (C-4, 5'' or 2''), 130.6 (C-4, 5'' or 2''), 130.5 (C-4, 5'' or 2''), 128.3 (C-4''), 126.7 (C-6''), 119.3 (C-5), 112.0 (C-3), 106.5 (C-5'), 46.1 (C-1'''), 21.4 (C-1''''), 13.5 (C-2'''); LCMS (MDAP): Rt = 16.0 min, >95% (Method 3); *m/z* (ESI$^+$) 330.9 [M + H]$^+$.

N-Isopropyl-*N*-propyl-4-pyrazolo[1,5-*b*]pyridazin-3-yl-pyrimidin-2-amine **107**

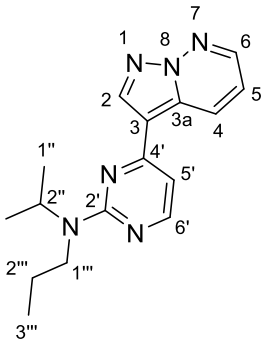

To a pressure vial containing 3-(2-chloropyrimidin-4-yl)pyrazolo[1,5-*b*]pyridazine (60 mg, 0.26 mmol) in 2-propanol (1.5 mL) was added *N*-isopropylpropan-1-amine (26 mg, 0.26 mmol). The vial was sealed and the reaction mixture was heated to 140 °C for 96 h. The reaction mixture was concentrated under reduced pressure. The residue was adsorbed onto solid load adsorbant. The crude was purified using flash silica column chromatography on a Biotage system (12 g silica, elution with 0-100% EtOAc / petroleum ether gradient). Desired fractions were combined and concentrated under reduced pressure. The crude was purified using reverse phase column chromatography on a Biotage system (12 g C-18, elution with 10-100% MeOH / water gradient) to afford the title compound, *N*-isopropyl-*N*-propyl-4-pyrazolo[1,5-*b*]pyridazin-3-yl-pyrimidin-2-amine, **107**, as a colourless oil (14 mg, 0.05 mmol, 18% yield). R_f 0.50 (EtOAc / petroleum ether 1:1); ^{1}H NMR (600 MHz, MeOD) δ_H 8.97 (1H, app d, *J* = 9.1 Hz, H-4), 8.65 (1H, s, H-2), 8.52 – 8.45 (1H, m, H-6), 8.33 – 8.26 (1H, m, H-6'), 7.40 – 7.35 (1H, m, H-5), 7.06 – 7.00 (1H, m, H-5'), 5.10 – 5.01 (1H, m, H-2''), 3.49 (2H, t, *J* = 8.1 Hz, H-1'''), 1.81 – 1.68 (2H, m, H-2'''), 1.30 (6H, d, *J* = 6.7 Hz, H-1''), 1.08 – 0.97 (3H, m, H-3'''); ^{13}C NMR (150 MHz, DMSO-d_6) δ_C 160.9 (C-4'), 158.8 (C-6'), 156.1 (C-2')*, 144.9 (C-6), 140.3 (C-2), 134.0 (C-3a), 130.3 (C-4), 119.6 (C-5), 111.3 (C-3), 105.7 (C-5'), 47.5 (C-2''), 45.2 (C-1'''), 23.6 (C-2'''), 20.7 (C-1''), 11.7 (C-3'''). *Tentatively assigned as C-2' as signal is weak; HRMS *m/z* (ESI$^+$) [Found: 297.1820., $C_{16}H_{21}N_6$ requires [M + H]$^+$ 297.1822]; LCMS (MDAP): Rt = 15.69 min, >95% (Method 3); *m/z* (ESI$^+$) 297.0 [M + H]$^+$

N-Cyclopropyl-*N*-isopropyl-4-pyrazolo[1,5-b]pyridazin-3-yl-pyrimidin-2-amine **108**

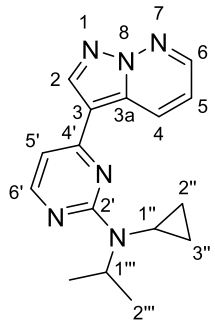

To a microwave vial containing a solution of *N*-cyclopropyl-4-pyrazolo[1,5-*b*]pyridazin-3-yl-pyrimidin-2-amine (10 mg, 0.04 mmol) in DMF (2 mL) was added sodium hydride (4.76 mg, 0.12 mmol) and the reaction mixture was stirred for 5 min at rt under nitrogen. 2-Iodopropane (0.01 mL, 0.10 mmol) was added to the reaction mixture and the reaction mixture was stirred at rt for 5 h. The reaction mixture was concentrated under reduced pressure. The residue was partitioned between EtOAc (20 mL) and water (20 mL) and separated. The aqueous layer was extracted with EtOAc (20 mL) two further times. The combined organic layers were dried over $MgSO_4$, filtered and concentrated under reduced pressure. The reaction was concentrated under reduced pressure. The crude was purified using flash silica column chromatography on an Isco Combiflash system (12 g silica, elution with 0-100% EtOAc / petroleum ether gradient) to afford a yellow oil. After trituration with petroleum ether the title compound, *N*-cyclopropyl-*N*-isopropyl-4-pyrazolo[1,5-*b*]pyridazin-3-yl-pyrimidin-2-amine, **108**, was obtained as a white solid (3 mg, 0.01 mmol, 24% yield). R_f 0.59 (EtOAc/ petroleum ether 1:1); ^{1}H NMR (500 MHz, MeOD) δ_H 9.14 (1H, dd, *J* = 9.1, 2.0 Hz, H-4), 8.69 (1H, s, H-2), 8.50 (1H, dd, *J* = 4.4, 1.9 Hz, H-6), 8.35 (1H, d, *J* = 5.3 Hz, H-6'), 7.39 (1H, dd, *J* = 9.0, 4.5 Hz, H-5), 7.16 (1H, d, *J* = 5.3 Hz, H-5'), 4.73 (1H, hept, *J* = 6.9 Hz, H-1'''), 2.66 (1H, tt, *J* = 7.1, 4.0 Hz, H-1''), 1.46 (6H, d, *J* = 6.9 Hz, H-2'''), 1.04 – 0.98 (2H, m, H-2'' and 3''), 0.78 – 0.73 (2H, m, H-2'' and 3''); ^{13}C NMR (150 MHz, MeOD) δ_C 163.5 (C-2'), 159.3 (C-4'), 158.3 (C-6'), 144.9 (C-6), 140.4 (C-2), 132.7 (C-3a), 130.7 (C-4), 119.7 (C-5), 111.1 (C-3), 106.8 (C-5'), 52.0 (C-1'''), 27.7 (C-1''), 21.8 (C-2'''), 9.8 (C-2'' and C-3''); LCMS (MDAP): Rt = 4.13 min, >95% (Method 3); *m/z* (ESI$^+$) 295.0 $[M + H]^+$

N-(2-Methoxyethyl)-N-propyl-4-pyrazolo[1,5-*b*]pyridazin-3-yl-pyrimidin-2-amine **109**

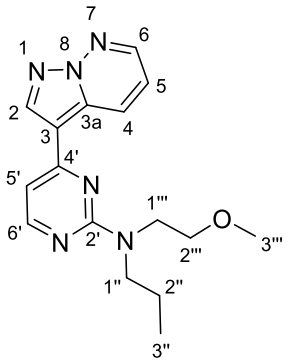

To a microwave vial containing a suspension of 3-(2-chloropyrimidin-4-yl)pyrazolo[1,5-*b*]pyridazine (80 mg, 0.35 mmol) in 2-propanol (2 mL) was added *N*-(2-methoxyethyl)propan-1-amine (81 mg, 0.69 mmol). The vial was sealed and the reaction mixture heated to 140 °C and stirred overnight. The reaction mixture was concentrated under reduced pressure. The crude was purified using flash silica column chromatography on an Isco Combiflash system (12 g silica, elution with 0-100% EtOAc / petroleum ether gradient). Desired fractions were combined and concentrated under reduced pressure. The crude was purified using reverse phase column chromatography on a Biotage system (12 g C-18, elution with 10-100% MeOH / water gradient) to afford the title compound, *N*-(2-methoxyethyl)-*N*-propyl-4-pyrazolo[1,5-*b*]pyridazin-3-yl-pyrimidin-2-amine, **109**, as a white solid (6 mg, 0.02 mmol, 5% yield). R_f 0.40 (EtOAc / petroleum ether 1:1); ^{1}H NMR (600 MHz, MeOD) δ_H 9.00 (1H, dd, *J*= 9.1, 2.0 Hz, H-4), 8.66 (1H, s, H-2), 8.51 – 8.48 (1H, m, H-6), 8.30 (1H, d, *J*= 5.2 Hz, H-6'), 7.39 – 7.34 (1H, m, H-5), 7.06 (1H, d, *J*= 5.2 Hz, H-5'), 3.88 (2H, d, *J*= 6.8 Hz, H-1'''), 3.69 (4H, t, *J*= 6.9 Hz, H-2''' and 1''), 3.40 (3H, s, H-1''''), 1.80 – 1.67 (2H, m, H-2''), 1.00 (3H, t, *J*= 7.6 Hz, H-3''); ^{13}C NMR (150 MHz, MeOD) δ_C 162.7 (C-2'), 161.0 (C-4'), 158.9 (C-6'), 144.9 (C-6), 140.3 (C-2), 134.1 (C-3a), 130.5 (C-4), 119.7 (C-5), 112.5 (C-3), 105.9 (C-5'), 71.7 (C-2'''), 59.2 (C-1''''), 51.9 (C-1''), 21.9 (C-2''), 11.6 (C-3''); HRMS *m/z* (ESI$^+$) [Found: 313.1769., $C_{16}H_{21}N_6O$ requires [M + H]$^+$ 313.1771]; LCMS (MDAP): Rt = 14.5 min, >95% (Method 3); *m/z* (ESI$^+$) 313.0 [M + H]$^+$.

3-[2-(Azetidin-1-yl)pyrimidin-4-yl]pyrazolo[1,5-*b*]pyridazine **110**

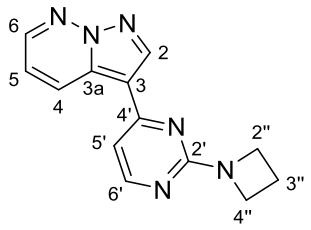

To a microwave vial containing 3-(2-chloropyrimidin-4-yl)pyrazolo[1,5-*b*]pyridazine (80 mg, 0.35 mmol) in 2-propanol (2 mL) was added azetidine (0.03 mL, 0.52 mmol). The vial was sealed and heated to 140 °C for 5 h. The reaction was concentrated under reduced pressure. The crude was purified using flash silica column chromatography on an Isco Combiflash system (12 g silica, elution with 0-100% EtOAc / petroleum ether gradient) to afford the title compound, 3-[2-(azetidin-1-yl)pyrimidin-4-yl]pyrazolo[1,5-*b*]pyridazine, **110**, as a pale yellow solid (46 mg, 0.17 mmol, 50% yield). R_f 0.23 (EtOAc / petroleum ether 1:1); m.p. 212-214 °C; $\bar{\nu}_{max}$ (neat)/cm^{-1} 3065 (C-H, w), 3009 (C-H, w), 2983 (C-H, w), 2871 (C-H, m), 1623 (C=N, m), 1565 (C=C, m), 1527 (C=C, m); ^{1}H NMR (500 MHz, DMSO-d$_6$) δ_H 8.99 – 8.91 (1H, m, H-4), 8.84 (1H, s, H-2), 8.62 – 8.55 (1H, m, H-6), 8.33 (d, *J*= 5.2 Hz, H-6'), 7.44 (1H, dd, *J*= 9.1, 4.4 Hz, H-5), 7.19 (1H, d, *J*= 5.2 Hz, H-5'), 4.13 (4H, t, *J*= 7.6 Hz, H-2'' and 4''), 2.35 (2H, p, *J*= 7.4 Hz, H-3''); ^{1}H NMR (600 MHz, DMSO-d$_6$) δ_H 8.94 – 8.88 (1H, m, H-4), 8.82 – 8.77 (1H, m, H-2), 8.59 – 8.52 (1H, m, H-6), 8.33 – 8.25 (1H, m, H-6'), 7.44 – 7.37 (1H, m, H-5), 7.18 – 7.11 (1H, m, H-5'), 4.20 – 3.98 (4H, m, H-2'' and 4''), 2.38 – 2.26 (2H, m, H-3''); ^{13}C NMR (150 MHz, DMSO-d$_6$) δ_C 162.7 (C-2'), 159.1 (C-4'), 158.0 (C-6'), 143.9 (C-6), 139.6 (C-2), 132.5 (C-3a), 129.4 (C-4), 118.9 (C-5), 110.1 (C-3), 105.4 (C-5'), 49.8 (C-2'' and C-4''), 15.8 (C-3''); HRMS *m/z* (ESI$^+$) [Found: 253.1198., $C_{13}H_{13}N_6$ requires [M + H]$^+$ 253.1196]; LCMS (MDAP): Rt = 13.3 min, >95% (Method 3); *m/z* (ESI$^+$) 253.0 [M + H]$^+$.

4-{Pyrazolo[1,5-*b*]pyridazin-3-yl}-2-(pyrrolidin-1-yl)pyrimidine **111**

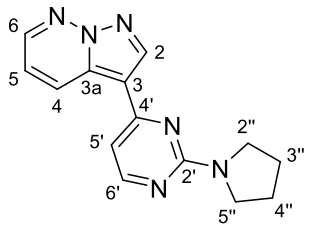

To a microwave vial containing 3-(2-chloropyrimidin-4-yl)pyrazolo[1,5-*b*]pyridazine (80 mg, 0.35 mmol) in 2-propanol (2 mL) was added pyrrolidine (0.03 mL, 0.41 mmol). The vial was sealed and heated to 140 °C for 5 h. The reaction mixture was concentrated under reduced pressure. The crude was purified using reverse phase column chromatography on a Biotage system (12 g C-18, elution with 10-100% MeOH / water gradient) to afford title compound, 3-(2-pyrrolidin-1-ylpyrimidin-4-yl)pyrazolo[1,5-*b*]pyridazine, **111**, as a bronze solid (25.mg, 0.09 mmol, 26% yield). R_f 0.43 (EtOAc / petroleum ether 1:1); Decomposed > 248 °C; $\bar{\nu}_{max}$ (neat)/cm^{-1} 3095 (C-H, w), 3062 (C-H, w), 2957 (C-H, w), 1623 (C=N, m), 1564 (C=C, m), 1532 (C=C, m); ^{1}H NMR (500 MHz, DMSO-d$_6$) δ_H 8.90 – 8.81 (2H, m, H-2 and 4), 8.62 – 8.57 (1H, m, H-6), 8.35 (1H, d, *J* = 5.1 Hz, H-6'), 7.46 (1H, dd, *J* = 9.0, 4.5 Hz, H-5), 7.16 (1H, d, *J* = 5.1 Hz, H-5'), 3.79 – 3.66 (4H, m, H-2'' and 5''), 2.84 – 2.73 (4H, m, H-3'' and 4'').

^{13}C NMR (125 MHz, DMSO-d$_6$) δ_C 160.0 (C-2'), 158.0 (C-6'), 143.9 (C-6), 139.6 (C-2), 132.4 (C-3a), 129.4 (C-4), 118.9 (C-5), 110.9 (C-3), 104.5 (C-5'), 46.4 (C-2'' and C-5''), 25.1 (C-3'' and C-4''); HRMS *m/z* (ESI$^+$) [Found: 267.1358., $C_{14}H_{15}N_6$ requires [M + H]$^+$ 267.1353]; LCMS (LCQ): Rt = 0.5 min (Method 1); *m/z* (ESI$^+$) 267.3 [M + H]$^+$; LCMS (MDAP): Rt = 13.5 min, >95% (Method 3); *m/z* (ESI$^+$) 267.0 [M + H]$^+$.

3-[2-(1-Piperidyl)pyrimidin-4-yl]pyrazolo[1,5-*b*]pyridazine **112**

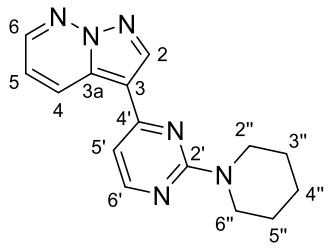

To a microwave vial containing 3-(2-chloropyrimidin-4-yl)pyrazolo[1,5-*b*]pyridazine (80 mg, 0.35 mmol) in 2-propanol (2 mL) was added piperidine (0.04 mL, 0.52 mmol). The vial was sealed and irradiated with microwaves at 140 °C for 22 min. The reaction was concentrated under reduced pressure. The crude was purified using flash silica column chromatography on an Isco Combiflash system (12 g silica, elution with 0-100% 10% MeOH in CH_2Cl_2 / CH_2Cl_2 gradient) to afford the title compound, 3-[2-(1-piperidyl)pyrimidin-4-yl]pyrazolo[1,5-*b*]pyridazine, **112**, as a pale orange solid (70 mg, 0.24 mmol, 69% yield). R_f 0.40 (EtOAc / petroleum ether 1:4); m.p. 162-164 °C; $\bar{\nu}_{max}$ (neat)/cm^{-1} 2987 (C-H, w), 2938 (C-H, w), 2848 (C-H, w), 1620 (C=N, m), 1561 (C=C, s), 1524 (C=C, m); ^{1}H NMR (500 MHz, DMSO-d$_6$) δ_H 8.88 – 8.81 (2H, m, H-2 and 4), 8.62 – 8.57 (1H, m, H-6), 8.35 (1H, d, *J*= 5.1 Hz, H-6'), 7.47 (1H, dd, *J*= 9.0, 4.4 Hz, H-5), 7.13 (1H, d, *J*= 5.1 Hz, H-5'), 3.82 (4H, t, *J*= 5.3 Hz, 4H, H-2'' and 6''), 1.69 – 1.62 (2H, m, H-4''), 1.62 – 1.53 (4H, m, H-3'' and 5''); ^{1}H NMR (600 MHz, DMSO-d$_6$) δ_H 8.86 – 8.76 (2H, m, H-2 and 4), 8.60 – 8.53 (1H, m, H-6), 8.32 (1H, d, *J* = 5.1 Hz, H-6'), 7.44 (1H, dd, *J* = 9.4, 4.4 Hz, H-5), 7.10 (1H, d, *J* = 5.1 Hz, H-5'), 3.85 – 3.72 (4H, m, H-2'' and 6''), 1.68 – 1.51 (6H, m, H-4'', 3'' and 5''); ^{13}C NMR (150 MHz, DMSO-d$_6$) δ_C 161.4 (C-6), 159.0 (C-4'), 158.1 (C-6'), 143.8 (C-6), 139.7 (C-2), 132.2 (C-3a), 128.8 (C-4), 118.9 (C-5), 110.5 (C-3), 105.0 (C-5'), 44.5 (C-2'' and C-6''), 25.3 (C-3'' and C-5''), 24.4 (C-4''); HRMS *m/z* (ESI$^+$) [Found: 281.1513., $C_{15}H_{17}N_6$ requires [M + H]$^+$ 281.1509]; LCMS (MDAP): Rt = 16.6 min, >95% (Method 3); *m/z* (ESI$^+$) 281.0 [M + H]$^+$

3-(2-Piperazin-1-ylpyrimidin-4-yl)pyrazolo[1,5-*b*]pyridazine **113**

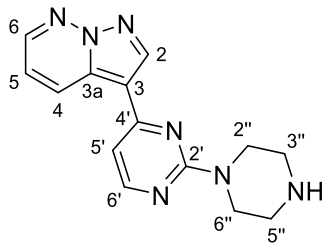

To a microwave vial containing 3-(2-chloropyrimidin-4-yl)pyrazolo[1,5-*b*]pyridazine (80 mg, 0.35 mmol) in 2-propanol (2 mL) was added piperazine (0.06 mL, 0.69 mmol). The vial was sealed and heated to 110 °C for 5 h. The reaction was concentrated under reduced pressure. The crude was purified using flash silica column chromatography on an Isco Combiflash system (12 g silica, elution with 0-100% ammonia/ MeOH/ CH_2Cl_2 1:10:90 gradient) to afford the title compound, 3-(2-piperazin-1-ylpyrimidin-4-yl)pyrazolo[1,5-*b*]pyridazine, **113**, as a peach coloured solid (56 mg, 0.19 mmol, 55% yield). R_f 0.14 (ammonia / MeOH / CH_2Cl_2 1:10:90); m.p. 176-178 °C; $\bar{\nu}_{max}$ (neat)/cm^{-1} 3492 (N-H, w), 3215 (N-H, w), 3095 (C-H, w), 3062(C-H, w), 2938 (C-H, w), 2803 (C-H, w), 1661 (N-H, w), 1623 (C=N, m), 1564 (C=C, m); ^{1}H NMR (500 MHz, DMSO-d_6) δ_H 9.03 – 8.97 (1H, m, H-2), 8.84 (1H, s, H-4), 8.61 – 8.56 (1H, m, H-6), 8.33 (1H, d, *J*= 5.2 Hz, H-6'), 7.45 (1H, dd, *J*= 9.0, 4.5 Hz, H-5), 7.13 (1H, d, *J*= 5.2 Hz, H-5'), 3.76 – 3.43 (4H, m, H-2'' and 6''), 2.07 – 1.89 (4H, m, H-3'' and 5''); ^{1}H NMR (600 MHz, DMSO-d_6) δ_H 8.92 – 8.80 (2H, m, H-2 and 4), 8.67 – 8.55 (1H, m, H-6), 8.40 – 8.31 (1H, m, H-6'), 7.51 – 7.42 (1H, m, H-5), 7.20 – 7.10 (1H, m, H-5'), 3.82 – 3.70 (4H, m, H-2'' and 6''), 2.87 – 2.75 (4H, m, H-3'' and 5''); ^{13}C NMR (150 MHz, DMSO-d_6) δ_C 161.6 (C-2'), 159.0 (C-4'), 158.0 (C-6'), 143.9 (C-6), 139.8 (C-2), 132.2 (C-3a), 129.0 (C-4), 119.0 (C-5), 110.4 (C-3), 105.4 (C-5'), 45.5 (C-3'' and C-5''), 44.8 (C-2'' and C-6''); HRMS *m/z* (ESI^+) [Found: 282.1452., $C_{14}H_{16}N_7$ requires $[M + H]^+$ 282.1462]; LCMS (MDAP): Rt = 12.3 min, >95% (Method 3); *m/z* (ESI^+) 282.0 $[M + H]^+$

3-[2-(4-Methylpiperazin-1-yl)pyrimidin-4-yl]pyrazolo[1,5-*b*]pyridazine **114**

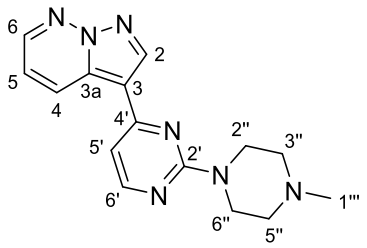

To a microwave vial containing 3-(2-chloropyrimidin-4-yl)pyrazolo[1,5-*b*]pyridazine (80 mg, 0.35 mmol) in 2-propanol (2 mL) was added 1-methylpiperazine (0.07 mL, 0.69 mmol). The vial was sealed and irradiated to 140 °C for 21 min with microwaves. The reaction was concentrated under reduced pressure. The crude was purified using flash silica column chromatography on an Isco Combiflash system (12 g silica, elution with 0-100% ammonia/ MeOH/ CH_2Cl_2 1:10:90 gradient) to afford the title compound, 3-[2-(4-methylpiperazin-1-yl)pyrimidin-4-yl]pyrazolo[1,5-*b*]pyridazine, **114**, as a red-brown solid (80 mg, 0.26 mmol, 75% yield). R_f 0 (EtOAc / petroleum ether 1:1); m.p. 154-156 °C; $\bar{\nu}_{max}$ (neat)/cm^{-1} 3077 (C-H, w), 2938 (C-H, w), 2912 (C-H, w), 2844 (C-H, w), 1623 (C=N, m), 1567 (C=C, s), 1529 (C=C, m); ^{1}H NMR (500 MHz, DMSO-d$_6$) δ_H 8.89 – 8.83 (2H, m, H-2 and 4), 8.62 – 8.58 (1H, m, H-6), 8.37 (d, *J* = 5.2 Hz, H-6'), 7.46 (1H, dd, *J* = 9.0, 4.4 Hz, H-5), 7.18 (1H, d, *J* = 5.2 Hz, H-5'), 3.85 – 3.75 (4H, m, H-2'' and 6''), 2.44 – 2.37 (4H, m, H-3'' and 5''), 2.23 (3H, s, H-1'''); ^{1}H NMR (600 MHz, DMSO-d$_6$) δ_H 8.84 – 8.74 (2H, m, H-2 and 4), 8.58 – 8.50 (1H, m, H-6), 8.31 (d, *J* = 5.2 Hz, H-6'), 7.40 (1H, dd, *J* = 9.5, 4.8 Hz, H-5), 7.12 (1H, d, *J* = 5.2 Hz, H-5'), 3.81 – 3.68 (4H, m, H-2'' and 6''), 2.42 – 2.29 (4H, m, H-3'' and 5''), 2.19 (3H, s, H-1'''); ^{13}C NMR (150 MHz, DMSO-d$_6$) δ_C 161.5 (C-2'), 159.1 (C-4'), 158.0 (C-6'), 143.8 (C-6), 139.8 (C-2), 132.2 (C-3a), 128.9 (C-4), 119.0 (C-5), 110.3 (C-3), 105.6 (C-5'), 54.5 (C-3'' and C-5''), 45.8 (C-1'''), 43.5 (C-2'' and C-6''); HRMS *m/z* (ESI$^+$) [Found: 296.1625., $C_{15}H_{18}N_7$ requires [M + H]$^+$ 296.1618]; LCMS (MDAP): Rt = 12.4 min, >95% (Method 3); *m/z* (ESI$^+$) 296.0 [M + H]$^+$

4-(4-Pyrazolo[1,5-*b*]pyridazin-3-ylpyrimidin-2-yl)morpholine **115**

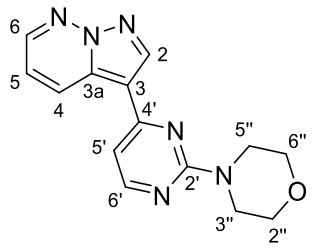

To a microwave vial containing 3-(2-chloropyrimidin-4-yl)pyrazolo[1,5-*b*]pyridazine (80 mg, 0.35 mmol) in 2-propanol (1 mL) was added morpholine (0.05 mL, 0.52 mmol). The vial was sealed and irradiated with microwaves at 140 °C for 22 min. The reaction was concentrated under reduced pressure. The crude was purified using flash reverse phase column chromatography on a Biotage system (12 g silica, elution with 10-100% MeOH / water gradient) to afford the title compound, 4-(4-pyrazolo[1,5-*b*]pyridazin-3-ylpyrimidin-2-yl)morpholine, **115**, as a pale yellow solid (65 mg, 0.22 mmol, 63% yield). R_f 0.45 (EtOAc / petroleum ether 1:1); m.p. 196-198 °C; $\bar{\nu}_{max}$ (neat)/cm^{-1} 2979 (C-H, w), 2923 (C-H, w), 2889 (C-H, w), 2856 (C-H, w), 1620 (C=N, m), 1562 (C=C, m), 1524 (C=C, m), 1115 (C-O, m); ^{1}H NMR (500 MHz, DMSO-d$_6$) δ_H 8.92 – 8.83 (2H, m, H-2 and 4), 8.62 – 8.56 (1H, m, H-6), 8.40 (1H, d, *J*= 5.2 Hz, H-6'), 7.45 (1H, dd, *J*= 9.2, 4.5 Hz, H-5), 7.23 (1H, d, *J*= 5.2 Hz, H-5'), 3.81 – 3.67 (8H, m, H-2'' and 6'', 3'' and 5''); ^{1}H NMR (600 MHz, DMSO-d$_6$) δ_H 8.82 – 8.75 (2H, m, H-2 and 4), 8.53 – 8.50 (1H, m, H-6), 8.34 – 8.26 (1H, m, H-6'), 7.40 – 7.33 (1H, m, H-5), 7.17 – 7.10 (1H, m, H-5'), 3.73 – 3.61 (8H, m, H-2'' and 6'', 3'' and 5''); ^{13}C NMR (150 MHz, DMSO-d$_6$) δ_C 161.6 (C-2'), 159.2 (C-4'), 158.1 (C-6'), 144.0 (C-6), 140.0 (C-2), 132.3 (C-3a), 129.1 (C-4), 119.13 (C-5), 110.3 (C-3), 106.1 (C-5'), 66.1 (C-2'' and C-6''), 44.1 (C-3'' and C-5''); HRMS *m/z* (ESI$^+$) [Found: 283.1309., $C_{14}H_{15}N_6O$ requires [M + H]$^+$ 283.1302]; LCMS (MDAP): Rt = 16.8 min, >95% (Method 3); *m/z* (ESI$^+$) 283.0 [M + H]$^+$

4-Iodo-2-methylsulfanyl-pyrimidine **117**

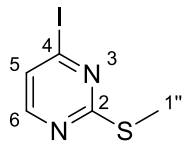

In darkness, 4-chloro-2-(methylthio)pyrimidine (5 g, 31.13 mmol) was added dropwise to hydroiodic acid (25 mL, 332.46 mmol) at 0 °C and the reaction mixture was stirred at 0 °C for 30 min, before warming to rt and stirring for 24 h. Aqueous sodium bicarbonate was then added and the resultant suspension basified to pH 9 by addition of sodium carbonate. The suspension that formed was then filtered and washed with water to afford the desired product, 4-iodo-2-methylsulfanyl-pyrimidine, **117**, as a yellow solid (7.8 g, 29.4 mmol, 94% yield). ^{1}H NMR (500 MHz, DMSO-d_6) δ_H 8.21 (1H, d, *J* = 5.1 Hz, H-6), 7.71 (1H, d, *J* = 5.2 Hz, H-5), 2.48 (3H, s, H-1''). The spectroscopic data are in good agreement with the literature values. Literature reference: ASTRAZENECA AB; ASTRAZENECA UK LIMITED - WO2003/87057, 2003, A1. Location in patent: Page/Page column 63

4-Ethynyl-2-methylsulfanyl-pyrimidine **118**

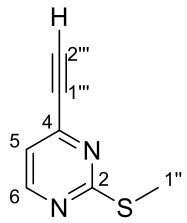

To a solution of 4-iodo-2-methylsulfanyl-pyrimidine (6 g, 23.8 mmol) in DMF (10 mL) was added (trimethylsilyl)acetylene (6.6 mL, 47.64 mmol), TEA (10.12 mL, 72.61 mmol), copper iodide (452 mg, 2.37 mmol), and bis(triphenylphosphine)palladium(II) dichloride (1.08 g, 1.54 mmol). The reaction mixture was heated to 50 °C for 1 h. The reaction mixture was diluted with water (200 mL) and extracted with EtOAc (400 mL x 2). The combined organic layers were dried over $MgSO_4$, filtered, and concentrated under reduced pressure. The crude was purified using flash silica column chromatography on an Isco Combiflash system (12 g silica, elution with 5-40% EtOAc / petroleum ether gradient) to afford a brown oil. To the brown oil was added MeOH (20 mL). Potassium fluoride (1.38 g, 23.8 mmol) was added slowly, and the reaction mixture was stirred at rt for 1h. Water (50 mL) was added and the mixture was extracted with EtOAc (200 mL x 3). The combined organic layers were washed with brine (200 mL), dried over MgSO4, filtered and concentrated under reduced pressure. The crude was purified using flash silica column chromatography on an Isco Combiflash system (12 g silica, elution with 20-50% EtOAc / petroleum ether gradient) to afford the title compound, 4-ethynyl-2-methylsulfanyl-pyrimidine, **118**, as a pale yellow solid (1.1 g, 6.96mmol, 29% yield). ^{1}H NMR (600 MHz, $CDCl_3$) δ_H 8.52 (1H, d, *J* = 5.0 Hz, H-6'), 7.08 (1H, d, *J* = 5.0 Hz, H-5'), 3.35 (1H, s, H-2'''), 2.59 (3H, s, H-1''); LCMS (LCQ): Rt = 0.6 min (Method 1); *m/z* (ESI$^+$) 151.2 [M + H]$^+$; The spectroscopic data are in good agreement with the literature values. Literature reference: F. Tibiletti et al. / Tetrahedron 66 (2010) 1280–1288.

3-(2-Methylsulfanylpyrimidin-4-yl)pyrazolo[1,5-*b*]pyridazine **119**

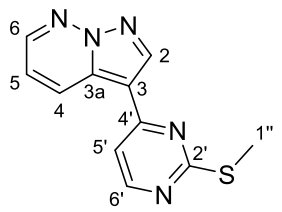

A mixture of (*E*)-3-(dimethylamino)-1-pyrazolo[1,5-*b*]pyridazin-3-yl-prop-2-en-1-one (4.3 g, 19.89 mmol), thiourea (15.13 g, 19.89 mmol) and sodium methoxide (1.29 g, 23.86 mmol) were heated at 90 °C in 1-butanol (10 mL) overnight. The reaction mixture was allowed to cool to 30 °C. Iodomethane (2.48 mL, 39.77 mmol) was then added and the reaction mixture stirred at 30 °C for 4 h. The reaction was concentrated under reduced pressure. Water (50 mL) was added to the residue. A suspension was formed and was filtered to afford the title compound, 3-(2-methylsulfanylpyrimidin-4-yl)pyrazolo[1,5-*b*]pyridazine, **119**, as a brown solid (1.4 g, 5.47 mmol, 27% yield). Decomposed > 178 °C; $\bar{\nu}_{max}$ (neat)/cm^{-1} 3103 (N-H, m), 3069 (C-H, w), 3050 (C-H, w), 3028 (C-H, w), 2919 (C-H, w), 1623 (C=N, m), 1571 (C=C, m); ^{1}H NMR (500 MHz, DMSO-d$_6$) δ_H 8.97 (1H, s, H-2), 8.93 (1H, dd, *J* = 9.1, 2.0 Hz, H-4), 8.64 (1H, dd, *J* = 4.5, 2.0 Hz, H-6), 8.59 (1H, d, *J* = 5.3 Hz, H-6'), 7.72 (1H, d, *J* = 5.3 Hz, H-5'), 7.52 (1H, dd, *J* = 9.1, 4.5 Hz, H-5), 2.62 (3H, s, H-1''); HRMS *m/z* (ESI$^+$) [Found: 244.0649., $C_{11}H_{10}N_5S$ requires [M + H]$^+$ 244.0651]; LCMS (LCQ): Rt = 1.9 min (Method 1); *m/z* (ESI$^+$) 244.2 [M + H]$^+$. The spectroscopic data are in good agreement with the literature values. Literature reference: Tavares FX, Boucheron JA, Dickerson SH, Griffin RJ, Preugschat F, Thomson SA, Wang TY, Zhou HQ. J Med Chem. 2004 Sep 9;47(19):4716-30.

3-(2-Methylsulfonylpyrimidin-4-yl)pyrazolo[1,5-*b*]pyridazine **120**

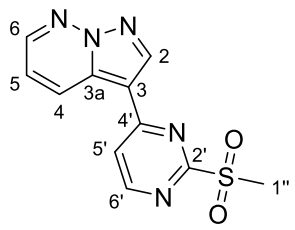

To a suspension of 3-(2-methylsulfanylpyrimidin-4-yl)pyrazolo[1,5-*b*]pyridazine (0.92 g, 3.78 mmol) in CH_2Cl_2 (50 mL), cooled to 0°C, was slowly added 3-chloroperbenzoic acid (2.18 g, 9.45 mmol). Once the addition was complete, the reaction was allowed to warm to rt and was stirred overnight. The reaction mixture was diluted with CH_2Cl_2 (100 mL), quenched with sat.aq. sodium thiosulfate (100 mL), washed with sat. aq. sodium bicarbonate solution (3 x 100 mL) and brine (100 mL), dried over $MgSO_4$, filtered, and concentrated under reduced pressure to afford the desired product, 3-(2-methylsulfonylpyrimidin-4-yl)pyrazolo[1,5-*b*]pyridazine, **120**, as a pale yellow solid (780 mg, 2.55 mmol, 67% yield). R_f 0.24 (EtOAc / petroleum ether 1:1); ^{1}H NMR (600 MHz, DMSO-d_6) δ_H 9.12 (1H, s, H-2), 9.02 – 8.98 (2H, m, H-4 and 6), 8.74 – 8.70 (1H, m, H-6'), 8.30 (1H, d, *J* = 5.4 Hz, H-5'), 7.63 (1H, dd, *J* = 9.1, 4.5 Hz, H-5), 3.51 (3H, s, H-1''); HRMS *m/z* (ESI$^+$) [Found: 298.0365., $C_{11}H_9N_5NaO_2S$ requires [M + Na]$^+$ 298.0369]; LCMS (LCQ): Rt = 0.6 min (Method 1); *m/z* (ESI$^+$) 276.1 [M + H]$^+$. The spectroscopic data are in good agreement with the literature values. Literature reference: Tavares FX, Boucheron JA, Dickerson SH, Griffin RJ, Preugschat F, Thomson SA, Wang TY, Zhou HQ. J Med Chem. 2004 Sep 9;47(19):4716-30.

3-[2-(3-Fluoro-3-methyl-azetidin-1-yl)pyrimidin-4-yl]pyrazolo[1,5-*b*]pyridazine **121**

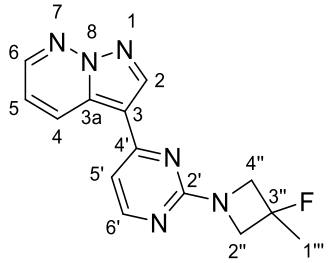

To a microwave vial containing a suspension of 3-fluoro-3-methylazetidine HCl (65 mg, 0.52 mmol) in 2-propanol (1.5 mL) was added 3-(2-chloropyrimidin-4-yl)pyrazolo[1,5-*b*]pyridazine (60 mg, 0.26 mmol). The vial was sealed and the reaction mixture was heated to 140 °C for 16 h. The reaction mixture was concentrated under reduced pressure. The crude was purified using flash silica column chromatography on an Isco Combiflash system (12 g silica, elution with 0-100% EtOAc / petroleum ether gradient) to afford Desired fractions were concentrated under reduced pressure. The crude was purified using reverse phase column chromatography on a Biotage system (12 g C-18, elution with 10-100% MeOH / water gradient) to afford the title compound, 3-[2-(3-fluoro-3-methyl-azetidin-1-yl)pyrimidin-4-yl]pyrazolo[1,5-*b*]pyridazine, **121**, as a pale yellow solid (12 mg, 0.04 mmol, 15% yield). R_f 0.34 (EtOAc / petroleum ether 1:1); m.p. 184-186 °C; $\bar{\nu}_{max}$ (neat)/cm^{-1} 3102 (C-H, w), 2933 (C-H, w), 2867 (C-H, w), 1623 (C=N, m), 1566 (C=C, m), 1526 (C=C, m); ^{1}H NMR (600 MHz, DMSO-d$_6$) δ_H 8.96 (1H, dd, *J* = 9.0, 2.4 Hz, H-4), 8.85 (1H, s, H-2), 8.59 (1H, dd, *J*= 4.4, 2.4 Hz, H-6), 8.36 (1H, d, *J*= 5.2 Hz, H-6'), 7.43 (1H, dd, *J*= 9.0, 4.4 Hz, H-5), 7.26 (1H, d, *J*= 5.2 Hz, H-5'), 4.29 – 4.16 (4H, m, H-2'' and 4''), 1.67 (3H, d, *J*= 22.1 Hz, H-1'''); ^{13}C NMR (150 MHz, DMSO-d$_6$) δ_C 162.8 (C-2'), 159.4 (C-4'), 158.2 (C-6'), 144.1 (C-6), 139.8 (C-2), 132.6 (C-3a), 129.6 (C-4), 119.2 (C-5), 109.9 (C-3), 106.4 (C-5'), 91.54 (d, *J* = 200.6 Hz, C-3''), 61.66 (d, *J* = 25.9 Hz, C-2'' and C-4''), 22.71 (d, *J* = 25.0 Hz, C-1'''); HRMS *m/z* (ESI$^+$) [Found: 285.1249., $C_{14}H_{14}FN_6$ requires [M + H]$^+$ 285.1258]; LCMS (MDAP): Rt = 14.3 min, >95% (Method 3); *m/z* (ESI$^+$) 284.9 [M + H]$^+$

6-(4-{Pyrazolo[1,5-*b*]pyridazin-3-yl}pyrimidin-2-yl)-2-oxa-6-azaspiro[3.3]heptane **122**

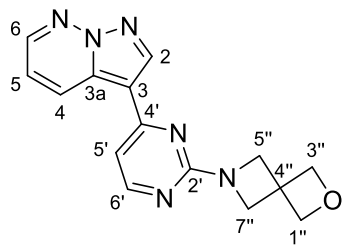

To a microwave vial containing 3-(2-methylsulfonylpyrimidin-4-yl)pyrazolo[1,5-*b*]pyridazine (96 mg, 0.35 mmol) in 2-propanol (2 mL) was added 2-oxa-6-azaspiro[3.3]heptane (35 mg, 0.35 mmol). The vial was sealed and irradiated at 140 °C for 45 min. The reaction mixture was concentrated under reduced pressure. The crude was purified using reverse phase column chromatography on a Biotage system (12 g C-18, elution with 10-100% MeOH / water gradient) to afford the title compound, 6-(4-pyrazolo[1,5-*b*]pyridazin-3-ylpyrimidin-2-yl)-2-oxa-6-azaspiro[3.3]heptane, **122**, as a pale pink solid (10 mg, 0.03 mmol, 9% yield). R_f 0.53 (MeOH/ CH_2Cl_2 1:9); Decomposed > 226°C; $\bar{\nu}_{max}$ (neat)/cm^{-1} 3095 (C-H, w), 2927 (C-H, w), 2863 (C-H, w), 1620 (C=N, m), 1563 (C=C, m), 1522 (C=C, m); ^{1}H NMR (600 MHz, DMSO-d$_6$) δ_H 8.97 (1H, dd, *J* = 9.0, 2.0 Hz, H-4), 8.83 (1H, s, H-2), 8.59 (1H, dd, *J* = 4.4, 2.0 Hz, H-6), 8.33 (1H, d, *J* = 5.2 Hz, H-6'), 7.45 (1H, dd, *J* = 9.0, 4.4 Hz, H-5), 7.21 (1H, d, *J* = 5.2 Hz, H-5'), 4.75 (4H, s, H-1'' and 3''), 4.30 (4H, s, H-5'' and 7''); ^{13}C NMR (150 MHz, DMSO-d$_6$) δ_C 162.6 (C-2'), 159.2 (C-4'), 158.1 (C-6'), 144.0 (C-6), 139.7 (C-2), 132.5 (C-3a), 129.5 (C-4), 119.0 (C-5), 110.0 (C-3), 105.9 (C-5'), 79.9 (C-1'' and C-3''), 59.2 (C-5'' and C-7''), 38.2 (C-4''); HRMS *m/z* (ESI$^+$) [Found: 295.1307., $C_{15}H_{15}N_6O$ requires [M + H]$^+$ 295.1302]; LCMS (LCQ): Rt = 0.5 min (Method 1); *m/z* (ESI$^+$) 295.2 [M + H]$^+$; LCMS (MDAP): Rt = 10.5 min, >95% (Method 3); *m/z* (ESI$^+$) 295.0 [M + H]$^+$.

1-(4-Pyrazolo[1,5-*b*]pyridazin-3-ylpyrimidin-2-yl)-6-oxa-1-azaspiro[3.3]heptane **123**

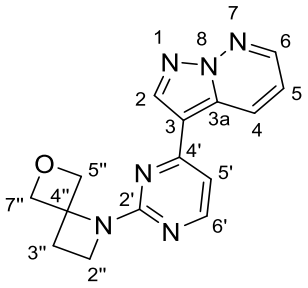

To a pressure vial containing 3-(2-chloropyrimidin-4-yl)pyrazolo[1,5-*b*]pyridazine (60 mg, 0.26 mmol) in 2-propanol (2 mL) was added 6-oxa-1-azaspiro[3.3]heptane (51 mg, 0.52 mmol). The vial was sealed and heated to 140 °C for 16 h. The reaction mixture was concentrated under reduced pressure. The residue was adsorbed onto solid load material. The crude was purified using flash silica column chromatography on a Biotage system (12 g silica, elution with 0-100% EtOAc / petroleum ether gradient). Desired fractions were combined and concentrated under reduced pressure. The crude was purified using reverse phase column chromatography on a Biotage system (12 g C-18, elution with 10-100% MeOH / water gradient) to afford the title compound, 1-(4-pyrazolo[1,5-*b*]pyridazin-3-ylpyrimidin-2-yl)-6-oxa-1-azaspiro[3.3]heptane, **123**, as a colourless solid (17 mg, 0.05 mmol, 21% yield). R_f 0.29 (EtOAc); Decomposed > 246 °C; $\bar{\nu}_{max}$ (neat)/cm^{-1} 3093 (C-H, w), 2931 (C-H, w), 2864 (C-H, w), 1623 (C=N, m), 1563 (C=C, m), 1529 (C=C, m); ^{1}H NMR (600 MHz, MeOD) δ_H 8.74 (1H, s, H-2), 8.51 – 8.48 (1H, m, H-6), 8.33 (1H, d, *J* = 5.3 Hz, H-6'), 7.34 (1H, dd, *J* = 8.9, 4.4 Hz, H-5), 7.24 (1H, d, *J* = 5.3 Hz, H-5'), 5.63 (2H, d, *J* = 7.1 Hz, H-5'' and 7''), 4.90 – 4.79 (2H, m, H-5'' and 7''), 4.02 (2H, t, *J* = 7.1 Hz, H-2''), 2.70 (2H, t, *J* = 7.1 Hz, H-3''). H-4 suspected to be broad signal at δ 9.49; ^{1}H NMR (600 MHz, $CDCl_3$) δ_H 9.56 – 9.22 (1H, m, H-4), 8.53 – 8.44 (1H, m, H-2), 8.38 – 8.29 (2H, m, H-6 and 6'), 7.22 – 7.11 (1H, m, H-5), 7.00 – 6.93 (1H, m, H-5'), 5.76 – 5.46 (2H, m, H-5'' and 7''), 4.89 – 4.67 (2H, m, H-5'' and 7''), 4.13 – 3.87 (2H, m, H-2''), 2.71 – 2.53 (2H, m, H-3''); ^{13}C NMR (150 MHz, $CDCl_3$) δ_C 160.9 (C-2'), 159.8 (C-4'), 158.3 (C-6'), 143.2 (C-6), 139.5 (C-2), 130.5 (C-4), 118.4 (C-5), 110.8 (C-3), 106.2 (C-5'), 81.4 (C-5'' and C-7''), 68.3 (C-4''), 45.6 (C-2''), 29.1 (C-3''); HRMS *m/z* (ESI$^+$) [Found: 295.1301., $C_{15}H_{15}N_6O$ requires [M + H]$^+$ 295.1302]; LCMS (MDAP): Rt = 11.9 min, >95% (Method 3); *m/z* (ESI$^+$) 295.0 [M + H]$^+$

2-(4-{Pyrazolo[1,5-*b*]pyridazin-3-yl}pyrimidin-2-yl)-7-oxa-2-azaspiro[3.5]nonane **124**

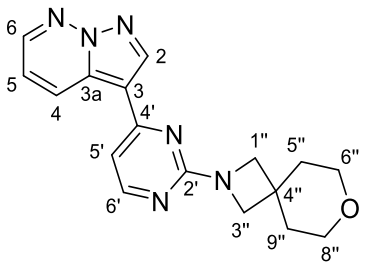

To a microwave vial containing 3-(2-methylsulfonylpyrimidin-4-yl)pyrazolo[1,5-*b*]pyridazine (80 mg, 0.29 mmol) in 2-propanol (2 mL) was added 7-oxa-2-azaspiro[3.5]nonane (74 mg, 0.58 mmol). The vial was sealed and heated to 140 °C overnight. The reaction was concentrated under reduced pressure. The crude was purified using flash silica column chromatography on an Isco Combiflash system (12 g silica, elution with 0-100% 10% MeOH in CH_2Cl_2 / CH_2Cl_2 gradient) to afford the title compound, 2-(4-pyrazolo[1,5-*b*]pyridazin-3-ylpyrimidin-2-yl)-7-oxa-2-azaspiro[3.5]nonane, **124**, as an off-white solid (55 mg, 0.16 mmol, 56% yield). R_f 0.73 (MeOH/ CH_2Cl_2 1:9); Decomposed > 240 °C; $\bar{\nu}_{max}$ (neat)/cm^{-1} 2961 (C-H, w), 2931 (C-H, w), 2859 (C-H, w), 1623 (C=N, m), 1563 (C=C, m), 1528 (C=C, m), 1100 (C-O, m); ^{1}H NMR (500 MHz, DMSO-d$_6$) δ_H 8.98 (1H, dd, *J* = 9.0, 2.0 Hz, H-4), 8.85 (1H, s, H-2), 8.63 – 8.58 (1H, m, H-6), 8.33 (1H, d, *J* = 5.2 Hz, H-6'), 7.45 (1H, dd, *J* = 9.0, 4.4 Hz, H-5), 7.20 (1H, d, *J* = 5.2 Hz, H-5'), 3.89 (4H, s, H-1'' and 3''), 3.58 (4H, t, *J* = 4.9 Hz, H-6'' and 8''), 1.78 (4H, t, *J* = 5.1 Hz, H-5'' and 9''); ^{13}C NMR (125 MHz, DMSO-d$_6$) δ_C 162.6 (C-2'), 159.1 (C-4'), 158.0 (C-6'), 144.0 (C-6), 139.6 (C-2), 132.5 (C-3a), 129.5 (C-4), 119.0 (C-5), 110.0 (C-3), 105.5 (C-5'), 64.1 (C-6'' and C-8''), 59.8 (C-1'' and C-3''), 35.9 (C-5'' and C-9''), 33.2 (C-4''); HRMS *m/z* (ESI$^+$) [Found: 323.1622., $C_{17}H_{19}N_6O$ requires [M + H]$^+$ 323.1615]; LCMS (LCQ): Rt = 4.9 min (Method 1); *m/z* (ESI$^+$) 323.2 [M + H]$^+$; LCMS (MDAP): Rt = 18.6 min, >95% (Method 3); *m/z* (ESI$^+$) 323.0 [M + H]$^+$

3-[2-(2-Methylpyrrolidin-1-yl)pyrimidin-4-yl]pyrazolo[1,5-*b*]pyridazine **125**

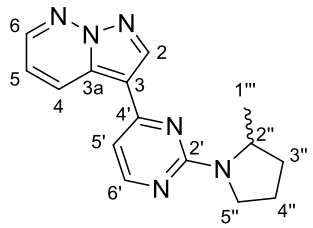

To a microwave vial containing 3-(2-methylsulfonylpyrimidin-4-yl)pyrazolo[1,5-*b*]pyridazine (100 mg, 0.33 mmol) in 2-propanol (1 mL) was added 2-methylpyrrolidine (0.03 mL, 0.33 mmol). The vial was sealed and heated to 140 °C overnight. The reaction mixture was concentrated under reduced pressure. The crude was purified using flash silica column chromatography on an Isco Combiflash system (12 g silica, elution with 0-100% EtOAc / petroleum ether gradient) to afford the title compound 3-[2-(2-methylpyrrolidin-1-yl)pyrimidin-4-yl]pyrazolo[1,5-*b*]pyridazine, **125**, as a white solid (96 mg, 0.33 mmol, 99% yield). R_f 0.38 (EtOAc / petroleum ether 1:1); m.p. 205-207 °C; $\bar{\nu}_{max}$ (neat)/cm^{-1} 2968 (C-H, w), 2942 (C-H, w), 2927 (C-H, w), 2871 (C-H, w), 1623 (C=N, w), 1563 (C=C, s), 1528 (C=C, m); ^{1}H NMR (600 MHz, DMSO-d$_6$) δ_H 8.98 (1H, d, *J* = 9.1 Hz, H-4), 8.84 (1H, s, H-2), 8.60 – 8.57 (1H, m, H-6), 8.34 (1H, d, *J* = 5.0 Hz, H-6'), 7.48 – 7.43 (1H, m, H-5), 7.13 (1H, d, *J* = 5.1 Hz, H-5'), 4.33 (1H, s, H-2''), 3.75 – 3.41 (2H, m, H-5''), 2.12 – 2.01 (2H, m, H-4''), 2.01 – 1.88 (1H, m, H-3''), 1.76 – 1.65 (1H, m, H-3''), 1.34 – 1.12 (3H, m, H-1'''); ^{13}C NMR (150 MHz, DMSO-d$_6$) δ_C 159.8 (C-2'), 158.9 (C-4'), 158.0 (C-6'), 143.9 (C-6), 139.6 (C-2), 132.4 (C-3a), 129.2 (C-4), 118.8 (C-5), 110.4 (C-3), 104.5 (C-5'), 52.6 (C-2''), 46.8 (C-5''), 32.3 (C-3''), 22.8 (C-4''), 19.3 (C-1'''); HRMS *m/z* (ESI$^+$) [Found: 281.1519., $C_{15}H_{17}N_6$ requires [M + H]$^+$ 281.1509]; LCMS (MDAP): Rt = 11.2 min, >95% (Method 3); *m/z* (ESI$^+$) 281.0 [M + H]$^+$.

3-[2-(2,2-Dimethylpyrrolidin-1-yl)pyrimidin-4-yl]pyrazolo[1,5-*b*]pyridazine **126**

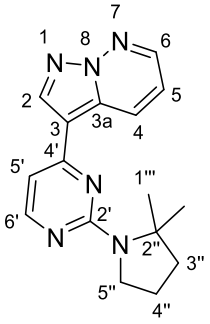

To a pressure vial containing 3-(2-chloropyrimidin-4-yl)pyrazolo[1,5-*b*]pyridazine (60 mg, 0.26 mmol) in 2-propanol (2 mL) was added 2,2-dimethylpyrrolidine (51 mg, 0.52 mmol). The vial was sealed and heated to 140 °C for 16 h. The reaction mixture was concentrated under reduced pressure. The crude was purified using flash silica column chromatography on an Isco Combiflash system (12 g silica, elution with 0-100% EtOAc / petroleum ether gradient) to afford. Desired fractions were combined and concentrated under reduced pressure. The crude was purified using reverse phase column chromatography on a Biotage system (12 g C-18, elution with 10-100% MeOH / water gradient) to afford the title compound, 3-[2-(2,2-dimethylpyrrolidin-1-yl)pyrimidin-4-yl]pyrazolo[1,5-*b*]pyridazine, **126**, as a colourless solid (40 mg, 0.13 mmol, 50% yield). R_f 0.51 (EtOAc / petroleum ether 1:1); m.p. 195-197 °C; $\bar{\nu}_{max}$ (neat)/cm^{-1} 2970 (C-H, w), 2943 (C-H, w), 2924 (C-H, w), 1623 (C=N, m), 1563 (C=C, m), 1527 (C=C, m); ^{1}H NMR (600 MHz, MeOD) δ_H 9.04 (1H, d, *J* = 9.0 Hz, H-4), 8.64 (1H, s, H-2), 8.51 – 8.47 (1H, m, H-6), 8.29 (1H, d, *J* = 5.3 Hz, H-6'), 7.40 – 7.34 (1H, m, H-5), 7.04 – 6.99 (1H, m, H-5'), 3.83 – 3.71 (2H, m, H-5''), 2.05 – 1.95 (4H, m, H-3'' and 4''), 1.64 (6H, s, H-1'''); ^{13}C NMR (150 MHz, MeOD) δ_C 163.2 (C-2'), 160.2 (C-4'), 158.4 (C-6'), 144.8 (C-6), 140.3 (C-2), 133.8 (C-3a), 119.6 (C-5), 111.4 (C-3), 105.4 (C-5'), 62.1 (C-2''), 50.7 (C-5''), 44.6 (C-3''), 26.2 (C-1'''), 22.9 (C-4''). C-4 expected to be weak signal at 129.3 ppm in line with analogues; HRMS *m/z* (ESI$^+$) [Found: 295.1663., $C_{16}H_{19}N_6$ requires [M + H]$^+$ 295.1666]; LCMS (MDAP): Rt = 12.6 min, >95% (Method 3); *m/z* (ESI$^+$) 295.0 [M + H]$^+$

3-[2-[(2*S*)-2-(Methoxymethyl)pyrrolidin-1-yl]pyrimidin-4-yl]pyrazolo[1,5-*b*]pyridazine **127**

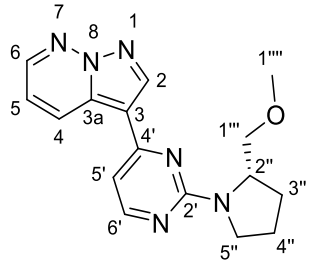

To a pressure vial containing 3-(2-chloropyrimidin-4-yl)pyrazolo[1,5-*b*]pyridazine (60 mg, 0.26 mmol) in 2-propanol (2 mL) was added (2*S*)-2-(methoxymethyl)pyrrolidine (59 mg, 0.52 mmol). The vial was sealed and heated to 140 °C for 16 h. The reaction mixture was concentrated under reduced pressure. The crude was purified using flash silica column chromatography on a Biotage system (12 g silica, elution with 0-100% EtOAc / petroleum ether gradient). Desired fractions were combined and concentrated under reduced pressure. The crude was purified using reverse phase column chromatography on a Biotage system (12 g C-18, elution with 10-100% MeOH / water gradient) to afford the title compound, 3-[2-[(2*S*)-2-(methoxymethyl)pyrrolidin-1-yl]pyrimidin-4-yl]pyrazolo[1,5-*b*]pyridazine, **127**, as a colourless solid (37 mg, 0.11 mmol, 44% yield). R_f 0.25 (1:1 EtOAc / petroleum ether); $[\alpha]_D^{25} = -157.9$ (c = 2.67 x 10^{-3} g / mL, $CHCl_3$); m.p. 145-147 °C; $\bar{\nu}_{max}$ (neat)/cm^{-1} 3032 (C-H, w), 2968 (C-H, w), 2933 (C-H, w), 2916 (C-H, w), 2892 (C-H, w), 2823 (C-H, w), 1623 (C=N, m), 1568 (C=C, m), 1527 (C=C, m); ^{1}H NMR (600 MHz, MeOD) δ_H 9.09 (1H, d, *J* = 9.1 Hz, H-4), 8.68 (1H, s, H-2), 8.52 – 8.48 (1H, m, H-6), 8.30 (1H, d, *J* = 5.2 Hz, H-6'), 7.38 (1H, dd, *J* = 9.1, 4.2 Hz, H-5), 7.11 (1H, d, *J* = 5.2 Hz, H-5'), 4.50 – 4.35 (1H, m, H-2''), 3.86 – 3.37 (7H, m, H-5'', 1''', 1''''), 2.20 – 2.00 (4H, m, H-3'' and 4''); ^{13}C NMR (150 MHz, MeOD) δ_C 161.6 (C-2'), 161.2 (C-4'), 158.7 (C-6'), 144.9 (C-6), 140.3 (C-2), 134.2 (C-3a), 130.8 (C-4), 119.8 (C-5), 112.2 (C-3), 106.0 (C-5'), 73.8 (C-1'''), 59.4 (C-1''''), 58.8 (C-2''), 29.6 (C-3''), 24.3 (C-4''). Signal corresponding to C-5'' suspected to be beneath solvent signal at 48.5 ppm; HRMS *m/z* (ESI^+) [Found: 311.1611., $C_{16}H_{19}N_6O$ requires $[M + H]^+$ 311.1615]; LCMS (MDAP): Rt = 11.7 min, >95% (Method 3); *m/z* (ESI^+) 311.0 $[M + H]^+$

3-[2-(3-Methylpyrrolidin-1-yl)pyrimidin-4-yl]pyrazolo[1,5-*b*]pyridazine **128**

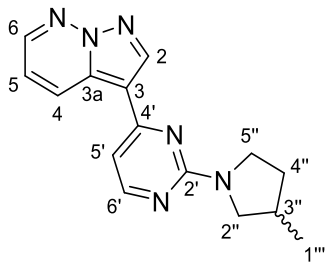

To a microwave vial containing 3-(2-methylsulfonylpyrimidin-4-yl)pyrazolo[1,5-*b*]pyridazine (60 mg, 0.20 mmol) in 2-propanol (1 mL) was added TEA (0.04 mL, 0.29 mmol) and 3-methylpyrrolidine hydrochloride (24 mg, 0.20 mmol). The vial was sealed and heated to 140 °C for 6 h. The reaction mixture was concentrated under reduced pressure. The crude was purified using flash silica column chromatography on an Isco Combiflash system (12 g silica, elution with 0-100% EtOAc / petroleum ether gradient) to afford the title compound, 3-[2-(3-methylpyrrolidin-1-yl)pyrimidin-4-yl]pyrazolo[1,5-*b*]pyridazine, **128**, as a white solid (40 mg, 0.14 mmol, 69% yield). R_f 0.40 (EtOAc / petroleum ether 1:1); m.p. 214-216 °C; $\bar{\nu}_{max}$ (neat)/cm^{-1} 3095 (C-H, w), 3054 (C-H, w), 2961 (C-H, w), 2934 (C-H, w), 2871 (C-H, w), 2841 (C-H, w), 1623 (C=N, m), 1562 (C=C, m), 1527 (C=C, m); ^{1}H NMR (600 MHz, DMSO-d$_6$) δ_H 9.00 (1H, d, *J* = 9.0 Hz, H-4), 8.83 (1H, s, H-2), 8.59 (1H, dd, *J* = 4.4, 1.9 Hz, H-6), 8.33 (1H, d, *J* = 5.2 Hz, H-6'), 7.46 (1H, dd, *J* = 9.0, 4.4 Hz, H-5), 7.12 (1H, d, *J* = 5.2 Hz, H-5'), 3.91 – 3.41 (3H, m, H-5'' and 2''), 3.21 – 3.02 (1H, m, H-2''), 2.44 – 2.28 (1H, m, H-3''), 2.21 – 2.04 (1H, m, H-4''), 1.68 – 1.53 (1H, m, H-4''), 1.12 (3H, s, H-1'''); ^{13}C NMR (150 MHz, DMSO-d$_6$) δ_C 160.0 (C-2'), 159.0 (C-4'), 158.0 (C-6'), 143.9 (C-6), 139.6 (C-2), 132.4 (C-3a), 129.4 (C-4), 118.9 (C-5), 110.4 (C-3), 104.4 (C-5'), 53.4 (C-2''), 46.1 (C-5''), 32.9 (C-3'' or C-4''), 32.6 (C-3'' or C-4''), 17.9 (C-1'''); HRMS *m/z* (ESI$^+$) [Found: 281.1520., $C_{15}H_{17}N_6$ requires [M + H]$^+$ 281.1509]; LCMS (LCQ): Rt = 0.7 min (Method 1); *m/z* (ESI$^+$) 281.0 [M + H]$^+$; LCMS (MDAP): Rt = 11.3 min, >95% (Method 3); *m/z* (ESI$^+$) 281.0 [M + H]$^+$

3-[2-(3,3-Dimethylpyrrolidin-1-yl)pyrimidin-4-yl]pyrazolo[1,5-*b*]pyridazine **129**

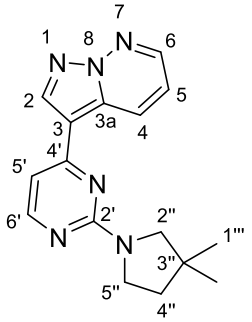

To a high-pressure vial containing 3-(2-methylsulfonylpyrimidin-4-yl)pyrazolo[1,5-*b*]pyridazine (100 mg, 0.33 mmol) in 2-propanol (2 mL) was added 3,3-dimethylpyrrolidine (33 mg, 0.33 mmol). The vial was sealed and heated to 140 °C overnight. The reaction mixture was concentrated under reduced pressure. The crude was purified using flash silica column chromatography on an Isco Combiflash system (12 g silica, elution with 0-100% EtOAc / petroleum ether gradient). Desired fractions were combined and concentrated under reduced pressure. The crude was purified using reverse phase column chromatography on a Biotage system (12 g C-18, elution with 10-100% MeOH / water gradient) to afford the title compound, 3-[2-(3,3-dimethylpyrrolidin-1-yl)pyrimidin-4-yl]pyrazolo[1,5-*b*]pyridazine, **129**, as a pale yellow solid (6 mg, 0.02 mmol, 6% yield). R_f 0.70 (EtOAc / petroleum ether 7:3); ^{1}H NMR (600 MHz, DMSO-d$_6$) δ_H 9.05 – 8.88 (1H, m, H-4), 8.82 (1H, s, H-2), 8.63 – 8.53 (1H, m, H-6), 8.38 – 8.24 (1H, m, H-6'), 7.51 – 7.37 (1H, m, H-5), 7.12 (1H, d, *J*= 5.2 Hz, H-5'), 3.81 – 3.50 (2H, m, H-5''), 3.47 – 3.37 (2H, m, H-2''), 1.79 (2H, s, H-4''), 1.13 (6H, s, H-1'''); ^{13}C NMR (150 MHz, DMSO-d$_6$) δ_C 160.1 (C-2'), 159.0 (C-4'), 158.0 (C-6'), 143.9 (C-6), 139.6 (C-2), 132.3 (C-3a), 129.3 (C-4), 118.9 (C-5), 110.3 (C-3), 104.5 (C-5'), 59.0 (C-2''), 45.7 (C-5''), 38.5 (C-4''), 37.6 (C-3''), 26.2 (C-1'''); HRMS *m/z* (ESI$^+$) [Found: 295.1666., $C_{16}H_{19}N_6$ requires [M + H]$^+$ 295.1666]; LCMS (MDAP): Rt = 12.3 min, >95% (Method 3); *m/z* (ESI$^+$) 295.0 [M + H]$^+$

3-[2-[(3*S*)-3-Methylpyrrolidin-1-yl]pyrimidin-4-yl]pyrazolo[1,5-*b*]pyridazine **130**

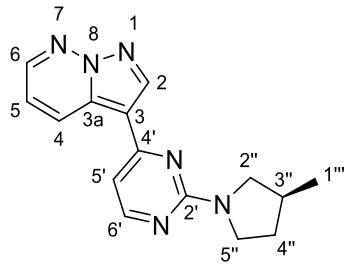

To a microwave vial containing a suspension of 3-(2-chloropyrimidin-4-yl)pyrazolo[1,5-*b*]pyridazine (60 mg, 0.26 mmol) in 2-propanol (2 mL) was added (*S*)-3-methyl-pyrrolidine hydrochloride (63 mg, 0.52 mmol). The vial was sealed and the reaction mixture was heated to 140 °C for 16 h. The reaction mixture was concentrated under reduced pressure. The crude was purified using flash silica column chromatography on an Isco Combiflash system (12 g silica, elution with 0-100% EtOAc / petroleum ether gradient). Desired fractions were combined and concentrated under reduced pressure. The crude was purified using flash reverse phase column chromatography on a Biotage system (12 g silica, elution with 10-100% MeOH / water gradient) to afford the title compound, 3-[2-[(3*S*)-3-methylpyrrolidin-1-yl]pyrimidin-4-yl]pyrazolo[1,5-*b*]pyridazine, **130**, as a colourless solid (21 mg, 0.07 mmol, 27% yield). R_f 0.34 (EtOAc / petroleum ether 1:1); $[\boldsymbol{\alpha}]_{\boldsymbol{D}}^{\mathbf{25}} = -60.1$ (c = 3.3 x 10^{-4} g / mL, $CHCl_3$); m.p. 213-215 °C; $\bar{\nu}_{max}$ (neat)/cm^{-1} 2959 (C-H, w), 2927 (C-H, w), 2871 (C-H, w), 2847 (C-H, w), 1623 (C=N, m), 1563 (C=C, s), 1509 (C=C, s); ^{1}H NMR (600 MHz, DMSO-d_6) δ_H 8.99 (1H, app. d, *J*= 9.0 Hz, H-4), 8.83 (1H, s, H-2), 8.59 (1H, dd, *J*= 4.3, 2.2 Hz, H-6), 8.32 (1H, d, *J*= 5.1 Hz, H-6'), 7.45 (1H, dd, *J*= 9.0, 4.3 Hz, H-5), 7.12 (1H, d, *J*= 5.1 Hz, H-5'), 3.96 – 2.97 (4H, m, H-2'' and 5''), 2.45 – 2.30 (1H, m, H-3''), 2.20 – 2.01 (1H, m, H-4''), 1.67 – 1.55 (1H, m, H-4''), 1.12 (3H, s, H-1'''); ^{13}C NMR (150 MHz, DMSO-d_6) δ_C 159.9 (C-2'), 158.9 (C-4'), 158.0 (C-6'), 143.9 (C-6), 139.6 (C-2), 132.4 (C-3a), 129.3 (C-4), 118.9 (C-5), 110.3 (C-3), 104.4 (C-5'), 53.4 (C-5''), 46.1 (C-2''), 32.9 (C-4''), 32.6 (C-3''), 17.9 (C-1'''); HRMS *m/z* (ESI$^+$) [Found: 281.1508., $C_{15}H_{17}N_6$ requires $[M + H]^+$ 281.1509]; LCMS (MDAP): Rt = 11.6 min, >95% (Method 3); *m/z* (ESI$^+$) 281.0 $[M + H]^+$; Chiral HPLC, Chiralcel OJ column (20:80 heptane : isopropanol (0.2% v/v NH_3), 1.0 ml min^{-1}) Retention Time = 8.04 min > 98% e.e.

3-[2-[(3*R*)-3-Methylpyrrolidin-1-yl]pyrimidin-4-yl]pyrazolo[1,5-*b*]pyridazine **131**

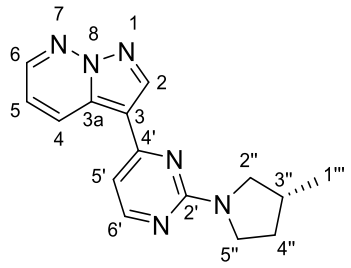

To a microwave vial containing a suspension of 3-(2-chloropyrimidin-4-yl)pyrazolo[1,5-*b*]pyridazine (60 mg, 0.26 mmol) in 2-propanol (2 mL) was added (*R*)-3-methyl-pyrrolidine hydrochloride (63 mg, 0.52 mmol). The vial was sealed and the reaction mixture was heated to 140 °C for 16 h. The reaction mixture was concentrated under reduced pressure. The crude was purified using flash silica column chromatography on an Isco Combiflash system (12 g silica, elution with 0-100% EtOAc / petroleum ether gradient). Desired fractions were combined and concentrated under reduced pressure. The crude was purified using flash reverse phase column chromatography on a Biotage system (12 g silica, elution with 10-100% MeOH / water gradient) to afford the title compound, 3-[2-[(3*R*)-3-methylpyrrolidin-1-yl]pyrimidin-4-yl]pyrazolo[1,5-*b*]pyridazine, **131**, as a pale yellow solid (13 mg, 0.04 mmol, 17% yield). R_f 0.34 (EtOAc / petroleum ether 1:1); $[\boldsymbol{\alpha}]_{\boldsymbol{D}}^{\mathbf{25}} = +60.1$ (c = 3.3 x 10^{-4} g / mL, $CHCl_3$); m.p. 213-215 °C; $\bar{\nu}_{max}$ (neat)/cm^{-1} 2957 (C-H, w), 2934 (C-H, w), 2860 (C-H, w), 2840 (C-H, w), 1622 (C=N, m), 1562 (C=C, s), 1509 (C=C, s); ^{1}H NMR (600 MHz, DMSO-d_6) δ_H 8.99 (1H, app. d, *J*= 9.0 Hz, H-4), 8.83 (1H, s, H-2), 8.59 (1H, dd, *J*= 4.3, 2.2 Hz, H-6), 8.33 (1H, d, *J*= 5.1 Hz, H-6'), 7.46 (1H, dd, *J*= 9.0, 4.3 Hz, H-5), 7.12 (1H, d, *J*= 5.1 Hz, H-5'), 3.93 – 2.88 (4H, m, H-2'' and 5''), 2.44 – 2.29 (1H, m, H-3''), 2.19 – 2.03 (1H, m, H-4''), 1.68 – 1.52 (1H, m, H-4''), 1.12 (3H, s, H-1'''); ^{13}C NMR (150 MHz, DMSO-d_6) δ_C 159.9 (C-2'), 158.9 (C-4'), 158.0 (C-6'), 143.9 (C-6), 139.6 (C-2), 132.4 (C-3a), 129.3 (C-4), 118.9 (C-5), 110.3 (C-3), 104.4 (C-5'), 53.4 (C-5''), 46.1 (C-2''), 32.9 (C-4''), 32.6 (C-3''), 18.0 (C-1'''); HRMS *m/z* (ESI$^+$) [Found: 281.1508., $C_{15}H_{17}N_6$ requires $[M + H]^+$ 281.1509]; LCMS (MDAP): Rt = 11.6 min, >95% (Method 3); *m/z* (ESI$^+$) 281.0 $[M + H]^+$; Chiral HPLC, Chiralcel OJ column (20:80 heptane : isopropanol (0.2% v/v NH_3), 1.0 ml min^{-1}) Retention Time = 7.07 min > 96% e.e.

3-[2-(3,3-Difluoropyrrolidin-1-yl)pyrimidin-4-yl]pyrazolo[1,5-*b*]pyridazine **132**

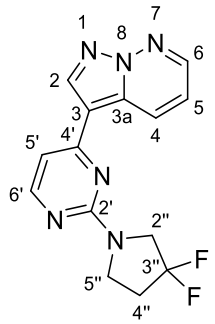

To a microwave vial containing 3-(2-methylsulfonylpyrimidin-4-yl)pyrazolo[1,5-*b*]pyridazine (90 mg, 0.33 mmol) in 2-propanol (1 mL) was added TEA (0.07 mL, 0.49 mmol) and 3,3-difluoropyrrolidine hydrochloride (47 mg, 0.33 mmol). The vial was sealed and irradiated at 140 °C for 5 h. The reaction mixture was concentrated under reduced pressure. The crude was purified using flash silica column chromatography on an Isco Combiflash system (12 g silica, elution with 0-100% EtOAc / petroleum ether gradient) to afford the title compound, 3-[2-(3,3-difluoropyrrolidin-1-yl)pyrimidin-4-yl]pyrazolo[1,5-*b*]pyridazine, **132**, as a white solid (26 mg, 0.08 mmol, 25% yield). R_f 0.47 (EtOAc / petroleum ether 7/3); m.p. 240-242 °C; $\bar{\nu}_{max}$ (neat)/cm^{-1} 3095 (C-H, w), 2926 (C-H, w), 2851 (C-H, w), 1619 (C=N, m), 1565 (C=C, s), 1525 (C=C, m); ^{1}H NMR (600 MHz, DMSO-d$_6$) δ_H 8.99 (1H, d, *J* = 9.0 Hz, H-4), 8.88 (1H, s, H-2), 8.61 (1H, d, *J* = 4.4 Hz, H-6), 8.41 (1H, d, *J* = 5.2 Hz, H-6'), 7.47 (1H, dd, *J* = 9.0, 4.4 Hz, H-5), 7.28 (1H, d, *J* = 5.2 Hz, H-5'), 4.12 – 3.93 (2H, m, H-2''), 3.93 – 3.72 (2H, m, H-5''), 2.63 – 2.53 (2H, m, H-4''); ^{1}H NMR (600 MHz, MeOD) δ_H 9.05 (1H, d, *J* = 9.1 Hz, H-4), 8.70 (1H, s, H-2), 8.52 (1H, d, *J* = 4.5 Hz, H-6), 8.36 (1H, d, *J* = 5.2 Hz, H-6'), 7.42 (1H, dd, *J* = 9.1, 4.5 Hz, H-5), 7.20 (1H, d, *J* = 5.2 Hz, H-5'), 4.05 (2H, app. t, *J* = 12.8 Hz, H-2''), 3.94 – 3.73 (2H, m, H-5), 2.59 (2H, app. tt, J = 14.1, 7.4 Hz, H-4''); ^{13}C NMR (150 MHz, MeOD) δ_C 159.9 (C-2'), 159.0 (C-4'), 158.0 (C-6'), 143.9 (C-6), 139.6 (C-2), 132.4 (C-3a), 129.3 (C-4), 119.0 (C-5), 110.3 (C-3), 104.7 (C-5'), 64.8 (C-3''), 50.6 (C-2''), 45.6 (C-5''), 43.9 (C-1''), 29.6 (C-4''); HRMS *m/z* (ESI$^+$) [Found: 325.0982., $C_{14}H_{12}F_2N_6Na$ requires [M + Na]$^+$ 325.0984]; LCMS (MDAP): Rt = 16.8 min, >95% (Method 3); *m/z* (ESI$^+$) 303.0 [M + H]$^+$

3-[2-[(3*S*)-3-Fluoropyrrolidin-1-yl]pyrimidin-4-yl]pyrazolo[1,5-*b*]pyridazine **133**

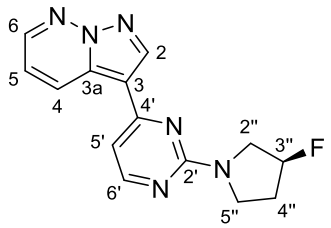

To a microwave vial containing 3-(2-chloropyrimidin-4-yl)pyrazolo[1,5-*b*]pyridazine (67 mg, 0.29 mmol) in 2-propanol (1 mL) was added (*S*)-3-fluoropyrrolidine hydrochloride (36 mg, 0.29 mmol). The vial was sealed and heated to 140 °C for 6 h. The reaction mixture was concentrated under reduced pressure. The crude was purified using flash silica column chromatography on an Isco Combiflash system (12 g silica, elution with 0-100% EtOAc / petroleum ether gradient) to afford the title compound, 3-[2-[(3*S*)-3-fluoropyrrolidin-1-yl]pyrimidin-4-yl]pyrazolo[1,5-*b*]pyridazine, **133**, as a white solid (70 mg, 0.23 mmol, 80% yield). R_f 0.25 (EtOAc / petroleum ether 1:1); $[\boldsymbol{\alpha}]_{\boldsymbol{D}}^{\mathbf{25}} = +47.6$ (c = 2.1 x 10^{-3} g / mL, $CHCl_3$); m.p. 228-230 °C; $\bar{\nu}_{max}$ (neat)/cm^{-1} 3092 (C-H, w), 2983 (C-H, w), 2886 (C-H, w), 2867 (C-H, w), 1620 (C=N, m), 1566 (C=C, m), 1525 (C=C, m); ^{1}H NMR (600 MHz, DMSO-d_6) δ_H 9.02 (1H, d, *J* = 9.0 Hz, H-4), 8.87 (1H, s, H-2), 8.61 (1H, dd, *J* = 4.4, 1.9 Hz, H-6), 8.38 (1H, d, *J* = 5.2 Hz, H-6'), 7.47 (1H, dd, *J* = 9.0, 4.4 Hz, H-5), 7.21 (1H, d, *J* = 5.2 Hz, H-5'), 5.49 (1H, d, *J* = 53.1 Hz, H-3''), 4.09 – 3.44 (4H, m, H-2'' and 5''), 2.34 – 2.14 (2H, m, H-4''); ^{13}C NMR (150 MHz, DMSO-d_6) δ_C 160.0 (C-2'), 159.1 (C-4'), 158.1 (C-4'), 143.9 (C-6), 139.7 (C-2), 132.5 (C-3a), 129.4 (C-4), 119.0 (C-5), 110.2 (C-3), 105.1 (C-5'), 93.2 (d, *J* = 173.4 Hz, C-3''), 53.2 (d, *J* = 22.3 Hz, C-2''), 44.2 (C-5''), 31.6 (d, *J* = 21.2 Hz, C-4''); HRMS *m/z* (ESI$^+$) [Found: 285.1261., $C_{14}H_{14}FN_6$ requires [M + H]$^+$ 285.1258]; LCMS (LCQ): Rt = 0.6 min (Method 1); *m/z* (ESI$^+$) 285.3 [M + H]$^+$; LCMS (MDAP): Rt = 11.6 min, >95% (Method 3); *m/z* (ESI$^+$) 285.0 [M + H]$^+$; Chiral SFC, Lux A2 column (50:50 isopropanol:CO_2 (0.2% v/v NH_3), 4.0 ml min^{-1}) Retention Time = 2.57 min > 97% e.e.

3-[2-[(3*R*)-3-Fluoropyrrolidin-1-yl]pyrimidin-4-yl]pyrazolo[1,5-*b*]pyridazine **134**

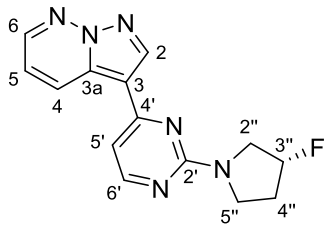

To a microwave vial containing 3-(2-chloropyrimidin-4-yl)pyrazolo[1,5-*b*]pyridazine (67 mg, 0.29 mmol) in 2-propanol (1 mL) was added *R*-(-)-3-fluoropyrrolidine hydrochloride (36 mg, 0.29 mmol). The vial was sealed and heated to 140 °C for 6 h. . The reaction mixture was concentrated under reduced pressure. The crude was purified using flash silica column chromatography on an Isco Combiflash system (12 g silica, elution with 0-100% EtOAc / petroleum ether gradient) to afford the title compound 3-[2-[(3*R*)-3-fluoropyrrolidin-1-yl]pyrimidin-4-yl]pyrazolo[1,5-*b*]pyridazine, **134**, as a cream solid (70 mg, 0.23 mmol, 80% yield). R_f 0.24 (EtOAc / petroleum ether 1:1); $[\boldsymbol{\alpha}]_{\boldsymbol{D}}^{\mathbf{25}} = -60.1$ (c = 3.67 x 10^{-3} g / mL, $CHCl_3$); m.p. 228-230 °C; $\bar{\nu}_{max}$ (neat)/cm^{-1} 3099 (C-H, w), 3061 (C-H, w), 2979 (C-H, w), 2871(C-H, w), 1620 (C=N, m), 1566 (C=C, m), 1525 (C=C, m); ^{1}H NMR (600 MHz, DMSO-d_6) δ_H 9.02 (1H, d, *J* = 9.0 Hz, H-4), 8.87 (1H, s, H-2), 8.61 (1H, dd, *J* = 4.4, 1.9 Hz, H-6), 8.38 (1H, d, *J* = 5.2 Hz, H-6'), 7.47 (1H, dd, *J* = 9.0, 4.4 Hz, H-5), 7.21 (1H, d, *J* = 5.2 Hz, H-5'), 5.49 (1H, d, *J* = 53.4 Hz, H-3''), 4.05 – 3.43 (4H, m, H-2'' and 5''), 2.36 – 2.13 (2H, m, H-4''); ^{13}C NMR (150 MHz, DMSO-d_6) δ_C 160.0 (C-2'), 159.1 (C-4'), 158.1 (C-6'), 143.9 (C-6), 139.7 (C-2), 132.4 (C-3a), 129.4 (C-4), 119.0 (C-5), 110.2 (C-3), 105.1 (C-5'), 93.21 (d, *J* = 170.8 Hz, C-3''), 53.17 (d, *J* = 22.4 Hz, C-2''), 44.2 (C-5''), 31.57 (d, *J* = 21.2 Hz, C-4''); HRMS *m/z* (ESI^+) [Found: 285.1267., $C_{14}H_{14}FN_6$ requires $[M + H]^+$ 285.1258]; LCMS (LCQ): Rt = 0.6 min (Method 1); *m/z* (ESI^+) 285.3 $[M + H]^+$; LCMS (MDAP): Rt = 11.6 min, >95% (Method 3); *m/z* (ESI^+) 285.0 $[M + H]^+$; Chiral SFC, Lux A2 column (50:50 isopropanol:CO_2 (0.2% v/v NH_3), 4.0 ml min^{-1}) Retention Time = 2.04 min > 99% e.e.

N,N-Dimethyl-1-(4-pyrazolo[1,5-*b*]pyridazin-3-ylpyrimidin-2-yl)pyrrolidin-3-amine **135**

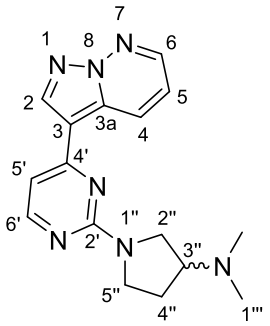

To a high-pressure vial containing 3-(2-methylsulfonylpyrimidin-4-yl)pyrazolo[1,5-*b*]pyridazine (100 mg, 0.33 mmol) in 2-propanol (2 mL) was added *N,N*-dimethylpyrrolidin-3-amine (75 mg, 0.66 mmol). The vial was sealed and heated to 140 °C overnight. The reaction mixture was concentrated under reduced pressure. The reaction was concentrated under reduced pressure. The crude was purified using flash silica column chromatography on an Isco Combiflash system (12 g silica, elution with 0-10% MeOH / CH_2Cl_2 gradient). Desired fractions were combined and concentrated under reduced pressure. The crude was purified using reverse phase column chromatography on a Biotage system (12 g C-18, elution with 10-100% MeOH / water gradient) to afford the title compound, *N,N*-dimethyl-1-(4-pyrazolo[1,5-*b*]pyridazin-3-ylpyrimidin-2-yl)pyrrolidin-3-amine, **135**, as a colourless solid (69.4 mg, 0.21 mmol, 65% yield). R_f 0.38 (MeOH/ CH_2Cl_2 1:9); m.p. 119-121 °C; ^{1}H NMR (600 MHz, DMSO-d_6) δ_H 8.98 (1H, d, *J*= 9.1 Hz, H-4), 8.84 (1H, H-2), 8.59 (1H, d, *J*= 4.3 Hz, H-6), 8.34 (1H, d, *J*= 5.1 Hz, H-6'), 7.51 – 7.41 (1H, m, H-5), 7.15 (1H, d, *J*= 5.1 Hz, H-5'), 3.97 – 3.38 (4H, m, H-2'' and H-5''), 2.91 – 2.71 (1H, m, H-3''), 2.30 – 2.08 (7H, m, H-4'' and H-1'''), 1.90 – 1.80 (1H, m, H-4''); ^{13}C NMR (150 MHz, DMSO-d_6) δ_C 159.9 (C-2'), 159.0 (C-4'), 158.0 (C-6'), 143.9 (C-6), 139.6 (C-2), 132.4 (C-3a), 129.3 (C-4), 119.0 (C-5), 110.3 (C-3), 104.7 (C-5'), 64.8 (C-3''), 50.6 (C-2''), 45.6 (C-5''), 43.9 (C-1''), 29.6 (C-4''); HRMS *m/z* (ESI$^+$) [Found: 310.1770., $C_{16}H_{20}N_7$ requires [M + H]$^+$ 310.1775]; LCMS (MDAP): Rt = 8.16 min, >95% (Method 3); *m/z* (ESI$^+$) 310.0 [M + H]$^+$

(3*S*)-1-(4-pyrazolo[1,5-*b*]pyridazin-3-ylpyrimidin-2-yl)pyrrolidin-3-amine **136**

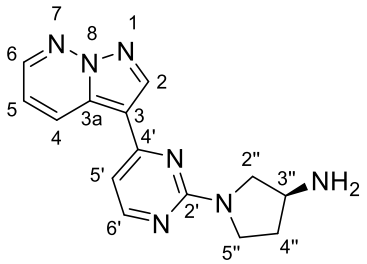

To a microwave vial containing a suspension of 3-(2-chloropyrimidin-4-yl)pyrazolo[1,5-*b*]pyridazine (60 mg, 0.26 mmol) in 2-propanol (2 mL) was added (3*S*)-(-)-3-aminopyrrolidine (22 mg, 0.26 mmol). The vial was sealed and the reaction mixture was heated to 140 °C for 16 h. The reaction mixture was concentrated under reduced pressure. The crude was purified using flash silica column chromatography on an Isco Combiflash system (12 g silica, elution with 0-50% 20% MeOH in CH_2Cl_2 / CH_2Cl_2 gradient) to afford the title compound. Desired fractions were combined and concentrated under reduced pressure. The crude was purified using flash reverse phase column chromatography on a Biotage system (12 g silica, elution with 10-100% MeOH / water gradient) to afford the title compound, (3*S*)-1-(4-pyrazolo[1,5-*b*]pyridazin-3-ylpyrimidin-2-yl)pyrrolidin-3-amine, **136**, as a pale yellow solid (32 mg, 0.11 mmol, 42% yield). R_f 0.09 (MeOH/ CH_2Cl_2 1:9); $[\boldsymbol{\alpha}]_{\boldsymbol{D}}^{\mathbf{25}} = +89.6$ (c = 6.7 x 10^{-4} g / mL, $CHCl_3$); Decomposed > 210 °C; $\bar{\nu}_{max}$ (neat)/cm^{-1} 3341 (N-H, w), 3098 (C-H, w), 2940 (C-H, w), 2859 (C-H, w), 1622 (C=N, m), 1563 (C=C, s), 1528 (C=C, m); ^{1}H NMR (600 MHz, DMSO-d_6) δ_H 8.99 (1H, app. d, *J*= 9.0 Hz, H-4), 8.83 (1H, s, H-2), 8.63 – 8.55 (1H, m, H-6), 8.32 (1H, d, *J*= 5.1 Hz, H-6'), 7.45 (1H, dd, *J*= 9.0, 4.4 Hz, H-5), 7.11 (1H, d, *J*= 5.1 Hz, H-5'), 4.11 – 2.89 (5H, m, H-2'', 3'', 5''), 2.43 – 1.58 (4H, m, H-4'', -NH_2); ^{13}C NMR (150 MHz, DMSO-d_6) δ_C 160.1 (C-2'), 158.9 (C-4'), 158.0 (C-6'), 143.9 (C-6), 139.6 (C-2), 132.4 (C-3a), 129.3 (C-4), 118.8 (C-5), 110.4 (C-3), 104.4 (C-5'), 54.7 (C-2''), 50.7 (C-3''), 44.9 (C-5''), 34.0 (C-4''); HRMS *m/z* (ESI$^+$) [Found: 282.1455., $C_{14}H_{16}N_7$ requires $[M + H]^+$ 282.1462]; LCMS (MDAP): Rt = 8.1 min, >95% (Method 3); *m/z* (ESI$^+$) 282.0 $[M + H]^+$; Chiral HPLC, Lux C1 column (50:50 heptane : EtOH (0.2% v/v NH_3), 1.0 ml min^{-1}) Retention Time = 12.50 min > 99% e.e.

(3*R*)-1-(4-pyrazolo[1,5-*b*]pyridazin-3-ylpyrimidin-2-yl)pyrrolidin-3-amine **137**

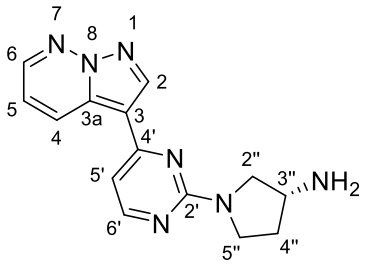

To a microwave vial containing a suspension of 3-(2-chloropyrimidin-4-yl)pyrazolo[1,5-*b*]pyridazine (60 mg, 0.26 mmol) in 2-propanol (2 mL) was added (*R*)-pyrrolidin-3-amine (22 mg, 0.26 mmol). The vial was sealed and the reaction mixture was heated to 140 °C for 16 h. The reaction mixture was concentrated under reduced pressure. The crude was purified using flash silica column chromatography on an Isco Combiflash system (12 g silica, elution with 0-50% 20% MeOH in CH_2Cl_2 / CH_2Cl_2 gradient) to afford the title compound. Desired fractions were combined and concentrated under reduced pressure. The crude was purified using flash reverse phase column chromatography on a Biotage system (12 g silica, elution with 10-100% MeOH / water gradient) to afford the title compound, (3*R*)-1-(4-pyrazolo[1,5-*b*]pyridazin-3-ylpyrimidin-2-yl)pyrrolidin-3-amine, **137**, as a pale yellow solid (36 mg, 0.12 mmol, 44% yield). R_f 0.09 (MeOH/ CH_2Cl_2 1:9); $[\boldsymbol{\alpha}]_{\boldsymbol{D}}^{\mathbf{25}} = -59.7$ (c = 6.7 x 10^{-4} g / mL, $CHCl_3$); Decomposed > 210 °C; $\bar{\nu}_{max}$ (neat)/cm^{-1} 3352 (N-H, w), 3094 (C-H, w), 2933 (C-H, w), 2859 (C-H, w), 1622 (C=N, m), 1563 (C=C, s), 1528 (C=C, m); ^{1}H NMR (600 MHz, DMSO-d_6) δ_H 8.99 (1H, app. d, *J* = 9.0 Hz, H-4), 8.83 (1H, s, H-2), 8.63 – 8.54 (1H, m, H-6), 8.32 (1H, d, *J* = 5.1 Hz, H-6'), 7.45 (1H, dd, *J* = 9.0, 4.4 Hz, H-5), 7.11 (1H, d, *J* = 5.1 Hz, H-5'), 4.01 – 2.74 (5H, m, H-2'', 3'', 5''), 2.43 – 1.59 (4H, m, H-4'', -NH_2); ^{13}C NMR (150 MHz, DMSO-d_6) δ_C 160.1 (C-2'), 158.9 (C-4'), 158.0 (C-6'), 143.9 (C-6), 139.6 (C-2), 132.4 (C-3a), 129.3 (C-4), 118.8 (C-5), 110.4 (C-3), 104.4 (C-5'), 54.7 (C-2''), 50.7 (C-3''), 44.9 (C-5''), 34.0 (C-4''); HRMS *m/z* (ESI$^+$) [Found: 282.1456., $C_{14}H_{16}N_7$ requires [M + H]$^+$ 282.1462]; LCMS (MDAP): Rt = 7.9 min, >95% (Method 3); *m/z* (ESI$^+$) 282.0 [M + H]$^+$; Chiral HPLC, Lux C1 column (50:50 heptane : EtOH (0.2% v/v NH_3), 1.0 ml min^{-1}) Retention Time = 9.55 min > 99% e.e.

Tert-butyl *N*-[(3*R*)-1-(4-pyrazolo[1,5-*b*]pyridazin-3-ylpyrimidin-2-yl)pyrrolidin-3-yl]carbamate **138**

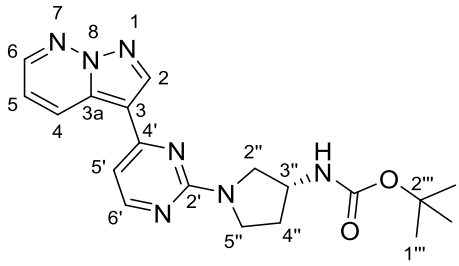

To a microwave vial containing a suspension of 3-(2-chloropyrimidin-4-yl)pyrazolo[1,5-*b*]pyridazine (60 mg, 0.26 mmol) in 2-propanol (2 mL) was added *tert*-butyl *N*-[(3*R*)-pyrrolidin-3-yl]carbamate (96 mg, 0.52 mmol). The vial was sealed and the reaction mixture was heated to 140 °C for 16 h. The reaction mixture was concentrated under reduced pressure. The crude was purified using flash silica column chromatography on an Isco Combiflash system (12 g silica, elution with 0-100% EtOAc / petroleum ether gradient). Desired fractions were combined and concentrated under reduced pressure. The crude was purified using flash reverse phase column chromatography on a Biotage system (12 g silica, elution with 10-100% MeOH / water gradient) to afford the title compound, *tert*-butyl *N*-[(3*R*)-1-(4-pyrazolo[1,5-*b*]pyridazin-3-ylpyrimidin-2-yl)pyrrolidin-3-yl]carbamate, **138**, as a pale yellow solid (45 mg, 0.11 mmol, 43% yield). R_f 0.11 (EtOAc / petroleum ether 1:1); $[\boldsymbol{\alpha}]_{\boldsymbol{D}}^{\mathbf{25}} = -30.5$ (c = 3.9 x 10^{-3} g / mL, $CHCl_3$); m.p. 208-210 °C; $\bar{\nu}_{max}$ (neat)/cm^{-1} 3309 (N-H, w), 2978 (C-H, w), 2874 (C-H, w), 1697 (C=O, s), 1623 (C=N, m), 1567 (C=C, m), 1529 (C=C, m); ^{1}H NMR (600 MHz, DMSO-d_6) δ_H 9.03 – 8.91 (1H, m, H-4), 8.84 (1H, s, H-2), 8.62 – 8.56 (1H, m, H-6), 8.34 (1H, d, *J*= 5.1 Hz, H-6'), 7.46 (1H, dd, *J*= 9.3, 4.4 Hz, H-5), 7.23 (1H, s, NH), 7.14 (1H, d, *J*= 5.1 Hz, H-5'), 4.23 – 4.04 (1H, m, H-3''), 3.89 – 3.37 (4H, m, H-2'' and 5''), 2.25 – 2.10 (1H, m, H-4''), 1.98 – 1.82 (1H, m, H-4''), 1.40 (9H, s, H-1'''); ^{13}C NMR (150 MHz, DMSO-d_6) δ_C 160.0 (C-2'), 159.0 (C-4'), 158.0 (C-6'), 155.3 (C=O), 143.9 (C-6), 139.6 (C-2), 132.4 (C-3a), 129.3 (C-4), 118.9 (C-5), 110.3 (C-3), 104.7 (C-5'), 77.8 (C-2'''), 51.7 (C-2''), 49.9 (C-3''), 44.7 (C-5''), 30.9 (C-4''), 28.2 (C-1'''); HRMS *m/z* (ESI$^+$) [Found: 404.1800., $C_{19}H_{23}N_7NaO_2$ requires [M + Na]$^+$ 404.1805]; LCMS (MDAP): Rt = 13.2 min, >95% (Method 3); *m/z* (ESI$^+$) 382.0 [M + H]$^+$.

2-(4-Pyrazolo[1,5-b]pyridazin-3-ylpyrimidin-2-yl)isoxazolidine **139**

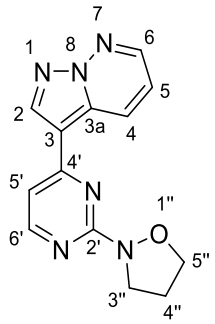

To a pressure vial containing 3-(2-chloropyrimidin-4-yl)pyrazolo[1,5-b]pyridazine (80 mg, 0.35 mmol)in 2-propanol (1.6mL) was added isoxazolidine hydrochloride (76 mg, 0.69 mmol) and TEA (0.1 mL, 0.69 mmol). The vial was sealed and heated to 140 °C for 16 h. The reaction mixture was concentrated under reduced pressure. The crude was purified using flash silica column chromatography on an Isco Combiflash system (12 g silica, elution with 0-100% EtOAc / petroleum ether gradient). Desired fractions were combined and concentrated under reduced pressure. The crude was purified using reverse phase column chromatography on a Biotage system (12 g C-18, elution with 10-100% MeOH / water gradient) to afford the title compound, 2-(4-pyrazolo[1,5-*b*]pyridazin-3-ylpyrimidin-2-yl)isoxazolidine, **139**, as a pale yellow solid (20 mg, 0.07 mmol, 21% yield). R_f 0.16 (EtOAc/ petroleum ether 1:1); m.p. 128-130 °C; $\bar{\nu}_{max}$ (neat)/cm^{-1} 3059 (C-H, w), 3032 (C-H, w), 2993 (C-H, w), 2954 (C-H, w), 2879 (C-H, w), 1623 (C=N, m), 1572 (C=C, s), 1560 (N-O, s), 1525 (C=C, s); ^{1}H NMR (500 MHz, MeOD) δ_H 9.10 (1H, dd, *J* = 9.0, 1.9 Hz, H-4), 8.76 (1H, s, H-2), 8.54 (1H, dd, *J* = 4.4, 1.9 Hz, H-6), 8.45 (1H, d, *J* = 5.4 Hz, H-6'), 7.45 (1H, dd, *J* = 9.0, 4.4 Hz, H-5), 7.41 (1H, d, *J* = 5.4 Hz, H-5'), 4.09 – 4.01 (4H, m, H-3'' and 5''), 2.37 (2H, p, *J* = 7.1 Hz, H-5''); ^{13}C NMR (125 MHz, MeOD) δ_C 166.6 (C-2'), 161.8 (C-4'), 158.9 (C-6'), 145.2 (C-6), 140.7 (C-2), 134.5 (C-3a), 130.7 (C-4), 120.3 (C-5), 111.6 (C-3), 110.1 (C-5'), 68.8 (C-5''), 50.2 (C-3''), 28.9 (C-4''); HRMS *m/z* (ESI$^+$) [Found: 291.0959., $C_{13}H_{12}N_6NaO$ requires [M + Na]$^+$ 291.0965]; LCMS (MDAP): Rt = 4.1 min, >95% (Method 3); *m/z* (ESI$^+$) 268.9 [M + H]$^+$

3-[2-(3-Azabicyclo[3.1.0]hexan-3-yl)pyrimidin-4-yl]pyrazolo[1,5-*b*]pyridazine **140**

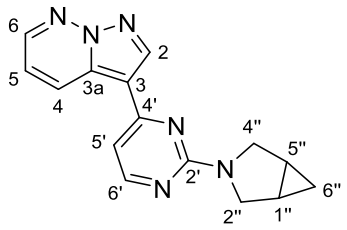

To a microwave vial containing 3-(2-methylsulfonylpyrimidin-4-yl)pyrazolo[1,5-*b*]pyridazine (90 mg, 0.33 mmol) in 2-propanol (2 mL) was added TEA (0.07 mL, 0.49 mmol) and 3-azabicyclo[3.1.0]petroleum ether hydrochloride (39 mg, 0.33 mmol). The vial was sealed and irradiated with microwaves at 140 °C for 45 min. The reaction mixture was concentrated under reduced pressure. The crude was purified using flash silica column chromatography on an Isco Combiflash system (12 g silica, elution with 0-100% EtOAc / petroleum ether gradient) to afford the title compound, 3-[2-(3-azabicyclo[3.1.0]hexan-3-yl)pyrimidin-4-yl]pyrazolo[1,5-*b*]pyridazine, **140**, as a white solid (56 mg, 0.19 mmol, 58% yield). R_f 0.56 (EtOAc / petroleum ether 4:1); m.p. 211-213 °C; $\bar{\nu}_{max}$ (neat)/cm^{-1} 2983 (C-H, w), 2923 (C-H, w), 2904 (C-H, w), 2867 (C-H, w), 1623 (C=N, m), 1563 (C=C, s), 1528 (C=C, m); ^{1}H NMR (600 MHz, DMSO-d$_6$) δ_H 8.88 – 8.84 (1H, m, H-4), 8.73 – 8.69 (1H, m, H-2), 8.51 – 8.44 (m, H-6), 8.24 – 8.15 (1H, m, H-6’), 7.38 – 7.30 (1H, m, H-5), 7.06 – 7.00 (1H, m, H-5’), 3.92 – 3.30 (4H, m, H-2’’ and 4’’), 1.65 – 1.51 (2H, m, H-1’’ and 5’’), 0.71 – 0.58 (1H, m, H-6’’), 0.13 – 0.01 (1H, m, H-6’’); ^{13}C NMR (150 MHz, DMSO-d$_6$) δ_C 160.8 (C-2’), 159.0 (C-4’), 158.0 (C-6’), 143.9 (C-6), 139.6 (C-2), 132.4 (C-3a), 129.4 (C-4), 119.0 (C-5), 110.2 (C-3), 105.0 (C-5’), 48.9 (C-2’’ and C-4’’), 15.6 (C-1’’ and C-5’’), 10.3 (C-6’’); HRMS *m/z* (ESI$^+$) [Found: 279.1352., $C_{15}H_{15}N_6$ requires [M + H]$^+$ 279.1353]; LCMS (MDAP): Rt = 11.7 min, >95% (Method 3); *m/z* (ESI$^+$) 279.0 [M + H]$^+$

3-[2-(3,3a,4,5,6,6a-Hexahydro-1*H*-cyclopenta[*c*]pyrrol-2-yl)pyrimidin-4-yl]pyrazolo[1,5-*b*]pyridazine **141**

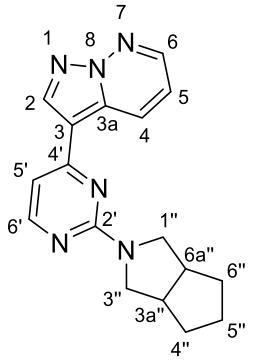

To a microwave vial containing a suspension of 1,2,3,3a,4,5,6,6a-octahydrocyclopenta[*c*]pyrrole (38 mg, 0.35 mmol) in 2-propanol (2 mL) was added 3-(2-chloropyrimidin-4-yl)pyrazolo[1,5-*b*]pyridazine (80 mg, 0.35 mmol). The vial was sealed and the reaction mixture was heated to 140 °C for 16 h. The reaction mixture was concentrated under reduced pressure. The crude was purified using flash silica column chromatography on an Isco Combiflash system (12 g silica, elution with 0-100% EtOAc / petroleum ether gradient). Desired fractions were combined and concentrated under reduced pressure. The crude was purified using reverse phase column chromatography on a Biotage system (12 g C-18, elution with 10-100% MeOH / water gradient) to afford the title compound, 3-[2-(3,3a,4,5,6,6a-hexahydro-1*H*-cyclopenta[*c*]pyrrol-2-yl)pyrimidin-4-yl]pyrazolo[1,5-*b*]pyridazine, **141**, as a cream solid (15 mg, 0.05 mmol, 13% yield). R_f 0.40 (EtOAc / petroleum ether 1:1); m.p. 213-215 °C; ^{1}H NMR (600 MHz, DMSO-d$_6$) δ_H 8.98 (1H, dd, *J*= 9.0, 1.8 Hz, H-4), 8.83 (1H, s, H-2), 8.59 (1H, dd, *J*= 4.4, 1.8 Hz, H-6), 8.33 (1H, d, *J*= 5.1 Hz, H-6'), 7.46 (1H, dd, *J*= 9.0, 4.4 Hz, H-5), 7.14 (1H, d, *J*= 5.1 Hz, H-5'), 3.91 – 3.70 (2H, m, H-1'' and 3''), 3.49 – 3.34 (2H, m, H-1'' and 3''), 2.84 – 2.72 (2H, m, H-3a'' and 6a''), 1.90 – 1.81 (2H, m, H-4'' and 6''), 1.81 – 1.70 (1H, m, H-5''), 1.66 – 1.47 (3H, m, H-5'', 4'' and 6''); ^{13}C NMR (150 MHz, DMSO-d$_6$) δ_C 160.2 (C-2'), 158.9 (C-4'), 158.0 (C-6'), 143.9 (C-6), 139.6 (C-2), 132.4 (C-3a), 129.4 (C-4), 118.9 (C-5), 110.3 (C-3), 104.7 (C-5'), 52.7 (C-1'' and C-3''), 42.4 (C-3a'' and C-6a''), 32.0 (C-4'' and C-6''), 25.2 (C-5''); HRMS *m/z* (ESI$^+$) [Found: 329.1485., $C_{17}H_{18}N_6Na$ requires [M + Na]$^+$ 329.1485]; LCMS (MDAP): Rt = 13.1 min, >95% (Method 3); *m/z* (ESI$^+$) 307.0 [M + H]$^+$

3-[2-(3,3a,4,5,6,6a-Hexahydro-2*H*-pyrrolo[2,3-*c*]pyrrol-1-yl)pyrimidin-4-yl]pyrazolo[1,5-*b*]pyridazine **142**

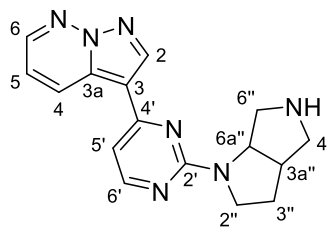

To a microwave vial containing 3-(2-methylsulfonylpyrimidin-4-yl)pyrazolo[1,5-*b*]pyridazine (100 mg, 0.33 mmol) in 2-propanol (1 mL) was added *tert*-butyl hexahydropyrrolo[3,4-*b*]pyrrole-5(1*H*)-carboxylate (105 mg, 0.49 mmol). The vial was sealed and heated to 140 °C overnight. The reaction mixture was concentrated under reduced pressure. The crude was purified using flash silica column chromatography on an Isco Combiflash system (12 g silica, elution with 0-100% ammonia/ MeOH / CH_2Cl_2 1:10:90 gradient). Desired fractions were combined and concentrated under reduced pressure to afford a yellow solid. To the solid was added 4 M HCl in dioxane (5 mL) and the reaction mixture stirred at rt for 5 h. The reaction mixture was concentrated under reduced pressure to afford the title compound, 3-[2-(3,3a,4,5,6,6a-hexahydro-2*H*-pyrrolo[2,3-*c*]pyrrol-1-yl)pyrimidin-4-yl]pyrazolo[1,5-*b*]pyridazine, **142**, as a pale yellow solid (40 mg, 0.12 mmol, 36% yield). R_f 0.05 (MeOH/ CH_2Cl_2 1:9); m.p. 214-216 °C; $\bar{\nu}_{max}$ (neat)/cm^{-1} 3369 (N-H, m), 2942 (C-H, w), 2867 (C-H, w), 1623 (C=N, m), 1563 (C=C, m), 1526 (C=C, m); ^{1}H NMR (600 MHz, MeOD) δ_H 8.85 (1H, d, *J* = 9.0 Hz, H-4), 8.57 (1H, s, H-2), 8.45 – 8.41 (1H, m, H-6), 8.24 (1H, d, *J* = 5.3 Hz, H-6'), 7.29 (1H, dd, *J* = 9.0, 4.5 Hz, H-5), 7.00 (1H, d, *J* = 5.3 Hz, H-5'), 4.56 – 4.53 (1H, m, H-6a''), 3.80 – 3.68 (2H, m, H-2''), 3.36 (1H, s, NH), 3.24 – 3.17 (2H, m, H-6''), 3.15 – 3.09 (1H, m, H-4''), 3.08 – 3.01 (1H, m, H-3a''), 2.95 – 2.89 (1H, m, H-4''), 2.28 – 2.19 (1H, m, H-3''), 1.97 – 1.89 (1H, m, H-3''); ^{13}C NMR (150 MHz, MeOD) δ_C 161.3 (C-2'), 161.0 (C-4'), 158.6 (C-6'), 144.9 (C-6), 140.3 (C-2), 134.1 (C-3a), 130.5 (C-4), 119.8 (C-5), 112.1 (C-3), 106.2 (C-5'), 64.8 (C-6a''), 54.7 (C-6''), 53.1 (C-4''), 48.4 (C-2''), 44.7 (C-3a''), 30.3 (C-3''); HRMS *m/z* (ESI$^+$) [Found: 308.1615., $C_{16}H_{18}N_7$ requires [M + H]$^+$ 308.1618]; LCMS (MDAP): Rt = 8.88 min, >90% (Method 3); *m/z* (ESI$^+$) 308.0 [M + H]$^+$.

7-(4-Pyrazolo[1,5-*b*]pyridazin-3-ylpyrimidin-2-yl)-2-oxa-7-azaspiro[4.4]nonane **143**

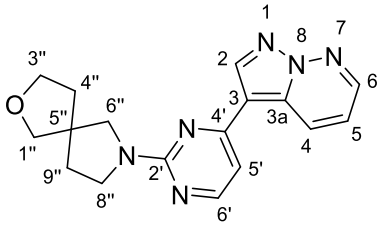

To a pressure vial containing 3-(2-chloropyrimidin-4-yl)pyrazolo[1,5-*b*]pyridazine (60 mg, 0.26 mmol) in 2-propanol (2 mL) was added 2-oxa-7-azaspiro[4.4]nonane (65 mg, 0.52 mmol). The vial was sealed and heated to 140 °C for 16 h. The reaction mixture was concentrated under reduced pressure. The crude was purified using flash silica column chromatography on a Biotage system (12 g silica, elution with 0-100% EtOAc / petroleum ether gradient). Desired fractions were combined and concentrated under reduced pressure. The crude was purified using reverse phase column chromatography on a Biotage system (12 g C-18, elution with 10-100% MeOH / water gradient) to afford the title compound, 7-(4-pyrazolo[1,5-*b*]pyridazin-3-ylpyrimidin-2-yl)-2-oxa-7-azaspiro[4.4]nonane, **143**, as a colourless solid (33 mg, 0.10 mmol, 38% yield). R_f 0.38 (100% EtOAc); m.p. 164-166 °C; $\bar{\nu}_{max}$ (neat)/cm^{-1} 3060(C-H, w), 2859 (C-H, w), 1622 (C=N, m), 1563 (C=C, m), 1529 (C=C, m); ^{1}H NMR (600 MHz, MeOD) δ_H 9.02 (1H. d, *J* = 9.1 Hz, H-4), 8.64 (1H, s, H-2), 8.48 (1H, dd, *J* = 4.4, 1.9 Hz, H-6), 8.26 (1H, d, *J* = 5.3 Hz, H-6'), 7.37 (1H, dd, *J* = 9.1, 4.4 Hz, H-5), 7.06 (1H, d, *J* = 5.3 Hz, 1H, H-5'), 3.98 (2H, t, *J* = 7.1 Hz, H-3'') 3.87 – 3.52 (6H, m, H-1'', 6'' and 8''), 2.18 – 1.98 (4H, m, H-4'' and -9''); ^{13}C NMR (150 MHz, MeOD) δ_C 160.0 (C-4' or C-2'), 159.9 (C-4' or C-2'), 157.1 (C-6'), 143.5 (C-6), 138.9 (C-2), 132.9 (C-3a), 129.4(C-4), 118.5 (C-5), 110.8 (C-3), 104.4 (C-5'), 75.9 (C-1''), 67.4 (C-3''), 55.5 (C-6''), 49.2 (C-5'' or C-8''), 46.0 (C-5'' or C-8''), 36.1 (C-9''), 34.3 (C-4''); HRMS *m/z* (ESI$^+$) [Found: 323.1612., $C_{17}H_{19}N_6O$ requires [M + H]$^+$ 323.1615]; LCMS (MDAP): Rt = 10.8 min, >95% (Method 3); *m/z* (ESI$^+$) 323.0 [M + H]$^+$.

(1*S*,4*S*)-5-(4-pyrazolo[1,5-*b*]pyridazin-3-ylpyrimidin-2-yl)-2-oxa-5-azabicyclo[2.2.1]heptane **144**

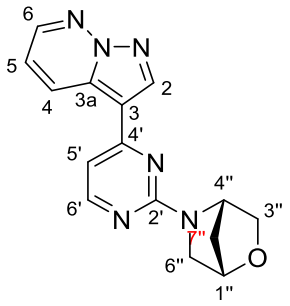

To a microwave vial containing 3-(2-methylsulfonylpyrimidin-4-yl)pyrazolo[1,5-*b*]pyridazine (90 mg, 0.33 mmol) in 2-propanol (2 mL) was added TEA (0.07 mL, 0.49 mmol) and (1*S*,4*S*)-2-oxa-5-azabicyclo[2.2.1]heptane hydrochloride (50 mg, 0.33 mmol). The vial was sealed and irradiated with microwaves at 140 °C for 45 min. The reaction mixture was concentrated under reduced pressure. The crude was purified using flash silica column chromatography on an Isco Combiflash system (12 g silica, elution with 0-100% EtOAc / petroleum ether gradient) to afford the title compound, (1*S*,4*S*)-5-(4-pyrazolo[1,5-*b*]pyridazin-3-ylpyrimidin-2-yl)-2-oxa-5-azabicyclo[2.2.1]heptane, **144**, as white solid (26 mg, 0.08 mmol, 26% yield). R_f (100% EtOAc) 0.70; $[\boldsymbol{\alpha}]_{\boldsymbol{D}}^{\mathbf{25}} = -100.0$ (c = 1 x 10^{-3} g / mL, $CHCl_3$); m.p. 214-216 °C; $\bar{\nu}_{max}$ (neat)/cm^{-1} 3058 (C-H, w), 2987(C-H, w), 2949 (C-H, w), 2871 (C-H, w), 1623 (C=N, m), 1562 (C=C, m), 1521 (C=C, m); ^{1}H NMR (600 MHz, DMSO-d_6) δ_H 8.97 – 8.88 (1H, m, H-4), 8.83 (1H, s, H-2), 8.59 – 8.55 (1H, m, H-6), 8.33 (1H, d, *J* = 5.2 Hz, H-6'), 7.42 (1H, dd, *J* = 9.0, 4.4 Hz, H-5), 7.17 (1H, d, *J* = 5.2 Hz, H-5'), 5.15 – 4.85 (1H, m, H-6''), 4.76 – 4.60 (1H, m, H-3''), 3.89 – 3.36 (4H, m, H-1'' and 4''), 2.01 – 1.81 (2H, m, H-7''); ^{13}C NMR (150 MHz, DMSO-d_6) δ_C 160.7 (C-2'), 159.9 (C-4'), 158.5 (C-6'), 144.4 (C-6), 140.1 (C-2), 132.9 (C-3a), 129.8 (C-4), 119.5 (C-5), 110.6 (C-3), 105.7 (C-5'), 76.2 (C-3''), 73.6 (C-1''), 57.0 (C-6''), 56.3 (C-4''), 36.7 (C-7''); HRMS *m/z* (ESI$^+$) [Found: 295.1303., $C_{15}H_{15}N_6O$ requires $[M + H]^+$ 295.1302]; LCMS (MDAP): Rt = 10.6 min, >95% (Method 3); *m/z* (ESI$^+$) 295.0 $[M + H]^+$.

Tert-butyl 2-(4-pyrazolo[1,5-*b*]pyridazin-3-ylpyrimidin-2-yl)-1,3,3a,4,6,6a-hexahydropyrrolo[3,4-*c*]pyrrole-5-carboxylate **145**

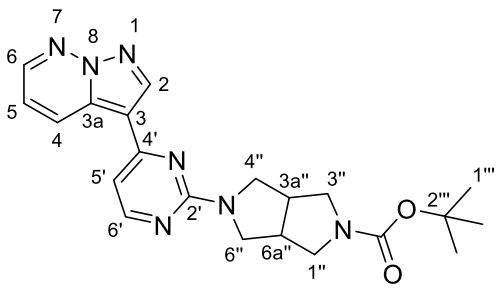

To a microwave vial containing a suspension of 3-(2-chloropyrimidin-4-yl)pyrazolo[1,5-*b*]pyridazine (60 mg, 0.26 mmol) in 2-propanol (2 mL) was added 2-boc-hexahydro-pyrrolo[3,4-*c*]pyrrole (55 mg, 0.26 mmol). The vial was sealed and the reaction mixture was heated to 140 °C for 16 h. The reaction mixture was concentrated under reduced pressure. The crude was purified using flash silica column chromatography on an Isco Combiflash system (12 g silica, elution with 0-50% 20% MeOH in CH_2Cl_2 / CH_2Cl_2 gradient). Desired fractions were combined and concentrated under reduced pressure. The crude was purified using flash reverse phase column chromatography on a Biotage system (12 g silica, elution with 10-100% MeOH / water gradient) to afford the title compound, *tert*-butyl 2-(4-pyrazolo[1,5-*b*]pyridazin-3-ylpyrimidin-2-yl)-1,3,3a,4,6,6a-hexahydropyrrolo[3,4-*c*]pyrrole-5-carboxylate, **145**, as a pale yellow solid (40 mg, 0.09 mmol, 36% yield). R_f 0.47 (MeOH/ CH_2Cl_2 1:9); m.p. 217-219 °C; $\bar{\nu}_{max}$ (neat)/cm^{-1} 2971 (C-H, w), 2878 (C-H, w), 1683 (C=O, s), 1623 (C=N, m), 1563 (C=C, s); ^{1}H NMR (600 MHz, DMSO-d_6) δ_H 9.00 (1H, app. d, *J* = 9.1 Hz, H-4), 8.84 (1H, s, H-2), 8.61 – 8.57 (1H, m, H-6), 8.34 (1H, d, *J*= 5.0 Hz, H-6'), 7.45 (1H, dd, *J*= 9.1, 4.4 Hz, H-5), 7.17 (1H, d, *J*= 5.0 Hz, H-5'), 3.96 – 2.89 (8H, m, H-1'', 3'', 4'' and 6''), 3.08 – 2.92 (2H, m, H-3a'' and 6a''), 1.39 (9H, s, H-1'''); ^{13}C NMR (150 MHz, DMSO-d_6) δ_C 160.1 (C-2'), 159.0 (C-4', 158.0 (C-6'), 153.6 (C=O), 143.9 (C-6), 139.6 (C-2), 132.4 (C-3a), 129.5 (C-4), 119.0 (C-5), 110.2 (C-3), 104.9 (C-5'), 78.4 (C-2'''), 50.4 (C-1'', C-3'', C-4'' or C-6''), 49.9 (C-1'', C-3'', C-4'' and C-6''), 41.5 (C-3a'' and C-6a''), 28.1 (C-1'''). Signals present at δ_C 40.5 and 49.8 ppm consistent with rotamers; HRMS *m/z* (ESI$^+$) [Found: 430.1963., $C_{21}H_{25}N_7NaO_2$ requires [M + Na]$^+$ 430.1962]; LCMS (MDAP): Rt = 14.4 min, >95% (Method 3); *m/z* (ESI$^+$) 408.0 [M + H]$^+$

3-[2-[(1*S*,4*S*)-5-Methyl-2,5-diazabicyclo[2.2.1]heptan-2-yl]pyrimidin-4-yl]pyrazolo[1,5-*b*]pyridazine **147**

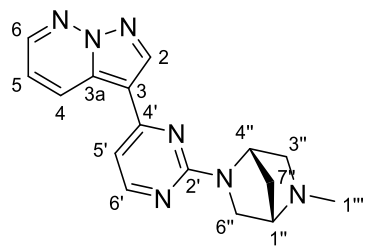

To a microwave vial containing 3-(2-chloropyrimidin-4-yl)pyrazolo[1,5-*b*]pyridazine (80 mg, 0.35 mmol) in 2-propanol (2 mL) was added (1*S*,4*S*)-2-methyl-2,5-diazabicyclo[2.2.1]heptane dihydrobromide (114 mg, 0.41 mmol) and TEA (0.1 mL, 0.69 mmol). The vial was sealed and irradiated with microwaves at 140 °C for 45 min. The reaction mixture was concentrated under reduced pressure. The crude was purified using flash silica column chromatography on an Isco Combiflash system (12 g silica, elution with 0-100% ammonia/ MeOH/ CH_2Cl_2 1:10:90 gradient) to afford the title compound, 3-[2-[(1*S*,4*S*)-5-methyl-2,5-diazabicyclo[2.2.1]heptan-2-yl]pyrimidin-4-yl]pyrazolo[1,5-*b*]pyridazine, **147**, as a pale pink solid (56 mg, 0.17 mmol, 50% yield). R_f 0.36 (ammonia / MeOH / CH_2Cl_2 1:10:90); $[\alpha]_D^{25} = -38.0$ (c = 3.17 x 10^{-3} g / mL, $CHCl_3$); Decompose > 226 °C; $\bar{\nu}_{max}$ (neat)/cm^{-1} 3492 (N-H, m), 2991 (C-H, w), 2949 (C-H, w), 2859 (C-H, w), 2799 (C-H, w), 1679 (N-H, w), 1623 (C=N, m), 1563 (C=C, s), 1530 (C=C, m); ^{1}H NMR (500 MHz, DMSO-d_6) δ_H 9.01 – 8.82 (2H, m, H-2 and 4), 8.63 – 8.57 (1H, m, H-6), 8.40 – 8.30 (1H, m, H-6'), 7.45 (1H, dd, *J*= 9.1, 4.5 Hz, H-5), 7.21 (1H, d, *J*= 5.1 Hz, H-5'), 5.06 – 4.73 (1H, m, H-4''), 3.92 – 3.51 (3H, m, H-1'', 3'' or 6''), 3.14 – 2.79 (2H, m, H-3'' or 6''), 2.54 (3H, s, H-1'''), 2.21 – 1.81 (2H, m, H-7''); ^{1}H NMR (600 MHz, DMSO-d_6) δ_H 8.91 – 8.65 (2H, m, H-2 and 4), 8.52 – 8.44 (1H, m, H-6), 8.28 – 8.16 (1H, m, H-6'), 7.33 (1H, dd, *J* = 9.2, 4.5 Hz, H-5), 7.13 – 7.03 (1H, m, H-5'), 4.94 – 4.63 (1H, m, H-4''), 3.84 – 3.48 (3H, m, H-1'', 3'' or 6''), 3.05 – 2.66 (2H, m, H-3'' or 6''), 2.44 (3H, s, H-1'''), 2.03 – 1.77 (2H, m, H-7''); ^{13}C NMR (150 MHz, DMSO-d_6) δ_C 159.9 (C-2' or C-4'), 159.1 (C-2' or C-4'), 158.1 (C-6'), 144.0 (C-6), 139.8 (C-2), 132.4 (C-3a), 129.3 (C-4), 119.1 (C-5), 110.1 (C-3), 105.5 (C-5'), 63.8 (C-1''), 61.2 (C-3'' or C-6''), 56.7 (C-4''), 50.3 (C-3'' or C-6''), 41.0 (C-1'''), 34.6 (C-7''); HRMS *m/z* (ESI^+) [Found: 308.1618., $C_{16}H_{18}N_7$ requires $[M + H]^+$ 308.1618]; LCMS (MDAP): Rt = 16.8 min, >95% (Method 3); *m/z* (ESI^+) 308.0 $[M + H]^+$

3-[2-[(3a*R*,6a*R*)-1-Methyl-2,3,3a,4,6,6a-hexahydropyrrolo[2,3-*c*]pyrrol-5-yl]pyrimidin-4-yl]pyrazolo[1,5-*b*]pyridazine **148**

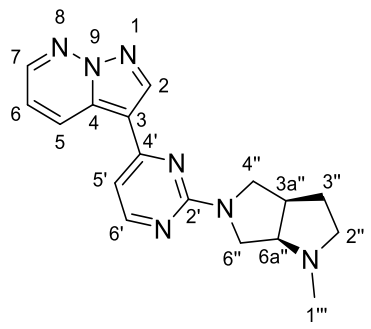

To a microwave vial containing a suspension of 3-(2-chloropyrimidin-4-yl)pyrazolo[1,5-*b*]pyridazine (60 mg, 0.26 mmol) in 2-propanol (2 mL) was added rac-(3*aR*,6*aR*)-1-methyl-octahydropyrrolo[2,3-*c*]pyrrole (65 mg, 0.52 mmol). The vial was sealed and the reaction mixture was heated to 140 °C for 16 h. The crude was purified using flash silica column chromatography on an Isco Combiflash system (12 g silica, elution with 0-50% 20% MeOH in CH_2Cl_2 / CH_2Cl_2 gradient). Desired fractions were concentrated under reduced pressure. The crude was purified using reverse phase column chromatography on a Biotage system (12 g C-18, elution with 10-100% MeOH / water gradient) to afford the title compound, 3-[2-[(3a*R*,6a*R*)-1-methyl-2,3,3a,4,6,6a-hexahydropyrrolo[2,3-*c*]pyrrol-5-yl]pyrimidin-4-yl]pyrazolo[1,5-*b*]pyridazine, **148**, as a pale yellow solid (14 mg, 0.04 mmol, 16% yield). R_f 0.55 (MeOH/ CH_2Cl_2 1:9); $[\boldsymbol{\alpha}]_{\boldsymbol{D}}^{\mathbf{25}} = +12.0$ (c = 1.67 x 10^{-3} g / mL, $CHCl_3$); m.p. 163-165 °C; $\bar{\nu}_{max}$ (neat)/cm^{-1} 3092 (C-H, w), 2950 (C-H, w), 2865 (C-H, w), 2773 (C-H, w), 1620 (C=N, m), 1562 (C=C, m), 1528 (C=C, m); ^{1}H NMR (600 MHz, DMSO-d_6) δ_H 8.98 (1H, app. d, *J* = 9.0 Hz, H-4), 8.83 (1H, s, H-2), 8.64 – 8.55 (1H, m, H-6), 8.32 (1H, d, *J*= 5.1 Hz, H-6'), 7.46 (1H, dd, *J*= 9.0, 4.4 Hz, H-5), 7.13 (1H, d, *J*= 5.1 Hz, H-5'), 3.96 – 3.69 (2H, m, H-4'' and 6''), 3.63 – 3.35 (2H, m, H-4'' and 6''), 3.05 (1H, t, *J*= 8.6 Hz, H-2''), 2.94 – 2.81 (2H, m, H-3a'' and 6a''), 2.33 – 2.22 (4H, m, H-1''' and 2''), 2.10 – 1.97 (1H, m, H-3''), 1.76 – 1.59 (1H, m, H-3''); ^{13}C NMR (150 MHz, DMSO-d_6) δ_C 160.1 (C-2'), 158.9 (C-4'), 158.0 (C-6'), 143.9 (C-6), 139.6 (C-2), 132.4 (C-3a), 129.3 (C-4), 118.9 (C-5), 110.3 (C-3), 104.7 (C-5'), 69.8 (C-6a''), 57.1 (C-2''), 53.7 (C-4''), 50.3 (C-6''), 41.4 (C-3a''), 40.3 (C-1'''), 29.5 (C-3''); HRMS *m/z* (ESI^+) [Found: 322.1766., $C_{17}H_{20}N_7$ requires $[M + H]^+$ 322.1775]; LCMS (MDAP): Rt = 8.7 min, >95% (Method 3); *m/z* (ESI^+) 322.0 $[M + H]^+$.

3-[2-[3-(3,5-Dimethylpyrazol-1-yl)pyrrolidin-1-yl]pyrimidin-4-yl]pyrazolo[1,5-*b*]pyridazine **149**

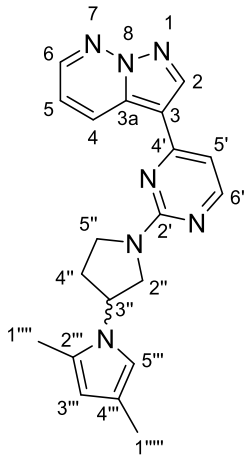

To a pressure vial containing 3-(2-chloropyrimidin-4-yl)pyrazolo[1,5-b]pyridazine (60 mg, 0.26 mmol) in 2-propanol (2 mL) was added 3,5-dimethyl-1-pyrrolidin-3-yl-pyrazole (85 mg, 0.52 mmol). The vial was sealed and heated to 140 °C for 16 h. The reaction mixture was concentrated under reduced pressure. The crude was purified using flash silica column chromatography on an Isco Combiflash system (12 g silica, elution with 0-50% 20% MeOH in CH_2Cl_2 / CH_2Cl_2 gradient). Desired fractions were combined and concentrated under reduced pressure. The crude was purified using reverse phase column chromatography on a Biotage system (12 g C-18, elution with 10-100% MeOH / water gradient) to afford the title compound, 3-[2-[3-(3,5-dimethylpyrazol-1-yl)pyrrolidin-1-yl]pyrimidin-4-yl]pyrazolo[1,5-*b*]pyridazine, **149**, as a colourless solid (33 mg, 0.09 mmol, 34% yield). R_f 0.05 (EtOAc / petroleum ether 1/1); m.p. 236-238 °C; $\bar{\nu}_{max}$ (neat)/cm^{-1} 3057 (C-H, w), 2969 (C-H, w), 2863 (C-H, w), 1624 (C=N, m), 1567 (C=C, m), 1527 (C=C, m); ^{1}H NMR (600 MHz, DMSO-d$_6$) δ_H 9.08 – 8.88 (1H, m, H-4), 8.86 (1H, s, H-2), 8.62 – 8.55 (1H, m, H-6), 8.41 – 8.30 (1H, m, H-6’), 7.49 – 7.40 (1H, m, H-5), 7.18 (1H, d, *J* = 5.1 Hz, H-5’), 5.83 (1H, s, H-3’’’), 5.14 – 4.90 (1H, m, H-3’’), 4.22 – 3.60 (4H, m, H-2’’ and H-5’’), 2.46 – 2.33 (2H, m, H-4’’), 2.29 (3H, s, H-1’’’’), 2.08 (3H, s, H-1’’’’’); ^{13}C NMR (150 MHz, DMSO-d$_6$) δ_C 159.9 (C-2’), 159.1 (C-4’), 158.1 (C-6’), 146.0 (C-4’’’), 143.9 (C-6), 139.7 (C-2), 138.7 (C-2’’’), 129.3 (C-4), 119.0 (C-5), 110.2 (C-3), 104.9 (C-5’ and C-3’’’), 55.7 (C-3’’), 51.2 (C-2’’), 45.3 (C-5’’), 31.1 (C-4’’), 13.6 (C-1’’’’), 10.6 (C-1’’’’’); HRMS *m/z* (ESI$^+$) [Found: 383.1696., $C_{19}H_{20}N_8Na$ requires [M + Na]$^+$ 383.1703]; LCMS (MDAP): Rt = 12.8 min, >95% (Method 3); *m/z* (ESI$^+$) 361.1 [M + H]$^+$.

3-[2-[4-(Trifluoromethyl)-1-piperidyl]pyrimidin-4-yl]pyrazolo[1,5-*b*]pyridazine **150**

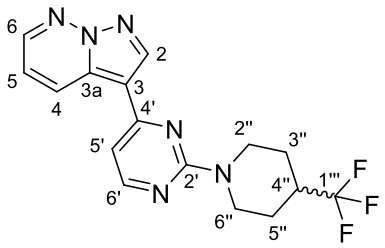

To a microwave vial containing 3-(2-chloropyrimidin-4-yl)pyrazolo[1,5-*b*]pyridazine (50 mg, 0.22 mmol) in 2-propanol (1 mL) was added TEA (0.05 mL, 0.32 mmol) and 4-(trifluoromethyl)piperidine hydrochloride (40 mg, 0.22 mmol). The vial was sealed and heated to 140 °C for 6 h. The reaction mixture was concentrated under reduced pressure. The crude was purified using flash silica column chromatography on an Isco Combiflash system (12 g silica, elution with 0-100% EtOAc / petroleum ether gradient) to afford the title compound, 3-[2-[4-(trifluoromethyl)-1-piperidyl]pyrimidin-4-yl]pyrazolo[1,5-*b*]pyridazine, **150**, as a white solid (52 mg, 0.14 mmol, 66% yield). R_f 0.55 (EtOAc / petroleum ether 1:1); m.p. 203-205 °C; $\bar{\nu}_{max}$ (neat)/cm^{-1} 2957 (C-H, w), 2934 (C-H, w), 2852 (C-H, w), 1623 (C=N, m), 1564 (C=C, m), 1527 (C=C, m); ^{1}H NMR (600 MHz, DMSO-d$_6$) δ_H 8.90 – 8.83 (2H, m, H-2 and 4), 8.61 (1H, dd, *J* = 4.4, 1.9 Hz, H-6), 8.39 (1H, d, *J* = 5.2 Hz, H-6'), 7.47 (1H, dd, *J* = 9.0, 4.4 Hz, H-5), 7.20 (1H, d, *J* = 5.2 Hz, H-5'), 4.85 (2H, d, *J* = 13.4 Hz, H-2'' and 6''), 3.05 – 2.96 (2H, m, H-2'' and 6''), 2.74 – 2.65 (1H, m, H-4''), 1.95 (2H, d, *J* = 12.5 Hz, H-3'' and 5''), 1.49 – 1.38 (2H, m, H-3'' and 5''); ^{13}C NMR (150 MHz, DMSO-d$_6$) δ_C 161.2 (C-2'), 159.2 (C-4'), 158.2 (C-6'), 143.9 (C-6), 139.8 (C-2), 132.2 (C-3a), 128.9 (C-4), 127.7 (q, *J* = 278.5 Hz, C-1'''), 119.1 (C-5), 110.3 (C-3), 105.7 (C-5'), 42.3 (C-2'' and C-6''), 39.2 (C-4), 23.8 (C-3'' and C-5''); HRMS *m/z* (ESI$^+$) [Found: 349.1396., $C_{16}H_{16}F_3N_6$ requires [M + H]$^+$ 349.1383]; LCMS (LCQ): Rt = 2.9 min (Method 1); *m/z* (ESI$^+$) 349.3 [M + H]$^+$; LCMS (MDAP): Rt = 19.5 min, >95% (Method 3); *m/z* (ESI$^+$) 349.0 [M + H]$^+$

4-Ethyl-1-(4-pyrazolo[1,5-*b*]pyridazin-3-ylpyrimidin-2-yl)piperidine-4-carbonitrile **151**

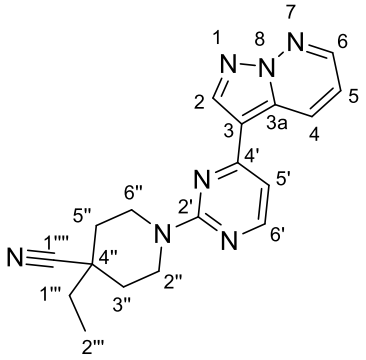

To a pressure vial containing 3-(2-chloropyrimidin-4-yl)pyrazolo[1,5-*b*]pyridazine (60 mg, 0.26 mmol) in 2-propanol (2 mL) was added 4-ethylpiperidine-4-carbonitrile (71 mg, 0.52 mmol). The vial was sealed and heated to 140 °C for 16h. The reaction mixture was concentrated under reduced pressure. The residue was adsorbed onto solid load material. The crude was purified using flash silica column chromatography on a Biotage system (12 g silica, elution with 0-100% EtOAc / petroleum ether gradient). Desired fractions were combined and concentrated under reduced pressure. The crude was purified using reverse phase column chromatography on a Biotage system (12 g C-18, elution with 10-100% MeOH / water gradient) to afford the title compound, 4-ethyl-1-(4-pyrazolo[1,5-*b*]pyridazin-3-ylpyrimidin-2-yl)piperidine-4-carbonitrile, **151**, as a colourless solid (26 mg, 0.07 mmol, 29% yield). R_f 0.33 (EtOAc / petroleum ether 1/1); m.p. 202-204 °C; $\bar{\nu}_{max}$ (neat)/cm^{-1} 3104 (C-H, w), 3063 (C-H, w), 2919 (C-H, w), 2858 (C-H, w), 2230 ($CN_{nitrile}$, m), 1622 (C=N, m), 1566 (C=C, m), 1528 (C=C, m); ^{1}H NMR (600 MHz, DMSO-d$_6$) δ_H 8.90 – 8.84 (2H, m, H-2 and 4), 8.62 – 8.59 (1H, m, H-6), 8.39 (d, *J* = 5.3 Hz, H-6'), 7.48 – 7.44 (1H, m, H-5), 7.22 – 7.18 (1H, m, H-5'), 4.78 (2H, d, *J* = 13.8 Hz, H-6'' and 2''), 3.13 (2H, t, *J* = 13.1 Hz, H-6'' and 2''), 2.03 (2H, d, *J* = 13.5 Hz, H-3'' and 5''), 1.65 (2H, q, *J* = 7.6 Hz, H-1'''), 1.53 (2H, t, *J* = 12.6 Hz, H-3'' and 5''), 1.08 – 0.95 (3H, m, H-2'''); ^{13}C NMR (150 MHz, DMSO-d$_6$) δ_C 161.1 (C-2'), 159.2 (C-4'), 158.2 (C-6'), 144.0 (C-6), 139.9 (C-2), 132.3 (C-3a), 129.0 (C-4), 122.7 (C-1'''', CN), 119.1 (C-5), 110.3 (C-3), 105.8 (C-5'), 41.1 (C-6'' and C-2''), 38.5 (C-4''), 33.4 (C-3'' and C-5''), 31.7 (C-1'''), 8.6 (C-2'''); HRMS *m/z* (ESI$^+$) [Found: 356.1590., $C_{18}H_{19}N_7Na$ requires [M + Na]$^+$ 356.1594]; LCMS (MDAP): Rt = 18.4 min, >95% (Method 3); *m/z* (ESI$^+$) 334.0 [M + H]$^+$

N,*N*-Dimethyl-1-(4-pyrazolo[1,5-*b*]pyridazin-3-ylpyrimidin-2-yl)piperidin-4-amine **152**

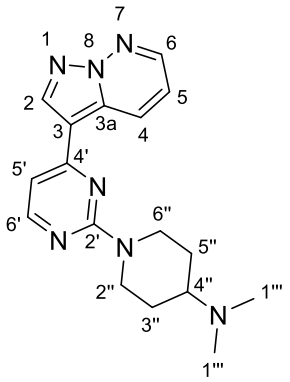

To a microwave vial containing a suspension of 3-(2-chloropyrimidin-4-yl)pyrazolo[1,5-*b*]pyridazine (80 mg, 0.35 mmol) in 2-propanol (2 mL) was added *N*,*N*-dimethylpiperidin-4-amine (88 mg, 0.69 mmol). The vial was sealed and the reaction mixture heated to 140 °C and stirred overnight. The reaction mixture was concentrated under reduced pressure. The crude was purified using flash silica column chromatography on an Isco Combiflash system (12 g silica, elution with 0-50% 20% MeOH in CH_2Cl_2 / CH_2Cl_2 gradient). Desired fractions were combined and concentrated under reduced pressure. The crude was purified using reverse phase column chromatography on a Biotage system (12 g C-18, elution with 10-100% MeOH / water gradient) to afford the title compound, *N*,*N*-dimethyl-1-(4-pyrazolo[1,5-*b*]pyridazin-3-ylpyrimidin-2-yl)piperidin-4-amine, **152**, as a white solid (6 mg, 0.02 mmol, 5% yield). R_f 0.30 (MeOH/ CH_2Cl_2 1:9); ^{1}H NMR (600 MHz, MeOD) δ_H 8.87 (1H, app. d, *J* = 9.0 Hz, H-4), 8.61 (1H, s, H-2), 8.49 – 8.45 (1H, m, H-6), 8.28 (1H, d, *J* = 5.3 Hz, H-6'), 7.35 (1H, dd, *J* = 9.0, 4.4 Hz, H-5), 7.01 (1H, d, *J* = 5.3 Hz, H-5'), 4.85 (2H, app. s, H-2'' and 6''), 2.96 (2H, td, *J* = 12.9, 2.5 Hz, H-2'' and 6''), 2.59 – 2.48 (1H, m, H-4''), 2.34 (6H, s, H-1'''), 2.02 (2H, d, *J* = 12.5 Hz, H-3'' and 5''), 1.48 (2H, qd, *J* = 12.4, 4.2 Hz, H-3'' and 5''); ^{13}C NMR (150 MHz, MeOD) δ_C 162.8 (C-2'), 161.1 (C-4'), 158.9 (C-6'), 144.8 (C-6), 140.4 (C-2), 134.0 (C-3a), 130.3 (C-4), 119.9 (C-5), 112.4 (C-3), 106.4 (C-5'), 64.0 (C-4''), 44.6 (C-6'' and C-2''), 41.7 (C-1'''), 29.1 (C-3'' and C-5''); HRMS *m/z* (ESI$^+$) [Found: 324.1920., $C_{17}H_{22}N_7$ requires [M + H]$^+$ 324.1931]; LCMS (MDAP): Rt = 9.5 min, >95% (Method 3); *m/z* (ESI$^+$) 324.0 [M + H]$^+$

1-(4-Pyrazolo[1,5-*b*]pyridazin-3-ylpyrimidin-2-yl)piperidin-3-ol **153**

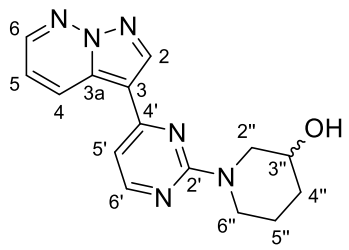

To a microwave vial containing 3-(2-methylsulfonylpyrimidin-4-yl)pyrazolo[1,5-*b*]pyridazine (60 mg, 0.20 mmol) in 2-propanol (1 mL) was added piperidin-3-ol (30 mg, 0.29 mmol). The vial was sealed and heated to 140 °C for 6 h. The reaction mixture was concentrated under reduced pressure. The crude was purified using reverse phase column chromatography on a Biotage system (12 g C-18, elution with 10-100% MeOH / water gradient). Desired fractions were combined and concentrated under reduced pressure to afford a yellow oil. The oil was sonicated in diethyl ether. The resulting beige solid was triturated further with diethyl ether and EtOAc to afford the title compound, 1-(4-pyrazolo[1,5-*b*]pyridazin-3-ylpyrimidin-2-yl)piperidin-3-ol, **153**, as a beige solid (50 mg, 0.15 mmol, 77% yield). R_f 0.0 (EtOAc / petroleum ether 1:1); m.p. 181-183 °C; $\bar{\nu}_{max}$ (neat)/cm^{-1} 3511 (O-H, s), 3107 (C-H, w), 3073 (C-H, w), 2942 (C-H, w), 2908 (C-H, w), 2856 (C-H, w), 1623 (C=N, m), 1567 (C=C, m), 1527 (C=C, m); ^{1}H NMR (600 MHz, DMSO-d$_6$) δ_H 8.87 (1H, d, *J* = 9.1 Hz, H-4), 8.83 (1H, s, H-2), 8.62 – 8.58 (1H, m, H-6), 8.34 (1H, d, *J* = 5.1 Hz, H-6'), 7.50 – 7.43 (1H, m, H-5), 7.12 (1H, d, *J* = 5.1 Hz, H-5'), 4.95 (1H, s, OH), 4.52 (1H, d, *J* = 12.7 Hz, H-2''), 4.37 (1H, d, *J* = 13.1 Hz, H-6''), 3.56 – 3.49 (1H, m, H-3''), 3.11 (1H, t, *J* = 11.3 Hz, H-6''), 2.96 (1H, t, *J* = 10.8 Hz, H-2''), 1.98 – 1.89 (1H, m, H-4''), 1.82 – 1.73 (1H, m, H-5''), 1.49 – 1.37 (2H, m, H-4'' and 5''); ^{13}C NMR (150 MHz, DMSO-d$_6$) δ_C 161.4 (C-2'), 159.1 (C-4'), 158.1 (C-6'), 143.9 (C-6), 139.8 (C-2), 132.2 (C-3a), 128.9 (C-4), 119.0 (C-5), 110.5 (C-3), 105.2 (C-5'), 65.3 (C-3''), 51.0 (C-2''), 43.6 (C-6''), 33.4 (C-4''), 22.8 (C-5''); HRMS *m/z* (ESI$^+$) [Found: 297.1470., $C_{15}H_{17}N_6O$ requires [M + H]$^+$ 297.1458]; LCMS (LCQ): Rt = 0.6 min (Method 1); *m/z* (ESI$^+$) 297.2 [M + H]$^+$; LCMS (MDAP): Rt = 10.9 min, >95% (Method 3); *m/z* (ESI$^+$) 297.0 [M + H]$^+$

3-[2-[3-(Trifluoromethyl)-1-piperidyl]pyrimidin-4-yl]pyrazolo[1,5-*b*]pyridazine **154**

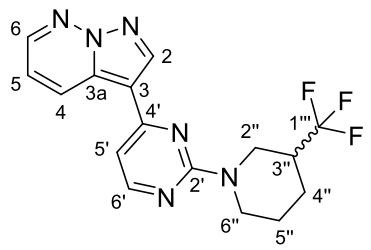

To a microwave vial containing 3-(2-chloropyrimidin-4-yl)pyrazolo[1,5-*b*]pyridazine (50 mg, 0.22 mmol) in 2-propanol (1 mL) was added DL-3-(trifluoromethyl)piperidine (33 mg, 0.22 mmol). The vial was sealed, heated to 140 °C and stirred overnight. The reaction mixture was concentrated under reduced pressure. The crude was purified using flash silica column chromatography on an Isco Combiflash system (12 g silica, elution with 0-100% EtOAc / petroleum ether gradient) to afford the title compound, 3-[2-[3-(trifluoromethyl)-1-piperidyl]pyrimidin-4-yl]pyrazolo[1,5-*b*]pyridazine, **154**, as a white solid (48 mg, 0.13 mmol, 61% yield). R_f 0.57 (EtOAc / petroleum ether 7:3); m.p. 146-148 °C; $\bar{\nu}_{max}$ (neat)/cm^{-1} 3080 (C-H, w), 3028 (C-H, w), 2931 (C-H, w), 2871 (C-H, w), 1620 (C=N, m), 1565 (C=C, m), 1526 (C=C, m); ^{1}H NMR (600 MHz, DMSO-d$_6$) δ_H 8.87 – 8.77 (2H, m, H-2 and 4), 8.61 – 8.54 (1H, m, H-6), 8.41 – 8.35 (1H, m, H-6'), 7.47 – 7.38 (1H, m, H-5), 7.21 – 7.15 (1H, m, H-5'), 4.85 (1H, d, *J* = 13.1 Hz, H-2''), 4.63 (1H, d, *J* = 13.3 Hz, H-6''), 3.13 – 2.98 (2H, m, H-2'' and 6''), 2.58 – 2.43 (1H, m, H-3''), 2.06 – 1.92 (1H, m, H-4''), 1.84 – 1.75 (1H, m, H-5''), 1.68 – 1.58 (1H, m, H-4''), 1.56 – 1.44 (1H, m, H-5''); ^{13}C NMR (150 MHz, DMSO-d$_6$) δ_C 161.1 (C-2'), 159.3 (C-4'), 158.3 (C-6'), 143.9 (C-6), 139.9 (C-2), 132.2 (C-3a), 128.6 (C-4), 118.9 (C-5), 110.3 (C-3a), 105.8 (C-5'), 43.7 (C-6''), 42.5 (C-2''), 38.68 (q, *J* = 25.5 Hz, C-3''), 23.3 (C-4''), 22.9 (C-5''). Signals at 127.6 ppm with J_1 = 279.3 Hz is consistent with trifluoromethyl group; HRMS *m/z* (ESI$^+$) [Found: 349.1379., $C_{16}H_{16}F_3N_6$ requires [M + H]$^+$ 349.1383]; LCMS (LCQ): Rt = 3.3 min (Method 1); *m/z* (ESI$^+$) 349.3 [M + H]$^+$; LCMS (MDAP): Rt = 21.2 min, >95% (Method 3); *m/z* (ESI$^+$) 349.0 [M + H]$^+$

3-[2-(3-Pyrimidin-4-yl-1-piperidyl)pyrimidin-4-yl]pyrazolo[1,5-*b*]pyridazine **155**

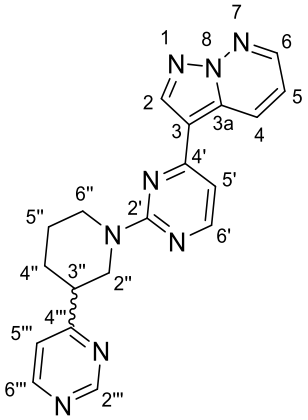

To a pressure vial containing 3-(2-methylsulfonylpyrimidin-4-yl)pyrazolo[1,5-*b*]pyridazine (60 mg, 0.22 mmol) in 2-propanol (2 mL) was added 4-(3-piperidyl)pyrimidine (71 mg, 0.44 mmol) and TEA (0.06 mL, 0.44 mmol). The vial was sealed and heated to 140 °C for 16 h. The reaction mixture was concentrated under reduced pressure. The residue was adsorbed onto solid load material. The crude was purified using flash silica column chromatography on a Biotage system (12 g silica, elution with 0-100% EtOAc / petroleum ether gradient). Desired fractions were combined and concentrated under reduced pressure. The crude was purified using reverse phase column chromatography on a Biotage system (12 g C-18, elution with 10-100% MeOH / water gradient) to afford the title compound, 3-[2-(3-pyrimidin-4-yl-1-piperidyl)pyrimidin-4-yl]pyrazolo[1,5-*b*]pyridazine, **155**, as a colourless solid (19 mg, 0.05 mmol, 24% yield). R_f 0.25(100% EtOAc); m.p. 158-160 °C; $\bar{\nu}_{max}$ (neat)/cm^{-1} 3088 (C-H, w), 3056 (C-H, w), 2924 (C-H, w), 2858 (C-H, w), 1616 (C=N, m), 1562 (C=C, s), 1524 (C=C, s); ^{1}H NMR (600 MHz, MeOD) δ_H 9.16 (1H, s, H-2’’’), 9.02 – 8.95 (1H, m, H-4), 8.73 (1H, d, *J* = 5.2 Hz, H-6’’’), 8.65 (1H, s, H-2), 8.49 (1H, dd, *J* = 4.5, 2.0 Hz, H-6), 8.33 (1H, d, *J* = 5.2 Hz, H-6’), 7.55 (1H, d, *J* = 5.2 Hz, H-5’’’), 7.34 (1H, dd, *J* = 9.3, 4.5 Hz, H-5), 7.07 (1H, d, *J* = 5.2 Hz, H-5’), 5.00 (1H, d, *J* = 13.2 Hz, H-2’’), 4.80 (1H, app. d, *J* = 13.6 Hz, H-6’’), 3.36 – 3.28 (1H, m, H-2’’), 3.23 – 3.12 (1H, m, H-6’’), 3.07 – 2.98 (1H, m, H-3’’), 2.24 – 2.14 (1H, m, H-4’’), 2.09 – 1.99 (1H, m, H-4’’), 1.97 – 1.89 (1H, m, H-5’’), 1.79 – 1.68 (1H, m, H-5’’); ^{13}C NMR (150 MHz, MeOD) δ_C 173.3 (C-4’’’), 163.0 (C-2’), 161.3 (C-4’), 159.2 (C-2’’’ or C-6’), 159.1 (C-2’’’ or C-6’), 158.3 (C-6’’’), 144.9 (C-6), 140.4 (C-2), 134.1 (C-3a), 130.5 (C-4), 121.2 (C-5’), 119.9 (C-5), 112.5 (C-3), 106.6 (C-5’), 50.0 (C-2’’), 45.9 (C-6’’), 44.7 (C-3’’). 31.1 (C-4’’), 25.7 (C-5’’); HRMS *m/z* (ESI$^+$) [Found: 359.1724., $C_{19}H_{19}N_8$ requires [M + H]$^+$ 359.1727]; LCMS (MDAP): Rt = 14.1 min, >95% (Method 3); *m/z* (ESI$^+$) 359.0 [M + H]$^+$

2,2,6,6-Tetramethyl-4-(4-pyrazolo[1,5-*b*]pyridazin-3-ylpyrimidin-2-yl)morpholine **156**

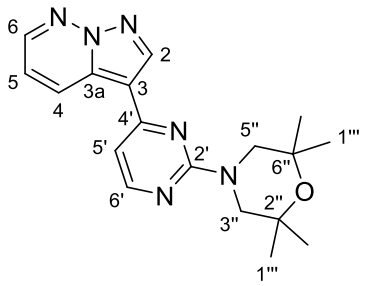

To a microwave vial containing 3-(2-methylsulfonylpyrimidin-4-yl)pyrazolo[1,5-*b*]pyridazine (100 mg, 0.33 mmol) in 2-propanol (1 mL) was added 2,2,6,6-tetramethylmorpholine (47 mg, 0.33 mmol). The vial was sealed and heated to 140 °C for 6 h. The reaction mixture was concentrated under reduced pressure. The crude was purified using flash silica column chromatography on an Isco Combiflash system (12 g silica, elution with 0-100% EtOAc / petroleum ether gradient) to afford the title compound 2,2,6,6-tetramethyl-4-(4-pyrazolo[1,5-*b*]pyridazin-3-ylpyrimidin-2-yl)morpholine, **156**, as a white solid (53 mg, 0.15 mmol, 45% yield). R_f 0.43 (EtOAc / petroleum ether 1:1); m.p. 178-180 °C; $\bar{\nu}_{max}$ (neat)/cm^{-1} 2968 (C-H, w), 2923 (C-H, w), 2859 (C-H, w), 1620 (C=N, m), 1562 (C=C, m), 1528 (C=C, m); ^{1}H NMR (600 MHz, DMSO-d$_6$) δ_H 8.89 – 8.80 (2H, m, H-2 and 4), 8.62 – 8.58 (1H, m, H-6), 8.37 (1H, d, *J* = 5.2 Hz, H-6'), 7.52 (1H, dd, *J* = 9.0, 4.4 Hz, H-5), 7.18 (1H, d, *J* = 5.2 Hz, H-5'), 3.72 (4H, s, H-3'' and 5''), 1.22 (12H, s, H-1'''); ^{13}C NMR (150 MHz, DMSO-d$_6$) δ_C 161.6 (C-2'), 159.1 (C-4'), 158.2 (C-6'), 143.9 (C-6), 139.9 (C-2), 132.2 (C-3a), 128.7 (C-4), 119.2 (C-5), 110.4 (C-3), 105.4 (C-5'), 71.2 (C-3'' and C-5''), 52.0 (C-2'' and C-6''), 28.3 (C-1'''); HRMS *m/z* (ESI$^+$) [Found: 339.2026., $C_{18}H_{23}N_6O$ requires [M + H]$^+$ 339.1928]; LCMS (LCQ): Rt = 2.7 min (Method 1); *m/z* (ESI$^+$) 339.1 [M + H]$^+$; LCMS (MDAP): Rt = 18.9 min, >95% (Method 3); *m/z* (ESI$^+$) 339.0 [M + H]$^+$

Cis-2,6-dimethyl-4-(4-{pyrazolo[1,5-*b*]pyridazin-3-yl}pyrimidin-2-yl)morpholine **157**

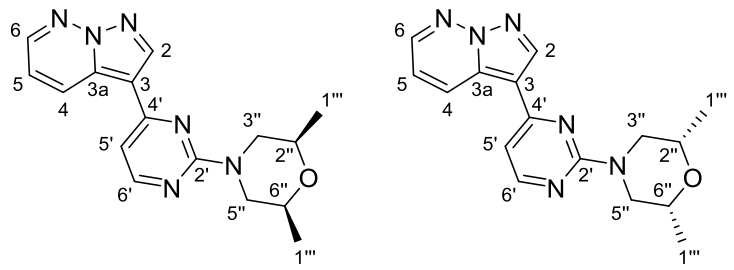

To a microwave vial containing 3-(2-methylsulfonylpyrimidin-4-yl)pyrazolo[1,5-*b*]pyridazine (90 mg, 0.33 mmol) in 2-propanol (1 mL) was added 2,6-dimethylmorpholine (0.06 mL, 0.49 mmol). The vial was sealed and heated conventionally at 140 °C for 4 h. The reaction mixture was concentrated under reduced pressure. The crude was purified using reverse phase column chromatography on a Biotage system (12 g C-18, elution with 10-100% MeOH / water gradient). Desired fractions were combined and concentrated under reduced pressure. The crude was purified using flash silica column chromatography on an Isco Combiflash system (12 g silica, elution with 0-100% EtOAc / petroleum ether gradient) to afford the title compound, *cis*-2,6-dimethyl-4-(4-pyrazolo[1,5-*b*]pyridazin-3-ylpyrimidin-2-yl)morpholine, **157**, as a white solid (56 mg, 0.17 mmol, 52% yield). R_f 0.50 (EtOAc / petroleum ether 3:2); $[\boldsymbol{\alpha}]_{\boldsymbol{D}}^{\mathbf{25}} = +13.3$ (c = 1.5 x 10^{-3} g / mL, $CHCl_3$); m.p. 152-154 °C; $\bar{\nu}_{max}$ (neat)/cm^{-1} 3097 (C-H, w), 2978 (C-H, w), 2933 (C-H, w), 1622 (C=N, m), 1563 (C=C, m), 1524 (C=C, m); ^{1}H NMR (600 MHz, DMSO-d_6) δ_H 8.85 – 8.77 (2H, m, H-2 and 4), 8.58 (1H, dd, *J* = 4.4, 1.9 Hz, H-6), 8.35 (1H, d, *J* = 5.2 Hz, H-6'), 7.46 (1H, dd, *J* = 9.0, 4.4 Hz, H-5), 7.17 (1H, d, *J* = 5.2 Hz, H-5'), 4.53 (2H, dd, *J* = 12.9, 2.3Hz, H-3'' and 5''), 3.65 – 3.53 (2H, m, H-2'' and 6''), 2.58 (2H, t, *J* = 11.8 Hz, H-3'' and 5''), 1.18 (6H, s, H-1'''); ^{13}C NMR (150 MHz, DMSO-d_6) δ_C 161.2 (C-2'), 159.1 (C-4'), 158.1 (C-6'), 143.9 (C-6), 139.9 (C-2), 132.2 (C-3a), 128.8 (C-4), 119.1 (C-5), 110.3 (C-3), 105.9 (C-5'), 71.0 (C-2'' and C-6''), 49.1 (C-3'' and C-5''), 18.8 (C-1'''); HRMS *m/z* (ESI$^+$) [Found: 311.1613., $C_{16}H_{19}N_6O$ requires [M + H]$^+$ 311.1615]; LCMS (LCQ): Rt = 2.1 min (Method 1); *m/z* (ESI$^+$) 311.1 [M + H]$^+$; LCMS (MDAP): Rt = 16.7 min, >95% (Method 3); *m/z* (ESI$^+$) 311.0 [M + H]$^+$

Trans-2,6-dimethyl-4-(4-{pyrazolo[1,5-*b*]pyridazin-3-yl}pyrimidin-2-yl)morpholine **158**

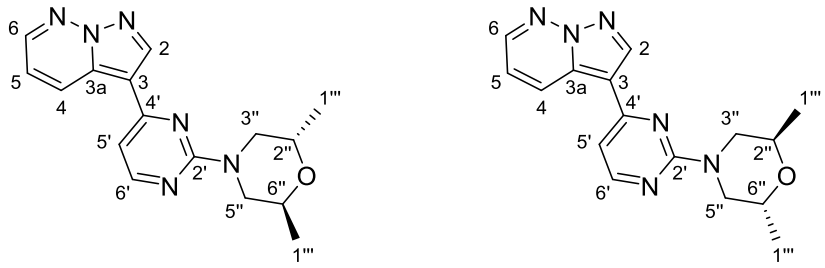

To a microwave vial containing 3-(2-methylsulfonylpyrimidin-4-yl)pyrazolo[1,5-*b*]pyridazine (90 mg, 0.33 mmol) in 2-propanol (1 mL) was added 2,6-dimethylmorpholine (0.06 mL, 0.49 mmol). The vial was sealed and heated conventionally at 140 °C for 4 h. The reaction mixture was concentrated under reduced pressure. The crude was purified using reverse phase column chromatography on a Biotage system (12 g C-18, elution with 10-100% MeOH / water gradient). Desired fractions were combined and concentrated under reduced pressure. The crude was purified using flash silica column chromatography on an Isco Combiflash system (12 g silica, elution with 0-100% EtOAc / petroleum ether gradient) to afford the title compound, *trans*-2,6-dimethyl-4-(4-pyrazolo[1,5-*b*]pyridazin-3-ylpyrimidin-2-yl)morpholine, **158**, as a white solid. (5 mg, 0.01 mmol, 4% yield). R_f 0.38 (EtOAc / petroleum ether 3:2); ^{1}H NMR (600 MHz, DMSO-d$_6$) δ_H 8.87 – 8.75 (2H, m, H-2 and 4), 8.58 (1H, dd, *J* = 4.5, 1.8 Hz, H-6), 8.35 (1H, d, *J* = 5.1 Hz, H-6'), 7.46 (1H, dd, *J* = 9.1, 4.5 Hz, H-5), 7.16 (1H, d, *J* = 5.1 Hz, H-5'), 4.07 – 3.96 (2H, m, H-2'' and 6''), 3.93 – 3.83 (2H, m, H-3'' and 5''), 3.56 – 3.45 (2H, m, H-3'' and 5''), 1.16 (6H, d, *J* = 6.4 Hz, H-1'''); ^{13}C NMR (150 MHz, DMSO-d$_6$) δ_C 161.8 (C-2'), 159.1 (C-4'), 158.1 (C-6'), 143.9 (C-6), 139.9 (C-2), 132.2 (C-3a), 128.9 (C-4), 119.1 (C-5), 110.3 (C-3), 105.6 (C-5'), 65.4 (C-2'' and C-6''), 48.4 (C-3'' and C-5''), 17.7 (C-1'''); HRMS *m/z* (ESI$^+$) [Found: 311.1614., $C_{16}H_{19}N_6O$ requires [M + H]$^+$ 311.1615]; LCMS (LCQ): Rt = 1.8 min (Method 1); *m/z* (ESI$^+$) 311.1 [M + H]$^+$; LCMS (MDAP): Rt = 15.5 min, >95% (Method 3); *m/z* (ESI$^+$) 311.0 [M + H]$^+$

3-[2-(3,4-Dimethylpiperazin-1-yl)pyrimidin-4-yl]pyrazolo[1,5-*b*]pyridazine **159**

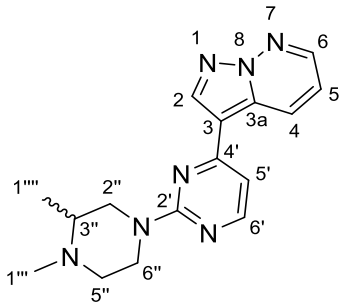

To a pressure vial containing 3-(2-chloropyrimidin-4-yl)pyrazolo[1,5-*b*]pyridazine (60 mg, 0.26 mmol) in 2-propanol (2 mL) was added 1,2-dimethylpiperazine (59 mg, 0.52 mmol). The vial was sealed and heated to 140 °C for 16 h. The reaction mixture was concentrated under reduced pressure. The residue was loaded onto solid load adsorbant. The crude was purified using flash silica column chromatography on an Isco Combiflash system (12 g silica, elution with 0-50% 20% MeOH in CH_2Cl_2 / CH_2Cl_2 gradient). Desired fractions were combined and concentrated under reduced pressure. The crude was purified using reverse phase column chromatography on a Biotage system (12 g C-18, elution with 10-100% MeOH / water gradient) to afford the title compound, 3-[2-(3,4-dimethylpiperazin-1-yl)pyrimidin-4-yl]pyrazolo[1,5-*b*]pyridazine, **159**, as a colourless solid (27 mg, 0.08 mmol, 33% yield). R_f 0.56 (MeOH/ CH_2Cl_2 1:9); m.p. 78-80 °C; $\bar{\nu}_{max}$ (neat)/cm^{-1} 3091 (C-H, w), 2951 (C-H, w), 2843 (C-H, w), 2789 (C-H, w), 1622 (C=N, m), 1563 (C=C, m), 1526 (C=C, m); ^{1}H NMR (600 MHz, DMSO-d$_6$) δ_H 8.87 – 8.81 (2H, m, H-4 and H-2), 8.60 – 8.56 (1H, m, H-6), 8.35 (1H, d, *J* = 5.1 Hz, H-6'), 7.47 (1H, dd, *J* = 9.1, 4.4 Hz, H-5), 7.16 (1H, d, *J* = 5.1 Hz, H-5'), 4.48 (1H, app. d, *J* = 13.0 Hz, H-6''), 4.42 (1H, d, *J* = 12.8 Hz, H-2''), 3.13 (1H, t, *J* = 12.1 Hz, H-6''), 2.83 (1H, app. d, *J* = 11.5 Hz, H-5''), 2.75 (1H, app. t, *J* = 11.6 Hz, H-2''), 2.21 (3H, s, H-1'''), 2.18 – 2.09 (1H, m, H-5''), 2.08 – 2.00 (1H, m, H-3''), 1.07 (3H, d, *J* = 6.1 Hz, H-1''''); ^{13}C NMR (150 MHz, DMSO-d$_6$) δ_C 161.3 (C-2'), 159.1 (C-4'), 158.1 (C-6'), 143.9 (C-6), 139.8 (C-2), 132.2 (C-3a), 128.9 (C-4), 119.1 (C-5), 110.4 (C-3), 105.6 (C-5'), 57.1 (C-3''), 54.6 (C-5''), 50.0 (C-2''), 43.8 (C-6''), 42.3 (C-1'''), 16.6 (C-1''''); HRMS *m/z* (ESI$^+$) [Found: 310.1771., $C_{16}H_{20}N_7$ requires [M + H]$^+$ 310.1775]; LCMS (MDAP): Rt = 9.7 min, >95% (Method 3); *m/z* (ESI$^+$) 310.0 [M + H]$^+$.

3-[2-(4-Cyclopropylpiperazin-1-yl)pyrimidin-4-yl]pyrazolo[1,5-*b*]pyridazine **160**

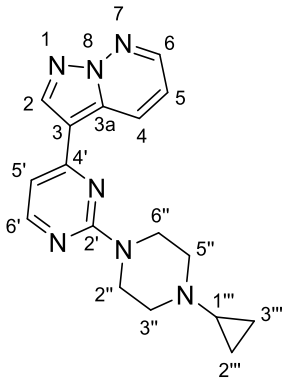

To a microwave vial containing a suspension of 3-(2-chloropyrimidin-4-yl)pyrazolo[1,5-*b*]pyridazine (80 mg, 0.35 mmol) in 2-propanol (2 mL) was added 1-cyclopropylpiperazine (87 mg, 0.69 mmol). The vial was sealed and the reaction mixture heated to 140 °C and stirred overnight. The reaction was concentrated under reduced pressure. The crude was purified using flash silica column chromatography on an Isco Combiflash system (12 g silica, elution with 0-50% 20% MeOH in CH_2Cl_2 / CH_2Cl_2 gradient). Desired fractions were combined and concentrated under reduced pressure. The crude was purified using reverse phase column chromatography on a Biotage system (12 g C-18, elution with 10-100% MeOH / water gradient) to afford the title compound, 3-[2-(4-cyclopropylpiperazin-1-yl)pyrimidin-4-yl]pyrazolo[1,5-*b*]pyridazine, **160**, as a yellow oil (7 mg, 0.02 mmol, 6% yield). R_f 0.73 (MeOH/ CH_2Cl_2 1:9); $\bar{\nu}_{max}$ (neat)/cm^{-1} 2939 (C-H, w), 2903 (C-H, w), 2809 (C-H, w), 1622 (C=N, m), 1562 (C=C, m), 1528 (C=C, m); ^{1}H NMR (600 MHz, MeOD) δ_H 8.96 (1H, app. d, *J* = 9.1 Hz, H-4), 8.68 (1H, s, H-2), 8.52 – 8.49 (1H, m, H-6), 8.34 (1H, d, *J*= 5.2 Hz, H-6'), 7.41 (1H, dd, *J*= 9.1, 4.4 Hz, H-5), 7.11 (1H, d, *J*= 5.2 Hz, H-5'), 3.89 (4H, t, *J*= 5.0 Hz, H-2'' and 6''), 2.78 (4H, t, *J*= 5.1 Hz, H-3'' and 5''), 1.78 – 1.72 (1H, m, H-1'''), 0.59 – 0.50 (4H, m, H-2''' and 3'''); ^{13}C NMR (150 MHz, MeOD) δ_C 161.2 (C-4'), 159.0 (C-6'), 144.9 (C-6), 140.5 (C-2), 132.1 (C-3a), 130.4 (C-4), 120.0 (C-5), 110.1 (C-3), 106.9 (C-5'), 54.3 (C-3'' and C-5''), 44.9 (C-2'' and C-6''), 39.6 (C-1'''), 5.97 (C-2''' and C-3'''). C-2' suspected to be weak signal at δ_C 161.3 ppm; HRMS *m/z* (ESI$^+$) [Found: 322.1770., $C_{17}H_{20}N_7$ requires [M + H]$^+$ 322.1775]; LCMS (MDAP): Rt = 9.6 min, >95% (Method 3); *m/z* (ESI$^+$) 322.0 [M + H]$^+$

3-[2-[(3*S*)-3-Isopropylpiperazin-1-yl]pyrimidin-4-yl]pyrazolo[1,5-*b*]pyridazine **161**

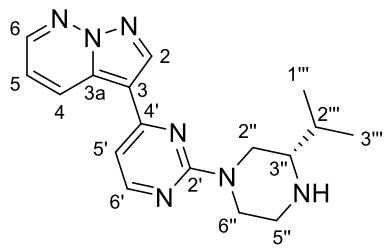

To a microwave vial containing 3-(2-methylsulfonylpyrimidin-4-yl)pyrazolo[1,5-*b*]pyridazine (100 mg, 0.33 mmol) in 2-propanol (1 mL) was added (*S*)-1-boc-2-Isopropylpiperazine (112 mg, 0.49 mmol). The vial was sealed and heated to 140 °C overnight. The reaction mixture was concentrated under reduced pressure. The crude was purified using flash silica column chromatography on an Isco Combiflash system (12 g silica, elution with 0-100% ammonia/ MeOH / CH_2Cl_2 1:10:90 gradient). Desired fractions were combined and concentrated under reduced pressure to afford a yellow solid. To the solid was added 4 M HCl in dioxane (5 mL) and the reaction mixture stirred at rt for 5 h. The reaction mixture was concentrated under reduced pressure to afford the title compound,3-[2-[(3*S*)-3-isopropylpiperazin-1-yl]pyrimidin-4-yl]pyrazolo[1,5-*b*]pyridazine, **161**, as a pale yellow solid (25 mg, 0.07 mmol, 22% yield). R_f 0.20 (MeOH/ CH_2Cl_2 1:9); Decomposed > 182 °C; $\bar{\nu}_{max}$ (neat)/cm^{-1} 3388 (N-H, s), 2961 (C-H, w), 2927 (C-H, w), 2874 (C-H, w), 1668 (N-H, w), 1620 (C=N, m), 1564 (C=C, m), 1527 (C=C, m); ^{1}H NMR (600 MHz, DMSO-d$_6$) δ_H 8.86 (1H, d, *J* = 9.1 Hz, H-4), 8.83 (1H, s, H-2), 8.61 – 8.57 (1H, m, H-6), 8.36 (1H, d, *J* = 5.1 Hz, H-6'), 7.43 (1H, dd, *J* = 9.1, 4.4 Hz, H-5), 7.14 (1H, d, *J* = 5.1 Hz, H-5'), 4.67 (1H, d, *J* = 12.6 Hz, H-2''), 4.55 (1H, d, *J* = 12.8 Hz, H-6''), 3.04 (1H, d, *J* = 12.0 Hz, 1H, H-5''), 2.93 (1H, t, *J* = 11.6 Hz, H-6''), 2.71 – 2.62 (2H, m, H-2'' and 5''), 2.36 – 2.32 (1H, m, H-3''), 1.65 (1H, dt, *J* = 13.4, 6.8 Hz, H-2'''), 1.01 – 0.92 (6H, m, H-1'''); ^{13}C NMR (150 MHz, DMSO-d$_6$) δ_C 161.4 (C-2'), 159.0 (C-4'), 158.1 (C-6'), 143.9 (C-6), 139.8 (C-2), 132.2 (C-8a), 128.8 (C-4), 118.8 (C-5), 110.4 (C-3), 105.2 (C-5'), 60.2 (C-3''), 46.9 (C-2''), 45.3 (C-5''), 44.1 (C-6''), 30.7 (C-2'''), 18.92 (d, J = 60.5 Hz, C-1''' and C-3''', possible rotamers); HRMS *m/z* (ESI$^+$) [Found: 324.1926., $C_{17}H_{22}N_7$ requires [M + H]$^+$ 324.1931]; LCMS (LCQ): Rt = 0.5 min (Method 1); *m/z* (ESI$^+$) 324.1 [M + H]$^+$; LCMS (MDAP): Rt = 10.3 min, >95% (Method 3); *m/z* (ESI$^+$) 324.0 [M + H]$^+$

3-[2-[(3*R*)-3-Isobutylpiperazin-1-yl]pyrimidin-4-yl]pyrazolo[1,5-*b*]pyridazine **162**

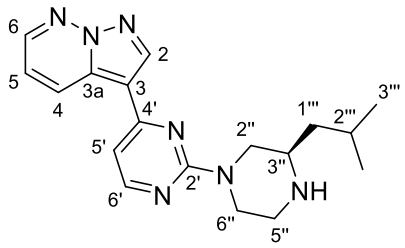

To a microwave vial containing 3-(2-methylsulfonylpyrimidin-4-yl)pyrazolo[1,5-*b*]pyridazine (100 mg, 0.33 mmol) in 2-propanol (1 mL) was added (*R*)-1-boc-2-isobutylpiperazine (120 mg, 0.49 mmol). The vial was sealed and heated to 140 °C overnight. The reaction mixture was concentrated under reduced pressure. The crude was purified using flash silica column chromatography on an Isco Combiflash system (12 g silica, elution with 0-100% ammonia/ MeOH / CH_2Cl_2 1:10:90 gradient). Desired fractions were combined and concentrated under reduced pressure to afford a pale yellow solid. To the solid was added 4 M HCl in dioxane (5 mL) and the reaction mixture stirred at rt for 5 h. The reaction mixture was concentrated under reduced pressure to afford the title compound, 3-[2-[(3*R*)-3-isobutylpiperazin-1-yl]pyrimidin-4-yl]pyrazolo[1,5-*b*]pyridazine, **162**, as a pale yellow solid (25 mg, 0.07 mmol, 21% yield). R_f 0.33 (MeOH/ CH_2Cl_2 1:9); Decomposed > 181 °C; $\bar{\nu}_{max}$ (neat)/cm^{-1} 3283 (N-H, w), 2957 (C-H, w), 2904 (C-H, w), 1672 (N-H, w), 1623 (C=N, m), 1564 (C=C, m), 1526 (C=C, m); ^{1}H NMR (600 MHz, DMSO-d_6) δ_H 8.88 – 8.83 (2H, m, H-2 and 4), 8.62 – 8.58 (1H, m, H-6), 8.37 (1H, d, *J*= 5.1 Hz, H-6'), 7.46 (1H, dd, *J*= 9.1, 4.4 Hz, H-5), 7.16 (1H, d, *J*= 5.1 Hz, H-5'), 4.66 – 4.50 (2H, m, H-2'' and 6''), 3.05 – 2.91 (2H, m, H-5'' and 6''), 2.75 – 2.56 (3H, m, H-2'', 3'' and 5''), 1.82 – 1.75 (1H, m, H-2'''), 1.31 – 1.26 (2H, m, H-1'''), 0.91 (6H, d, *J*= 6.7 Hz, H-3'''); ^{13}C NMR (150 MHz, DMSO-d_6) δ_C 161.3 (C-2'), 159.1 (C-4'), 158.2 (C-6'), 143.9 (C-6), 139.8 (C-2), 132.2 (C-3a), 128.8 (C-4), 118.9 (C-5), 110.4 (C-3), 105.3 (C-5'), 52.5 (C-3''), 49.5 (C-2''), 45.0 (C-5''), 44.2 (C-6''), 42.5 (C-1'''), 23.9 (C-2'''), 22.82 (d, J = 12.5 Hz, C3''', rotamers); HRMS *m/z* (ESI$^+$) [Found: 338.2082., $C_{18}H_{24}N_7$ requires [M + H]$^+$ 338.2088]; LCMS (LCQ): Rt = 0.5 min (Method 1); *m/z* (ESI$^+$) 338.1 [M + H]$^+$; LCMS (MDAP): Rt = 11.2 min, >95% (Method 3); *m/z* (ESI$^+$) 338.0 [M + H]$^+$.

3-[2-(1,4-Diazepan-1-yl)pyrimidin-4-yl]pyrazolo[1,5-*b*]pyridazine **163**

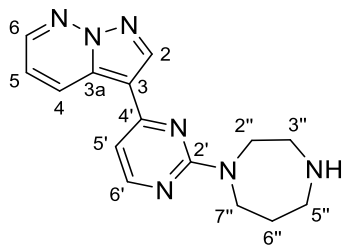

To a microwave vial containing 3-(2-methylsulfonylpyrimidin-4-yl)pyrazolo[1,5-*b*]pyridazine (100 mg, 0.33 mmol) in 2-propanol (1 mL) was added 2-methyl-2-propanyl 1,4-diazepane-1-carboxylate (99 mg, 0.49 mmol). The vial was sealed and heated to 140 °C overnight. The reaction mixture was concentrated under reduced pressure. The crude was purified using flash silica column chromatography on an Isco Combiflash system (12 g silica, elution with 0-100% ammonia/ MeOH / CH_2Cl_2 1:10:90 gradient). Desired fractions were combined and concentrated under reduced pressure to afford a pale yellow solid. To the solid was added 4 M HCl in dioxane (5 mL) and the reaction mixture stirred at rt for 5 h. The reaction mixture was concentrated under reduced pressure to afford the title compound, 3-[2-(1,4-diazepan-1-yl)pyrimidin-4-yl]pyrazolo[1,5-*b*]pyridazine, **163**, as a pale yellow solid (35 mg, 0.11 mmol, 34% yield). R_f 0.11 (MeOH/ CH_2Cl_2 1:9); Decomposed > 240 °C; $\bar{\nu}_{max}$ (neat)/cm^{-1} 3335 (N-H, w), 3091 (C-H, w), 2942 (C-H, w), 2897 (C-H, w), 2848 (C-H, w), 1623 (C=N, m), 1563 (C=C, m), 1526 (C=C, m); ^{1}H NMR (600 MHz, MeOD) δ_H 8.91 (1H, d, *J*= 9.0 Hz, H-4), 8.64 (1H, s, H-2), 8.50 – 8.46 (1H, m, H-6), 8.30 (1H, d, *J*= 5.2 Hz, H-6’), 7.36 (1H, dd, *J*= 9.0, 4.4 Hz, H-5), 7.06 (1H, d, *J*= 5.2 Hz, H-5’), 4.01 – 3.94 (4H, m, H-2’’ and 3’’, 5’’ and 7’’), 3.36 (1H, s, NH), 3.14 (2H, t, *J*= 5.2 Hz, H-2’’ and 3’’), 2.95 (2H, t, *J*= 5.7 Hz, H-5’’ and 7’’), 2.08 – 1.99 (2H, m, H-6’’); ^{13}C NMR (150 MHz, MeOD) δ_C 162.6 (C-2’), 161.1 (C-4’), 159.0 (C-6’), 144.9 (C-6), 140.4 (C-2), 134.0 (C-3a), 130.3 (C-4), 119.9 (C-5), 112.5 (C-3), 106.2 (C-5’), 48.3 (C-2’’ and C-3’’), 47.0 (C-5’’ and C-7’’) , 29.8 (C-6’’); HRMS *m/z* (ESI$^+$) [Found: 296.1613., $C_{15}H_{18}N_7$ requires [M + H]$^+$ 296.1618]; LCMS (MDAP): Rt = 9.0 min, >95% (Method 3); *m/z* (ESI$^+$) 296.0 [M + H]$^+$

3-(4-Pyrazolo[1,5-*b*]pyridazin-3-ylpyrimidin-2-yl)-8-oxa-3-azabicyclo[3.2.1]octane **164**

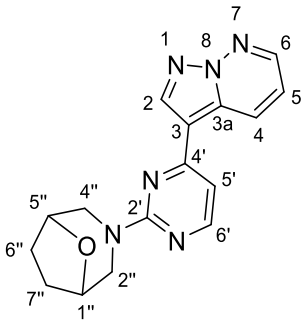

To a microwave vial containing 3-(2-chloropyrimidin-4-yl)pyrazolo[1,5-*b*]pyridazine (80 mg, 0.35 mmol) in 2-propanol (2 mL) was added 8-oxa-3-azabicyclo[3.2.1]octane (78 mg, 0.69 mmol. The vial was sealed and irradiated with microwaves, heating to 140 °C for 21 min. The reaction was concentrated under reduced pressure. The crude was purified using flash silica column chromatography on an Isco Combiflash system (12 g silica, elution with 0-100% EtOAc / petroleum ether gradient) to afford the title compound, 3-(4-pyrazolo[1,5-*b*]pyridazin-3-ylpyrimidin-2-yl)-8-oxa-3-azabicyclo[3.2.1]octane, **164**, as a pale yellow solid (80 mg, 0.25 mmol, 71% yield). R_f 0.36 (EtOAc / petroleum ether 1:1); m.p. 218-220 °C; $\bar{\nu}_{max}$ (neat)/cm^{-1} 2976 (C-H, w), 2957 (C-H, w), 2856 (C-H, w), 1623 (C=N, m), 1564 (C=C, m); ^{1}H NMR (500 MHz, DMSO-d$_6$) δ_H 8.92 – 8.87 (1H, m, H-4), 8.86 (1H, s, H-2), 8.62 – 8.58 (1H, m, H-6), 8.37 (1H, d, *J*= 5.2 Hz, H-6'), 7.46 (1H, dd, *J*= 9.0, 4.5 Hz, H-5), 7.22 (1H, d, *J*= 5.2 Hz, H-5'), 4.47 (2H, s, H-1'' and 5''), 4.24 (2H, d, *J*= 12.8 Hz, H-2'' and 4''), 3.14 (2H, d, *J*= 13.0 Hz, H-2'' and 4''), 1.88 – 1.80 (2H, m, H-6'' and 7''), 1.72 (2H, d, *J*= 7.1 Hz, H-6'' and 7''); ^{1}H NMR (600 MHz, MeOD) δ_H 8.97 (1H, dd, *J* = 9.1, 1.9 Hz, H-4), 8.68 (1H, s, H-2), 8.51 (1H, dd, *J* = 4.5, 1.9 Hz, H-6), 8.34 (1H, d, *J* = 5.2 Hz, H-6'), 7.41 (1H, dd, *J* = 9.1, 4.5 Hz, H-5), 7.15 (1H, d, *J* = 5.2 Hz, H-5'), 4.53 (2H, d, *J* = 5.1 Hz, H-1'' and 5''), 4.35 (2H, d, *J* = 12.8 Hz, H-2'' and 4''), 3.26 (2H, dd, *J* = 13.0, 2.5 Hz, H-2'' and 4''), 2.04 – 1.93 (2H, m, H-6'' and 7''), 1.93 – 1.82 (2H, m, H-6'' and 7''); ^{13}C NMR (150 MHz, MeOD) δ_C 164.1 (C-2'), 161.1 (C-4'), 158.9 (C-6'), 144.9 (C-6), 140.5 (C-2), 134.1 (C-3a)*, 130.5 (C-4), 120.0 (C-5), 111.5 (C-3)*, 107.1 (C-5'), 75.3 (C-1'' and C-5''), 51.2 (C-2'' and C-4''), 28.8 (C-6'' and C-7''). *Signals at δ_C 134.1 and 111.5 ppm weak but consistent with analogues; HRMS *m/z* (ESI$^+$) [Found: 309.1460., $C_{16}H_{17}N_6O$ requires [M + H]$^+$ 309.1458]; LCMS (MDAP): Rt = 21.11 min, >95% (Method 3); *m/z* (ESI$^+$) 309.0 [M + H]$^+$

Methyl pyrazolo[1,5-*b*]pyridazine-3-carboxylate **165**

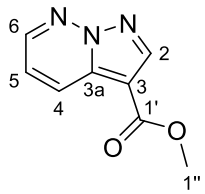

To a slurry of pyridazin-1-ium-1-amine iodide (3.13 g, 14.05 mmol) in CH_2Cl_2 (100 mL) was added methyl propiolate (0.5 mL, 5.62 mmol). The reaction flask was cooled in an ice bath before slowly adding a solution of potassium carbonate (2.33 g, 16.86 mmol) in water (100 mL) in one portion. The reaction mixture was stirred at rt for 16 h. The organic layer was separated. The aqueous layer was washed with CH_2Cl_2 (3 x 100 mL). The combined organic layers were washed with brine solution (200 mL), and dried over $MgSO_4$, filtered and concentrated under reduced. The crude was purified using flash silica column chromatography on an Isco Combiflash system (12 g silica, elution with 0-100% EtOAc / petroleum ether gradient) to afford the title compound, methyl pyrazolo[1,5-*b*]pyridazine-3-carboxylate, **165**, as a pale yellow solid (380 mg, 2.04 mmol, 36% yield). R_f 0.38 (CH_2Cl_2); m.p. 119-121 °C; $\bar{\nu}_{max}$ (neat)/cm^{-1} 3099 (C-H, w), 3013 (C-H, w), 1698 (C=O, s), 1623 (C=N, m), 1536 (C=C, m); ^{1}H NMR (500 MHz, DMSO-d$_6$) δ_H 8.70 – 8.65 (1H, m, H-4), 8.58 – 8.53 (2H, m, H-2 and 6), 7.55 (1H, dd, *J* = 9.1, 4.5 Hz, H-5), 3.86 (3H, s, H-1''); HRMS *m/z* (ESI$^+$) [Found: 178.0608., $C_8H_8N_3O_2$ requires [M + H]$^+$ 178.0611]; LCMS (LCQ): Rt = 1.0 min (Method 1); *m/z* (ESI$^+$) 178.1 [M + H]$^+$.

Pyrazolo[1,5-*b*]pyridazine-3-carboxylic acid **166**

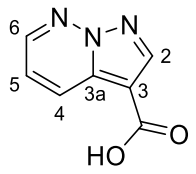

To a solution of methyl pyrazolo[1,5-*b*]pyridazine-3-carboxylate (350 mg, 1.98 mmol) in MeOH (2.5 mL) was added lithium hydroxide (135 mg, 3.22 mmol) in water (2.5 mL). The reaction mixture was stirred at rt for 16 h. The reaction mixture was concentrated under reduced pressure. Water (10 mL) was added to the residue and the resulting solution cooled in an ice bath. 1 M HCl (10 mL) was added and the mixture stirred at rt for 30 min. A suspension immediately formed and was filtered and washed with water. The resulting solid was dried under reduced pressure to afford the title compound pyrazolo[1,5-*b*]pyridazine-3-carboxylic acid, **166**, as a white solid (250 mg, 1.46 mmol, 74% yield). R_f 0 (EtOAc / petroleum ether 1:1); Decomposed > 295 °C; $\bar{\nu}_{max}$ (neat)/cm^{-1} 3136 (O-H, s), 2556 (C-H, w), 1703 (C=O, s), 1621 (C=N, m), 1542 (C=C, m), 1520 (C=C, m); ^{1}H NMR (500 MHz, DMSO-d$_6$) δ_H 12.83 (1H, s, COOH), 8.63 (1H, dd, *J* = 4.4, 2.1 Hz, H-6), 8.55 – 8.44 (2H, m, H-2 and 4), 7.50 (1H, dd, *J* = 9.1, 4.4 Hz, H-5); ^{13}C NMR (150 MHz, DMSO-d$_6$) δ_C 163.5 (C=O), 144.3 (C-6), 142.1 (C-2), 134.6 (C-3a), 127.9 (C-4), 120.2 (C-5), 104.5 (C-3); HRMS *m/z* (ESI$^+$) [Found: 186.0271., $C_7H_5N_3NaO_2$ requires [M + Na]$^+$ 186.0274]; LCMS (MDAP): Rt = 1.48 -4.65 min, >95% (Method 5); *m/z* (ESI$^+$) 164.1 [M + H]$^+$.

3-Bromopyrazolo[1,5-*b*]pyridazine **167**

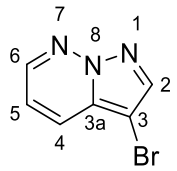

To a solution of pyrazolo[1,5-*b*]pyridazine-3-carboxylic acid (360 mg, 2.21 mmol) in DMF (4 mL) was added *N*-bromosuccinimide (790 mg, 4.41 mmol) and the reaction stirred at rt for 3 h. The reaction mixture was concentrated under reduced pressure. The crude was purified using flash silica column chromatography on an Isco Combiflash system (12 g silica, elution with 0-60% EtOAc / petroleum ether gradient) to afford 3-bromopyrazolo[1,5-*b*]pyridazine, **167**, as a white crystalline solid (360 mg, 1.73 mmol, 78% yield). R_f 0.74 (EtOAc / petroleum ether 1:1); m.p. 102-104 °C; $\bar{\nu}_{max}$ (neat)/cm^{-1} 3100 (C-H, w), 3084 (C-H, w), 3044 (C-H, w); ^{1}H NMR (500 MHz, DMSO-d$_6$) δ_H 8.52 (1H, dd, *J*= 4.4, 1.8 Hz, H-6), 8.28 (1H, s, H-2), 8.20 (1H, dd, *J*= 9.0, 1.8 Hz, H-4), 7.31 (1H, dd, *J*= 9.0, 4.4 Hz, H-5); ^{13}C NMR (125 MHz, DMSO-d$_6$) δ_C 143.7 (C-6), 139.3 (C-2), 131.5 (C-3a), 125.8 (C-4), 117.6 (C-5), 82.7 (C-3); HRMS *m/z* (ESI) no ionisation observed with +ve or -ve ion mode LRMS only EI$^+$ 198 [M]$^+$ m/z; LCMS (LCQ): Rt = 0.8 min (Method 1); *m/z* (ESI$^+$) 198.0 [M]$^+$ and 200.0 [M + 2]$^+$.

3-(4,4,5,5-Tetramethyl-1,3,2-dioxaborolan-2-yl)pyrazolo[1,5-*b*]pyridazine **168**

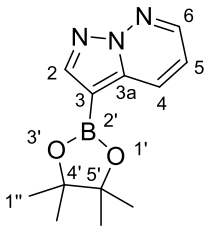

To a solution of 3-bromopyrazolo[1,5-*b*]pyridazine (100 mg, 0.50 mmol) in 1,4-dioxane (1 mL) was added bis(pinacolato)diboron (141 mg, 0.56 mmol), [1,1′-bis(diphenylphosphino)ferrocene]dichloropalladium(II), complex with CH_2Cl_2 (21 mg, 0.03 mmol) and potassium acetate (99 mg, 1.01 mmol). The reaction mixture was heated to 90 °C and stirred for 16 h. The reaction mixture was filtered through celite and concentrated under reduced pressure. The crude was purified using flash silica column chromatography on an Isco Combiflash system (12 g silica, elution with 0-50% EtOAc / petroleum ether gradient). Desired fractions were combined and concentrated under reduced pressure. The crude was purified using flash silica column chromatography on an Isco Combiflash system (12 g silica, elution with 0-50% 20% MeOH in CH_2Cl_2 / CH_2Cl_2 gradient) to afford the title compound, 3-(4,4,5,5-tetramethyl-1,3,2-dioxaborolan-2-yl)pyrazolo[1,5-*b*]pyridazine, **168**, as a white crystalline solid (30 mg, 0.12 mmol, 23% yield). R_f 0.38 (EtOAc / petroleum ether 1:1); m.p. 160-162 °C; $\bar{\nu}_{max}$ (neat)/cm^{-1} 2975 (C-H, w), 2932 (C-H, w), 1623 (C=N, m), 1536 (C=C, m); ^{1}H NMR (500 MHz, DMSO-d$_6$) δ_H 8.53 (1H, dd, *J*= 4.4, 1.9 Hz, H-6), 8.27 (1H, dd, *J*= 9.0, 1.9 Hz, H-4), 8.23 (1H, s, H-2), 7.34 (1H, dd, *J*= 9.0, 4.4 Hz, H-5), 1.30 (12H, s, H-1''); LCMS (LCQ): Rt = 2.4 min (Method 1); *m/z* (ESI$^+$) 246.2 [M + H]$^+$; LCMS (MDAP): Rt = 18.58 min, >95% (Method 3); *m/z* (ESI$^+$) 246.10 [M + H]$^+$.

4-Chloro-5-methoxy-*N*,*N*-dimethyl-pyrimidin-2-amine **169**

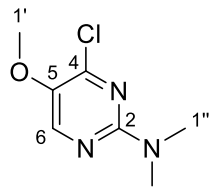

To a solution of 4-chloro-5-methoxy-2-pyrimidinamine (100 mg, 0.63 mmol) in THF (10 mL) was added sodium hydride (75 mg, 3.13 mmol) at 0 °C. After warming to rt and stirring for 5 min, iodomethane (0.08 mL, 1.36 mmol) was added dropwise and the reaction stirred at rt for 16 h. The reaction mixture was concentrated under reduced pressure and the residue was purified by using flash silica column chromatography on an Isco Combiflash system (12 g silica, elution with 0-50% EtOAc / petroleum ether gradient) to afford 4-chloro-5-methoxy-*N*,*N*-dimethyl-pyrimidin-2-amine, **169**, as a colourless oil (200 mg, 0.53 mmol, 83% yield). R_f 0.71 (EtOAc / petroleum ether 1:1); ^{1}H NMR (600 MHz, $CDCl_3$) δ_H 8.03 (1H, s, H-6), 3.85 (3H, s, H-1'), 3.14 (6H, s, H-1''); HRMS *m/z* (ESI$^+$) [Found: 186.0426., $C_7H_9ClN_3O$ requires [M + H]$^+$ 186.0429]; LCMS (MDAP): Rt = 2.4 min (Method 5); *m/z* (ESI$^+$) 188.0 [M + H]$^+$.

5-Methoxy-*N*,*N*-dimethyl-4-pyrazolo[1,5-*b*]pyridazin-3-yl-pyrimidin-2-amine **170**

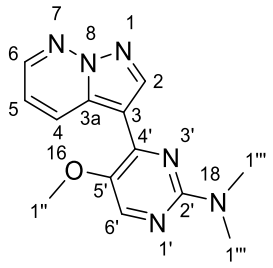

To a solution of 3-(4,4,5,5-tetramethyl-1,3,2-dioxaborolan-2-yl)pyrazolo[1,5-*b*]pyridazine (80 mg, 0.3 mmol) in acetonitrile (4.5 mL) and water (0.45 mL) was added sodium carbonate (70 mg, 0.65 mmol), bis[2-(di-*tert*-butylphosphanyl)cyclopenta-2,4-dien-1-yl]iron; dichloropalladium (11 mg, 0.02 mmol), and 4-chloro-5-methoxy-*N*,*N*-dimethyl-pyrimidin-2-amine (80 mg, 0.21 mmol). The reaction mixture was heated to 140 °C overnight. The reaction mixture was concentrated under reduced pressure. The residue was partitioned between EtOAc (10 mL) and water (10 mL), and extracted. The organic components were washed with water (2 x 30 mL), followed by saturated brine solution (1x 10 mL). The combined organic components were dried over $MgSO_4$, filtered and concentrated to dryness under reduced pressure. The crude was purified using flash silica column chromatography on an Isco Combiflash system (12 g silica, elution with 0-100% EtOAc / petroleum ether gradient) to afford the title compound, 5-methoxy-*N*,*N*-dimethyl-4-pyrazolo[1,5-*b*]pyridazin-3-yl-pyrimidin-2-amine, **170**, as a yellow solid (20 mg, 0.07 mmol, 22 % yield). R_f 0.21 (EtOAc/ petroleum ether 2:3); m.p. 181-183 °C; $\bar{\nu}_{max}$ (neat)/cm^{-1} 2931 (C-H, w), 2784 (C-H, w), 1620 (C=N, m), 1586 (C=C, m), 1558 (C=C, m); ^{1}H NMR (600 MHz, $CDCl_3$) δ_H 9.10 (1H, dd, *J* = 9.0, 2.0 Hz, H-4), 8.87 (1H, s, H-2), 8.39 (1H, dd, *J* = 4.5, 2.0 Hz, H-6), 8.17 (1H, s, H-6'), 7.17 (1H, dd, *J* = 9.0, 4.5 Hz, H-5), 3.95 (3H, s, H-1''), 3.26 (6H, s, H-1'''); ^{13}C NMR (150 MHz, $CDCl_3$) δ_C 158.2 (C-2'), 149.5 (C-5'), 143.2 (C-2 / 6 /6'), 142.9 (C-4'), 142.8 (C-2 or 6 or 6'), 142.5 (C-2 or 6 or 6'), 133.5 (C-3a), 130.1 (C-4), 117.5 (C-5), 108.9 (C-3), 57.4 (C-1''), 38.1 (C-1'''); HRMS *m/z* (ESI$^+$) [Found: 271.300., $C_{13}H_{15}N_6O$ requires [M + H]$^+$ 271.1302]; LCMS (MDAP): Rt = 12.45 min, >95% (Method 3); *m/z* (ESI$^+$) 271.9 [M + H]$^+$

4-Chloro-5-fluoro-*N*,*N*-dimethyl-pyrimidin-2-amine 171

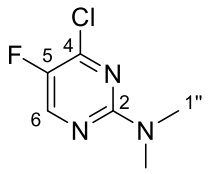

To a solution of 4-chloro-5-fluoropyrimidin-2-amine (100 mg, 0.68 mmol) in DMF (2 mL) was added sodium hydride (81 mg, 3.39 mmol) at 0 °C. After warming to rt and stirring for 5 min, iodomethane (0.08 mL, 1.36 mmol) was added dropwise and the reaction stirred at rt for 16 h. The reaction mixture was concentrated under reduced pressure. The crude was dissolved with water (100 mL) and extracted into EtOAc (3 x 100 mL). The combined EtOAc phases were dried over $MgSO_4$, filtered concentrated under reduced pressure to afford the title compound, 4-chloro-5-fluoro-*N*,*N*-dimethyl-pyrimidin-2-amine, **171**, as an orange solid (130 mg, 0.59 mmol, 87% yield). R_f 0.70 (EtOAc / petroleum ether 1:1); LCMS (LCQ): Rt = 3.0 min (Method 1); *m/z* (ESI^+) 176.1 $[M + H]^+$.

5-Fluoro-*N*,*N*-dimethyl-4-pyrazolo[1,5-*b*]pyridazin-3-yl-pyrimidin-2-amine **172**

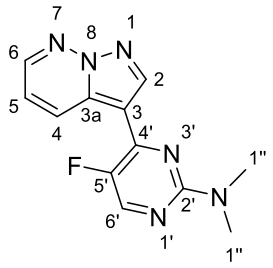

To a microwave vial containing 3-(2-chloro-5-fluoro-pyrimidin-4-yl)pyrazolo[1,5-*b*]pyridazine (80 mg, 0.32 mmol) was added dimethylamine (0.03 mL, 0.64 mmol). The vial was sealed and heated at 110 °C for 2h. The reaction mixture was concentrated under reduced pressure. The crude was purified using flash silica column chromatography on an Isco Combiflash system (12 g silica, elution with 0-60% EtOAc / petroleum ether gradient). Desired fractions were concentrated under reduced pressure. The crude was purified using flash reverse phase column chromatography on a Biotage system (12 g silica, elution with 10-100% MeOH / water gradient) to afford the title compound, 5-fluoro-*N*,*N*-dimethyl-4-pyrazolo[1,5-*b*]pyridazin-3-yl-pyrimidin-2-amine, **172**, as an off-white solid (50 mg, 0.18 mmol, 57% yield). R_f 0.57 (EtOAc / petroleum ether 1:1); m.p. 181-183 °C; $\bar{\nu}_{max}$ (neat)/cm^{-1} 3112 (C-H, w), 3030 (C-H, w), 2840 (C-H, w), 2894 (C-H, w), 2858 (C-H, w), 2796 (C-H, w), 1623 (C=N, m), 1574 (C=C, m), 1533 (C=C, m); ^{1}H NMR (600 MHz, $CDCl_3$) δ_H 9.01 (1H, dd, *J* = 9.0, 2.0 Hz, H-4), 8.67 (1H, app. d, *J* = 3.1 Hz, H-2), 8.42 (1H, dd, *J* = 4.4, 2.0 Hz, H-6), 8.25 (1H, d, *J* = 3.1 Hz, H-6'), 7.20 (1H, dd, *J* = 9.0, 4.4 Hz, H-5), 3.26 (6H, s, H-1''); ^{13}C NMR (150 MHz, $CDCl_3$) δ_C 159.2 (C-2'), 148.6 (d, *J* = 249.1 Hz, C-5'), 147.1 (d, *J* = 11.4 Hz, C-4'), 145.4 (d, *J* = 24.1 Hz, C-6'), 143.2 (C-6), 141.8 (d, *J* = 16.1 Hz, C-2), 133.4 (C-3a), 129.7 (C-4), 118.0 (C-5), 107.1 (C-3), 38.2 (C-1''); HRMS *m/z* (ESI$^+$) [Found: 281.0918., $C_{12}H_{11}FN_6Na$ requires [M + Na]$^+$ 281.0921]; LCMS (MDAP): Rt = 19.55 min, >95% (Method 3); *m/z* (ESI$^+$) 259.9 [M + H]$^+$

5-Chloro-*N*,*N*-dimethyl-4-pyrazolo[1,5-*b*]pyridazin-3-yl-pyrimidin-2-amine **174**

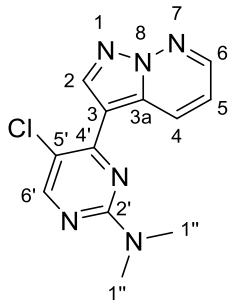

To a microwave vial containing a solution of 5-chloro-4-pyrazolo[1,5-*b*]pyridazin-3-yl-pyrimidin-2-amine (40 mg, 0.16 mmol) in DMF (2 mL) was added sodium hydride (19 mg, 0.49 mmol). The reaction mixture was stirred for 5 min at rt under nitrogen. Iodomethane (0.03 mL, 0.41 mmol) was added to the reaction mixture. The reaction mixture was stirred at rt for 5 h. The reaction mixture was concentrated under reduced pressure. The residue was partitioned between EtOAc (20 mL) and water (20 mL) and the layers separated. The aqueous layer was extracted with EtOAc (20 mL x 2). The combined organic layer was dried over $MgSO_4$, filtered and concentrated under reduced pressure. The crude was purified using flash silica column chromatography on an Isco Combiflash system (12 g silica, elution with 0-100% EtOAc / petroleum ether gradient). Trituration with petroleum ether afforded the title compound, 5-chloro-*N*,*N*-dimethyl-4-pyrazolo[1,5-*b*]pyridazin-3-yl-pyrimidin-2-amine, **174**, as a white solid (15 mg, 0.05 mmol, 32% yield). R_f 0.50 (EtOAc / petroleum ether 1:1); m.p. 206-208 °C; ^{1}H NMR (500 MHz, MeOD) δ_H 9.06 (1H, dd, *J*= 9.1, 1.9 Hz, H-4), 8.99 (1H, s, H-2), 8.55 (1H, dd, *J*= 4.5, 2.0 Hz, H-6), 8.35 (1H, s, H-6'), 7.43 (1H, dd, *J*= 9.1, 4.4 Hz, H-5), 3.28 (6H, s, H-1''); ^{1}H NMR (500 MHz, DMSO-d_6) δ_H 8.98 – 8.86 (2H, m, H-4 and 2), 8.69 – 8.59 (1H, m, H-6), 8.46 – 8.39 (1H, m, H-6'), 7.54 – 7.44 (1H, m, H-5), 3.18 (6H, s, H-1''); ^{13}C NMR (125 MHz, DMSO-d_6) δ_C 160.0 (C-2'), 158.1 (C-6'), 154.5 (C-4'), 144.4 (C-6), 140.8 (C-2), 133.6 (C-3a), 129.5 (C-4), 119.4 (C-5), 113.1 (C-5'), 108.3 (C-3), 37.4 (C-1''); HRMS *m/z* (ESI$^+$) [Found: 275.0800., $C_{12}H_{12}ClN_6$ requires $[M + H]^+$ 275.0806]; LCMS (MDAP): Rt = 17.8 min, >95% (Method 3); *m/z* (ESI$^+$) 274.9 $[M]^+$ and 276.8 $[M+2]^+$.

N,*N*-Dimethyl-4-pyrazolo[1,5-*b*]pyridazin-3-yl-5-(trifluoromethyl)pyrimidin-2-amine **176**

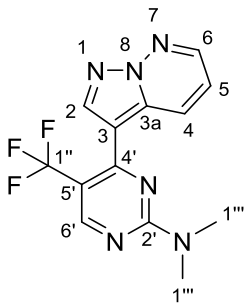

To a solution of 3-(4,4,5,5-tetramethyl-1,3,2-dioxaborolan-2-yl)pyrazolo[1,5-*b*]pyridazine (80 mg, 0.33 mmol) in DMF (1.6 mL) was added 2,4-dichloro-5-(trifluoromethyl)pyrimidine (85 mg, 0.39 mmol), 2 M potassium carbonate (0.5 mL, 1 mmol) and bis[2-(di-*tert*-butylphosphanyl)cyclopenta-2,4-dien-1-yl]iron; dichloropalladium (13 mg, 0.02 mmol). The reaction mixture was heated to 60 °C for 1.5 h. The reaction mixture was concentrated under reduced pressure. The residue was dissolved in 1,4-dioxane (0.50 mL), dimethylamine (0.5 mL, 1 mmol) was added and the solution was heated to 100°C for 2 h. The reaction mixture was concentrated under reduced pressure. The crude was purified using flash silica column chromatography on an Isco Combiflash system (12 g silica, elution with 0-70% EtOAc / petroleum ether gradient). Desired fractions were combined and concentrated under reduced pressure. The crude was purified using flash reverse phase column chromatography on a Biotage system (12 g silica, elution with 10-100% MeOH / water gradient) to afford the title compound, *N*,*N*-dimethyl-4-pyrazolo[1,5-*b*]pyridazin-3-yl-5-(trifluoromethyl)pyrimidin-2-amine, **176**, as a white solid (20 mg, 0.06 mmol, 18% yield). R_f 0.86 (EtOAc / petroleum ether 1:1); m.p. 124-126 °C; ^{1}H NMR (500 MHz, DMSO-d$_6$) δ_H 8.88 (1H, dd, *J*= 9.0, 1.9 Hz, H-4), 8.75 (1H, s, H-2), 8.67 (1H, s, H-6'), 8.63 (1H, dd, *J*= 4.5, 1.9 Hz, H-6), 7.51 (1H, dd, *J*= 9.0, 4.5 Hz, H-5), 3.24 (6H, s, H-1''); ^{13}C NMR (125 MHz, DMSO-d$_6$) δ_C 161.2 (C-4'), 159.5 (C-2'), 157.39 – 157.19 (m, C-6'), 144.4 (C-6), 141.5 (C-2), 133.8 (C-3a), 129.2 (C-4), 127.40 – 122.06 (m, CF_3), 119.9 (C-5), 111.2 (C-3), 103.0 (C-5'), 40.5 (C-1''); HRMS *m/z* (ESI$^+$) [Found: 331.0886., $C_{13}H_{11}F_3N_6Na$ requires [M + Na]$^+$ 331.0890]; LCMS (MDAP): Rt = 19.9 min, >95% (Method 3); *m/z* (ESI$^+$) 309.9 [M + H]$^+$.

N,*N*,5-Trimethyl-4-pyrazolo[1,5-*b*]pyridazin-3-yl-pyrimidin-2-amine **178**

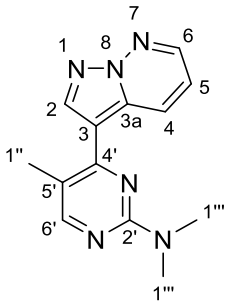

To a solution of 3-(4,4,5,5-tetramethyl-1,3,2-dioxaborolan-2-yl)pyrazolo[1,5-*b*]pyridazine (80 mg, 0.33 mmol) in DMF (1.6 mL) was added 2,4-dichloro-5-methylpyrimidine (64 mg, 0.39 mmol), 2 M potassium carbonate (0.5 mL, 1 mmol) and bis[2-(di-*tert*-butylphosphanyl)cyclopenta-2,4-dien-1-yl]iron; dichloropalladium (13 mg, 0.02 mmol). The reaction mixture was heated to 60 °C for 1.5 h. The reaction mixture was concentrated under reduced pressure. To the residue was added 1,4-dioxane (0.50 mL) and dimethylamine (0.05 mL, 1 mmol), the solution was heated to 100°C for 2h. The reaction mixture was concentrated under reduced pressure. The crude was purified using flash silica column chromatography on an Isco Combiflash system (12 g silica, elution with 0-70% EtOAc / petroleum ether gradient). Desired fractions were combined and concentrated under reduced pressure. The crude was purified using flash reverse phase column chromatography on a Biotage system (12 g silica, elution with 10-100% MeOH / water gradient) to afford the title compound, *N*,*N*,5-trimethyl-4-pyrazolo[1,5-*b*]pyridazin-3-yl-pyrimidin-2-amine, **178**, as a pale yellow solid (15 mg, 0.06 mmol, 17% yield). R_f 0.69 (EtOAc / petroleum ether 1:1); Decomposed > 180 °C; $\bar{\nu}_{max}$ (neat)/cm^{-1} 3101 (C-H, w), 2962 (C-H, w), 2931 (C-H, w), 2892 (C-H, w), 2857 (C-H, w), 1616 (C=N, m), 1579 (C=C, m), 1556 (C=C, m); ^{1}H NMR (500 MHz, DMSO-d$_6$) δ_H 8.96 (1H, dd, *J* = 9.1, 2.0 Hz, H-4), 8.64 – 8.60 (2H, m, H-2 and 6), 8.26 (1H, s, H-6’), 7.44 (1H, dd, *J* = 9.1, 4.5 Hz, H-5), 3.18 (6H, s, H-1’’’), 2.37 (3H, s, H-1’’); ^{13}C NMR (125 MHz, DMSO-d$_6$) δ_C 160.8 (C-2’), 159.8 (C-6’), 157.1 (C-4’), 144.0 (C-6), 140.2 (C-2), 133.1 (C-3a), 129.5 (C-4), 118.5 (C-5), 113.8 (C-5’), 110.6 (C-3), 37.1 (C-1’’’), 16.6 (C-1’’); HRMS *m/z* (ESI$^+$) [Found: 277.1168., $C_{13}H_{14}N_6Na$ requires [M + Na]$^+$ 277.1172]; LCMS (MDAP): Rt = 11.1 min, >95% (Method 3); *m/z* (ESI$^+$) 255.0 [M + H]$^+$.

N,*N*-5-trimethyl-2-pyrazolo[1,5-*b*]pyridazin-3-yl-pyrimidin-4-amine **178b** (regioisomer)

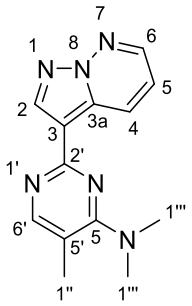

To a solution of 3-(4,4,5,5-tetramethyl-1,3,2-dioxaborolan-2-yl)pyrazolo[1,5-*b*]pyridazine (80 mg, 0.33 mmol) in DMF (1.6 mL) was added 2,4-dichloro-5-methylpyrimidine (64 mg, 0.39 mmol), 2 M potassium carbonate (0.5 mL, 1 mmol) and bis[2-(di-*tert*-butylphosphanyl)cyclopenta-2,4-dien-1-yl]iron; dichloropalladium (13 mg, 0.02 mmol). The reaction mixture was heated to 60 °C for 1.5 h. The reaction mixture was concentrated under reduced pressure. To the residue was added 1,4-dioxane (0.50 mL) and dimethylamine (0.05 mL, 1 mmol), the solution was heated to 100°C for 2h. The reaction mixture was concentrated under reduced pressure. The crude was purified using flash silica column chromatography on an Isco Combiflash system (12 g silica, elution with 0-70% EtOAc / petroleum ether gradient). Desired fractions were combined and concentrated under reduced pressure. The crude was purified using flash reverse phase column chromatography on a Biotage system (12 g silica, elution with 10-100% MeOH / water gradient) to afford the title compound, *N*,*N*-5-trimethyl-2-pyrazolo[1,5-*b*]pyridazin-3-yl-pyrimidin-4-amine, **178b**, as a colourless solid (2.5 mg, 0.01 mmol, 3% yield). R_f 0.69 (EtOAc / petroleum ether 1:1); ^{1}H NMR (600 MHz, DMSO-d$_6$) δ_H 8.88 (1H, dd, *J* = 9.0, 1.9 Hz, H-4), 8.60 (1H, s, H-2), 8.51 (1H, dd, *J* = 4.4, 1.9 Hz, H-6), 8.05 (1H, s, H-6'), 7.37 (1H, dd, *J* = 9.0, 4.4 Hz, H-4), 3.14 (6H, s, H-1'''), 2.27 (3H, s, H-1''); ^{13}C NMR (125 MHz, DMSO-d$_6$) δ_C 163.8 (C-4'), 157.5 (C-2'), 157.4 (C-6'), 143.8 (C-6), 140.0 (C-2), 132.8 (C-3a), 129.2 (C-4), 118.7 (C-5), 112.8 (C-5'), 112.3 (C-3), 40.2 (C-1'''), 18.1 (C-1''); HRMS *m/z* (ESI$^+$) [Found: 277.1167., $C_{13}H_{14}N_6Na$ requires [M + Na]$^+$ 277.1172]; LCMS (MDAP): Rt = 11.1 min, >95% (Method 3); *m/z* (ESI$^+$) 255.0 [M + H]$^+$

5-Bromo-*N*,*N*-dimethyl-4-pyrazolo[1,5-*b*]pyridazin-3-yl-pyrimidin-2-amine **181**

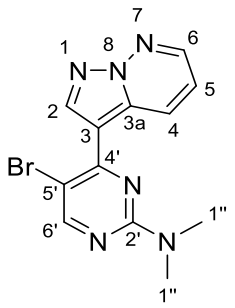

To a microwave vial containing a suspension of 4-pyrazolo[1,5-*b*]pyridazin-3-ylpyrimidin-2-amine (25 mg, 0.12 mmol) in acetonitrile (5 mL) was added *N*-bromosuccinimide (31 mg, 0.18 mmol). The microwave vial was sealed and stirred at rt for 2 h. The reaction mixture was concentrated under reduced pressure. The crude was purified using flash silica column chromatography on an Isco Combiflash system (12 g silica, elution with 0-50% 20% MeOH in CH_2Cl_2 / CH_2Cl_2 gradient). Desired fractions were combined and concentrated under reduced pressure. The crude was dissolved in THF (2 mL). Sodium hydride (8 mg, 0.35 mmol) was added slowly under nitrogen followed by iodomethane (0.02 mL, 0.29 mmol). The reaction mixture was stirred at rt overnight. The reaction mixture was concentrated under reduced pressure. The crude was purified using flash silica column chromatography on an Isco Combiflash system (12 g silica, elution with 0-100% EtOAc / petroleum ether gradient), trituration with petroleum ether afforded the title compound, 5-bromo-*N*,*N*-dimethyl-4-pyrazolo[1,5-*b*]pyridazin-3-yl-pyrimidin-2-amine, **181**, as a yellow solid (20 mg, 0.06 mmol, 51% yield). R_f 0.17 (EtOAc / petroleum ether 1:1); m.p. 208-210 °C; $\bar{\nu}_{max}$ (neat)/cm^{-1} 3114 (C-H, w), 3034 (C-H, w), 2895 (C-H, w), 2860 (C-H, w), 1617 (C=N, m), 1544 (C=C, s); ^{1}H NMR (500 MHz, DMSO-d$_6$) δ_H 8.99 (1H, s, H-2), 8.87 (1H, dd, *J* = 9.1, 1.9 Hz, H-4), 8.65 (1H, dd, *J* = 4.4, 1.9 Hz, H-6), 8.54 (1H, s, H-6'), 7.50 (1H, dd, *J* = 9.1, 4.4 Hz, H-5), 3.19 (6H, s, H-1''); ^{13}C NMR (125 MHz, DMSO-d$_6$) δ_C 160.7 (C-6'), 160.3 (C-2'), 155.9 (C-4'), 144.4 (C-6), 140.8 (C-2), 133.6 (C-3a), 129.4 (C-4), 119.4 (C-5), 109.7 (C-3), 101.9 (C-5'), 37.4 (C-1''); HRMS *m/z* (ESI$^+$) [Found: 341.0121., $C_{12}H_{12}BrN_6Na$ requires [M + Na]$^+$ 341.0121]; LCMS (MDAP): Rt = 18.0 min, >95% (Method 3); *m/z* (ESI$^+$) 318.9 [M]$^+$ and 320.8 [M+2]$^+$.

5-Iodo-*N*,*N*-dimethyl-4-pyrazolo[1,5-*b*]pyridazin-3-yl-pyrimidin-2-amine **183**

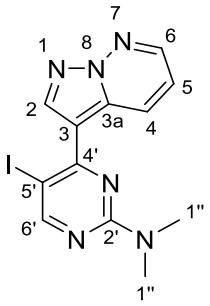

To a microwave vial containing a suspension of 4-pyrazolo[1,5-*b*]pyridazin-3-ylpyrimidin-2-amine (25 mg, 0.12 mmol) in acetonitrile (5 mL) was added *N*-iodosuccinimide (50 mg, 0.22 mmol). The microwave vial was sealed and stirred at rt for 2 h. The reaction mixture was concentrated under reduced pressure. The crude was purified using flash silica column chromatography on an Isco Combiflash system (12 g silica, elution with 0-50% 20% MeOH in CH_2Cl_2 / CH_2Cl_2 gradient). Desired fractions were combined and concentrated under reduced pressure. The crude was dissolved in THF (2 mL). Sodium hydride (8 mg, 0.35 mmol) was added slowly and was stirred for 5 min under nitrogen before iodomethane (0.02 mL, 0.29 mmol) was added. The reaction was stirred at rt overnight. The reaction mixture was concentrated under reduced pressure. The crude was purified using flash silica column chromatography on an Isco Combiflash system (12 g silica, elution with 0-100% EtOAc / petroleum ether gradient), trituration with petroleum ether afforded the title compound, 5-iodo-*N*,*N*-dimethyl-4-pyrazolo[1,5-*b*]pyridazin-3-yl-pyrimidin-2-amine, **183**, as a white solid (20 mg, 0.05 mmol, 44% yield). R_f 0.13 (EtOAc / petroleum ether 1:1); m.p. 204-206 °C; $\bar{\nu}_{max}$ (neat)/cm^{-1} 3114 (C-H, w), 2925 (C-H, w), 2857 (C-H, w), 1619 (C=N, m), 1558 (C=C, s); ^{1}H NMR (500 MHz, DMSO-d$_6$) δ_H 8.99 (1H, s, H-2), 8.73 (1H, dd, *J* = 9.1, 1.9 Hz, H-4), 8.68 (1H, s, H-6'), 8.62 (1H, dd, *J* = 4.5, 1.9 Hz, H-6), 7.45 (1H, dd, *J* = 9.1, 4.5 Hz, H-5), 3.16 (6H, s, H-1''); ^{13}C NMR (125 MHz, DMSO-d$_6$) δ_C 166.1 (C-6'), 160.5 (C-2'), 158.7 (C-4'), 144.2 (C-6), 140.6 (C-2), 133.2 (C-3'), 129.2 (C-4), 119.0 (C-5), 111.2 (C-3), 74.2 (C-5'), 37.0 (C-1''); HRMS *m/z* (ESI$^+$) [Found: 317.0154., $C_{12}H_{12}IN_6$ requires [M + H]$^+$ 367.0163]; LCMS (MDAP): Rt = 18.2 min, >95% (Method 3); *m/z* (ESI$^+$) 367.8 [M + H]$^+$.

2-(2-Chloro-5-fluoro-pyrimidin-4-yl)ethynyl-trimethyl-silane **184**

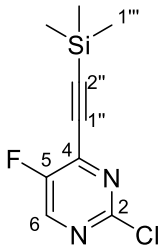

To a stirred solution of copper iodide (114 mg, 0.60 mmol) in THF (55 mL) was added bis(triphenylphosphine)palladium(II) dichloride (252 mg, 0.36 mmol), TEA (2.09 mL, 15 mmol), (trimethylsilyl)acetylene (2.12 mL, 14.97 mmol), followed by slow addition of 2,4-dichloro-5-fluoropyrimidine (2 g, 11.98 mmol). The reaction mixture was stirred at rt overnight. The reaction mixture was concentrated under reduced pressure. The crude was purified using flash silica column chromatography on an Isco Combiflash system (12 g silica, elution with 0-10% EtOAc / petroleum ether gradient) to afford the title compound, 2-(2-chloro-5-fluoro-pyrimidin-4-yl)ethynyl-trimethyl-silane, **184**, as a pale yellow solid (1.2 g, 4.98 mmol, 42% yield). R_f 0.77 (EtOAc / petroleum ether 1:9); ^{1}H NMR (600 MHz, $CDCl_3$) δ_H 8.50 (1H, d, J = 4.7 Hz, H-6), 0.31 (9H, s, H-1'''); LCMS (LCQ): Rt = 2.3 min (Method 1); *m/z* (ESI$^+$) 228.9 [M]$^+$ and 230.9 [M + 2]$^+$.

3-(2-Chloro-5-fluoro-pyrimidin-4-yl)pyrazolo[1,5-*b*]pyridazine **185**

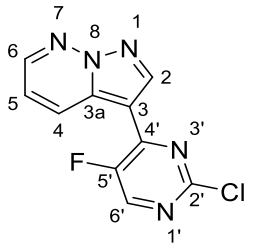

To a stirred solution of pyridazin-1-ium-1-amine iodide (3.25 g, 8.74 mmol) in acetonitrile (50 mL) was added 2-(2-chloro-5-fluoro-pyrimidin-4-yl)ethynyl-trimethyl-silane (1.0 g, 4.37 mmol) followed by DBU (0.98 mL, 6.56 mmol). The reaction mixture was stirred at 50 °C for 1 h. The reaction mixture concentrated under reduced pressure. The crude was purified using flash silica column chromatography on an Isco Combiflash system (12 g silica, elution with 0-60% EtOAc / petroleum ether gradient) to afford the title compound, 3-(2-chloro-5-fluoro-pyrimidin-4-yl)pyrazolo[1,5-*b*]pyridazine, **185**, as a pale pink solid (480 mg, 1.83 mmol, 42% yield). R_f 0.73 (EtOAc / petroleum ether 1:1); m.p. 196-198 °C; $\bar{\nu}_{max}$ (neat)/cm^{-1} 3096 (C-H, w), 3030 (C-H, w), 2923 (C-H, w), 1619 (C=N, m), 1581 (C=C, m), 1567 (C=C, m); ^{1}H NMR (600 MHz, DMSO-d$_6$) δ_H 8.91 – 8.84 (2H, m, H-4 and 6'), 8.76 – 8.70 (2H, m, H-6 and 2), 7.63 (1H, dd, *J* = 9.0, 4.4 Hz, H-5); ^{13}C NMR (150 MHz, DMSO-d$_6$) δ_C 154.1 (d, *J* = 2.8 Hz, C-2'), 153.7 (d, *J* = 263.5 Hz, C-5'), 149.7 (d, *J* = 12.8 Hz, C-4'), 147.8 (d, *J* = 24.7 Hz, C-6'), 145.0 (C-6), 141.5 (d, *J* = 14.6 Hz, C-2), 133.4 (C-3a), 128.9 (C-4), 120.7 (C-5), 103.79 (d, *J* = 5.4 Hz, C-3); LCMS (MDAP): Rt = 19.6 min, >95% (Method 3); *m/z* (ESI$^+$) 259.9 [M + H]$^+$.

4-Chloro-6-isopropyl-*N*,*N*-dimethyl-pyrimidin-2-amine **186**

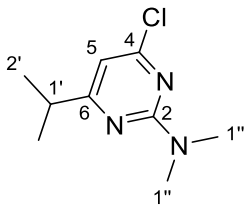

To a solution of 4-chloro-6-isopropyl-2-pyrimidinamine (240 mg, 1.39 mmol) in THF (10 mL) was added sodium hydride (167 mg, 6.97 mmol) at 0 °C. After warming to rt and stirring for 5 min, iodomethane (0.25 mL, 4.02 mmol) was added dropwise and the reaction stirred at rt for 16 h. The reaction mixture was concentrated under reduced pressure. The crude was purified using flash silica column chromatography on an Isco Combiflash system (12 g silica, elution with 0-100% EtOAc / petroleum ether gradient) to afford the title compound, 4-chloro-6-isopropyl-*N*,*N*-dimethyl-pyrimidin-2-amine, **186**, as a yellow oil (216 mg, 1.03 mmol, 74% yield). R_f 0.86 (EtOAc / petroleum ether 1:9); ^{1}H NMR (500 MHz, DMSO-d$_6$) δ_H 6.56 (1H, s, H-5), 3.08 (6H, s, H-1''), 2.76 (1H, hept, *J* = 6.9 Hz, H-1'), 1.15 (6H, d, *J* = 6.9 Hz, H-2'); ^{13}C NMR (125 MHz, DMSO-d$_6$) δ_C 177.8 (C-6), 161.5 (C-2), 160.0 (C-4), 104.9 (C-5), 36.5 (C-1''), 35.2 (C-1'), 21.3 (C-2'); LCMS (MDAP): Rt = 3.13 min, >95% (Method 5); *m/z* (ESI$^+$) 200.1 [M + H]$^+$

4-Isopropyl-*N*,*N*-dimethyl-6-pyrazolo[1,5-*b*]pyridazin-3-yl-pyrimidin-2-amine **187**

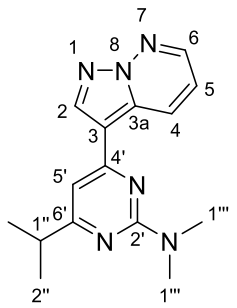

To a solution of 3-(4,4,5,5-tetramethyl-1,3,2-dioxaborolan-2-yl)pyrazolo[1,5-*b*]pyridazine (74 mg, 0.30 mmol) in 1,4-dioxane (1.25 mL) was added, bis[2-(di-*tert*-butylphosphanyl)cyclopenta-2,4-dien-1-yl]iron; dichloropalladium (10 mg, 0.02 mmol), 2 M potassium carbonate (0.45 mL, 0.90 mmol) and 4-chloro-6-isopropyl-*N*,*N*-dimethyl-pyrimidin-2-amine (90 mg, 0.45 mmol). The reaction mixture was heated for 2 h at 70 °C. The reaction mixture was concentrated under reduced pressure. The crude was purified using flash silica column chromatography on an Isco Combiflash system (12 g silica, elution with 0-100% EtOAc / petroleum ether gradient). Desired fractions were combined and concentrated under reduced pressure. The crude was purified using flash reverse phase column chromatography on a Biotage system (12 g silica, elution with 10-100% MeOH / water gradient) to afford the title compound, 4-isopropyl-*N*,*N*-dimethyl-6-pyrazolo[1,5-*b*]pyridazin-3-yl-pyrimidin-2-amine, **187**, as a white solid (49 mg, 0.16 mmol, 55% yield). R_f 0.88 (EtOAc / petroleum ether 4:1); m.p. 124-126 °C; $\bar{\nu}_{max}$ (neat)/cm^{-1} 3094 (C-H, w), 2962 (C-H, w), 2931 (C-H, w), 2865 (C-H, w), 1623 (C=N, m), 1575 (C=C, m), 1559 (C=C, m); ^{1}H NMR (500 MHz, MeOD) δ_H 9.07 (1H, dd, *J* = 9.1, 2.0 Hz, H-4), 8.67 (1H, s, H-2), 8.48 (1H, dd, *J* = 4.5, 2.0 Hz, H-6), 7.35 (1H, dd, *J* = 9.1, 4.5 Hz, H-5), 6.95 (1H, s, H-5'), 3.29 (6H, s, H-1'''), 2.94 – 2.85 (1H, m, H-1''), 1.32 (6H, d, *J* = 6.9 Hz, H-2''); ^{13}C NMR (125 MHz, MeOD) δ_C 177.7 (C-6'), 163.9 (C-2'), 160.6 (C-4'), 144.7 (C-6), 139.9 (C-2), 134.0 (C-3a), 130.8 (C-4), 119.3 (C-5), 113.1 (C-3), 102.5 (C-5'), 37.5 (C-1''), 37.3 (C-1'''), 22.2 (C-1''); HRMS *m/z* (ESI$^+$) [Found: 283.1670., $C_{15}H_{19}N_6$ requires [M + H]$^+$ 283.1666]; LCMS (MDAP): Rt = 9.5 min, >95% (Method 3); *m/z* (ESI$^+$) 283.0 [M + H]$^+$.

4,6-Dichloro-*N*,*N*-dimethyl-pyrimidin-2-amine **188**

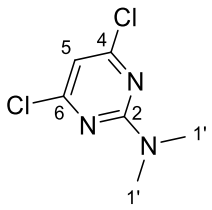

To a solution of 4,6-dichloro-2-pyrimidinamine (200 mg, 1.22 mmol) in THF (10 mL) was added sodium hydride (146 mg, 6.1 mmol) at 0 °C. After warming to rt and stirring for 5 min, iodomethane (0.25 mL, 4.02 mmol) was added dropwise and the reaction stirred at rt for 16 h. The reaction was concentrated under reduced pressure. The crude was purified using flash silica column chromatography on an Isco Combiflash system (12 g silica, elution with 0-100% EtOAc / petroleum ether gradient) to afford the title compound,4,6-dichloro-*N*,*N*-dimethyl-pyrimidin-2-amine, **188**, as a white solid (154 mg, 0.76 mmol, 62% yield). R_f 0.75 (EtOAc / petroleum ether 1:9); ^{1}H NMR (500 MHz, DMSO-d_6) δ_H 6.90 (1H, s, H-5), 3.10 (6H, s, H-1'); ^{13}C NMR (125 MHz, DMSO-d_6) δ_C 160.7 (C-6 and C-4), 160.7, (C-2), 106.6 (C-5), 36.8 (C-1'); LCMS (MDAP): Rt = 2.76 min, >95% (Method 5); *m/z* (ESI$^+$) 192.1 [M + H]$^+$.

4-Chloro-*N*,*N*-dimethyl-6-pyrazolo[1,5-*b*]pyridazin-3-yl-pyrimidin-2-amine **189**

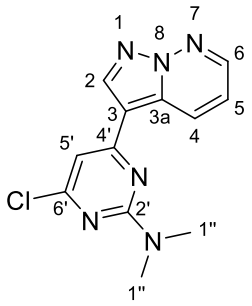

To a solution of 3-(4,4,5,5-tetramethyl-1,3,2-dioxaborolan-2-yl)pyrazolo[1,5-*b*]pyridazine (70 mg, 0.29 mmol) in 1,4-dioxane (2 mL) was added 4,6-dichloro-*N*,*N*-dimethyl-pyrimidin-2-amine (82 mg, 0.43 mmol), 2 M potassium carbonate (0.43 mL, 0.86 mmol) and bis[2-(di-*tert*-butylphosphanyl)cyclopenta-2,4-dien-1-yl]iron; dichloropalladium (19 mg, 0.03 mmol). The reaction mixture was heated for 2 h at 70 °C. The reaction mixture was concentrated under reduced pressure. The crude was purified using flash silica column chromatography on an Isco Combiflash system (12 g silica, elution with 0-100% EtOAc / petroleum ether gradient). Desired fractions were combined and concentrated under reduced pressure. The crude was purified using flash reverse phase column chromatography on a Biotage system (12 g silica, elution with 10-100% MeOH / water gradient) to afford the title compound, 4-chloro-*N*,*N*-dimethyl-6-pyrazolo[1,5-*b*]pyridazin-3-yl-pyrimidin-2-amine, **189**, as a pale yellow solid (29 mg, 0.10 mmol, 35% yield). R_f 0.75 (EtOAc / petroleum ether 4:1); m.p. 208-210 °C; $\bar{\nu}_{max}$ (neat)/cm^{-1} 3101 (C-H, w), 2938 (C-H, w), 2903 (C-H, w), 1623 (C=N, m), 1563 (C=C, m); ^{1}H NMR (500 MHz, MeOD) δ_H 9.02 (1H, dd, *J* = 9.1, 2.0 Hz, H-4), 8.70 (1H, s, H-2), 8.51 (1H, dd, *J* = 4.5, 2.0 Hz, H-6), 7.40 (1H, dd, *J* = 9.1, 4.5 Hz, H-5), 7.12 (1H, s, H-5'), 3.29 (6H, s, H-1''); ^{1}H NMR (500 MHz, DMSO-d$_6$) δ_H 8.87 (1H, s, H-2), 8.82 (1H, dd, *J* = 9.0, 2.0 Hz, H-4), 8.57 (1H, dd, *J* = 4.5, 2.0 Hz, H-6), 7.42 (1H, dd, *J* = 9.0, 4.5 Hz, H-5), 7.22 (1H, s, H-5'), 3.15 (6H, s, H-1''); ^{13}C NMR (150 MHz, DMSO-d$_6$) δ_C 161.5 (C-6'), 160.8 (C-2'), 160.2 (C-4'), 144.1 (C-6), 140.2 (C-2), 132.6 (C-3a), 129.1 (C-4), 119.4 (C-5), 109.5 (C-3), 103.0 (C-5'), 37.1 (C-1''); HRMS *m/z* (ESI$^+$) [Found: 297.0629., $C_{12}H_{11}ClN_6Na$ requires [M + Na]$^+$ 297.0626]; LCMS (MDAP): Rt = 19.0 min, >95% (Method 3); *m/z* (ESI$^+$) 274.9 [M]$^+$ and 276.9 [M+2]$^+$.

4-Chloro-*N*,*N*,6-trimethyl-pyrimidin-2-amine **190**

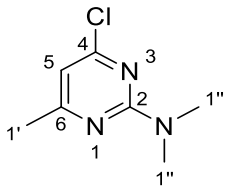

To a solution of 4-chloro-6-methyl-2-pyrimidinamine (200 mg, 1.39 mmol) in THF (10 mL) was added sodium hydride (117 mg, 4.88 mmol) at 0 °C. After warming to rt and stirring for 5 min, iodomethane (0.25 mL, 4.02 mmol) was added dropwise and the reaction stirred at rt for 16 h. The reaction mixture was concentrated under reduced pressure. The crude was purified using flash silica column chromatography on an Isco Combiflash system (12 g silica, elution with 0-100% EtOAc / petroleum ether gradient) to afford the title compound,s 4-chloro-*N*,*N*,6-trimethyl-pyrimidin-2-amine, **190**, as a colourless liquid (74 mg, 0.41 mmol, 29% yield). R_f 0.75 (EtOAc / petroleum ether 1:9); ^{1}H NMR (500 MHz, DMSO-d_6) δ_H 6.13 (1H, s, H-5), 3.86 (3H, s, H-1'), 3.10 (6H, s, H-1''); LCMS (MDAP): Rt = 1.8 min, >95% (Method 5); *m/z* (ESI$^+$) 188.1 [M + H]$^+$.

N,*N*-4-Trimethyl-6-pyrazolo[1,5-*b*]pyridazin-3-yl-pyrimidin-2-amine **191**

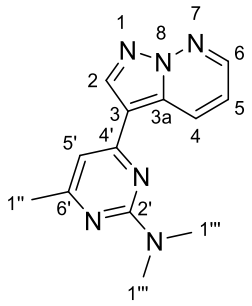

To a solution of 3-(4,4,5,5-tetramethyl-1,3,2-dioxaborolan-2-yl)pyrazolo[1,5-*b*]pyridazine (70 mg, 0.29 mmol) in 1,4-dioxane (2 mL) was added 4-chloro-*N*,*N*,6-trimethyl-pyrimidin-2-amine (74 mg, 0.43 mmol), 2 M potassium carbonate (0.43 mL, 0.86 mmol) and bis[2-(di-*tert*-butylphosphanyl)cyclopenta-2,4-dien-1-yl]iron; dichloropalladium (19 mg, 0.03 mmol). The reaction mixture was heated for 2 h at 70 °C. The reaction mixture was concentrated under reduced pressure. The crude was purified using flash silica column chromatography on an Isco Combiflash system (12 g silica, elution with 0-100% EtOAc / petroleum ether gradient). Desired fractions were combined and concentrated under reduced pressure. The crude was purified using flash reverse phase column chromatography on a Biotage system (12 g silica, elution with 10-100% MeOH / water gradient) to afford the title compound, *N*,*N*,4-trimethyl-6-pyrazolo[1,5-*b*]pyridazin-3-yl-pyrimidin-2-amine, **191**, as a pale yellow solid (52 mg, 0.19 mmol, 68% yield). R_f 0.71 (EtOAc / petroleum ether 4:1); m.p. 195-197 °C; $\bar{\nu}_{max}$ (neat)/cm^{-1} 3113 (C-H, w), 2925 (C-H, w), 2861 (C-H, w), 1624 (C=N, m), 1560 (C=C, m); ^{1}H NMR (500 MHz, MeOD) δ_H 9.06 (1H, dd, *J* = 9.1, 2.0 Hz, H-4), 8.65 (1H, s, H-2), 8.48 (1H, dd, *J* = 4.4, 2.0 Hz, H-6), 7.36 (1H, dd, *J* = 9.1, 4.4 Hz, H-5), 6.98 (1H, s, H-5'), 3.28 (6H, s, H-1'''), 2.40 (3H, s, H-1''); ^{1}H NMR (600 MHz, DMSO-d$_6$) δ_H 8.94 (1H, dd, *J* = 9.0, 1.9 Hz, H-4), 8.79 (1H, s, H-2), 8.57 (1H, dd, *J* = 4.4, 1.9 Hz, H-6), 7.42 (1H, dd, *J* = 9.0, 4.4 Hz, H-5), 7.04 (1H, s, H-5'), 3.20 (6H, s, H-1'''), 2.32 (3H, s, H-1''); ^{13}C NMR (125 MHz, DMSO-d$_6$) δ_C 167.0 (C-6'), 162.0 (C-2'), 158.6 (C-4'), 143.8 (C-6), 139.4 (C-2), 132.3 (C-3a), 129.2 (C-4), 118.6 (C-5), 110.6 (C-3), 103.8 (C-5'), 36.9 (C-1'''), 24.1 (C-1''); HRMS *m/z* (ESI$^+$) [Found: 255.1350., $C_{13}H_{15}N_6$ requires [M + H]$^+$ 255.1353]; LCMS (MDAP): Rt = 3.71 min, >95% (Method 3); *m/z* (ESI$^+$) 254.9 [M + H]$^+$.

4-Chloro-6-methoxy-*N*,*N*-dimethyl-pyrimidin-2-amine **192**

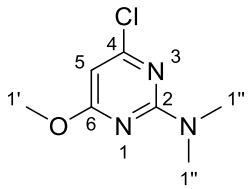

To a solution of 4-chloro-6-methoxy-pyrimidin-2-ylamine (200 mg, 1.25 mmol) in THF (10 mL) was added sodium hydride (105 mg, 4.39 mmol) at 0 °C. After warming to rt and stirring for 5 min, iodomethane (0.25 mL, 4.02 mmol) was added dropwise and the reaction stirred at rt for 16 h. The reaction mixture was concentrated under reduced pressure. The crude was purified using flash silica column chromatography on an Isco Combiflash system (12 g silica, elution with 0-100% EtOAc / petroleum ether gradient) to afford the title compound,4-chloro-6-methoxy-*N*,*N*-dimethyl-pyrimidin-2-amine, **192**, as a white solid (127 mg, 0.64 mmol, 51% yield). R_f 0.90 (EtOAc / petroleum ether 1:4); ^{1}H NMR (500 MHz, DMSO-d$_6$) δ_H 6.13 (1H, s, H-5), 3.86 (3H, s, H-1'), 3.10 (6H, s, H-1''); ^{13}C NMR (125 MHz, DMSO-d$_6$) δ_C 170.3 (C-6), 160.9 (C-2), 159.7 (C-4), 93.3 (C-5), 53.5 (C-1'), 36.5 (C-1''); LCMS (MDAP): Rt = 1.8 min, >95% (Method 5); *m/z* (ESI$^+$) 188.1 [M + H]$^+$.

4-Methoxy-*N*,*N*-dimethyl-6-pyrazolo[1,5-*b*]pyridazin-3-yl-pyrimidin-2-amine **193**

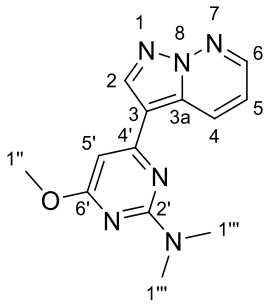

To a solution of 3-(4,4,5,5-tetramethyl-1,3,2-dioxaborolan-2-yl)pyrazolo[1,5-*b*]pyridazine (70 mg, 0.29 mmol) in 1,4-dioxane (2 mL) was added 4-chloro-6-methoxy-*N*,*N*-dimethyl-pyrimidin-2-amine (80 mg, 0.43 mmol), 2 M potassium carbonate (0.43 mL, 0.86 mmol) and bis[2-(di-*tert*-butylphosphanyl)cyclopenta-2,4-dien-1-yl]iron; dichloropalladium (19 mg, 0.03 mmol). The reaction mixture was heated for 2 h at 70 °C. The reaction mixture was concentrated under reduced pressure. The crude was purified using flash silica column chromatography on an Isco Combiflash system (12 g silica, elution with 0-100% EtOAc / petroleum ether gradient). Desired fractions were combined and concentrated under reduced pressure. The crude was purified using flash reverse phase column chromatography on a Biotage system (12 g silica, elution with 10-100% MeOH / water gradient) to afford the title compound, 4-methoxy-*N*,*N*-dimethyl-6-pyrazolo[1,5-*b*]pyridazin-3-yl-pyrimidin-2-amine, **193**, as a white solid (50 mg, 0.18 mmol, 62% yield). R_f 0.83 (EtOAc / petroleum ether 4:1); m.p. 180-182 °C; $\bar{\nu}_{max}$ (neat)/cm^{-1} 3108 (C-H, w), 3036 (C-H, w), 2948 (C-H, w), 2891 (C-H, w), 1625 (C=N, m), 1571 (C=C, m); ^{1}H NMR (500 MHz, MeOD) δ_H 9.03 (1H, dd, *J* = 9.1, 2.0 Hz, H-4), 8.59 (1H, s, H-2), 8.45 (1H, dd, *J* = 4.4, 2.0 Hz, H-6), 7.32 (1H, dd, *J* = 9.1, 4.4 Hz, H-5), 6.47 (1H, s, H-5'), 3.96 (3H, s, H-1''), 3.28 (6H, s, H-1'''); ^{1}H NMR (500 MHz, DMSO-d$_6$) δ_H 8.90 (1H, dd, *J* = 9.0, 2.0 Hz, H-4), 8.77 (1H, s, H-2), 8.53 (1H, dd, *J* = 4.4, 2.0 Hz, H-6), 7.37 (1H, dd, *J* = 9.0, 4.4 Hz, H-5), 6.57 (1H, s, H-5'), 3.86 (3H, s, H-1''), 3.17 (6H, s, H-1'''); ^{13}C NMR (125 MHz, DMSO-d$_6$) δ_C 170.1 (C-6'), 161.9 (C-2'), 159.7 (C-5'), 143.7 (C-6), 139.3 (C-2), 132.1 (C-3a), 129.3 (C-4), 118.5 (C-5), 110.7 (C-3), 89.8 (C-5'), 52.8 (C-1''), 36.2 (C-1'''); HRMS *m/z* (ESI$^+$) [Found: 271.1306., $C_{13}H_{15}N_6O$ requires [M + H]$^+$ 271.1302]; LCMS (MDAP): Rt = 17.7 min, >95% (Method 3); *m/z* (ESI$^+$) 270.9 [M + H]$^+$.

N,*N*-Dimethyl-4-pyrazolo[1,5-*b*]pyridazin-3-yl-5,7-dihydrofuro[3,4-*d*]pyrimidin-2-amine **195**

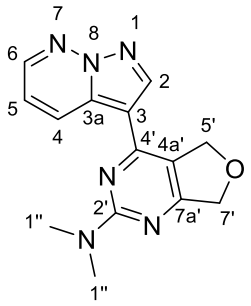

To a solution of 3-(4,4,5,5-tetramethyl-1,3,2-dioxaborolan-2-yl)pyrazolo[1,5-*b*]pyridazine (74 mg, 0.30 mmol) in 1,4-dioxane (1.25 mL) was added, bis[2-(di-*tert*-butylphosphanyl)cyclopenta-2,4-dien-1-yl]iron; dichloropalladium (10 mg, 0.02 mmol), 2 M potassium carbonate (0.45 mL, 0.90 mmol) and 2,4-dichloro-5,7-dihydrofuro[3,4-*d*]pyrimidine (86 mg, 0.45 mmol). The reaction mixture was heated for 4 h at 110 °C. To the reaction mixture was added dimethylamine (0.15 mL, 0.30 mmol) in THF (2 mL). The reaction mixture was heated overnight at 110 °C. The reaction mixture was concentrated under reduced pressure. The crude was purified using flash silica column chromatography on an Isco Combiflash system (12 g silica, elution with 0-100% EtOAc / petroleum ether gradient). Desired fractions were combined and concentrated under reduced pressure. The crude was purified using flash reverse phase column chromatography on a Biotage system (12 g silica, elution with 10-100% MeOH / water gradient) to afford the title compound, *N*,*N*-dimethyl-4-pyrazolo[1,5-*b*]pyridazin-3-yl-5,7-dihydrofuro[3,4-*d*]pyrimidin-2-amine, **195**, as a pale yellow solid (22 mg, 0.07 mmol, 25% yield). R_f 0.80 (EtOAc / petroleum ether 1:1); Decomposed > 238 °C; $\bar{\nu}_{max}$ (neat)/cm^{-1} 2920(C-H, w), 2848 (C-H, w), 1624 (C=N, m), 1567 (C=C, m), 1516(C=C, m); ^{1}H NMR (500 MHz, DMSO-d$_6$) δ_H 9.05 (1H, dd, *J* = 9.0, 1.9 Hz, H-4), 8.65 (1H, dd, *J* = 4.5, 1.9 Hz, H-6), 8.32 (1H, s, H-2), 7.51 (1H, dd, *J* = 9.0, 4.5 Hz, H-5), 5.29 (2H, s, H-5'), 4.82 (2H, s, H-7'), 3.23 (6H, s, H-1''); ^{13}C NMR (150 MHz, DMSO-d$_6$) δ_C 171.2 (C-7a'), 162.3 (C-2'), 152.2 (C-4'), 144.3 (C-6), 140.0 (C-2), 132.8 (C-3a), 129.5 (C-4), 119.2 (C-5), 112.1 (C-4a'), 109.6 (C-3), 71.4 (C-7'), 71.1 (C-5'), 37.4 (C-1''); HRMS *m/z* (ESI$^+$) [Found: 283.1306., $C_{14}H_{15}N_6O$ requires [M + H]$^+$ 283.1302]; LCMS (MDAP): Rt = 12.7 min, >95% (Method 3); *m/z* (ESI$^+$) 282.9 [M + H]$^+$

6-Bromo-*N*,*N*-dimethyl-pyridin-2-amine **196**

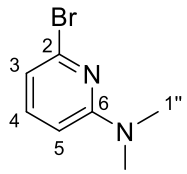

To a solution of 2,6-dibromopyridine (300 mg, 0.63 mmol) in THF (1 mL) was added dimethylamine (4 mL, 8 mmol) and the reaction mixture was heated in a sealed tube at 80 °C overnight. The reaction mixture was concentrated under reduced pressure. The residue was dissolved in EtOAc (50 mL) and was washed with water (2 x 50 mL), followed by sat brine solution (50 mL). The organic component was dried over $MgSO_4$, filtered and concentrated under reduced pressure. The residue was purified using flash silica column chromatography on an Isco Combiflash system (12 g silica, elution with 0-10% EtOAc / petroleum ether gradient) to afford the title compound, 6-bromo-*N*,*N*-dimethyl-pyridin-2-amine, **196**, as an off-white gum (250 mg, 1.18 mmol, 93% yield). $\bar{\nu}_{max}$ (neat)/cm^{-1} 2931 (C-H, w), 2867 (C-H, w), 1623 (C=N, m), 1586 (C=C, m); ^{1}H NMR (500 MHz, DMSO-d$_6$) δ_H 7.74 – 7.66 (1H, m, NH), 7.37 (1H, dd, *J*= 8.5, 7.4 Hz, H-4), 6.68 (1H, d, *J*= 7.4 Hz, H-3), 6.58 (1H, d, *J*= 8.4 Hz, H-5), 2.97 (6H, d, *J*= 1.3 Hz, H-1''); LCMS (LCQ): Rt = 2.9 min (Method 1); *m/z* (ESI$^+$) 201.2 [M + H]$^+$ and 203.1 [M + 2]$^+$.

N,*N*-Dimethyl-6-pyrazolo[1,5-*b*]pyridazin-3-yl-pyridin-2-amine **197**

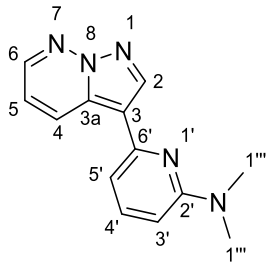

To a solution of 3-(4,4,5,5-tetramethyl-1,3,2-dioxaborolan-2-yl)pyrazolo[1,5-*b*]pyridazine (80 mg, 0.33 mmol) in acetonitrile (0.6 mL)and water (0.1 mL) was added sodium carbonate (69 mg, 0.65 mmol), bis[2-(di-*tert*-butylphosphanyl)cyclopenta-2,4-dien-1-yl]iron; dichloropalladium (11 mg, 0.02 mmol), and 6-bromo-*N*,*N*-dimethyl-pyridin-2-amine (131 mg, 0.65 mmol). The reaction mixture was heated at 140 °C overnight. The reaction mixture was concentrated under reduced pressure. The residue was partitioned between EtOAc (10 mL) and water (10 mL), and extracted. The organic components were washed with water (2 x 30 mL), followed by saturated brine solution (1x 10 mL). The combined organic components were dried over $MgSO_4$, filtered and concentrated to dryness under reduced pressure. The crude was purified using flash silica column chromatography on an Isco Combiflash system (12 g silica, elution with 0-40% EtOAc / petroleum ether gradient). Desired fractions were combined and concentrated under reduced pressure. The crude was purified using flash reverse phase column chromatography on a Biotage system (12 g silica, elution with 10-100% MeOH / water gradient) to afford the title compound, *N*,*N*-dimethyl-6-pyrazolo[1,5-*b*]pyridazin-3-yl-pyridin-2-amine, **197**, as a yellow solid (30 mg, 0.12 mmol, 36% yield). R_f 0.71 (EtOAc/ petroleum ether 2:3); Decomposed > 210 °C; $\bar{\nu}_{max}$ (neat)/cm^{-1} 3096 (C-H, w), 2927 (C-H, w), 2899 (C-H, w), 1619 (C=N, m), 1566 (C=C, m), 1537 (C=C, m); ^{1}H NMR (600 MHz, $CDCl_3$) δ_H 8.96 (1H, dd, *J* = 9.0, 2.0 Hz, H-4), 8.41 (1H, s, H-2), 8.29 (1H, dd, *J* = 4.4, 2.0 Hz, H-6), 7.53 – 7.48 (1H, m, H-4'), 7.05 (1H, dd, *J* = 9.0, 4.4 Hz, H-5), 6.97 (1H, d, *J* = 7.4 Hz, H-5'), 6.42 (1H, d, *J* = 8.4 Hz, H-3'), 3.18 (6H, s, H-1'''); ^{13}C NMR (150 MHz, $CDCl_3$) δ_C 159.3 (C-2'), 150.4 (C-6'), 142.4 (C-6), 138.2 (C-2), 137.9 (C-4'), 132.1 (C-3a), 129.8 (C-4), 116.5 (C-5), 113.8 (C-3), 107.9 (C-5'), 103.6 (C-3'), 99.2, 38.6 (C-1'''); HRMS *m/z* (ESI$^+$) [Found: 262.1057., $C_{13}H_{13}N_5Na$ requires [M + Na]$^+$ 262.1063]; LCMS (MDAP): Rt = 14.51 min, >95% (Method 3); *m/z* (ESI$^+$) 240.9 [M + H]$^+$.

4-Bromo-*N*,*N*-dimethyl-pyridin-2-amine **198**

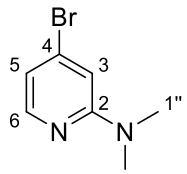

To a solution of 2-amino-4-bromopyridine (300 mg, 1.73 mmol) in THF (10 mL) was added sodium hydride (208 mg, 8.67 mmol) at 0 °C. After warming to rt and stirring for 5 min, iodomethane (0.11 mL, 1.73 mmol) was added dropwise and the reaction stirred at rt for 16 h. The reaction mixture was concentrated under reduced pressure. The crude was dissolved with water (100 mL) and extracted into EtOAc (3 x 100 mL). The combined EtOAc phases were dried over $MgSO_4$, filtered concentrated under reduced pressure to afford the title compound, 4-bromo-*N*,*N*-dimethyl-pyridin-2-amine, **198**, as an off-white solid (320 mg, 1.43 mmol, 83% yield). R_f 0.63 (EtOAc / petroleum ether 1:9); ^{1}H NMR (500 MHz, DMSO-d_6) δ_H 7.93 (1H, d, *J*= 5.3 Hz, H-6), 6.80 (1H, d, *J*= 1.6 Hz, H-3), 6.72 (1H, dd, *J*= 5.3, 1.6 Hz, H-5'), 2.99 (6H, s, H-1''); LCMS (LCQ): Rt = 1.7 min (Method 1); *m/z* (ESI$^+$) 201.1 [M]$^+$ and 203.1 [M+2]$^+$.

N,*N*-Dimethyl-4-pyrazolo[1,5-*b*]pyridazin-3-yl-pyridin-2-amine **199**

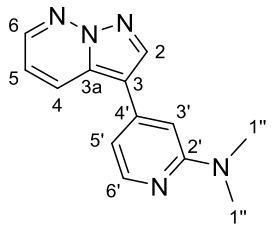

To a microwave vial containing a solution of 3-(4,4,5,5-tetramethyl-1,3,2-dioxaborolan-2-yl)pyrazolo[1,5-*b*]pyridazine (30 mg, 0.12 mmol) in acetonitrile (0.60 mL) and water (0.10 mL) was added bis[2-(di-*tert*-butylphosphanyl)cyclopenta-2,4-dien-1-yl]iron; dichloropalladium (4 mg, 0.01 mmol), sodium carbonate (32 mg, 0.31 mmol) and 4-bromo-*N*,*N*-dimethyl-pyridin-2-amine (49 mg, 0.24 mmol). The vial was sealed and irradiated with microwaves at 140 °C for 20 min. The reaction mixture was concentrated under reduced pressure. The residue was dissolved in EtOAc (10 mL) and washed with water (2 x 10 mL), followed by brine solution (10 mL). The organic component was then dried over $MgSO_4$, filtered and concentrated under reduced pressure. The crude was purified using flash silica column chromatography on an Isco Combiflash system (4 g silica, elution with 0-40% EtOAc / petroleum ether gradient). Desired fractions were combined and concentrated under reduced pressure. The crude was purified using flash reverse phase column chromatography on a Biotage system (12 g silica, elution with 10-100% MeOH / water gradient) to afford the title compound, *N*,*N*-dimethyl-4-pyrazolo[1,5-*b*]pyridazin-3-yl-pyridin-2-amine, **199**, as an off-white solid (10 mg, 0.04 mmol, 32% yield). R_f 0.13 (EtOAc / petroleum ether 3:2); m.p. 132-134 °C; $\bar{\nu}_{max}$ (neat)/cm^{-1} 2975 (C-H, w), 2933 (C-H, w), 1623 (C=N, m), 1536 (C=C, m); ^{1}H NMR (600 MHz, DMSO-d$_6$) δ_H 8.60 (1H, s, H-2), 8.58 (1H, dd, *J* = 9.1, 1.8 Hz, H-4), 8.52 (1H, dd, *J* = 4.4, 1.8 Hz, H-6), 8.12 (1H, d, *J* = 5.2 Hz, H-6'), 7.32 (1H, dd, *J* = 9.1, 4.4 Hz, H-5), 6.92 (1H, dd, *J* = 5.2, 1.4 Hz, H-5'), 6.85 (1H, s, H-3'), 3.08 (6H, s, H-1''); ^{13}C NMR (150MHz, DMSO-d$_6$) δ_C 159.73 (C-2'), 148.33 (C-6'), 143.37 (C-4), 140.12 (C-4'), 138.42 (C-2), 130.72 (C-3a), 127.59 (C-6), 117.74 (C-5), 110.98 (C-3), 109.45 (C-5'), 102.47 (C-3'), 37.81 (C-1''); HRMS *m/z* (ESI$^+$) [Found: 240.1252., $C_{13}H_{13}N_5$ requires [M + H]$^+$ 240.1244]; LCMS (LCQ): Rt = 0.4 min (Method 1); *m/z* (ESI$^+$) 240.3 [M + H]$^+$; LCMS (MDAP): Rt = 8.6 min, >95% (Method 3); *m/z* (ESI$^+$) 240.1 [M + H]$^+$.

N,*N*-Dimethyl-4-pyrazolo[1,5-*b*]pyridazin-3-yl-1,3,5-triazin-2-amine **201**

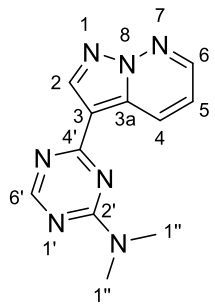

To a solution of 2,4-dichloro-1,3,5-triazine (200 mg, 1.33 mmol) in THF (0.80 mL) was added dimethylamine hydrochloride (120 mg, 1.47 mmol) and *N*,*N*-diisopropylethylamine (0.7 mL, 4.01 mmol). The reaction mixture was stirred at rt for 3 h. The reaction mixture was concentrated under reduced pressure. The crude was triturated with water and dried under reduced pressure. The crude was dissolved in 1,4-dioxane (2 mL). To the crude was added 3-(4,4,5,5-tetramethyl-1,3,2-dioxaborolan-2-yl)pyrazolo[1,5-*b*]pyridazine (80 mg, 0.33 mmol), 2 M potassium carbonate (0.5 mL, 1 mmol) and bis[2-(di-*tert*-butylphosphanyl)cyclopenta-2,4-dien-1-yl]iron; dichloropalladium (15 mg, 0.02 mmol). The reaction mixture was heated to 80 °C overnight. The reaction mixture was concentrated under reduced pressure. The crude was purified using flash silica column chromatography on an Isco Combiflash system (12 g silica, elution with 0-100% EtOAc / petroleum ether gradient) to afford the title compound, *N*,*N*-dimethyl-4-pyrazolo[1,5-*b*]pyridazin-3-yl-1,3,5-triazin-2-amine, **201**, as a white solid (15 mg, 0.06 mmol, 4% yield). R_f 0.25 (EtOAc / petroleum ether 1:1); m.p. 204-206 °C; $\bar{\nu}_{max}$ (neat)/cm^{-1} 3091 (C-H, w), 3074 (C-H, w), 2868 (C-H, w), 1624 (C=N, m), 1568 (C=C, m); ^{1}H NMR (500 MHz, MeOD) δ_H 9.01 (1H, dd, *J* = 9.0, 2.0 Hz, H-4), 8.75 (1H, s, H-2), 8.55 – 8.52 (2H, m, H-6 and 6'), 7.45 (1H, dd, *J* = 9.0, 4.5 Hz, H-5), 3.36 (3H, s, H-1''), 3.28 (3H, s, H-1''); ^{1}H NMR (500 MHz, DMSO-d$_6$) δ_H 8.86 (1H, dd, *J* = 9.0, 1.9 Hz, H-4), 8.72 (1H, s, H-2), 8.61 (1H, dd, *J* = 4.5, 1.9 Hz, H-6), 8.55 (1H, s, H-6'), 7.48 (1H, dd, *J* = 9.0, 4.5 Hz, H-5), 3.24 (3H, s, H-1''), 3.16 (3H, s, H-1''); ^{13}C NMR (125 MHz, DMSO-d$_6$) δ_C 166.1 (C-4'), 165.7 (C-6'), 163.5 (C-2'), 144.1 (C-6), 141.2 (C-2), 133.8 (C-3a), 129.0 (C-4), 119.8 (C-5), 109.9 (C-3), 36.1 (C-1''); HRMS *m/z* (ESI$^+$) [Found: 242.1143., $C_{11}H_{12}N_7$ requires [M + H]$^+$ 242.1149]; LCMS (MDAP): Rt = 9.6 min, >95% (Method 3); *m/z* (ESI$^+$) 241.9 [M + H]$^+$.

N,*N*-Dimethyl-4-(6-methylpyrazolo[1,5-*b*]pyridazin-3-yl)pyrimidin-2-amine **202**

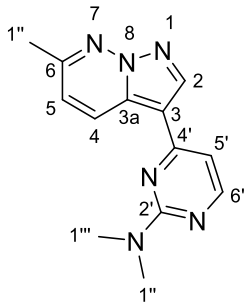

To a solution of 3-methylpyridazine (0.1 mL, 1.06 mmol) in pH 8 phosphate buffer (1.5 mL) was added aminosulfuric acid (180 mg, 1.59 mmol) in water (0.1 mL). The reaction mixture was neutralized to pH 7.5 by slow addition of 2.4 M potassium bicarbonate (0.77 mL, 1.85 mmol). The reaction mixture was heated to 70 °C and was stirred for 2 h. The reaction mixture was cooled to rt and CH_2Cl_2 (1.8 mL) was added. The reaction mixture was cooled in an ice bath and 3-butyn-2-one (0.04 mL, 0.45 mmol) was added in one portion followed by dropwise addition of potassium hydroxide (67 mg, 1.19 mmol) in water (0.18 mL). The reaction mixture was allowed to warm to rt and stirred overnight. The aqueous layer was extracted with CH_2Cl_2 (2 x 20 mL). The combined organic layers were washed with water (10 mL), dried over $MgSO_4$, filtered and concentrated under reduced pressure. To the residue was added *N*,*N*-dimethylformamide dimethyl acetal (3.68 mL, 27.70 mmol). The reaction mixture was heated to 75 °C for 16 h. The reaction mixture was concentrated under reduced pressure. To the crude was added 2-methoxyethanol (30 mL), 1,1-dimethylguanidine sulfate salt (178 mg, 0.66 mmol) and potassium carbonate (125 mg, 0.90 mmol). The reaction mixture was heated to 125 °C overnight. The reaction mixture was concentrated under reduced pressure. The residue was partitioned between EtOAc (50 mL) and water (50 mL) and the organic layer separated. The aqueous layer was extracted with further EtOAc (2 x 50 mL). The combined organics were dried over $MgSO_4$, filtered and concentrated to dryness under reduced pressure. The crude was purified using flash silica column chromatography on an Isco Combiflash system (12 g silica, elution with 0-100% EtOAc / petroleum ether gradient), trituration with petroleum ether followed by recrystallisation in EtOAc furnished the title compound, *N*,*N*-dimethyl-4-(6-methylpyrazolo[1,5-*b*]pyridazin-3-yl)pyrimidin-2-amine, **202**, as a white solid (15 mg, 0.05 mmol, 12% yield). R_f 0.63 (EtOAc); m.p. 190-192 °C; $\bar{\nu}_{max}$ (neat)/cm^{-1} 3099 (C-H, w), 2924 (C-H, w), 2858 (C-H, w), 1624 (C=N, m), 1566 (C=C, s); ^{1}H NMR (600 MHz, DMSO-d$_6$) δ_H 8.82 (1H, d, *J* = 9.1 Hz, H-4), 8.72 (1H, s, H-2), 8.33 (1H, d, *J* = 5.2 Hz, 1H, H-6'), 7.36 (1H, d, J = 9.1 Hz, H-5), 7.10 (1H, d, *J* = 5.2 Hz, H-5'), 3.20 (6H, s, H-1'''), 2.57 (3H, s, H-1''); ^{13}C NMR (150 MHz, DMSO-d$_6$) δ_C 161.9 (C-2'), 159.0 (C-4'), 157.9 (C-6'), 152.5 (C-6), 139.0 (C-2), 130.6 (C-3a), 128.4 (C-4), 120.7 (C-5), 110.3 (C-3), 104.5

(C-5’), 36.9 (C-1’’’), 21.2 (C-1’’); HRMS *m/z* (ESI$^+$) [Found 277.1167., $C_{13}H_{14}N_6Na$ requires [M + Na]$^+$ 277.1172]; LCMS (MDAP): Rt = 11.7 min, >92% (Method 3); *m/z* (ESI$^+$) 255.9 [M + H]$^+$.

4-(6-Methoxypyrazolo[1,5-*b*]pyridazin-3-yl)-*N*,*N*-dimethyl-pyrimidin-2-amine **203**

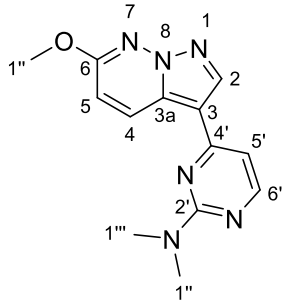

To a solution of 3-methoxypyridazine (100 mg, 0.91 mmol) in pH 8 phosphate buffer (1.5 mL) was added aminosulfuric acid (154 mg, 1.36 mmol) in water (0.1 mL). The reaction mixture was neutralized to pH 7.5 by slow addition of 2.4 M potassium bicarbonate (0.66 mL, 1.58 mmol). The reaction mixture was heated to 70 °C and was stirred for 2 h. The reaction mixture was cooled to rt and CH_2Cl_2 (1.5 mL) was added. The reaction mixture was cooled in an ice bath and 3-butyn-2-one (0.03 mL, 0.38 mmol) was added in one portion followed by dropwise addition of potassium hydroxide (57 mg, 1.02 mmol) in water (0.15 mL). The reaction mixture was allowed to warm to rt and stirred overnight. The aqueous layer was extracted with CH_2Cl_2 (2 x 20 mL). The combined organic layers were washed with water (10 mL), dried over $MgSO_4$, filtered and concentrated under reduced pressure. To the residue was added *N*,*N*-dimethylformamide dimethyl acetal (3.37 mL, 25.38 mmol). The reaction mixture was heated to 75 °C for 16 h. The reaction mixture was concentrated under reduced pressure. To the crude was added 2-methoxyethanol (30 mL), 1,1-dimethylguanidine sulfate salt (167 mg, 0.61 mmol) and potassium carbonate (117 mg, 0.84 mmol). The reaction mixture was heated to 125 °C overnight. The reaction mixture was concentrated under reduced pressure. The residue was partitioned between EtOAc (50 mL) and water (50 mL) and the organic layer separated. The aqueous layer was extracted with further EtOAc (2 x 50 mL). The combined organics were dried over $MgSO_4$, filtered and concentrated to dryness under reduced pressure. The crude was purified using flash silica column chromatography on an Isco Combiflash system (12 g silica, elution with 0-100% EtOAc / petroleum ether gradient), trituration with petroleum ether followed by recrystallisation in EtOAc furnished the title compound, 4-(6-methoxypyrazolo[1,5-*b*]pyridazin-3-yl)-*N*,*N*-dimethyl-pyrimidin-2-amine, **203**, as a yellow solid (15 mg, 0.05 mmol, 13% yield). R_f 0.35 (EtOAc/ petroleum ether 1:1); m.p. 161-163 °C; $\bar{\nu}_{max}$ (neat)/cm^{-1} 3096 (C-H, w), 2924 (C-H, w), 2858 (C-H, w), 1567 (C=C, s); ^{1}H NMR (600 MHz, DMSO-d$_6$) δ_H 8.80 (1H, d, *J* = 9.6 Hz, H-4), 8.62 (1H, s, H-2), 8.32 (1H, d, *J* = 5.1 Hz, H-6'), 7.14 (1H, d, *J* = 9.6 Hz, H-5), 7.08 (1H, d, *J* = 5.1 Hz, H-5'), 3.99 (3H, s, H-1''), 3.19 (6H, s, H-1'''); ^{13}C NMR (150 MHz, DMSO-d$_6$) δ_C 161.9 (C-2'), 159.6 (C-6), 158.9 (C-4'), 157.9 (C-6'), 137.9 (C-2), 130.4 (C-4), 129.2 (C-3a), 113.2 (C-5), 111.0 (C-3),

104.4 (C-5'), 54.7 (C-1''), 36.9 (C-1'''); HRMS *m/z* (ESI^+) [Found 293.1117., $C_{13}H_{14}N_6NaO$ requires $[M + Na]^+$ 293.1121]; LCMS (MDAP): Rt = 12.7 min, >95% (Method 3); *m/z* (ESI^+) 271.9 $[M + H]^+$.

N,*N*-Dimethyl-4-(5-methylpyrazolo[1,5-*b*]pyridazin-3-yl)pyrimidin-2-amine **204**

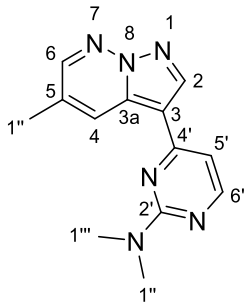

To a solution of 4-methylpyridazine (256 mg, 2.72 mmol) in pH 5 acetate buffer (1.5 mL) was added aminosulfuric acid (462 mg, 1.36 mmol) in water (0.1 mL). The reaction mixture was neutralized to pH 7.5 by slow addition of 2.4 M potassium bicarbonate (1.98 mL, 4.75 mmol). The reaction mixture was heated to 70 °C and was stirred for 2 h. The reaction mixture was cooled to rt and CH_2Cl_2 (4.5 mL) was added. The reaction mixture was cooled in an ice bath and 3-butyn-2-one (0.09 mL, 1.15 mmol) was added in one portion followed by dropwise addition of potassium hydroxide (171 mg, 3.05 mmol) in water (0.45 mL). The reaction mixture was allowed to warm to rt and stirred overnight. The aqueous layer was extracted with CH_2Cl_2 (2 x 20 mL). The combined organic layers were washed with water (10 mL), dried over $MgSO_4$, filtered and concentrated under reduced pressure. To the residue was added *N*,*N*-dimethylformamide dimethyl acetal (3.37 mL, 25.38 mmol). The reaction mixture was heated to 75 °C for 16 h. The reaction mixture was concentrated under reduced pressure. To the crude was added 1,1-dimethylguanidine sulfate salt (600 mg, 2.2 mmol), 2-methoxyethanol (30 mL) and potassium carbonate (400 mg, 2.89mmol). The reaction mixture was heated to 125 °C overnight. The reaction mixture was concentrated under reduced pressure. The residue was partitioned between EtOAc (50 mL) and water (50 mL) and the organic layer separated. The aqueous layer was extracted with further EtOAc (2 x 50 mL). The combined organics were dried over $MgSO_4$, filtered and concentrated to dryness under reduced pressure. The crude was purified using flash silica column chromatography on an Isco Combiflash system (12 g silica, elution with 0-100% EtOAc / petroleum ether gradient), trituration with petroleum ether followed by recrystallisation in EtOAc furnished the title compound, *N*,*N*-dimethyl-4-(5-methylpyrazolo[1,5-*b*]pyridazin-3-yl)pyrimidin-2-amine, **204**, as a salmon pink solid (15 mg, 0.05 mmol, 9% yield). R_f 0.46 (EtOAc/ petroleum ether 2:3); m.p. 236-238 °C; $\bar{\nu}_{max}$ (neat)/cm^{-1} 3090 (C-H, w), 2925 (C-H, w), 2859 (C-H, w), 1630 (C=N, m), 1591 (C=C, s); ^{1}H NMR (600 MHz, DMSO-d$_6$) δ_H 8.75 (1H, s, H-2), 8.68 – 8.64 (1H, m, H-4), 8.46 (1H, d, *J* = 2.4 Hz, H-6), 8.32 (1H, d, *J* = 5.1 Hz, H-6'), 7.09 (1H, d, *J* = 5.1 Hz, H-5'), 3.20 (6H, s, H-1'''), 2.44 (3H, s, H-1''); ^{13}C NMR (150 MHz, DMSO-d$_6$) δ_C 161.9 (C-2'), 159.0 (C-4'), 157.8 (C-6'), 145.8 (C-6), 139.9 (C-2), 132.1 (C-3a), 129.3 (C-5), 126.7 (C-4), 109.2 (C-3), 104.4 (C-5'), 36.9 (C-1'''), 18.3 (C-1''); HRMS *m/z* (ESI$^+$) [Found 255.1350., $C_{13}H_{15}N_6$

requires $[M + H]^+$ 255.1353]; LCMS (MDAP): Rt = 11.6 min, >95% (Method 3); *m/z* (ESI^+) 255.9 $[M + H]^+$

N,*N*-Dimethyl-4-(4-methylpyrazolo[1,5-*b*]pyridazin-3-yl)pyrimidin-2-amine **205**

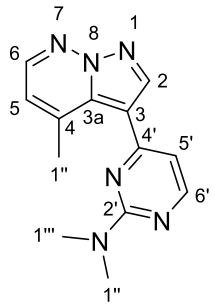

To a solution of 4-methylpyridazine (256 mg, 2.72 mmol) in pH 5 acetate buffer (1.5 mL) was added aminosulfuric acid (462 mg, 1.36 mmol) in water (0.1 mL). The reaction mixture was neutralized to pH 7.5 by slow addition of 2.4 M potassium bicarbonate (1.98 mL, 4.75 mmol). The reaction mixture was heated to 70 °C and was stirred for 2 h. The reaction mixture was cooled to rt and CH_2Cl_2 (4.5 mL) was added. The reaction mixture was cooled in an ice bath and 3-butyn-2-one (0.09 mL, 1.15 mmol) was added in one portion followed by dropwise addition of potassium hydroxide (171 mg, 3.05 mmol) in water (0.45 mL). The reaction mixture was allowed to warm to rt and stirred overnight. The aqueous layer was extracted with CH_2Cl_2 (2 x 20 mL). The combined organic layers were washed with water (10 mL), dried over $MgSO_4$, filtered and concentrated under reduced pressure. To the residue was added *N*,*N*-dimethylformamide dimethyl acetal (3.37 mL, 25.38 mmol). The reaction mixture was heated to 75 °C for 16 h. The reaction mixture was concentrated under reduced pressure. To the crude was added 1,1-dimethylguanidine sulfate salt (600 mg, 2.2 mmol), 2-methoxyethanol (30 mL) and potassium carbonate (400 mg, 2.89mmol). The reaction mixture was heated to 125 °C overnight. The reaction mixture was concentrated under reduced pressure. The residue was partitioned between EtOAc (50 mL) and water (50 mL) and the organic layer separated. The aqueous layer was extracted with further EtOAc (2 x 50 mL). The combined organics were dried over $MgSO_4$, filtered and concentrated to dryness under reduced pressure. The crude was purified using flash silica column chromatography on an Isco Combiflash system (12 g silica, elution with 0-100% EtOAc / petroleum ether gradient), trituration with petroleum ether followed by recrystallisation in EtOAc furnished the title compound, *N*,*N*-dimethyl-4-(4-methylpyrazolo[1,5-*b*]pyridazin-3-yl)pyrimidin-2-amine, **205**, as a cream solid (10 mg, 0.04 mmol, 6% yield). R_f 0.43 (EtOAc/ petroleum ether 1:1); m.p. 135-137 °C; $\bar{\nu}_{max}$ (neat)/cm^{-1} 2925 (C-H, w), 2864 (C-H, w), 2790 (C-H, w), 1609 (C=N, m), 1570 (C=C, s), 1545 (C=C, s); ^{1}H NMR (600 MHz, DMSO-d$_6$) δ_H 8.42 (1H, d, *J* = 4.6 Hz, H-6), 8.40 (1H, s, H-2), 8.36 (1H, d, *J* = 5.0 Hz, H-6'), 7.17 (1H, d, *J* = 4.6, H-5), 6.92 (1H, d, *J* = 5.0 Hz, H-5'), 3.15 (6H, s, H-1'''), 2.68 (3H, s, H-1''); ^{13}C NMR (150 MHz, DMSO-d$_6$) δ_C 161.7 (C-2'), 159.7 (C-4'), 157.7 (C-6'), 143.1 (C-6), 140.6 (C-2), 140.4 (C-4), 132.1 (C-3a), 118.2 (C-5), 113.0 (C-3), 108.7 (C-5'), 36.8 (C-1'''), 20.3 (C-1''); HRMS *m/z* (ESI$^+$) [Found 255.1349.,

$C_{13}H_{15}N_6$ requires $[M + H]^+$ 255.1353]; LCMS (MDAP): Rt = 12.4 min, >95% (Method 3); *m/z* (ESI^+) 255.9 $[M + H]^+$.

4-(4-Methoxypyrazolo[1,5-*b*]pyridazin-3-yl)-*N*,*N*-dimethyl-pyrimidin-2-amine **206**

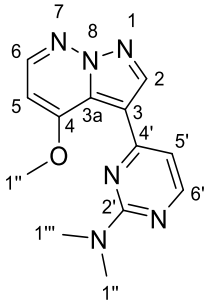

To a solution of 4-methoxypyridazine (300 mg, 2.72 mmol) in pH 5 acetate buffer (1.5 mL) was added aminosulfuric acid (462 mg, 1.36 mmol) in water (0.1 mL). The reaction mixture was neutralized to pH 7.5 by slow addition of 2.4 M potassium bicarbonate (1.98 mL, 4.75 mmol). The reaction mixture was heated to 70 °C and was stirred for 2 h. The reaction mixture was cooled to rt and CH_2Cl_2 (4.5 mL) was added. The reaction mixture was cooled in an ice bath and 3-butyn-2-one (0.09 mL, 1.15 mmol) was added in one portion followed by dropwise addition of potassium hydroxide (171 mg, 3.05 mmol) in water (0.45 mL). The reaction mixture was allowed to warm to rt and stirred overnight. The aqueous layer was extracted with CH_2Cl_2 (2 x 20 mL). The combined organic layers were washed with water (10 mL), dried over $MgSO_4$, filtered and concentrated under reduced pressure. To the residue was added *N*,*N*-dimethylformamide dimethyl acetal (3.37 mL, 25.38 mmol). The reaction mixture was heated to 75 °C for 16 h. The reaction mixture was concentrated under reduced pressure. To the crude was added 1,1-dimethylguanidine sulfate salt (600 mg, 2.2 mmol), 2-methoxyethanol (30 mL) and potassium carbonate (400 mg, 2.89 mmol). The reaction mixture was heated to 125 °C overnight. The reaction mixture was concentrated under reduced pressure. The residue was partitioned between EtOAc (50 mL) and water (50 mL) and the organic layer separated. The aqueous layer was extracted with further EtOAc (2 x 50 mL). The combined organics were dried over $MgSO_4$, filtered and concentrated to dryness under reduced pressure. The crude was purified using flash silica column chromatography on an Isco Combiflash system (12 g silica, elution with 0-100% EtOAc / petroleum ether gradient), trituration with petroleum ether followed by recrystallisation in EtOAc furnished the title compound, 4-(4-methoxypyrazolo[1,5-*b*]pyridazin-3-yl)-*N*,*N*-dimethyl-pyrimidin-2-amine, **206**, as a white solid (12 mg, 0.04 mmol, 8% yield). R_f 0.41 (EtOAc); m.p. 180-182 °C; $\bar{\nu}_{max}$ (neat)/cm^{-1} 3063 (C-H, w), 2924 (C-H, w), 2857 (C-H, w), 1579 (C=C, s), 1562 (C=C, s), 1550 (C=C, s); ^{1}H NMR (600 MHz, DMSO-d$_6$) δ_H 8.53 (1H, s, H-2), 8.40 (1H, d, *J* = 5.6 Hz, H-6), 8.33 (1H, d, *J* = 5.1 Hz, H-6'), 7.12 (1H, d, *J* = 5.1 Hz, H-5'), 6.87 (1H, d, *J* = 5.6 Hz, H-5), 4.07 (3H, s, H-1''), 3.17 (6H, s, H-1'''); ^{13}C NMR (150 MHz, DMSO-d$_6$) δ_C 161.8 (C-2'), 158.3 (C-4), 157.9 (C-4'), 157.7 (C-6'), 144.0 (C-6), 126.5 (C-3a), 112.6 (C-3), 108.2 (C-5'), 96.9 (C-

5), 56.8 (C-1''), 36.6 (C-1'''); HRMS *m/z* (ESI^+) [Found 271.1298., $C_{13}H_{15}N_6O$ requires $[M + H]^+$ 271.1302]; LCMS (MDAP): Rt = 11.5 min, >95% (Method 3); *m/z* (ESI^+) 271.9 $[M + H]^+$

2-Methylsulfanyl-4-prop-1-ynyl-pyrimidine **207**

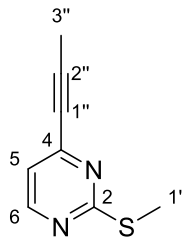

To a stirred solution of copper iodide (38 mg, 0.20 mmol) in THF (20 mL) was added bis(triphenylphosphine)palladium(II) dichloride (84 mg, 0.0.12mmol), TEA (0.69 mL, 4.96 mmol), propyne (ca. 5% in THF, ca. 1 mol/L) (5 mL, 4.96 mmol), followed by slow addition of 4-iodo-2-methylsulfanyl-pyrimidine (1 g, 3.97 mmol). The reaction mixture was stirred at rt overnight. The reaction mixture was concentrated under reduced pressure. The crude was purified using flash silica column chromatography on an Isco Combiflash system (24 g silica, elution with 0-40% EtOAc / petroleum ether gradient) to afford the title compound, 2-methylsulfanyl-4-prop-1-ynyl-pyrimidine, **207**, as a yellow liquid (600 mg, 3.47 mmol, 87% yield). R_f 0.85 (EtOAc / petroleum ether 1:9); ^{1}H NMR (600 MHz, DMSO-d_6) δ_H 8.58 (1H, d, *J* = 5.1 Hz, H-6), 7.20 (1H, d, *J* = 5.1 Hz, H-5), 2.48 (3H, s, H-1'), 2.13 (3H, s, H-3''); LCMS (MDAP): Rt = 2.0 min (Method 5); *m/z* (ESI$^+$) 164.9 [M + H]$^+$.

2-Methyl-3-(2-methylsulfanylpyrimidin-4-yl)pyrazolo[1,5-*b*]pyridazine **208**

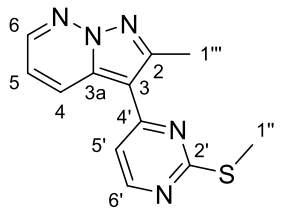

To a suspension of pyridazin-1-ium-1-amine iodide (217 mg, 0.97 mmol) in acetonitrile (5 mL) was added 2-methylsulfanyl-4-prop-1-ynyl-pyrimidine (100 mg, 0.61 mmol) followed by DBU (0.14 mL, 0.91 mmol). The reaction mixture was stirred at 50 °C for 16 h. The reaction mixture was concentrated under reduced pressure. The residue was partitioned between water (50 mL) and diethyl ether (50 mL). The aqueous was extracted further with diethyl ether (2 x 50 mL). The combined organic layer was washed with brine (50 mL). The combined organics were dried over $MgSO_4$, filtered and concentrated under reduced pressure. . The crude was purified using flash silica column chromatography on an Isco Combiflash system (12 g silica, elution with 0-100% EtOAc / petroleum ether gradient) to afford the title compound, 2-methyl-3-(2-methylsulfanylpyrimidin-4-yl)pyrazolo[1,5-*b*]pyridazine, **208**, as a white solid (120 mg, 0.44 mmol, 73% yield). R_f 0.25 (EtOAc / petroleum ether 1:1); ^{1}H NMR (600 MHz, DMSO-d_6) δ_H 8.78 (1H, dd, *J* = 9.1, 1.9 Hz, H-4), 8.61 (1H, d, *J* = 5.4 Hz, H-6'), 8.55 (1H, dd, *J* = 4.4, 1.9 Hz, H-6), 7.49 – 7.42 (2H, m, H-5 and 5'), 2.72 (3H, s, H-1'' or 1'''), 2.60 (3H, s, H-1'' or 1'''); HRMS *m/z* (ESI$^+$) [Found: 258.0803., $C_{12}H_{12}N_5S$ requires [M + H]$^+$ 258.0808]; LCMS (MDAP): Rt = 2.0 min (Method 5); *m/z* (ESI$^+$) 258.0 [M + H]$^+$. The spectroscopic data are in good agreement with the literature values. Literature reference: Tavares FX, Boucheron JA, Dickerson SH, Griffin RJ, Preugschat F, Thomson SA, Wang TY, Zhou HQ. J Med Chem. 2004 Sep 9;47(19):4716-30.

2-Methyl-3-(2-methylsulfonylpyrimidin-4-yl)pyrazolo[1,5-*b*]pyridazine **209**

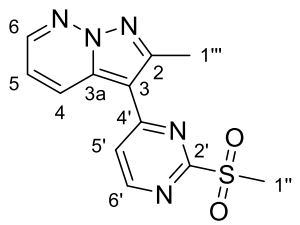

To a suspension of 2-methyl-3-(2-methylsulfanylpyrimidin-4-yl)pyrazolo[1,5-*b*]pyridazine (120 mg, 0.47 mmol) in CH_2Cl_2 (5 mL), cooled to 0°C, was slowly added 3-chloroperbenzoic acid (268 mg, 1.17 mmol). Once the addition was complete, the reaction was allowed to warm to rt and was stirred overnight. The reaction mixture was diluted with CH_2Cl_2 (100 mL), quenched with sat.aq. sodium thiosulfate (100 mL), washed with sat. aq. sodium bicarbonate solution (3 x 100 mL) and brine (100 mL), dried over $MgSO_4$, filtered, and concentrated under reduced pressure to afford the title compound, 2-methyl-3-(2-methylsulfonylpyrimidin-4-yl)pyrazolo[1,5-*b*]pyridazine, **209**, as a pale yellow solid (180 mg, 0.37 mmol, 80% yield) and benzoic acid impurity. R_f 0.25 (EtOAc / petroleum ether 1:1); ^{1}H NMR (600 MHz, DMSO-d_6) δ_H 9.01 (1H, d, *J* = 5.4 Hz, H-6'), 8.90 (1H, dd, *J* = 9.1, 1.8 Hz, H-4), 8.63 (1H, dd, *J* = 4.5, 1.8 Hz, H-6), 8.03 (1H, d, *J* = 5.4 Hz, H-5'), 7.58 – 7.50 (1H, m, H-5), 3.48 (3H, s, H-1''), 2.78 (3H, s, H-1'''); The spectroscopic data are in good agreement with the literature values. Literature reference: Tavares FX, Boucheron JA, Dickerson SH, Griffin RJ, Preugschat F, Thomson SA, Wang TY, Zhou HQ. J Med Chem. 2004 Sep 9;47(19):4716-30.

N,*N*-Dimethyl-4-(2-methylpyrazolo[1,5-*b*]pyridazin-3-yl)pyrimidin-2-amine **210**

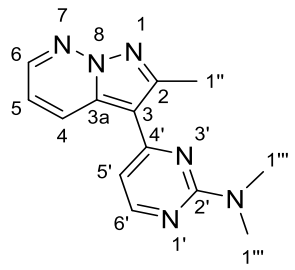

To a microwave vial containing 2-methyl-3-(2-methylsulfonylpyrimidin-4-yl)pyrazolo[1,5-*b*]pyridazine (80 mg, 0.28 mmol) was added dimethylamine (0.02 mL, 0.55 mmol). The vial was sealed and heated conventionally at 110 °C for 2h. The reaction mixture was concentrated under reduced pressure. The crude was purified using flash silica column chromatography on an Isco Combiflash system (12 g silica, elution with 0-100% EtOAc / petroleum ether gradient), trituration of the residue with petroleum ether afforded the title compound, *N*,*N*-dimethyl-4-(2-methylpyrazolo[1,5-*b*]pyridazin-3-yl)pyrimidin-2-amine, **210**, as an off-white solid (55 mg, 0.21 mmol, 74% yield). R_f 0.50 (EtOAc); m.p. 134-136 °C; $\bar{\nu}_{max}$ (neat)/cm^{-1} 3063 (C-H, w), 2976 (C-H, w), 2849 (C-H, w), 1619 (C=N, m), 1574 (C=C, s), 1561 (C=C, s); ^{1}H NMR (600 MHz, DMSO-d$_6$) δ_H 8.78 (1H, dd, *J* = 9.1, 1.9 Hz, H-4), 8.50 (1H, dd, *J* = 4.5, 1.9 Hz, H-6), 8.38 (1H, d, *J* = 5.2 Hz, H-6'), 7.37 (1H, dd, *J* = 9.1, 4.5 Hz, H-5), 6.90 (1H, d, *J* = 5.2 Hz, H-5'), 3.19 (6H, s, H-1'''), 2.69 (3H, s, H-1''); ^{13}C NMR (150 MHz, DMSO-d$_6$) δ_C 161.9 (C-2'), 159.1 (C-4'), 158.1 (C-6'), 148.7 (C-2), 142.9 (C-6), 133.6 (C-3a), 128.1 (C-4), 118.5 (C-5), 107.9 (C-3), 106.0 (C-5'), 36.9 (C-1'''), 14.9 (C-1'); HRMS *m/z* (ESI$^+$) [Found 277.1168., $C_{13}H_{14}N_6Na$ requires [M + Na]$^+$ 277.1172]; LCMS (MDAP): Rt = 11.0 min, >95% (Method 3); *m/z* (ESI$^+$) 255.9 [M + H]$^+$.

4-Chloro-*N*,*N*-dimethyl-pyrimidin-2-amine **211**

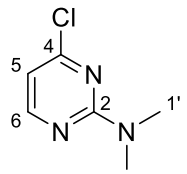

To a solution of 2-amino-4-chloropyrimidin-2-amine (500 mg, 3.86 mmol) in THF (20 mL) was added sodium hydride (463 mg, 19.3 mmol) at 0 °C. After warming to rt and stirring for 5 min, iodomethane (0.48 mL, 7.72 mmol) was added dropwise and the reaction stirred at rt for 16 h. The reaction mixture was concentrated under reduced pressure. The crude was dissolved with water (100 mL) and extracted into EtOAc (3 x 100 mL). The combined EtOAc phases were dried over $MgSO_4$, filtered concentrated under reduced pressure to afford the title compound, 4-chloro-*N*,*N*-dimethyl-pyrimidin-2-amine, **211**, as an orange solid (600 mg, 3.43 mmol, 89% yield). R_f 0.63 (EtOAc / petroleum ether 1:9); ^{1}H NMR (500 MHz, DMSO-d_6) δ_H 8.28 (1H, d, *J*= 5.1 Hz, H-6), 6.66 (1H, d, *J*= 5.1 Hz, H-5), 3.09 (6H, s, H-1'); LCMS (LCQ): Rt = 0.9 min (Method 1); *m/z* (ESI$^+$) 158.2 [M + H]$^+$.

N,*N*-Dimethyl-4-(1*H*-pyrrolo[2,3-*b*]pyridin-3-yl)pyrimidin-2-amine **212**

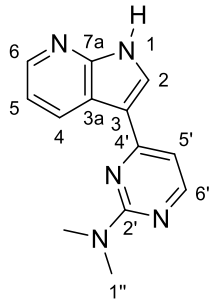

2-Methyl-2-propanyl 3-(4,4,5,5-tetramethyl-1,3,2-dioxaborolan-2-yl)-1*H*-pyrrolo[2,3-*b*]pyridine-1-carboxylate (150 mg, 0.44 mmol), potassium fluoride (101 mg, 1.74 mmol), tris(dibenzylideneacetone)dipalladium(0) (20 mg, 0.02 mmol), tri-*tert*-butylphosphonium tetrafluoroborate (9 mg, 0.03 mmol) and 4-chloro-*N*,*N*-dimethyl-pyrimidin-2-amine (69 mg, 0.44 mmol) were combined in acetonitrile (2mL) and water (0.50 mL) and heated in the microwave for 20 min at 120 °C. The reaction mixture was concentrated under reduced pressure. The residue was partitioned between water (20 mL) and EtOAc (20 mL). The organic layer was separated. The aqueous layer was extracted further with EtOAc (2 x 20 mL). The combined organic components were washed with brine solution (50 mL), dried over $MgSO_4$, filtered and concentrated under reduced pressure. The residue was taken up in MeOH (1 mL) and then 4N HCl in dioxane (4 mL) was added. The reaction mixture was stirred at rt for 2 h. The reaction mixture was concentrated under reduced pressure. The crude was purified using flash silica column chromatography on an Isco Combiflash system (12 g silica, elution with 0-50% 20% MeOH in CH_2Cl_2 / CH_2Cl_2 gradient), trituration with hot EtOH followed by recrystallization in minimum amount of hot EtOH afforded the title compound, *N*,*N*-dimethyl-4-(1*H*-pyrrolo[2,3-*b*]pyridin-3-yl)pyrimidin-2-amine, **212**, as a white crystalline solid (100 mg, 0.40 mmol, 91% yield). R_f 0.34 (MeOH / CH_2Cl_2 1:9); Decomposed > 283 °C; $\bar{\nu}_{max}$ (neat)/cm^{-1} 3425 (N-H, m), 3403 (N-H, m), 3069 (C-H, m), 2916 (C-H, m), 2852 (C-H, m), 1626 (C=N, m), 1587 (C=C, s), 1527 (C=C, m); ^{1}H NMR (600 MHz, MeOD) δ_H 8.87 (1H, d, *J* = 8.0 Hz, H-4), 8.63 (1H, s, H-2), 8.43 – 8.36 (1H, m, H-6), 8.07 (1H, d, *J* = 6.7 Hz, H-6'), 7.42 – 7.34 (2H, m, H-5 and 5'), 3.45 (6H, s, H-1''); ^{13}C NMR (150 MHz, MeOD) δ_C 156.6 (C-2' or C-4')*, 154.7 (C-2' or C-4'), 150.8 (C-7a or C-3a)*, 145.6 (C-6), 135.4 (C-2), 132.5 (C-4), 119.69 (C-7a or C-3a), 119.59 (C-5), 113.8 (C-3), 111.4 (C-6'), 105.6 (C-5'), 38.5 (C-1''); HRMS *m/z* (ESI$^+$) [Found 240.1245., $C_{13}H_{14}N_5$ requires [M + H]$^+$ 240.1244]; LCMS (MDAP): Rt = 10.8min, >95% (Method 3); *m/z* (ESI$^+$) 240.0 [M + H]$^+$.

N,*N*-Dimethyl-4-(1-methylpyrrolo[2,3-*b*]pyridin-3-yl)pyrimidin-2-amine **213**

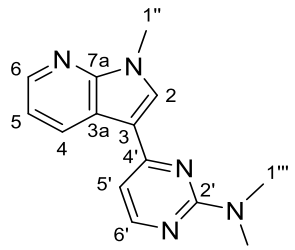

To a solution of *N*,*N*-dimethyl-4-(1*H*-pyrrolo[2,3-*b*]pyridin-3-yl)pyrimidin-2-amine (30 mg, 0.13 mmol) in DMF (2 mL) was added sodium hydride (12 mg, 0.50 mmol) and the mixture stirred in an ice bath for 10 min. Iodomethane (0.03 mL, 0.48 mmol) was added and the reaction mixture was stirred at rt for 1 h. The reaction mixture was concentrated under reduced pressure. The crude was purified using flash silica column chromatography on an Isco Combiflash system (12 g silica, elution with 0-20% 20% MeOH in CH_2Cl_2 / CH_2Cl_2 gradient) to afford the title compound, *N*,*N*-dimethyl-4-(1-methylpyrrolo[2,3-*b*]pyridin-3-yl)pyrimidin-2-amine, **213**, as an off-white solid (20 mg, 0.08 mmol, 60% yield). R_f 0.12 (CH_2Cl_2); m.p. 120-122 °C; $\bar{\nu}_{max}$ (neat)/cm^{-1} 3106 (C-H, w), 2923 (C-H, w), 2859 (C-H, w), 1558 (C=C, m), 1531 (C=C, s); ^{1}H NMR (500 MHz, DMSO-d$_6$) δ_H 8.70 (1H, d, *J* = 7.9 Hz, H-4), 8.38 (1H, s, H-2), 8.27 (1H, d, *J* = 4.6 Hz, H-6), 8.17 (1H, d, *J* = 5.3 Hz, H-6'), 7.19 (1H, dd, *J* = 7.9, 4.6 Hz, H-5), 6.92 (1H, d, *J* = 5.3 Hz, H-5'), 3.81 (3H, s, H-1''), 3.14 (6H, s, H-1'''); ^{13}C NMR (150 MHz, DMSO-d$_6$) δ_C 162.1 (C-2'), 161.2 (C-4'), 157.1 (C-6'), 148.2 (C-7a), 143.3 (C-6), 132.4 (C-2'), 130.2 (C-4), 118.1 (C-3), 117.2 (C-5), 111.5 (C-3a), 103.8 (C-5'), 36.9 (C-1'''), 31.3 (C-1''); HRMS *m/z* (ESI$^+$) [Found 254.1405., $C_{14}H_{16}N_5$ requires [M + H]$^+$ 254.1400]; LCMS (MDAP): Rt = 11.3 min, >95% (Method 3); *m/z* (ESI$^+$) 254.0 [M + H]$^+$.

4-{1-Ethyl-1*H*-pyrrolo[2,3-*b*]pyridin-3-yl}-*N*,*N*-dimethylpyrimidin-2-amine **214**

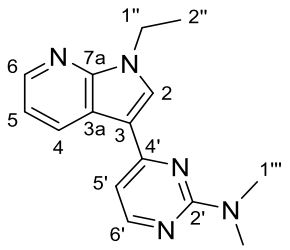

To a solution of *N*,*N*-dimethyl-4-(1*H*-pyrrolo[2,3-*b*]pyridin-3-yl)pyrimidin-2-amine (30 mg, 0.13 mmol) in DMF (2 mL) was added sodium hydride (12 mg, 0.50 mmol) and the mixture stirred in an ice bath under nitrogen for 10 min. Iodoethane (0.03 mL, 0.48 mmol) was added and the reaction mixture was stirred at rt for 1 h. The reaction was concentrated under reduced pressure. The crude was purified using flash silica column chromatography on an Isco Combiflash system (12 g silica, elution with 0-20% 20% MeOH in CH_2Cl_2 / CH_2Cl_2 gradient) to afford the title compound, 4-(1-ethylpyrrolo[2,3-*b*]pyridin-3-yl)-*N*,*N*-dimethyl-pyrimidin-2-amine, **214**, as an off-white solid (20 mg, 0.07 mmol, 57% yield). R_f 0.53 (CH_2Cl_2); m.p. 116-118 °C; $\bar{\nu}_{max}$ (neat)/cm^{-1} 3092 (C-H, w), 2972 (C-H, w), 2927 (C-H, w), 1555 (C=C, s), 1528 (C=C, s); ^{1}H NMR (500 MHz, DMSO-d$_6$) δ_H 8.90 (1H, d, *J* = 7.9 Hz, H-4), 8.64 (1H, s, H-2), 8.48 – 8.42 (1H, m, H-6), 8.37 (1H, d, *J* = 5.1 Hz, H-6'), 7.42 – 7.32 (1H, m, H-5), 7.14 (1H, d, *J* = 5.1 Hz, H-5'), 4.47 (2H, q, *J* = 6.8 Hz, H-1''), 3.33 (6H, s, H-1'''), 1.56 (3H, t, *J* = 6.8 Hz, H-2''); ^{13}C NMR (125 MHz, DMSO-d$_6$) δ_C 162.1 (C-2'), 161.2 (C-4'), 157.0 (C-6'), 147.7 (C-7a), 143.2 (C-6), 131.0 (C-2), 130.3 (C-4), 118.2 (C-3), 117.2 (C-5), 111.7 (C-3a), 103.9 (C-5'), 39.3 (C-1''), 36.9 (C-1'''), 15.4 (C-2''); HRMS *m/z* (ESI$^+$) [Found 268.1560., $C_{15}H_{18}N_5$ requires [M + H]$^+$ 268.1557]; LCMS (MDAP): Rt = 12.0 min, >95% (Method 3); *m/z* (ESI$^+$) 267.0 [M + H]$^+$.

N,*N*-Dimethyl-4-pyrazolo[1,5-*a*]pyridin-3-yl-pyrimidin-2-amine **215**

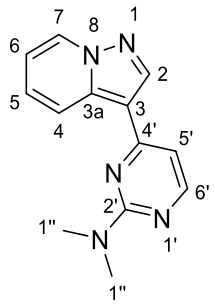

To a solution of 4-chloro-*N*,*N*-dimethyl-pyrimidin-2-amine (80 mg, 0.51 mmol) in 1,4-dioxane (2 mL) was added bis[2-(di-*tert*-butylphosphanyl)cyclopenta-2,4-dien-1-yl]iron; dichloropalladium (20 mg, 0.03 mmol), 3-(4,4,5,5-tetramethyl-1,3,2-dioxaborolan-2-yl)pyrazolo[1,5-*a*]pyridine (70 mg, 0.29 mmol) and 2 M potassium carbonate (0.4 mL, 0.80 mmol). The reaction mixture was heated to 70 °C for 16 h. The reaction mixture was concentrated under reduced pressure. The crude was purified using flash silica column chromatography on an Isco Combiflash system (12 g silica, elution with 0-100% EtOAc / petroleum ether gradient) to afford the title compound, *N*,*N*-dimethyl-4-pyrazolo[1,5-*a*]pyridin-3-yl-pyrimidin-2-amine, **215**, as a pale yellow solid (60 mg, 0.24 mmol, 83% yield). R_f 0.42 (EtOAc/ petroleum ether 1:1); m.p. 152-154 °C; $\bar{\nu}_{max}$ (neat)/cm^{-1} 3060 (C-H, w), 3047 (C-H, w), 2926 (C-H, w), 2893 (C-H, w), 1635 (C=N, m), 1566 (C=C, s), 1520 (C=C, s); ^{1}H NMR (600 MHz, DMSO-d$_6$) δ_H 8.80 (1H, d, *J* = 6.9 Hz, H-7), 8.74 (1H, s, H-2), 8.55 (1H, d, *J* = 8.8 Hz, H-4), 8.27 (1H, d, *J* = 5.2 Hz, H-6'), 7.50 (1H, dd, *J* = 8.8, 6.8 Hz, H-5), 7.09 – 7.05 (2H, m, H-6 and 5'), 3.21 (6H, s, H-1''); ^{13}C NMR (150 MHz, DMSO-d$_6$) δ_C 162.0 (C-2'), 159.6 (C-4'), 157.4 (C-6'), 142.4 (C-2), 138.0 (C-3a), 129.7 (C-7), 126.7 (C-5), 119.6 (C-4), 113.7 (C-6), 109.7 (C-3), 104.4 (C-5'), 36.9 (C-1''); HRMS *m/z* (ESI$^+$) [Found 240.1240., $C_{13}H_{14}N_5$ requires [M + H]$^+$ 240.1244]; LCMS (MDAP): Rt = 11.5 min, >95% (Method 3); *m/z* (ESI$^+$) 239.9 [M + H]$^+$.

1-(*p*-Tolylsulfonyl)pyrrolo[2,3-*c*]pyridine **216**

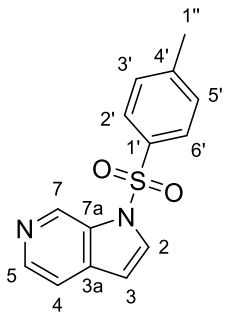

1*H*-Pyrrolo[2,3-*c*]pyridine (4.5 g, 38.09 mmol) was suspended in toluene (100 mL) and to this suspension was added tetrabutylammonium hydrogensulfate (1.95 g, 5.71 mmol). At 0 °C, approx. 33% sodium hydroxide (100 mL, 272.25 mmol) was added followed by *p*-toluenesulfonyl chloride (10.89 g, 57.14 mmol). The reaction was stirred at rt overnight. The organic layer was separated. The aqueous layer was extracted with toluene (2 x 100 mL). The combined organic components were washed with water (100 mL), sat aq NH_4Cl solution (100 mL) and water (100 mL). The combined organic components were dried over $MgSO_4$, filtered and concentrated under reduced pressure to afford 1-(*p*-tolylsulfonyl)pyrrolo[2,3-*c*]pyridine, **216**, as a beige solid (10.05 g, 35.06 mmol, 92% yield). R_f 0.41 (EtOAc / petroleum ether 1:1); ^{1}H NMR (500 MHz, DMSO-d_6) δ_H 9.20 (1H, s, H-7), 8.37 (1H, d, *J* = 5.3 Hz, H-5), 8.05 (1H, d, *J* = 3.5 Hz, H-2), 7.96 (2H, d, *J* = 8.3 Hz, H-2' and 6), 7.63 (1H, d, *J* = 5.3 Hz, H-4), 7.41 (1H, d, *J* = 8.1 Hz, H-3' and 5'), 6.91 (1H, d, *J* = 3.5 Hz, H-3), 2.32 (3H, s, H-1''). The spectroscopic data are in good agreement with the literature values. Literature reference: MERCK PATENT GMBH; BURGDORF, Lars; KUHN, Daniel; ROSS, Tatjana; DEUTSCH, Carl - WO2014/23385, 2014, A1. Location in patent: Page/Page column 123

3-Bromo-1-(*p*-tolylsulfonyl)pyrrolo[2,3-*c*]pyridine **217**

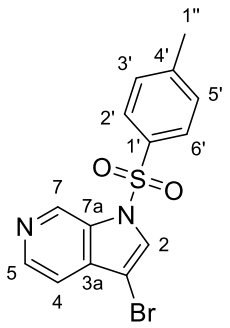

To a suspension of 1-(*p*-tolylsulfonyl)pyrrolo[2,3-*c*]pyridine (4 g, 14.69 mmol) in DMF (10 mL) was added *N*-bromosuccinimide (3.92 g, 22.03 mmol) and the resulting solution stirred at rt overnight. The reaction mixture was concentrated under reduced pressure. The crude was purified using flash silica column chromatography on an Isco Combiflash system (12 g silica, elution with 0-60% EtOAc / petroleum ether gradient) to afford the title compound, 3-bromo-1-(*p*-tolylsulfonyl)pyrrolo[2,3-*c*]pyridine, **217**, as a pale yellow solid (770 mg, 2.08 mmol, 14% yield). R_f 0.71 (EtOAc / petroleum ether 3:2); ^{1}H NMR (500 MHz, DMSO-d_6) δ_H 9.26 (1H, s, H-7), 8.49 (1H, d, *J* = 5.3 Hz, H-5), 8.43 (1H, s, H-2), 8.03 (2H, d, *J* = 8.0 Hz, H-2' and 6'), 7.53 (1H, d, *J* = 5.3 Hz, H-4), 7.44 (2H, d, J = 8.0 Hz, H-3' and 5'), 2.34 (3H, s, H-1''); LCMS (LCQ): Rt = 2.5 min (Method 1); *m/z* (ESI$^+$) 351.0 [M]$^+$ and 353.0 [M + 2]$^+$. The spectroscopic data are in good agreement with the literature values. Literature reference: MERCK PATENT GMBH; BURGDORF, Lars; KUHN, Daniel; ROSS, Tatjana; DEUTSCH, Carl - WO2014/23385, 2014, A1. Location in patent: Page/Page column 123

1-(*p*-Tolylsulfonyl)-3-(4,4,5,5-tetramethyl-1,3,2-dioxaborolan-2-yl)pyrrolo[2,3-*c*]pyridine **218**

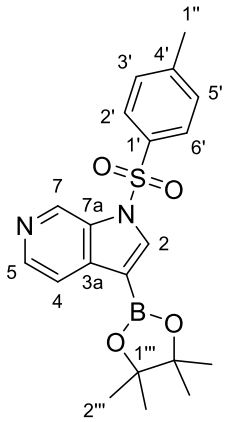

To a solution of bis(pinacolato)diboron (1.52 g, 5.98 mmol) in 1,4-dioxane (3 mL) was added potassium acetate (391 mg, 3.99 mmol), bis(triphenylphosphine)palladium(II) dichloride (70 mg, 0.10 mmol) and 3-bromo-1-(*p*-tolylsulfonyl)pyrrolo[2,3-*c*]pyridine (700 mg, 1.99 mmol). The reaction mixture was heated to 100 °C and stirred for 2 h. The reaction mixture was concentrated under reduced pressure. The residue was partitioned between water (50 mL) and EtOAc (50 mL), and the aqueous layer separated. The aqueous layer was extracted further with EtOAc (2 x 50 mL). The combined organic components were washed with water (100 mL), dried over $MgSO_4$, filtered and concentrated under reduced pressure to afford the title compound, 1-(*p*-tolylsulfonyl)-3-(4,4,5,5-tetramethyl-1,3,2-dioxaborolan-2-yl)pyrrolo[2,3-*c*]pyridine, **218**, as a brown solid (960 mg, 1.69 mmol, 85% yield) plus impurities. The material was used without further purification. LCMS (LCQ): Rt = 0.7 min (Method 1); *m/z* (ESI$^+$) 317.1 $[M + H]^+$ for boronic acid. The spectroscopic data are in good agreement with the literature values. Literature reference: MERCK PATENT GMBH; BURGDORF, Lars; KUHN, Daniel; ROSS, Tatjana; DEUTSCH, Carl - WO2014/23385, 2014, A1. Location in patent: Page/Page column 123

N,*N*-Dimethyl-4-(1*H*-pyrrolo[2,3-*c*]pyridin-3-yl)pyrimidin-2-amine **219**

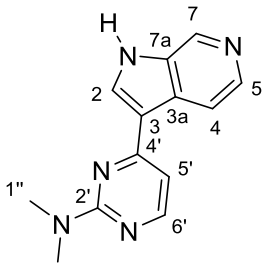

1-(*p*-tolylsulfonyl)-3-(4,4,5,5-tetramethyl-1,3,2-dioxaborolan-2-yl)pyrrolo[2,3-*c*]pyridine (250 mg, 0.63 mmol), potassium fluoride (146 mg, 2.51 mmol), tris(dibenzylideneacetone)dipalladium(0) (29 mg, 0.03 mmol), tri-*tert*-butylphosphonium tetrafluoroborate (14 mg, 0.05 mmol) and 4-chloro-*N*,*N*-dimethyl-pyrimidin-2-amine (198 mg, 1.26 mmol) were combined in acetonitrile (2 mL) and water (0.50 mL) and heated for 5 h at 120 °C. 1 M NaOH (1 mL) was added and the reaction mixture was heated to 100 °C for 1 h in the microwave. The reaction was concentrated under reduced pressure. The crude was purified using flash silica column chromatography on an Isco Combiflash system (12 g silica, elution with 0-100% 10% MeOH in CH_2Cl_2 / CH_2Cl_2 gradient) to afford the title compound, *N*,*N*-dimethyl-4-(1*H*-pyrrolo[2,3-*c*]pyridin-3-yl)pyrimidin-2-amine, **219**, as a beige solid (20 mg, 0.08 mmol, 12% yield). R_f 0.27 (MeOH / CH_2Cl_2 1:9); m.p. 220-222 °C; ^{1}H NMR (500 MHz, DMSO-d_6) δ_H 12.21 (1H, s, NH), 8.81 (1H, s, H-7), 8.48 (1H, s, H-2), 8.34 (1H, d, *J* = 5.2 Hz, H-6'), 8.29 – 8.19 (2H, m, H-6'and 5), 7.07 (1H, d, *J* = 5.2 Hz, H-5'), 3.22 (6H, s, H-1''); ^{13}C NMR (150 MHz, DMSO-d_6) δ_C 162.2 (C-2'), 161.5 (C-4'), 157.3 (C-6'), 139.5 (C-5), 135.2 (C-7), 134.4 (C-7a), 132.0 (C-2), 129.9 (C-3a), 116.4 (C-4), 113.9 (C-3), 104.4 (C-5'), 37.1 (C-1''); HRMS *m/z* (ESI$^+$) [Found 240.1253., $C_{13}H_{14}N_5$ requires [M + H]$^+$ 240.1244]; LCMS (MDAP): Rt = 21.4 min, >90% (Method 3); *m/z* (ESI$^+$) 240.0 [M + H]$^+$.

N,*N*-Dimethyl-4-(1-methylpyrrolo[2,3-*c*]pyridin-3-yl)pyrimidin-2-amine **220**

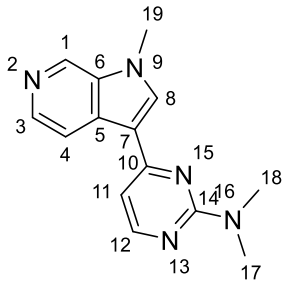

To a solution of *N*,*N*-dimethyl-4-(1*H*-pyrrolo[2,3-*c*]pyridin-3-yl)pyrimidin-2-amine (30 mg, 0.13 mmol) in DMF (2 mL) was added sodium hydride (3 mg, 0.14 mmol) and the mixture was stirred in an ice bath for 10 min. Iodomethane (0.01 mL, 0.13 mmol) was added and the reaction mixture was stirred at rt for 30 min. The reaction mixture was concentrated under reduced pressure. The crude was purified using flash silica column chromatography on an Isco Combiflash system (12 g silica, elution with 0-50% 20% MeOH in CH_2Cl_2 / CH_2Cl_2 gradient) to afford the title compound *N*,*N*-dimethyl-4-(1-methylpyrrolo[2,3-*c*]pyridin-3-yl)pyrimidin-2-amine, **220**, as a white solid (5 mg, 0.02 mmol, 15% yield). R_f 0.50 (MeOH / CH_2Cl_2 1:9); m.p. 169-171 °C; $\bar{\nu}_{max}$ (neat)/cm^{-1} 3028 (C-H, w), 2893 (C-H, w), 2848 (C-H, w), 1623 (C=N, m), 1566 (C=C, s); ^{1}H NMR (500 MHz, DMSO-d$_6$) δ_H 8.92 (1H, s, H-7), 8.46 (1H, s, H-2), 8.35 – 8.23 (3H, m, H-4, 5 and 6'), 6.99 (1H, d, *J* = 5.2 Hz, H-5'), 3.97 (3H, s, H-1''), 3.22 (6H, s, H-1'''); ^{13}C NMR (125 MHz, DMSO-d$_6$) δ_C 162.1 (C-2'), 160.9 (C-4'), 157.2 (C-6'), 139.8 (C-5), 135.5 (C-2), 133.9 (C-7a), 130.0 (C-3a), 115.9 (C-4), 112.6 (C-3), 104.1 (C-5), 36.8 (C-1''), 33.3 (C-1'''); HRMS *m/z* (ESI$^+$) [Found 254.1405., $C_{14}H_{16}N_5$ requires [M + H]$^+$ 254.1400]; LCMS (MDAP): Rt = 5.3 min, >95% (Method 3); *m/z* (ESI$^+$) 254.1 [M + H]$^+$.

4-(1,6-Dimethylpyrrolo[2,3-*c*]pyridin-6-ium-3-yl)-*N*,*N*-dimethyl-pyrimidin-2-amine iodide **221**

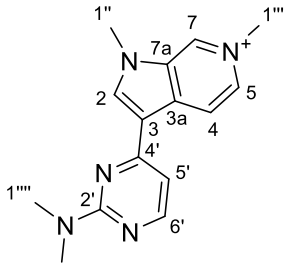

To a solution of *N*,*N*-dimethyl-4-(1*H*-pyrrolo[2,3-*c*]pyridin-3-yl)pyrimidin-2-amine (30 mg, 0.13 mmol) in DMF (2 mL) was added sodium hydride (3 mg, 0.14 mmol) and the mixture stirred in an ice bath for 10 min under nitrogen. Iodomethane (0.01 mL, 0.13 mmol) was added and the reaction mixture stirred at rt for 30 min. The reaction mixture was concentrated under reduced pressure. The crude was purified using flash silica column chromatography on an Isco Combiflash system (12 g silica, elution with 0-50% 20% MeOH in CH_2Cl_2 / CH_2Cl_2 gradient) to afford the title compound, 4-(1,6-dimethylpyrrolo[2,3-*c*]pyridin-6-ium-3-yl)-*N*,*N*-dimethyl-pyrimidin-2-amine iodide, **221**, as an orange solid (40 mg, 0.10 mmol, 77% yield). R_f 0.50 (MeOH / CH_2Cl_2 1:9); Decomposed > 300 °C; $\bar{\nu}_{max}$ (neat)/cm^{-1} 3388, 3039 (C-H, w), 3013 (C-H, w), 2986 (C-H, w), 2964 (C-H, w), 1646 (C=N, m), 1573 (C=C, s); ^{1}H NMR (500 MHz, DMSO-d$_6$) δ_H 9.58 (1H, s, H-7), 9.08 (1H, s, H-2), 8.76 (1H, d, *J* = 6.6 Hz, H-5), 8.45 (1H, d, *J* = 6.6 Hz, H-4), 8.38 (1H, d, *J* = 5.2 Hz, H-6'), 7.08 (1H, d, *J* = 5.2 Hz, H-5'), 4.37 (3H, s, H-1'''), 4.06 (3H, s, H-1''), 3.21 (6H, s, H-1''''); ^{13}C NMR (150 MHz, DMSO-d$_6$) δ_C 159.2 (C-2'), 158.0 (C-4'), 143.4 (C-2), 134.2 (C-4), 133.3 (C-7a), 132.8 (C-7), 131.6 (C-3a), 118.2 (C-5), 114.6 (C-3), 104.4 (C-5'), 47.1 (C-1'''), 37.0 (C-1''''), 34.4 (C-1''); HRMS *m/z* (ESI$^+$) [Found 268.1549., $C_{15}H_{18}N_5$ requires [M + H]$^+$ 268.1557]; LCMS (MDAP): Rt = 0.4 min, >95% (Method 3); *m/z* (ESI$^+$) 268.3 [M + H]$^+$.

1-Imidazo[1,2-*a*]pyrimidin-3-ylethanone **222**

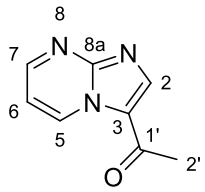

Pyrimidin-2-amine (1 g, 10.52 mmol) was dissolved in toluene (7 mL) and *N*,*N*-dimethylformamide dimethyl acetal (3 mL, 22.58 mmol) was added. The reaction mixture was heated to 90 °C for 2 h. The reaction mixture was concentrated under reduced pressure. The crude was dissolved in EtOH (10 mL) and chloroacetone (1.6 mL, 20.1 mmol) was added to the mixture. The reaction mixture was heated to reflux and stirred overnight. The reaction mixture was concentrated under reduced pressure. The crude was purified using flash silica column chromatography on an Isco Combiflash system (24 g silica, elution with 0-50% 20% MeOH in CH_2Cl_2 / CH_2Cl_2 gradient) to afford 1-imidazo[1,2-*a*]pyrimidin-3-ylethanone, **222**, as a gold solid (800 mg, 4.59 mmol, 44% yield). R_f 0.10 (EtOAc); ^{1}H NMR (600 MHz, DMSO-d_6) δ_H 9.77 (1H, dd, *J* = 6.8, 2.0 Hz, H-5), 8.82 (1H, dd, *J* = 4.2, 2.0 Hz, H-7), 8.77 (1H, s, H-2), 7.38 (1H, dd, *J* = 6.8, 4.2 Hz, H-6), 2.57 (3H, s, H-2'); LCMS (LCQ): Rt = 0.6 min (Method 1); *m/z* (ESI$^+$) 162.2 [M + H]$^+$.

1-Imidazo[1,2-*a*]pyridin-3-ylethanone **223**

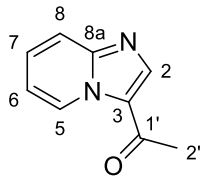

2-Amino pyridine (1 g, 10.63 mmol) was dissolved in toluene (7 mL) and *N*,*N*-dimethylformamide dimethyl acetal (3 mL, 22.58 mmol) was added. The reaction mixture was heated to 90 °C overnight. The reaction mixture was concentrated under reduced pressure. The crude was dissolved in EtOH (10 mL) and chloroacetone (1.6 mL, 20.1 mmol) was added to the mixture. The reaction mixture was heated to reflux and stirred overnight. The reaction mixture was concentrated under reduced pressure. The crude was purified using flash silica column chromatography on an Isco Combiflash system (24 g silica, elution with 0-50% 20% MeOH in CH_2Cl_2 / CH_2Cl_2 gradient) to afford 1-imidazo[1,2-*a*]pyridin-3-ylethanone, **223**, as a gold solid (700 mg, 4.15 mmol, 39% yield). R_f 0.12 (EtOAc); ^{1}H NMR (600 MHz, DMSO-d_6) δ_H 9.54 – 9.49 (1H, m, H-5), 8.61 (1H, s, H-2), 7.85 – 7.79 (1H, m, H-8), 7.65 – 7.59 (1H, m, H-7), 7.29 – 7.23 (1H, m, H-6), 2.56 (3H, s, H-2'); LCMS (LCQ): Rt = 0.7 min (Method 1); *m/z* (ESI$^+$) 161.2 [M + H]$^+$.

1-Imidazo[1,2-*b*]pyridazin-3-ylethanone **224**

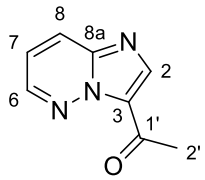

Pyridazin-3-amine (1 g, 10.52 mmol) was dissolved in toluene (7 mL) and *N*,*N*-dimethylformamide dimethyl acetal (3 mL, 22.58 mmol) was added. The reaction mixture was heated to 90 °C overnight. The reaction mixture was concentrated under reduced pressure. The crude was dissolved in EtOH (10 mL) and chloroacetone (1.6 mL, 20.1 mmol) was added to the mixture. The reaction mixture was heated to reflux and stirred overnight. The reaction mixture was concentrated under reduced pressure. The residue was partitioned between EtOAc (100 mL) and water (100 mL) and the organic layer separated. The aqueous layer was extracted further with EtOAc (2 x 100 mL). The combined organics were washed with 1 N NaOH solution (100 mL), water (100 mL), dried over $MgSO_4$, filtered and concentrated under reduced pressure. The crude was purified using flash silica column chromatography on an Isco Combiflash system (12 g silica, elution with 0-100% EtOAc / petroleum ether gradient) to afford the title compound, 1-imidazo[1,2-*b*]pyridazin-3-ylethanone, **224**, as a cream solid (500 mg, 2.79 mmol, 27% yield). R_f 0.17 (EtOAc); ^{1}H NMR (600 MHz, DMSO-d_6) δ_H 8.77 (1H, dd, *J* = 4.4, 1.6 Hz, H-6), 8.55 (1H, s, H-2), 8.32 (1H, dd, *J* = 9.2, 1.6 Hz, H-8), 7.50 (1H, dd, *J* = 9.2, 4.4 Hz, H-7), 2.65 (3H, s, H-2'); LCMS (LCQ): Rt = 0.5 min (Method 1); *m/z* (ESI$^+$) 162.2 [M + H]$^+$.

(*E*)-3-(Dimethylamino)-1-imidazo[1,2-*a*]pyrimidin-3-yl-prop-2-en-1-one **225**

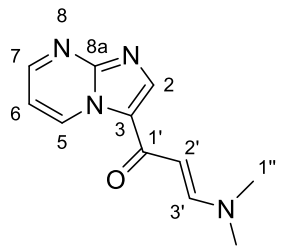

To 1-imidazo[1,2-*a*]pyrimidin-3-ylethanone (100 mg, 0.62 mmol) was added *N*,*N*-dimethylformamide dimethyl acetal (4 mL, 30.11 mmol). The reaction mixture was heated to 75 °C for 16 h. The reaction mixture was concentrated under reduced pressure to afford the title compound, (*E*)-3-(dimethylamino)-1-imidazo[1,2-*a*]pyrimidin-3-yl-prop-2-en-1-one, **225**, as a red solid (150 mg, 0.62 mmol, 99% yield) plus impurities. R_f 0.23 (MeOH / CH_2Cl_2 5:95); ^{1}H NMR (600 MHz, $CDCl_3$) δ_H 10.06 (1H, dd, *J* = 6.9, 2.1 Hz, H-5), 8.67 (1H, dd, *J* = 4.1, 2.1 Hz, H-7), 8.36 (1H, s, H-2), 7.80 (1H, d, *J* = 12.3 Hz, H-3'), 7.04 (1H, dd, *J* = 6.9, 4.1 Hz, H-6), 5.67 (1H, d, *J* = 12.3 Hz, H-2'), 3.19 (3H, s, H-1''), 2.97 (3H, s, H-1''); LCMS (LCQ): Rt = 0.6 min (Method 1); *m/z* (ESI$^+$) 217.2 [M + H]$^+$.

(*E*)-3-(Dimethylamino)-1-imidazo[1,2-*a*]pyridin-3-yl-prop-2-en-1-one **226**

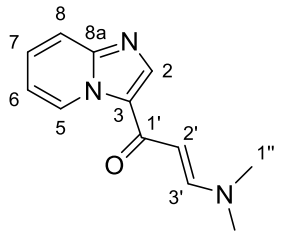

To 1-imidazo[1,2-*a*]pyridin-3-ylethanone (100 mg, 0.62 mmol) was added *N*,*N*-dimethylformamide dimethyl acetal (4 mL, 30.11 mmol). The reaction mixture was heated to 75 °C for 16 h. The reaction mixture was concentrated under reduced pressure to afford the title compound, (*E*)-3-(dimethylamino)-1-imidazo[1,2-*a*]pyridin-3-yl-prop-2-en-1-one, **226**, as a red solid (150 mg, 0.63 mmol, 99% yield) plus impurities. R_f 0.44 (MeOH / CH_2Cl_2 5:95); ^{1}H NMR (600 MHz, $CDCl_3$) δ_H 9.81 (1H, d, *J* = 7.0 Hz, H-5), 8.22 (1H, s, H-2), 7.78 (1H, d, *J* = 12.3 Hz, H-3'), 7.69 (1H, d, *J* = 9.0 Hz, H-8), 7.40 – 7.33 (1H, m, H-7), 7.03 – 6.92 (1H, m, H-6), 5.69 (1H, d, *J* = 12.3 Hz, H-2'), 3.27 – 2.74 (6H, m, 1''); LCMS (LCQ): Rt = 0.5 min (Method 1); *m/z* (ESI$^+$) 216.2 [M + H]$^+$.

(*E*)-3-(Dimethylamino)-1-imidazo[1,2-*b*]pyridazin-3-yl-prop-2-en-1-one **227**

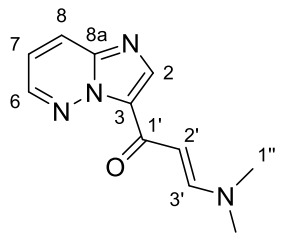

To 1-imidazo[1,2-*b*]pyridazin-3-ylethanone (100 mg, 0.62 mmol) was added *N*,*N*-dimethylformamide dimethyl acetal (4 mL, 30.11 mmol). The reaction mixture was heated to 75 °C for 16 h. The reaction mixture was concentrated under reduced pressure to afford the title compound, (E)-3-(dimethylamino)-1-imidazo[1,2-*b*]pyridazin-3-yl-prop-2-en-1-one, **227**, as a red solid (100 mg, 0.23 mmol, 37% yield) plus impurities. R_f 0.23 (MeOH / CH_2Cl_2 5:95); ^{1}H NMR (600 MHz, $CDCl_3$) δ_H 8.53 – 8.49 (1H, m, H-6), 8.38 (1H, s, H-2), 8.05 – 8.00 (1H, m, H-8), 7.93 (1H, d, *J* = 12.4 Hz, H-3'), 7.14 (1H, dd, *J* = 9.1, 4.4 Hz, H-7), 6.21 (1H, d, *J* = 12.5 Hz, H-2'), 3.18 (3H, s, H-1''), 2.97 (3H, s, H-1''); LCMS (LCQ): Rt = 0.6 min (Method 1); *m/z* (ESI$^+$) 217.1 [M + H]$^+$.

4-Imidazo[1,2-*a*]pyrimidin-3-yl-*N*,*N*-dimethyl-pyrimidin-2-amine **228**

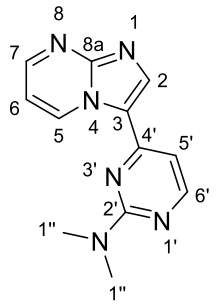

To a solution of (*E*)-3-(dimethylamino)-1-imidazo[1,2-*a*]pyrimidin-3-yl-prop-2-en-1-one (100 mg, 0.46 mmol) in 2-methoxyethanol (35 mg, 0.46 mmol) was added 1,1-dimethylguanidine sulfate salt (190 mg, 0.70 mmol) and potassium carbonate (133 mg, 0.96 mmol). The reaction mixture was heated to 125 °C overnight. The reaction mixture was concentrated under reduced pressure. The residue was partitioned between EtOAc (50 mL) and water (50 mL) and the organic layer separated. The aqueous layer was extracted with further EtOAc (2 x 50 mL). The combined organics were dried over $MgSO_4$, filtered and concentrated to dryness under reduced pressure. The crude was purified using flash silica column chromatography on an Isco Combiflash system (12 g silica, elution with 0-50% 20% MeOH in CH_2Cl_2 / CH_2Cl_2 gradient) to afford the title compound, 4-imidazo[1,2-*a*]pyrimidin-3-yl-*N*,*N*-dimethyl-pyrimidin-2-amine, **228**, as a pale yellow solid (21 mg, 0.08 mmol, 18% yield). R_f 0.63 (EtOAc); m.p. 237-239 °C; $\bar{\nu}_{max}$ (neat)/cm^{-1} 3110 (C-H, w), 3002 (C-H, w), 2931 (C-H, w), 1657 (C=N, m), 1564 (C=C, s); ^{1}H NMR (600 MHz, DMSO-d$_6$) δ_H 10.14 (1H, dd, *J* = 7.0, 2.0 Hz, H-5), 8.71 – 8.66 (2H, m, H-2 and 7), 8.36 (1H, d, *J* = 5.2 Hz, H-6'), 7.33 (1H, dd, *J* = 7.0, 4.1 Hz, H-6), 7.19 (1H, d, *J* = 5.2 Hz, H-5'), 3.21 (6H, s, H-1''); ^{13}C NMR (150 MHz, DMSO-d$_6$) δ_C 161.5 (C-2'), 157.9 (C-6'), 156.3 (C-4), 151.4 (C-7), 150.2 (C-8a), 138.8 (C-2), 136.5 (C-5), 120.2 (C-3), 110.3 (C-6), 104.0 (C-5'), 37.2 (C-1''); HRMS *m/z* (ESI$^+$) [Found 263.1012., $C_{12}H_{12}N_6Na$ requires [M + Na]$^+$ 263.1016]; LCMS (MDAP): Rt = 10.1 min, >95% (Method 3); *m/z* (ESI$^+$) 241.7 [M + H]$^+$.

4-Imidazo[1,2-*a*]pyridin-3-yl-*N*,*N*-dimethyl-pyrimidin-2-amine **229**

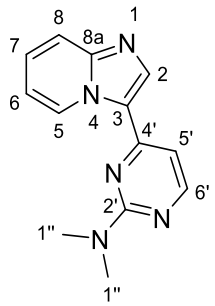

To a solution of (*E*)-3-(dimethylamino)-1-imidazo[1,2-*a*]pyridin-3-yl-prop-2-en-1-one (100 mg, 0.46 mmol) in 2-methoxyethanol (30 mL) was added 1,1-dimethylguanidine sulfate salt (191 mg, 0.70 mmol) and potassium carbonate (134 mg, 0.97 mmol). The reaction was heated to 125 °C overnight. The reaction mixture was concentrated under reduced pressure. The residue was partitioned between EtOAc (50 mL) and water (50 mL) and the organic layer separated. The aqueous layer was extracted with further EtOAc (2 x 50 mL). The combined organics were dried over $MgSO_4$, filtered and concentrated to dryness under reduced pressure. The crude was purified using flash silica column chromatography on an Isco Combiflash system (12 g silica, elution with 0-100% EtOAc / petroleum ether gradient), trituration with petroleum ether afforded the title compound, 4-imidazo[1,2-*a*]pyridin-3-yl-*N*,*N*-dimethyl-pyrimidin-2-amine, **229**, as a yellow solid (30 mg, 0.12 mmol, 26% yield). R_f 0.29 (EtOAc/ petroleum ether 1:1); m.p. 135-137 °C; $\bar{\nu}_{max}$ (neat)/cm^{-1} 3112 (C-H, w), 2925 (C-H, w), 2859 (C-H, w), 1569 (C=C, s), 1558 (C=C, s); ^{1}H NMR (600 MHz, DMSO-d$_6$) δ_H 9.93 – 9.89 (1H, m, H-5), 8.52 (1H, s, H-2), 8.32 (1H, d, *J* = 5.3 Hz, H-6'), 7.76 – 7.72 (1H, m, H-8), 7.48 – 7.44 (1H, m, H-7), 7.21 – 7.16 (1H, m, H-6), 7.15 (1H, d, *J* = 5.3 Hz, H-5'), 3.21 (6H, s, H-1''); ^{13}C NMR (150 MHz, DMSO-d$_6$) δ_C 161.5 (C-2'), 157.4 (C-6'), 156.6 (C-4'), 147.7 (C-8a), 138.0 (C-2), 128.4 (C-5), 126.7 (C-7), 121.6 (C-3), 117.4 (C-8), 113.9 (C-6), 104.1 (C-5'), 37.1 (C-1''); HRMS *m/z* (ESI$^+$) [Found 240.1240., $C_{13}H_{14}N_5$ requires [M + H]$^+$ 240.1244]; LCMS (MDAP): Rt = 10.6 min, >95% (Method 3); *m/z* (ESI$^+$) 240.9 [M + H]$^+$.

4-Imidazo[1,2-*b*]pyridazin-3-yl-*N*,*N*-dimethyl-pyrimidin-2-amine **230**

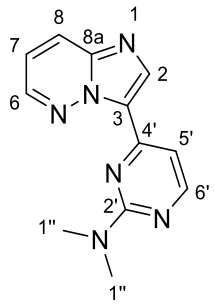

To a solution of (*E*)-3-(dimethylamino)-1-imidazo[1,2-*b*]pyridazin-3-yl-prop-2-en-1-one (100 mg, 0.46 mmol) in 2-methoxyethanol (30 mL) was added 1,1-dimethylguanidine sulfate salt (190 mg, 0.70 mmol) and potassium carbonate (133 mg, 0.96 mmol). The reaction was heated to 125 °C overnight. The reaction mixture was concentrated under reduced pressure. The residue was partitioned between EtOAc (50 mL) and water (50 mL) and the organic layer separated. The aqueous layer was extracted with further EtOAc (2 x 50 mL). The combined organics were dried over $MgSO_4$, filtered and concentrated to dryness under reduced pressure. The crude was purified using flash silica column chromatography on an Isco Combiflash system (12 g silica, elution with 0-100% EtOAc / petroleum ether gradient) to afford the title compound, 4-imidazo[1,2-*b*]pyridazin-3-yl-*N*,*N*-dimethyl-pyrimidin-2-amine, **230**, as a white solid (50 mg, 0.20 mmol, 43% yield). R_f 0.50 (EtOAc); m.p. 159-161 °C; ^{1}H NMR (600 MHz, DMSO-d_6) δ_H 8.75 (1H, d, *J* = 4.4 Hz, H-6), 8.58 (1H, s, H-2), 8.49 (1H, d, *J* = 5.1 Hz, H-6'), 8.29 (1H, d, *J* = 9.2 Hz, H-8), 7.75 (1H, d, *J* = 5.1 Hz, H-5'), 7.40 (1H, dd, *J* = 9.2, 4.4 Hz, H-7), 3.19 (6H, s, H-1''); ^{13}C NMR (150 MHz, DMSO-d_6) δ_C 161.6 (C-2'), 158.9 (C-6'), 153.9 (C-4'), 144.4 (C-6), 141.6 (C-8a), 136.7 (C-2), 126.33 (C-8), 126.26 (C-3), 118.4 (C-7), 104.4 (C-5'), 36.5 (C-1''); HRMS *m/z* (ESI$^+$) [Found 241.1192., $C_{12}H_{13}N_6$ requires [M + H]$^+$ 241.1196]; LCMS (MDAP): Rt = 12.4 min, >95% (Method 3); *m/z* (ESI$^+$) 241.9 [M + H]$^+$.

4-Imidazo[1,2-*a*]pyrimidin-2-yl-*N*,*N*-dimethyl-pyrimidin-2-amine **231**

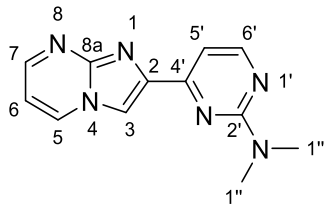

To a solution of (*E*)-3-(dimethylamino)-1-imidazo[1,2-*a*]pyrimidin-3-yl-prop-2-en-1-one (100 mg, 0.46 mmol) in 2-methoxyethanol (30 mL) was added 1,1-dimethylguanidine sulfate salt (190 mg, 0.70 mmol) and potassium carbonate (133 mg, 0.96 mmol). The reaction was heated to 125 °C overnight. The reaction mixture was concentrated under reduced pressure. The residue was partitioned between EtOAc (50 mL) and water (50 mL) and the organic layer separated. The aqueous layer was extracted with further EtOAc (2 x 50 mL). The combined organics were dried over $MgSO_4$, filtered and concentrated to dryness under reduced pressure. The crude was purified using flash silica column chromatography on an Isco Combiflash system (12 g silica, elution with 0-50% 20% MeOH in CH_2Cl_2 / CH_2Cl_2 gradient). Desired fractions were combined and concentrated under reduced pressure. The crude was purified using flash silica column chromatography on an Isco Combiflash system (12 g silica, elution with 0-100% acetone / petroleum ether gradient), trituration with petroleum ether afforded the title compound, 4-imidazo[1,2-*a*]pyrimidin-2-yl-*N*,*N*-dimethyl-pyrimidin-2-amine, **231**, as a cream solid (40 mg, 0.16 mmol, 34% yield). R_f 0.83 (acetone); m.p. 208-210 °C; $\bar{\nu}_{max}$ (neat)/cm^{-1} 3145 (C-H, w), 3058 (C-H, w), 2997 (C-H, w), 1622 (C=N, m), 1576 (C=C, s); ^{1}H NMR (600 MHz, DMSO-d$_6$) δ_H 9.00 (1H, dd, *J* = 6.6, 2.0 Hz, H-5), 8.59 (1H, dd, *J* = 4.0, 2.0 Hz, H-7), 8.55 (1H, s, H-3), 8.45 (1H, d, *J* = 4.9 Hz, H-6'), 7.26 (1H, d, *J* = 4.9 Hz, H-5'), 7.12 – 7.09 (1H, m, H-6), 3.19 (6H, s, H-1''); ^{13}C NMR (150 MHz, DMSO-d$_6$) δ_C 161.9 (C-2'), 159.3 (C-4'), 158.8 (C-6'), 151.5 (C-7), 147.8 (C-8a), 143.9 (C-2), 135.7 (C-5), 111.4 (C-3), 109.4 (C-6), 104.9 (C-5'), 36.5 (C-1''); HRMS *m/z* (ESI$^+$) [Found 263.1012., $C_{12}H_{12}N_6Na$ requires [M + Na]$^+$ 263.1016]; LCMS (MDAP): Rt = 10.7 min, >95% (Method 3); *m/z* (ESI$^+$) 241.7 [M + H]$^+$.

4-(1-Isopropylpyrazol-3-yl)-*N*,*N*-dimethyl-pyrimidin-2-amine **232**

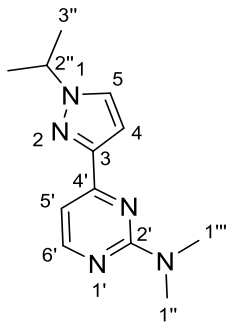

To a solution of 4-chloro-*N*,*N*-dimethyl-pyrimidin-2-amine (70 mg, 0.44 mmol) in 1,4-dioxane (2 mL) was added bis[2-(di-*tert*-butylphosphanyl)cyclopenta-2,4-dien-1-yl]iron; dichloropalladium (20 mg, 0.03 mmol), 1-isopropyl-1*H*-pyrazole-4-boronic acid pinacol ester (105 mg, 0.44 mmol) and 2 M potassium carbonate (0.4 mL, 0.80 mmol). The reaction mixture was heated to 80 °C for 16 h. The reaction mixture was concentrated under reduced pressure. The crude was purified using flash silica column chromatography on an Isco Combiflash system (12 g silica, elution with 0-100% EtOAc / petroleum ether gradient) to afford the title compound, 4-(1-isopropylpyrazol-3-yl)-*N*,*N*-dimethyl-pyrimidin-2-amine, **232**, as a colourless oil (26 mg, 0.11 mmol, 24% yield). R_f 0.50 (EtOAc/ petroleum ether 1:1); $\bar{\nu}_{max}$ (neat)/cm^{-1} 2978 (C-H, w), 2934 (C-H, w), 2864 (C-H, w), 1568 (C=C, m), 1534 (C=C, s); ^{1}H NMR (600 MHz, DMSO-d$_6$) δ_H 8.39 (1H, app. s, H-4 or 5), 8.24 (1H, d, *J* = 5.2 Hz, H-6'), 8.03 (1H, app. s, H-4 or 5), 6.82 (1H, d, *J* = 5.2 Hz, H-5'), 4.54 (1H, hept, *J* = 6.6 Hz, H-2''), 3.14 (6H, s, H-1'''), 1.44 (6H, d, *J* = 6.7 Hz, H-3''); ^{13}C NMR (150 MHz, DMSO-d$_6$) δ_C 161.9 (C-2'), 158.7 (C-4'), 157.7 (C-6'), 137.5 (C-5 or C-4), 127.7 C-4 or C-5), 121.0 (C-3), 104.3 (C-5'), 53.4 (C-2''), 36.5 (C-1'''), 22.6 (C-3''); HRMS *m/z* (ESI$^+$) [Found 232.1556., $C_{12}H_{18}N_5$ requires [M + H]$^+$ 232.1557]; LCMS (MDAP): Rt = 4.1 min, >95% (Method 3); *m/z* (ESI$^+$) 232.0 [M + H]$^+$.

5-[2-(Dimethylamino)pyrimidin-4-yl]-1-methyl-pyridin-2-one **233**

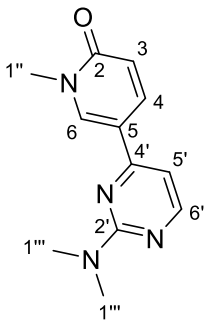

To a solution of 4-chloro-*N*,*N*-dimethyl-pyrimidin-2-amine (70 mg, 0.44 mmol) in 1,4-dioxane (2 mL) was added bis[2-(di-*tert*-butylphosphanyl)cyclopenta-2,4-dien-1-yl]iron; dichloropalladium (20 mg, 0.03 mmol), and 2 M potassium carbonate (0.4 mL, 0.80 mmol). The reaction mixture was heated to 80 °C for 16 h. The reaction mixture was concentrated under reduced pressure. The crude was purified using flash silica column chromatography on an Isco Combiflash system (12 g silica, elution with 0-100% EtOAc / petroleum ether gradient) to afford the title compound, 5-[2-(dimethylamino)pyrimidin-4-yl]-1-methyl-pyridin-2-one, **233**, as a pale yellow solid (48 mg, 0.2 mmol, 45% yield). R_f 0.17 (EtOAc/ petroleum ether 1:1); m.p. 140-142 °C; $\bar{\nu}_{max}$ (neat)/cm^{-1} 3071 (C-H, w), 2939 (C-H, w), 1655 (C=O, s), 1622 (C=N, m), 1573 (C=C, s); ^{1}H NMR (600 MHz, MeOD) δ_H 8.56 (1H, d, *J* = 2.5 Hz, H-6), 8.30 – 8.24 (2H, m, H-6' and 4), 6.93 (1H, d, *J* = 5.3 Hz, H-5'), 6.63 (1H, d, *J* = 9.5 Hz, H-3), 3.68 (3H, s, H-1''), 3.23 (6H, s, H-1'''); ^{13}C NMR (150 MHz, MeOD) δ_C 165.2 (C=O), 163.3 (C-2'), 161.9 (C-4'), 159.2 (C-6'), 141.0 (C-6), 139.8 (C-4), 119.7 (C-3), 119.1 (C-5), 103.9 (C-5'), 38.6 (C-1''), 37.4 (C-1'''); HRMS *m/z* (ESI$^+$) [Found 253.1059., $C_{12}H_{14}N_4NaO$ requires [M + Na]$^+$ 253.1060]; LCMS (MDAP): Rt = 3.7 min, >95% (Method 3); *m/z* (ESI$^+$) 230.9 [M + H]$^+$.

5-[2-(Dimethylamino)pyrimidin-4-yl]indolin-2-one **234**

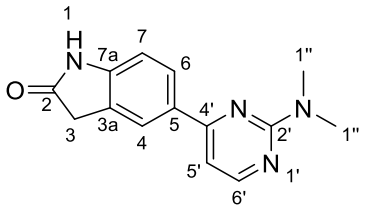

To a solution of 4-chloro-*N*,*N*-dimethyl-pyrimidin-2-amine (70 mg, 0.44 mmol) in 1,4-dioxane (2 mL) was added bis[2-(di-*tert*-butylphosphanyl)cyclopenta-2,4-dien-1-yl]iron; dichloropalladium (20 mg, 0.03 mmol), 5-(4,4,5,5-tetramethyl-1,3,2-dioxaborolan-2-yl)-1,3-dihydro-2*H*-indol-2-one (115 mg, 0.44 mmol) and 2 M potassium carbonate (0.4 mL, 0.80 mmol). The reaction mixture was heated to 80 °C for 16 h. The reaction mixture was concentrated under reduced pressure. The crude was purified using flash silica column chromatography on an Isco Combiflash system (12 g silica, elution with 0-100% EtOAc / petroleum ether gradient) to afford the title compound, 5-[2-(dimethylamino)pyrimidin-4-yl]indolin-2-one, **234**, as a pale yellow solid (18 mg, 0.07 mmol, 15% yield). R_f 0.57 (EtOAc); m.p. 196-198 °C; ^{1}H NMR (600 MHz, DMSO-d_6) δ_H 10.59 (1H, s, N-H), 8.33 (1H, d, *J* = 5.2 Hz, H-6'), 8.04 – 7.98 (2H, m, H-4 and 6), 7.07 (1H, d, *J* = 5.2 Hz, H-5'), 6.91 (1H, d, *J* = 8.0 Hz, H-7), 3.56 (2H, s, H-3), 3.18 (6H, s, H-1''); ^{13}C NMR (150 MHz, DMSO-d_6) δ_C 176.6 (C=O), 162.9 (C-4'), 161.9 (C-2'), 158.3 (C-6'), 146.1 (C-3a), 130.2 (C-5), 126.8 (C-6), 126.3 (C-7a), 122.8 (C-4), 109.1 (C-7), 103.8 (C-5'), 36.6 (C-1''), 35.8 (C-3); HRMS *m/z* (ESI$^+$) [Found 255.1238., $C_{14}H_{15}N_4O$ requires [M + H]$^+$ 255.1240]; LCMS (MDAP): Rt = 3.9 min, >95% (Method 3); *m/z* (ESI$^+$) 256.0 [M + H]$^+$.

4-(2-Methoxythiazol-5-yl)-*N*,*N*-dimethyl-pyrimidin-2-amine **235**

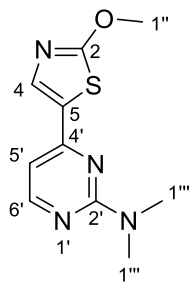

To a solution of 4-chloro-*N*,*N*-dimethyl-pyrimidin-2-amine (70 mg, 0.44 mmol) in 1,4-dioxane (2 mL) was added bis[2-(di-*tert*-butylphosphanyl)cyclopenta-2,4-dien-1-yl]iron; dichloropalladium (20 mg, 0.03 mmol), 2-methoxy-5-(tetramethyl-1,3,2-dioxaborolan-2-yl)-1,3-thiazole (107 mg, 0.44 mmol) and 2 M potassium carbonate (0.4 mL, 0.80 mmol). The reaction mixture was heated to 80 °C for 16 h. The reaction mixture was concentrated under reduced pressure. The crude was purified using flash silica column chromatography on an Isco Combiflash system (12 g silica, elution with 0-100% EtOAc / petroleum ether gradient) to afford the title compound, 4-(2-methoxythiazol-5-yl)-*N*,*N*-dimethyl-pyrimidin-2-amine, **235**, as a colourless solid (48 mg, 0.19 mmol, 44% yield). R_f 0.57 (EtOAc/ petroleum ether 1:1); m.p. 106-108 °C; $\bar{\nu}_{max}$ (neat)/cm^{-1} 2949 (C-H, w), 2871 (C-H, w), 1571 (C=C, s); ^{1}H NMR (600 MHz, MeOD) δ_H 8.23 (1H, d, *J* = 5.3 Hz, H-6'), 7.87 (1H, s, H-4), 6.91 (1H, d, *J* = 5.3 Hz, H-5'), 4.12 (3H, s, H-1''), 3.18 (6H, s, CH-1'''); ^{13}C NMR (150 MHz, MeOD) δ_C 178.9 (C-2), 163.1 (C-2'), 159.5 (C-4'), 158.6 (C-6'), 138.5 (C-4), 133.0 (C-5), 103.8 (C-5'), 59.4 (C-1''), 37.2 (C-1'''); LCMS (MDAP): Rt = 8.7 min, >95% (Method 3); *m/z* (ESI$^+$) 237.9 [M + H]$^+$.

N,*N*-Dimethyl-4-[3-(trifluoromethyl)-1*H*-pyrazol-4-yl]pyrimidin-2-amine **236**

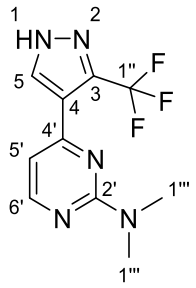

To a solution of 4-chloro-*N*,*N*-dimethyl-pyrimidin-2-amine (70 mg, 0.44 mmol) in 1,4-dioxane (2 mL) was added bis[2-(di-*tert*-butylphosphanyl)cyclopenta-2,4-dien-1-yl]iron; dichloropalladium (20 mg, 0.03 mmol), 4-(tetramethyl-1,3,2-dioxaborolan-2-yl)-3-(trifluoromethyl)-1*H*-pyrazole (116 mg, 0.44 mmol) and 2 M potassium carbonate (0.4 mL, 0.80 mmol). The reaction mixture was heated to 80 °C for 16 h. The reaction mixture was concentrated under reduced pressure. The crude was purified using flash silica column chromatography on an Isco Combiflash system (12 g silica, elution with 0-100% EtOAc / petroleum ether gradient) to afford the title compound, *N*,*N*-dimethyl-4-[3-(trifluoromethyl)-1*H*-pyrazol-4-yl]pyrimidin-2-amine, **236**, as a white solid (31 mg, 0.12 mmol, 26% yield). R_f 0.50 (EtOAc/ petroleum ether 1:1); m.p. 201-203 °C; $\bar{\nu}_{max}$ (neat)/cm^{-1} 3132 (N-H, w), 2863 (C-H, w), 1579 (C=C, s), 1523 (C=C, m); ^{1}H NMR (600 MHz, DMSO-d$_6$) δ_H 13.88 (1H, s, NH), 8.65 (1H, s, H-5), 8.33 (1H, d, *J* = 5.1 Hz, H-6'), 6.88 (1H, d, *J* = 5.1 Hz, H-5'), 3.13 (6H, s, H-1'''); ^{13}C NMR (150 MHz, DMSO-d$_6$) δ_C 161.8 (C-2'), 158.1 (C-6'), 157.3 (C-4'), 138.2 (C-3)*, 132.6 (C-5), 123.9-119.8 (m, CF_3-1''), 119.0 (C-4)*, 105.6 (C-5'), 36.4 (C-1'''). * assigned with HMBC; LCMS (MDAP): Rt = 7.2 min, >95% (Method 3); *m/z* (ESI$^+$) 258.0 [M + H]$^+$.

4-(2-Cyclopropylpyrimidin-5-yl)-*N*,*N*-dimethyl-pyrimidin-2-amine **237**

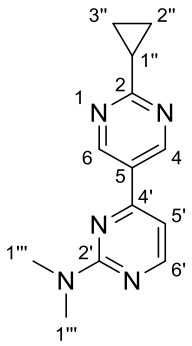

To a solution of 4-chloro-*N*,*N*-dimethyl-pyrimidin-2-amine (70 mg, 0.44 mmol) in 1,4-dioxane (2 mL) was added bis[2-(di-*tert*-butylphosphanyl)cyclopenta-2,4-dien-1-yl]iron; dichloropalladium (20 mg, 0.03 mmol), (2-cyclopropylpyrimidin-5-yl)boronic acid (87 mg, 0.53 mmol) and 2 M potassium carbonate (0.4 mL, 0.80 mmol). The reaction mixture was heated to 80 °C for 16 h. The reaction mixture was concentrated under reduced pressure. The crude was purified using flash silica column chromatography on an Isco Combiflash system (12 g silica, elution with 0-100% EtOAc / petroleum ether gradient) to afford the title compound, 4-(2-cyclopropylpyrimidin-5-yl)-*N*,*N*-dimethyl-pyrimidin-2-amine, **237**, as a pale yellow solid (38 mg, 0.15 mmol, 34% yield). R_f 0.55 (EtOAc/ petroleum ether 1:1); m.p. 112-114 °C; $\bar{\nu}_{max}$ (neat)/cm^{-1} 3004 (C-H, w), 2932 (C-H, w), 2868 (C-H, w), 1577 (C=C, m), 1557 (C=C, s); ^{1}H NMR (600 MHz, DMSO-d$_6$) δ_H 9.28 (2H, s, H-6 and 4), 8.45 (1H, d, *J* = 5.1 Hz, H-6'), 7.23 (1H, d, *J* = 5.1 Hz, H-5'), 3.18 (6H, s, H-1'''), 2.28 (1H, tt, *J* = 8.2, 4.7 Hz, H-1''), 1.14 – 1.04 (4H, m, H-2'' and 4''); ^{13}C NMR (150 MHz, DMSO-d$_6$) δ_C 172.7 (C-2), 161.8 (C-2'), 159.1 (C-6'), 159.0 (C-4'), 155.3 (C-6 and C-4), 127.1 (C-5), 104.4 (C-5'), 36.6 (C-1'''), 18.1 (C-1''), 11.1 (C-2'' and C-3''); HRMS *m/z* (ESI$^+$) [Found 242.1400., $C_{13}H_{16}N_5$ requires [M + H]$^+$ 242.1400]; LCMS (MDAP): Rt = 13.1 min, >95% (Method 3); *m/z* (ESI$^+$) 242.0 [M + H]$^+$.

4-(2,4-Dimethoxypyrimidin-5-yl)-*N*,*N*-dimethyl-pyrimidin-2-amine **238**

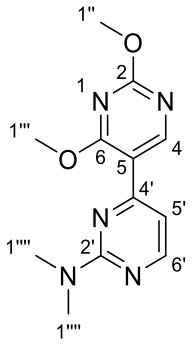

To a solution of 4-chloro-*N*,*N*-dimethyl-pyrimidin-2-amine (70 mg, 0.44 mmol) in 1,4-dioxane (2 mL) was added 2,4-dimethoxy-5-pyrimidinylboronic acid (100 mg, 0.54 mmol), 2 M potassium carbonate (0.4 mL, 0.80 mmol) and bis[2-(di-*tert*-butylphosphanyl)cyclopenta-2,4-dien-1-yl]iron; dichloropalladium (20 mg, 0.03 mmol). The reaction mixture was heated to 80 °C for 16 h. The reaction mixture was concentrated under reduced pressure. The crude was purified using flash silica column chromatography on an Isco Combiflash system (12 g silica, elution with 0-100% EtOAc / petroleum ether gradient) to afford the title compound, 4-(2,4-dimethoxypyrimidin-5-yl)-*N*,*N*-dimethyl-pyrimidin-2-amine, **238**, as a white solid (61 mg, 0.22 mmol, 50% yield). R_f 0.53 (EtOAc/ petroleum ether 1:1); m.p. 120-122 °C; $\bar{\nu}_{max}$ (neat)/cm^{-1} 3018 (C-H, w), 2932 (C-H, w), 2898 (C-H, w), 1689 (C=N, m), 1564 (C=C, s); ^{1}H NMR (600 MHz, MeOD) δ_H 9.13 (1H, s, H-4), 8.31 (1H, d, *J* = 5.3 Hz, H-6'), 7.21 (1H, d, *J* = 5.3 Hz, H-5'), 4.15 (3H, s, H-1''), 4.07 (3H, s, H-1'''), 3.22 (6H, s, H-1''''); ^{13}C NMR (150 MHz, MeOD) δ_C 170.5 (C-2), 167.0 (C-6), 163.1 (C-2'), 161.2 (C-4), 160.0 (C-4'), 159.0 (C-6'), 113.4 (C-5), 109.2 (C-5'), 55.8 (C-1'''), 55.0 (C-1''), 37.4 (C-1''''); HRMS *m/z* (ESI$^+$) [Found 284.1117., $C_{12}H_{15}N_5NaO_2$ requires [M + H]$^+$ 284.1118]; LCMS (MDAP): Rt = 8.9 min, >95% (Method 3); *m/z* (ESI$^+$) 261.9 [M + H]$^+$.

4-(1,3-Benzodioxol-5-yl)-*N*,*N*-dimethyl-pyrimidin-2-amine **239**

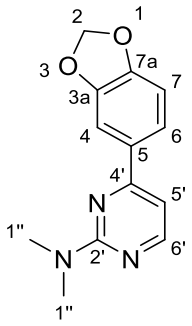

To a solution of 4-chloro-*N*,*N*-dimethyl-pyrimidin-2-amine (80 mg, 0.50 mmol) in 1,4-dioxane (2 mL) was added (2*H*-1,3-benzodioxol-5-yl)boronic acid (70 mg, 0.42 mmol), 2 M potassium carbonate (0.4mL, 0.80 mmol) and bis[2-(di-*tert*-butylphosphanyl)cyclopenta-2,4-dien-1-yl]iron; dichloropalladium (20 mg, 0.03 mmol). The reaction mixture was heated to 80 °C overnight. The reaction mixture was concentrated under reduced pressure. The crude was purified using flash silica column chromatography on an Isco Combiflash system (12 g silica, elution with 0-100% EtOAc / petroleum ether gradient), trituration with petroleum ether furnished the title compound, 4-(1,3-benzodioxol-5-yl)-*N*,*N*-dimethyl-pyrimidin-2-amine, **239**, as a peach solid (102 mg, 0.40 mmol, 94% yield). R_f 0.30 (EtOAc/ petroleum ether 1:1); m.p. 152-154 °C; $\bar{\nu}_{max}$ (neat)/cm^{-1} 2937 (C-H, w), 2902 (C-H, w), 2861 (C-H, w), 1576 (C=C, s); ^{1}H NMR (600 MHz, MeOD) δ_H 8.28 (1H, d, *J* = 5.3 Hz, H-6'), 7.70 (1H, dd, *J* = 8.0, 1.7 Hz, H-6), 7.67 (1H, d, *J* = 1.7 Hz, H-4), 7.00 (1H, d, *J* = 5.3 Hz, H-5'), 6.93 (1H, d, *J* = 8.0 Hz, H-7), 6.04 (2H, s, H-2), 3.25 (6H, s, H-1''); HRMS *m/z* (ESI$^+$) [Found 244.1080., $C_{13}H_{14}N_3O_2$ requires [M + H]$^+$ 244.1081]; LCMS (MDAP): Rt = 8.9 min, >95% (Method 3); *m/z* (ESI$^+$) 243.9 [M + H]$^+$.

1-(5-Fluoro-4-pyrazolo[1,5-*b*]pyridazin-3-yl-pyrimidin-2-yl)-6-oxa-1-azaspiro[3.3]heptane **240**

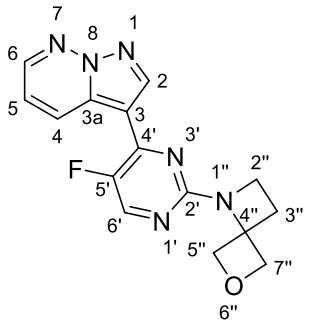

To 3-(2-chloro-5-fluoro-pyrimidin-4-yl)pyrazolo[1,5-*b*]pyridazine (80 mg, 0.32 mmol) in 2-propanol (2.5 mL)was added 6-oxa-1-azaspiro[3.3]heptane (64 mg, 0.64 mmol). The vial was sealed and heated to 120 °C for 16 h. The reaction mixture was concentrated under reduced pressure. The crude was purified using flash silica column chromatography on an Isco Combiflash system (12 g silica, elution with 0-100% EtOAc / petroleum ether gradient), trituration with petroleum ether afforded the title compound, 1-(5-fluoro-4-pyrazolo[1,5-*b*]pyridazin-3-yl-pyrimidin-2-yl)-6-oxa-1-azaspiro[3.3]heptane, **240**, as a cream solid (45 mg, 0.14 mmol, 43% yield). R_f 0.53 (EtOAc); m.p. 271-273 °C; $\bar{\nu}_{max}$ (neat)/cm^{-1} 3096 (C-H, w), 3046 (C-H, w), 2952 (C-H, w), 2936 (C-H, w), 2870 (C-H, w), 1623 (C=N, m), 1573 (C=C, s); ^{1}H NMR (600 MHz, $CDCl_3$) δ_H 9.45 (1H, s, H-4), 8.74 (1H, d, *J* = 3.2 Hz, H-2), 8.43 (1H, dd, *J* = 4.4, 1.9 Hz, H-6), 8.30 (1H, d, *J* = 3.2 Hz, H-6'), 7.24 (1H, dd, *J* = 9.1, 4.4 Hz, H-5), 5.59 (2H, d, *J* = 7.1 Hz, H-7'' and 5''), 4.80 (2H, d, *J* = 7.1 Hz, H-7'' and 5''), 4.02 (2H, t, *J* = 7.1 Hz, H-2''), 2.66 (2H, t, *J* = 7.1 Hz, H-3''); ^{13}C NMR (150 MHz, $CDCl_3$) δ_C 157.4 (C-2'), 149.6 (d, *J* = 251.3 Hz, C-5'), 147.92 (d, *J* = 11.0 Hz, C-4'), 145.88 (d, *J* = 24.3 Hz, C-6'), 143.4 (C-6), 142.12 (d, *J* = 17.9 Hz, C-2), 133.9 (C-3a), 130.4 (C-4), 118.7 (C-5), 106.43 (d, *J* = 5.8 Hz, C-3), 81.3 (C-5'' and C-7''), 45.9 (C-2''), 28.6 (C-3''); HRMS *m/z* (ESI$^+$) [Found 335.1031., $C_{15}H_{13}FN_6NaO$ requires [M + Na]$^+$ 335.1027]; LCMS (MDAP): Rt = 18.1 min, >95% (Method 3); *m/z* (ESI$^+$) 313.9 [M + H]$^+$.

N-Cyclopropyl-5-fluoro-N-methyl-4-pyrazolo[1,5-*b*]pyridazin-3-yl-pyrimidin-2-amine **241**

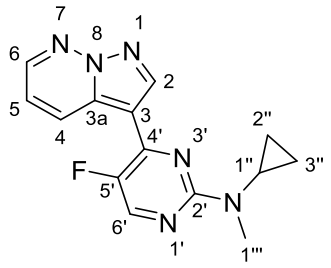

To 3-(2-chloro-5-fluoro-pyrimidin-4-yl)pyrazolo[1,5-*b*]pyridazine (80 mg, 0.32 mmol) in 2-propanol (2.5 mL) was added TEA (0.04 mL, 0.32 mmol). The vial was sealed and heated to 120 °C for 16 h. The reaction mixture was concentrated under reduced pressure. The crude was purified using flash silica column chromatography on an Isco Combiflash system (12 g silica, elution with 0-60% EtOAc / petroleum ether gradient). Desired fractions were combined and concentrated under reduced pressure. The crude was purified using flash reverse phase column chromatography on a Biotage system (12 g silica, elution with 10-100% MeOH / water gradient), trituration with petroleum ether afforded the title compound, *N*-cyclopropyl-5-fluoro-N-methyl-4-pyrazolo[1,5-*b*]pyridazin-3-yl-pyrimidin-2-amine, **241**, as a white solid (50 mg, 0.17 mmol, 52% yield). R_f 0.70 (EtOAc); m.p. 157-159 °C; $\bar{\nu}_{max}$ (neat)/cm^{-1} 3096 (C-H, w), 3018 (C-H, w), 2788 (C-H, w), 1622 (C=N, m), 1573 (C=C, s); ^{1}H NMR (600 MHz, DMSO-d$_6$) δ_H 9.14 (1H, d, *J* = 9.0 Hz, H-4), 8.68 – 8.64 (1H, m, H-6), 8.63 – 8.60 (1H, m, H-2), 8.52 – 8.46 (1H, m, H-6'), 7.53 (1H, dd, *J* = 9.0, 4.3 Hz, H-5), 3.15 (3H, s, H-1'''), 2.90 – 2.79 (1H, m, H-1''), 0.98 – 0.86 (2H, m, H-2'' and 3''), 0.72 – 0.61 (2H, m, H-2'' and 3''); ^{13}C NMR (150 MHz, DMSO-d$_6$) δ_C 159.8 (C-2'), 148.5 (d, *J* = 249.4 Hz, C-5'), 146.10 (d, *J* = 10.9 Hz, C-4'), 145.41 (d, *J* = 23.4 Hz, C-6'), 144.4 (C-6), 140.73 (d, *J* = 15.6 Hz, C-2), 133.0 (C-3a), 129.3 (C-4), 119.4 (C-5), 105.65 (d, *J* = 5.8 Hz, C-3), 36.3 (C-1'''), 31.9 (C-1''), 8.4 (C-2'' and C-3''); HRMS *m/z* (ESI$^+$) [Found 307.1074., $C_{14}H_{13}FN_6Na$ requires [M + Na]$^+$ 307.1078]; LCMS (MDAP): Rt = 20.6 min, >95% (Method 3); *m/z* (ESI$^+$) 285.9 [M + H]$^+$.

1-(5-Fluoro-4-imidazo[1,2-*a*]pyrimidin-3-yl-pyrimidin-2-yl)-6-oxa-1-azaspiro[3.3]heptane **242**

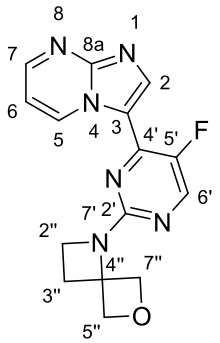

To a microwave vial containing 3-(2-chloro-5-fluoro-pyrimidin-4-yl)imidazo[1,2-*a*]pyrimidine (60 mg, 0.24 mmol) was added 6-oxa-1-azaspiro[3.3]heptane (48 mg, 0.48 mmol). The vial was sealed and heated to 120 °C for 16 h. The reaction mixture was concentrated under reduced pressure. The crude was purified using flash reverse phase column chromatography on a Biotage system (12 g C-18, elution with 10-100% MeOH / water gradient) to afford the title compound, 1-(5-fluoro-4-imidazo[1,2-*a*]pyrimidin-3-yl-pyrimidin-2-yl)-6-oxa-1-azaspiro[3.3]heptane, **242**, as a beige solid (15 mg, 0.05 mmol, 19% yield). R_f 0.08 (EtOAc); m.p. 290-292 °C; $\bar{\nu}_{max}$ (neat)/cm^{-1} 3108 (C-H, w), 2944 (C-H, w), 2874 (C-H, w), 2849 (C-H, w), 1615 (C=N, m), 1570 (C=C, s); ^{1}H NMR (600 MHz, $CDCl_3$) δ_H 10.67 (1H, s, H-5), 8.79 – 8.59 (2H, m, 2H, H-7 and H-2 or H-6'), 8.34 (1H, d, *J* = 3.7 Hz, H-2 or H-6'), 7.10 (1H, dd, *J* = 7.0, 4.1 Hz, H-6), 5.52 (2H, d, *J* = 7.4 Hz, H-5'' and 7''), 4.91 – 4.79 (2H, m, H-5'' and 7''), 4.03 (2H, t, *J* = 7.1 Hz, H-2''), 2.66 (2H, t, *J* = 7.1 Hz, H-3''); HRMS *m/z* (ESI$^+$) [Found 335.1026., $C_{15}H_{13}FN_6NaO$ requires [M + Na]$^+$ 335.1027]; LCMS (MDAP): Rt = 14.9 min, >95% (Method 3); *m/z* (ESI$^+$) 313.9 [M + H]$^+$.

5-Fluoro-4-imidazo[1,2-*a*]pyrimidin-3-yl-*N*,*N*-dimethyl-pyrimidin-2-amine **243**

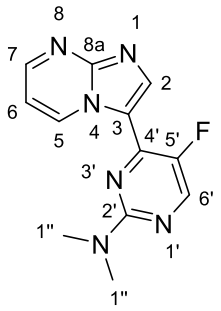

To a microwave vial containing 3-(2-chloro-5-fluoro-pyrimidin-4-yl)imidazo[1,2-*a*]pyrimidine (60 mg, 0.24 mmol) was added dimethylamine (0.24 mL, 0.48 mmol). The vial was sealed and heated to 120 °C for 2 h. The reaction mixture was concentrated under reduced pressure. The crude was purified using flash reverse phase column chromatography on a Biotage system (12 g C-18, elution with 10-100% MeOH / water gradient) to afford the title compound, 5-fluoro-4-imidazo[1,2-*a*]pyrimidin-3-yl-*N*,*N*-dimethyl-pyrimidin-2-amine, **243**, as a pale yellow solid (7 mg, 0.02 mmol, 10% yield). R_f 0.13 (EtOAc/ petroleum ether 1:1); ^{1}H NMR (600 MHz, $CDCl_3$) δ_H 10.30 (1H, dd, *J* = 7.0, 2.0 Hz, H-5), 8.72 (1H, dd, *J* = 4.1, 2.0 Hz, H-7), 8.64 (1H, d, *J* = 3.6 Hz, H-2 or H-6'), 8.30 (1H, d, *J* = 3.3 Hz, H-2 or H-6'), 7.09 (1H, dd, *J* = 7.0, 4.1 Hz, H-6), 3.27 (6H, s, H-1''); HRMS *m/z* (ESI$^+$) [Found 281.0919., $C_{12}H_{11}FN_6Na$ requires [M + Na]$^+$ 281.0921]; LCMS (MDAP): Rt = 15.7 min, >95% (Method 3); *m/z* (ESI$^+$) 258.9 [M + H]$^+$.

4-[(*E*)-2-Butoxyvinyl]-2-chloro-5-fluoro-pyrimidine **244**

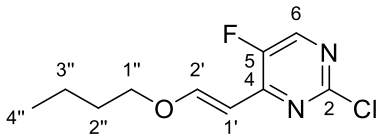

To a solution of 2,4-dichloro-5-fluoropyrimidine (2.2 g, 13.18 mmol) and butoxyethene (5 mL, 38.64 mmol) in polyethylene glycol 500 (6 mL) was added TEA (1.93 mL, 13.85 mmol) and palladium(II) acetate (150 mg, 0.67 mmol) and the solution was stirred under nitrogen at 80 °C overnight. The reaction mixture was partitioned between water (50 mL) and CH_2Cl_2 (100 mL) and the layers were separated. The mixture was washed through with CH_2Cl_2 (100 mL x 3). The combined organics were washed with water (200 mL x 2), brine (60 mL), dried over $MgSO_4$, filtered and concentrated under reduced pressure. The crude was purified using flash silica column chromatography on an Isco Combiflash system (40 g silica, elution with 0-10% EtOAc / petroleum ether gradient) to afford the title compound, 4-[(*E*)-2-butoxyvinyl]-2-chloro-5-fluoro-pyrimidine, **244**, as a yellow liquid (2.1 g, 7.28 mmol, 55% yield) plus residual impurities. R_f 0.34 (EtOAc / petroleum ether 1:9); ^{1}H NMR (600 MHz, $CDCl_3$) δ_H 8.21 (1H, d, *J* = 2.2 Hz, H-6), 8.00 (1H, d, *J* = 12.3 Hz, H-2'), 5.91 (1H, d, *J* = 12.3 Hz, H-1'), 4.01 (2H, t, *J* = 6.5 Hz, H-1''), 1.77 – 1.70 (2H, m, H-2''), 1.49 – 1.42 (2H, m, H-3''), 0.97 (3H, t, *J* = 7.5 Hz, H-4''); LCMS (MDAP): Rt = 4.8 min (Method 5); *m/z* (ESI$^+$) 230.9 [M]$^+$ and 232.9 [M + 2]$^+$; The spectroscopic data are in good agreement with the literature values. Literature reference: Ward RA *et al*. J Med Chem, 2013, vol. 56, # 17, p. 7025 – 7048

3-(2-Chloro-5-fluoro-pyrimidin-4-yl)imidazo[1,2-*a*]pyrimidine **245**

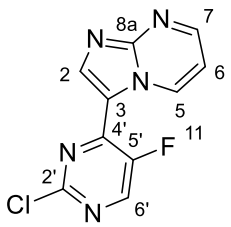

N-bromosuccinimide (180 mg, 1.04 mmol) was added to a stirred solution of 4-[(*E*)-2-butoxyvinyl]-2-chloro-5-fluoro-pyrimidine (200 mg, 0.87 mmol) in 1,4-dioxane (3 mL) : water (1 mL) and the reaction mixture was stirred for 1 h at rt. Pyrimidin-2-amine (80 mg, 0.86 mmol) was added and the reaction mixture was heated to 85 °C for 2 h. The reaction mixture was concentrated under reduced pressure. The crude was purified using flash silica column chromatography on an Isco Combiflash system (12 g silica, elution with 0-100% EtOAc / petroleum ether gradient) to afford the title compound, 3-(2-chloro-5-fluoro-pyrimidin-4-yl)imidazo[1,2-*a*]pyrimidine, **245**, as a yellow solid (450 mg, 0.72 mmol, 83% yield) plus impurities. R_f 0.61 (MeOH / CH_2Cl_2 1:9); ^{1}H NMR (600 MHz, DMSO-d_6) δ_H 10.00 (1H, dd, *J* = 6.9, 2.0 Hz, H-5), 8.93 (1H, d, *J* = 3.2 Hz, 1H, H-6' or 2), 8.86 (1H, dd, *J* = 4.2, 2.0 Hz, H-7), 8.67 (1H, d, *J* = 3.8 Hz, H-6' or 2), 7.50 (1H, dd, *J* = 7.0, 4.1 Hz, H-6). *50 mg of the impure material isolated was purified by flash reverse phase column chromatography on a Biotage system (12 g silica, elution with 10-100% MeOH / water ether gradient. LCMS (MDAP): Rt = 4.8 min (Method 5); *m/z* (ESI$^+$) 249.9 [M]$^+$ and 251.9 [M + 2]$^+$.

6-(4-Pyridyl)-3-[3-(trifluoromethoxy)phenyl]imidazo[1,2-*b*]pyridazine **247**

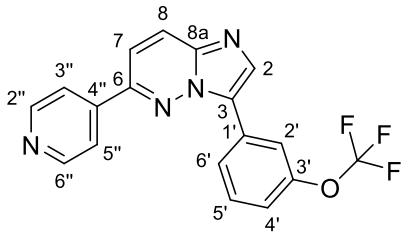

To a sealed and degassed microwave vial containing 6-chloro-3-[3-(trifluoromethoxy)phenyl]imidazo[1,2-*b*]pyridazine (40 mg, 0.13 mmol), pyridine-4-boronic acid hydrate (16 mg, 0.13 mmol), sodium carbonate (27 mg, 0.26 mmol) and bis(triphenylphosphine)palladium(II) dichloride (5 mg, 0.01 mmol) was added water (0.10 mL) and acetonitrile (0.50 mL). The reaction mixture was irradiated with microwaves for 15 min at 150°C. The reaction mixture was concentrated under reduced pressure. The residue was partitioned between EtOAc (30 mL) and water (30 mL), and extracted. The organic components were washed with water (2 x 30 mL), saturated brine solution (1 x 30 mL), and finally sodium hydroxide (2 x 30 mL). The combined organic components were dried over $MgSO_4$, filtered and concentrated to dryness under reduced pressure. The residue was purified using flash silica column chromatography on an Isco Combiflash system (12 g silica, elution with 0-50% 20% MeOH in CH_2Cl_2/ CH_2Cl_2 gradient) to afford the title compound, 6-(4-pyridyl)-3-[3-(trifluoromethoxy)phenyl]imidazo[1,2-*b*]pyridazine, **247**, as a yellow solid (25 mg, 0.07 mmol, 55% yield). R_f 0.41 (MeOH/CH_2Cl_2 1:9); m.p. 166-168 °C; $\bar{\nu}_{max}$ (neat)/cm^{-1} 2975 (C-H, m), 2918 (C-H, m), 1615 (C=N, m), 1478 (C=C, m), 1152 (C-O, s); ^{1}H NMR (600 MHz, DMSO-d$_6$) δ_H 8.82 – 8.77 (2H, m, H-2'' and 6''), 8.48 (1H, s, H-2), 8.41 (1H, d, *J* = 9.5 Hz, 1H, H-7), 8.36 – 8.33 (1H, m, H-2'), 8.25 – 8.22 (1H, m, H-6'), 8.10 – 8.06 (2H, m, H-3'' and 5''), 8.01 (d, *J* = 9.5 Hz, 1H, H-8), 7.69 (t, *J* = 8.0 Hz, 1H, H-5'), 7.43 – 7.39 (1H, m, H-4'); ^{13}C (150 MHz, DMSO-d$_6$) δ_C 150.5 (C-2'' and 6''); 149.1 (C-6); 148.7 (d, *J* = 1.5 Hz, C-3'); 142.2 (C-4''); 139.8 (C-8a); 134.9 (C-2); 130.3 (C-5'); 130.8 (C-1'); 126.8 (C-7), 126.1 (C-3); 125.1 (C-6'); 120.9 (C-3'' and 5''); 120.1 (C-4); 118.1 (C-2'); 116.0 (C-8). Signals at 120.50 ppm with J_1 = 240.6 Hz are consistent with trifluoromethyl group. HRMS *m/z* (ESI$^+$) [Found: 357.0959., $C_{18}H_{11}F_3N_4O$ requires [M + H]$^+$ 357.0958]; LCMS (LCQ): Rt = 3.4 min (Method 1); *m/z* (ESI$^+$) 357.3 [M + H]$^+$; LCMS (MDAP): Rt = 13.8 min, >95% (Method 3); *m/z* (ESI$^+$) 357.0 [M + H]$^+$.

6-Chloro-3-[3-(trifluoromethoxy)phenyl]imidazo[1,2-*b*]pyridazine **252**

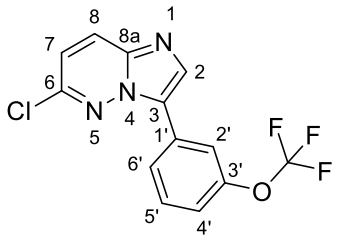

To a sealed and degassed microwave vial containing 3-bromo-6-chloroimidazo[1,2-*b*]pyridazine (250 mg, 1.08 mmol), [3-(trifluoromethoxy)phenyl]boronic acid (220 mg, 1.08 mmol), cesium carbonate (700 mg, 2.15 mmol) and [1,1'-bis(diphenylphosphino)ferrocene]dichloropalladium(II) (4 mg, 0.05 mmol) was added water (0.5 mL) and 1,4-dioxane (3 mL). The reaction mixture was heated to 110°C for 16 h. The reaction mixture was concentrated under reduced pressure. The residue was purified using flash silica column chromatography on an Isco Combiflash system (12 g silica, elution with 15% EtOAc / petroleum ether gradient). Recrystallisation in petroleum ether afforded the title compound, 6-chloro-3-[3-(trifluoromethoxy)phenyl]imidazo[1,2-*b*]pyridazine, **252**, as a pale yellow solid (0.20 g, 0.61 mmol, 56% yield). R_f 0.55 (EtOAc/ petroleum ether 1:1); m.p. 71-73 °C; $\bar{\nu}_{max}$ (neat)/cm^{-1} 3055 (C-H, m), 3030 (C-H, m), 1610 (C=N, m), 1514 (C=C, m); 1132 (C-O, s); ^{1}H NMR (600 MHz, DMSO-d$_6$) δ_H 8.25 (1H, s, H-2), 8.12 (1H, d, *J* = 9.5 Hz, H-7), 7.98 – 7.95 (1H, m, H-2'), 7.93 (2H, d, J = 7.9 Hz, H-6'), 7.48 (1H, t, *J* = 8.0 Hz, H-5'), 7.27 (1H, d, *J* = 9.5 Hz,H-8), 7.21 (1H, d, *J* = 8.2 Hz,H-4'); ^{13}C NMR (150 MHz, DMSO-d$_6$) δ_C 148.65 (d, *J* = 1.5 Hz, C-3'), 146.5 (C-6), 139.0 (C-8a), 134.4 (C-2), 130.7 (C-5'), 129.8 (C-1'), 128.1 (C-7), 126.1 (C-3), 125.0 (C-6'), 120.16 (q, *J* = 256.6 Hz, CF$_3$), 120.2 (C-4'), 119.3 (C-8), 119.1 (C-2'); HRMS *m/z* (ESI$^+$) [Found: 314.0311., $C_{13}H_7ClF_3N_3O$ requires [M + H]$^+$ 314.0303]; LCMS (LCQ): Rt = 4.8 min (Method 1); *m/z* (ESI$^+$) 314.3 [M + H]$^+$; LCMS (MDAP): Rt = 18.4 min, >95% (Method 3); *m/z* (ESI$^+$) 314.0 [M + H]$^+$; The spectroscopic data are in good agreement with the literature values Literature reference: US2009093475A1

6-Phenyl-3-[3-(trifluoromethoxy)phenyl]imidazo[1,2-*b*]pyridazine **253**

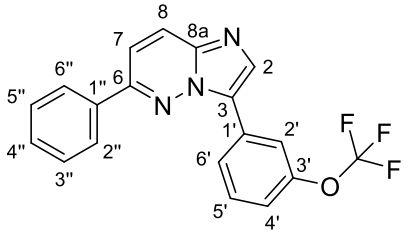

To a sealed and degassed microwave vial containing 6-chloro-3-[3-(trifluoromethoxy)phenyl]imidazo[1,2-*b*]pyridazine (188 mg, 0.48 mmol), phenylboronic acid (175 mg, 1.43 mmol), sodium carbonate (101 mg, 0.96 mmol) and bis(triphenylphosphine)palladium(II) dichloride (17 mg, 0.02 mmol) was added water (0.10 mL) and acetonitrile (0.50 mL). The reaction mixture was irradiated with microwaves for 15 min at 140 °C. The reaction mixture was concentrated under reduced pressure and the residue was taken up in EtOAc (30 mL). The organic components were washed with water (2 x 30 mL), saturated brine solution (1 x 30 mL), and finally sodium hydroxide (2 x 30 mL). The combined organic components were dried over $MgSO_4$, filtered and concentrated to dryness under reduced pressure. The residue was purified using flash silica column chromatography on an Isco Combiflash system (12 g silica, elution with 0-50% 20% MeOH in CH_2Cl_2/ CH_2Cl_2 gradient). Desired fractions were combined and concentrated under reduced pressure to afford a yellow solid. The solid was The residue was purified using flash silica column chromatography on an Isco Combiflash system (12 g silica, elution with 30-100% EtOAc/ petroleum ether gradient) to afford the title compound, 6-phenyl-3-[3-(trifluoromethoxy)phenyl]imidazo[1,2-*b*]pyridazine, **253**, as a yellow solid (78 mg, 0.21 mmol, 44% yield). R_f 0.47 (EtOAc); m.p. 115-117 °C; $\bar{\nu}_{max}$ (neat)/cm^{-1} 3105 (C-H, m), 3031 (C-H, m), 1614 (C=N, m), 1579 (C=C, m), 1580 (C=C, m), 1549 (C=C, m); 1474 (C=C, m), 1155 (C-O, s); ^{1}H NMR (600 MHz, DMSO-d$_6$) δ_H 8.41 (1H, s, H-2), 8.40 – 8.37 (1H, m, H-2'), 8.31 (1H, d, *J* = 9.5 Hz, 1H, H-7), 8.20 (1H, d, *J* = 7.9 Hz, H-6'), 8.10 (2H, dd, *J* = 7.8, 1.7 Hz, H-2'' and 6''), 7.91 (1H, d, *J* = 9.5 Hz, H-8), 7.66 (1H, t, *J* = 8.0 Hz, H-5'), 7.58 – 7.51 (3H, m, H-3'', 4'' and 5''), 7.39 – 7.33 (1H, m, H-4'); ^{13}C (150 MHz, DMSO-d$_6$) δ_C 151.4 (C-6), 148.71 (d, *J* = 1.6 Hz, C-3'), 139.6 (C-8a), 135.0 (C-1''), 134.2 (C-2), 130.9 (C-5'), 130.6 (C-1'), 130.4 (C-4''), 129.2 (C-3'' and 5''), 127.0 (C-2'' and 6''), 126.5 (C-7), 126.0 (C-3), 125.2 (C-6'), 120.1 (C-4'), 119.3 (q, *J* = 257.4 Hz, CF_3), 118.1 (C-2'), 116.7 (C-8); HRMS *m/z* (ESI$^+$) [Found: 356.1009., $C_{19}H_{12}F_3N_3O$ requires [M + H]$^+$ 356.1005]; LCMS (LCQ): Rt = 5.4 min (Method 1); *m/z* (ESI$^+$) 356.3 [M + H]$^+$; LCMS (MDAP): Rt = 22.7 min, >95% (Method 3); *m/z* (ESI$^+$) 356.0 [M + H]$^+$.

6-(3-Methoxyphenyl)-3-[3-(trifluoromethoxy)phenyl]imidazo[1,2-*b*]pyridazine **254**

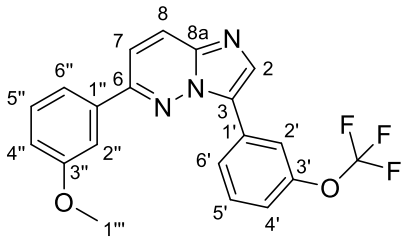

To a sealed and degassed microwave vial containing 6-chloro-3-[3-(trifluoromethoxy)phenyl]imidazo[1,2-*b*]pyridazine (80 mg, 0.26 mmol), (3-methoxyphenyl) boronic acid (78 mg, 0.51 mmol), sodium carbonate (54 mg, 0.51 mmol) and bis(triphenylphosphine)palladium(II) dichloride (9 mg, 0.01 mmol) was added water (0.10 mL) and acetonitrile (0.60 mL). The reaction mixture was irradiated with microwaves for 15 min at 140 °C. The reaction mixture was concentrated under reduced pressure and the residue was taken up in EtOAc (30 mL). The organic components were washed with water (2 x 30 mL), saturated brine solution (1 x 30 mL), and finally sodium hydroxide (2 x 30 mL). The combined organic components were dried over $MgSO_4$, filtered and concentrated to dryness under reduced pressure. The residue was purified using flash silica column chromatography on an Isco Combiflash system (12 g silica, elution with 20-100% EtOAc/ petroleum ether gradient). Desired fractions were combined and concentrated under reduced pressure to afford a yellow solid. Desired fractions were combined and concentrated under reduced pressure to afford a yellow solid. The solid was purified using flash silica column chromatography on an Isco Combiflash system (12 g silica, elution with 0-100% 10% MeOH in CH_2Cl_2/ CH_2Cl_2 gradient) to afford the title compound, 6-(3-methoxyphenyl)-3-[3-(trifluoromethoxy)phenyl]imidazo[1,2-*b*]pyridazine, **254**, as a yellow solid (52 mg, 0.13 mmol, 50% yield). R_f 0.18 (CH_2Cl_2); m.p. 150-152 °C; $\bar{\nu}_{max}$ (neat)/cm^{-1} 3059 (C-H, m), 3019 (C-H, m), 1610 (C=N, m), 1592 (C=C, m), 1544 (C=C, m); 1481 (C=C, m), 1142 (C-O, s); ^{1}H NMR (600 MHz, DMSO-d$_6$) δ_H 8.47 – 8.42 (2H, m, H-4 and 2'), 8.33 (1H, d, *J* = 9.5 Hz, H-7), 8.22 (1H, d, *J* = 7.9 Hz, H-6'), 7.96 (1H, d, *J* = 9.5 Hz, H-8), 7.72 – 7.65 (3H, m, H-4'', 5'' and 6''), 7.50 (1H, t, *J* = 8.0 Hz, H-5'), 7.42 – 7.37 (1H, m, H-4''), 7.14 (1H, dd, *J* = 8.2, 2.5 Hz, H-4'), 3.87 (3H, s, H-1'''); ^{13}C (150 MHz, DMSO-d$_6$) δ_C 159.9 (C-3''), 151.3 (C-6), 148.8 (m, C-3'), 139.7 (C-8a), 136.4 (C-1''), 134.2 (C-2), 130.9 (C-6''), 130.7 (C-1'), 130.4 (C-5'), 126.4 (C-7), 125.9 (C-3), 125.2 (C-6'), 120.0 (q, *J* = 258.1 Hz, CF_3), 120.1 (C-4''), 119.4 (C-5''), 118.1 (C-2'), 116.9 (C-8), 116.3 (C-4'), 112.2 (C-2''), 55.3 (C-1'''); HRMS *m/z* (ESI$^+$) [Found: 386.1113., $C_{20}H_{14}F_3N_3O_2$ requires [M + H]$^+$ 386.1111]; LCMS (LCQ): Rt = 5.4 min (Method 1); *m/z* (ESI$^+$) 386.3 [M + H]$^+$; LCMS (MDAP): Rt = 23.0 min, >95% (Method 3); *m/z* (ESI$^+$) 386.0 [M + H]$^+$.

6-[3-Methoxymethyl)phenyl]-3-[3-(trifluoromethoxy)phenyl]imidazo[1,2-*b*]pyridazine **255**

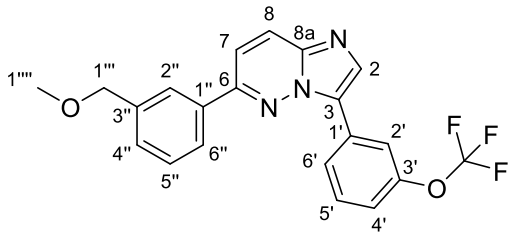

To a sealed and degassed microwave vial containing 6-chloro-3-[3-(trifluoromethoxy)phenyl]imidazo[1,2-*b*]pyridazine (80 mg, 0.26 mmol), [3-(methoxymethyl)phenyl]boronic acid (85 mg, 0.51 mmol), sodium carbonate (54 mg, 0.51 mmol) and bis(triphenylphosphine)palladium(II) dichloride (9 mg, 0.01 mmol) was added water (0.10 mL) and acetonitrile (0.60 mL). The reaction mixture was irradiated with microwaves for 15 min at 140 °C. The reaction mixture was concentrated under reduced pressure and the residue was taken up in EtOAc (30 mL). The organic components were washed with water (2 x 30 mL), saturated brine solution (1 x 30 mL), and finally sodium hydroxide (2 x 30 mL). The combined organic components were dried over $MgSO_4$, filtered and concentrated to dryness under reduced pressure. The residue was purified using flash silica column chromatography on an Isco Combiflash system (12 g silica, elution with 30-100% EtOAc/ petroleum ether gradient). Desired fractions were combined and concentrated under reduced pressure to afford a yellow solid. The solid was purified using flash silica column chromatography on an Isco Combiflash system (12 g silica, elution with 0-100% 10% MeOH/ CH_2Cl_2 gradient) to afford the title compound, 6-[3-methoxymethyl)phenyl]-3-[3-(trifluoromethoxy)phenyl]imidazo[1,2-*b*]pyridazine, **255**, as a yellow solid (78 mg, 0.19 mmol, 73% yield). R_f 0.21 (MeOH/ CH_2Cl_2 1:9); m.p. 110-111 °C; $\bar{\nu}_{max}$ (neat)/cm^{-1} 3108 (C-H, w), 3043(C-H, w), 1614 (C=N, m), 1582(C=C, m), 1547 (C=C, m); 1206 (C-O, s), 1145 (C-O, s); ^{1}H NMR (500 MHz, DMSO-d$_6$) δ_H 8.47 (1H, s, H-2'), 8.44 (1H, s, H-2), 8.33 (1H, d, *J* = 9.5 Hz, H-7), 8.22 – 8.18 (1H, m, H-6'), 8.08 (1H, s, H-2''), 8.07 – 8.03 (1H, m, H-6''), 7.94 (1H, d, *J* = 9.5 Hz, H-8), 7.68 (t, *J* = 8.0 Hz, H-5'), 7.57 (1H, t, *J* = 7.6 Hz, H-5''), 7.52 (1H, d, *J* = 7.6 Hz, H-4''), 7.42 – 7.37 (1H, m, H-4'), 4.53 (2H, s, H-1'''), 3.35 (3H, s, H-1''''); ^{13}C NMR (150 MHz, DMSO-d$_6$) δ_C 151.3 (C-6), 148.8 – 148.6 (m, C-3'), 139.7 (C-8a), 139.4 (C-3''), 135.0 (C-1''), 134.2 (C-2), 130.8 (C-5'), 130.6 (C-1'), 129.5 (C-4''), 129.1 (C-5''), 126.5 (C-7), 126.2 (C-6''), 125.91 (C-2''), 125.90 (C-3), 125.1 (C-6'), 120.0 (C-4'), 119.6 (q, *J* = 256.8 Hz, CF_3), 118.0 (C-2'), 116.6 (C-8), 73.4 (C-1'''), 57.7 (C-1''''); HRMS *m/z* (ESI$^+$) [Found: 400.1266., $C_{21}H_{16}F_3N_3O_2$ requires [M + H]$^+$ 400.1267]; LCMS (LCQ): Rt = 5.3min (Method 1); *m/z* (ESI$^+$) 400.3 [M + H]$^+$; LCMS (MDAP): Rt = 22.3 min, >95% (Method 3); *m/z* (ESI$^+$) 400.1 [M + H]$^+$.

3-[3-[3-(Trifluoromethoxy)phenyl]imidazo[1,2-*b*]pyridazin-6-yl]benzamide **256**

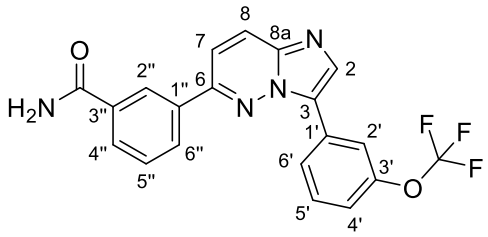

To a sealed and degassed microwave vial containing 6-chloro-3-[3-(trifluoromethoxy)phenyl]imidazo[1,2-*b*]pyridazine (80 mg, 0.26 mmol), (3-carbamoylphenyl)boronic acid (84 mg, 0.51 mmol), sodium carbonate (54 mg, 0.51 mmol) and bis(triphenylphosphine)palladium(II) dichloride (9 mg, 0.01 mmol) was added water (0.10 mL) and acetonitrile (0.60 mL). The reaction mixture was irradiated with microwaves for 15 min at 140 °C. The reaction mixture was concentrated under reduced pressure and the residue was taken up in EtOAc (30 mL). The organic components were washed with water (2 x 30 mL), saturated brine solution (1 x 30 mL), and finally sodium hydroxide (2 x 30 mL). The combined organic components were dried over $MgSO_4$, filtered and concentrated to dryness under reduced pressure. The residue was purified using flash silica column chromatography on an Isco Combiflash system (12 g silica, elution with 0-100% 10% MeOH/ CH_2Cl_2 gradient) to afford the title compound, **256**, as an off-white solid (34 mg, 0.081 mmol, 32% yield). R_f 0.22 (EtOAc/petroleum ether 3:1); m.p. 259-261 °C; $\bar{\nu}_{max}$ (neat)/cm^{-1} 3424 (N-H, s), 3189 (N-H, s), 3118(C-H, w), 3071(C-H, w), 1651 (C=O, s), 1610 (C=N, m), 1582 (C=C, m), 1548 (C=C, m); 1144 (C-O, s); ^{1}H NMR (500 MHz, DMSO-d$_6$) δ_H 8.58 – 8.55 (1H, m, H-2''), 8.45 (1H, s, H-2), 8.42 – 8.37 (2H, m, H-7 and 2'), 8.28 – 8.23 (2H, m, 2H, H-6' and 4''), 8.15 (1H, s, N*H*), 8.04 (1H, d, *J* = 7.7 Hz, H-6''), 8.00 (1H, d, *J* = 9.5 Hz, H-8), 7.71 – 7.64 (2H, m, H-5' and H-5''), 7.50 (1H, s, N*H*), 7.42 – 7.37 (1H, m, H-4'); ^{13}C NMR (150 MHz, DMSO-d$_6$) δ_C 167.4 (C=O), 151.1 (C-6), 148.7 (C-3'), 135.3 (C-1''or C-3''), 135.2 (C-1'' or C-3''), 134.6 (C-2), 130.8 (C-5'), 130.7 (C-1'), 129.5 (C-4''), 129.3 (C-6''), 129.2 (C-5''), 126.7 (C-7), 126.2 (C-3 and 2''), 125.2 (C-6'), 120.1 (C-4'), 119.8 (q, *J* = 256.6 Hz, CF_3), 118.2 (C-2'), 116.6 (C-8). C-8a not visible; HRMS *m/z* (ESI$^+$) [Found: 399.1067., $C_{20}H_{13}F_3N_4O_2$ requires [M + H]$^+$ 399.1063]; LCMS (LCQ): Rt = 0.7 min (Method 1); *m/z* (ESI$^+$) 399.1 [M + H]$^+$; LCMS (MDAP): Rt = 14.6 min, >95% (Method 3); *m/z* (ESI$^+$) 399.1 [M + H]$^+$.

3-[3-[3-(Trifluoromethoxy)phenyl]imidazo[1,2-*b*]pyridazin-6-yl]benzonitrile **257**

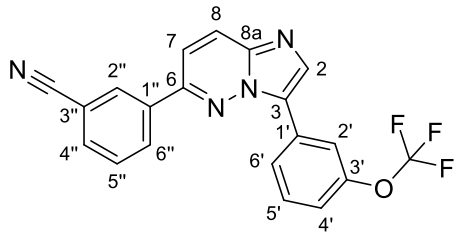

To a sealed and degassed microwave vial containing 6-chloro-3-[3-(trifluoromethoxy)phenyl]imidazo[1,2-*b*]pyridazine (80 mg, 0.26 mmol), 3-cyanophenylboronic acid (75 mg, 0.51 mmol), sodium carbonate (54 mg, 0.51 mmol) and bis(triphenylphosphine)palladium(II) dichloride (9 mg, 0.01 mmol) was added water (0.10 mL) and acetonitrile (0.60 mL). The reaction mixture was irradiated with microwaves for 15 min at 140 °C. The reaction mixture was concentrated under reduced pressure and the residue was taken up in EtOAc (30 mL). The organic components were washed with water (2 x 30 mL), saturated brine solution (1 x 30 mL), and finally sodium hydroxide (2 x 30 mL). The combined organic components were dried over $MgSO_4$, filtered and concentrated to dryness under reduced pressure. The residue was purified using flash silica column chromatography on an Isco Combiflash system (12 g silica, elution with 0-100% EtOAc/ petroleum ether gradient) to afford the title compound, 3-[3-[3-(trifluoromethoxy)phenyl]imidazo[1,2-*b*]pyridazin-6-yl]benzonitrile, **257**, as an off-white solid (30 mg, 0.08 mmol, 29% yield). R_f 0.18 (EtOAc/petroleum ether 1:1); m.p. 213-215 °C; $\bar{\nu}_{max}$ (neat)/cm^{-1} 3095 (C-H, w), 1614 (C=N, m), 1584 (C=C, m), 1545 (C=C, m); 1153 (C-O, s); ^{1}H NMR (600 MHz, DMSO-d$_6$) δ_H 8.57 – 8.54 (1H, m, H-6''), 8.48 – 8.43 (3H, m, H-2, 2' and 4''), 8.40 (1H, d, *J* = 9.5 Hz, H-7), 8.19 – 8.15 (1H, m, H-6'), 8.05 – 8.01 (2H, m, H-8 and H-2''), 7.80 (1H, t, *J* = 7.8 Hz, H-5''), 7.69 (1H, t, *J* = 8.1 Hz, H-5'), 7.43 – 7.39 (1H, m, H-4'); ^{13}C NMR (150 MHz, DMSO-d$_6$) δ_C 149.7 (C-6), 148.8-148.7 (m, C-3'), 139.7 (C-8a), 136.3 (C-1''), 134.6 (C-2), 133.8 (C-4''), 131.6 (C-6''), 130.9 (C-5'), 130.6 (C-2''), 130.43 (C-5''), 130.41 (C-1'), 126.8 (C-7), 126.1 (C-3), 125.4 (C-6'), 120.3 (C-4'), 119.4 (q, *J* = 256.1 Hz, CF_3), 118.3 (CN), 118.1 (C-2'), 116.4 (C-8), 112.4 (C-3''); HRMS *m/z* (ESI$^+$) [Found: 381.0961., $C_{20}H_{11}F_3N_4O$ requires [M + H]$^+$ 381.0958]; LCMS (LCQ): Rt = 4.8 min (Method 1); *m/z* (ESI$^+$) 381.8 [M + H]$^+$; LCMS (MDAP): Rt = 21.1 min, >95% (Method 3); *m/z* (ESI$^+$) 381.1 [M + H]$^+$.

6-(1,3-Benzodioxol-5-yl)-3-[3-(trifluoromethoxy)phenyl]imidazo[1,2-*b*]pyridazine **258**

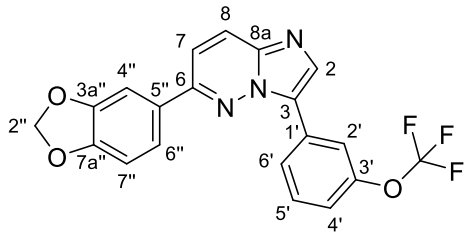

To a sealed and degassed microwave vial containing 6-chloro-3-[3-(trifluoromethoxy)phenyl]imidazo[1,2-*b*]pyridazine (80 mg, 0.26 mmol), (2*H*-1,3-benzodioxol-5-yl)boronic acid (85 mg, 0.51 mmol), sodium carbonate (54 mg, 0.51 mmol) and bis(triphenylphosphine)palladium(II) dichloride (9 mg, 0.01 mmol) was added water (0.10 mL) and acetonitrile (0.60 mL). The reaction mixture was irradiated with microwaves for 20 min at 140 °C. The reaction mixture was concentrated under reduced pressure and the residue was taken up in EtOAc (30 mL). The organic components were washed with water (2 x 30 mL), saturated brine solution (1 x 30 mL), and finally sodium hydroxide (2 x 30 mL). The combined organic components were dried over $MgSO_4$, filtered and concentrated to dryness under reduced pressure. The residue was purified using flash silica column chromatography on an Isco Combiflash system (12 g silica, elution with 0-50% EtOAc/ petroleum ether gradient) to afford the title compound, 6-(1,3-benzodioxol-5-yl)-3-[3-(trifluoromethoxy)phenyl]imidazo[1,2-*b*]pyridazine, **258**, as a yellow solid (86 mg, 0.21 mmol, 80% yield). R_f 0.36 (EtOAc/petroleum ether 1:1); m.p. 168-170 °C; $\bar{\nu}_{max}$ (neat)/cm^{-1} 3112 (C-H, w), 3045(C-H, w), 1609 (C=N, m), 1594 (C=C, m), 1546 (C=C, m); 1213 (C-O, s), 1144 (C-O, s); ^{1}H NMR (600 MHz, DMSO-d$_6$) δ_H 8.39 – 8.34 (2H, m, H-2'and H-2), 8.22 (1H, d, *J* = 9.5 Hz, H-7), 8.15 – 8.12 (1H, m, H-6'), 7.86 (1H, d, *J* = 9.6 Hz, H-8), 7.68 – 7.60 (3H, m, H-4'', 5' and 6''), 7.39 – 7.35 (1H, m, H-4'), 7.07 (1H, d, *J* = 8.1 Hz, H-7''), 6.11 (2H, s, H-2''); ^{13}C (150 MHz, DMSO-d$_6$) δ_C 151.3 (C-6), 149.6 (C-7a''), 148.94 – 148.83 (m, C-3'), 148.6 (C-3a''), 139.6 (C-8a), 133.7 (C-2), 131.1 (C-5'), 130.7 (C-1'), 129.1 (C-5''), 126.4 (C-7), 126.2 (C-3), 125.5 (C-6'), 122.0 (C-4'), 120.5 (q, *J* = 256.5 Hz, CF_3), 120.4 (C-2'), 118.2 (C-8), 117.0 (C-4''), 109.0 (C-7''), 106.8 (C-2''); HRMS *m/z* (ESI$^+$) [Found: 400.0903., $C_{20}H_{12}F_3N_3O_3$ requires [M + H]$^+$ 400.0904]; LCMS (LCQ): Rt = 3.6 min (Method 1); *m/z* (ESI$^+$) 400.3 [M + H]$^+$; LCMS (MDAP): Rt = 21.5 min, >95% (Method 3); *m/z* (ESI$^+$) 400.1 [M + H]$^+$.

6-(4-Chlorophenyl)-3-[3-(trifluoromethoxy)phenyl]imidazo[1,2-*b*]pyridazine **259**

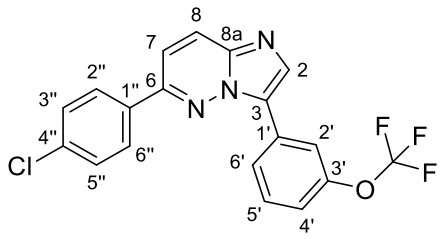

To a sealed and degassed microwave vial containing 6-chloro-3-[3-(trifluoromethoxy)phenyl]imidazo[1,2-*b*]pyridazine (80 mg, 0.26 mmol), 4-chlorophenylboronic acid (80 mg, 0.51 mmol), sodium carbonate (54 mg, 0.51 mmol) and bis(triphenylphosphine)palladium(II) dichloride (9 mg, 0.01 mmol) was added water (0.10 mL) and acetonitrile (0.60 mL). The reaction mixture was irradiated with microwaves for 15 min at 140 °C. The reaction mixture was concentrated under reduced pressure and the residue was taken up in EtOAc (30 mL). The organic components were washed with water (2 x 30 mL), saturated brine solution (1 x 30 mL), and finally sodium hydroxide (2 x 30 mL). The combined organic components were dried over $MgSO_4$, filtered and concentrated to dryness under reduced pressure. The residue was purified using flash silica column chromatography on an Isco Combiflash system (12 g silica, elution with 10-100% 10% MeOH in CH_2Cl_2/ CH_2Cl_2 gradient) to afford the title compound, 6-(4-chlorophenyl)-3-[3-(trifluoromethoxy)phenyl]imidazo[1,2-*b*]pyridazine, **259**, as a yellow solid (45 mg, 0.11 mmol, 43% yield). R_f 0.25 (CH_2Cl_2); m.p. 129-131 °C; $\bar{\nu}_{max}$ (neat)/cm^{-1} 3046 (C-H, w), 1617 (C=N, m), 1597 (C=C, m), 1546 (C=C, m); 1495 (C-O, s), 1145 (C-O, s); ^{1}H NMR (600 MHz, DMSO-d$_6$) δ_H 8.39 (1H, s, H-2), 8.33 – 8.26 (2H, m, H-7 and H-2'), 8.18 – 8.15 (1H, m, H-6'), 8.10 – 8.05 (2H, m, H-2'' and 6''), 7.87 (1H, d, *J* = 9.5 Hz, H-8), 7.65 (1H, t, *J* = 8.1 Hz, H-5'), 7.61 – 7.57 (2H, m, H-3'' and 5''), 7.39 – 7.33 (1H, m, H-4'); ^{13}C (150 MHz, DMSO-d$_6$) δ_C 150.4 (C-6); 148.8 (C-3'); 139.6 (C-8a); 135.4 (C-4''); 134.4 (C-2); 133.9 (C-1''); 130.9 (C-5'); 130.6 (C-1'); 129.2 (C-2'' and 6''); 128.8 (C-3'' and 5''); 126.6 (C-7), 126.1 (C-3); 125.2 (C-6'); 120.2 (C-4'); 119.7 (q, *J* = 257.3 Hz, CF_3); 118.1 (C-2'), 116.4 (C-8); HRMS *m/z* (ESI$^+$) [Found: 390.0618., $C_{19}H_{11}ClF_3N_3O$ requires [M + H]$^+$ 390.0616]; LCMS (LCQ): Rt = 3.6 min (Method 1); *m/z* (ESI$^+$) 400.3 [M + H]$^+$; LCMS (MDAP): Rt = 25.6 min, >95% (Method 3); *m/z* (ESI$^+$) 391.0 [M + H]$^+$.

3-[3-(Trifluoromethoxy)phenyl]-6-[4-(trifluoromethyl)phenyl]imidazo[1,2-*b*]pyridazine **260**

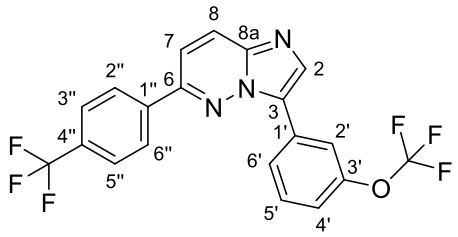

To a sealed and degassed microwave vial containing 6-chloro-3-[3-(trifluoromethoxy)phenyl]imidazo[1,2-*b*]pyridazine (80 mg, 0.26 mmol), [4-(trifluoromethyl)phenyl]boronic acid (97 mg, 0.51 mmol), sodium carbonate (54 mg, 0.51 mmol) and bis(triphenylphosphine)palladium(II) dichloride (9 mg, 0.01 mmol) was added water (0.10 mL) and acetonitrile (0.60 mL). The reaction mixture was irradiated with microwaves for 15 min at 140 °C. The reaction mixture was concentrated under reduced pressure and the residue was taken up in EtOAc (30 mL). The organic components were washed with water (2 x 30 mL), saturated brine solution (1 x 30 mL), and finally sodium hydroxide (2 x 30 mL). The combined organic components were dried over $MgSO_4$, filtered and concentrated to dryness under reduced pressure. The residue was purified using flash silica column chromatography on an Isco Combiflash system (12 g silica, elution with 0-100% EtOAc/ petroleum ether gradient) to afford the title compound, **260**, as a yellow solid (73 mg, 0.16 mmol, 64% yield). R_f 0.26 (CH_2Cl_2); m.p. 123-124 °C; $\bar{\nu}_{max}$ (neat)/cm^{-1} 3096(C-H, w), 1611 (C=N, m), 1585 (C=C, m), 1546 (C=C, m); 1153 (C-O, s); ^{1}H NMR (600 MHz, DMSO-d$_6$) δ_H 8.45 (s, 1H, H-2), 8.37 (1H, d, *J* = 9.5 Hz, H-7), 8.34 – 8.27 (3H, m, H-2', 2'' and 6''), 8.24 – 8.19 (1H, m, H-6'), 7.97 (1H, d, *J* = 9.5 Hz, H-8), 7.92 (2H, d, *J* = 8.2 Hz, H-3'' and H-5''), 7.67 (1H, t, *J* = 8.1 Hz, H-5'), 7.41 – 7.37 (1H, m, H-4'); ^{13}C NMR (150 MHz, DMSO-d$_6$) δ_C 150.1 (C-6), 148.8 – 148.7 (m, C-3'), 139.7 (C-8a), 139.0 (C-1''), 134.7 (C-2), 130.9 (C-5'), 130.5 (C-1'), 130.4 (q, *J* = 31.9 Hz, C-4''), 127.9 (C-2'' and 6''), 126.7 (C-7), 126.1 (C-3), 126.0 (q, *J* = 3.5 Hz, C-3'' and C-5''), 125.2 (C-6'), 124.3 (q, *J* = 271.6 Hz, CF_3), 120.2 (C-4'), 119.3 (q, *J* = 254.9 Hz, OCF_3), 118.2 (C-2'), 116.6 (C-8); HRMS *m/z* (ESI$^+$) [Found: 424.0880., $C_{20}H_{11}F_6N_3O$ requires [M + H]$^+$ 424.0879]; LCMS (MDAP): Rt = 25.4 min, >95% (Method 3); *m/z* (ESI$^+$) 424.0 [M + H]$^+$.

6-(3-Pyridyl)-3-[3-(trifluoromethoxy)phenyl]imidazo[1,2-*b*]pyridazine **261**

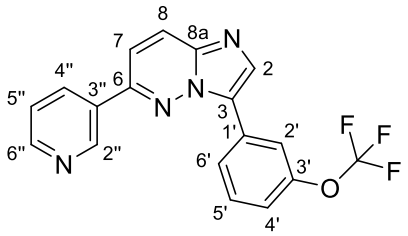

To a sealed and degassed microwave vial containing 6-chloro-3-[3-(trifluoromethoxy)phenyl]imidazo[1,2-*b*]pyridazine (100 mg, 0.32 mmol), pyridine-3-boronic acid hydrate (118 mg, 0.96 mmol), sodium carbonate (68 mg, 0.64 mmol) and bis(triphenylphosphine)palladium(II) dichloride (11 mg, 0.02 mmol) was added water (0.10 mL) and acetonitrile (0.50 mL). The reaction mixture was irradiated with microwaves for 20 min at 120 °C. The reaction mixture was concentrated under reduced pressure and the residue was taken up in EtOAc (30 mL). The organic components were washed with water (2 x 30 mL), saturated brine solution (1 x 30 mL), and finally sodium hydroxide (2 x 30 mL). The combined organic components were dried over $MgSO_4$, filtered and concentrated to dryness under reduced pressure. The residue was purified using flash silica column chromatography on an Isco Combiflash system (12 g silica, elution with 0-100% EtOAc/ petroleum ether gradient) to afford the title compound, 6-(3-pyridyl)-3-[3-(trifluoromethoxy)phenyl]imidazo[1,2-*b*]pyridazine, **261**, as a yellow solid (68 mg, 0.18 mmol, 56% yield). R_f 0.26 (EtOAc); m.p. 176-179 °C; $\bar{\nu}_{max}$ (neat)/cm^{-1} 3113 (C-H, m), 3049 (C-H, m), 1613 (C=N, m), 1592 (C=C, m), 1581 (C=C, m), 1551 (C=C, m); 1480 (C=C, m), 1149 (C-O, s); ^{1}H NMR (600 MHz, DMSO-d$_6$) δ_H 9.27 (1H, d, *J* = 2.3 Hz, H-2''), 8.71 (1H, dd, *J* = 4.8, 1.6 Hz, H-6''), 8.47 – 8.40 (2H, m, H-2 and 4''), 8.37 – 8.32 (2H, m, H-7 and 2'), 8.18 (1H, d, *J* = 7.9 Hz, H-6'), 7.95 (1H, d, *J* = 9.5 Hz, H-8), 7.65 (1H, t, *J* = 8.0 Hz, H-5'), 7.58 (1H, dd, *J* = 8.0, 4.8 Hz, H-5''), 7.38 – 7.33 (1H, m, H-4); ^{13}C (150 MHz, DMSO- d$_6$) δ_C 150.9 (C-6''); 149.4 (C-6), 148.73-148.66 (m, C-3');147.9 (C-2''); 139.7 (C-8a); 135.0 (C-4''); 134.9 (C-2); 131.4 (C-3''); 131.3 (C-5'); 130.5 (C-1'); 126.8 (C-7); 126.1 (C-3); 125.2 (C-6'); 124.1 (C-5''); 120.2 (C-4'), 119.9 (q, *J* = 257.4 Hz, CF_3), 118.1 (C-2'); 116.4 (C-8); HRMS *m/z* (ESI$^+$) [Found: 357.0961., $C_{18}H_{11}F_3N_4O$ requires [M + H]$^+$ 357.0958]; LCMS (LCQ): Rt = 2.4 min (Method 1); *m/z* (ESI$^+$) 357.2 [M + H]$^+$; LCMS (MDAP): Rt = 15.6 min, >95% (Method 3); *m/z* (ESI$^+$) 357.0 [M + H]$^+$.

6-(2-Methyl-4-pyridyl)-3-[3-(trifluoromethoxy)phenyl]imidazo[1,2-*b*]pyridazine **262**

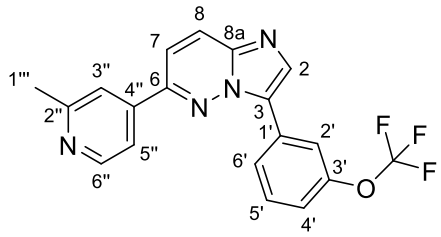

To a sealed and degassed microwave vial containing 6-chloro-3-[3-(trifluoromethoxy)phenyl]imidazo[1,2-*b*]pyridazine (80 mg, 0.26 mmol), (2-methylpyridin-4-yl) boronic acid (68 mg, 0.17 mmol), sodium carbonate (54 mg, 0.51 mmol) and bis(triphenylphosphine)palladium(II) dichloride (9 mg, 0.01 mmol) was added water (0.10 mL) and acetonitrile (0.50 mL). The reaction mixture was irradiated with microwaves for 30 min at 140 °C. The reaction mixture was concentrated under reduced pressure and the residue was taken up in EtOAc (30 mL). The organic components were washed with water (2 x 30 mL), saturated brine solution (1 x 30 mL), and finally sodium hydroxide (2 x 30 mL). The combined organic components were dried over $MgSO_4$, filtered and concentrated to dryness under reduced pressure. The residue was purified using flash silica column chromatography on an Isco Combiflash system (12 g silica, elution with 0-15% 10% MeOH in CH_2Cl_2/ CH_2Cl_2 gradient). Desired fractions were combined and concentrated under reduced pressure to afford a yellow solid. Desired fractions were combined and concentrated under reduced pressure to afford a yellow solid. The solid was purified using flash silica column chromatography on an Isco Combiflash system (12 g silica, elution with 70-100% EtOAc/ petroleum ether gradient) to afford the title compound, 6-(2-methyl-4-pyridyl)-3-[3-(trifluoromethoxy)phenyl]imidazo[1,2-*b*]pyridazine, **262**, as a yellow solid (68 mg, 0.174 mmol, 68% yield). R_f 0.69 (EtOAc); m.p. 155-157 °C; $\bar{\nu}_{max}$ (neat)/cm^{-1} 3096 (C-H, m), 3037 (C-H, m), 1615 (C=N, m), 1562 (C=C, m), 1542 (C=C, m); 1481 (C=C, m), 1136 (C-O, s); ^{1}H NMR (600 MHz, DMSO-d$_6$) δ_H 8.65 (1H, d, *J* = 5.2 Hz, H-6''), 8.48 (1H, s, H-2), 8.44 – 8.39 (2H, m, H-2' and 7), 8.20 (1H, d, *J* = 8.0 Hz, H-6'), 8.00 (1H, d, *J* = 9.5 Hz, H-8), 7.96 (1H, s, H-3''), 7.90 – 7.86 (1H, m, H-5''), 7.69 (1H, t, *J* = 8.0 Hz, H-5'), 7.43 – 7.39 (1H, m, H-4'), 2.59 (3H, s, H-1'''); ^{13}C (150 MHz, DMSO-d$_6$) δ_C 159.1 (C-2''), 149.9 (C-6''), 149.3 (C-6), 148.7 (C-3'), 142.5 (C-4''), 139. 9 (C-8a), 134.9 (C-2), 130.9 (C-5'), 130.4 (C-1'), 126.8 (C-7), 126.1 (C-3), 125.3 (C-6'), 120.3 (C-4'), 120.2 (C-3''), 120.0 (q, *J* = 245.2 Hz, CF_3), 118.3 (C-5''), 118.1 (C-2'), 116.2 (C-8), 24.1 (C-1'''); HRMS *m/z* (ESI$^+$) [Found: 371.1112., $C_{19}H_{13}F_3N_4O$ requires [M + H]$^+$ 371.1114]; LCMS (LCQ): Rt = 2.7 min (Method 1); *m/z* (ESI$^+$) 371.3 [M + H]$^+$; LCMS (MDAP): Rt = 10.7 min, >95% (Method 3); *m/z* (ESI$^+$) 371.0 [M + H]$^+$.

6-(3-Methyl-4-pyridyl)-3-[3-(trifluoromethoxy)phenyl]imidazo[1,2-*b*]pyridazine **263**

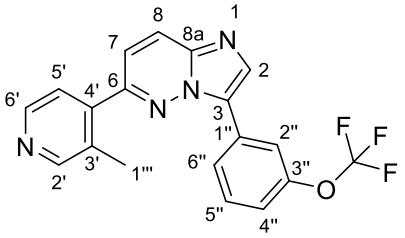

To a degassed microwave vial containing a solution of 6-chloro-3-[3-(trifluoromethoxy)phenyl]imidazo[1,2-*b*]pyridazine (143 mg, 0.32 mmol) in acetonitrile (0.80 mL) and water (0.20 mL) was added (3-methylpyridin-4-yl)boronic acid (87 mg, 0.64 mmol), bis[2-(di-*tert*-butylphosphanyl)cyclopenta-2,4-dien-1-yl]iron; dichloropalladium (10 mg, 0.02 mmol), and cesium carbonate (208 mg, 0.64 mmol). The reaction vial was sealed and irradiated with microwaves at 140 °C for 20 min. The reaction mixture was concentrated under reduced pressure. The residue was partitioned between EtOAc (30 mL) and water (30 mL) and the layers separated. The aqueous layer was extracted further with EtOAc (2 x 30 mL). The combined organic components were washed with saturated brine solution (50 mL), dried over $MgSO_4$, filtered and concentrated under reduced pressure. The crude was purified using flash reverse phase column chromatography on a Biotage system (12 g C-18, elution with 10-100% MeOH / water gradient). Desired fractions were combined and concentrated under reduced pressure. The crude was purified using flash silica column chromatography on an Isco Combiflash system (12 g silica, elution with 0-100% EtOAc / petroleum ether gradient). Desired fractions were combined and concentrated under reduced pressure to afford the desired product, 6-(3-methyl-4-pyridyl)-3-[3-(trifluoromethoxy)phenyl]imidazo[1,2-*b*]pyridazine, **263**, as a yellow solid (30 mg, 0.08 mmol, 24% yield). R_f 0.22 (100% EtOAc); m.p. 140-142 °C; $\bar{\nu}_{max}$ (neat)/cm^{-1} 3093 (C-H, w), 3035 (C-H, w), 1614 (C=N, m), 1593 (C=C, m), 1542 (C=C, m); 1247 (C-O, s), 1158 (C-O, s); ^{1}H NMR (500 MHz, DMSO-d$_6$) δ_H 8.65 (1H, s, H-2'), 8.60 (1H, d, *J*= 5.0 Hz, H-6'), 8.49 (1H, s, H-2), 8.39 (1H, d, *J*= 9.4 Hz, H-7), 8.26 (1H, s, H-2''), 8.18 (1H, d, *J*= 8.0 Hz, H-6''), 7.68 – 7.58 (3H, m, H-5', 5'' and 8), 7.41 – 7.35 (1H, m, H-4''), 2.44 (3H, s, H-1''''); ^{1}H NMR (600 MHz, DMSO- d$_6$) δ_H 8.69 – 8.51 (2H, m, H-2' and 6'), 8.41 (1H, s, H-2), 8.32 (1H, d, *J* = 9.5 Hz, H-7), 8.18 (1H, s, H-2''), 8.17 – 8.05 (1H, m, H-6''), 7.70 – 7.50 (3H, m, H-5', 5'' and 8), 7.30 (1H, d, *J* = 8.1 Hz, H-4''), 2.38 (3H, s, H-1''''); ^{13}C NMR (150 MHz, DMSO-d$_6$) δ_C 151.8 (C-2'), 151.4 (C-6), 148.7 (C-3''), 147.7 (C-6'), 142.8 (C-4'), 139.4 (C-8a), 134.6 (C-2), 130.9 (C-3'), 130.8 (C-5''), 130.5 (C-1''), 126.5 (C-7), 126.1 (C-3), 125.2 (C-6'''), 123.7 (C-5'), 120.1 (C-4''), 118.9 (C-8), 118.3 (C-2''). Signals at 120.14 ppm with (J_1 = 256.5 Hz) consistent with trifluoromethyl group; HRMS *m/z* (ESI$^+$) [Found: 371.1122., $C_{19}H_{14}F_3N_4O$ requires [M + H]$^+$ 371.1114]; LCMS (MDAP): Rt = 16.8 min, >95% (Method 3); *m/z* (ESI$^+$) 371.1 [M + H]$^+$.

6-(2-Methoxy-4-pyridyl)-3-[3-(trifluoromethoxy)phenyl]imidazo[1,2-*b*]pyridazine **264**

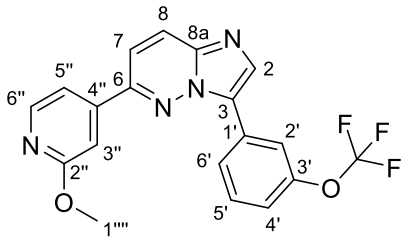

To a degassed microwave vial containing a solution of 6-chloro-3-[3-(trifluoromethoxy)phenyl]imidazo[1,2-*b*]pyridazine (80 mg, 0.26 mmol) in acetonitrile (0.80 mL) and water (0.20 mL) was added 2-methoxypyridine-4-boronic acid (78 mg, 0.51 mmol), bis[2-(di-*tert*-butylphosphanyl)cyclopenta-2,4-dien-1-yl]iron; dichloropalladium (8 mg, 0.01 mmol), and cesium carbonate (166 mg, 0.51 mmol). The vial was sealed and irradiated with microwaves at 140 °C for 20 min. The reaction mixture was concentrated under reduced pressure. The residue was partitioned between EtOAc (30 mL) and water (30 mL) and the layers separated. The aqueous layer was extracted further with EtOAc (2 x 30 mL). The organic components were combined and washed with saturated brine solution (50 mL), dried over $MgSO_4$, filtered and concentrated under reduced pressure. The crude was purified using flash reverse-phase column chromatography on a Biotage system (12 g C-18, elution with 10-100% MeOH / water gradient). Desired fractions were combined and concentrated under reduced pressure. The crude was purified using flash silica column chromatography on an Isco Combiflash system (12 g silica, elution with 0-50% 20% MeOH in CH_2Cl_2 / CH_2Cl_2 gradient). Desired fractions were combined and concentrated under reduced pressure to afford the desired product, 6-(2-methoxy-4-pyridyl)-3-[3-(trifluoromethoxy)phenyl]imidazo[1,2-*b*]pyridazine, **264**, as a yellow solid (55 mg, 0.14 mmol, 53% yield). R_f 0.43 (EtOAc / hexane 1:1); m.p. 138-140 °C; $\bar{\nu}_{max}$ (neat)/cm^{-1} 3068 (C-H, w), 3033(C-H, w), 1613 (C=N, m), 1560 (C=C, m), 1547 (C=C, m); 1244 (C-O, s), 1157 (C-O, s); ^{1}H NMR (500 MHz, DMSO-d$_6$) δ_H 8.49 (1H, s, H-2), 8.41 (1H, d, *J*= 9.4 Hz, H-7), 8.39 – 8.35 (2H, m, H-2' and 5''), 8.22 (1H, d, *J*= 7.9 Hz, H-6'), 8.02 (1H, d, *J*= 9.4 Hz, H-8), 7.74 – 7.66 (2H, m, H-5' and 6''), 7.54 (1H, s, H-3''), 7.44 – 7.39 (1H, m, H-4'), 3.94 (3H, s, H-1''''); ^{1}H NMR (600 MHz, DMSO-d$_6$) δ_H 8.40 (1H, s, H-2), 8.31 – 8.23 (3H, m, H-7, 2' and 5''), 8.11 (1H, d, *J* = 7.7 Hz, H-6'), 7.89 (1H, d, *J* = 9.5 Hz, H-8), 7.61 (1H, t, *J* = 8.0 Hz, H-5'), 7.58 – 7.54 (1H, m, H-6''), 7.40 (1H, s, H-3''), 7.35 – 7.29 (1H, m, H-4'), 3.87 (3H, s, H-1''''); ^{13}C NMR (150 MHz, DMSO-d$_6$) δ_C 164.5 (C-2''), 148.8 (C-6), 148.64 (d, *J* = 1.7 Hz, C-3'), 147.8 (C-5''), 145.2 (C-4''), 139.9 (C-8a), 134.9 (C-2), 130.7 (C-5'), 130.3 (C-1'), 126.6 (C-7), 126.0 (C-3), 125.0 (C-6'), 120.17 (q, *J* = 256.5 Hz, CF_3), 120.1 (C-4'), 118.0 (C-2'), 116.0 (C-8), 114.2 (C-6''), 108.0 (C-3''), 53.5 (C-1''''); HRMS *m/z* (ESI$^+$) [Found:

387.1075., $C_{19}H_{14}F_3N_4O_2$ requires $[M + H]^+$ 387.1063]; LCMS (LCQ): Rt = 3.68 min (Method 1); *m/z* (ESI^+) 387.25 $[M + H]^+$; LCMS (MDAP): Rt = 23.3 min, >95% (Method 3); *m/z* (ESI^+) 387.1 $[M + H]^+$.

6-(3-Methoxy-4-pyridyl)-3-[3-(trifluoromethoxy)phenyl]imidazo[1,2-*b*]pyridazine **265**

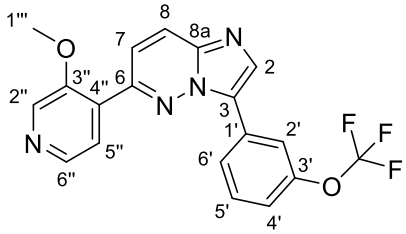

To a sealed and degassed microwave vial containing 6-chloro-3-[3-(trifluoromethoxy)phenyl]imidazo[1,2-*b*]pyridazine (100 mg, 0.32 mmol), 3-methoxy-4-(tetramethyl-1,3,2-dioxaborolan-2-yl)pyridine (150 mg, 0.64 mmol), sodium carbonate (68 mg, 0.64 mmol) and bis(triphenylphosphine)palladium(II) dichloride (11 mg, 0.02 mmol) was added water (0.10 mL) and acetonitrile (0.50 mL). The reaction mixture was irradiated with microwaves for 15 min at 140 °C. The reaction mixture was concentrated under reduced pressure and the residue was taken up in EtOAc (30 mL). The organic components were washed with water (2 x 30 mL), saturated brine solution (1 x 30 mL), and finally sodium hydroxide (2 x 30 mL). The combined organic components were dried over $MgSO_4$, filtered and concentrated to dryness under reduced pressure. The residue was purified using flash silica column chromatography on an Isco Combiflash system (12 g silica, elution with 0-15% 10% MeOH in CH_2Cl_2/ CH_2Cl_2 gradient). Desired fractions were combined and concentrated under reduced pressure to afford a yellow solid. The solid was purified using flash silica column chromatography on an Isco Combiflash system (12 g silica, elution with 70-100% EtOAc/ petroleum ether gradient). Trituration with diethyl ether afforded the title compound, 6-(3-methoxy-4-pyridyl)-3-[3-(trifluoromethoxy)phenyl]imidazo[1,2-*b*]pyridazine, **265**, as a yellow solid (60 mg, 0.15 mmol, 47% yield). R_f 0.41 (MeOH/ CH_2Cl_2 95:5); m.p. 167-169 °C; $\bar{\nu}_{max}$ (neat)/cm^{-1} 3106 (C-H, m), 3031 (C-H, m), 1613 (C=N, m), 1581 (C=C, m), 1580 (C=C, m), 1548 (C=C, m); 1475 (C=C, m), 1153 (C-O, s); ^{1}H NMR (600 MHz, DMSO-d$_6$) δ_H 8.61 (1H, s, H-2''), 8.43 (1H, s, H-2), 8.37 (1H, d, J = 4.8 Hz, H-6''), 8.32 – 8.25 (2H, m, H-2' and H-7), 8.16 (1H, d, *J* = 8.0 Hz, H-6'), 7.71 – 7.65 (2H, m, H-8 and H-5''), 7.61 (1H, t, *J* = 8.1 Hz, H-5'), 7.35 – 7.31 (1H, m, H-4'), 3.96 (3H, s, H-1'''); ^{13}C (150 MHz, DMSO-d$_6$) δ_C 152.7 (C-3''), 149.1 (C-6), 148.7 (C-3'), 142.5 (C-6''), 139.5 (C-8a), 135.6 (C-2''), 134.4 (C-2), 131.3 (C-4''), 130.8 (C-5'), 130.5 (C-1'), 126.0 (C-3), 125.5 (C-7), 125.1 (C-6'), 123.8 (C-5''), 120.2 (q, *J* = 255.6 Hz, CF_3), 120.0 (C-4'), 119.6 (C-8), 118.2 (C-2'), 56.7 (C-1'''); HRMS *m/z* (ESI$^+$) [Found: 387.1065., $C_{19}H_{13}F_3N_4O_2$ requires [M + H]$^+$ 387.1063]; LCMS (LCQ): Rt = 1.0 min (Method 1); *m/z* (ESI$^+$) 387.3 [M + H]$^+$; LCMS (MDAP): Rt = 15.4 min, >95% (Method 3); *m/z* (ESI$^+$) 387.0 [M + H]$^+$.

6-(4-Pyridyl)imidazo[1,2-*b*]pyridazine **266**

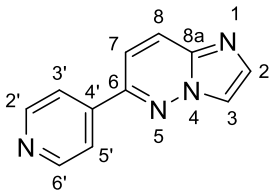

To a sealed and degassed microwave vial containing 6-chloroimidazo[1,2-*b*]pyridazine (1.0 g, 6.51 mmol), pyridine-4-boronic acid hydrate (1.2 g, 9.77 mmol), bis[2-(di-*tert*-butylphosphanyl)cyclopenta-2,4-dien-1-yl]iron; dichloropalladium (50 mg, 0.08 mmol), and sodium carbonate (1.38 g, 13.02 mmol) was added acetonitrile (10 mL) and water (0.5 mL) and the reaction mixture was heated to 80 °C overnight. The reaction mixture was concentrated under reduced pressure. The residue was partitioned between EtOAc (50 mL) and water (50 mL) and the aqueous layer removed. The aqueous layer was extracted with EtOAc (50 mL x 3). The organic components were combined and washed with brine solution (100 mL), dried over $MgSO_4$, filtered and concentrated under reduced pressure. The crude was purified using flash silica column chromatography on an Isco Combiflash system (12 g silica, elution with 0-50% 20% MeOH in CH_2Cl_2 / CH_2Cl_2 gradient). Desired fractions were concentrated under reduced pressure to afford the title compound, 6-(4-pyridyl)imidazo[1,2-*b*]pyridazine, **266**, as an off-white solid (400 mg, 1.94 mmol, 30% yield). R_f 0.66 (MeOH/ CH_2Cl_2 1:9); m.p. 146-148 °C; $\bar{\nu}_{max}$ (neat)/cm^{-1} 3132(C-H, w), 3091(C-H, w), 3076 (C-H, w), 1603 (C=N, m), 1557 (C=C, m), 1537 (C=C, m); ^{1}H NMR (500 MHz, DMSO-d$_6$) δ_H 8.63 (2H, d, *J* = 5.2 Hz, H-2' and 6'), 8.27 (1H, app. s, H-3), 8.15 (1H, d, *J* = 9.5 Hz, H-7), 7.89 (2H, d, *J* = 5.2 Hz, H-3' and 5'), 7.78 – 7.70 (2H, m, H-2 and 8); ^{13}C NMR (125 MHz, DMSO-d$_6$) δ_C 150.5 (C-2' and C-6'), 149.0 (C-6), 142.2 (C-4'), 138.1 (C-8a), 134.9 (C-2), 126.3 (C-7), 121.0 (C-3' and C-5'), 117.5 (C-3), 115.9 (C-8); HRMS *m/z* (ESI$^+$) [Found: 197.0819., $C_{11}H_9N_4$ requires [M + H]$^+$ 197.0822]; LCMS (LCQ): Rt = 0.6 min (Method 1); *m/z* (ESI$^+$) 197.3 [M + H]$^+$; LCMS (MDAP): Rt = 7.5 min, >95% (Method 3); *m/z* (ESI$^+$) 197.1 [M + H]$^+$.

3-[3-(Trifluoromethoxy)phenyl]imidazo[1,2-*b*]pyridazine **267**

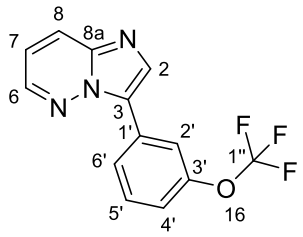

To 3-bromoimidazo[1,2-*b*]pyridazine (50 mg, 0.25 mmol) in water (0.5 mL):acetonitrile (3 mL) was added bis[2-(di-*tert*-butylphosphanyl)cyclopenta-2,4-dien-1-yl]iron; dichloropalladium (8 mg, 0.01 mmol), [3-(trifluoromethoxy)phenyl]boronic acid (52 mg, 0.25 mmol) and sodium carbonate (54 mg, 0.5 mmol). The reaction mixture was degassed for 2 min before it was irradiated with microwaves at 140 °C for 21 min. The reaction was concentrated under reduced pressure. The crude was purified using flash silica column chromatography on an Isco Combiflash system (12 g silica, elution with 0-100% EtOAc/ petroleum ether gradient). Desired fractions were combined and concentrated under reduced pressure to afford the title compound, 3-[3-(trifluoromethoxy)phenyl]imidazo[1,2-*b*]pyridazine, **267**, as a brown oil (65 mg, 0.22 mmol, 88% yield). R_f 0.16 (EtOAc / hexane 1:1); $\bar{\nu}_{max}$ (neat)/cm^{-1} 3099 (C-H, w), 3077(C-H, w), 1619 (C=N, m), 1585 (C=C, m), 1522 (C=C, m); 1146 (C-O, s); ^{1}H NMR (600 MHz, DMSO-d$_6$) δ_H 8.74 – 8.68 (1H, m, H-6), 8.43 (1H, s, H-2), 8.28 – 8.23 (2H, m, H-2' and 8), 8.21 (1H, d, *J*= 8.0 Hz, H-6'), 7.70 – 7.61 (1H, m, H-5'), 7.41 – 7.32 (2H, m, H-4' and 7); ^{13}C NMR (150 MHz, DMSO-d$_6$) δ_C 148.6 (C-3'), 144.1 (C-6), 140.3 (C-8a), 133.8 (C-2), 130.67 (C-1'or C-5'), 130.65 (C-1' or C-5'), 126.2 (C-8), 125.5 (C-3), 125.0 (C-6'), 120.1 (q, *J* = 256.4 Hz, C-1''), 119.8 (C-4'), 118.2 (C-2'), 117.7 (C-7); HRMS *m/z* (ESI$^+$) [Found: 280.0687., $C_{13}H_9F_3N_3O_1$ requires [M + H]$^+$ 280.0692]; LCMS (LCQ): Rt = 2.83 min (Method 1); *m/z* (ESI$^+$) 280.3 [M + H]$^+$;

3-Bromo-6-(4-pyridyl)imidazo[1,2-*b*]pyridazine **268**

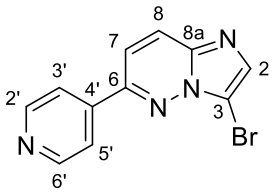

To a solution of 6-(4-pyridyl)imidazo[1,2-*b*]pyridazine (1 g, 5.1 mmol) in chloroform (15 mL) was added *N*-bromosuccinimide (1.09 g, 6.12 mmol) and the reaction mixture was stirred at rt overnight. The reaction was concentrated under reduced pressure. The crude was purified using flash silica column chromatography on an Isco Combiflash system (40 g silica, elution with 0-50% 20% MeOH in CH_2Cl_2 / CH_2Cl_2 gradient). Desired fractions combined and concentrated under reduced pressure to afford 3-bromo-6-(4-pyridyl)imidazo[1,2-*b*]pyridazine, **268**, as a peach solid (1.43 g, 2.6 mmol, 51% yield). R_f 0.15 (100% EtOAc); m.p. 218-220 °C; $\bar{\nu}_{max}$ (neat)/cm^{-1} 3099 (C-H, w), 3061 (C-H, w), 1600 (C=N, m), 1541 (C=C, m), 1407 (C=C, m); ^{1}H NMR (600 MHz, DMSO-d$_6$) δ_H 8.82 (2H, d, *J* = 5.0 Hz, H-2'' and 6''), 8.38 (1H, d, *J* = 9.5 Hz, H-7), 8.11 (2H, d, *J* = 5.0 Hz, H-3' and 5'), 8.05 (1H, s, H-2), 8.02 (1H, d, *J* = 9.5 Hz, H-8); ^{13}C NMR (150 MHz, DMSO-d$_6$) δ_C 150.6 (C-2'' and C-6''), 149.8 (C-6), 141.8 (C-4'), 139.1 (C-8a), 134.9 (C-2), 126.7 (C-7), 121.0 (C-3' and C-5'), 116.3 (C-8), 100.9 (C-3); HRMS *m/z* (ESI$^+$) [Found: 274.9916., $C_{11}H_7BrN_4$ requires [M]$^+$ 274.9927]; LCMS (LCQ): Rt = 0.59 min (Method 1); *m/z* (ESI$^+$) 275.2 [M]$^+$ and 277.2 [M+2]$^+$.

3-(3,6-Dihydro-2*H*-pyran-4-yl)-6-(4-pyridyl)imidazo[1,2-*b*]pyridazine **269**

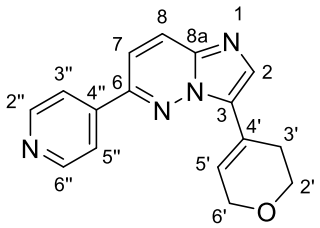

To a microwave vial containing a solution of 3-iodo-6-(4-pyridyl)imidazo[1,2-*b*]pyridazine (80 mg, 0.25 mmol) in water (0.5 mL):acetonitrile (3 mL) was added 3,6-dihydro-2*H*-pyran-4-boronic acid pinacol ester (104 mg, 0.5 mmol), potassium carbonate (69 mg, 0.5 mmol), and bis[2-(di-*tert*-butylphosphanyl)cyclopenta-2,4-dien-1-yl]iron; dichloropalladium (8 mg, 0.01 mmol). The vial was sealed and heated under microwave irradiation at 140 °C for 25 min. The reaction mixture was concentrated under reduced pressure. The crude was purified using flash reverse phase column chromatography on a Biotage system (12 g C-18, elution with 10-100% MeOH / water gradient). Desired fractions were combined and concentrated under reduced pressure. The residue was triturated with small amount of EtOH to afford the desired product, 3-(3,6-dihydro-2*H*-pyran-4-yl)-6-(4-pyridyl)imidazo[1,2-*b*]pyridazine, **269**, as a yellow solid (30 mg, 0.10 mmol, 41% yield). R_f 0.56 (MeOH/ CH_2Cl_2 1:9); m.p. 199-201 °C; $\bar{\nu}_{max}$ (neat)/cm^{-1} 3110 (C-H, w), 3036 (C-H, w), 2964 (C-H, w), 2907 (C-H, w), 2865 (C-H, w), 2813 (C-H, w), 1596 (C=C, m), 1546 (C=C, m); 1334 (C-O, s), 1213 (C-O, s), 1154 (C-O, s); ^{1}H NMR (500 MHz, DMSO-d$_6$) δ_H 8.76 (2H, app. d, *J* = 4.8 Hz, H-2'' and 6''), 8.33 (1H, d, *J*= 9.3 Hz, H-7), 8.08 – 8.05 (2H, m, H-3'' and 5''), 7.97 (1H, s, H-2), 7.94 (1H, d, *J*= 9.3 Hz, H-8), 7.32 – 7.26 (1H, m, H-5'), 4.39 – 4.31 (2H, m, H-6'), 3.88 (2H, t, *J*= 5.6 Hz, H-2'), 2.67 – 2.55 (2H, m, H-3'); ^{13}C NMR (150 MHz, DMSO-d$_6$) δ_C 150.6 (C-2'' and C-6''), 148.7 (C-4''), 142.3 (C-6), 139.5 (C-8a), 133.5 (C-2), 127.2 (C-3), 126.5 (C-7), 123.8 (C-5'), 122.3 (C-4'), 121.0 (C-3'' and C-5''), 115.2 (C-8), 64.9 (C-6'), 63.4 (C-2'), 26.1 (C-3'); HRMS *m/z* (ESI$^+$) [Found: 279.1251., $C_{16}H_{15}N_4O$ requires [M + H]$^+$ 279.1240]; LCMS (LCQ): Rt = 0.5 min (Method 1); *m/z* (ESI$^+$) 279.2 [M + H]$^+$; LCMS (MDAP): Rt = 10.8 min, >95% (Method 3); *m/z* (ESI$^+$) 279.2 [M + H]$^+$.

6-(4-Pyridyl)-3-tetrahydropyran-4-yl-imidazo[1,2-*b*]pyridazine **270**

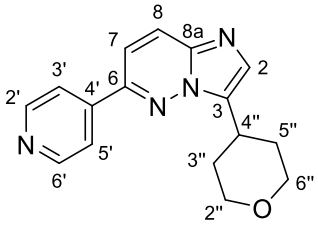

A two-neck flask containing a solution of 3-(3,6-dihydro-2*H*-pyran-4-yl)-6-(4-pyridyl)imidazo[1,2-*b*]pyridazine (100 mg, 0.36 mmol) in EtOH (2 mL) was evacuated and backfilled with nitrogen x 3. 10% palladium on carbon (4 mg, 0.04 mmol) was added followed by slow addition of ammonium formate (227 mg, 3.59mmol). The reaction mixture was heated to 75 °C for 32 h. The reaction mixture was filtered through celite under a shower of nitrogen. The filtrate was concentrated under reduced pressure. The crude was purified using flash silica column chromatography on an Isco Combiflash system (12 g silica, elution with 0-50% 20% MeOH in CH_2Cl_2 / CH_2Cl_2 gradient). Desired fractions were combined and concentrated under reduced pressure to afford yellow solid (30 mg). The residue was purified using flash reverse phase column chromatography on an Isco Combiflash system (12 g C-18, elution with 10-100% MeOH / water gradient). Desired fractions were combined and concentrated under reduced pressure to afford the desired product 6-(4-pyridyl)-3-tetrahydropyran-4-yl-imidazo[1,2-*b*]pyridazine, **270**, as a pale yellow solid (25 mg, 0.08 mmol, 22% yield). R_f 0.57 (MeOH/ CH_2Cl_2 1:9); m.p. 131-133 °C; $\bar{\nu}_{max}$ (neat)/cm^{-1} 3103 (C-H, w), 3047 (C-H, w), 2949 (C-H, m), 2923 (C-H, m), 2841 (C-H, m), 1597 (C=C, m), 1545 (C=C, m); 1306 (C-O, s), 1130 (C-O, s); ^{1}H NMR (600 MHz, DMSO-d$_6$) δ_H 8.80 (2H, d, *J*= 5.1 Hz, H-2' and 6'), 8.29 (1H, d, *J*= 9.5 Hz, H-7), 8.09 (2H, d, *J*= 5.7 Hz, H-3' and 5'), 7.89 (1H, d, *J*= 9.5 Hz, H-8), 7.74 (1H, s, H-2), 4.00 (2H, d, *J*= 12.0 Hz, H-2'' and 6''), 3.64 – 3.56 (2H, m, H-2'' and 6''), 3.54 – 3.47 (1H, m, H-4''), 2.08 (2H, d, *J*= 13.3 Hz, H-3'' and 5''), 1.90 – 1.79 (2H, m, H-3'' and 5''); ^{1}H NMR (600 MHz, $CDCl_3$) δ_H 8.87 – 8.68 (2H, m, H-2' and 6'), 8.04 (1H, d, *J* = 9.5 Hz, H-7), 7.86 (2H, d, *J* = 4.8 Hz, H-3' and 5'), 7.64 (1H, s, H-2), 7.47 (1H, d, *J* = 9.3 Hz, H-8), 4.10 (2H, d, *J* = 11.5 Hz, H-2'' and 6''), 3.66 (2H, t, *J* = 11.8 Hz, H-2'' and 6''), 3.55 – 3.47 (1H, m, H-4''), 2.13 (2H, d, *J* = 13.1 Hz, H-3'' and 5''), 2.03 – 1.90 (2H, m, H-3'' and 5''); ^{13}C NMR (150 MHz, $CDCl_3$) δ_C 150.8 (C-2' and C-6'), 148.7 (C-6), 143.1 (C-4'), 138.7 (C-3), 133.1 (C-8a), 131.5 (C-2), 126.4 (C-7), 121.0 (C-3' and C-5'), 114.2 (C-8), 68.0 (C-2'' and C-6''), 31.3 (C-4''), 30.7 (C-3'' and C-5''); HRMS *m/z* (ESI$^+$) [Found: 281.1396, $C_{16}H_{17}N_4O$ requires [M + H]$^+$ 281.1397]; LCMS (MDAP): Rt = 9.0 min, >95% (Method 3); *m/z* (ESI$^+$) 281.0 [M + H]$^+$.

6-(3,6-Dihydro-2*H*-pyran-4-yl)-3-[3-(trifluoromethoxy)phenyl]imidazo[1,2-*b*]pyridazine **271**

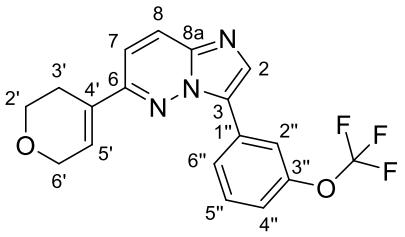

To a solution of 6-chloro-3-[3-(trifluoromethoxy)phenyl]imidazo[1,2-*b*]pyridazine (100 mg, 0.32 mmol) in water (0.5 mL):acetonitrile (3 mL) in a microwave vial was added 3,6-dihydro-2*H*-pyran-4-boronic acid pinacol ester (134 mg, 0.64 mmol), potassium carbonate (88 mg, 0.64 mmol), and bis[2-(di-*tert*-butylphosphanyl)cyclopenta-2,4-dien-1-yl]iron; dichloropalladium (10 mg, 0.02 mmol). The vial was sealed and heated under microwave irradiation to 140 °C for 25 min. The reaction mixture was concentrated under reduced pressure. The crude was purified using flash silica column chromatography on an Isco Combiflash system (12 g silica, elution with 100% EtOAc). Desired fractions were combined and concentrated under reduced pressure to afford the title compound, 6-(3,6-dihydro-2*H*-pyran-4-yl)-3-[3-(trifluoromethoxy)phenyl]imidazo[1,2-*b*]pyridazine, **271**, as a yellow solid (75 mg, 0.2 mmol, 62% yield). Rf. 0.40 (MeOH/ CH_2Cl_2 1:9); m.p. 140.2-142.1°C; $\bar{\nu}_{max}$ (neat)/cm^{-1} 3118 (C-H, w), 3043 (C-H, w), 2925 (C-H, w), 2857 (C-H, w), 1696 (C=C, w), 1613 (C=N, m), 1583 (C=C, m), 1549 (C=C, m); 1207 (C-O, s), 1155(C-O, s); ^{1}H NMR (500 MHz, DMSO-d$_6$) δ_H 8.37 (1H, s, H-2), 8.33 (1H, s, H-2''), 8.21 – 8.14 (2H, m, H-7 and 6'), 7.75 (1H, d, *J*= 9.6 Hz, H-8), 7.64 (1H, t, *J*= 8.1 Hz, H-5''), 7.36 (1H, d, *J*= 8.3 Hz, H-4''), 6.98 (1H, s, H-5'), 4.37 – 4.24 (2H, m, H-6'), 3.86 (2H, t, *J*= 5.5 Hz, H-2'), 2.64 (2H, d, *J*= 12.6 Hz, H-3'); ^{13}C NMR (125 MHz, DMSO-d$_6$) δ_C 151.1 (C-6), 148.7 (C-3''), 139.9 (C-8a), 133.8 (C-2), 130.9 (C-1'' or C-5' or C-5''), 130.8 (C-1'' or C-5' or C-5''), 130.7 (C-1'' or C-5' or C-5''), 125.9 (C-3), 125.6 (C-7), 125.0 (C-6''), 122.86 – 118.31 (m, CF_3), 120.0 (C-4''), 117.9 (C-2''), 115.0 (C-8), 65.0 (C-6'), 63.5 (C-2'), 24.7 (C-3'); HRMS *m/z* (ESI$^+$) [Found: 362.1103., $C_{18}H_{14}F_3N_3O_2$ requires [M + H]$^+$ 362.1111]; LCMS (LCQ): Rt = 2.23 min (Method 1); *m/z* (ESI$^+$) 362.15 [M + H]$^+$; LCMS (MDAP): Rt = 18.29 min, >95% (Method 3); *m/z* (ESI$^+$) 362.1 [M + H]$^+$.

6-Tetrahydropyran-4-yl-3-[3-(trifluoromethoxy)phenyl]imidazo[1,2-*b*]pyridazine **272**

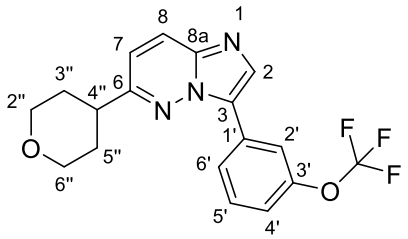

To a solution of 6-(3,6-dihydro-2*H*-pyran-4-yl)-3-[3-(trifluoromethoxy)phenyl]imidazo[1,2-*b*]pyridazine (25 mg, 0.07 mmol) in EtOH (3 mL) under nitrogen was added palladium on carbon 10% wetted with water (7 mg, 0.07 mmol) and the reaction mixture was stirred at rt. The reaction flask was evacuated and backfilled three times with nitrogen gas before adding a balloon filled with hydrogen gas. A second balloon filled with hydrogen was added and the reaction stirred at rt for 24 h. The reaction was filtered through celite and the filtrate concentrated under reduced pressure. The crude was purified using flash silica column chromatography on an Isco Combiflash system (12 g silica, elution with 0-100% EtOAc / petroleum ether gradient). Desired fractions were combined and concentrated under reduced pressure to afford the desired product, 6-tetrahydropyran-4-yl-3-[3-(trifluoromethoxy)phenyl]imidazo[1,2-*b*]pyridazine, **272**, as an off-white solid (25 mg, 0.07 mmol, 94% yield). R_f 0.35 (100% EtOAc); m.p. 178-180 °C; $\bar{\nu}_{max}$ (neat)/cm^{-1} 3110 (C-H, w), 3039 (C-H, w), 1675 (C=N, m), 1584 (C=C, m), 1552 (C=C, m); 1242 (C-O, s), 1156 (C-O, s); ^{1}H NMR (500 MHz, DMSO-d$_6$) δ_H 8.39 – 8.33 (2H, m, H-2, 2' or 6'), 8.21 – 8.15 (2H, m, H-7, 2' or 6'), 7.65 (1H, t, *J* = 8.1 Hz, H-5'), 7.40 – 7.33 (2H, m, H-4' and 8), 3.98 (2H, dd, *J* = 11.7, 4.0 Hz, H-2'' and 6''), 3.49 (2H, dd, *J* = 12.6, 10.6 Hz, H-2'' and 6''), 3.20 – 3.11 (1H, m, H-4''), 1.94 (2H, d, *J* = 13.0 Hz, H-3'' and 5''), 1.82 (2H, qd, *J* = 12.3, 4.3 Hz, H-3'' and 5''); ^{13}C NMR (125 MHz, DMSO-d$_6$) δ_C 158.4 (C-6), 148.7 (C-3'), 139.7 (C-8a), 133.6 (C-2), 130.9 (C-5' or/and C-1'), 126.2 (C-7), 125.6 (C-3), 125.0 (C-6'), 119.9 (C-4'), 118.2 (C-8), 117.9 (C-2'), 66.9 (C-2'' and 6''), 40.4 (C-4''), 31.2 (C-3'' and 5''). Signal at 120.1 with J_1 = 256.4 Hz consistent with trifluoromethyl group. HRMS *m/z* (ESI$^+$) [Found: 364.1259., $C_{18}H_{17}F_3N_3O_2$ requires [M + H]$^+$ 364.1267]; LCMS (LCQ): Rt = 1.88 min (Method 1); *m/z* (ESI$^+$) 364.3 [M + H]$^+$; LCMS (MDAP): Rt = 19.6 min, >95% (Method 3); *m/z* (ESI$^+$) 364.1 [M + H]$^+$.

4-[3-[3-(Trifluoromethoxy)phenyl]imidazo[1,2-*b*]pyridazin-6-yl]morpholine **273**

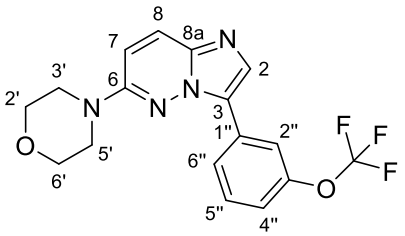

To a microwave vial containing a solution of 6-chloro-3-[3-(trifluoromethoxy)phenyl]imidazo[1,2-*b*]pyridazine (111 mg, 0.32 mmol) in 1,4-dioxane (2 mL) was added morpholine (0.08 mL, 0.96 mmol), XPhos (15 mg, 0.03 mmol), sodium hydroxide (26 mg, 0.64 mmol) and palladium(II)acetate (4 mg, 0.02 mmol) was then added to the vial and the reaction was heated to 90 °C over the weekend. Another equivalent morpholine (0.08 mL, 0.96 mmol) was added and the reaction mixture was heated to 110°C overnight. The reaction was concentrated under reduced pressure. The crude was purified using flash silica column chromatography on an Isco Combiflash system (12 g silica, elution with 0-10% 20% MeOH in CH_2Cl_2 / CH_2Cl_2 gradient). Desired fractions were concentrated under reduced pressure. The crude was purified using flash silica column chromatography on an Isco Combiflash system (12 g silica, elution with 100% EtOAc isocratic. Desired fractions were combined and concentrated under reduced pressure to afford the desired product, 4-[3-[3-(trifluoromethoxy)phenyl]imidazo[1,2-*b*]pyridazin-6-yl]morpholine, **273**, as a yellow solid (30 mg, 0.08 mmol, 25% yield). R_f 0.57 (MeOH/ CH_2Cl_2 1:9); m.p. 111-113 °C; $\bar{\nu}_{max}$ (neat)/cm^{-1} 3114(C-H, w), 2992 (C-H, w), 2929 (C-H, w), 2902 (C-H, w), 2860 (C-H, w), 1617 (C=N, m), 1584 (C=C, m), 1555 (C=C, m); 1250 (C-O, s), 1120 (C-O, s); ^{1}H NMR (500 MHz, DMSO-d$_6$) δ_H 8.29 (1H, s, H-2''), 8.12 (1H, s, H-2), 8.09 (1H, d, *J*= 8.0 Hz, H-6''), 7.97 (1H, d, *J*= 10.0 Hz, H-7), 7.58 (1H, t, *J*= 8.1 Hz, H-5''), 7.31 – 7.24 (2H, m, H-4'' and 8), 3.74 (4H, t, *J*= 4.8 Hz, H-2' and 6'), 3.48 (4H, t, *J*= 4.8 Hz, 4H, H-3' and 5'); ^{1}H NMR (600 MHz, $CDCl_3$) δ_H 8.19 (1H, s, H-2), 7.97 – 7.74 (3H, m, H-2'', 6'' and 7), 7.50 – 7.42 (1H, m, H-5''), 7.16 (1H, d, *J* = 8.3 Hz, H-4''), 6.86 (1H, d, *J* = 10.0 Hz, H-8), 3.87 (4H, q, *J* = 3.9, 2.7 Hz, H-2' and H-6'), 3.52 (4H, q, *J* = 3.9, 2.7 Hz, 4H, H-3' and 5'); ^{13}C NMR (150 MHz, $CDCl_3$) δ_C 155.1 (C-6), 149.6 (C-3'')*, 138.1 (C-8a)*, 131.9 (C-2)*, 131.3 (C-1''), 130.0 (C-5''), 126.9 (C-3)*, 126.6 (C-7)*, 124.7 (C-6'')*, 119.9 (C-4'')*, 118.6 (C-2'')*, 109.6 (C-8)*, 66.5 (C-2' and C-6'), 46.8 (C-3' and C-5'). Trifluoromethyl group signals not observed. Signals* assigned based on similarity to analogues. HRMS *m/z* (ESI$^+$) [Found: 365.1214., $C_{17}H_{16}F_3N_4O_2$ requires [M + H]$^+$ 365.1220]; LCMS (LCQ): Rt = 0.6 min (Method 1); *m/z* (ESI$^+$) 365.3 [M + H]$^+$; LCMS (MDAP): Rt = 15.6 min, >95% (Method 3); *m/z* (ESI$^+$) 365.1 [M + H]$^+$.

6-Chloro-2-methyl-imidazo[1,2-*b*]pyridazine **274**

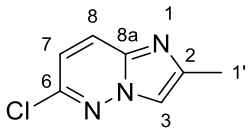

To a microwave vial containing 6-chloropyridazin-3-amine (2.35 g, 36.67 mmol) in EtOH (15 mL) was added chloroacetone (3.39 g, 36.67 mmol) and TEA (2.53 mL). The reaction mixture was heated to 150 °C and stirred for 1 h. The reaction mixture was concentrated under reduced pressure. The crude was purified using flash silica column chromatography on an Isco Combiflash system (40 g silica, elution with 30-50% EtOAc / petroleum ether gradient). Desired fractions were combined and concentrated under reduced pressure to afford 6-chloro-2-methyl-imidazo[1,2-*b*]pyridazine, **274**, as an off-white solid (2.8 g, 15.87 mmol, 87% yield). R_f 0.65 (MeOH/ CH_2Cl_2 1:9); ^{1}H NMR (500 MHz, DMSO- d_6) δ_H 8.10 (1H, s, H-3), 8.07 (1H, d, *J* = 9.5 Hz, H-7), 7.28 (1H, d, *J* = 9.5 Hz, H-8), 2.37 (3H, s, H-1'); LCMS (LCQ): Rt = 0.9 min (Method 1); *m/z* (ESI$^+$) 168.2 [M + H]$^+$; LCMS (MDAP): Rt = 10.8 min, (Method 3); *m/z* (ESI$^+$) 168.1 [M + H]$^+$.

2-Methyl-6-(4-pyridyl)imidazo[1,2-*b*]pyridazine **275**

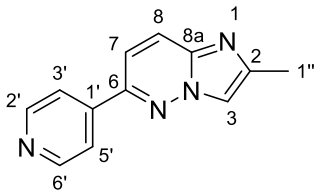

To a sealed and degassed vial containing pyridine-4-boronic acid hydrate (220 mg, 1.79 mmol), bis[2-(di-*tert*-butylphosphanyl)cyclopenta-2,4-dien-1-yl]iron; dichloropalladium (29 mg, 0.04 mmol), sodium carbonate (190 mg, 1.79 mmol), and 6-chloro-2-methyl-imidazo[1,2-*b*]pyridazine (150 mg, 0.89 mmol) was added acetonitrile (2 mL) and water (0.20 mL). The reaction mixture was heated to 80 °C and stirred overnight. Additional equivalents of pyridine-4-boronic acid hydrate (220 mg, 1.79 mmol), sodium carbonate (190 mg, 1.79 mmol) and bis[2-(di-*tert*-butylphosphanyl)cyclopenta-2,4-dien-1-yl]iron; dichloropalladium (29 mg, 0.04 mmol) were added, the vial was degassed, and the reaction was irradiated with microwaves at 140°C for 25 min. The reaction mixture was concentrated under reduced pressure. The residue was partitioned between EtOAc (30 mL) and water (30 mL), and the organic layers separated. The aqueous layer was extracted with EtOAc (2 x 30 mL). The organic components were combined, washed with brine solution (50 mL), dried over $MgSO_4$, filtered and concentrated under reduced pressure. The crude was purified using flash silica column chromatography on an Isco Combiflash system (12 g silica, elution with 0-50% 20% MeOH in CH_2Cl_2 / CH_2Cl_2 gradient). Desired fractions were combined and concentrated under reduced pressure to afford 2-methyl-6-(4-pyridyl)imidazo[1,2-*b*]pyridazine, **275**, as a pale yellow solid. (140 mg, 0.63 mmol, 71% yield). R_f 0.45 (MeOH/ CH_2Cl_2 1:9); m.p. 84-86 °C; $\bar{\nu}_{max}$ (neat)/cm^{-1} 3131 (C-H, w), 3040(C-H, w), 2927 (C-H, w), 1599 (C=N, m), 1594 (C=C, m), 1546 (C=C, m); 1531 (C=C, m); ^{1}H NMR (500 MHz, DMSO-d$_6$) δ_H 8.75 (2H, d, *J*= 4.5 Hz, H-2' and 6'), 8.20 – 8.12 (2H, m, H-3 and 7), 8.02 (2H, d, *J*= 4.5 Hz, H-3' and 5'), 7.84 (1H, d, *J*= 9.4 Hz, H-8), 2.42 (3H, s, H-1''); ^{1}H NMR (600 MHz, DMSO-d$_6$) δ_H 8.74 – 8.41 (2H, m, H-2' and 6'), 8.00 – 7.88 (2H, m, H-3 and 7), 7.87 – 7.71 (2H, m, H-3' and 5'), 7.60 (1H, d, *J* = 9.5 Hz, H-8), 2.24 (3H, s, H-1''); ^{13}C NMR (150 MHz, DMSO-d$_6$) δ_C 150.4 (C-2' and C-6'), 147.9 (C-6), 144.5 (C-2), 142.2 (C-4'), 137.6 (C-8a), 124.7 (C-7), 120.7 (C-3' and C-5'), 115.0 (C-8), 114.5 (C-3), 14.6 (C-1''); HRMS *m/z* (ESI$^+$) [Found: 211.0988., $C_{12}H_{11}N_4$ requires [M + H]$^+$ 211.0978]; LCMS (LCQ): Rt = 0.5 min (Method 1); *m/z* (ESI$^+$) 211.3 [M + H]$^+$; LCMS (MDAP): Rt = 8.0 min, >95% (Method 3); *m/z* (ESI$^+$) 211.1 [M + H]$^+$.

6-Chloro-2-isopropyl-imidazo[1,2-*b*]pyridazine **276**

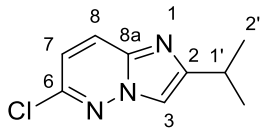

To a microwave vial containing 6-chloropyridazin-3-amine (1.50 g, 11.58 mmol) in 2-propanol (15 mL) was added 1-bromo-3-methyl-2-butanone (1.91 g, 11.58 mmol) and TEA (1.61 mL). The reaction mixture was heated to 120 °C and stirred for 2.5 h. The reaction mixture was concentrated under reduced pressure. The residue was partitioned between EtOAc (100 mL) and water (100 mL), and the organic layer separated. The aqueous layer was extracted with EtOAc (2 x 100 mL). The organic components were combined, washed with brine solution (100 mL), dried over $MgSO_4$, filtered and concentrated under reduced pressure. The crude was purified using flash silica column chromatography on an Isco Combiflash system (12 g silica, elution with 0-70% EtOAc / petroleum ether gradient). Desired fractions were combined and concentrated under reduced pressure to afford 6-chloro-2-isopropyl-imidazo[1,2-*b*]pyridazine, **276**, as a gold solid (900 mg, 4.37 mmol, 38% yield). R_f 0.55 (MeOH/ CH_2Cl_2 1:18); ^{1}H NMR (600 MHz, DMSO- d_6) δ_H 8.12 (1H, s, H-3), 8.10 (1H, d, *J* = 9.4 Hz, H-7), 7.29 (1H, d, *J* = 9.4 Hz, H-8), 3.04 (1H, hept, *J* = 6.9 Hz, H-1'), 1.29 (d, *J* = 6.9 Hz, 6H, H-2'); LCMS (MDAP): Rt = 3.88 min, (Method 5); *m/z* (ESI$^+$) 195.9 [M]$^+$ and 197.9 [M+2]$^+$.

6-(4-Pyridyl)pyridazin-3-amine **278**

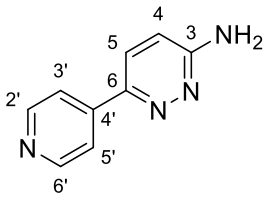

A microwave vial containing 6-chloropyridazin-3-amine (400 mg, 3.09 mmol), pyridine-4-boronic acid hydrate (570 mg, 4.64 mmol), potassium phosphate tribasic (692 mg, 3.26 mmol) and bis(triphenylphosphine)palladium(II)dichloride (108 mg, 0.15 mmol) in 1-butanol (6 mL): water (1.5 mL) was sealed and heated to 130 °C and stirred for 16 h. The residue was partitioned between EtOAc (100 mL) and water (10 mL), and the organic layers separated. The aqueous layer was extracted with EtOAc (100 mL). The organic components were combined, washed with brine solution (50 mL), dried over $MgSO_4$, filtered and concentrated under reduced pressure. The crude was purified using flash silica column chromatography on an Isco Combiflash system (40 g silica, elution with 0-50% 20% MeOH in CH_2Cl_2 / CH_2Cl_2 gradient). Desired fractions were combined and concentrated under reduced pressure to afford 6-(4-pyridyl)pyridazin-3-amine, **278**, as a pale yellow solid. (110 mg, 0.61 mmol, 20% yield). R_f 0.20 (MeOH/ CH_2Cl_2 1:9); ^{1}H NMR (500 MHz, DMSO- d_6) δ_H 8.64 (2H, d, *J* = 4.7 Hz, H-2' and 6'), 8.01 – 7.86 (3H, m, H-3', 5' and 5), 6.87 (1H, d, *J* = 9.3 Hz, H-4), 6.77 (2H, s, NH_2); LCMS (LCQ): Rt = 0.4 min (Method 1); *m/z* (ESI$^+$) 173.3 [M + H]$^+$. The spectroscopic data are in good agreement with the literature values. Literature reference: WO 2010/056875 PCT/US2009/064224 page 212

6-(4-Pyridyl)-2-(trifluoromethyl)imidazo[1,2-*b*]pyridazine **279**

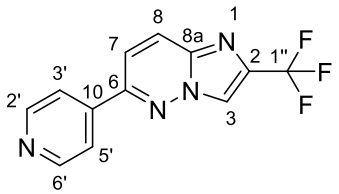

To a solution of 6-(4-pyridyl)pyridazin-3-amine (80 mg, 0.46 mmol) in EtOH (1.5 mL) was added TEA (0.06 mL, 0.46 mmol) and 1-bromo-3,3,3-trifluoroacetone (0.1 mL, 0.93 mmol). The reaction mixture was stirred at 150 °C for 4 h. The reaction mixture was concentrated under reduced pressure. The residue was purified using flash reverse phase column chromatography on an Isco Combiflash system (40 g C-18, elution with 10-100% MeOH / water gradient). Desired fractions were combined and concentrated under reduced pressure. The crude was purified using flash silica column chromatography on an Isco Combiflash system (12 g silica, elution with 30-100% EtOAc / petroleum ether gradient). Desired fractions were combined and concentrated under reduced pressure to afford the desired product, 6-(4-pyridyl)-2-(trifluoromethyl)imidazo[1,2-*b*]pyridazine, **279**, as a white solid (16 mg, 0.06 mmol, 12% yield). R_f 0.55 (MeOH/ CH_2Cl_2 1:9); m.p. 222-224 °C; $\bar{\nu}_{max}$ (neat)/cm^{-1} 3099 (C-H, w), 3077(C-H, w), 3039 (C-H, w), 1653 (C=N, m), 1597 (C=C, m), 1549 (C=C, m); ^{1}H NMR (500 MHz, DMSO-d$_6$) δ_H 9.12 (1H, s, H-3), 8.81 (2H, d, *J* = 4.9 Hz, H-2' and 6'), 8.46 (1H, d, *J* = 9.6 Hz, H-7), 8.11 (1H, d, J = 9.6 Hz, H-8), 8.07 (2H, d, *J* = 4.9 Hz, H-3' and 5'); ^{1}H NMR (600 MHz, MeOD) δ_H 8.81 – 8.73 (3H, m, H-2' and H-6', H-3), 8.27 (1H, d, *J* = 9.6 Hz, H-7), 8.17 – 8.11 (2H, m, H-3' and 5'), 8.04 (1H, d, *J* = 9.6 Hz, H-8); ^{13}C NMR (150 MHz, MeOD) δ_C 152.7 (C-6), 151.2 (C-2' and C-6'), 144.3 (C-4'), 140.6 (C-8a), 136.89 (d, *J* = 39.7 Hz, , C-2), 128.0 (C-7), 122.9 (C-3' and C-5'), 120.2 (C-8), 118.25 (q, *J* = 3.8 Hz, C-3). Quartet at 124.6 ppm with J_1 = 260.8 Hz is consistent with trifluoromethyl group. HRMS *m/z* (ESI$^+$) [Found: 265.0712., $C_{12}H_8F_3N_4$ requires [M + H]$^+$ 265.0696]; LCMS (MDAP): Rt = 21.1 min, >95% (Method 3); *m/z* (ESI$^+$) 265.0 [M + H]$^+$.

6-(4-Pyridyl)-2-[3-(trifluoromethoxy)phenyl]imidazo[1,2-*b*]pyridazine **280**

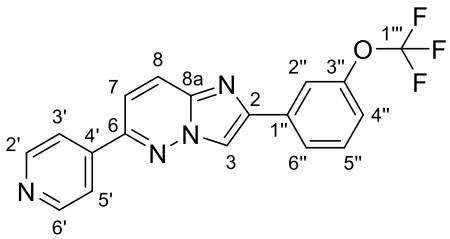

To a solution of 6-(4-pyridyl)pyridazin-3-amine (80 mg, 0.46 mmol) in EtOH (1.5 mL) was added TEA (0.06 mL, 0.46 mmol) and 2-bromo-1-[3-(trifluoromethoxy)phenyl]ethanone (263 mg, 0.93 mmol). The reaction mixture was stirred at 150 °C overnight. The reaction was concentrated under reduced pressure. The residue was purified using flash reverse phase column chromatography on an Isco Combiflash system (12 g C-18, elution with 10-100% MeOH / water gradient). Desired fractions were combined and concentrated under reduced pressure. The crude was purified using flash silica column chromatography on an Isco Combiflash system (12 g silica, elution with 30-100% EtOAc / petroleum ether gradient). Desired fractions were combined and concentrated under reduced pressure to afford the desired product, 6-(4-pyridyl)-2-[3-(trifluoromethoxy)phenyl]imidazo[1,2-*b*]pyridazine, **280**, as a pale yellow solid (10 mg, 0.03 mmol, 6% yield). R_f 0.57 (1/9 MeOH / CH_2Cl_2); m.p. 185-187 °C; $\bar{\nu}_{max}$ (neat)/cm^{-1} 3095 (C-H, w), 3058(C-H, w), 2916 (C-H, w), 2848 (C-H, w), 1604 (C=N, m), 1544 (C=C, 1206 (C-O, s), 1147 (C-O, s); ^{1}H NMR (500 MHz, DMSO-d$_6$) δ_H 9.14 (1H, s, H-3), 8.80 (2H, d, *J*= 4.6 Hz, H-2' and 6'), 8.36 (1H, d, *J*= 9.6 Hz, H-7), 8.13 (1H, d, *J*= 7.8 Hz, H-6''), 8.10 – 8.03 (3H, m, H-2'', 3' and 5'), 7.97 (1H, d, *J*= 9.6 Hz, 1H, H-8), 7.63 (1H, t, *J*= 8.1 Hz, H-5''), 7.38 (1H, d, *J*= 8.2 Hz, H-4''); ^{1}H NMR (600 MHz, MeOD) δ_H 8.82 – 8.67 (3H, m, H-2' and 6', 3), 8.19 – 8.11 (3H, m, H-3' and 5', 7), 8.03 – 8.00 (1H, m, H-6''), 7.96 (1H, s, H-2''), 7.91 (1H, d, *J* = 9.5 Hz, H-8), 7.59 (1H, t, *J* = 8.0 Hz, H-5''), 7.34 – 7.29 (1H, m, H-4''); ^{13}C NMR (150 MHz, MeOD) δ_C 151.2 – 151.16 (m, C-3''), 151.11 (C-2' and 6'), 151.0 (C-6), 146.1 (C-2), 144.9 (C-4'), 140.7 (C-8a), 136.6 (C-1''), 131.7 (C-5''), 126.4 (C-7), 125.9 (C-6''), 122.9 (C-3' and 5'), 122.0 (C4''), 119.5 (C-2''), 118.2 (C-8), 115.7 (C-3). Quartet at 122.0 ppm with J_1 = 255.9 Hz is consistent with trifluoromethyl group. HRMS *m/z* (ESI$^+$) [Found: 357.0973., $C_{18}H_{12}F_3N_4O$ requires [M + H]$^+$ 357.0958]; LCMS (MDAP): Rt = 25.0 min, >95% (Method 3); *m/z* (ESI$^+$) 357.0 [M + H]$^+$.

3-Bromo-2-methyl-6-(4-pyridyl)imidazo[1,2-*b*]pyridazine **281**

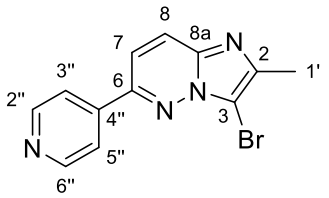

To a solution of 2-methyl-6-(4-pyridyl)imidazo[1,2-*b*]pyridazine (330 mg, 1.57 mmol) in DMF (3 mL) was added *N*-bromosuccinimide (300 mg, 1.69 mmol). The reaction mixture was stirred at rt overnight. The reaction mixture was concentrated under reduced pressure. The crude was purified using flash silica column chromatography on an Isco Combiflash system (24 g silica, elution with 0-50% 20% MeOH in CH_2Cl_2 / CH_2Cl_2 gradient). Desired fractions were combined and concentrated under reduced pressure to afford 3-bromo-2-methyl-6-(4-pyridyl)imidazo[1,2-*b*]pyridazine as a gold solid (600 mg, 1.04 mmol, 66% yield).

50 mg of the crude was purified using flash reverse phase column chromatography on a Biotage system (12 g C-18, elution with 10-100% MeOH / water gradient). Desired fractions were combined and concentrated under reduced pressure to afford 3-bromo-2-methyl-6-(4-pyridyl)imidazo[1,2-*b*]pyridazine, **281**, as a white solid (30 mg, 0.1 mmol). R_f 0.43 (MeOH/ CH_2Cl_2 1:9); ^{1}H NMR (600 MHz, DMSO- d_6) δ_H 8.81 – 8.76 (2H, m, H-2'' and 6''), 8.24 (1H, d, *J* = 9.4 Hz, H-7), 8.09 – 8.05 (2H, m, H-3'' and 5''), 7.96 (1H, d, *J* = 9.4 Hz, H-8), 2.44 (3H, s, H-1'); LCMS (LCQ): Rt = 1.0 min (Method 1); *m/z* (ESI$^+$) 289.2 [M]$^+$ and 291.2 [M+2]$^+$.

2-Methyl-6-(4-pyridyl)-3-[3-(trifluoromethoxy)phenyl]imidazo[1,2-*b*]pyridazine **282**

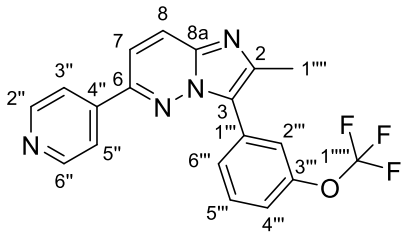

To a microwave vial containing bis[2-(di-*tert*-butylphosphanyl)cyclopenta-2,4-dien-1-yl]iron; dichloropalladium (23 mg, 0.03 mmol), [3-(trifluoromethoxy)phenyl]boronic acid (214 mg, 1.04 mmol), 3-bromo-2-methyl-6-(4-pyridyl)imidazo[1,2-*b*]pyridazine (200 mg, 0.35 mmol) and cesium carbonate (225 mg, 0.69 mmol) was added water (1 mL) and acetonitrile (8 mL). The reaction vial was evacuated and backflushed with nitrogen x 3 before the reaction mixture was heated to 110°C for 48 h. The reaction mixture was concentrated under reduced pressure. The crude was purified using flash silica column chromatography on an Isco Combiflash system (12 g silica, elution with 0-10% MeOH / EtOAc gradient). Desired fractions were combined and concentrated under reduced pressure. The residue was purified using flash reverse phase column chromatography on an Isco Combiflash system (20 g C-18, elution with 10-100% MeOH / water gradient). Desired fractions were combined and concentrated under reduced pressure. Desired fractions were combined and concentrated under reduced pressure to afford the desired product, 2-methyl-6-(4-pyridyl)-3-[3-(trifluoromethoxy)phenyl]imidazo[1,2-*b*]pyridazine, **282**, as a yellow solid (80 mg, 0.21 mmol, 59% yield). R_f 0.37 (MeOH/ CH_2Cl_2 1:9); m.p. 126-128 °C; $\bar{\nu}_{max}$ (neat)/cm^{-1} 3095 (C-H, w), 3031 (C-H, w), 2923 (C-H, w), 1608 (C=N, m), 1597 (C=C, m), 1544 (C=C, m); 1212 (C-O, s), 1144 (C-O, s); ^{1}H NMR (600 MHz, MeOD) δ_H 8.69 (2H, d, *J* = 5.4 Hz, H-2'' and 6''), 8.12 (1H, d, *J* = 9.5 Hz, H-7), 8.04 (1H, d, *J* = 5.4 Hz, H-3'' and 5''), 7.91 (1H, d, *J* = 9.5 Hz, H-8), 7.84 – 7.76 (2H, m, H-2''' and 6'''), 7.69 (1H, t, *J* = 8.0 Hz, H-5'''), 7.42 – 7.37 (1H, m, H-4'''), 2.63 (3H, s, H-1''''); ^{13}C NMR (150 MHz, MeOD) δ_C 151.0 (C-2'' and C-6''), 150.56 (d, *J* = 1.7 Hz, C-3'''), 150.0 (C-6), 145.0 (C-4''), 144.3 (C-2), 139.4 (C-8a), 131.6 (C-1'''), 131.5 (C-5'''), 129.1 (C-6'''), 125.9 (C-7), 125.3 (C-3), 122.8 (C-2'''), 122.6 (C-3'' and C-5''), 122.0 (C-4'''), 117.5 (C-8), 14.8 (C-1''''). Signals at 122.04 ppm with J_1 = 256.0 Hz consistent with trifluoromethyl group. HRMS *m/z* (ESI$^+$) [Found: 371.1113., $C_{19}H_{14}F_3N_4O$ requires [M + H]$^+$ 371.1114]; LCMS (MDAP): Rt = 17.6 min, >95% (Method 3); *m/z* (ESI$^+$) 371.9 [M + H]$^+$.

3-Bromo-2-isopropyl-6-(4-pyridyl)imidazo[1,2-*b*]pyridazine **283**

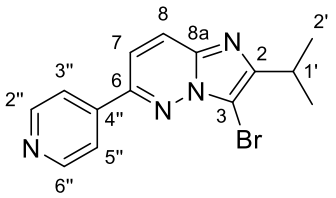

To a solution of 2-isopropyl-6-(4-pyridyl)imidazo[1,2-*b*]pyridazine (180 mg, 0.42 mmol) in DMF (1.44 mL) was added *N*-bromosuccinimide (79 mg, 0.45 mmol). The reaction mixture was stirred at rt overnight. The reaction mixture was concentrated under reduced pressure. The crude was purified using flash silica column chromatography on an Isco Combiflash system (24 g silica, elution with 0-50% 20% MeOH in CH_2Cl_2 / CH_2Cl_2 gradient). Desired fractions were combined and concentrated under reduced pressure to afford 3-bromo-2-isopropyl-6-(4-pyridyl)imidazo[1,2-*b*]pyridazine, **283**, as a yellow solid (255 mg, 0.4 mmol, 97% yield). R_f 0.45 (MeOH/ CH_2Cl_2 1:9); ^{1}H NMR (600 MHz, DMSO- d_6) δ_H 8.81 – 8.76 (2H, m, H-2'' and 6''), 8.27 (1H, d, *J* = 9.4 Hz, H-7), 8.10 – 8.05 (2H, m, H-3'' and 5''), 7.96 (1H, d, *J* = 9.4 Hz, H-8), 3.23 (1H, hept, *J* = 6.9 Hz, H-1'), 1.32 (6H, d, *J* = 6.9 Hz, H-2'); LCMS (LCQ): Rt = 1.30 min (Method 1); *m/z* (ESI$^+$) 317.2 [M]$^+$ and 319.2 [M+2]$^+$.

2-Isopropyl-6-(4-pyridyl)-3-[3-(trifluoromethoxy)phenyl]imidazo[1,2-*b*]pyridazine **284**

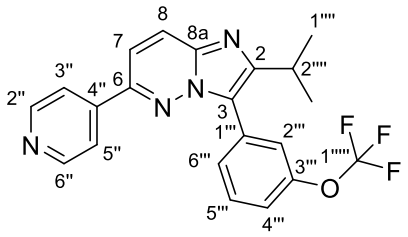

To a microwave vial containing bis[2-(di-*tert*-butylphosphanyl)cyclopenta-2,4-dien-1-yl]iron; dichloropalladium (15 mg, 0.02 mmol), [3-(trifluoromethoxy)phenyl]boronic acid (146 mg, 0.71 mmol), 3-bromo-2-isopropyl-6-(4-pyridyl)imidazo[1,2-*b*]pyridazine (150 mg, 0.24 mmol) and cesium carbonate (154 mg, 0.47 mmol) was added water (1 mL) and acetonitrile (10 mL). The reaction vial was evacuated and backflushed with nitrogen x 3 before the reaction mixture was heated to 110 °C for 48 h conventionally. The crude was purified using flash silica column chromatography on an Isco Combiflash system (12 g silica, elution with 0-10% MeOH / EtOAc gradient). Desired fractions were combined and concentrated under reduced pressure. The residue was purified using flash reverse phase column chromatography on an Isco Combiflash system (20 g C-18, elution with 10-100% MeOH / water gradient). Desired fractions were combined and concentrated under reduced pressure to afford the desired product, 2-isopropyl-6-(4-pyridyl)-3-[3-(trifluoromethoxy)phenyl]imidazo[1,2-*b*]pyridazine, **284**, as a yellow solid (60 mg, 0.14 mmol, 61% yield). R_f 0.50 (MeOH/ CH_2Cl_2 1:9); m.p. 98-100 °C; $\bar{\nu}_{max}$ (neat)/cm^{-1} 3071 (C-H, w), 3026(C-H, w), 2972 (C-H, m), 2923 (C-H, w), 1609 (C=N, m), 1595 (C=C, m), 1212 (C-O, s), 1144 (C-O, s); ^{1}H NMR (600 MHz, MeOD) δ_H 8.68 (2H, d, *J* = 5.2 Hz, H-2'' and 6''), 8.15 (1H, d, *J* = 9.5 Hz, H-7), 8.03 (2H, d, *J* = 5.2 Hz, H-3'' and 5''), 7.93 (1H, d, *J* = 9.5 Hz, H-8), 7.74 – 7.67 (3H, m, H-2''', H-5''' and H-6'''), 7.46 – 7.40 (1H, m, H-4'''), 3.41 – 3.34 (1H, m, H-2''''), 1.43 (6H, d, *J* = 6.9 Hz, H-1''''); ^{13}C NMR (150 MHz, MeOD) δ_C 153.4 (C-2), 151.0 (C-2'' and C-6''), 150.60 (d, *J* = 1.7 Hz, C-3'''), 150.0 (C-6), 145.1 (C-4''), 139.7 (C-8a), 131.5 (C-2''', C-5''' or C-6'''), 129.8 (C-2''', C-5''' or C-6'''), 126.0 (C-7), 124.3 (C-1'''), 123.4 (C-2''', C-5''' or C-6'''), 122.5 (C-3'' and C-5''), 122.2 (C-4'''), 117.6 (C-8), 28.1 (C-2''''), 23.0 (C-1''''); Signals at 122.03 ppm J_1 = 255.8 Hz are consistent with trifluoromethyl group. HMBC shows correlation between carbon at 122.5 ppm and protons of phenyl ring suggesting that C-1''' is present at 122.5 ppm. HRMS *m/z* (ESI$^+$) [Found: 399.1428., $C_{21}H_{18}F_3N_4O$ requires [M + H]$^+$ 399.1427]; LCMS (MDAP): Rt = 20.1 min, >95% (Method 3); *m/z* (ESI$^+$) 399.0 [M + H]$^+$.

4-[(6-Chloro-2-methyl-imidazo[1,2-*b*]pyridazin-3-yl)methyl]morpholine **285**

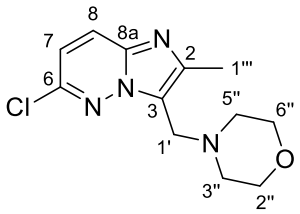

To a microwave vial containing morpholine (0.05 mL, 0.60 mmol) in MeOH (0.50 mL) was added formaldehyde solution (0.44 mL, 5.97 mmol) and the reaction mixture was stirred at rt for 10 min. To the vial was then added 6-chloro-2-methyl-imidazo[1,2-*b*]pyridazine (100 mg, 0.60 mmol) and acetic acid (0.3 mL, 5.24 mmol). The reaction mixture was heated to 65 °C and stirred overnight. The reaction was concentrated under reduced pressure. The crude was purified using flash silica column chromatography on an Isco Combiflash system (12 g silica, elution with 0-50% 20% MeOH in CH_2Cl_2 / CH_2Cl_2 gradient). Desired fractions were combined and concentrated under reduced pressure to afford the desired product, 4-[(6-chloro-2-methyl-imidazo[1,2-*b*]pyridazin-3-yl)methyl]morpholine, **285**, as a cream solid (150 mg, 0.53 mmol, 90% yield). R_f 0.59 (MeOH/ CH_2Cl_2 1:9); m.p. 145-147 °C; $\bar{\nu}_{max}$ (neat)/cm^{-1} 3084 (C-H, w), 3035 (C-H, w), 1608 (C=N, m), 1516 (C=C, m), 1294 (C-O, s); ^{1}H NMR (600 MHz, DMSO-d$_6$) δ_H 8.08 (1H, d, *J* = 9.4 Hz, H-7), 7.29 (1H, d, *J* = 9.4 Hz, H-8), 3.84 (2H, s, H-1'), 3.53 (4H, t, *J* = 4.6 Hz, H-2'' and 6''), 2.46 – 2.34 (7H, m, C-3'', 5'' and 1'''); ^{13}C NMR (150 MHz, DMSO-d$_6$) δ_C 145.2 (C-6), 143.8 (C-2), 136.3 (C-8a), 126.4 (C-7), 121.5 (C-3), 117.7 (C-8), 66.1 (C-2'' and C-6''), 53.0 (C-3'' and C-5''), 49.1 (C-1'), 14.0 (C-1'''); HRMS *m/z* (ESI$^+$) [Found: 267.1014., $C_{12}H_{16}ClN_4O$ requires [M + H]$^+$ 267.1007]; LCMS (LCQ): Rt = 0.4min (Method 1); *m/z* (ESI$^+$) 267.0 [M + H]$^+$.

4-[[2-Methyl-6-(4-pyridyl)imidazo[1,2-*b*]pyridazin-3-yl]methyl]morpholine **286**

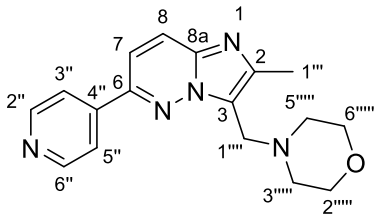

To a sealed microwave vial containing 4-[(6-chloro-2-methyl-imidazo[1,2-*b*]pyridazin-3-yl)methyl]morpholine (100 mg, 0.37 mmol), pyridine-4-boronic acid hydrate (138 mg, 1.12 mmol), bis[2-(di-*tert*-butylphosphanyl)cyclopenta-2,4-dien-1-yl]iron; dichloropalladium (12 mg, 0.02 mmol) and potassium carbonate (78 mg, 0.56 mmol) was added acetonitrile (1.6 mL) and water (0.40 mL). The vial was then subjected to microwave irradiation at 120 °C for 21 min. The reaction mixture was concentrated under reduced pressure. The crude was purified using flash reverse phase column chromatography on a Biotage system (12 g C-18, elution with 10-100% MeOH / water gradient). Desired fractions were combined and concentrated under reduced pressure to afford the desired product, 4-[[2-methyl-6-(4-pyridyl)imidazo[1,2-*b*]pyridazin-3-yl]methyl]morpholine, **286**, as a brown solid (50 mg, 0.15 mmol, 41% yield). R_f 0.50 (MeOH/ CH_2Cl_2 1:9); m.p. 208-210 °C; $\bar{\nu}_{max}$ (neat)/cm^{-1} 3058 (C-H, w), 2960 (C-H, w), 2863 (C-H, w), 2818 (C-H, w), 2803 (C-H, w), 1602 (C=N, m), 1543 (C=C, m); 1340 (C-O, s), 1110 (C-O, s); ^{1}H NMR (600 MHz, DMSO-d$_6$) δ_H 8.78 (2H, d, *J* = 4.9 Hz, H-2'' and 6''), 8.16 (1H, d, *J* = 9.4 Hz, H-7), 8.09 (2H, d, *J* = 4.9 Hz, H-3'' and 5''), 7.87 (1H, d, *J* = 9.4 Hz, H-8), 4.00 (2H, s, H-1''''), 3.59 – 3.48 (4H, m, H-2''''' and 6'''''), 2.49 – 2.45 (7H, m, H-3''''', H-5''''' and H-1'''); ^{13}C NMR (150 MHz, DMSO-d$_6$) δ_C 150.6 (C-2'' and C-6''), 147.5 (C-4''), 144.2 (C-2), 142.6 (C-6), 137.3 (C-8a), 124.8 (C-7), 121.4 (C-3), 120.9 (C-3'' and C-5''), 114.7 (C-8), 66.2 (C-2''''' and C-6'''''), 53.0 (C-3''''' and C-5'''''), 49.0 (C-1''''), 14.1 (C-1'''); HRMS *m/z* (ESI$^+$) [Found: 310.1658., $C_{17}H_{20}N_5O$ requires [M + H]$^+$ 310.1662]; LCMS (LCQ): Rt = 0.4 min (Method 1); *m/z* (ESI$^+$) 310.1 [M + H]$^+$; LCMS (MDAP): Rt = 5.3 min, >95% (Method 3); *m/z* (ESI$^+$) 310.0 [M + H]$^+$.

6-Chloro-7-methyl-imidazo[1,2-*b*]pyridazine **291**

6-Chloro-8-methyl-imidazo[1,2-*b*]pyridazine **292**

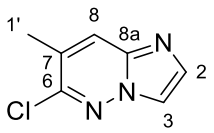

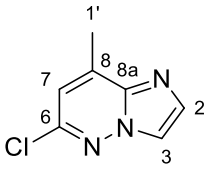

To a microwave vial containing of 3,6-dichloro-4-methylpyridazine (1.0 g, 6.13 mmol) was added aminoacetaldehyde dimethyl acetal (3.86 g, 36.71 mmol). The reaction mixture was heated to 100 °C and stirred for 4 h. The reaction mixture was concentrated under reduced pressure. Sulfuric acid (5 mL) was added to the crude and the reaction mixture was heated to 100 °C and stirred for 1 h. The reaction mixture was cooled in an ice bath before being basified with 20% sodium hydroxide solution slowly. The resulting solution was extracted with CH_2Cl_2 (2 x 100 mL). The organics were combined and concentrated under reduced pressure. The residue was purified using flash silica column chromatography on an Isco Combiflash system (12 g silica, elution with 0-50% EtOAc / petroleum ether gradient). Desired fractions were combined and concentrated under reduced pressure to afford 6-chloro-7-methyl-imidazo[1,2-*b*]pyridazine, **291**, as an off-white solid (430 mg, 2.44 mmol, 40% yield) and 6-chloro-8-methyl-imidazo[1,2-*b*]pyridazine, **292**, as a colourless oil (215 mg, 1.22 mmol, 20% yield).

292: R_f 0.31 (EtOAc/ petroleum ether 1:1); ^{1}H NMR (500 MHz, DMSO-d_6) δ_H 8.28 (1H, s, H-2), 7.76 (1H, s, H-3), 7.26 (1H, s, H-7), 2.56 (s, 3H, H-1'); LCMS (LCQ): Rt = 1.1 min (Method 1); *m/z* (ESI$^+$) 168.3 [M + H]$^+$; LCMS (MDAP): Rt = 12.3 min, (Method 3); *m/z* (ESI$^+$) 168.1 [M + H]$^+$.

291: R_f 0.47 (EtOAc/ petroleum ether 1:1); ^{1}H NMR (500 MHz, DMSO- d_6) δ_H 8.25 (1H, s, H-3), 8.15 (1H, s, H-2), 7.75 (1H, s, H-3), 2.38 (3H, s, H-1'); LCMS (LCQ): Rt = 0.6 min (Method 1); *m/z* (ESI$^+$) 168.3 [M + H]$^+$; LCMS (MDAP): Rt = 9.8 min, (Method 3); *m/z* (ESI$^+$) 168.1 [M + H]$^+$. The spectroscopic data are in good agreement with the literature values. Literature reference: Pollak *et al*. Tetrahedron, 1968, vol. 24, p. 2623

7-Methyl-6-(4-pyridyl)imidazo[1,2-*b*]pyridazine **293**

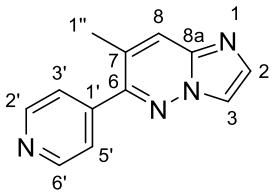

To a sealed microwave vial containing 6-chloro-7-methyl-imidazo[1,2-*b*]pyridazine (150 mg, 0.89 mmol), pyridine-4-boronic acid hydrate (132 mg, 1.07 mmol), bis[2-(di-*tert*-butylphosphanyl)cyclopenta-2,4-dien-1-yl]iron; dichloropalladium (29 mg, 0.04 mmol) and potassium carbonate (186 mg, 1.34 mmol) was added EtOH (1.6 mL) and water (0.40 mL). The reaction vial was degassed for 5 min and then subjected to microwave irradiation at 120 °C for 21 min. Additional equivalents of pyridine-4-boronic acid hydrate (132 mg, 1.07 mmol), bis[2-(di-*tert*-butylphosphanyl)cyclopenta-2,4-dien-1-yl]iron; dichloropalladium (29 mg, 0.04 mmol), and potassium carbonate (186 mg, 1.34 mmol) were added to the vial. The reaction vial was degassed for 5 min and then subjected to microwave irradiation at 120 °C for 41 min. The reaction mixture was concentrated under reduced pressure. The crude was purified using flash reverse phase column chromatography on a Biotage system (12 g C-18, elution with 10-100% MeOH / water gradient). Desired fractions were combined and concentrated under reduced pressure to afford the desired product, 7-methyl-6-(4-pyridyl)imidazo[1,2-*b*]pyridazine, **293**, as an off-white solid (90 mg, 0.41 mmol, 45% yield). R_f 0.12 (MeOH/ CH_2Cl_2 1:9); m.p. 196-198 °C; $\bar{\nu}_{max}$ (neat)/cm^{-1} 3133 (C-H, w), 3080 (C-H, w), 3050 (C-H, w), 3039 (C-H, w), 3028 (C-H, w), 2923 (C-H, w), 1602 (C=N, m), 1530 (C=C, m); ^{1}H NMR (500 MHz, DMSO-d$_6$) δ_H 8.75 (2H, d, *J*= 4.4 Hz, H-2' and 6'), 8.28 (1H, s, H-2 or 3), 8.11 (1H, s, H-8), 7.77 (1H, s, H-2 or 3), 7.64 (2H, d, *J*= 4.4 Hz, H-3' and 5'), 2.30 (3H, s, H-1''); ^{1}H NMR (600 MHz, DMSO-d$_6$) δ_H 8.77 – 8.64 (2H, m, H-2' and 6'), 8.22 (1H, s, H-2 or 3), 8.09 – 7.99 (1H, m, H-8), 7.72 (1H, s, H-2 or 3), 7.64 – 7.54 (2H, m, H-3' and 5'), 2.25 (3H, s, H-1''); ^{13}C NMR (150 MHz, DMSO-d$_6$) δ_C 152.5 (C-6), 149.8 (C-2' and C-6'), 143.5 (C-4'), 138.4 (C-8a), 134.0 (C-2 or C-3), 126.5 (C-7), 125.1 (C-8), 123.8 (C-3' and C-5'), 116.2 (C-2 or C-3), 19.3 (C-1''); HRMS *m/z* (ESI$^+$) [Found: 211.0973., $C_{12}H_{11}N_4$ requires [M + H]$^+$ 211.0978]; LCMS (MDAP): Rt = 5.3 min, >95% (Method 3); *m/z* (ESI$^+$) 211.1 [M + H]$^+$.

8-Methyl-6-(4-pyridyl)imidazo[1,2-*b*]pyridazine **294**

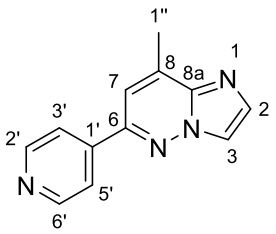

To a sealed microwave vial containing 6-chloro-8-methyl-imidazo[1,2-*b*]pyridazine (150 mg, 0.89 mmol), pyridine-4-boronic acid hydrate (132 mg, 1.07 mmol),bis[2-(di-*tert*-butylphosphanyl)cyclopenta-2,4-dien-1-yl]iron; dichloropalladium (29 mg, 0.04 mmol) and potassium carbonate (186 mg, 1.34 mmol) was added EtOH (1.6 mL) and water (0.4 mL). The vial was degassed for 5 min. The vial was then subjected to microwave irradiation at 120 °C for 21 min. The reaction mixture was concentrated under reduced pressure. The crude was purified using flash reverse phase column chromatography on a Biotage system (12 g C-18, elution with 10-100% MeOH / water gradient). Desired fractions were combined and concentrated under reduced pressure to afford the desired product, 8-methyl-6-(4-pyridyl)imidazo[1,2-*b*]pyridazine, **294**, as an off-white solid (131 mg, 0.59 mmol, 66% yield). R_f 0.25 (100% EtOAc); m.p. 165-167 °C; $\bar{\nu}_{max}$ (neat)/cm^{-1} 3067 (C-H, m), 3035(C-H, w), 2990 (C-H, w), 1602 (C=N, m), 1567 (C=C, m), 1546 (C=C, m); ^{1}H NMR (500 MHz, DMSO-d$_6$) δ_H 8.77 (2H, d, *J*= 6.0 Hz, H-2' and 6'), 8.40 – 8.33 (1H, m, H-3), 8.03 (2H, d, *J*= 6.0 Hz, H-3' and 5'), 7.84 – 7.78 (2H, m, H-2 and 7), 2.66 (3H, s, H-1''); ^{1}H NMR (600 MHz, DMSO-d$_6$) δ_H 8.69 – 8.63 (2H, m, H-2' and 6'), 8.24 (1H, s, H-3), 7.93 – 7.89 (2H, m, H-3' and 5'), 7.71 (1H, s, H-2), 7.66 (1H, s, H-7), 2.55 (3H, s, H-1''); ^{13}C NMR (150 MHz, DMSO-d$_6$) δ_C 150.5 (C-2' and C-6'), 148.7 (C-6), 142.4 (C-4'), 139.2 (C-8a), 137.5 (C-8), 133.9 (C-2), 121.0 (C-3' and C-5'), 117.7 (C-3), 114.8 (C-7), 16.3 (C-1''); HRMS *m/z* (ESI$^+$) [Found: 211.0975., $C_{12}H_{11}N_4$ requires [M + H]$^+$ 211.0978]; LCMS (LCQ): Rt = 0.6 min (Method 1); *m/z* (ESI$^+$) 211.3 [M + H]$^+$; LCMS (MDAP): Rt = 8.2 min, >95% (Method 3); *m/z* (ESI$^+$) 211.1 [M + H]$^+$.

(6-Chloro-4-methyl-pyridazin-3-yl)hydrazine **295**

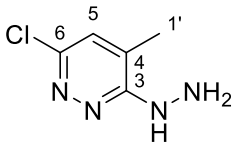

To 3,6-dichloro-4-methylpyridazine (5.0 g, 30.67 mmol) was added hydrazine hydrate (30 mL, 615.46 mmol) and the reaction heated to 80 °C overnight. The reaction was cooled down to rt; the resulting solid was filtered off, washed with water and dried under reduced pressure. Recrystallisation in hot EtOH followed by trituration with EtOH afforded the title product, (6-chloro-4-methyl-pyridazin-3-yl)hydrazine, **295**, as a white solid (2.0 g, 11.98 mmol, 39% yield). R_f 0.54 (MeOH/ CH_2Cl_2 1:9); ^{1}H NMR (500 MHz, DMSO- d_6) δ_H 7.73 (1H, s, NH), 7.21 (1H, s, H-5), 4.25 (2H, s, NH_2), 1.98 (3H, s, H-1'); LCMS (LCQ): Rt = 0.50 min (Method 1); *m/z* (ESI$^+$) 159.1 [M + H]$^+$. The spectroscopic data are in good agreement with the literature values. Literature reference: US 2014/0349990 A1 p104 paragraph [1046]

6-Chloro-8-methyl-[1,2,4]triazolo[4,3-*b*]pyridazine **296**

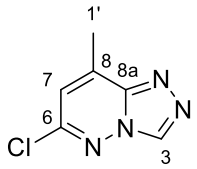

To a microwave vial containing of (6-chloro-4-methyl-pyridazin-3-yl)hydrazine (200 mg, 1.26 mmol) was added formic acid (0.05 mL, 1.26 mmol). The reaction mixture was heated to 100 °C and stirred for 6 h. The reaction mixture was diluted with CH_2Cl_2 (50 mL) and poured into saturated $NaHCO_3$ solution (50 mL). The organic layer was separated and the aqueous layer was extracted with CH_2Cl_2 (50 mL). The combined organic components were concentrated under reduced pressure. The residue was purified using flash silica column chromatography on an Isco Combiflash system (12 g silica, elution with 0-100% EtOAc / petroleum ether gradient). Desired fractions were combined and concentrated under reduced pressure to afford 6-chloro-8-methyl-[1,2,4]triazolo[4,3-*b*]pyridazine, **296**, as an off-white solid (180 mg, 1.01 mmol, 80% yield). R_f 0.30 (EtOAc/ petroleum ether 7:3); ^{1}H NMR (500 MHz, DMSO- d_6) δ_H 9.63 (1H, s, H-3), 7.39 (1H, s, H-7), 2.61 (3H, s, H-1'); LCMS (LCQ): Rt = 0.5 min (Method 1); *m/z* (ESI$^+$) 169.3 [M + H]$^+$; LCMS (MDAP): Rt = 11.9 min, (Method 3); *m/z* (ESI$^+$) 169.1 [M + H]$^+$. The spectroscopic data are in good agreement with the literature values. Literature reference: US 2014/0349990 A1 Nov 27 2014 page 104-105 [1045]

8-Methyl-6-(4-pyridyl)-[1,2,4]triazolo[4,3-*b*]pyridazine **297**

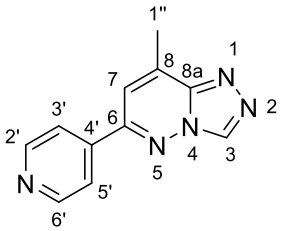

To a sealed microwave vial containing 6-chloro-8-methyl-[1,2,4]triazolo[4,3-*b*]pyridazine (100 mg, 0.59 mmol), 6-chloro-8-methyl-[1,2,4]triazolo[4,3-*b*]pyridazine (100 mg, 0.59 mmol), pyridine-4-boronic acid hydrate (88 mg, 0.71 mmol), pyridine-4-boronic acid hydrate (88 mg, 0.71 mmol), bis[2-(di-*tert*-butylphosphanyl)cyclopenta-2,4-dien-1-yl]iron; dichloropalladium (19 mg, 0.03 mmol) and potassium carbonate (123 mg, 0.89 mmol) was added EtOH (1.6mL) and water (0.4 mL). The vial was degassed for 5 min. The reaction vial was then subjected to microwave irradiation at 120 °C for 21 min. Additional equivalents ofPyridine-4-boronic acid hydrate (88 mg, 0.71 mmol),bis[2-(di-*tert*-butylphosphanyl)cyclopenta-2,4-dien-1-yl]iron; dichloropalladium (19 mg, 0.03 mmol) and potassium carbonate (123 mg, 0.89 mmol) were added to the vial. The vial was degassed for 5 min. The vial was then subjected to microwave irradiation at 120 °C for 41 min. The reaction mixture was concentrated under reduced pressure. The crude was purified using flash silica column chromatography on an Isco Combiflash system (12 g silica, elution with 0-50% 20% MeOH in CH_2Cl_2 / CH_2Cl_2 gradient). Desired fractions were combined and concentrated under reduced pressure to afford the desired product, 8-methyl-6-(4-pyridyl)-[1,2,4]triazolo[4,3-*b*]pyridazine, **297**, as a white solid (15 mg, 0.07 mmol, 11% yield). R_f 0.32 (MeOH/ CH_2Cl_2 1:9); m.p. 198-200 °C; $\bar{\nu}_{max}$ (neat)/cm^{-1} 3107 (C-H, w), 3058 (C-H, w), 2916 (C-H, w), 1604 (C=N, m), 1564 (C=C, m); ^{1}H NMR (500 MHz, DMSO-d$_6$) δ_H 9.76 (1H, s, H-3), 8.81 (2H, d, *J*= 4.8 Hz, H-2' and 6'), 8.05 (2H, d, *J*= 4.8 Hz, H-3' and 5'), 7.93 (1H, s, H-7), 2.72 (3H, s, H-1''); ^{1}H NMR (600 MHz, $CDCl_3$) δ_H 9.16 (1H, s, H-3), 8.81 (2H, d, *J* = 5.1 Hz, H-2' and 6'), 7.84 (2H, d, *J* = 5.4 Hz, H-3' and 5'), 7.37 (1H, s, H-7), 2.83 (3H, s, H-1''); ^{13}C NMR (150 MHz, $CDCl_3$) δ_C 152.1 (C-6), 151.0 (C-2' and C-6'), 145.4 (C-8), 141.9 (C-4'), 139.6 (C-3), 138.3 (C-8a), 121.3 (C-3' and C-5'), 117.7 (C-7), 17.1 (C-1''); LCMS (MDAP): Rt = 15.6 min, >95% (Method 3); *m/z* (ESI$^+$) 365.1 [M + H]$^+$.

6-(4-Pyridyl)imidazo[1,2-*a*]pyrimidine **298**

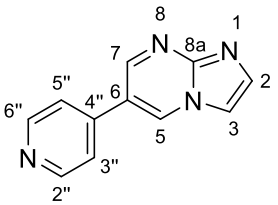

To a sealed and degassed vial containing 6-bromoimidazo[1,2-*a*]pyrimidine (40 mg, 0.20 mmol), pyridine-4-boronic acid hydrate (60 mg, 0.49 mmol), bis[2-(di-*tert*-butylphosphanyl)cyclopenta-2,4-dien-1-yl]iron; dichloropalladium (6.0 mg, 0.01 mmol), and cesium carbonate (184 mg, 0.57 mmol) was added acetonitrile (2 mL) and water (0.2 mL). The reaction mixture was irradiated with microwaves for 25 min at 140 °C. The reaction was concentrated under reduced pressure. The crude was purified using flash silica column chromatography on an Isco Combiflash system (12 g silica, elution with 0-50% 20% MeOH in CH_2Cl_2 / CH_2Cl_2 gradient). Desired fractions were combined and concentrated under reduced pressure to afford the desired product, 6-(4-pyridyl)imidazo[1,2-*a*]pyrimidine, **298**, as a yellow/brown solid (13 mg, 0.06 mmol, 31% yield). R_f 0.12 (MeOH/ CH_2Cl_2 1:9); m.p. 280-282 °C; $\bar{\nu}_{max}$ (neat)/cm^{-1} 3091(C-H, w), 3029 (C-H, w), 2989 (C-H, w), 2920 (C-H, w), 1626 (C=N, m), 1596 (C=C, m), 1550 (C=C, m); ^{1}H NMR (600 MHz, DMSO-d_6) δ_H 9.53 (1H, d, *J* = 2.5 Hz, H-5), 9.00 (1H, d, *J* = 2.5 Hz, H-7), 8.70 (2H, d, *J* = 5.2 Hz, H-2'' and 6''), 7.96 (1H, s, H-2), 7.84 (2H, d, *J* = 5.2 Hz, H-3'' and 5''), 7.81 (1H, s, H-3); ^{13}C NMR (150 MHz, DMSO-d_6) δ_C 150.4 (C-2'' and C-6''), 148.9 (C-7), 147.6 (C-8a), 141.4 (C-4''), 135.4 (C-3), 133.4 (C-5), 121.0 (C-3'' and C-5''), 118.5 (C-6), 112.5 (C-2); LCMS (MDAP): Rt = 4.80 min, >95% (Method 3); *m/z* (ESI$^+$) 197.0 [M + H]$^+$.

6-(4-Pyridyl)imidazo[1,2-*a*]pyridine **300**

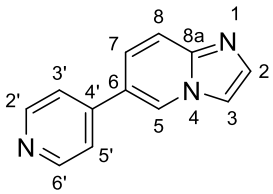

To a sealed and degassed vial containing pyridine-4-boronic acid hydrate (125 mg, 1.02 mmol), bis[2-(di-*tert*-butylphosphanyl)cyclopenta-2,4-dien-1-yl]iron; dichloropalladium (17 mg, 0.03 mmol), cesium carbonate (331 mg, 1.02 mmol) and 6-bromoimidazo[1,2-*a*]pyridine (100 mg, 0.51 mmol) was added acetonitrile (2 mL) and water (0.2 mL). The reaction mixture was heated to 80 °C and stirred overnight. Additional equivalents of Pyridine-4-boronic acid hydrate (125 mg, 1.02 mmol) and bis[2-(di-*tert*-butylphosphanyl)cyclopenta-2,4-dien-1-yl]iron; dichloropalladium (17 mg, 0.03 mmol) and cesium carbonate (331 mg, 1.02 mmol) were added. The reaction mixture was irradiated with microwaves for 25 min at 140 °C. The reaction mixture was concentrated under reduced pressure. The residue was partitioned between water (30 mL) and EtOAc (30 mL) and the layers separated. The aqueous layer was extracted with EtOAc (30 mL x 2). The combined organic components were washed with sat. brine solution (50 mL), dried over $MgSO_4$, filtered and concentrated under reduced pressure. The crude was purified using flash silica column chromatography on an Isco Combiflash system (12 g silica, elution with 0-50% 20% MeOH in CH_2Cl_2 / CH_2Cl_2 gradient). Desired fractions were combined and concentrated under reduced pressure to afford the desired product, 6-(4-pyridyl)imidazo[1,2-*a*]pyridine, **300**, as a mauve solid (50 mg, 0.24 mmol, 48% yield). R_f 0.42 (MeOH/ CH_2Cl_2 1:9); m.p. 75-77 °C; $\bar{\nu}_{max}$ (neat)/cm^{-1} 3118(C-H, w), 3103(C-H, w), 1636 (C=N, m), 1598 (C=C, m), 1537 (C=C, m); ^{1}H NMR (500 MHz, DMSO-d_6) δ_H 9.16 (1H, s, H-5), 8.66 (2H, d, *J*= 5.7 Hz, H-2' and 6'), 7.99 (1H, s, H-3), 7.76 (2H, d, *J*= 5.7 Hz, H-3' and 5'), 7.71 – 7.66 (2H, m, H-7 and 8), 7.64 (1H, s, H-2); ^{13}C NMR (125 MHz, DMSO-d_6) δ_C 150.3 (C-2' and C-6'), 144.1 (C-4' or C-6' or 8a), 143.9 (C-4' or C-6' or 8a), 134.1 (C-2), 125.6 (C-5), 123.4 (C-7), 122.1 (C-4' or C-6' or 8a), 120.7 (C-3' and C-5'), 117.2 (C-8), 114.0 (C-3); HRMS *m/z* (ESI$^+$) [Found: 196.0875., $C_{12}H_{10}N_3$ requires [M + H]$^+$ 196.0869]; LCMS (LCQ): Rt = 0.39 min (Method 1); *m/z* (ESI$^+$) 196.4 [M + H]$^+$; LCMS (MDAP): Rt = 3.3 min, >95% (Method 3); *m/z* (ESI$^+$) 196.1 [M + H]$^+$. Literature compound: THE ARIZONA BOARD OF REGENTS ON BEHALF OF THE UNIVERSITY OF ARIZONA; HULME, ChristopherWO2017/40993, 2017, A1

N-[5-(3-Pyridyl)-1*H*-pyrazolo[3,4-*c*]pyridazin-3-yl]cyclopropanecarboxamide **301**

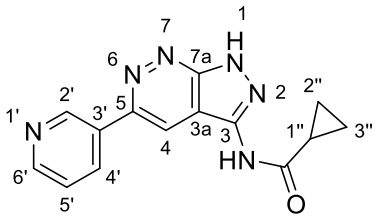

To 5-(3-pyridyl)-1*H*-pyrazolo[3,4-*c*]pyridazin-3-amine (30 mg, 0.14 mmol) in 1,4-dioxane (5 mL) was added cyclopropanecarbonyl chloride (0.01 mL, 0.14 mmol) and TEA (0.03 mL, 0.21 mmol). The reaction mixture was heated under reflux for 30 min. The reaction was concentrated under reduced pressure. To the residue was added piperidine (2 mL) and the mixture was stirred at rt overnight. The reaction mixture was concentrated under reduced pressure. The residue was purified using flash silica column chromatography on an Isco Combiflash system (12 g silica, elution with 0-50% 20% MeOH in CH_2Cl_2 / CH_2Cl_2 gradient) to afford the title compound, *N*-[5-(3-pyridyl)-1*H*-pyrazolo[3,4-*c*]pyridazin-3-yl]cyclopropanecarboxamide, **301**, as an off-white solid (20 mg, 0.07 mmol, 48% yield). R_f. 0.33 (MeOH/ CH_2Cl_2 1:9); $\bar{\nu}_{max}$ (neat)/cm^{-1} 3172 (N-H, m), 3154 (N-H, m), 3026 (C-H, w), 2988 (C-H, w), 1662 (C=O, s), 1608 (N-H, m); ^{1}H NMR (500 MHz, DMSO-d_6) δ_H 11.34 (1H, s, NH_{amide}), 9.24 (1H, s, H-2'), 8.72 (1H, s, H-4), 8.67 (1H, d, *J* = 4.8 Hz, H-6'), 8.42 (1H, d, *J* = 8.0 Hz, H-4'), 7.57 (1H, dd, *J* = 8.0 Hz, 4.8 Hz, H-5'), 2.03-1.98 (1H, m, 1'-C*H*), 0.96 – 0.84 (4H, m, H-2'' and H-3''); HRMS *m/z* (ESI$^+$) [Found: 281.1152., $C_{14}H_{12}N_6O$ requires [M + H]$^+$ 281.1145]; LCMS (LCQ): Rt = 0.5 min (Method 1); *m/z* (ESI$^+$) 281.2 [M + H]$^+$; LCMS (MDAP): Rt = 9.4 min, >95% (Method 3); *m/z* (ESI$^+$) 281.1 [M + H]$^+$. The spectroscopic data are in good agreement with the literature values. Lit Reference: J Witherington et al. Bioorganic and Medicinal Chemistry Letters, 2003, vol. 13, 9 p. 1581 – 1584.

5-Chloro-*1H*-pyrazolo[3,4-*c*]pyridazin-3-amine **305**

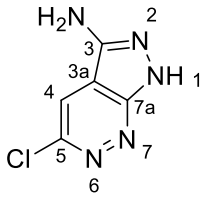

To a solution of 3,6-dichloropyridazine-4-carbonitrile (290 mg, 1.67 mmol) in MeOH (4 mL) was added hydrazine hydrate (0.16 mL, 3.33 mmol). The reaction stirred at 60 °C for 3 h. The reaction mixture was concentrated under reduced pressure to afford a brown residue. Water was added to the residue and a brown suspension was formed. The suspension was filtered to afford a brown solid. The filtrate was concentrated under reduced pressure and was purified by flash silica column chromatography on an Isco Combiflash system (12 g silica, elution with 80-100% 10% MeOH in CH_2Cl_2 / CH_2Cl_2 gradient). Desired fractions were combined and concentrated under reduced pressure. The solids were combined to afford the title compound, 5-chloro-1*H*-pyrazolo[3,4-*c*]pyridazin-3-amine, **305**, as a brown solid (250 mg, 1.40 mmol, 84% yield). R_f. 0.42 (MeOH: CH_2Cl_2 1:9); ^{1}H NMR (500 MHz, DMSO-d_6) δ_H 12.83 (1H, s, NH), 8.16 (1H, s, H-4), 6.02 (2H, s, NH_2); LCMS (LCQ): Rt = 0.6 min (Method 1); *m/z* (ESI$^+$) 170.3 [M + H]$^+$. The spectroscopic data are in good agreement with the literature values. Literature reference: WO 2015/025025 p. 408

3,6-Dichloropyridazine-4-carboxamide **307**

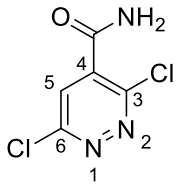

To a solution of 3,6-dichloropyridazine-4-carboxylic acid (800 mg, 4.2 mmol) in CH_2Cl_2 (5 mL) was added oxalyl chloride (0.39 mL, 4.56 mmol) and a few drops of DMF. The reaction mixture was stirred at rt overnight. The reaction mixture was concentrated under reduced pressure. The residue was dissolved in acetone (4 mL) before being carefully added to ammonium hydroxide solution (1 mL, 28% w/w ammonia in water) and stirred at rt for 2 h. The reaction mixture was concentrated under reduced pressure and the crude was purified using flash silica column chromatography on an Isco Combiflash system (24 g silica, elution with 0-100% 10% MeOH in CH_2Cl_2 / CH_2Cl_2 gradient). Desired fractions were combined and concentrated under reduced pressure to afford the title compound, 3,6-dichloropyridazine-4-carboxamide, **307**, as an orange solid (350 mg, 1.83 mmol, 44% yield). R_f 0.40 (MeOH:CH_2Cl_2 5:95); ^{1}H NMR (500 MHz, DMSO- d_6) δ_H 8.35 – 8.02 (3H, m, NH_2 and H-5); LCMS (LCQ): Rt = 0.6 min (Method 1); *m/z* (ESI$^+$) 192.1 [M + H]$^+$. The spectroscopic data are in good agreement with the literature values. Literature reference: WO 2015/025025 p. 408

3,6-Dichloropyridazine-4-carbonitrile **308**

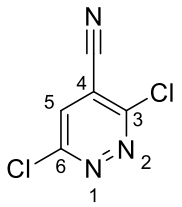

To 3,6-dichloropyridazine-4-carboxamide (500 mg, 2.6 mmol) was added phosphorus (v) oxychloride (2.9 mL, 31.6 mmol). The reaction mixture was stirred at 90 °C for 2.5 h. The resulting mixture was concentrated under reduced pressure. To the residue was added CH_2Cl_2 (15 mL) followed by careful addition of water (15 mL). The contents of the flask were stirred vigorously to quench. The solution was partitioned between CH_2Cl_2 (50 mL) and water (50 mL) and extracted. The combined organic components were washed with brine (50 mL x 2), dried over $MgSO_4$, filtered and concentrated under reduced pressure to afford the title compound, 3,6-dichloropyridazine-4-carbonitrile, **308**, as a brown solid (300 mg, 1.6 mmol, 62% yield). R_f 0.53 (EtOAc/petroleum ether 1:5); ^{1}H NMR (500 MHz, DMSO-d_6) δ_H 8.82 (1H, s, H-5); LCMS (LCQ): Rt = 0.6 min (Method 1); *m/z* (ESI$^+$) 174.0 $[M + H]^+$. The spectroscopic data are in good agreement with the literature values. Literature reference: WO 2015/025025 p. 408.

5-(3-Pyridyl)-1*H*-pyrazolo[3,4-*c*]pyridazin-3-amine **310**

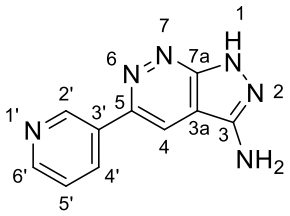

To a suspension of 3-chloro-6-(3-pyridyl)pyridazine-4-carbonitrile (500 mg, 2.31 mmol) in EtOH (10 mL) was added hydrazine hydrate (0.27 mL, 5.55 mmol) and the reaction mixture was heated to 80 °C for 4 h. The reaction mixture was concentrated under reduced pressure. The crude was purified using flash silica column chromatography on an Isco Combiflash system (12 g silica, elution with 0-50% 20% MeOH in CH_2Cl_2 / CH_2Cl_2 gradient) to afford the title compound, 5-(3-pyridyl)-1*H*-pyrazolo[3,4-*c*]pyridazin-3-amine, **310**, as an off-white solid (100 mg, 0.42 mmol, 18% yield). R_f. 0.25 (CH_2Cl_2:MeOH 9:1); ^{1}H NMR (500 MHz, DMSO-d_6) δ_H 12.82 (1H, s, $NH_{indazole}$), 9.26 – 9.19 (1H, m, H-2'), 8.68 – 8.63 (1H, m, H-6'), 8.60 (1H, s, H-4), 8.47 – 8.39 (1H, m, H-4'), 7.58 (1H, dd, *J* = 8.0, 4.8 Hz, H-5'), 6.03 (2H, s, NH_2); LCMS (LCQ): Rt = 0.4 min (Method 1); *m/z* (ESI^+) 213.3 $[M + H]^+$. The spectroscopic data are in good agreement with the literature values. Lit Reference: J Witherington et al. Bioorganic and Medicinal Chemistry Letters, 2003, vol. 13, 9 p. 1581 – 1584.

Diethyl 2-hydroxy-2-[2-oxo-2-(3-pyridyl)ethyl]propanedioate **314**

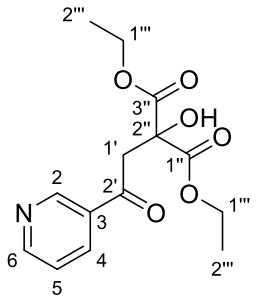

To a mixture of diethyl ketomalonate (2.42 mL, 15.89 mmol) and 3-acetylpyridine (1.50 mL, 13.65 mmol) was added pyridine (0.60 mL, 10 mmol). The reaction mixture was stirred at 125 °C overnight. The reaction mixture was concentrated under reduced pressure. The residue was purified by flash silica column chromatography on an Isco Combiflash system (12 g silica, elution with 0-10% MeOH/CH_2Cl_2 gradient) to afford the title compound, diethyl 2-hydroxy-2-[2-oxo-2-(3-pyridyl)ethyl]propanedioate, **314**, as a brown oil (1.50 g, 4.57 mmol, 34% yield). R_f 0.67 (MeOH:CH_2Cl_2 1:9); ^{1}H NMR (500 MHz, DMSO-d_6) δ_H 9.14 – 9.10 (1H, m, H-2), 8.85 – 8.80 (1H, m, H-6), 8.34 – 8.27 (1H, m, H-4), 7.62 – 7.56 (1H, m, H-5), 6.45 (1H, s, OH), 4.19 (4H, q, *J* = 7.1 Hz, H-1'''), 3.77 (2H, s, H-1'), 1.22 (6H, t, *J* = 7.1 Hz, H-2'''); LCMS (LCQ): Rt = 0.5 min (Method 1); *m/z* (ESI$^+$) 296.1 [M + H]$^+$. The spectroscopic data are in good agreement with the literature values. Literature reference: Hoelder S, WO 2004/046117A1.

Ethyl 6-oxo-3-(3-pyridyl)-*1H*-pyridazine-5-carboxylate **315**

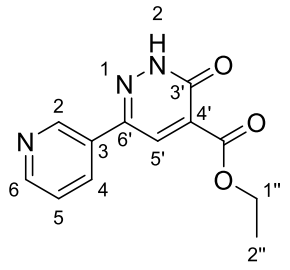

To a solution of diethyl 2-hydroxy-2-[2-oxo-2-(3-pyridyl)ethyl]propanedioate (1.50 g, 5.08 mmol) in EtOH (25 mL) was added hydrazine dihydrochloride (0.64 g, 6.1 mmol). The reaction mixture was heated under reflux and stirred overnight. The reaction mixture was concentrated under reduced pressure. The crude was recrystallized with minimum hot EtOH. Once cooled, the suspension was filtered and washed with cool EtOH to afford the title compound, ethyl 6-oxo-3-(3-pyridyl)-1*H*-pyridazine-5-carboxylate, **315**, as a brown solid (0.73 g, 2.53 mmol, 50% yield). R_f 0.54 (MeOH:CH_2Cl_2 1:9); ^{1}H NMR (500 MHz, DMSO-d_6) δ_H 13.88 (1H, s, NH), 9.22 (1H, d, *J* = 2.2 Hz, H-2), 8.80 (1H, dd, *J* = 5.2, 1.4 Hz, H-6), 8.63 (1H, d, *J* = 8.5 Hz, H-4), 8.47 (1H, s, H-5'), 7.84 (1H, dd, *J* = 8.1, 5.4 Hz, H-5), 4.32 (2H, q, *J* = 7.1 Hz, H-1''), 1.31 (3H, t, *J* = 7.1 Hz, H-2''); LCMS (LCQ): Rt = 0.6 min (Method 1); *m/z* (ESI$^+$) 246.2 [M + H]$^+$; The spectroscopic data are in good agreement with the literature values. Literature reference: Hoelder S, WO 2004/046117A1.

3-Chloro-6-(3-pyridyl)pyridazine-4-carbonitrile **316**

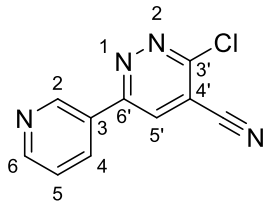

To a solution of ammonium hydroxide (5 mL, 28% v/v) was added ethyl 6-oxo-3-(3-pyridyl)-1*H*-pyridazine-5-carboxylate (4.0 g, 16.31 mmol). The reaction mixture was stirred for 48 h at rt. A suspension formed and was filtered to afford a brown solid. The solid was dried overnight. To the brown solid (1.80 g, 8.33 mmol) was added phosphorus (V) oxychloride (23.35 mL, 249.77 mmol). The reaction mixture was heated under reflux for 2 h. The reaction mixture was concentrated under reduced pressure. Water (20 mL) and CH_2Cl_2 (20 mL) were added slowly to the mixture. The aqueous component was neutralized with saturated $NaHCO_3$ solution. A precipitate formed and was filtered to afford the desired product, 3-chloro-6-(3-pyridyl)pyridazine-4-carbonitrile, **316**, as a brown solid (0.75 g, 3.12 mmol, 40% yield). ^{1}H NMR (500 MHz, DMSO-d_6) δ_H 9.38 – 9.29 (1H, m, H-2), 9.15 (1H, s, H-5'), 8.79 (1H, d, *J* = 4.9 Hz, H-6), 8.56 (1H, d, *J* = 8.4 Hz, H-4), 7.65 (1H, dd, *J* = 8.1, 4.8 Hz, H-5); LCMS (LCQ): Rt = 0.4 min (Method 1); *m/z* (ESI$^+$) 217.3 [M + H]$^+$. The spectroscopic data are in good agreement with the literature values. Lit Reference: J Witherington *et al*. Bioorganic and Medicinal Chemistry Letters, 2003, vol. 13, 9 p. 1581 – 1584

5-(3-Pyridyl)-1*H*-indazol-3-amine **317**

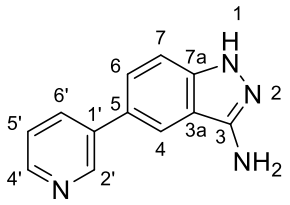

To a microwave vial containing a solution of 5-bromo-1*H*-indazol-3-amine (140 mg, 0.66 mmol) in water (1.25 mL) and acetonitrile (2.5 mL) was added pyridine-3-boronic acid (120 mg, 0.99 mmol), tetrakis(triphenylphosphine)palladium(0) (80 mg, 0.07 mmol) and sodium carbonate (240 mg, 2.26 mmol). The vial sealed and the reaction mixture was heated to 150 °C under microwave irradiation for 20 min. The reaction was concentrated under reduced pressure. The crude was purified using flash silica column chromatography on an Isco Combiflash system (12 g silica, elution with 0-100% EtOAc/ petroleum ether gradient) to afford the desired product, 5-(3-pyridyl)-1*H*-indazol-3-amine, **317**, as an off-white solid (60 mg, 0.27 mmol, 41 % yield). R_f 0.44 (MeOH/CH_2Cl_2 1:9); m.p. 140-141 °C; $\bar{\nu}_{max}$ (neat)/cm^{-1} 3267 (N-H, m), 3132 (N-H, s), 3046 (C-H, m), 2871 (C-H, w), 1620 (C=N, m), 1533 (C=C, s); ^{1}H NMR (500 MHz, DMSO-d$_6$) δ_H 11.49 (1H, s, NH$_{indazole}$), 8.92 – 8.79 (1H, m, H-2'), 8.51 (1H, dd, *J* = 4.7, 1.6 Hz, H-4'), 8.11 – 8.07 (1H, m, H-4), 8.03 (1H, ddd, *J* = 7.9, 2.5, 1.6 Hz, H-6'), 7.60 (1H, dd, *J* = 8.6, 1.8 Hz, H-6), 7.47 (1H, ddd, *J* = 7.9, 4.7, 0.9 Hz, H-5'), 7.34 (1H, dd, *J* = 8.6, 0.9 Hz, H-7), 5.42 (2H, s, NH_2); HRMS *m/z* (ESI$^+$) [Found: 211.0974., $C_{12}H_{10}N_4$ requires [M + H]$^+$ 211.0978]; LCMS (LCQ): Rt = 0.4 min (Method 1); *m/z* (ESI$^+$) 211.3 [M + H]$^+$.

N-[5-(3-Pyridyl)-1*H*-indazol-3-yl]cyclopropanecarboxamide **318**

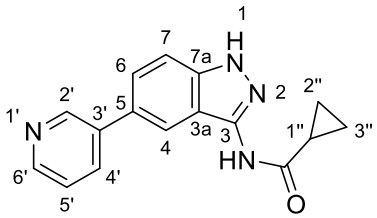

To a solution of 5-(3-pyridyl)-1*H*-indazol-3-amine (50 mg, 0.24 mmol) in 1,4-dioxane (1 mL) was added cyclopropanecarbonyl chloride (0.02 mL, 0.24 mmol) and TEA (0.05 mL, 0.36 mmol). The reaction mixture was heated to 60 °C for 1 h. The reaction mixture was concentrated under reduced pressure. Piperidine (2 mL) was added and the reaction mixture was stirred overnight at rt. The reaction was concentrated under reduced pressure. The crude was purified using flash silica column chromatography on an Isco Combiflash system (12 g silica, elution with 0-50% 20% MeOH in CH_2Cl_2/ CH_2Cl_2 gradient) to afford the desired product *N*-[5-(3-pyridyl)-1*H*-indazol-3-yl]cyclopropanecarboxamide, **318**, as an off-white solid (50 mg, 0.15 mmol, 64% yield). R_f. 0.50 (MeOH/ CH_2Cl_2 1:9); m.p. 229-231 °C; $\bar{\nu}_{max}$ (neat)/cm^{-1}3169 (N-H, m), 3039(C-H, w), 2935 (C-H, w), 2820 (C-H, w), 1659 (C=O, s), 1625 (C=N, m), 1568 (C=C, m); ^{1}H NMR (500 MHz, DMSO-d$_6$) δ_H 12.73 (1H, s, NH$_{indazole}$), 10.71 (1H, s, NH$_{amide}$), 8.84 (1H, d, *J* = 1.8 Hz, H-2'), 8.54 (1H, dd, *J* = 4.8, 1.6 Hz, H-6'), 8.11 – 8.07 (1H, m, H-4), 8.02 (1H, dt, *J* = 7.9, 2.1 Hz, H-4'), 7.68 (1H, dd, *J* = 8.7, 1.7 Hz, H-6), 7.55 (1H, d, *J* = 8.7 Hz, H-7), 7.48 (1H, ddd, *J* = 7.9, 4.7, 0.9 Hz, H-5'), 2.03 – 1.87 (1H, m, H-1''), 0.93 – 0.73 (4H, m, H-2'' and 3''); ^{13}C (125 MHz, DMSO-d$_6$) δ_C 171.8 (C=O), 147.8 (C-6'), 147.7 (C-2'), 141.1 (C-3), 140.7 (C-7a), 136.4 (C-3'), 134.1 (C-4'), 128.9 (C-5), 125.9 (C-6), 123.9 (C-5'), 121.0 (C-4), 116.6 (C-3a), 110.9 (C-7), 13.8 (C-1''), 7.4 (C-2'' and 3''); HRMS *m/z* (ESI$^+$) [Found: 279.1233., $C_{16}H_{14}N_4O$ requires [M + H]$^+$ 279.1240]; LCMS (LCQ): Rt = 0.5 min (Method 1); *m/z* (ESI$^+$) 279.3 [M + H]$^+$; LCMS (MDAP): Rt = 8.9 min, >95% (Method 3); *m/z* (ESI$^+$) 279.1 [M + H]$^+$.

5-(3-Pyridyl)-1*H*-pyrazolo[3,4-*b*]pyridin-3-amine **319**

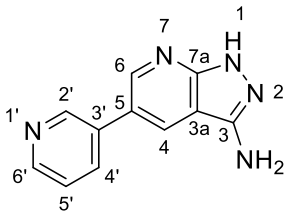

To a microwave vial containing a solution of 5-bromo-1*H*-pyrazolo[3,4-*b*]pyridin-3-amine (140 mg, 0.66 mmol) in acetonitrile (2.5 mL) and water (1.25 mL) was added pyridine-3-boronic acid (120 mg, 0.99 mmol), tetrakis(triphenylphosphine)palladium(0) (70 mg, 0.06 mmol) and sodium carbonate (240 mg, 2.26 mmol). The vial was sealed and the reaction mixture was subjected to microwave irradiation, heating to 150 °C for 20 min. The reaction mixture was concentrated under reduced pressure. The crude was purified using flash silica column chromatography on an Isco Combiflash system (12 g silica, elution with 0-50% 20% MeOH in CH_2Cl_2/ CH_2Cl_2 gradient) to afford the desired product 5-(3-pyridyl)-1*H*-pyrazolo[3,4-*b*]pyridin-3-amine, **319**, as a yellow solid (60 mg, 0.27 mmol, 41% yield). R_f. 0.15 (MeOH/CH_2Cl_2 1:9); ^{1}H NMR (500 MHz, DMSO-d_6) δ_H 12.08 (1H, s, $NH_{indazole}$), 8.93 – 8.88 (1H, m, H-2'), 8.71 (1H, d, *J* = 2.2 Hz, H-4), 8.57 (1H, dd, *J* = 4.8, 1.5 Hz, H-6'), 8.48 (1H, d, *J* = 2.2 Hz, H-6), 8.09 (1H, ddd, *J* = 8.0, 2.5, 1.5 Hz, H-4'), 7.51 (1H, ddd, *J* = 8.0, 4.8, 0.9 Hz, H-5'), 5.64 (2H, s, NH_2); HRMS *m/z* (ESI$^+$) [Found: 212.0929., $C_{11}H_9N_5$ requires [M + H]$^+$ 212.0931]; LCMS (LCQ): Rt = 0.4 min (Method 1); *m/z* (ESI$^+$) 212.3 [M + H]$^+$.

N-[5-(3-Pyridyl)-1*H*-pyrazolo[3,4-*b*]pyridin-3-yl]cyclopropanecarboxamide **320**

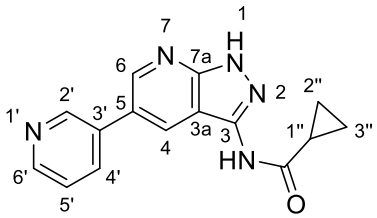

To a solution of 5-(3-pyridyl)-1*H*-pyrazolo[3,4-*b*]pyridin-3-amine (40 mg, 0.19 mmol) in 1,4-dioxane (1 mL) was added cyclopropanecarbonyl chloride (0.02 mL, 0.19 mmol) and TEA (0.04 mL, 0.28 mmol). The reaction mixture was heated to 60 °C for 1 h. The reaction mixture was concentrated under reduced pressure. To the crude was added piperidine (2 mL) and the reaction mixture was stirred overnight at rt. The reaction mixture was concentrated under reduced pressure. The crude was purified using flash silica column chromatography on an Isco Combiflash system (12 g silica, elution with 0-50% 20% MeOH in CH_2Cl_2/ CH_2Cl_2 gradient) to afford the desired product, *N*-[5-(3-pyridyl)-1*H*-pyrazolo[3,4-*b*]pyridin-3-yl]cyclopropanecarboxamide, **320**, as an off-white solid (30 mg, 0.10 mmol, 54% yield). R_f. 0.38 (MeOH/ CH_2Cl_2 1:9); m.p. 266-268 °C; $\bar{\nu}_{max}$ (neat)/cm^{-1} 3180 (N-H, m), 3045 (C-H, m), 2928 (C-H, m), 2812 (C-H, w), 1662 (C=O, s), 1613 (C=N, s), 1584 (C=C, m), 1562 (C=C, m); ^{1}H NMR (500 MHz, DMSO-d$_6$) δ_H 13.32 (1H, s, NH$_{indazole}$), 11.02 (1H, s, NH$_{amide}$), 8.91 – 8.88 (1H, m, H-2'), 8.82 (1H, d, *J* = 2.2 Hz, H-4), 8.64 (1H, d, *J* = 2.2 Hz, H-6), 8.60 (1H, dd, *J* = 4.8, 1.6 Hz, H-6'), 8.10 (1H, ddd, *J* = 7.9, 2.5, 1.6 Hz, H-4'), 7.52 (1H, ddd, *J* = 8.0, 4.8, 0.9 Hz, H-5'), 2.02 – 1.92 (1H, m, H-1''), 0.91 – 0.87 (2H, m, H-2'' and 3''), 0.87 – 0.82 (2H, m, H-2'' and 3''); ^{13}C NMR (125 MHz, DMSO-d$_6$) δ_C 171.8 (C=O), 151.4 (C-7a), 148.45 (C-4 or 6), 148.39 (C-4 or 6), 147.8 (C-2'), 140.4 (C-3), 134.5 (C-4'), 134.8 (C-3'), 131.2 (C-4), 125.4 (C-5), 124.0 (C-5'), 107.7 (C-3a), 13.7 (C-1''), 7.5 (C-2'' and C-3''); HRMS *m/z* (ESI$^+$) [Found: 280.1186., $C_{15}H_{13}N_5O$ requires [M + H]$^+$ 280.1193]; LCMS (LCQ): Rt = 0.6 min (Method 1); *m/z* (ESI$^+$) 280.3 [M + H]$^+$; LCMS (MDAP): Rt = 9.1 min, >95% (Method 3); *m/z* (ESI$^+$) 280.0 [M + H]$^+$. The spectroscopic data are in good agreement with the literature values. Literature reference: Garland, Stephen; Haigh, David; Hickey, Deidre Mary Bernadette; Liddle, John; Smith, David Glynn; Ward, Robert William; Witherington, Jason; US2004/19052 A1, 2004 ; Page/Page column 17; 19.

N-[5-(3-Pyridyl)-1*H*-pyrazolo[3,4-*b*]pyrazin-3-yl]cyclopropanecarboxamide **322**

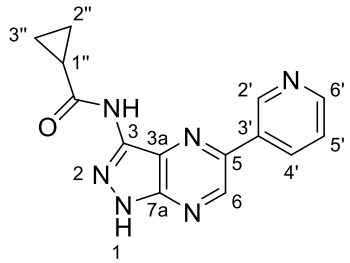

To a microwave vial was added 5-bromo-1*H*-pyrazolo[3,4-*b*]pyrazin-3-amine (50 mg, 0.23 mmol), pyridine-3-boronic acid (43 mg, 0.35 mmol), bis[2-(di-*tert*-butylphosphanyl)cyclopenta-2,4-dien-1-yl]iron; dichloropalladium (15 mg, 0.02 mmol) and sodium carbonate (74 mg, 0.70 mmol). The vial was sealed. Water (0.2 mL) and acetonitrile (1.2 mL) were added to the vial and the reaction heated to 100 °C over the weekend. The reaction was concentrated under reduced pressure. The residue was dissolved in minimum amount of MeOH and filtered through celite, before being concentrated under reduced pressure. The residue was dissolved in 1,4-dioxane (5mL). cyclopropanecarbonyl chloride (0.06 mL, 0.70 mmol) and TEA (0.03 mL, 0.23 mmol) were added to the reaction. The vial was heated to 80 °C for 3 h. The reaction mixture was concentrated under reduced pressure. Piperidine (5 mL, 50.62 mmol) was added to the residue and the reaction mixture was stirred overnight at rt. The reaction was concentrated under reduced pressure. The crude was purified using flash reverse phase column chromatography on a Biotage system (12 g C-18, elution with 10-100% MeOH / water gradient). Desired fractions were concentrated under reduced pressure. The crude was purified using flash amino-functionalised silica column chromatography on an Isco Combiflash system (12 g silica, elution with 0-50% 20% MeOH in CH_2Cl_2 / CH_2Cl_2 gradient). Desired fractions were combined and concentrated under reduced pressure. The resulting brown solid was triturated with minimum amount of EtOH to afford the desired product, *N*-[5-(3-pyridyl)-1*H*-pyrazolo[3,4-*b*]pyrazin-3-yl]cyclopropanecarboxamide, **322**, as an off-white solid (30 mg, 0.10 mmol, 44% yield). R_f 0.53 (MeOH/ CH_2Cl_2 1:9); m.p. 292-294 °C; $\bar{\nu}_{max}$ (neat)/cm^{-1} 3255 (N-H, m), 3205 (N-H, m), 3088 (C-H, m), 3023 (C-H, w), 1660 (C=O, s), 1594 (C=C, m), 1549 (C=C, s); ^{1}H NMR (500 MHz, DMSO-d$_6$) δ_H 13.83 (1H, s, NH$_{indazole}$), 10.60 (1H, s, NH$_{amide}$), 9.31 (1H, d, *J* = 2.2 Hz, H-6), 9.24 (1H, s, H-2'), 8.66 (1H, dd, *J* = 4.9, 1.5 Hz, H-6'), 8.48 (1H, d, *J* = 8.1 Hz, H-4'), 7.56 (1H, dd, *J* = 8.0, 4.8 Hz, H-5'), 2.01 – 1.81 (1H, m, H-1''), 0.89 – 0.75 (4H, m, H-2'' and 3''); 13C NMR (125 MHz, DMSO-d$_6$) δ_C 150.1 (C-6'), 148.0 (C-2' and C-3, C-3a or C-7a), 145.4 (C-5), 143.7 (C-3, C-3a or C-7a), 141.9 (C-6 and C-3, C-3a or C-7a), 134.3 (C-4'), 132.3 (C-3'), 123.9 (C-5'), 13.7 (C-1''), 7.5 (C-2'' and C-3''). Signal for C=O at 173.0 visible in HMBC; HRMS *m/z* (ESI$^+$) [Found: 281.1139., $C_{14}H_{13}N_6O$ requires [M + H]$^+$ 281.1145]; LCMS (MDAP): Rt = 9.1 min, >95% (Method 3); *m/z* (ESI$^+$) 281.1 [M + H]$^+$.

N-[5-(3-Pyridyl)-1*H*-pyrazolo[3,4-*c*]pyridin-3-yl]cyclopropanecarboxamide **324**

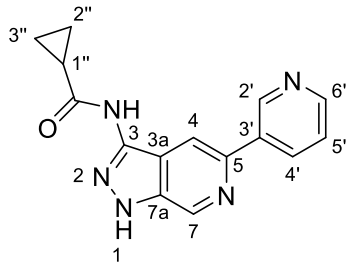

To a microwave vial containing a solution of 2-bromo-5-fluoropyridine-4-carbonitrile (100 mg, 0.50 mmol) in DMSO (0.50 mL) was added hydrazine hydrate (0.36 mL, 7.39 mmol). The reaction vial was sealed and heated to 120 °C for 3 h. The reaction mixture was diluted with water (10 mL) and the aqueous was extracted with EtOAc (3 x 10 mL). The combined organics were washed with saturated brine solution (2 x 5 mL), dried over $MgSO_4$, filtered and then dried concentrated under reduced pressure. The residue was dissolved in water (2 mL) and acetonitrile (8 mL) and added to a microwave vial containing pyridine-3-boronic acid (86 mg, 0.70 mmol), bis[2-(di-*tert*-butylphosphanyl)cyclopenta-2,4-dien-1-yl]iron; dichloropalladium (30 mg, 0.05 mmol) and sodium carbonate (149 mg, 1.41 mmol). The vial was sealed and the reaction mixture was heated to 100 °C overnight. The reaction mixture was concentrated under reduced pressure. The residue was dissolved in minimum amount of MeOH and filtered through celite, before being concentrated under reduced pressure. The residue was dissolved in 1,4-dioxane (4.29 mL). Cyclopropanecarbonyl chloride (0.13 mL, 1.41 mmol) and TEA (0.07 mL, 0.47 mmol) were added to the reaction. The vial was heated to 80 °C for 3 h. The reaction mixture was concentrated under reduced pressure. Piperidine (10 mL, 101.7 mmol) was added to the residue and stirred overnight at rt. The reaction mixture was concentrated under reduced pressure. The crude was purified using flash reverse phase column chromatography on a Biotage system (12 g C-18, elution with 10-100% MeOH / water gradient). Desired fractions were concentrated under reduced pressure. The crude was purified using flash amino-functionalised silica column chromatography on an Isco Combiflash system (12 g silica, elution with 0-50% 20% MeOH in CH_2Cl_2 / CH_2Cl_2 gradient). Desired fractions were combined and concentrated under reduced pressure. The resulting brown solid was triturated with petroleum ether, diethyl ether and finally a minimum amount of EtOH to afford the desired product, *N*-[5-(3-pyridyl)-1*H*-pyrazolo[3,4-*c*]pyridin-3-yl]cyclopropanecarboxamide, **324**, as a pale brown solid (30 mg, 0.10 mmol, 19% yield). R_f 0.33 (MeOH / CH_2Cl_2 1/9); m.p. 296-298 °C; $\bar{\nu}_{max}$ (neat)/cm^{-1} 3182 (N-H, m), 3144 (N-H, m), 3016 (C-H, w), 2930 (C-H, w), 2814 (C-H, w), 1657 (C=O, s), 1603 (C=C, m), 1550 (C=C, s); ^{1}H NMR (600 MHz, DMSO-d_6) δ_H 13.30 (1H, s, $NH_{indazole}$), 10.99 (1H, s, NH_{amide}), 9.22 – 9.13 (1H, m, H-2'), 9.06 (1H, s, H-7), 8.56 (1H, dd, *J*= 4.8, 1.6 Hz, H-6'), 8.37 (1H,

s, H-4), 8.35 – 8.30 (1H, m, H-4'), 7.49 (1H, dd, *J*= 8.0, 4.7 Hz, H-5'), 2.02 – 1.89 (1H, m, H-1'), 0.94 – 0.77 (4H, m, H-2'' and 3''); ^{13}C NMR (150 MHz, DMSO-d_6) δ_C 171.9 (C=O), 148.6 (C-6'), 147.4 (C-2'), 142.5 (C-5), 141.2 (C-3a), 137.4 (C-3), 135.1 (C-7), 135.0 (C-3), 133.5 (C-4'), 123.8 (C5'), 120.3 (C-7a), 113.5 (C-4), 13.7 (C-1''), 7.6 (C-2'' and C-3''); HRMS *m/z* (ESI$^+$) [Found: 302.1010., $C_{15}H_{13}N_5NaO$ requires [M + Na]$^+$ 302.1012]; LCMS (MDAP): Rt = 9.5 min, >95% (Method 3); *m/z* (ESI$^+$) 280.8 [M + H]$^+$.

1-Methyl-5-(3-pyridyl)pyrazolo[3,4-*c*]pyridazin-3-amine **325**

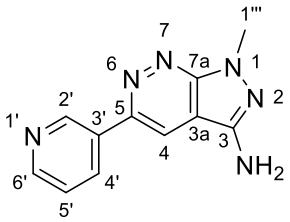

To 3-chloro-6-(3-pyridyl)pyridazine-4-carbonitrile (100 mg, 0.46 mmol) was added copper iodide (10 mg, 0.03 mmol), cesium carbonate (230 mg, 0.69 mmol) and 1,10-phenanthroline (20 mg, 0.10 mmol). DMF (1.5 mL) was added followed by methylhydrazine (0.15 mL, 2.77 mmol). The reaction mixture was heated to 60 °C and stirred overnight. The reaction mixture was concentrated under reduced pressure. The crude was purified using flash reverse phase column chromatography on a Biotage system (12 g C-18, elution with 10-100% MeOH / water gradient) to afford the desired product, 1-methyl-5-(3-pyridyl)pyrazolo[3,4-*c*]pyridazin-3-amine, **325**, as a brown solid (80 mg, 0.32 mmol, 69% yield). R_f 0.33 (MeOH/CH_2Cl_2 1:9); ^{1}H NMR (500 MHz, DMSO-d_6) δ_H 9.26 – 9.21 (m, 1H, H-2'), 8.68 – 8.63 (2H, m, H-6' and H-4), 8.46 – 8.37 (1H, m, H-4'), 7.58 (1H, dd, *J* = 8.0, 4.8 Hz, H-5'), 6.25 – 6.12 (2H, app. m, NH_2), 3.17 (3H, app. d, *J* = 3.0 Hz, H-1'''); LCMS (LCQ): Rt = 0.6 min (Method 1); *m/z* (ESI$^+$) 227.4 [M + H]$^+$.

N-[1-Methyl-5-(3-pyridyl)pyrazolo[3,4-*c*]pyridazin-3-yl]cyclopropanecarboxamide **326**

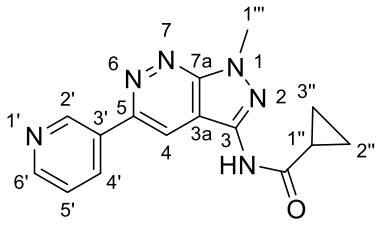

To a suspension of 1-methyl-5-(3-pyridyl)pyrazolo[3,4-*c*]pyridazin-3-amine (50 mg, 0.24 mmol) in 1,4-dioxane (1 mL) was added TEA (0.03 mL, 0.24 mmol) followed by cyclopropanecarbonyl chloride (0.02 mL, 0.24 mmol). The reaction mixture was heated to 60 °C for 30 min. The reaction mixture was concentrated under reduced pressure. The residue was dissolved in 1,4-dioxane (1 mL). Piperidine (1 mL, 0.24 mmol) was then added and the reaction mixture was stirred at rt overnight. The reaction mixture was concentrated under reduced pressure. The crude was purified using flash silica column chromatography on an Isco Combiflash system (12 g silica, elution with 0-50% 20% MeOH in CH_2Cl_2/ CH_2Cl_2 gradient). Trituration with diethyl ether and EtOAc afforded the desired product, *N*-[1-methyl-5-(3-pyridyl)pyrazolo[3,4-*c*]pyridazin-3-yl]cyclopropanecarboxamide, **326**, as an off-white solid (60 mg, 0.13 mmol, 55% yield). R_f. 0.40 (MeOH/CH_2Cl_2 1:9); m.p. 206-208 °C; ^{1}H NMR (500 MHz, DMSO-d_6) δ_H 11.40 (1H, s, NH_{amide}), 9.28 – 9.22 (1H, m, H-2'), 8.75 (1H, s, H-4), 8.71 – 8.66 (1H, m, H-6'), 8.43 (1H, ddd, *J* = 8.0, 2.4, 1.7 Hz, H-4'), 7.59 (1H, ddd, *J* = 7.9, 4.8, 0.9 Hz, H-5'), 4.22 (3H, s, H-1'''), 2.02 – 1.95 (1H, m, H-1''), 0.97 – 0.92 (2H, m, H-2''and H-3''), 0.92 – 0.87 (2H, m, H-2'' and H-3''); ^{13}C NMR (125 MHz, DMSO-d_6) δ_C 172.0 (C=O), 152.3 (C-7a), 149.7 (C-6'), 148.2 (C-5), 147.6 (C-2'), 139.3 (C-3), 134.2 (C-4'), 132.9 (C-3'), 124.0 (C-5'), 120.0 (C-4), 110.0 (C-3a), 34.2 (C-1'''), 13.7 (C-1''), 7.87 (C-2'' and C-3''); HRMS *m/z* (ESI$^+$) [Found: 295.1293., $C_{15}H_{14}N_6O$ requires [M + H]$^+$ 295.1302]; LCMS (LCQ): Rt = 0.5 min (Method 1); *m/z* (ESI$^+$) 295.3 [M + H]$^+$; LCMS (MDAP): Rt = 10.1 min, >95% (Method 3); *m/z* (ESI$^+$) 295.1 [M + H]$^+$.

5-Phenyl-1*H*-indazol-3-amine **327**

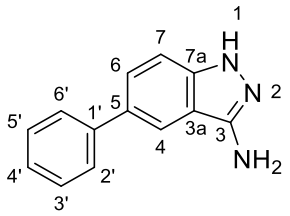

To a solution of 5-bromo-1*H*-indazol-3-amine (140 mg, 0.66 mmol) in water (1.25 mL) and acetonitrile (2.5 mL) was added phenylboronic acid (120 mg, 0.99 mmol) and tetrakis(triphenylphosphine)palladium(0) (70 mg, 0.06 mmol). The reaction mixture was heated to 150 °C under microwave irradiation for 20 min. The reaction mixture was concentrated under reduced pressure. The crude was purified using flash silica column chromatography on an Isco Combiflash system (12 g amino silica, elution with 0-30% 20% MeOH in CH_2Cl_2 / CH_2Cl_2 gradient) to afford the desired product, 5-phenyl-1*H*-indazol-3-amine, **327**, as an off-white solid (60 mg, 0.27 mmol, 41% yield). R_f 033 (MeOH/ CH_2Cl_2 1:9); ^{1}H NMR (500 MHz, DMSO-d_6) δ_H 11.39 (1H, s, $NH_{indazole}$), 8.05 – 7.96 (1H, m, H-4), 7.67 – 7.60 (2H, m, H-2' and 6'), 7.55 (1H, dd, *J* = 8.6, 1.8 Hz, H-6), 7.48 – 7.40 (2H, m, H-7- and 4'), 7.35 – 7.24 (2H, m, H-3' and 5'), 5.38 (2H, s, NH_2); HRMS *m/z* (ESI$^+$) [Found: 210.1024., $C_{13}H_{11}N_3$ requires [M + H]$^+$ 210.1026]; LCMS (LCQ): Rt = 1.3 min (Method 1); *m/z* (ESI$^+$) 210.3 [M + H]$^+$. The spectroscopic data are in good agreement with the literature values. Literature reference: WO2005/123688 A2, 2005; Page/Page column 71

N-(5-Phenyl-1*H*-indazol-3-yl)cyclopropanecarboxamide **328**

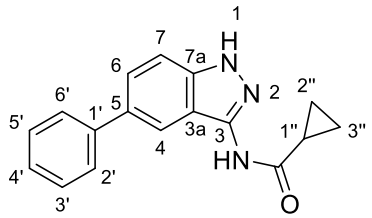

To a solution of 5-phenyl-1*H*-indazol-3-amine (50 mg, 0.24 mmol) in 1,4-dioxane (1 mL) was added cyclopropanecarbonyl chloride (0.02 mL, 0.24 mmol) and TEA (0.05 mL, 0.36 mmol). The reaction mixture was heated to 60 °C for 1 h. The reaction mixture was concentrated under reduced pressure. To the crude was added piperidine (2 mL) and the reaction mixture was stirred overnight at rt. The reaction mixture was concentrated under reduced pressure. The crude was purified using flash silica column chromatography on an Isco Combiflash system (12 g silica, elution with 0-50% 20% MeOH in CH_2Cl_2/ CH_2Cl_2 gradient) to afford the desired compound, *N*-(5-phenyl-1*H*-indazol-3-yl)cyclopropanecarboxamide, **328**, as an off-white solid (50 mg, 0.17 mmol, 72% yield). R_f. 0.44 (MeOH/ CH_2Cl_2 1:9); m.p. 201-203 °C; $\bar{\nu}_{max}$ (neat)/cm^{-1} 3198 (N-H, m), 3162 (N-H, m), 3030 (C-H, m), 2935 (C-H, w), 1660 (C=O, s), 1625 (C=N, m), 1547 (C=C, m); ^{1}H NMR (500 MHz, DMSO-d$_6$) δ_H 12.66 (1H, s, NH$_{indazole}$), 10.66 (1H, s, NH$_{amide}$), 8.04 – 8.00 (1H, m, H-4), 7.66 – 7.58 (3H, m, H-6, 6' and 2'), 7.51 (1H, d, *J* = 8.7 Hz, H-7), 7.46 (2H, app. t, *J* = 7.7 Hz, H-3' and 5'), 7.36 – 7.30 (1H, m, H-4'), 2.01 – 1.89 (1H, m, H-1''), 0.89 – 0.78 (4H, m, H-2'' and 3''); ^{13}C (125 MHz, DMSO-d$_6$) δ_C 171.8 (C=O), 140.99 (C-7a or 3), 140.95 (C-7a or 3), 140.5 (C-1' or 5), 131.9 (C-1' or 5), 128.9 (C-3' and 5'), 126.8 (C-2' and 6'), 126.7 (C-4'), 126.0 (C-6), 120.4 (C-4), 116.7 (C-3a), 110.6 (C-7), 13.8 (C-1''), 7.3 (C-2'' and 3''); HRMS *m/z* (ESI$^+$) [Found: 278.1283., $C_{17}H_{15}N_3O$ requires [M + H]$^+$ 278.1288]; LCMS (LCQ): Rt = 2.2 min (Method 1); *m/z* (ESI$^+$) 278.1 [M + H]$^+$; LCMS (MDAP): Rt = 17.5 min, >95% (Method 3); *m/z* (ESI$^+$) 278.1 [M + H]$^+$.

N-[5-(4-Pyridyl)-1*H*-indazol-3-yl]cyclopropanecarboxamide **330**

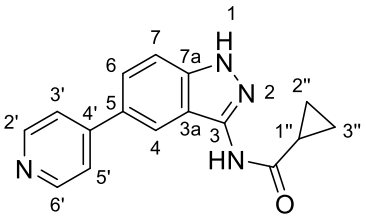

To a solution of 5-phenyl-1*H*-indazol-3-amine (200 mg, 0.94 mmol) in acetonitrile (0.6 mL) and water (0.10 mL) was added sodium carbonate (250 mg, 2.36 mmol), pyridine-4-boronic acid hydrate (170 mg, 1.41 mmol), tetrakis(triphenylphosphine)palladium(0) (50 mg, 0.05 mmol). The reaction mixture was degassed for 2 min before it was heated to 150 °C for 40 min. The reaction mixture was concentrated to dryness under reduced pressure. The crude was dissolved in MeOH and filtered through celite. The filtrate was concentrated under reduced pressure. The residue was dissolved in 1,4-dioxane (3 mL). Cyclopropanecarbonyl chloride (0.17 mL, 1.89 mmol) and TEA (0.26 mL, 1.89 mmol) were added. The reaction mixture was heated to 80 °C for 5 h. The reaction mixture was concentrated under reduced pressure. Piperidine (0.09 mL, 0.94 mmol) was added and the reaction mixture was stirred at rt overnight. The reaction mixture was concentrated under reduced pressure. The crude was purified using flash reverse phase column chromatography on a Biotage system (12 g C-18, elution with 10-100% MeOH / water gradient) to afford the desired product, *N*-[5-(4-pyridyl)-1*H*-indazol-3-yl]cyclopropanecarboxamide, **330**, as an off-white solid (50 mg, 0.17 mmol, 18% yield). R_f 0.27 (MeOH/CH_2Cl_2 1:9); m.p. 257-258 °C; $\bar{\nu}_{max}$ (neat)/cm^{-1} 3264 (N-H, m), 3142 (N-H, m), 3031 (C-H, m), 2928(C-H, w), 1660 (C=O, s), 1642 (C=N, m), 1598 (C=C, s), 1553 (C=C, s); ^{1}H NMR (500 MHz, DMSO-d$_6$) δ_H 12.79 (1H, s, NH$_{indazole}$), 10.77 (1H, s, NH$_{amide}$), 8.63 – 8.48 (2H, m, H-2' and 6'), 8.20 (1H, s, H-4), 7.72 (1H, d, *J* = 9.1 Hz, H-6), 7.63 (2H, d, *J* = 5.1 Hz, H-3' and 5'), 7.52 (1H, d, *J* = 8.7 Hz, H-7), 2.01 – 1.84 (1H, m, H-1''), 0.90 – 0.77 (4H, m, H-2'' and 3''); ^{13}C (125 MHz, DMSO-d$_6$) δ_C 171.8 (C=O), 150.2 (C-2' and 6'), 147.7 (C-4'), 141.3 (C-7a or 3), 141.2 (C-7a or 3), 128.6 (C-4'), 125.5 (C-6), 121.4 (C-5), 121.2 (C-3' and 5'), 116.5 (C-3a), 111.0 (C-7), 13.8 (C-1''), 7.4 (C-2'' and 3''); HRMS *m/z* (ESI$^+$) [Found: 279.1234., $C_{16}H_{14}N_4O$ requires [M + H]$^+$ 279.1201]; LCMS (LCQ): Rt = 0.6 min (Method 1); *m/z* (ESI$^+$) 279.3 [M + H]$^+$; LCMS (MDAP): Rt = 8.5 min, >95% (Method 3); *m/z* (ESI$^+$) 279.1 [M + H]$^+$.

References

[1] Salazar, D.E., Gormley, G., Clinical and Translational Science, Principles of Human Research Second Edition, Robertson, D., Williams, G.H. (Eds.), **2017**, 719. Academic Press

[2] Lindsay, M.A. *Nat. Rev. Drug Discov*, **2003**. 2, 831.

[3] Whittaker, P. A. *Drug Discov. Today Technol*. **2004**, 1, 125.

[4] Jain, K.K. *Drug Discovery Today*, **2004**, *9*(7), 307.

[5] Myers, R.A., Cruz, L.J., Rivier, J.E., Olivera, B.M. *Chem. Rev*., **1993**, *93*(5), 1923.

[6] Visintin, M., Quondam, M., Cattaneo, A. *Methods*, **2004**, *34*(2), 200.

[7] Beswick, P., Bowers, K. *The Handbook of Medicinal Chemistry: Principles and Practice*. Davis, A., Ward, S.E. (Eds.), Royal Society of Chemistry, **2015**, 486.

[8] Furber, M., Narjes, F., Steele, J. *The Handbook of Medicinal Chemistry: Principles and Practice*. Davis, A., Ward, S.E. (Eds.), Royal Society of Chemistry, **2015**, 505.

[9] Kola, I., Landis, J. *Nat. Rev. Drug Discov*. **2004**, *3*(8), 711.

[10] Arrowsmith, C.H., Audia, J.E., Austin, C., Baell, J., Bennett, J., Blagg, J., Bountra, C., Brennan, P.E., Brown, P.J., Bunnage, M.E., Buser-Doepner, C., Campbell, R.M., Carter, A.J., Cohen, P., Copeland, R.A., Cravatt, B., Dahlin, J.L., Dhanak, D., Edwards, A.M., Frederiksen, M., Frye, S.V., Gray, N., Grimshaw, C.E., Hepworth, D., Howe, T., Huber, K.V., Jin, J., Knapp, S., Kotz, J.D., Kruger, R.G., Lowe, D., Mader, M.M., Marsden, B., Mueller-Fahrnow, A., Müller, S., O'Hagan, R.C., Overington, J.P., Owen, D.R., Rosenberg, S.H., Roth, B., Ross, R., Schapira, M., Schreiber, S.L., Shoichet, B., Sundström, M., Superti-Furga, G., Taunton, J., Toledo-Sherman, L., Walpole, C., Walters, M.A., Willson, T.M., Workman, P., Young, R.N, Zuercher, W.J. *Nat Chem Biol*. **2015**, *11*(8), 536.

[11] Garbaccio, R.M., Parmee, E.R. *Cell Chem. Biol*. **2016**, *23*(1), 10.

[12] Workman, P., Collins, I. *Chem*. *Biol*. **2010**, *17*(6), 561.

[13] Antolin, A.A., Tym, J.E., Komianou, A., Collins, I., Workman, P., Al-Lazikani, B. *Cell Chem. Biol*. **2018**, *25*(2), 194.

[14] Baell, J., Walters, M.A. *Nature*. **2014**, *513*(7519), 481.

[15] De la Torre, R., de Sola, S., Hernandez, G., Farré, M., Pujol, J., Rodriguez, J., Espadaler, J.M., Langohr, K., Cuenca-Royo, A., Principe, A., Xicota, L., Janel, N., Catuara-Solarz, S., Sanchez-Benavides, G., Bléhaut, H., Dueñas-Espín, I., Del Hoyo, L., Benejam, B., Blanco-Hinojo, L., Videla, S., Fitó, M., Delabar, J.M., Dierssen, M. TESDAD study group. *Lancet Neurol*. **2016**, *15*(8), 801.

[16] De la Torre, R., De Sola, S., Pons, M., Duchon, A., de Lagran, M.M., Farré, M., Fitó, M., Benejam, B., Langohr, K., Rodriguez, J., Pujadas, M., Bizot, J.C., Cuenca, A., Janel, N., Catuara, S., Covas, M.I., Blehaut, H., Herault, Y., Delabar, J.M., Dierssen, M. *Mol. Nutr. Food Res*. **2014**, *58*(2), 278.

[17] Hughes, B. *Nat. Rev. Drug Discov*. **2008**, 7, 107.

[18] Frearson, J., Wyatt, P. *Expert Opin. Drug Discov*. **2010**, *5*(10), 909.

[19] Elkins, J.M., Fedele, V., Szklarz, M., Abdul Azeez, K.R., Salah, E., Mikolajczyk, J., Romanov, S., Sepetov, N., Huang, X.P., Roth, B.L., Al Haj Zen, A., Fourches, D., Muratov, E., Tropsha, A., Morris, J., Teicher, B.A., Kunkel, M., Polley, E., Lackey, K.E., Atkinson, F.L., Overington, J.P., Bamborough, P., Müller, S., Price, D.J., Willson, T.M., Drewry, D.H., Knapp, S., Zuercher, W.J. *Nat. Biotechnol*. **2016**, *34*(1), 95.

[20] European Bioinformatics Institute. https://www.ebi.ac.uk/chembldb/extra/PKIS/ (accessed Nov 30, 2018).

[21] Drewry, D.H., Wells, C.I., Andrews, D.M., Angell, R., Al-Ali, H., Axtman, A.D., Capuzzi, S.J., Elkins, J.M., Ettmayer, P., Frederiksen, M., Gileadi, O., Gray, N., Hooper, A., Knapp, S., Laufer, S., Luecking, U., Michaelides, M., Müller, S., Muratov, E., Denny, R.A., Saikatendu, K.S., Treiber, D.K., Zuercher, W.J., Willson, T.M. *PLoS One*. **2017**, *12*(8), e0181585.

[22] Meanwell, N.A. *Chem. Res. Toxicol*., **2011**, 24, 1420.

[23] Gleeson, M.P., Leeson, P.D., van de Waterbeemd, H. *The Handbook of Medicinal Chemistry: Principles and Practice*. Davis, A., Ward, S.E. (Eds.), Royal Society of Chemistry, **2015**, 1.

[24] Lipinski, C.A., Lombardo, F., Dominy, B.W., Feeney, P.J. *Adv. Drug Deliv. Rev.* **1997**, 23, 3.

[25] Curatolo, W. *Pharm. Sci. Technol. Today.* **1998**, 1, 387.

[26] Hann, M.M. *Med. Chem. Commun*., **2011**, 2, 349.

[27] Hopkins, A.L., Keserü, G.M., Leeson, P.D., Rees, D.C., Reynolds, C.H. *Nat. Rev. Drug Discov*. **2014**, *13*(2), 105.

[28] Hopkins, A. L., Groom, C. R., Alex, A. *Drug Discov. Today*. **2004**, 9, 430.

[29] Kuntz, I. D., Chen, K., Sharp, K. A., Kollman, P. A. *Proc. Natl Acad. Sci. USA*. **1999**, 96, 9997.

[30] Wager, T.T, Hou, X., Verhoest, P.R., Villalobos, A. *ACS Chem. Neurosci*. **2010**, *1*(6), 435.

[31] Heffron, T.P. *J. Med. Chem*. **2016**, 59, 10030.

[32] Heffron T.P., Salphati, L., Alicke, B., Cheong, J., Dotson, J., Edgar, K., Goldsmith, R., Gould, S.E., Lee, L.B., Lesnick, J.D., Lewis, C., Ndubaku, C., Nonomiya, J., Olivero, A.G., Pang, J., Plise, E.G., Sideris, S., Trapp, S., Wallin, J., Wang, L., Zhang, X. *J Med Chem*. **2012**, 55, 8007.

[33] KNIME | Open for Innovation. KNIME | Open for Innovation, https://www.knime.org/.

[34] Hill, A.P., Young, R.J. *Drug Discov. Today*. **2010**, *15*(15-16), 648.

[35] Norinder, U., Haeberlein, M. *Adv. Drug Deliv. Rev*. **2002**, *54*(3), 291.

[36] Vilar, S., Chakrabarti, M., Costanzi, S. *J. Mol. Graph Model*. **2010**, *28*(8), 899.

[37] Shire, S.J., Cromwell, M., Liu, J. *AAPS J*. **2006**, *8*(4), E729.

[38] Egan, W.J., Merz, K.M. Jr., Baldwin, J.J. *J. Med. Chem*. **2000**, 43, 3867.

[39] Martin, Y.C. *J. Med. Chem*. **2005**, 48, 3164.

[40] Gaulton, A., Bellis, L.J., Bento, A.P., Chambers, J., Davies, M., Hersey, A., Light, Y., McGlinchey, S., Michalovich, D., Al-Lazikani, B., Overington, J.P. *Nucleic Acids Res*. **2012**, 40(Database issue):D1100.

[41] Metz, J.T., Johnson, E.F., Soni, N.B., Merta, P.J., Kifle, L., Hajduk, P. *Nat. Chem. Biol*. **2011**, *7*(4), 200.

[42] Laboratoires Servier (FR) and Vernalis (UK). WO055530; **2017**.

[43] IUPAC Gold Book radical (free radical).

[44] Romero, N.A., Nicewicz, D.A. *Chem. Rev*. **2016**, 116, 10075.

[45] Curran, D.P. *Synthesis*. **1988**, 417.

[46] McAtee, R.C., McClain, E.J., Stephenson, C.R.J. *Trends in Chemistry*. **2019**, 1(1).

[47] Arias-Rotondo, D.M., McCusker, J.K. *Chem. Soc. Rev*., **2016**, 45, 5803.

[48] Le, C.C., Wismer, M.K., Shi, Z.C., Zhang, R., Conway, D.V., Li, G., Vachal, P., Davies, I.W., MacMillan, D.W.C. *ACS Cent. Sci*. **2017**, *3*(6), 647.

[49] Beatty, J.W., Douglas, J.J., Miller, R., McAtee, R.C., Cole, K.P., Stephenson, C.R.J. *Chem*. **2016**, *1*(3), 456.

[50] Shaw, M.H., Twilton, J., MacMillan, D.W.C. *J. Org. Chem*. **2016**, 81, 6898.

[51] Douglas, J.J., Sevrin, M.J., Stephenson, C.R.J. *J. Org. Process Res. Dev*. **2016**, 20, 1134.

[52] Pitre, S.P., McTiernan, C.D., Ismaili,H., Scaiano, J.C. *ACS Catal*. **2014**, 4, 2530.

[53] Lipton, S.A. *NeuroRx*. **2004**, 1, 101

[54] Coyle, J.T. *Mol Neurobiol*. **2006**, 26, 365.

[55] Meldrum, B.S. *Curr. Opin. Neurol. Neurosurg*. **1992**, 5, 508.

[56] Chen, H.S., Lipton, S.A. *J. Neurochem*. **2006**, 97, 1611.

[57] Pittenger, C., Sanacora, G., Krystal, J.H. *CNS Neurol. Disord. Drug Targets*. **2007**, 6, 101.

[58] McShane, R., Areosa Sastre, A., Minakaran, N. *Cochrane Database Syst Rev*. **2006**, 2, CD003154.

[59] Fadda, E., Danysz, W., Wroblewski, J.T., Costa, E. *Neuropharmacology*. **1988**, 27, 1183.

[60] Wolosker, H., Sheth, K.N., Takahashi, M., Mothet, J.P., Brady, R.O. Jr., Ferris, C.D., Snyder, S.H. *Proc. Natl. Acad. Sci. USA*. **1999**, 96, 721.

[61] Basu, A.C., Tsai, G.E., Ma, C.L., Ehmsen, J.T., Mustafa, A.K., Han, L., Jiang, Z.I., Benneyworth, M.A., Froimowitz, M.P., Lange, N., Snyder, S.H., Bergeron, R., Coyle, J.T. *Mol. Psychiatry.* **2009**, 14, 719.

[62] Turpin, F.R., Potier, B., Dulong, J.R., Sinet, P.M., Alliot, J., Oliet, S.H., Dutar, P., Epelbaum, J., Mothet, J.P., Billard, J.M. *Neurobiol Aging.* **2011**, *32*(8), 1495.

[63] Inoue, R., Hashimoto, K., Harai, T., Mori, H. *J. Neurosci*. **2008**, 28, 14486.

[64] Mustafa, A.K., Ahmad, A.S., Zeynalov, E., Gazi, S.K., Sikka, G., Ehmsen, J.T., Barrow, R.K., Coyle, J.T., Snyder, S.H., Doré, S. *J. Neurosci*. **2010**, 30, 1413.

[65] Sasabe, J., Chiba, T., Yamada, M., Okamoto, K., Nishimoto, I., Matsuoka, M., Aiso, S. *EMBO J*. **2007**, 26, 4149.

[66] Heresco-Levy, U., Durrant, A.R., Ermilov, M., Javitt, D.C., Miya, K., Mori, H. *Biol. Psychiatry*. **2015**, *77*(6), 27.

[67] Jirásková-Vaníčková, J., Ettrich, R., Vorlová, B., Hoffman, H.E., Lepšík, M., Jansa, P., Konvalinka, J. *Curr. Drug Targets*. **2011**, 12, 1037.

[68] Smith M.A., Mack, V., Ebneth, A., Moraes, I., Felicetti, B., Wood, M., Schonfeld, D., Mather, O., Cesura, A., Barker, J. *J. Biol. Chem*. **2010**, 285, 12873.

[69] Wada, M., Nakamori, S., Takagi, H. *FEMS. Microbiol. Lett*. **2003**, 225, 189.

[70] Wolosker, H., Blackshaw, S., Snyder, S.H. *Proc. Natl. Acad. Sci. USA*. **1999**, 96, 13409.

[71] Yoshikawa, M., Nakajima, K., Takayasu, N., Noda, S., Sato, Y., Kawaguchi, M., Oka, T., Kobayashi, H., Hashimoto, A. *Eur. J. Pharmacol*. **2006**, 548, 74.

[72] Miya, K., Inoue, R., Takata, Y., Abe, M., Natsume, R., Sakimura, K., Hongou, K., Miyawaki, T., Mori, H. *J Comp Neurol*. **2008**, 510, 641.

[73] Verrall, L., Walker, M., Rawlings, N., Benzel, I., Kew, J.N., Harrison, P.J., Burnet, P,W. *Eur. J. Neurosci*. **2007**, 26, 1657.

[74] Stevens, E.R., Esguerra, M., Kim, P.M. *Proc. Natl. Acad. Sci. USA*. **2003**, 100, 6789.

[75] Wu, S., Barger, S.W., Sims, T.J. *Brain Res*. **2004**, 1020, 161.

[76] Xia, M., Liu, Y., Figueroa, D.J., Chiu, C.S., Wei, N., Lawlor, A.M., Lu, P., Sur, C., Koblan, K.S., Connolly, T.M. *Brain Res. Mol. Brain Res*. **2004**, 125, 96.

[77] Chen, Z., Huang, W., Srinivas, S.R., Jones, C.R., Ganapathy, V., Prasad, P.D. *J. Soc. Gynecol. Investig*. **2004**, 11, 294.

[78] Percudani, R., Peracchi, A. *BMC Bioinformat*. **2009**, 10, 273.

[79] Dunathan, H.C. *Proc. Natl. Acad. Sci. USA*. **1966**, 55, 712.

[80] Goto, M., Takae, Y., Kamiya, N., Miyahara, I., Yoshimura, T., Mihara, H., Kurihara, T., Hirotsu, K., Esaki, N. *J. Biol. Chem*. **2009**, 38, 25944.

[81] Nitoker, N., Major, D.T. *Biochemistry*. **2015**, 54, 516.

[82] Baumgart, F., Rodriguez-Crespo, I. *FEBS. J*. **2008**, 275, 3538.

[83] Hoffman, H., Jiraskova, J., Zvelebil, M., Konvalinka, J. *Collect. Czech Chem. Commun*. **2010**, 75, 59.

[84] Baumgart, F., Mancheno, J.M., Rodriguez-Crespo, I. *FEBS. J.* **2007**, 274, 4561.

[85] De Miranda, J., Panizzutti, R., Foltyn, V., Wolosker, H. *Proc. Natl. Acad. Sci. USA.* **2002**, 22, 14542

[86] Foltyn, V., Bendikov, I., De Miranda, J., Panizzutti, R., Dumin, E., Shelper, M., Li, P., Toney, M.D., Kartvelishvily, E., Wolosker, H. *J. Biol. Chem*. **2005**, 280, 1754.

[87] Marchetti, M., Bruno, S., Campanini, B., Peracchi, A., Mai, N., Mozzarelli, A. *FEBS. J*. **2013**, *280*(22), 5853.

[88] Kubala, M., Teisinger, J., Ettrich R, Hofbauerová, K., Kopecký, V. Jr., Baumruk, V., Krumscheid, R., Plásek, J., Schoner, W., Amler, E. *Biochemistry*. **2003**, 42, 6446.

[89] Tomitsuka, E., Hirawake, H., Goto, Y., Taniwaki, M., Harada, S., Kita, K. *J. Biochem*. **2003**, 134, 191.

[90] Vorlova, B., Nachtigallova, D., Jiraskova-Vanickova, J., Ajani, H., Jansa, P., Rezac, J., Fanfrlik, J., Otyepka, M., Hobza, P., Konvalinka, J., Lepsik, M. *Eur. J. Med. Chem*. **2015**, 89, 189.

[91] Strisovsky, K., Jiraskova, J., Mikulova, A., Rulisek, L., Konvalinka, J. *Biochemistry*. **2005**, 44, 13091.

[92] Henneberger, C., Papouin, T., Oliet, S.H., Rusakov, D.A. *Nature*. **2010**, 463, 169.

[93] Hoffman, H.E., Jiraskova, J., Cigler, P., Sanda, M., Schraml, J., Konvalinka, J. *J. Med. Chem*. **2009**, 52, 6032.

[94] Dixon, S.M, Li, P., Liu, R., Wolosker, H., Lam, K.S., Kurth, M.J., Toney, M.D. *J. Med. Chem*. **2006**, 49, 2388.

[95] Otvos, L., Jr., Wade, J.D. *Front. Chem*. **2014**, 2, 62.

[96] Mori, H.,Wada, R., Li, J., Ishimoto, T., Mizuguchi, M., Obita, T., Gouda, H., Hirono, S., Toyooka, N. *Bioorg. Med. Chem. Lett*. **2014**, 24, 3732.

[97] Mori, H. EP 2808014A1.

[98] Irwin, J.J., Sterling, T., Mysinger, M.M., Bolstad, E.S., Coleman, R.G. *J. Chem. Inf. Model*. **2012**, *52*(7), 1757.

[99] Dellafiora, L., Marchetti, M., Spyrakis, F., Orlandi, V., Campanini, B., Cruciani, G., Cozzinia, P., Mozzarelli, A. *Bioorg. Med. Chem. Lett*. **2015**, 25, 4297.

[100]Mori, H., Wada, R., Takahara, S., Horino, Y., Izumi, H., Ishimoto, T., Yoshida, T., Mizuguchi, M., Obita, T., Gouda, H., Hirono, S., Toyooka, N. *Bioorg. Med. Chem*. **2017**, 25, 3736.

[101] Takahara, S., Nakagawa, K., Uchiyama, T., Yoshida, T., Matsumoto, K., Kawasumi, Y., Mizuguchi, M., Obita, T., Watanabe, Y., Hayakawa, D., Gouda, H., Mori, H., Toyooka, N. *Bioorg. Med. Chem. Lett*. **2018**, 28, 441.

[102] Koshland, D.E. *Proc. Natl. Acad. Sci. U S A*., **1958**, *44*(2) 98.

[103] Jin, Y., Wan, Z., Zhang, Q. WO 2012076435A1

[104] Johnson, L. N. *Biochem. Soc. Trans*. **2009**, 37, 627.

[105] Manning, G., Whyte, D. B., Martinez, R., Hunter, T., Sudarsanam, S. *Science.* **2002**, 298, 1912.

[106] Manning, G., Plowman, G. D., Hunter, T., Sudarsanam, S. *Trends. Biochem. Sci*. **2002**, 27, 514.

[107] Knighton, D.R., Zheng, J.H., Ten Eyck, L.F., Ashford, V.A., Xuong, N.H., Taylor, S.S., Sowadski, J.M. *Science*. **1991**. *253*(5018), 407.

[108] Endicottm, J.A., Noble, M.E., Johnson, L.N. *Annu. Rev. Biochem*. **2012**, 81, 587.

[109] Schwartz, P. A., Murray, B. W. *Bioorg. Chem*. **2011**, 39, 192.

[110] Eswaran, J., Knapp, S. *Biochim. Biophys. Acta.* **2010**, 1804, 429.

[111] Roskoski R. Jr. *Pharmacol. Res*. **2015**, 100, 1.

[112] Cohen, P., *Nat. Rev. Drug Discov*., **2002**, 1, 309.

[113] Rosokoski, R., *Pharmacol. Res*. **2019**, 144, 19.

[114] https://www.fda.gov/NewsEvents/Newsroom/PressAnnouncements/ucm635906.htm

[115] Carles, F., Bourg, S., Meyer, C., Bonnet, P. *Molecules*. **2018**, *23*(4), E908.

[116] Fischer, P.M., *Med. Res. Rev*. **2017**, 37, 314.

[117] Knapp, S. *Br. J. Cancer*. **2018**, *118*(7), 936.

[118] Roth, B.L., Sheffler, D.J., Kroeze, W.K. *Nat. Rev. Drug. Discov*. **2004**, *3*(4), 353.

[119] Takata, M., Tanaka, H., Kimura, M., Nagahara, Y., Tanaka, K., Kawasaki, K., Seto, M., Tsuruma, K., Shimazawa, M., Hara, H. *Br. J. Pharmacol*. **2013**, *170*(2), 341.

[120] Ward, R.A., Goldberg, F.W. (Eds.). *Kinase Drug Discovery: Modern Approaches (RSC Drug Discovery Series)*. Royal Society of Chemistry, **2019**, 1.

[121] Dar, A.C., Shokat, K.M. *Annu. Rev. Biochem*. **2011**, 80, 769.

[122] Zuccotto, F., Ardini, E., Casale, E., Angiolini, M. *J. Med. Chem*. **2010**, 53, 2691.

[123] Roskoski, R. Jr. *Pharmacol. Res*. **2016**, 103, 26.

[124] Gavrin, L.K., Saiah, E. *Med. Chem. Commun*. **2013**, 4, 41.

[125] Lamba, V., Ghosh, I. *Curr. Pharm. Des*. **2012**, 18, 2936.

[126] De Bruin, G., Barf, T. *Kinase Drug Discovery: Modern Approaches (RSC Drug Discovery Series)*. Ward, R.A., Goldberg, F.W. (Eds.) Royal Society of Chemistry, **2019**, 61.

[127] Vijayan, R.S., He, P., Modi, V., Duong-Ly, K.C., Ma, H., Peterson, J.R., Dunbrack, R.L. Jr, Levy, R.M. *J. Med. Chem*. **2015**, 58, 466.

[128] Kwarcinski, F.E., Brandvold, K.R., Phadke, S., Beleh, O.M., Johnson, T.K., Meagher, J.L., Seeliger, M.A., Stuckey, J.A., Soellner, M.B. *ACS Chem. Biol*. **2016**, 11, 1296.

[129] Zhao, Z., Wu, H., Wang, L., Liu, Y., Knapp, S., Liu, Q., Gray, N.S. *ACS Chem. Biol*. **2014**, *9*(6), 1230.

[130] Knuutila, S., Bjorkqvist, A.M., Autio, K., Tarkkanen, M., Wolf, M., Monni, O., Szymanska, J., Larramendy, M.L., Tapper, J., Pere, H., El-Rifai, W., Hemmer, S., Wasenius, V.M., Vidgren, V., Zhu, Y. *Am. J. Pathol*. **1998**, 152, 107.

[131] Aranda, S., Laguna, A., de la Luna, S. *FASEB J*. **2011**, 25, 449.

[132] Becker, W., Joost, H.G. *Prog. Nucleic. Acid. Res. Mol. Biol*. **1999**, 62, 1.

[133] Park, J., Song, W.J., Chung, K.C. *Cell. Mol. Life Sci*. **2009**, 66, 3235.

[134] Okui, M., Ide, T., Morita, K., Funakoshi, E., Ito, F., Ogita, K., Yoneda, Y., Kudoh, J., Shimizu, N. *Genomics*. **1999**, 62, 165.

[135] Soundararajan, M., Roos, A.K., Savitsky, P., Filippakopoulos, P., Kettenbach, A.N., Olsen, J.V., Gerber, S.A., Eswaran, J., Knapp, S., Elkins, J.M. *Structure*. **2013**, *21*(6), 986.

[136] Lochhead, P.A., Sibbet, G., Morrice, N., Cleghon, V. *Cell*, **2005**, 121, 925.

[137] Himpel, S., Tegge, W., Frank, R., Leder, S., Joost, H.G., Becker, W. *J. Biol. Chem*. **2000**, 275, 2431.

[138] Skurat, A.V., Dietrich, A.D. *J. Biol.Chem*. **2004**, 279, 2490.

[139] Laguna, A., Aranda, S., Barallobre, M.J., Barhoum, R., Fernández, E., Fotaki, V., Delabar, J.M., de la Luna, S., de la Villa, P., Arbonés, M.L. *Dev. Cell*. **2008**, 15, 841.

[140] Fernandez-Martinez, J., Vela, E.M., Tora-Ponsioen, M., Ocaña, O.H., Nieto, M.A., Galceran, J. *J. Cell Sci*. **2009**, 122, 1574.

[141] Roewenstrunk, J., Di Vona, C., Chen, J., Borras, E., Dong, C., Arató, K., Sabidó, E., Huen, M.S.Y., de la Luna, S. *Sci. Rep*. **2019**, *9*(1), 6014.

[142] Munoz, L., Selig, R., Yeung, Y., Peifer, C., Laufer, S. *Anal. Biochem*. **2010**, 401, 125.

[143] Kim, E.J., Sung, J.Y., Lee, H.J., Rhim, H., Hasegawa, M., Iwatsubo, T., Min, D.S., Kim, J., Paik, S.R., Chung, K.C. *J. Biol. Chem*. **2006**, 281, 33250.

[144] Kang, J.E., Choi, S.A., Park, J.B., Chung, K.C. *Cells. J. Neurosci. Res*, **2005**, 81, 62.

[145] Jakob-Roetne, R., Jacobsen, H. *Agnew. Chem. Int. Ed*. **2009**, 48, 3030.

[146] Rang, H.P., Dale, M.M., Ritter, J.M. *Pharmacology Fifth Edition*. **1987**. Churchill Livingston. 504.

[147] Wolfe, M.S. *Emerging Drug Targets for Alzheimer's Disease*. **2010**, 1, 3.

[148] Smith, B., Medda, F., Gokhale, V., Dunckley, T., Hulme, C. *ACS Chem. Neurosci*. **2012**, 3, 857.

[149] Ryu, Y.S., Park, S.Y., Jung, M.S., Yoon, S.H., Kwen, M.Y., Lee, S.Y., Choi, S.H., Radnabaazar, C., Kim, M.K., Kim, H., Kim, K., Song, W.J., Chung, S.H. *J. Neurochem*. **2010** 115, 574.

[150] Kimura, R., Kamino, K., Yamamoto, M., Nuripa, A., Kida, T., Kazui, H., Hashimoto, R., Tanaka, T., Kudo, T., Yamagata, H., Tabara, Y., Miki, T., Akatsu, H., Kosaka, K., Funakoshi, E., Nishitomi, K., Sakaguchi, G., Kato, A., Hattori, H., Uema, T., Takeda, M. *Disease. Hum. Mol. Genet*. **2007**, 16, 15.

[151] Goedert, M., Jakes, R. *Biochem. Biophys. Acta*. **2005**, 1739, 240.

[152] Shi, J., Zhang, T., Zhou, C., Chohan, M. O., Gu, X., Wegiel, J., Zhou, J., Hwang, Y. W., Iqbal, K., Grundke-Iqbal, I., Gong, C. X., Liu, F. *J. Biol. Chem*. **2008**, 283, 28660.

[153] Jung, M.S., Park, J.H., Ryu, Y.S., Choi, S.H., Yoon, S.H., Kwen, M.Y., Oh, J.Y., Song, W.J., Chung, S.H. *J. Biol. Chem*. **2011**, *286*(46), 40401.

[154] Sadowski, M., Wisniewski, H.M., Tarnawski, M., Kozlowski, P.B., Lach, B., Wegiel, *J. Acta. Neuropathol*. **1999**, *97*(2), 156.

[155] Abbassi, R., Johns, T.G., Kassiou, M., Munoz, L. *Pharmacol. Ther*. **2015**, 151, 87.

[156] Reeves, R.H., Irving, N.G., Moran, T.H., Wohn, A., Kitt, C.,Sisodia, S.S., Schmidt, C., Bronson, R.T., Davisson, M.T. *Nat. Genet*. **1995**, 11, 177.

[157] Sago, H., Carlson, E. J., Smith, D. J., Kilbridge, J., Rubin, E. M.,Mobley, W. C., Epstein, C. J., Huang, T. T. *Proc. Natl. Acad. Sci. U.S.A*. **1998**, 95, 6256.

[158] Belichenko, N. P., Belichenko, P. V., Kleschevnikov, A. M., Salehi, A., Reeves, R. H., Mobley, W. C. *J. Neurosci*. **2009**, 29, 5938.

[159] Belichenko, P. V., Masliah, E., Kleschevnikov, A. M., Villar, A. J., Epstein, C. J., Salehi, A., Mobley, W. C. *J. Comp. Neurol*. **2004**, 480, 281.

[160] Belchenko, P. V., Kleschevnikov, A. M., Salehi, A., Epstein, C. J., Mobley, W. C. *J. Comp. Neurol*. **2007**, 504, 329.

[161] Smith, D. J., Stevens, M. E., Sudanagunta, S. P., Bronson, R. T.,Makhinson, M., Watabe, A. M., O'Dell, T. J., Fung, J., Weier, H. U.,Cheng, J. F., Rubin, E. M. *Nat. Genet*. **1997**, 16, 28.

[162] Branchi, I., Bichler, Z., Minghetti, L., Delabar, J. M., Malchoidi-Abedi, F., Gonzalez, M. C., Chettouh, C., Niccolini, A., Chabert, C., Smith, D. J., Rubin, E. M., Migliore-Samour, D., Alleva, E. *J.Neuropathol. Exp. Neurol*. **2004**, 63, 429.

[163] Chabert, C., Jamon, M., Cherfouh, A., Duquenne, V., Smith, D.J., Rubin, E., Roubertoux, P.L. *Behav. Genet*. **2004**, 34, 559.

[164] Feki, A., Hibaoui, Y. *Brain Sci*. **2018**, *8*(10), 187.

[165] Schnabel, F., Smogavec, M., Funke, R., Pauli, S., Burfeind, P., Bartels, I. *Mol. Cytogenet*. **2018**, 11, 62.

[166] Yang, Q., Rasmussen, S. A., Friedman, J. M. *Lancet*. **2002**, 359, 1019.

[167] Baek, K. -H., Zaslavsky, A., Lynch, R.C., Britt, C., Okada, Y., Siarey, R.J, Lensch, M.W., Park, I.H., Yoon, S.S., Minami, T., Korenberg, J.R., Folkman, J., Daley, G.Q., Aird, W.C., Galdzicki, Z., Ryeom, S. *Nature*. **2009**, 459, 1126.

[168] Liu, Q., Liu, N., Zang, S., Liu, H., Wang, P., Ji, C., Sun, X. *PLoS One*. **2014**, 9(6), e98853.

[169] Liao, J. -M., Zhou, X., Zhang, Y., Lu, H. *Cell Cycle*. **2012**, 11, 2624.

[170] Chang, H. -S., Lin, C. -H., Yang, C. -H., Yen, M. -S., Lai, C. -R., Chen, Y. -R., Liang, Y.J., Yu, W.C. *Int. J. Cancer*. **2007**, 120, 2377.

[171] Pozo, N., Zahonero, C., Fernandez, P., Linares, J. M., Ayuso, A., Hagiwara, M., Perez, A., Ricoy, J. R., Hernandez-Lain, A., Sepulveda, J. M., Sanchez- Gomez, P. *J. Clin. Invest*. **2013**, *123*(6), 2475.

[172] Pozo, N.; Zahonero, C.; Fernandez, P.; Linares, J. M.; Ayuso, A.; Hagiwara, M.; Perez, A.; Ricoy, J. R.; Hernandez-Lain, A.; Sepulveda, J. M.; Sanchez- Gomez, P. *J. Clin. Invest*. **2013**, *123*(6), 2475.

[173] Mahindroo, N., Punchihewa, C., Fujii, N. *J. Med. Chem*. **2009**, 52, 3829.

[174] Masuda, M., Wakasaki, T., Suzui, M. Toh, S., Joe, A.K., Weinstein, I.B. *Curr. Cancer Drug Targets*. **2010**, 10, 117.

[175] Liu, Y., Li, C., Lin, J. *Anticancer Agents Med. Chem*. **2010**, 10, 512.

[176] Guschin, D., Rogers, N., Briscoe, J., Witthuhn, B., Watling, D., Horn, F., Pellegrini, S., Yasukawa, K., Heinrich, P., Stark, G.R., Ihle, J.N., Ke, I.M. *EMBO J*. **1995**, 14, 1421.

[177] Harmes, D.C., DiRenzo, J. *J. Mammary Gland Biol. Neoplasia*. **2009**, 14, 19.

[178] Litovchick, L., Florens, L.A., Swanson, S.K, Washburn, M.P., DeCaprio, J.A. *Genes Dev*. **2011**, 25, 801.

[179] Boichuk, S., Parry, J.A., Makielski, K.R., Litovchick, L., Baron, J.L., Zewe, J.P., Wozniak, A., Mehalek, K.R., Korzeniewski, N., Seneviratne, D.S., Schöffski, P., Debiec-Rychter, M., DeCaprio, J.A., Duensing, A. *Cancer Res*. **2013**, 73, 5120.

[180] Seifert, A., Allan, L.A., Clarke, P.R. *FEBS J*. **2008**, 275, 6268.

[181] Seifert, A.; Clarke, P.R. *Cell Signal*. **2009**, 21, 1626.

[182] Ionescu, A., Dufrasne, F., Gelbcke, M., Jabin, I., Kiss, R., Lamoral-Theys, D. *Mini. Rev. Med. Chem*. **2012**. *12*(13), 1315.

[183] Kang, J. E., Choi, S. A., Park, J. B., Chung, K. C. *J. Neurosci. Res*. **2005**, *81*(1), 62.

[184] Kim, E. J.; Sung, J. Y.; Lee, H. J.; Rhim, H.; Hasegawa, M.; Iwatsubo, T.; Min, D. S.; Kim, J.; Paik, S. R.; Chung, K. C. *J. Biol. Chem*. **2006**, *281*(44), 33250.

[185] Im, E., Chung, K.C. J. *Neurochem*. **2015**, 134, 756.

[186] Møller, R.S., Kübart, S., Hoeltzenbein, M., Heye, B., Vogel, I., Hansen, C.P., Menzel, C., Ullmann, R., Tommerup, N., Ropers, H.H., Tümer, Z., Kalscheuer, V.M. *Am J Hum Genet*. **2008**, *82*(5), 1165.

[187] Arbones, M.L., Thomazeau, A., Nakano-Kobayashi, A., Hagiwara, M., Delabar, J.M. *Pharmacol. Ther*. **2019**, 194, 199.

[188] van Bon, B.W., Coe, B.P., Bernier, R., Green, C., Gerdts, J., Witherspoon, K., Kleefstra, T., Willemsen, M.H., Kumar, R., Bosco, P., Fichera, M., Li, D., Amaral, D., Cristofoli, F., Peeters, H., Haan, E., Romano, C., Mefford, H.C., Scheffer, I., Gecz, J., de Vries, B.B., Eichler, E.E. *Mol. Psychiatry*. **2016**, *21*(1), 126.

[189] Ashcroft, F.M., Rorsman, P. *Cell*. **2012**, 148, 1160.

[190] Nathan, D.M. *N. Engl. J. Med*. **2002**, 347, 1342.

[191] Vetere, A., Choudhary, A., Burns, S.M., Wagner, B.K. *Nat. Rev. Drug Discov*. **2014**, 13, 278.

[192] Belgardt, B-F., Lammert, E. *Diabetes*. **2016**, *65*(6), 1496.

[193] Smith, B., Medda, F., Gokhale, V., Dunckley, T., Hulme, C. *ACS Chem. Neurosci*. **2012**, 3, 857.

[194] Stotani, S., Giordanetto, F., Medda, F. *Future Med. Chem*. **2016**, 8, 681.

[195] Nguyen, T.L., Fruit, C., Hérault, Y., Meijer, L., Besson, T. *Expert Opin. Ther. Pat*. **2017**, *27*(11), 1183.

[196] Jarhad, D.B., Mashelkar, K.K., Kim, H.R., Noh, M., Jeong, L.S. *J. Med. Chem*. **2018**, 61, 9791.

[197] Adayev, T., Chen-Hwang, M.C., Murakami, N., Wegiel, J., Hwang, Y. W. *Biochemistry.* **2006**, 45, 12011.

[198] McLauchlan, H., Elliott, M., Cohen, P. *Biochem. J*. **2003**, 371, 199.

[199] Guedj, F., Sebrie, C., Rivals, I., Ledru, A., Paly, E., Bizot, J. C., Smith, D., Rubin, E., Gillet, B., Arbones, M., Delabar, J. M. *PLoS One*. **2009**, 4, e4606.

[200] de la Torre, R., de Sola, S., Hernandez, G., Farré, M., Pujol, J., Rodriguez, J., Espadaler, J.M., Langohr, K., Cuenca-Royo, A., Principe, A., Xicota, L., Janel, N., Catuara-Solarz, S., Sanchez-Benavides, G., Bléhaut, H., Dueñas-Espín, I., Del Hoyo, L., Benejam, B., Blanco-Hinojo, L., Videla, S., Fitó, M., Delabar, J.M., Dierssen, M. TESDAD study group. *Lancet Neurol*. **2016**, *15*(8), 801.

[201] Lambert, J.D., Sang, S., Yang, C.S. *Mol.Pharmaceutics*. **2007**, 4, 819.

[202] Stringer, M., Goodlett, C. R., Roper, R. J. *Mol. Genet. Genomic Med*. **2017**, 5, 451.

[203] Abeysekera, I., Thomas, J., Georgiadis, T. M., Berman, A. G., Hammond, M. A., Dria, K. J., Wallace, J. M., Roper, R. J. *Mol.Nutr. Food Res*. **2016**, 60, 717.

[204] Baell, J. B., Holloway, G. *J. Med. Chem*. **2010**, 53, 2719.

[205] Ingolfsson, H.I., Thakur, P., Herold, K.F., Hobart, E.A., Ramsey, N.B., Periole, X., de Jong, D.H., Zwama, M., Yilmaz, D., Hall, K., Maretzky, T., Hemmings, H.C., Jr., Blobel, C., Marrink, S.J., Kocer, A., Sack, J. T., Andersen, O. S. *ACS Chem. Biol*. **2014**, 9, 1788.

[206] Araldi, G.L. Avanti Biosciences Inc., **2018**. US20180000774.

[207] Bain, J., Plater, L., Elliott, M., Shpiro, N., Hastie, C.J., Mclauchlan, H., Klevernic, I., Arthur, J.S.; Alessi, D.R., Cohen, P. *Biochem. J*. **2007**, 408, 297.

[208] Morales-García, J.A., de la Fuente Revenga, M., Alonso-Gil, S., Rodríguez-Franco, M.I., Feilding, A., Perez-Castillo, A., Riba, J. *Sci. Rep*. **2017**, *7*(1), 5309.

[209] Li, C., Wang, Y., Wang, C., Yi, X., Li, M., He, X. *Phytomedicine*. **2017**, 28, 10.

[210] Malinge, S., Bliss-Moreau, M., Kirsammer, G., Diebold, L., Chlon, T., Gurbuxani, S., Crispino, J.D. *J. Clin. Invest*. **2012**, 122, 948.

[211] Waki, H., Park, K. W., Mitro, N., Pei, L., Damoiseaux, R., Wilpitz, D. C., Reue, K., Saez, E., Tontonoz, P. *Cell Metab*. **2007**, 5, 357.

[212] Park, K. W., Waki, H., Villanueva, C. J., Monticelli, L. A., Hong, C., Kang, S., MacDougald, O.A., Goldrath, A.W., Tontonoz, P. *Mol. Endocrinol*. **2008**, 22, 2038.

[213] Kumar, B., Gupta, V.P., Kumar, V. *Curr. Drug Targets*. **2017**, *18*(1), 87.

[214] Ogawa, Y., Nonaka, Y., Goto, T., Ohnishi, E., Hiramatsu, T., Kii I., Yoshida, M., Ikura, T., Onogi, H., Shibuya, H., Hosoya, T., Ito, N., Hagiwara, M. *Nat. Commun*. **2010**, 5(1), 86.

[215] Rüben, K., Wurzlbauer, A., Walte, A., Sippl, W., Bracher, F., Becker, W. *PLoS One*. **2015**, 10, e0132453.

[216] Balint, B., Weber, C., Cruzalegui, F., Burbridge, M., Kotschy, A. *ChemMedChem*. **2017**, 12, 932.

[217] Kumar, K., Wang, P., Sanchez, R., Swartz, E.A., Stewart, A.F., DeVita, R.J. *J. Med. Chem*. **2018**, 61, 7687.

[218] Chan, G.W., Mong, S., Hemling, M.E., Freyer, A.J., Offen, P.M., De Brosse, C.W., Sarau, H.M., Westley, J.W. *J. Nat. Prod*. **1993**, 56, 116.

[219] Loaec, N., Attanasio, E., Villiers, B., Durieu, E., Tahtouh, T., Cam, M., Davis, R. A., Alencar, A., Roue, M., Bourguet-Kondracki,´ M.-L., Proksch, P., Limanton, E., Guiheneuf, S., Carreaux, F., Bazureau, J.-P., Klautau, M., Meijer, L. *Mar. Drugs*. **2017**, 15, 316.

[220] Bidinosti, M., Botta, P., Kruttner, S., Proenca, C. C., Stoehr, N., Bernhard, M., Fruh, I., Mueller, M., Bonenfant, D., Voshol, H., Carbone, W., Neal, S. J., McTighe, S. M., Roma, G., Dolmetsch, R. E., Porter, J. A., Caroni, P., Bouwmeester, T., Luthi, A., Galimberti, I. *Science*. **2016**, 351, 1199.

[221] Kallen, J., Bergsdorf, C., Arnaud, B., Bernhard, M., Brichet, M., Cobos-Correa, A., Elhajouji, A., Freuler, F., Galimberti, I., Guibourdenche, C., Haenni, S., Holzinger, S., Hunziker, J., Izaac, A., Kaufmann, M., Leder, L., Martus, H.J., von Matt, P., Polyakov, V., Roethlisberger, P., Roma, G., Stiefl, N., Uteng, M., Lerchner, A. *ChemMedChem*. **2018**, *13*(18), 1997.

[222] Debdab, M., Renault, S., Soundararajan, M., Fedorov, O., Filippakopoulos, P., Lozach, O., Babault, L., Tahtouh, T., Baratte, B., Ogawa, Y., Hagiwara, M., Eisenreich, A., Rauch, U., Knapp, S., Meijer, L., Bazureau, J.-P. *J. Med. Chem*. **2011**, 54, 4172.

[223] Debdab, M., Renault, S., Eid, S., Lozach, O., Meijer, L., Carreaux, F., Bazureau, J.-P. Tett. Lett. **2009**, 78, 1191.

[224] Tahtouh, T., Elkins, J.M., Filippakopoulos, P., Soundararajan, M., Burgy, G., Durieu, E., Cochet, C., Schmid, R.S., Lo, D.C., Delhommel, F., Oberholzer, A.E., Pearl, L.H., Carreaux, F., Bazureau, J.P., Knapp, S., Meijer, L. *J. Med. Chem*. **2012**, 55, 9312.

[225] Song, W.J., Song, E.A., Jung, M.S., Choi, S.H., Baik, H.H., Jin, B.K., Kim, J.H., Chung, S.H. *J. Biol. Chem*. **2015**, *290*(4), 2321.

[226] Souchet, B., Audrain, M., Billard, J.M., Dairou, J., Fol, R., Orefice, N.S., Tada, S., Gu, Y., Dufayet-Chaffaud, G., Limanton, E., Carreaux, F., Bazureau, J.P., Alves, S., Meijer, L., Janel, N., Braudeau, J., Cartier, N. *Acta. Neuropathol. Commun*. **2019**, 18, *7*(1), 46.

[227] Naert, G., Ferré, V., Meunier, J., Keller, E., Malmström, S., Givalois, L., Carreaux, F., Bazureau, J.P., Maurice, T. *Eur. Neuropsychopharmacol*. **2015**, *25*(11), 2170.

[228] Nguyen, T.L., Duchon, A., Manousopoulou, A., Loaëc, N., Villiers, B., Pani, G., Karatas, M., Mechling, A.E., Harsan, L.A., Limanton, E., Bazureau, J.P., Carreaux, F., Garbis, S.D., Meijer, L., Herault, Y. *Dis. Model Mech*. **2018**, 11 (9).

[229] Radwan, M.A.A., El-Sherbiny, M. *Bioorg. Med. Chem*. **2007**, 15, 1206.

[230] Giraud, F., Alves, G., Debiton, E., Nauton, L., Thery, V., Durieu, E., Ferandin, Y., Lozach, O., Meijer, L., Anizon, F., Pereira, E., Moreau, P. *J. Med. Chem*. **2011**, 54, 4474.

[231] Echalier, A., Bettayeb, K., Ferandin, Y., Lozach, O., Clement, M., Valette, A., Liger, F., Marquet, B., Morris, J. C., Endicott, J. A., Joseph, B., Meijer, L. *J. Med. Chem*. **2008**, 51, 737.

[232] Radwan, M.A.A., El-Sherbiny, M. *Bioorg. Med. Chem*. **2007**, 15, 1206.

[233] Trimurtulu, G., Faulkner, D.J., Perry, N.B., Ettouati, L., Litaudon, M., Blunt, J.W., Munro, M.H.G., Jameson, G.B. *Tetrahedron*. **1994**, 50, 3993.

[234] Walker, S.R., Carter, E.J., Huff, B.C., Morris, J. C. *Chem. Rev*. **2009**, 109, 3080.

[235] Bettayeb, K., Tirado, O.M., Marionneau-Lambot, S., Ferandin, Y., Lozach, O., Morris, J.C., Mateo-Lozano, S., Drueckes, P., Schächtele, C., Kubbutat, M.H., Liger, F., Marquet, B., Joseph, B., Echalier, A., Endicott, J.A., Notario, V., Meijer, L. *Cancer Res*. **2007**, *67*(17), 8325.

[236] Ogawa, Y., Nonaka, Y., Goto, T., Ohnishi, E., Hiramatsu, T., Kii, I., Yoshida, M., Ikura, T., Onogi, H., Shibuya, H., Hosoya, T., Ito, N., Hagiwara, M. *Nat. Commun*. **2010**, *1*(7), 86.

[237] Mott, B.T., Tanega, C., Shen, M., Maloney, D.J., Shinn, P., Leister, W., Marugan, J.J., Inglese, J., Austin, C.P., Misteli, T., Auld, D.S., Thomas, C.J. *Bioorg. Med. Chem. Lett*. **2009**, *19*(23), 6700.

[238] Chaikuad, A., Diharce, J., Schröder, M., Foucourt, A., Leblond, B., Casagrande, A.S., Désiré, L., Bonnet, P., Knapp, S., Besson, T. *J. Med. Chem*. **2016**, 59, 10315.

[239] Exonhit SA (FR/US). **2013**. WO 026806A1.

[240] Foucourt, A., Hédou, D., Dubouilh-Benard, C., Désiré, L., Casagrande, A.S., Leblond, B., Loäec, N., Meijer, L., Besson, T. *Molecules*. **2014**, 19, 15546.

[241] Foucourt, A., Hédou, D., Dubouilh-Benard, C., Désiré, L., Casagrande, A.S., Leblond, B., Loäec, N., Meijer, L., Besson, T. Molecules. **2014**, 19, 15411.

[242] Stotani, S., Giordanetto, F., Medda, F. *Future Med. Chem*. **2016**, 8, 681.

[243] Coutadeur, S., Benyamine, H., Delalonde, L., de Oliveira, C., Leblond, B., Foucourt, A., Besson, T., Casagrande, A.S., Taverne, T., Girard, A., Pando, M.P., Désiré, L. *J. Neurochem*. **2015**, *133*(3), 440.

[244] Heffron, T.P. *J. Med. Chem*. **2016**, *59* (22), 10030.

[245] Cummings, J., Lee, G., Mortsdorf, T., Ritter, A., Zhong, K. *Alzheimers Dement. (N Y)*. **2017**, *3*(3), 367.

[246] Shi, Y., Mader, M. *Bioorg. Med. Chem. Lett*. **2018**, 28, 1981.

[247] Smyth, L.A., Collins, I. *J. Chem*. *Biol*. **2009**, *2*(3), 131.

[248] Cheng, Y-C., Prusoff, W.H. *Biochem. Pharmacol*. **1973**, *22*(23), 3099.

[249] Knight, Z.A., Shokat, K.M. *Chem. Biol*. **2005**, *12*(6), 621.

[250] Stevens, K.L., Reno, M.J., Alberti, J.B., Price, D.J., Kane-Carson, L.S., Knick, V.B., Shewchuk, L.M., Hassell, A.M., Veal, J.M., Davis, S.T., Griffin, R.J., Peel, M.R. *Bioorg. Med. Chem. Lett*. **2008**, *18*(21), 5758.

[251] Tavares, F.X., Boucheron, J.A., Dickerson, S.H., Griffin, R.J., Preugschat, F., Thomson, S.A., Wang, T.Y., Zhou, H.Q. *J. Med. Chem*. **2004**, *47*(19), 4716.

[252] Griffen, E., Leach, A.G., Robb, G.R., Warner, D.J. *J. Med. Chem*. **2011**, *54*(22), 7739.

[253] Kettle, J.G., Ballard, P., Bardelle, C., Cockerill, M., Colclough, N., Critchlow, S.E., Debreczeni, J., Fairley, G., Fillery, S., Graham, M.A., Goodwin, L., Guichard, S., Hudson, K., Ward, R.A., Whittaker, D. *J. Med. Chem*. **2015**, *58*(6), 2834.

[254] Pierce, A.C., Jacobs, M., Stuver-Moody, C. *J. Med. Chem*. **2008**, 51, 1972.

[255] Pierce, A. C., Sandretto, K.L., Bemis, G. *Proteins*. **2002**, 49, 567.

[256] Taylor, R., Kennard, O. *J. Am.Chem. Soc*. **1982**, 104, 5063.

[257] Gill, A.L., Verdonk, M., Boyle, R.G., Taylor, R.A. *Curr. Top. Med. Chem*. **2007**, 7, 1408.

[258] Leeson, P.D., Springthorpe, B. *Nat. Rev. Drug. Discovery*. **2007**, 6, 881.

[259] Imai, Y.N., Inoue, Y., Yamamoto, Y. *J. Med. Chem*. **2007**, 50, 1189.

[260] de Witte, W.E.A., Danhof, M., van der Graaf, P.H., de Lange, E.C.M. *Trends Pharmacol. Sci*. **2016**, *37*(10), 831.

[261] Tonge, P.J. *ACS Chem. Neurosci*. **2018**, *9*(1), 29.

[262] Copeland, R.A., Pompliano, D.L., Meek, T.D. *Nat. Rev. Drug Discov*. **2006**, *5*(9), 730.

[263] Heroven, C., Georgi, V., Ganotra, G.K., Brennan, P., Wolfreys, F., Wade, R.C., Fernández-Montalván, A.E., Chaikuad, A., Knapp, S. *Angew. Chem. Int. Ed*. **2018**, 57, 7220.

[264] Hassner, A., Keogh, J. *J. Org. Chem*. **1986**, *51*(14), 2767.

[265] Dorn, H., Ozegowski, R., Griindemann, E., *J. Prakt. Chem*. **1979**, 321, 555.

[266] Jasiński, R. *Computational and Theoretical Chemistry*. **2018**, 1125, 77.

[267] Henderson, S.H., West, R.A., Ward, S.E., Honey, M.A. *R. Soc. Open Sci*. **2018**, 5(6):180333.

[268] Jung, S.h., Choi, K., Pae, A.N., Lee, J.K., Choo, H., Keum, G., Cho, Y.S., Min, S. *J. Org. Biomol. Chem*. **2014**, 12, 9674.

[269]Browne, D.L., Helm, M.D., Plant, A., Harrity, J.P. *Angew. Chem. Int. Ed*. **2007**, 46, 8656.

[270]Davies, M.W., Wybrow, R.A., Johnson, C.N., Harrity, J.P. *Chem. Commun*. **2001**, 1558.

[271] Huisgen, R. *Angew. Chem. internat. Edit.* **1963**, *2*(10), 565.

[272] Hilt, G., Bolze, P. *Synthesis*. **2005**, 13, 2091.

[273] Noble, A., McCarver, S.J, MacMillan, D.W. *J. Am. Chem. Soc*. **2015**, 137, 624.

[274] Zuo, Z., Cong, H., Li, W., Choi, J., Fu, G.C., MacMillan, D.W. *J. Am. Chem. Soc.* **2016**, 138, 1832.

[275] Zuo, Z., Ahneman, D.T., Chu, L., Terrett, J.A., Doyle, A.G., MacMillan, D.W. *Science*. **2014**, 345, 437.

[276] Nagib, D.A., MacMillan, D.W. *Nature*. **2011**, 480, 224.

[277] Czarna, A., Wang, J., Zelencova, D., Liu, Y., Deng, X., Choi, H.G., Zhang, T., Zhou, W., Chang, J.W., Kildalsen, H., Seternes, O.M., Gray, N.S., Engh, R.A., Rothweiler, U. *J. Med. Chem*. **2018**, *61*(17), 7560.

[278] Hu, Y., Stumpfe, D., Bajorath, J. *J. Med. Chem*. **2017**, 60, 1238.

[279] Pennington, L.D., Moustakas, D.T. *J. Med. Chem*. **2017**, *60*(9), 3552.

[280] Li, P., Maier, J.M., Vik, E.C., Yehl, C.J., Dial, B.E., Rickher, A.E., Smith, M.D., Pellechia, P.J., Shimizu, K.D. *Angew. Chem. Int. Ed*. **2017**, 56, 7209.

[281] https://openlabnotebooks.org/category/past-scientist/carla-alamillo/

[282] Hynes, J. Jr., Doubleday, W.W., Dyckman, A.J., Godfrey, J.D. Jr., Grosso, J.A., Kiau, S., Leftheris, K. *J. Org. Chem*. **2004**, *69*(4), 1368.

[283] Böhm, H.J., Flohr, A., Stahl, M. *Drug Discov. Today Technol*. **2004**, *1*(3), 217.

[284] Spyrakis, F., Ahmed, M.H., Bayden, A.S., Cozzini, P., Mozzarelli, A., Kellogg, G.E. *J. Med. Chem*. **2017**, *60*(16), 6781.

[285] Burgdorf, L.; Kuhn, D., Ross, T., Deutsch, Carl. MERCK PATENT GMBH. **2014**.WO2014/23385.

[286] Chatzopoulou, M., Martínez, R.F., Willis, N.J., Claridge, T.D.W., Wilson, F.X., Wynne, G.M., Davies, S.G., *Tetrahedron*, **2018**, 74, 5280.

[287] Ellis, J.M., Altman, M.D., Bass, A., Butcher, J.W., Byford, A.J., Donofrio, A., Galloway, S., Haidle, A.M., Jewell, J., Kelly, N., Leccese, E.K., Lee, S., Maddess, M., Miller, J.R., Moy, L.Y., Osimboni, E., Otte, R.D., Reddy, M.V., Spencer, K., Sun, B., Vincent, S.H., Ward, G.J., Woo, G.H.C., Yang, C., Houshyar, H., Northrup, A.B. *J. Med. Chem*. **2015**, 58, 1929.

[288] Bendjeddou, L.Z., Loaëc, N., Villiers, B., Prina, E., Späth, G.F., Galons, H., Meijer, L., Oumata, N. *Eur. J. Med. Chem*. **2017**, 125, 696

[289] The Arizona Board of Regents on behalf of the University of Arizona (US). **2017.** WO040993.

[290] Alelyunas, Y.W., Empfield, J.R., McCarthy, D., Spreen, R.C., Bui, K., Pelosi-Kilby, L., Shen, C. *Bioorg. Med. Chem. Lett*. **2010**, 20, 7312.

[291] Ishikawa, M., Hashimoto, Y. *J. Med. Chem*. **2011**, 54, 1539.

[292] Ran, Y., Yalkowsky, S.H. *J. Chem. Inf. Comput. Sci*. **2001**, 41, 354.

[293] Ritchie, T.J., Macdonald, S.J. *Drug Discov. Today*. **2009**, *14*(21-22), 1011.

[294] Hou, T.J., Xia, K., Zhang, W., Xu, X.J. *J. Chem. Inf. Comput. Sci*. **2004**, 44, 266.

[295] Young, R.J., Green, D.V., Luscombe, C.N., Hill, A.P. *Drug Discov. Today*. **2011**, *16*(17-18), 822.

[296] Funnell, T., Tasaki, S., Oloumi, A., Araki, S., Kong, E., Yap, D., Nakayama, Y., Hughes, C.S., Cheng, S.G., Tozaki, H., Iwatani, M., Sasaki, S., Ohashi, T., Miyazaki, T., Morishita, N., Morishita, D., Ogasawara-Shimizu, M., Ohori, M., Nakao, S., Karashima, M., Sano, M., Murai, A., Nomura, T., Uchiyama, N., Kawamoto, T., Hara, R., Nakanishi, O., Shumansky, K., Rosner, J., Wan, A., McKinney, S., Morin, G.B., Nakanishi, A., Shah, S., Toyoshiba, H., Aparicio, S. *Nat. Commun*. **2017**, *8*(1), 7.

[297] Barbosa, A., **2010**. WO 2010/056875. PCT/US2009/064224.

[298] Lombardino, J.G. *J. Heterocycl Chem*. **1968**, 5(1), 35.

[299] Cernak, T., Schçnherr, H. *Angew. Chem. Int. Ed*. **2013**, 52, 12256.

[300] Witherington, J., Bordas, V., Haigh, D., Hickey, D.M.B., Ife, R.J., Rawlings, A.D., Slingsby, B.P., Smith, D.G., Ward, R.W. *Bioorg. Med. Chem. Lett*. **2003**, 13, 1581.

[301]Braña, M.F., Cacho, M., García, M.L., Mayoral, E.P., López, B., de Pascual-Teresa, B., Ramos, A., Acero, N., Llinares, F., Muñoz-Mingarro, D., Lozach, O., Meijer, L. *J. Med. Chem*. **2005**, 48, 6843.

[302] Blaquiere, N. WO 2015/025025.

[303] Kurti, L., Czako, B. *Strategic Applications of Named Reactions in Organic Synthesis*. Elsevier. **2005**, 448.

[304] Hood, J., Sunil Kumar, K.C - WO2013/40215, **2013**, A1.

[305] Deshmukh, V., Murphy, E.A., Hood, J. - WO2018/75858, **2018**, A1

[306] Nakano-Kobayashi, A., Awaya, T., Kii, I., Sumida, Y., Okuno, Y., Yoshida, S., Sumida, T., Inoue, H., Hosoya, T., Hagiwara, M. *Proc. Natl. Acad. Sci. U S A*. **2017**, *114*(38), 10268.

[307] Karaman, M.W., Herrgard, S., Treiber, D.K., Gallant, P., Atteridge, C.E., Campbell, B.T., Chan, K.W., Ciceri, P., Davis, M.I., Edeen, P.T., Faraoni, R., Floyd, M., Hunt, J.P., Lockhart, D.J., Milanov, Z.V., Morrison, M.J., Pallares, G., Patel, H.K., Pritchard, S., Wodicka, L.M., Zarrinkar, P.P. *Nat. Biotechnol*. **2008**, *26*(1), 127.

[308] Gu, S., Cui, D., Chen, X., Xiong, X., Zhao, Y. *BioEssays*. **2018**, 40, 1700247.